DOGGER BANK D WIND FARM

Preliminary Environmental Information Report

Volume 2
Appendix 8.3 Marine Physical Processes Modelling Report

Document Reference No: 2.8.3
Date: June 2025
Revision: V1

sse Renewables equinor

www.doggerbankd.com

Document Title:	**Volume 2, Appendix 8.3 Marine Physical Processes Modelling Report**
Document BIM No.	**PC6250-RHD-XX-OF-RP-EV-0052**
Prepared By:	**Royal HaskoningDHV**
Prepared For:	**Dogger Bank D Offshore Wind Farm**

Revision No.	Date	Status / Reason for Issue	Author	Checked By	Approved By
V1	04/02/2025	Final	SB/TC/DXL	GA	RH

Table of Contents

8.3 Marine Physical Processes Modelling Report 6
8.3.1 Introduction 6
8.3.2 Data Collection 6
8.3.2.1 Bathymetry 6
8.3.2.2 Wind and Wave Data 9
8.3.2.3 Water Level Data 10
8.3.2.4 Tidal Current Data 12
8.3.3 Model Layout 12
8.3.3.1 DBD Wind farm Layouts 13
8.3.3.2 Baseline 16
8.3.3.3 DBD Option 16
8.3.3.4 Scenario 1 17
8.3.3.5 Scenario 2 18
8.3.4 Wave Modelling 19
8.3.4.1 Model Configuration 19
8.3.4.2 Model Verification 23
8.3.4.3 Offshore Extreme Wave and Wind Analysis 33
8.3.4.4 Sensitivity Model Runs 34
8.3.4.5 Model Simulations for Assessing Potential Impact 40
8.3.4.6 Baseline and Option Model Run Results 40
8.3.4.7 Cumulative Model Run Results 59
8.3.4.8 Discussions of Wave Model Results 76
8.3.5 Hydrodynamic Modelling 77
8.3.5.1 Model Description 77
8.3.5.2 Model Boundary Conditions 81
8.3.5.3 Model Calibration 82
8.3.5.4 Hydrodynamic Model Production Runs 92
8.3.5.5 Hydrodynamic Model Results and Discussions 93
8.3.6 Suspended Sediment Dispersion Modelling 101
8.3.6.1 Model Configuration 101
8.3.6.2 Construction Activities and Sediment Release 102
8.3.6.3 Seabed Sediment Properties 105

8.3.6.4 Model Simulations 106
8.3.6.5 Discussion of Suspended Sediment Dispersion Model Results 108
References 112
List of Figures, Tables and Plates 113
List of Acronyms 120

List of Appendices

Term	Definition
Appendix A	Hydrodynamic Modelling Baseline Run Results
Appendix B	Hydrodynamic Modelling Cumulative Run Results – Layout C, Offshore Platform 2
Appendix C	Hydrodynamic Modelling Cumulative Run Results – Layout B, Offshore Platform 2
Appendix D	Predicted Maximum Suspended Sediment Concentration and Sediment Depositions from Laying Export Cables
Appendix E	Predicted Maximum Suspended Sediment Concentration and Sediment Depositions from Drilling Foundation of Turbines and Platforms
Appendix F	Time Series of Predicted Suspended Sediment Concentration at Selected Points during Trenching Export Cable Corridor

Glossary

Term	Definition
Array Area	The area within which the wind turbines, inter-array cables and Offshore Platform(s) will be located.
Design	All of the decisions that shape a development throughout its design and pre-construction, construction / commissioning, operation and, where relevant, decommissioning phases.
Development Consent Order (DCO)	A consent required under Section 37 of the Planning Act 2008 to authorise the development of a Nationally Significant Infrastructure Project, which is granted by the relevant Secretary of State following an application to the Planning Inspectorate.
Effect	An effect is the consequence of an impact when considered in combination with the receptor's sensitivity / value / importance, defined in terms of significance.
Impact	A change resulting from an activity associated with the Project, defined in terms of magnitude.
Offshore Export Cable Corridor (ECC)	The area within which the offshore export cables will be located, extending from the DBD Array Area to Mean High Water Springs at the landfall.
Offshore Export Cables	Cables which bring electricity from the offshore platform(s) to the transition joint bays at landfall.
Offshore Platform(s)	Fixed structures located within the DBD Array Area that contain electrical equipment to aggregate and, where required, convert the power from the wind turbines, into a more suitable voltage for transmission through the export cables to the Onshore Converter Station. Such structures could include (but are not limited to): Offshore Converter Station(s) and an Offshore Switching Station.
Significant Wave Height (Hs)	The average height of the highest of one third of the waves in a given sea state.
The Project	Dogger Bank D (DBD) Offshore Wind Farm Project, also referred to as DBD in PEIR.

8.3 Marine Physical Processes Modelling Report

8.3.1 Introduction

1. This document presents the methodology and results of the Project-specific marine physical processes modelling work undertaken to inform the Dogger Bank D Offshore Wind Farm Project (hereafter referred to as 'the Project' or 'DBD') Preliminary Environmental Information Report.

2. This report details the methodology, inputs into the model and final results of the modelling work in relation to the following modelling campaigns:

   - Wave modelling;
   - Hydrodynamic modelling; and
   - Sediment dispersion modelling.

8.3.2 Data Collection

8.3.2.1 Bathymetry

3. Detailed bathymetry survey data was provided by the Project covering the DBD Wind Farm Area (**Figure 8.3-1**), Dogger Bank Tranche A (surveyed 2010) and Tranche B (surveyed 2012) Wind farm Areas (**Figure 8.3-2**). Bathymetry data covering Dogger Bank South (DBS) West and DBS East Wind farm Areas (**Figure 8.3-3**) and DBS's Offshore Export Cable Corridor (ECC) (**Figure 8.3-4**) were obtained from a site specific survey undertaken for the DBS project (Fugro, 2023a; 2023b).

4. For offshore areas where there was no detailed bathymetry available, EMODnet bathymetry data has been downloaded from the EMODnet Bathymetry Portal and used in the wave and local hydrodynamic model (**Figure 8.3-4**). The Export Cable Corridor and additional section of the array is currently being surveyed, and these data will be used at the Development Consent Order (DCO) application stage.

5. In the regional hydrodynamic model which provides boundary conditions for the local hydrodynamic model, the bathymetry was based on C-Map data supplemented by more recent bathymetry data from the UK Hydrographic Office's Admiralty Maritime Data Solutions (**Figure 8.3-5**).

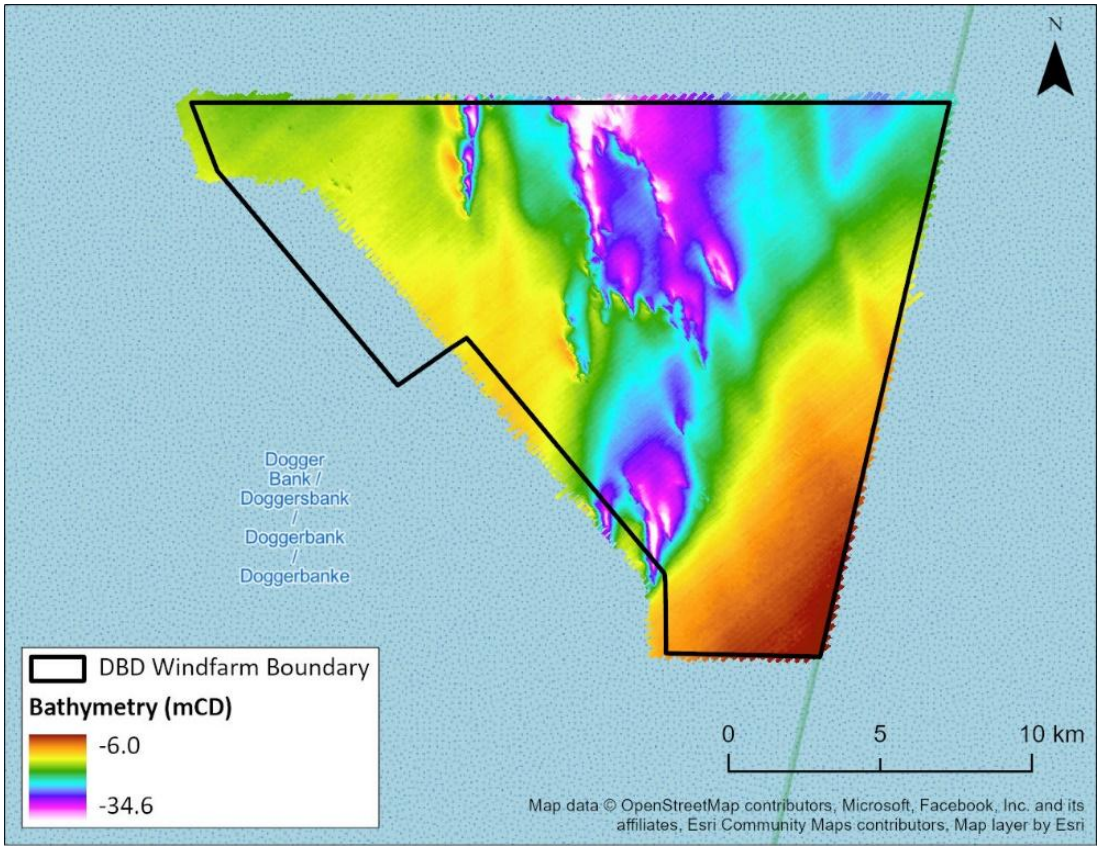

Figure 8.3-1: Detailed Bathymetry of DBD Wind Farm Area

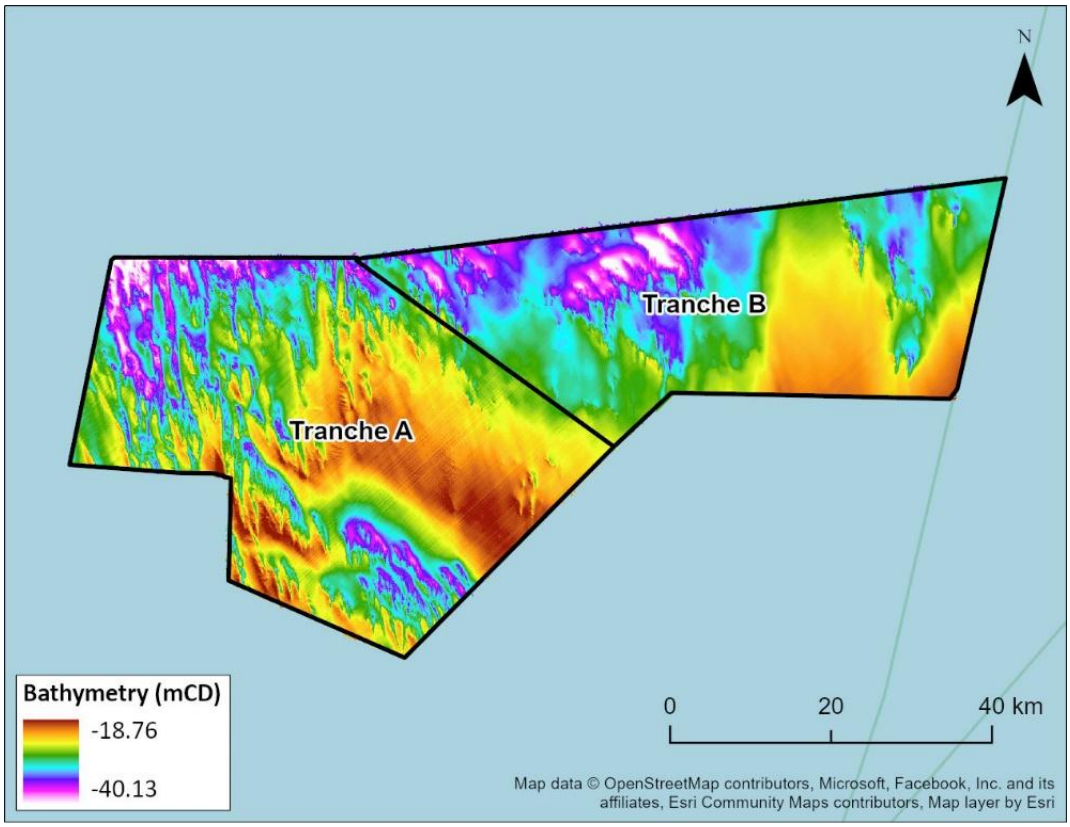

Figure 8.3-2: Detailed Bathymetry of Dogger Bank Tranche A and Tranche B Wind Farm Areas

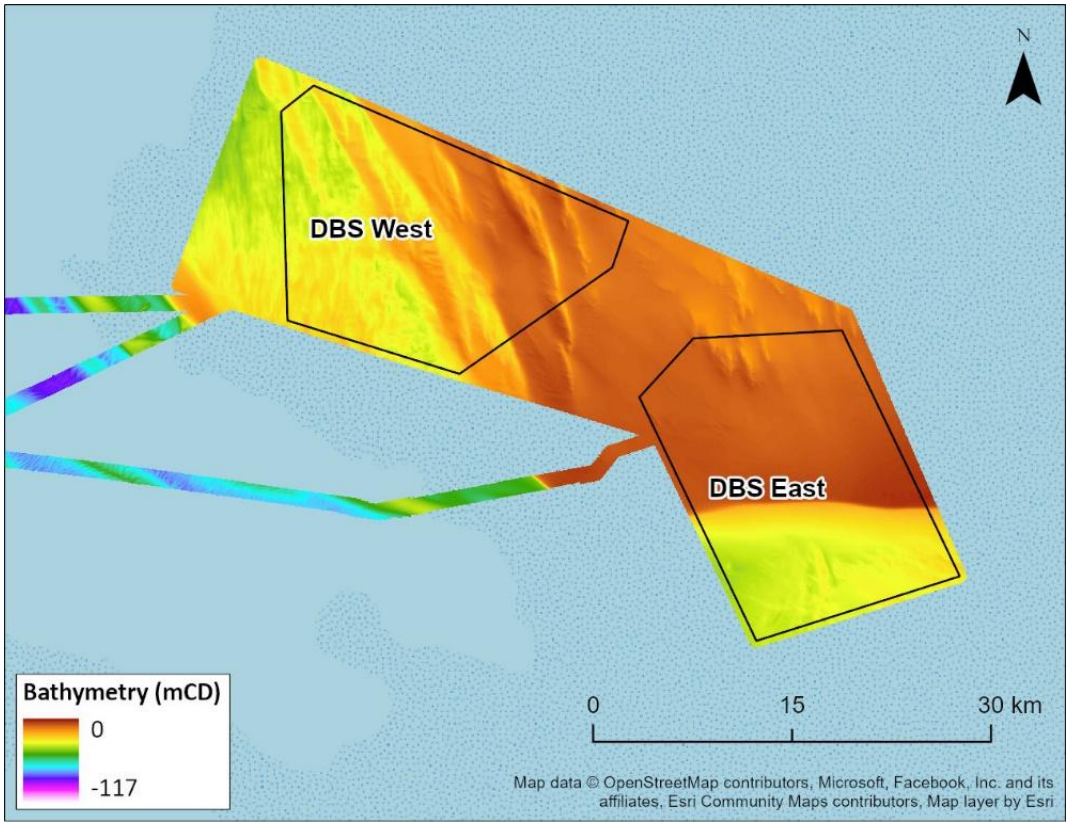

Figure 8.3-3: Detailed Bathymetry of Areas DBS West and DBS East

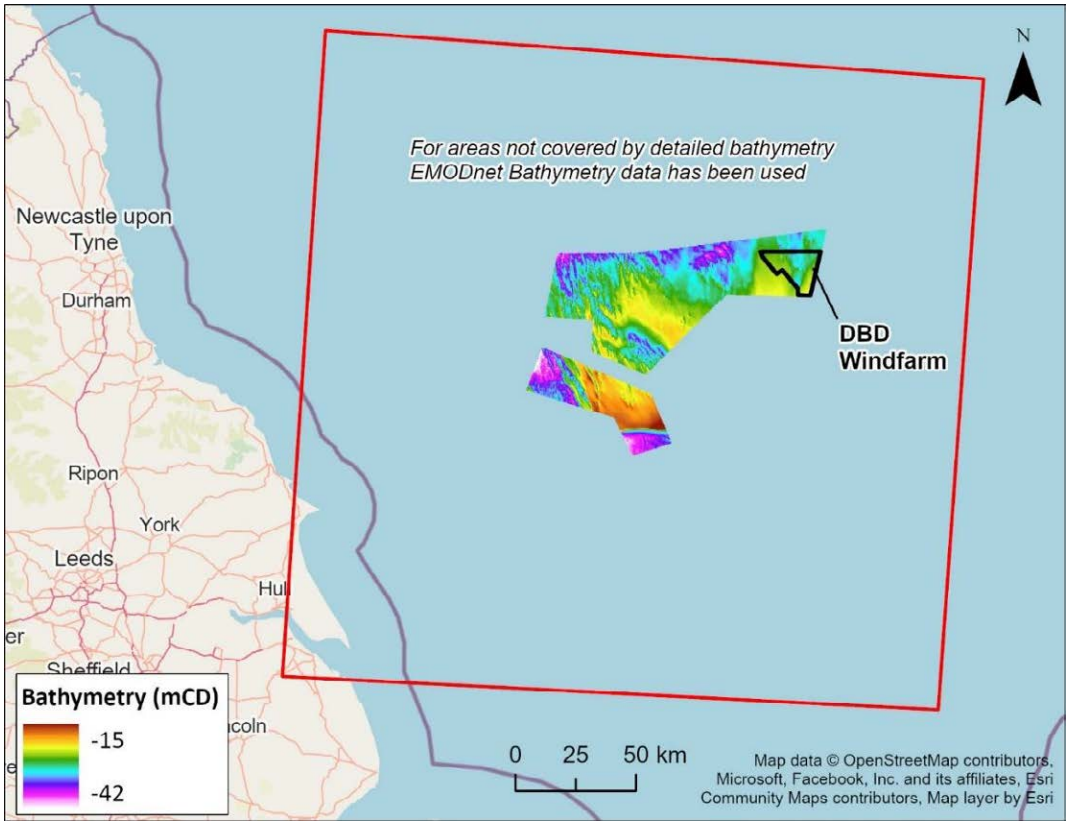

Figure 8.3-4: Coverage of Detailed Bathymetry Data used in the Wave and Local Hydrodynamic Model

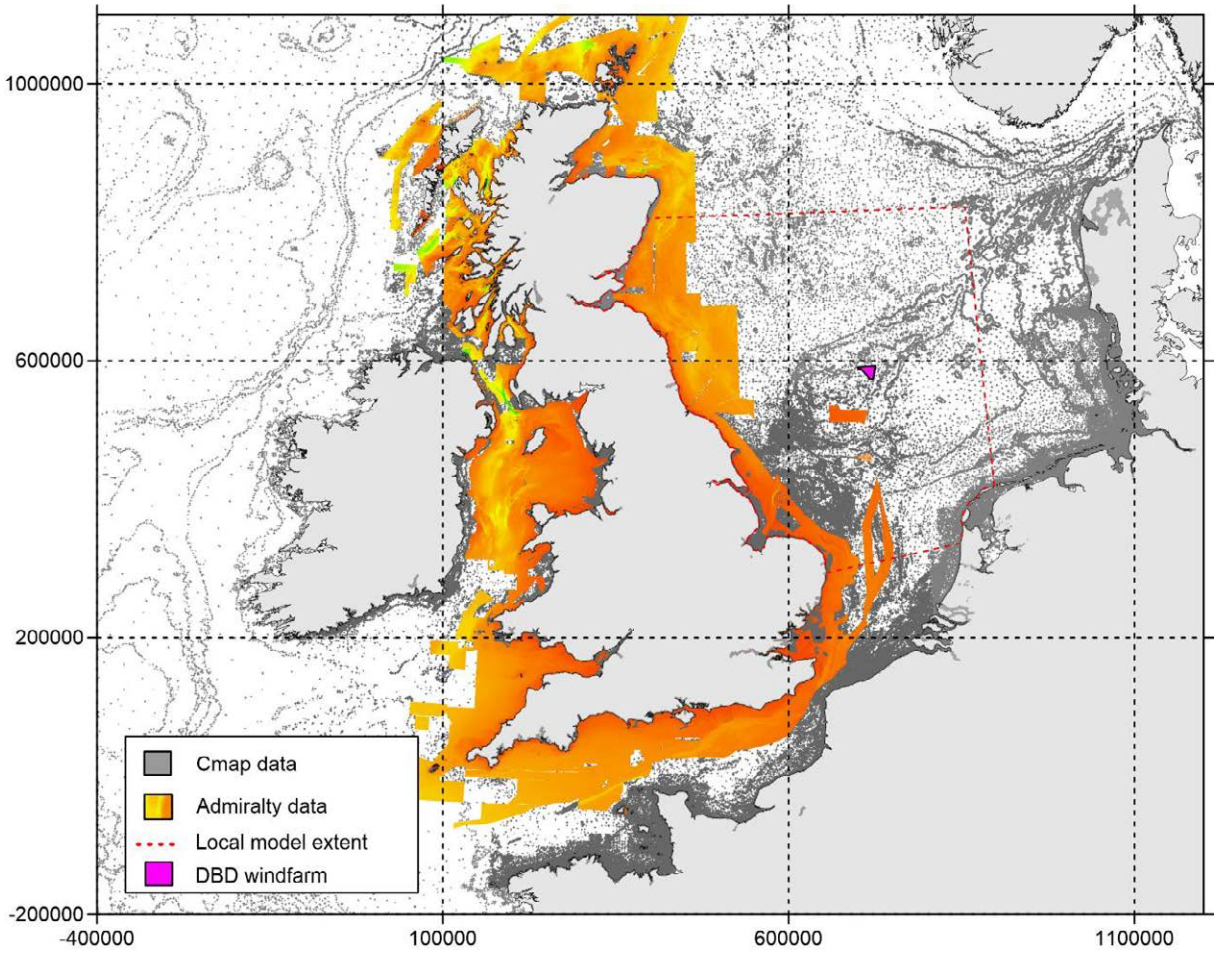

Figure 8.3-5: C-map and Admiralty Maritime Data Solutions Data used in the Regional Hydrodynamic Model

8.3.2.2 Wind and Wave Data

8.3.2.2.1 Measured Wave Data

6. Measured wave buoy data (collected by Partrac; hereafter referred to Partrac wave buoy data) was provided by the Project at three locations (as shown on **Figure 8.3-6**) for the stated time periods:

- Dogger Bank North; 25/09/2022 to 08/01/2024;
- Dogger Bank South; 30/06/2022 to 29/12/2023; and
- Dogger Bank B; 16/09/2023 to 15/02/2024.

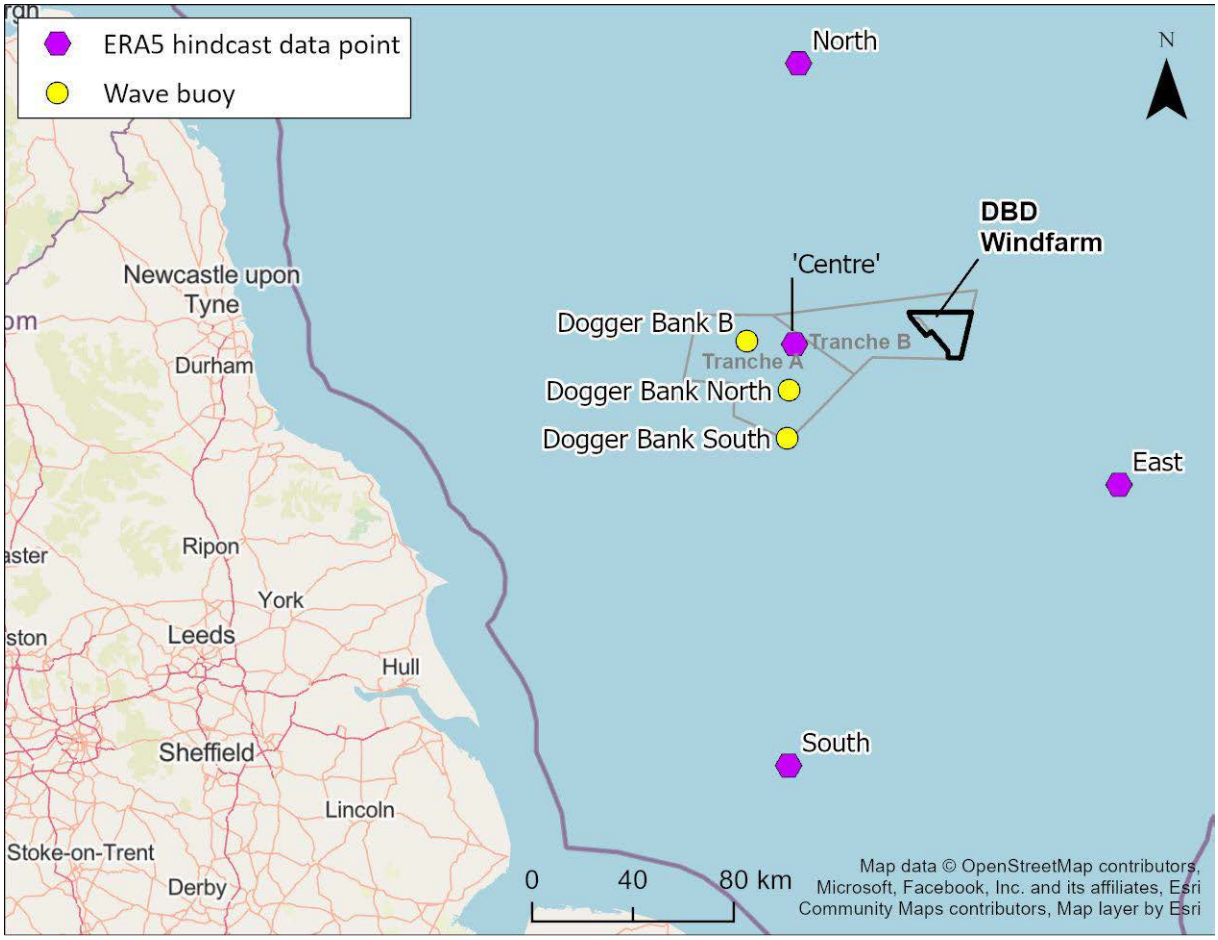

Figure 8.3-6: Locations of wave buoys North and South and ERA5 Hindcast Data Points

8.3.2.2.1.1. Hindcast Wind and Wave Data

7. Atmospheric hindcast wave and wind data (at approximately 10m above water surface) close to the wave model boundary and close to the calibration wave buoys has been downloaded from European Centre for Medium-Range Weather Forecasts (ECMRWF) covering the time period between January 1979 and May 2023 (**Figure 8.3-6**).

8.3.2.3 Water Level Data

8. Measured water levels from 1st March 2012 to 31st May 2013 were downloaded from British Oceanographic Data Centre (BODC) at three locations; North Shields, Whitby and Cromer. The locations (1, 2 and 3) are shown on **Figure 8.3-7** and the coordinates in **Table 8.3-1**. These measured water levels were used to calibrate the regional and the local hydrodynamic models.

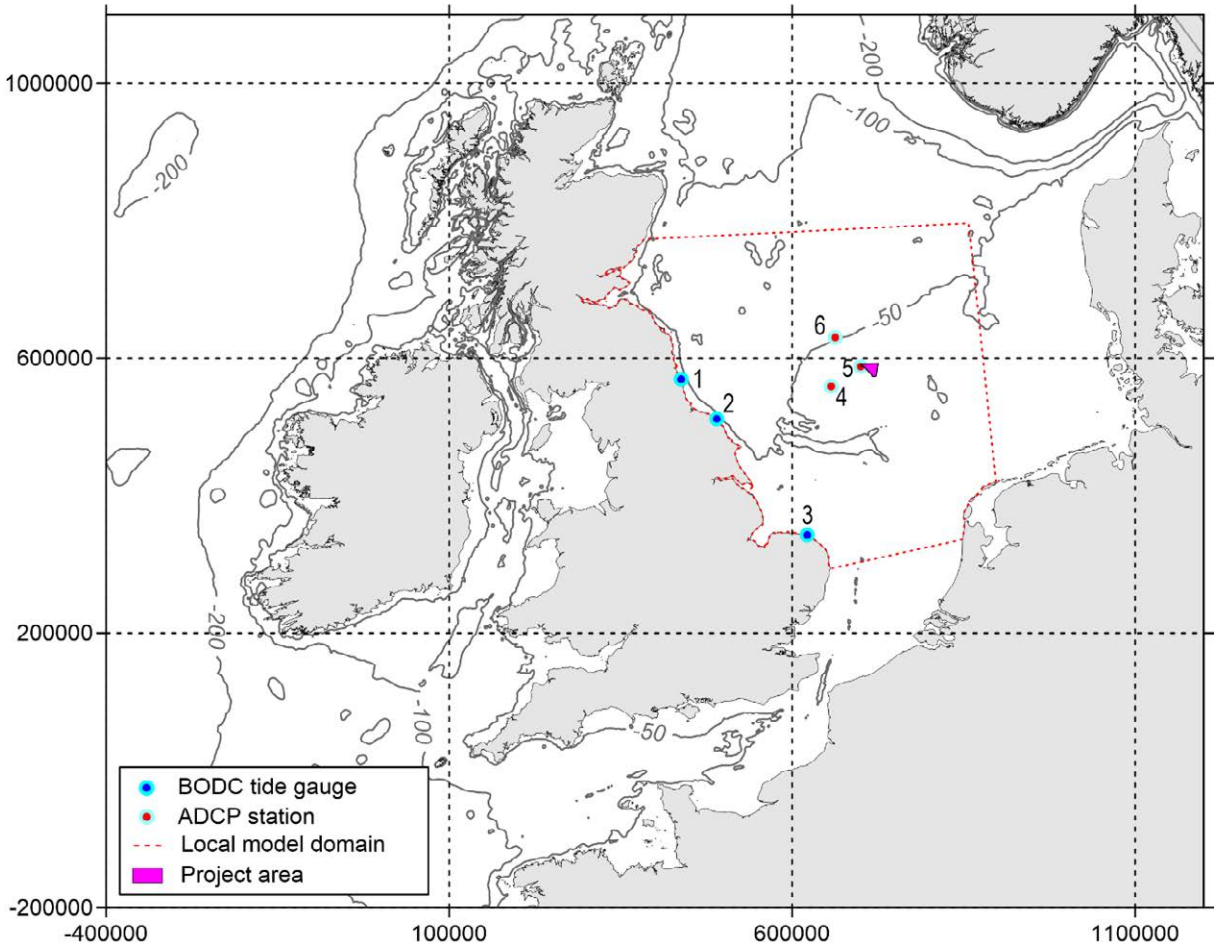

Figure 8.3-7: Locations of Tidal Gauges and Current Stations (Gauge and Station Detailed are Given in Table 8.3-1 and Table 8.3-2)

Table 8.3-1: Locations of the Measured Water Levels

ID	Station name	Longitude (degrees)	Latitude (degrees)	Time interval (minutes)	Duration
1	North Shields	-1.40	55.01	60	3/2012 – 3/2013
2	Whitby	-0.61	54.49	60	3/2012 – 3/2013
3	Cromer	1.30	52.93	60	3/2012 – 3/2013

8.3.2.4 Tidal Current Data

9. Measured current data was collected by Gardline shown on **Figure 8.3-7**. This data was used in the calibration of the Local Hydrodynamic Model. A description of the measured data including locations is provided in **Table 8.3-2**.

Table 8.3-2: Locations of the Measured Currents

ID	Station name	Longitude (degrees)	Latitude (degrees)	Time interval (minutes)	Duration
4	West Met Mast	1.99	54.86	10	2/2012 – 2/2013
5	East Met Mast	2.69	55.09	10	2/2012 – 3/2013
6	North Dogger	2.15	55.49	10	5/2012 – 9/2012

8.3.3 Model Layout

10. For the Project, there are 4 different DBD turbine layouts that have been carried out as Sensitivity Tests for the Wave Modelling and as Production Runs for Hydrodynamic Modelling. These are:

- Four turbine layouts, namely A, B, C and D; and
- Three offshore platform options for each array layout.

11. For the Sensitivity Runs for the Wave Modelling, the following test conditions were used, namely:

- Two wave directions, namely 'North' and 'South'; and
- One wave condition, namely 50 percentile (chosen for its shorter wave length for worst-case).

12. For the Project, there are 4 different offshore wind farm scenarios that have been carried out as Production Runs for both Wave and Hydrodynamic Modelling for assessing potential cumulative impact. These are:

- Baseline (no offshore wind farm structures);
- DBD Option;
- Scenario 1 (DBD and existing offshore wind farms, inclusive of those under construction); and
- Scenario 2 (DBD, existing offshore wind farms and planned DBS).

8.3.3.1 DBD Wind farm Layouts

13. **Table 8.3-3** shows the details of the four turbine layouts A to D and the three offshore platform options 1 to 3.

14. It should be noted that the number of turbines stated in **Table 8.3-3** excludes five 'spare' locations which have been removed; the 'spare' turbines were excluded from the north-east corner of each array based on advice given by engineers as being the most likely region to be used for spare locations.

15. It should also be noted that each offshore platform in the model is represented by six legs, defined as monopiles, with dimensions shown in **Table 8.3-4**. The use of monopiles with diameter of 15.5m (of two smaller offshore platforms) and 18.5m (of single larger offshore platform) for jacket legs is considered to be a conservative model option. The maximum diameters for smaller and larger offshore platforms are 15m and 18m respectively. An extra 0.5m was added to account for hammer, boat ladder and any other protrusions.

16. The four turbine layouts A to D and the three offshore platform options are shown on **Figure 8.3-8** to **Figure 8.3-11** respectively.

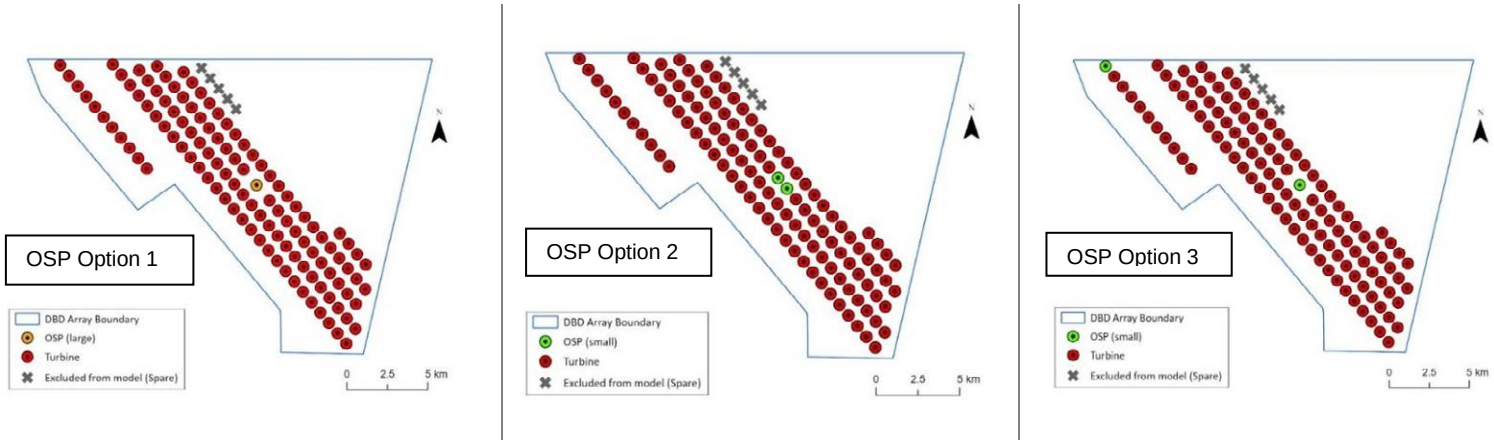

*Figure 8.3-8: Wind Farm Array **Layout A** with Offshore Platform Options 1 to 3*

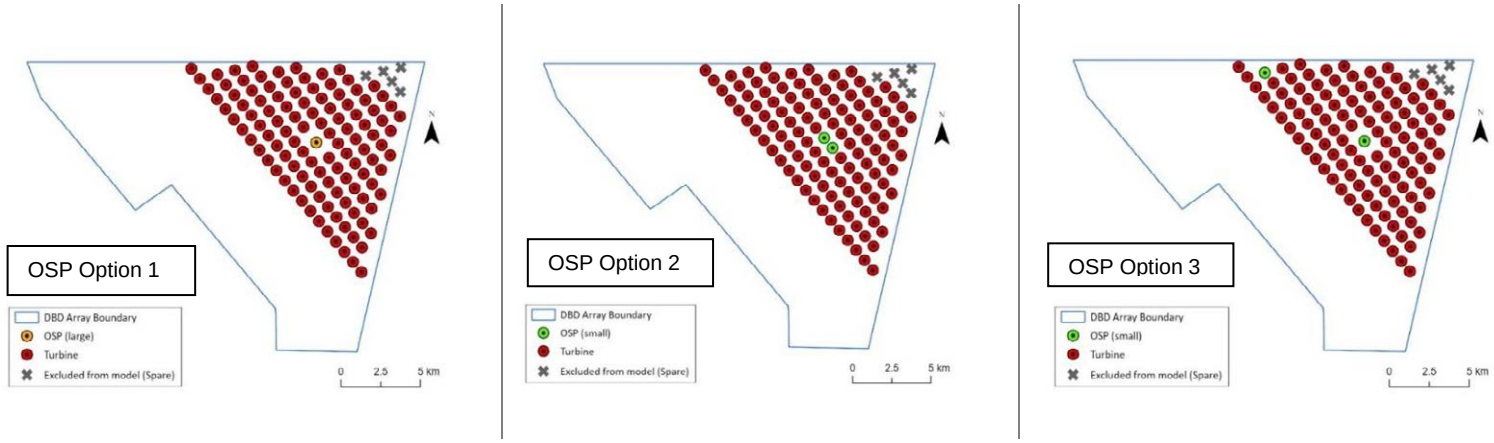

*Figure 8.3-9: Wind Farm Array **Layout B** with Offshore Platform Options 1 to 3*

Table 8.3-3: Details of Array Layouts A to D and Offshore Platform Options 1 to 3

Turbine Layout	Offshore Platform Option	No. of Offshore Platforms*	Offshore Platform Location	Offshore Platform Leg Diameter (m)	No. of Turbines**	Turbine Foundation Diameter (m)	Approx Turbine Spacing (m)
A	1	1	Central	18.5	113	18.5	NW to SE: 800m; NE to SW: 1,000m
	2	2	Central	15.5			
	3	2	Central / north-west	15.5			
B	1	1	Central	18.5	113	18.5	NW to SE: 800m; NE to SW: 1,000m
	2	2	Central	15.5			
	3	2	Central / north-west	15.5			
C	1	1	Central	18.5	113	18.5	NW to SE: 1,400m; NE to SW: 1,200m
	2	2	Central	15.5			
	3	2	Central / north-west	15.5			
D	1	1	Central	18.5	70	18.5	NW to SE: 1,500m; NE to SW: 1,500m
	2	2	Central	15.5			
	3	2	Central / north-west	15.5			

*Each offshore platform is modelled with six legs

**Excluding 5 spare turbines

Table 8.3-4: Dimensions of Large and Small Offshore Platform

Large Offshore Platform (leg diameter: ø18.5m)	Small Offshore Platform (leg diameter: ø15.5m)
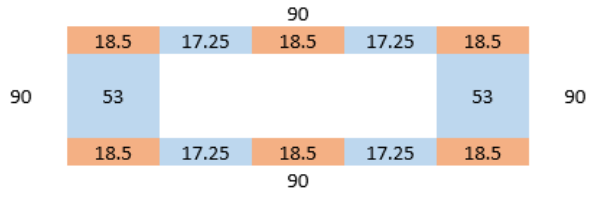	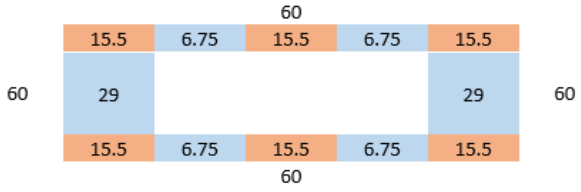

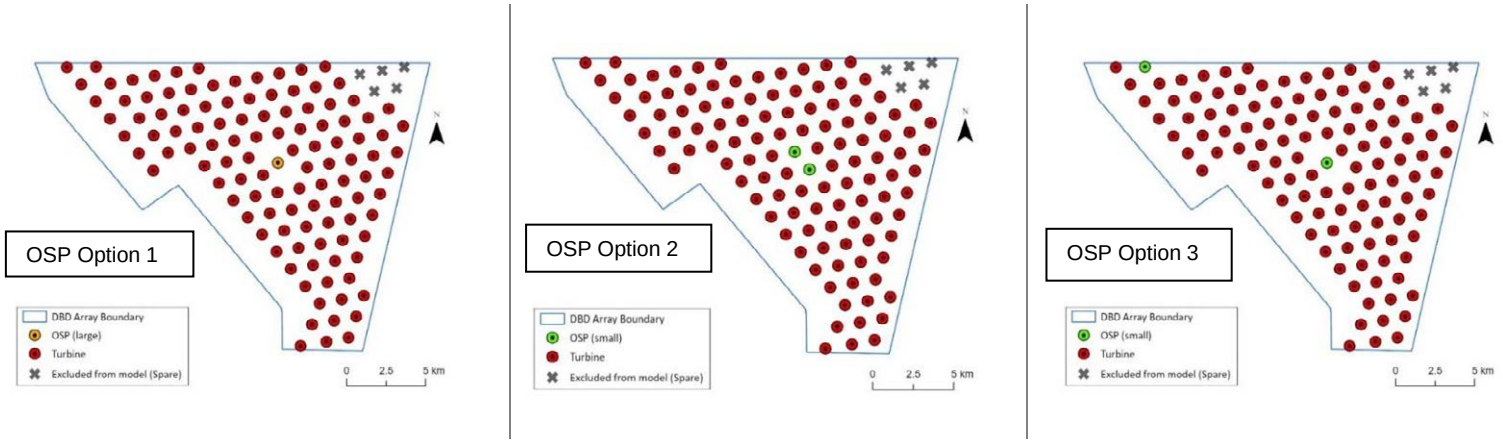

*Figure 8.3-10: DBD Turbine **Layout C** with Offshore Platform Options 1 to 3*

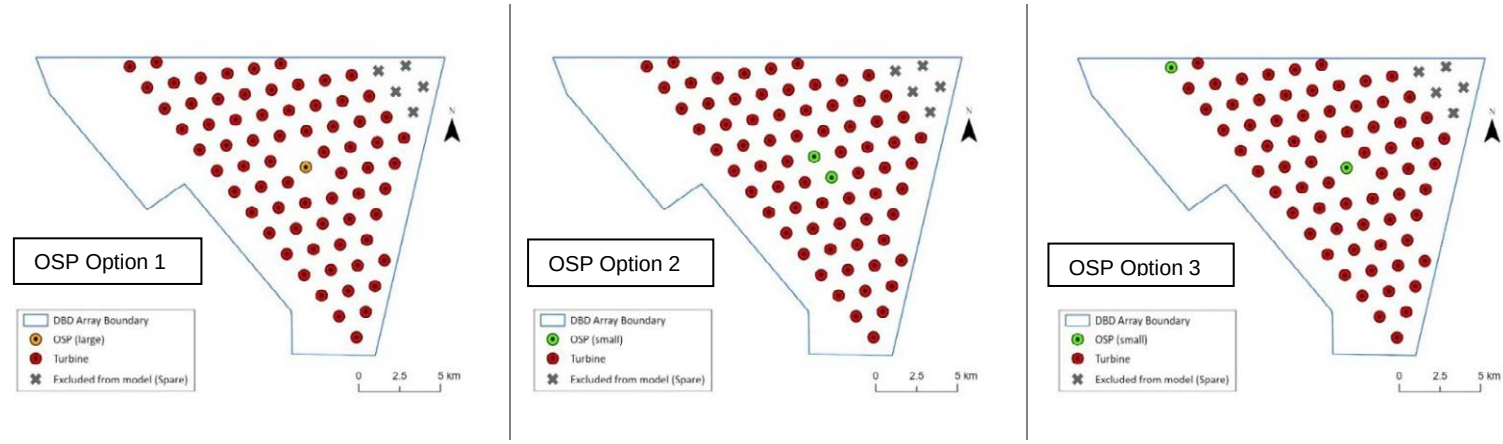

*Figure 8.3-11: DBD Turbine **Layout D** with Offshore Platform Options 1 to 3*

8.3.3.2 Baseline

17. The 'Baseline' model layout takes forward the parameters assuming there is no wind farm development.

8.3.3.3 DBD Option

18. Turbine Layout C with two small Offshore Platforms at the centre was chosen as the "worst-case" DBD layout, which includes 113 turbines and two small Offshore Platforms in the centre of the array area (**Figure 8.3-12**). The "worst-case" layout is discussed in **Section 8.3.4.4** and **Section 8.3.5.5**.

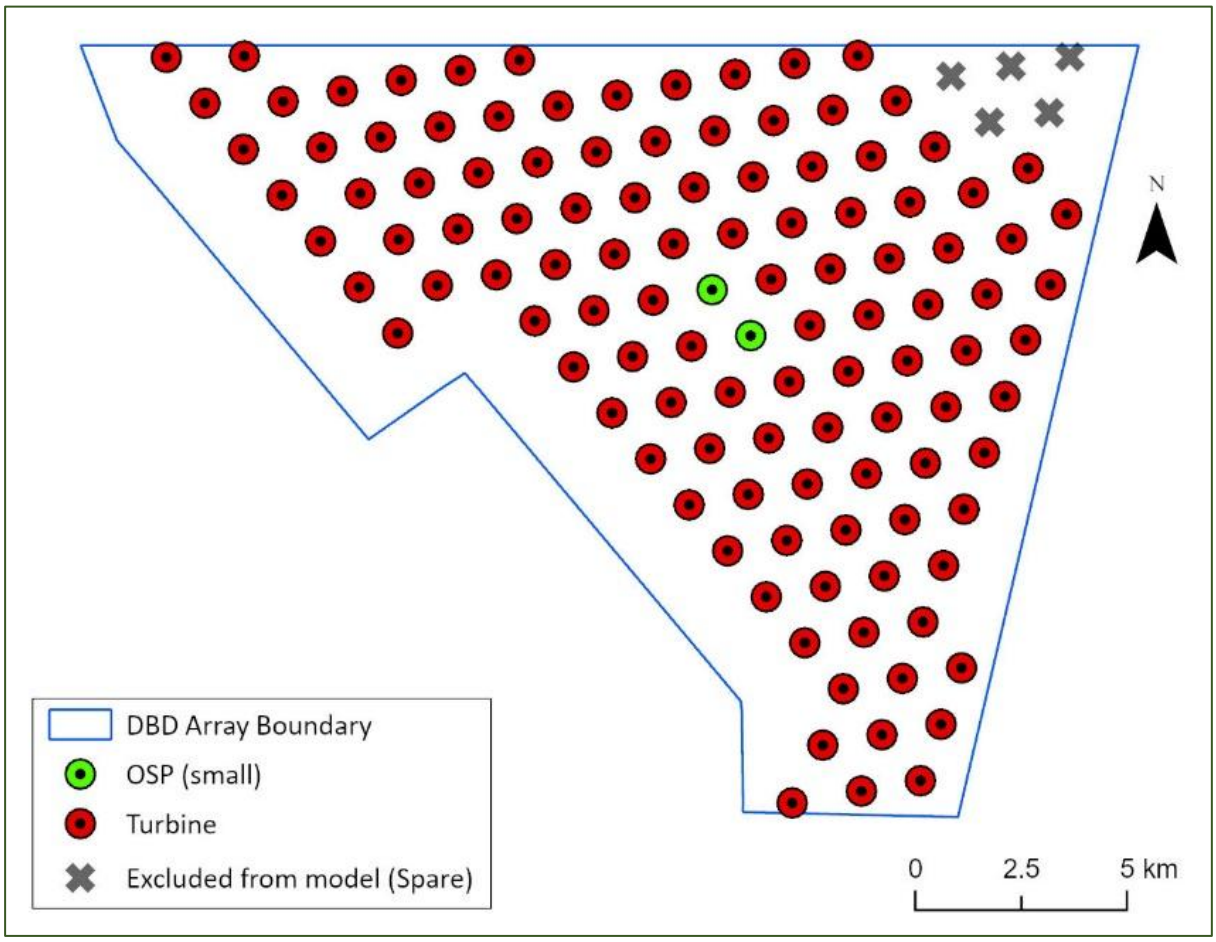

Figure 8.3-12: DBD Option

19. The 113 turbines are spaced at approx. 1,400m spread across the entire DBD array area. Each turbine foundation measures 18.5m in diameter and is defined as monopile in the model. There are two Offshore Platforms situated at the centre of the Array Area, each Offshore Platform has six legs which are defined as monopile in the model measuring 15.5m in diameter.

20. It should be noted that the two Offshore Platform locations have been chosen indicatively at the most likely future position based on advice given by engineers.

8.3.3.4 Scenario 1

21. The 'Scenario 1' wind farm layout takes forward the parameters including the "worst-case" 'DBD Option', and existing wind farms Dogger Bank A (DBA), Dogger Bank B (DBB), Dogger Bank C (DBC) and Sofia (**Figure 8.3-13**).

22. The proposed wind farm array layouts for 'Scenario 1' are explained in **Table 8.3-5**.

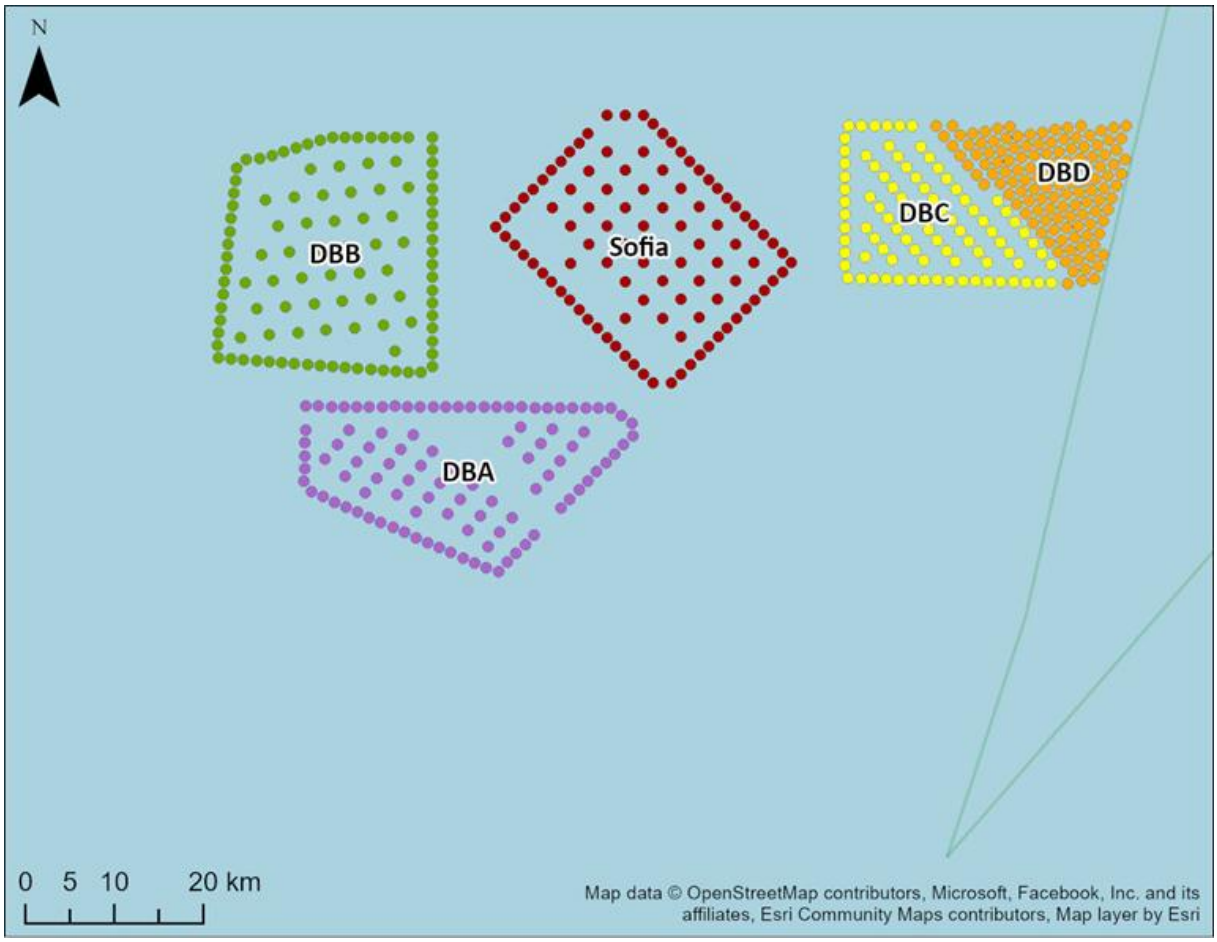

Figure 8.3-13: Wind Farm Layouts included in 'Scenario 1'

Table 8.3-5: Details of Wind Farm Layouts for Cumulative Scenarios

Scenario	Wind farm	No. of Turbines	Turbine foundation diameter (m)	No. of Offshore Platforms	Offshore Platform Foundation Diameter (m)
1&2	DBD	113	18.5	2 (6 pin piles each)	15.5
1	DBA	95	8.6	1 (4 pin piles)	2.438
1	DBB	95	8.6	1 (4 pin piles)	2.438
1	DBC	87	8.4	1 (4 pin piles)	2.438
1	Sofia	100	8.8	1 (8 pin piles)	2.438
2	Dogger Bank South (A + B) [spread out design]	200	15.0	8 (+1 along cable corridor)	65.0

8.3.3.5 Scenario 2

23. The 'Scenario 2' model layout takes forward the parameters including the proposed wind farm development from 'DBD Option', and existing wind farms DBA, DBB, DBC and Sofia, as well as the planned DBS wind farm array (**Figure 8.3-14**).

24. The proposed wind farm arrays' layouts for 'Scenario 2' are explained in **Table 8.3-5**.

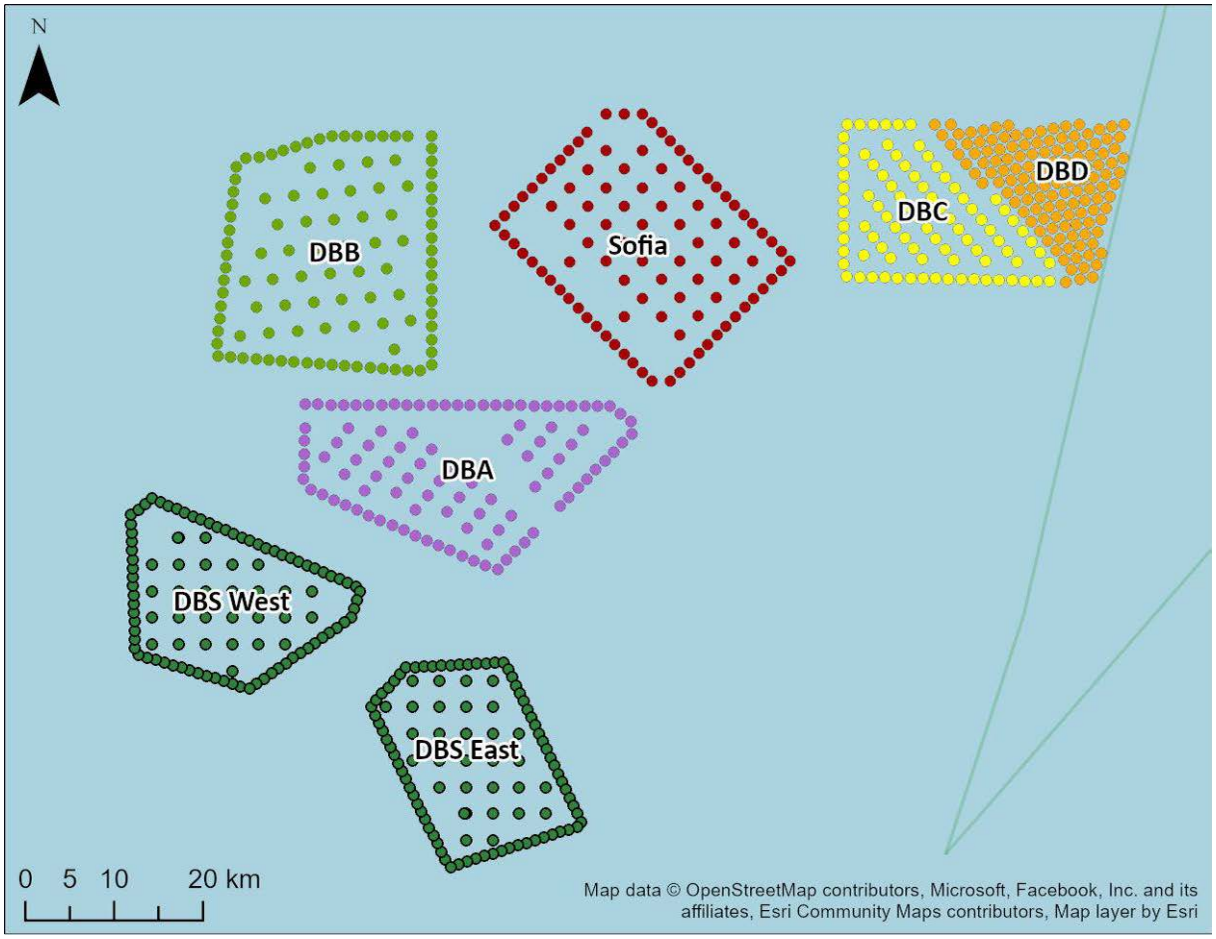

Figure 8.3-14: Wind Farm Layouts included in 'Scenario 2'

8.3.4 Wave Modelling

8.3.4.1 Model Configuration

25. Royal HaskoningDHV has an established wave transformation model covering the Dogger Bank. The model was built in MIKE21-SW software developed by Danish Hydraulic Institute (DHI). For this project, the model mesh was refined, and bathymetry updated using the data described in **Section 8.3.2.1**.

26. The south-west corner of the model is located near Spurn Head encompassing the mouth of the Humber Estuary and extending approx. 268km northwards and 270km eastwards. The wave model domain and bathymetry are shown on **Figure 8.3-15**.

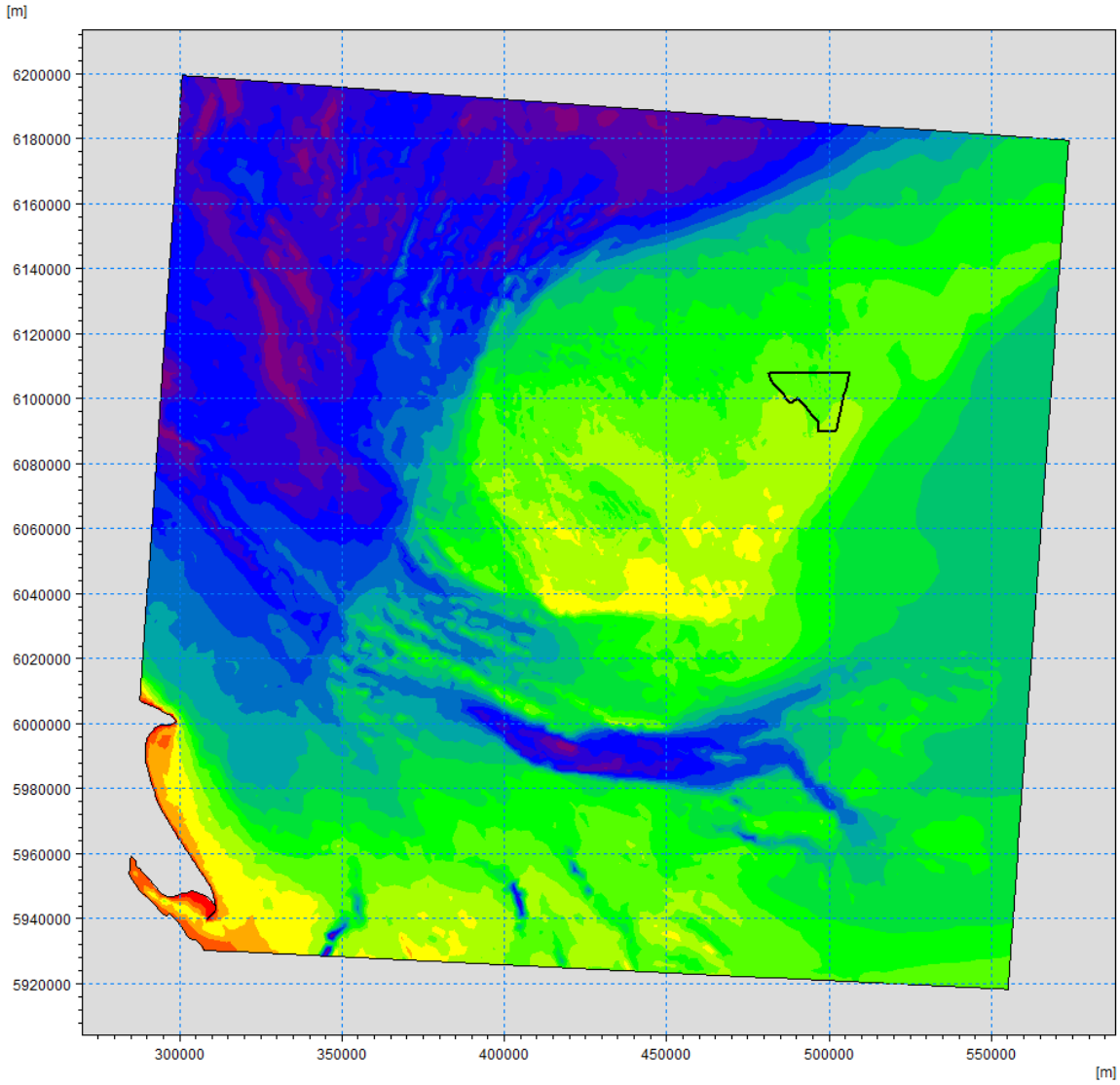

Figure 8.3-15: Extent of MIKE21-SW-FM Model Domain and Bathymetry used for Model Verification

27. The MIKE21-SW modelling software allows unstructured triangular meshes which enables the model to use a coarser grid (2,000m) in the areas further away from the proposed development site and a finer mesh in the areas of greatest interest (200m). This approach enables higher computational efficiency whilst still maintaining sufficient accuracy of mesh coverage in areas of greatest interest in the present study. **Figure 8.3-16** shows the different mesh resolutions used in the wave model.

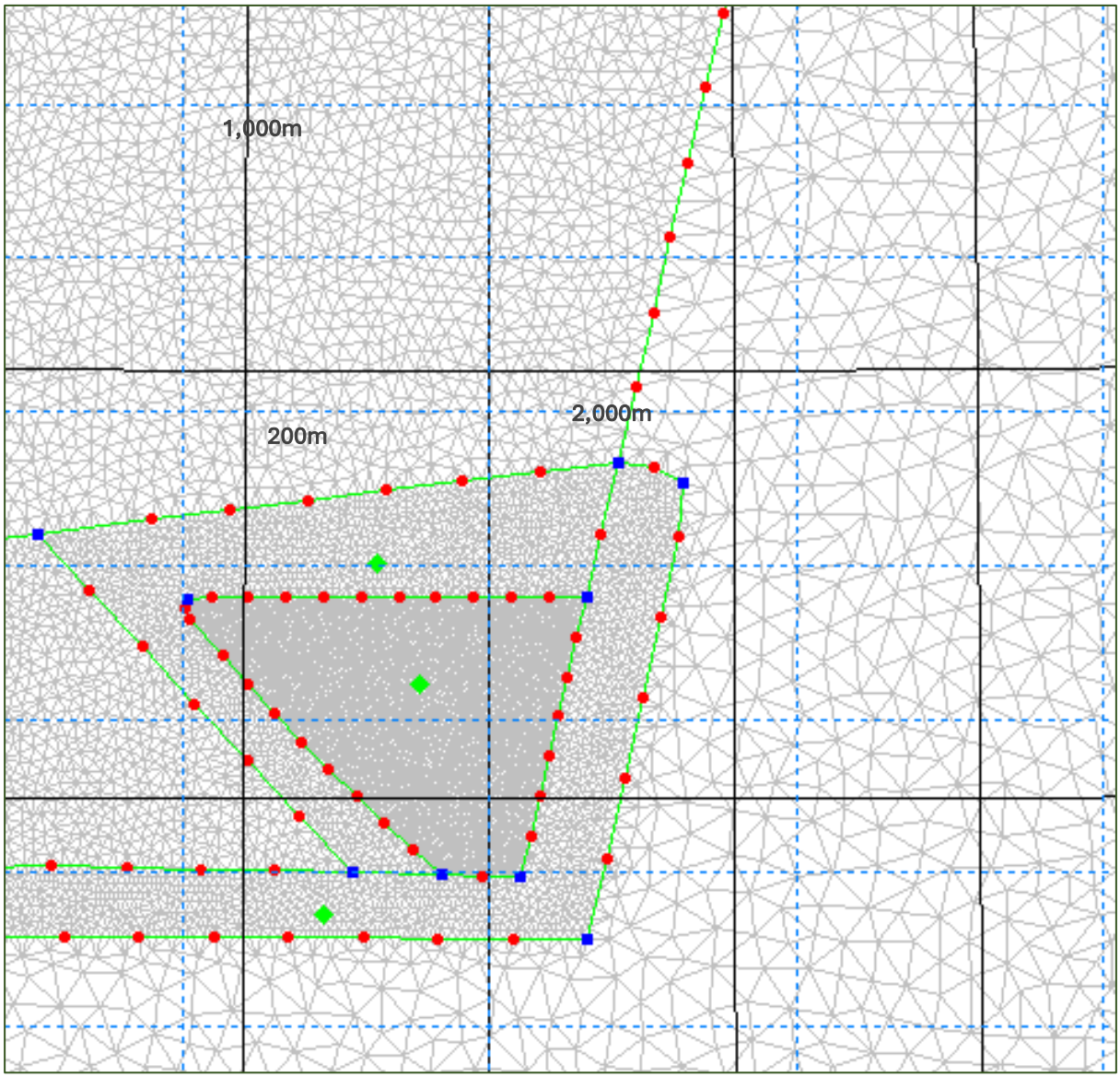

Figure 8.3-16: Wave Model Mesh Resolution

28. The wave model has been run with a Mean High Water Spring (MHWS) water level of 6.1mCD based on the Admiralty Tide Table at Bridlington. Considering relatively deep water at the site, model results are not sensitive to water level (between high and low tides).

29. ERA5 hindcast hourly wind data has been applied to the model boundary. **Table 8.3-6** shows the wave model settings that have been used.

Table 8.3-6: MIKE21-SW Model Settings

MIKE 21 Parameter	Chosen Parameter
Basic Equations	Spectral Formulation: Fully spectral Time Formulation: Quasi Stationary
Spectral Discretization	360 degrees rose: 36 directions
Solution Technique	Low order, fast algorithm Iterations: 500
Diffraction	None
Wave Breaking	Gamma data: Constant value of 0.8 Alpha: 1
White Capping	Dissipation coefficient Cdis: 1.33 DELTA: 0.5
Bottom Friction (roughness height)	0.001m

30. The MIKE21-SW model was run to transform the ERA5 hindcast hourly wave data from offshore to the wind farm site. The following wave input data were applied at the model boundary:

- Significant wave height, Hs;
- Spectral peak period, Tp;
- Mean wave direction, MWD; and
- Directional standard deviation, DSD (set to 30 degrees).

31. Please note, the model has been run only with the most relevant wave directions. In this study, we applied northerly waves from 345degN, which has the largest waves, and easterly waves from 90degN, which has the shortest travel distance to the UK coastline (also see explanation in **paragraph 44**).

32. The wave model is based on Royal HaskoningDHV's established and already calibrated wave model, therefore no further calibration was required.

8.3.4.2 Model Verification

33. Model verification against the provided wave buoy data was carried out to ensure that the wave model produces reasonably accurate wave conditions around Dogger Bank for storm events.

34. For the verification process ERA5 hindcast wave and wind data have been downloaded for the same time period as the measured Partrac wave buoy data. The hindcast wave and wind data has been downloaded at four locations: at three locations around the model boundaries, namely 'North', 'East' and 'South', and one location called 'Centre', which is located approximately 20km north of the Partrac wave buoys and 50km west of the DBD wind farm site. The four hindcast data points, three model boundaries and the three Partrac wave buoy locations 'North', 'South' and 'Dogger Bank B' are shown on **Figure 8.3-17**.

35. The largest storm events (of the most relevant wave directions to the Project) that have been recorded during the wave buoy deployment between June 2022 to February 2024 have been chosen for model verification, and the ERA5 offshore wave and wind conditions for these events have then been applied to the model domain boundary.

36. The offshore wave conditions for each storm event have been applied to the wave model using the ERA5 hindcast point 'North', 'East' and 'South' for the three model boundaries respectively (as shown on **Figure 8.3-17**). Wind conditions for each storm event have been applied to the wave model using the ERA5 hindcast point closer to the wave buoy locations. The model results for these storm events have been extracted at the same location as the three Partrac wave buoys of 'North', 'South' and 'Dogger Bank B'.

37. **Figure 8.3-18** to **Figure 8.3-31** show a comparison between the measured and modelled wave height at wave buoys 'North' and 'South'. The measured heights are presented as small crosses, the modelled height are drawn as a solid line. On the figures, the 'North' buoy data is shown in blue and the 'South' buoy data in red.

38. **Figure 8.3-23** and **Figure 8.3-29** are the exception in that they show a comparison between the measured and modelled wave data at the wave buoy 'Dogger Bank B'. The measured data are presented as small blue crosses, the modelled data are drawn as a solid line.

39. All verification figures also show the ERA5 offshore hindcast wave height and wave direction, and the 'local' ERA5 wind speed and wind direction that have been applied to the model boundary. The ERA5 offshore wind speed is also shown on the figures to illustrate the effect that the wind has on the wave height, and also to explain the need to apply the wind from a location closer to the wave buoys.

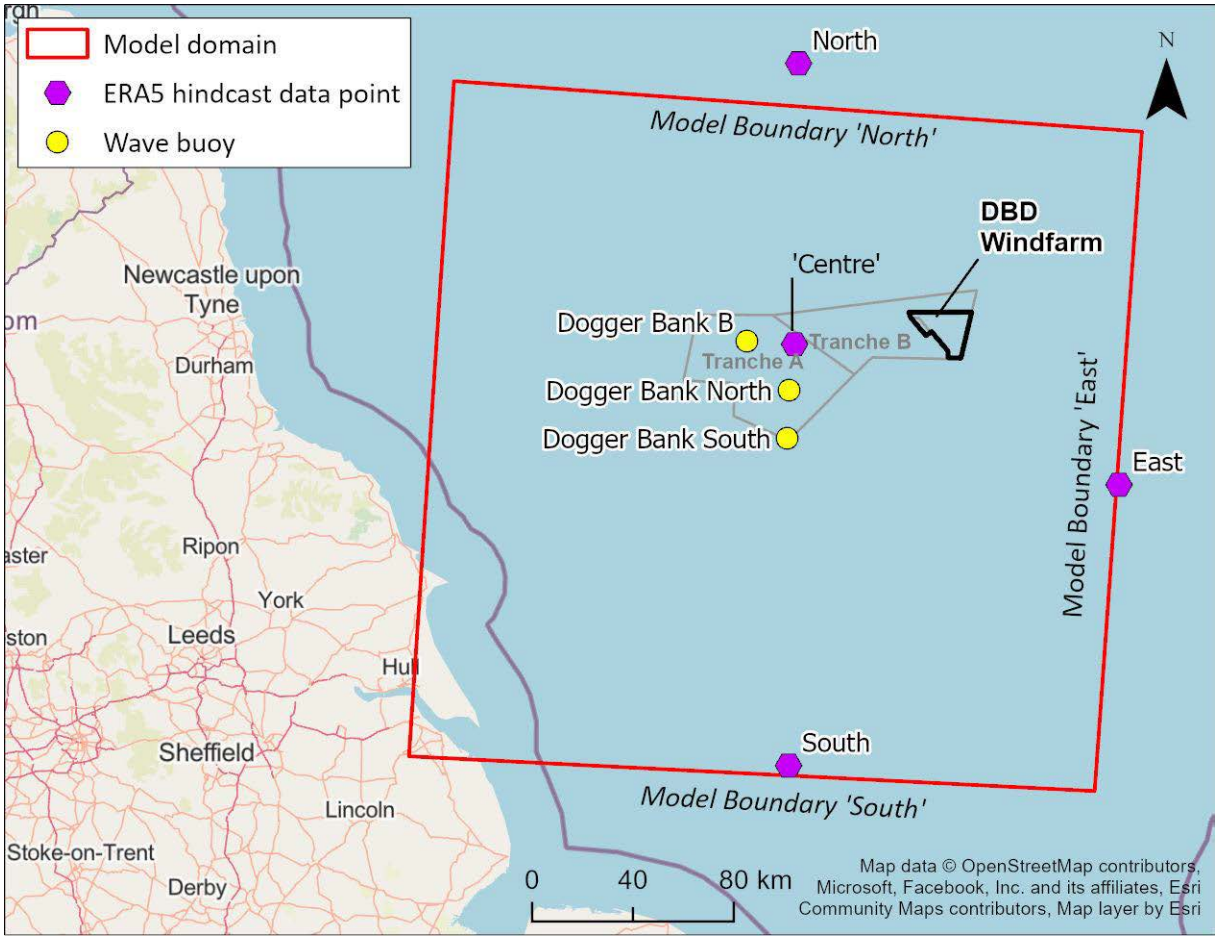

Figure 8.3-17: Partrac Wave Buoy Locations and ERA5 Hindcast Model Points Used for Wave Model Verification

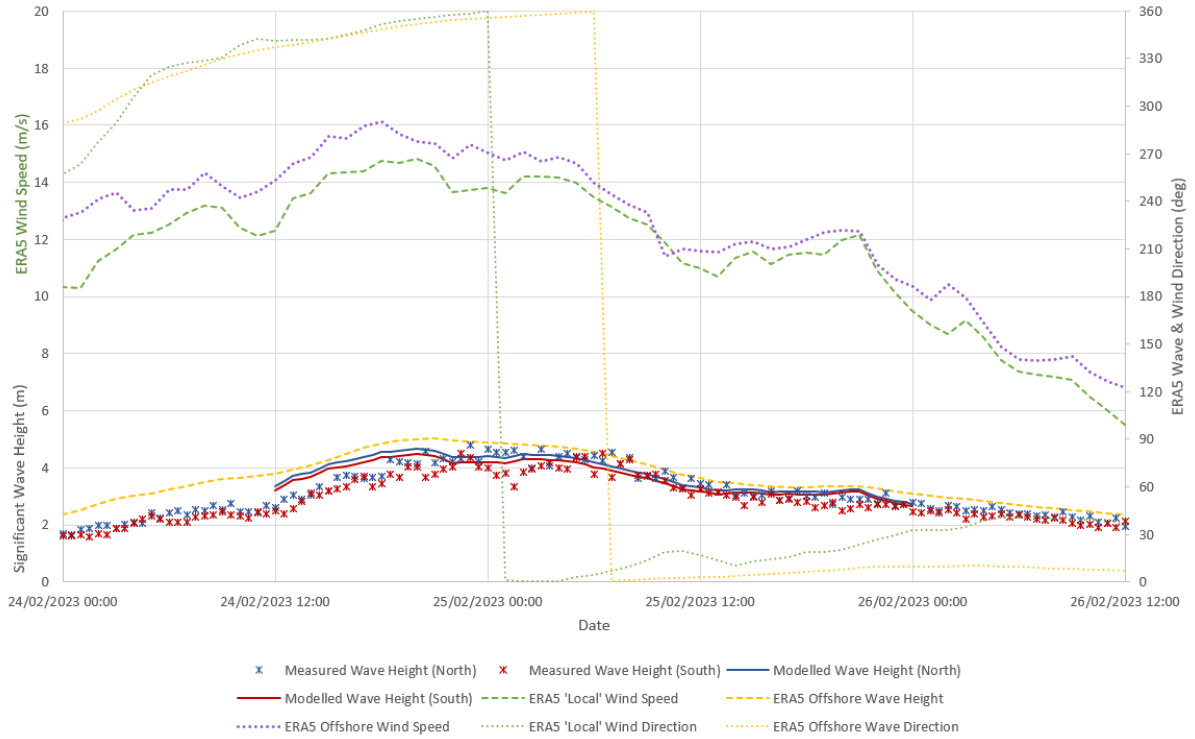

Figure 8.3-18: Comparison of Measured and Modelled Wave Height for Waves Coming from Northerly Direction - Event 1

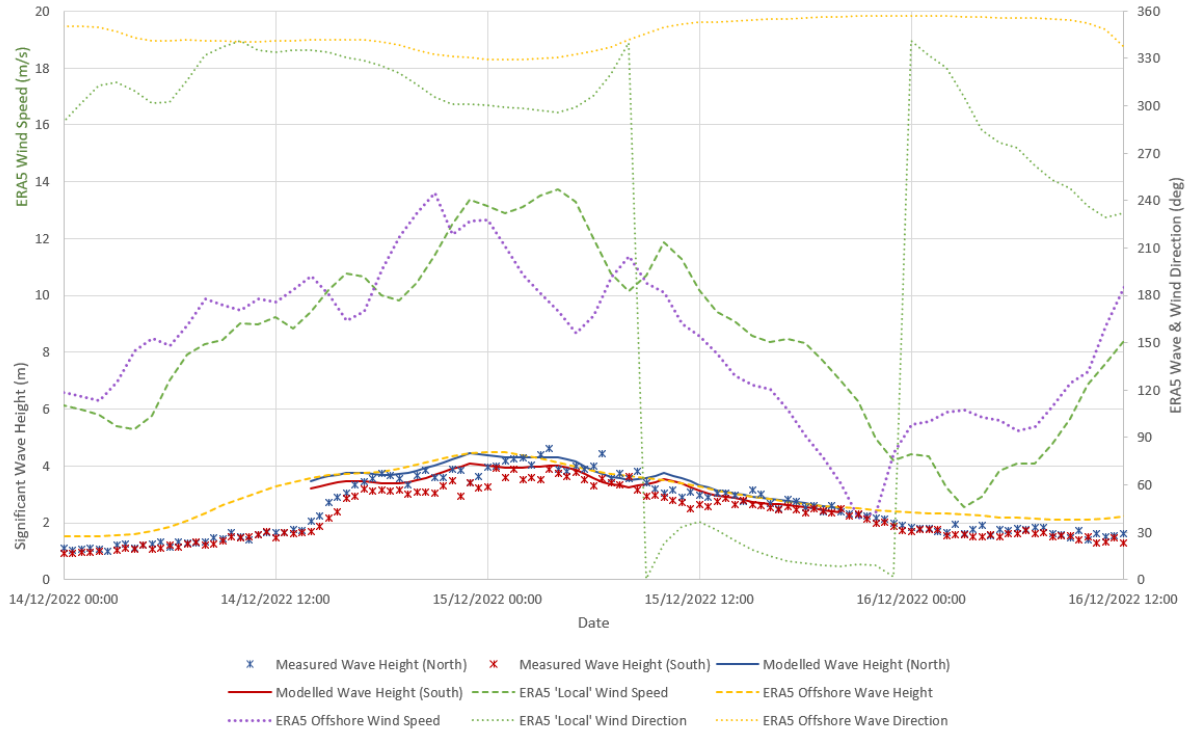

Figure 8.3-19: Comparison of Measured and Modelled Wave Height for Waves Coming from Northerly Direction - Event 2

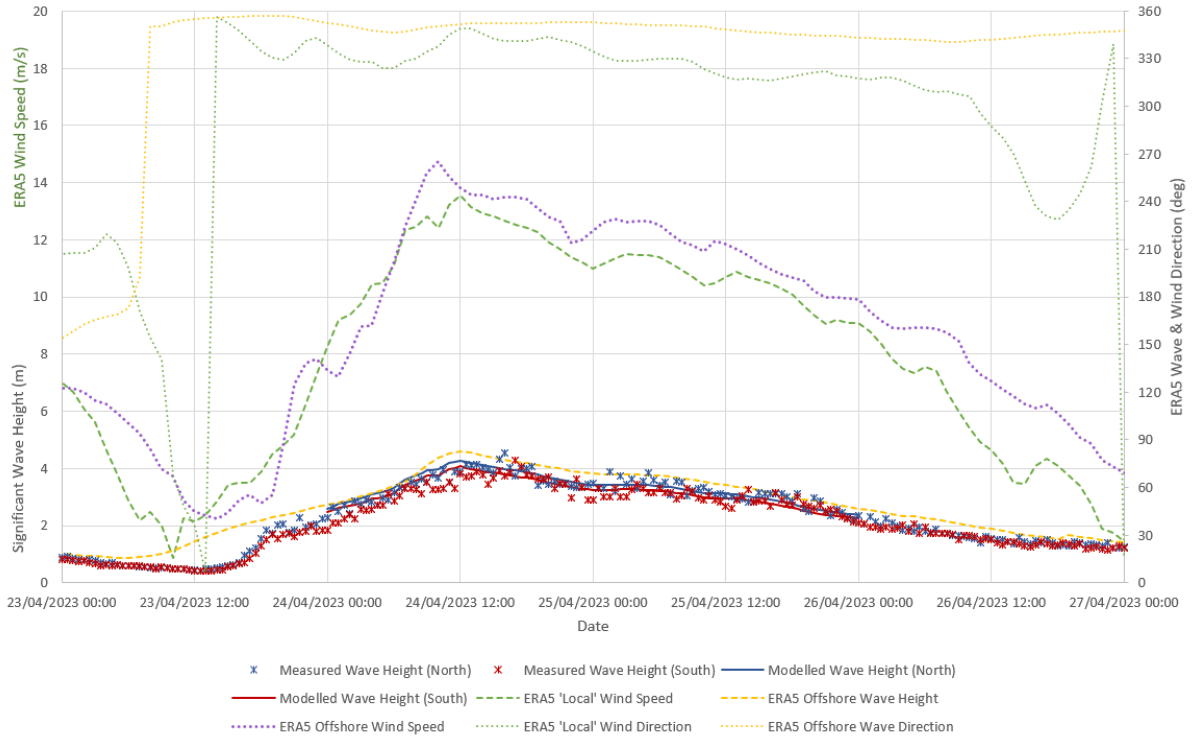

Figure 8.3-20: Comparison of Measured and Modelled Wave Height for Waves Coming from Northerly Direction - Event 3

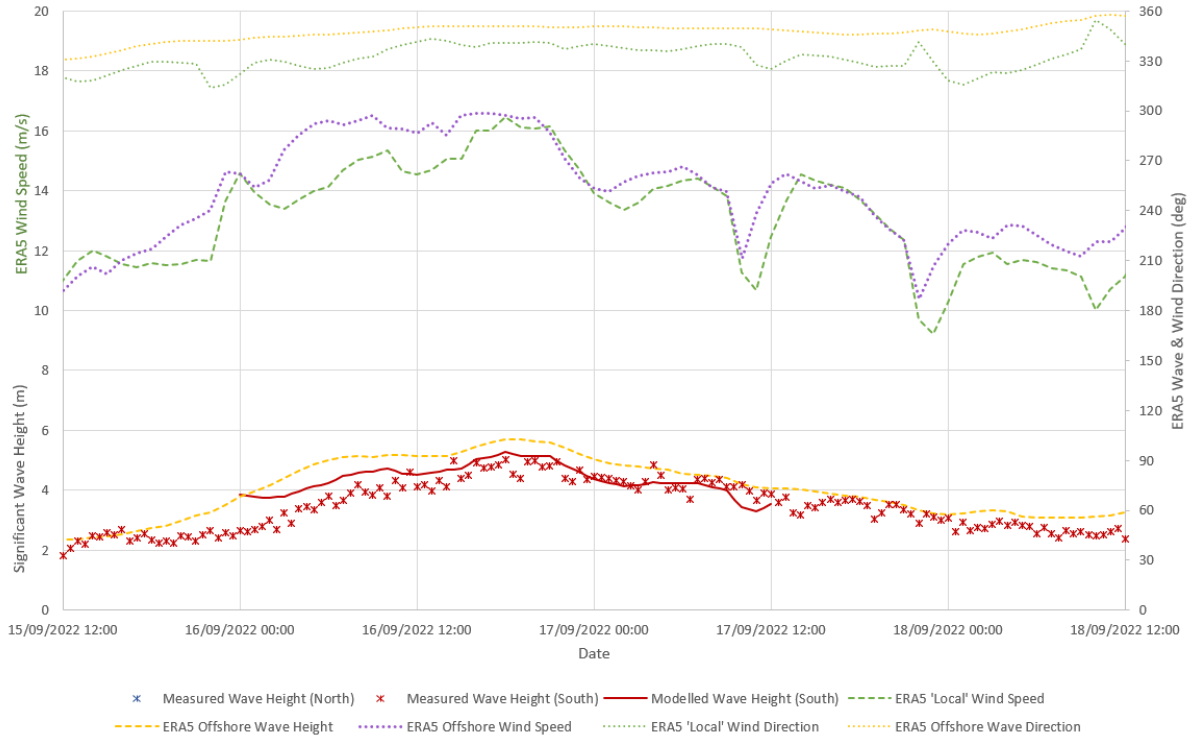

Figure 8.3-21: Comparison of Measured and Modelled Wave Height for Waves Coming from Northerly Direction - Event 4 (please note that there was no measured data available for wave buoy 'North' for this storm event)

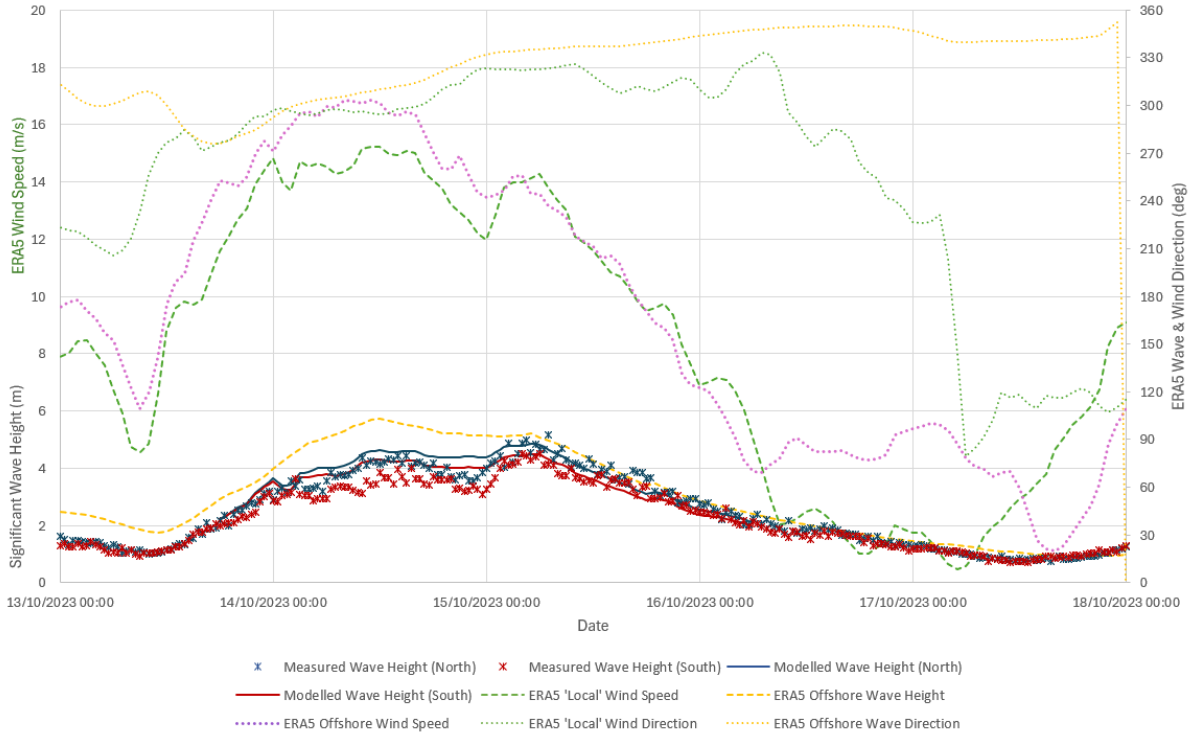

Figure 8.3-22: Comparison of Measured and Modelled Wave Height for Waves Coming from the Northerly Direction at Dogger Bank "North" and "South" - Event 5

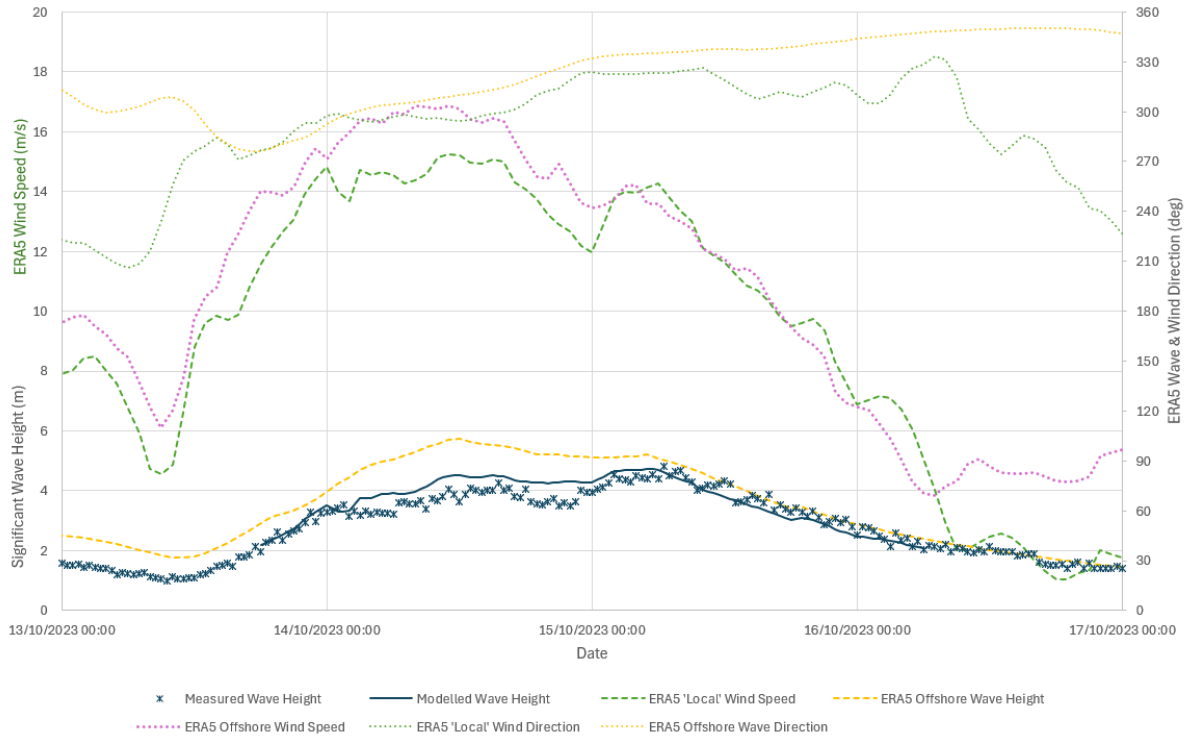

Figure 8.3-23: Comparison of Measured and Modelled Wave Height for Waves Coming from Northerly Direction at Dogger Bank B Wave Buoy - Event 5

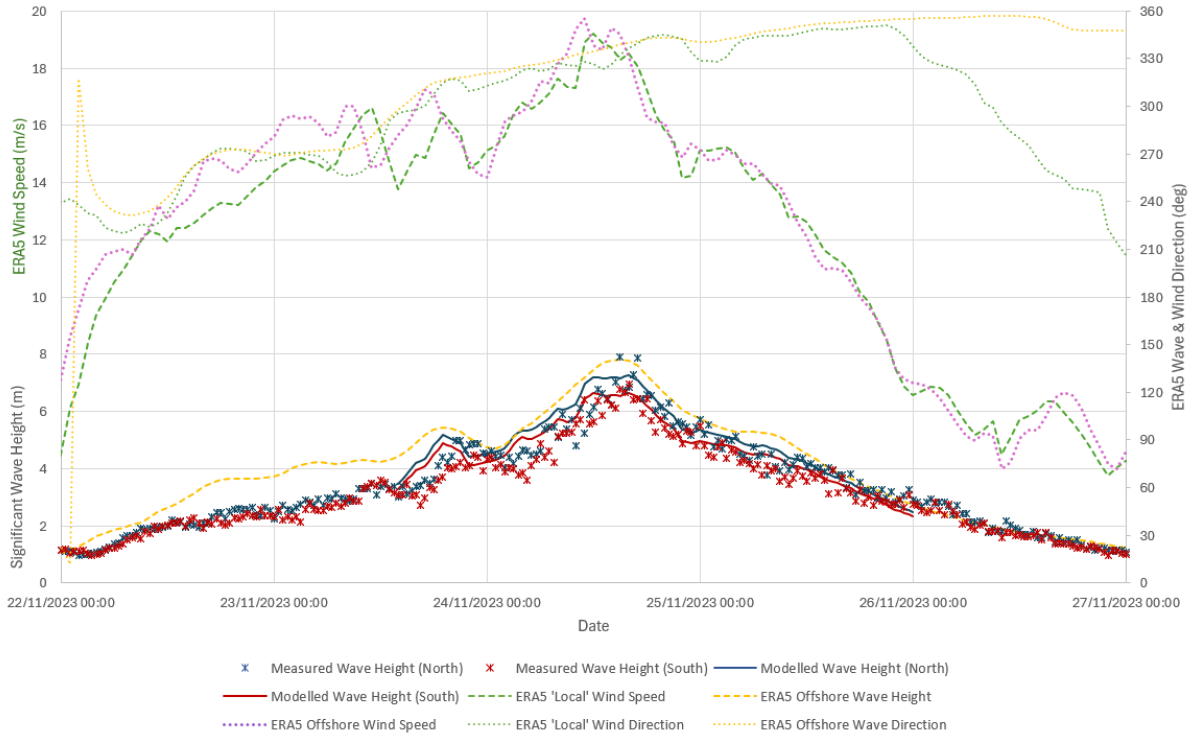

Figure 8.3-24: Comparison of Measured and Modelled Wave Height for Waves Coming from Northerly Direction - Event 6

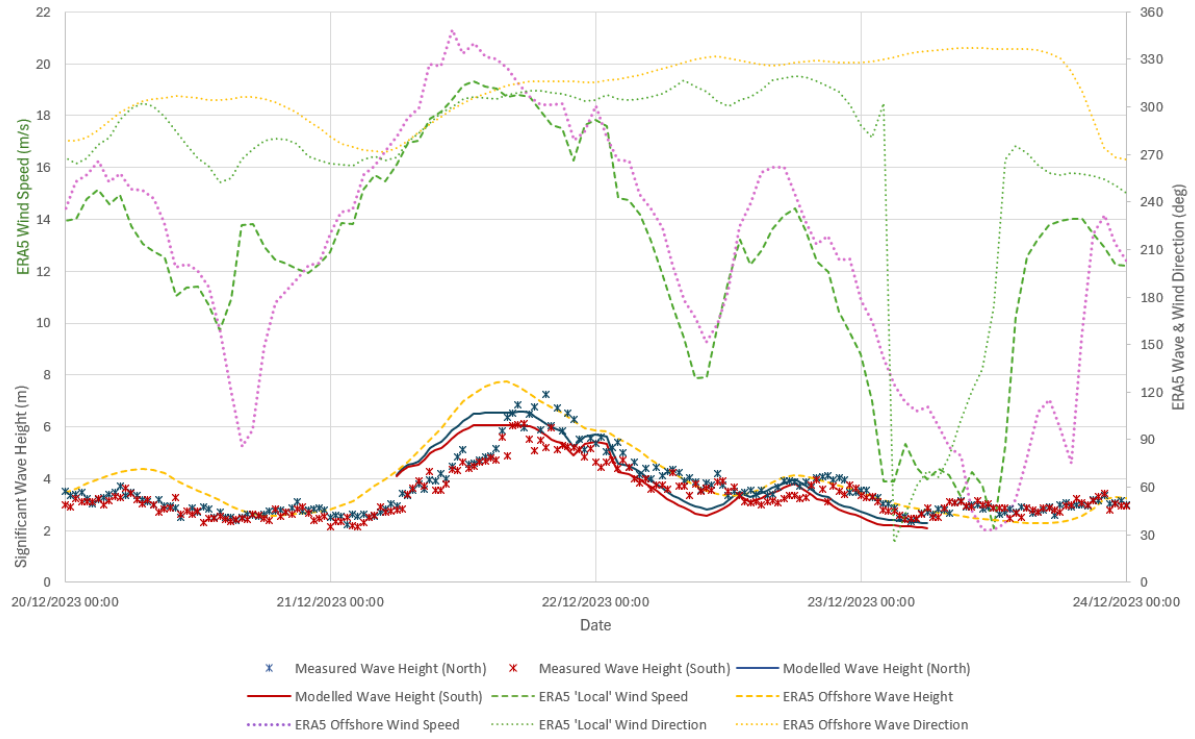

Figure 8.3-25: Comparison of Measured and Modelled Wave Height for Waves Coming from Northerly Direction - Event 7

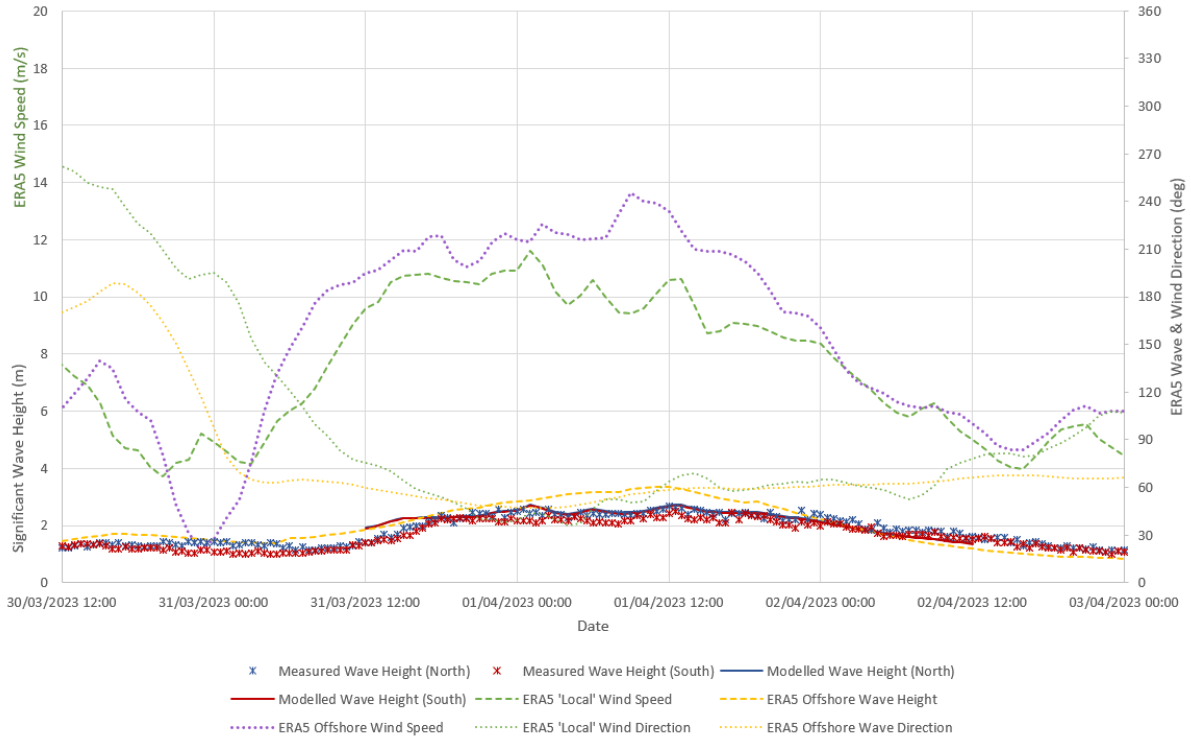

Figure 8.3-26: Comparison of Measured and Modelled Wave Height for Waves Coming from North-easterly Direction - Event 8

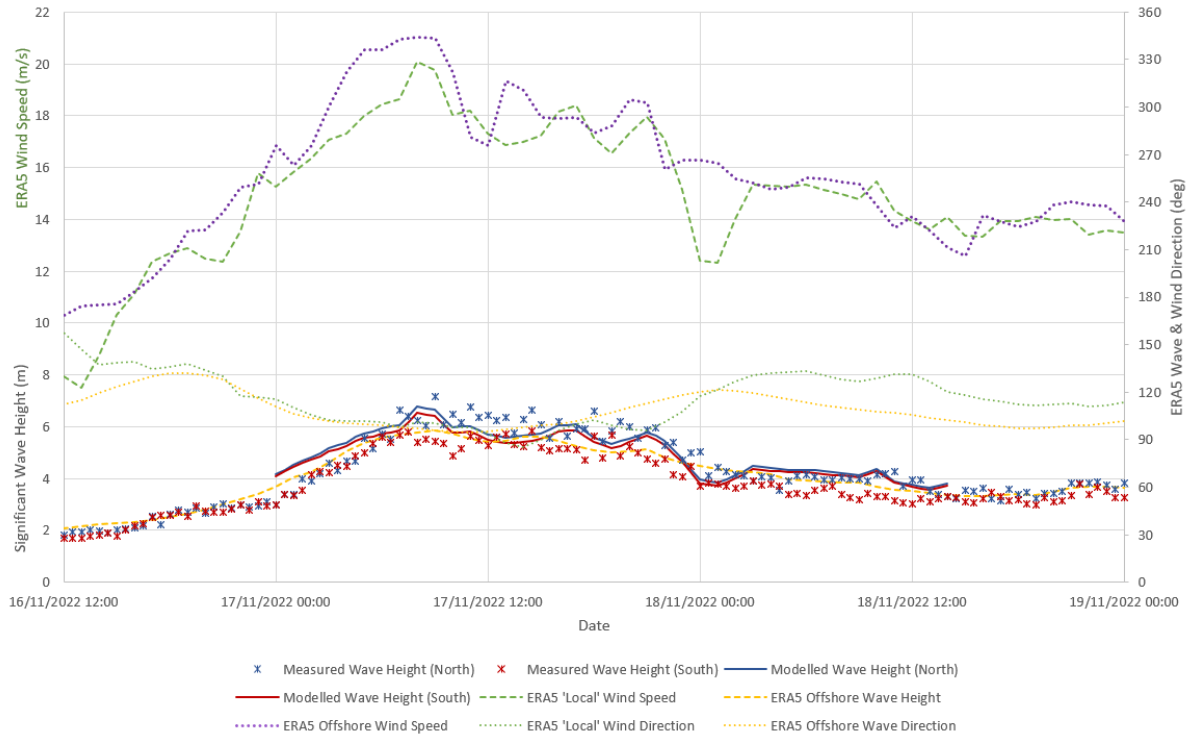

Figure 8.3-27: Comparison of Measured and Modelled Wave Height for Waves Coming from Easterly Direction - Event 9

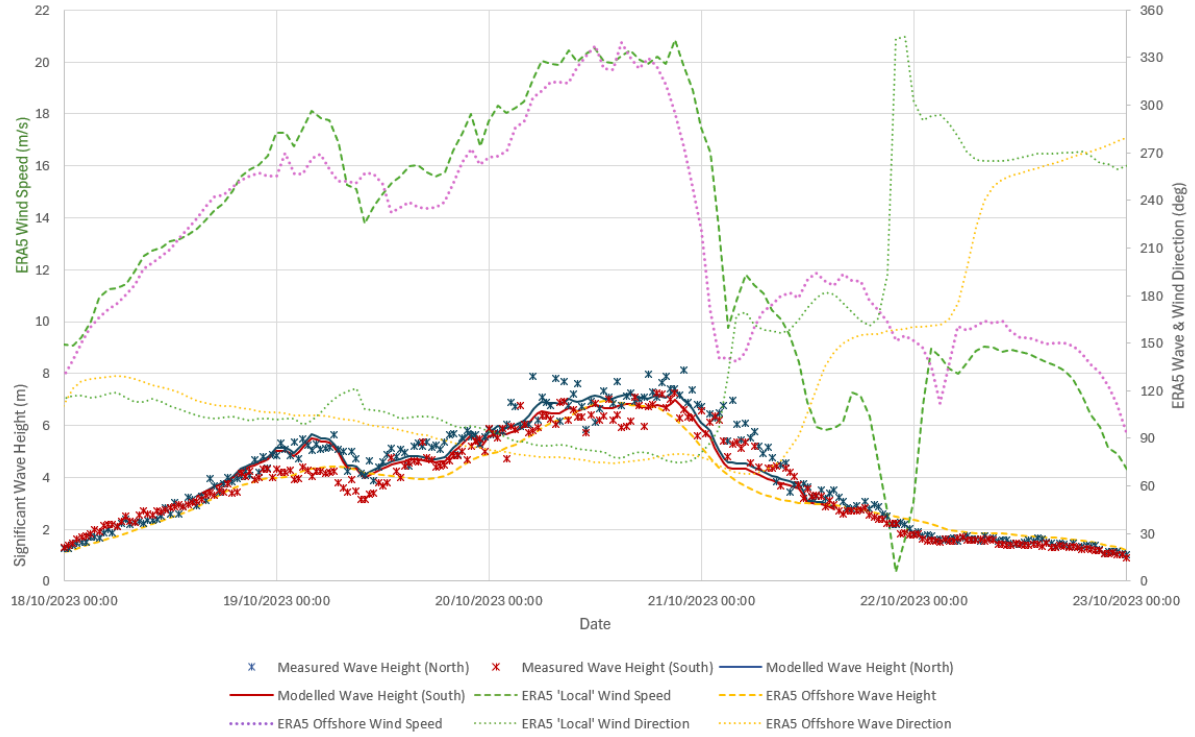

Figure 8.3-28: Comparison of Measured and Modelled Wave Height for Waves Coming from Easterly Direction at Dogger Bank "North" and "South" - Event 10

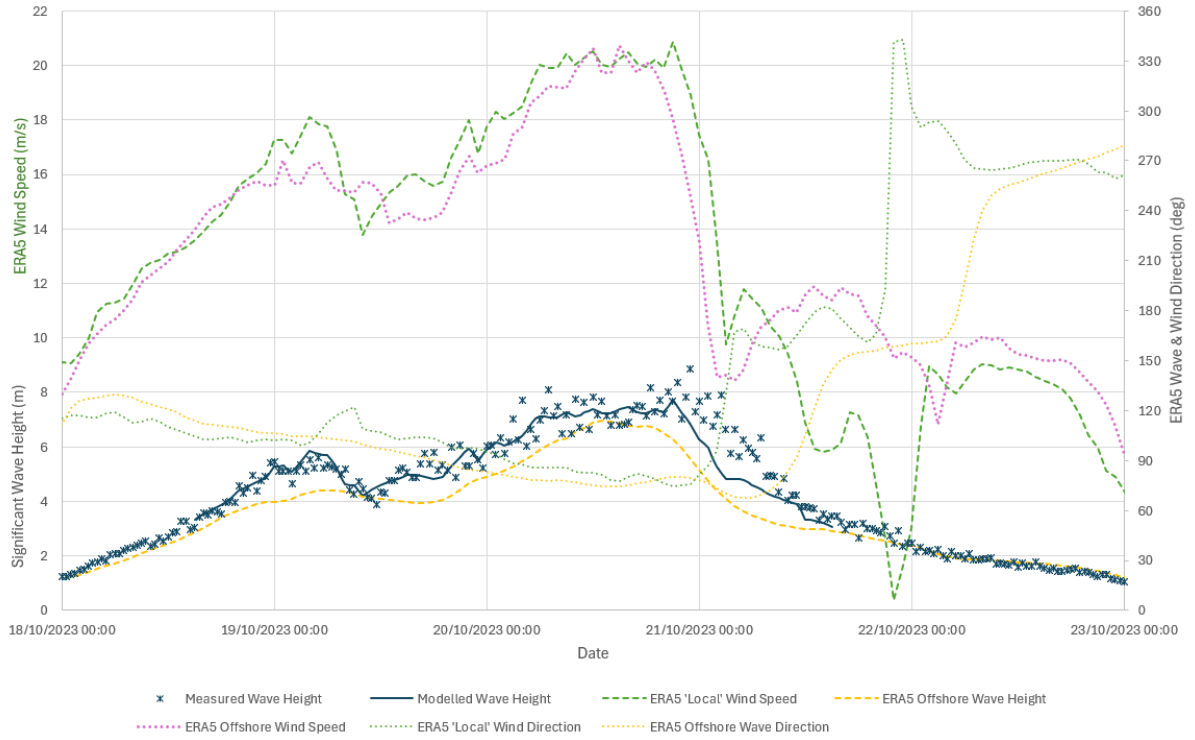

Figure 8.3-29: Comparison of Measured and Modelled Wave Height for Waves Coming from Easterly Direction at Dogger Bank B Wave Buoy - Event 10

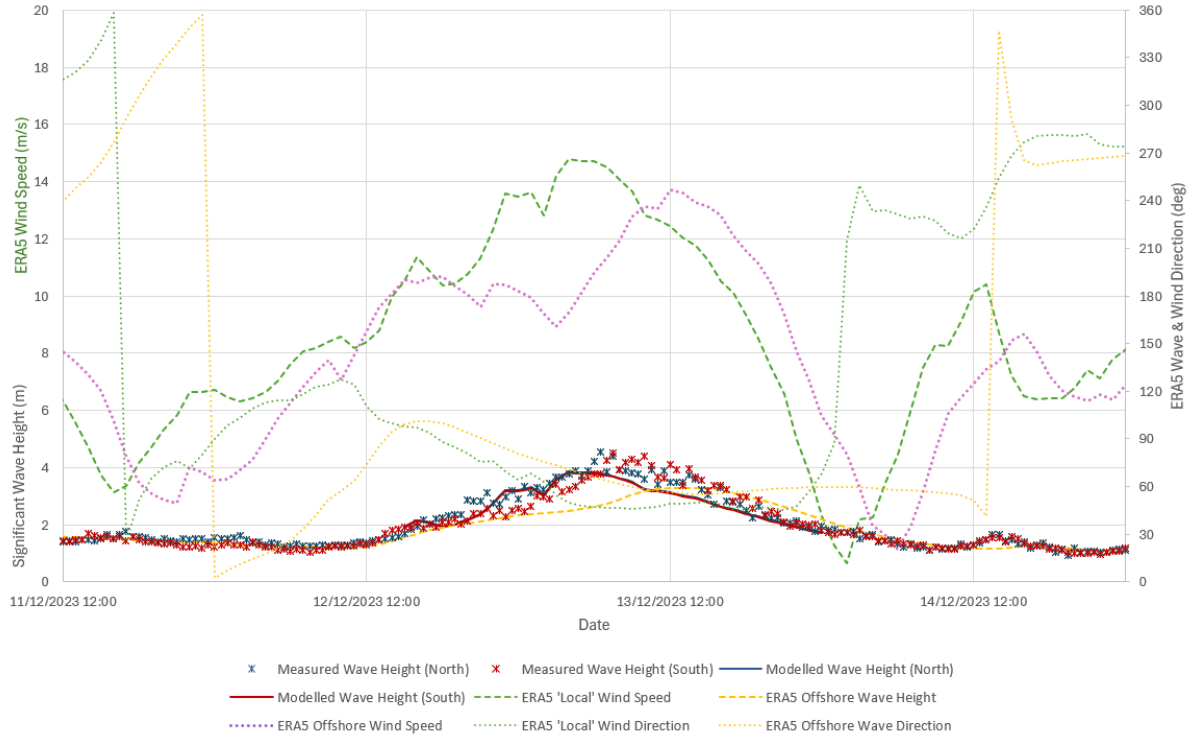

Figure 8.3-30: Comparison of Measured and Modelled Wave Height for Waves Coming from Easterly Direction - Event 11

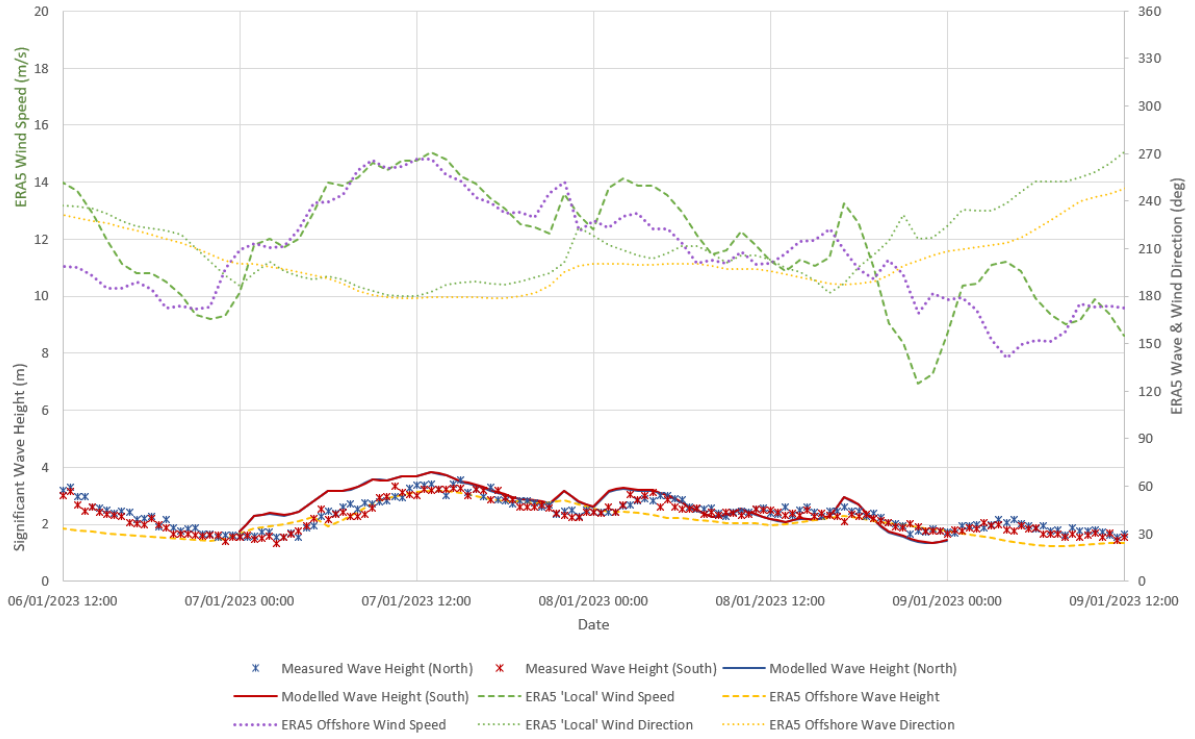

Figure 8.3-31: Comparison of Measured and Modelled Wave Height for Waves Coming from Southerly Direction - Event 12

40. Overall there is a good agreement between the measured and modelled wave height of the chosen storm events. In general, the modelled data matches the measured wave data well, and any over- or under-predictions in wave height are due to the effect of the ERA5 wind data applied to the model. Localised weather conditions at the wave buoy deployment site and spatial variation of wind conditions were not captured by the ERA5 global weather model with coarse mesh and therefore lead to discrepancies in the verification.

41. A summary of the 12 calibration storm events is presented in **Table 8.3-7**.

Table 8.3-7: Summary of Calibration Storm Events

Calibration Storm event	Wave Direction	Date	Comments
Event 1	Northerly	23/02/23 – 26/02/23	Overall, the modelled wave height matches the measured wave height well; but on the first day the modelled wave height is slightly over-estimated. This is likely caused by over-estimated hindcast wind speed. The graph shows significant difference in hindcast wind speed between “local” and “boundary”.
Event 2	Northerly	14/02/22 - 16/02/22	Good agreement.
Event 3	Northerly	23/04/23 - 27/04/23	Good agreement.
Event 4	Northerly	15/09/23 - 18/09/23	Good agreement; similar to Event 1.
Event 5	Northerly	13/10/23 – 17/10/23	Good agreement; during the first day of the storm event, the modelled wave height matches well with the measured at wave buoy “North” but is slightly overestimated at wave buoy “South”. This indicates local variation of weather system which cannot be picked up by the ERA5 global weather model.
Event 6	Northerly	22/11/23 - 27/11/23	Good agreement.
Event 7	Northerly	20/12/23 - 24/12/23	Good agreement; similar to Event 1.
Event 8	North-Easterly	30/03/23 – 02/04/23	Good agreement.

Calibration Storm event	Wave Direction	Date	Comments
Event 9	Easterly	16/11/23 - 19/11/23	Good agreement; the modelled data for wave buoy 'North' is slightly underestimated; however, the modelled wave height compares better with the wave buoy "South" data, which indicates local weather variation which cannot be picked up by global ERA5 weather model.
Event 10	Easterly	18/10/23 – 19/10/23	Good agreement; similar to Event 9.
Event 11	Easterly	11/12/23 - 14/12/23	Reasonable agreement; during the peak of the storm event the modelled wave height is underestimated which is likely due to the ERA5 wind speed being too low. There also seems to be a bigger difference between the ERA5 offshore and 'local' wind speed just before the peak of the storm. This may indicate spatial variation of wind speed and local weather system which is difficult to be picked up by global ERA5 weather model.
Event 12	Southerly	06/11/23 – 09/11/23	Reasonable agreement; modelled data overestimates the wave height during the first day of the storm event, which is likely due to the ERA5 wind speed being too high during this period. In the second half when the ERA5 wind speed drops, the agreement is better.

42. Overall the model verification achieved good results. Some mismatches were due to the ERA5 hindcast data either under- or over-predicting the wind speed because local weather systems were not being picked up by the global ERA5 weather model.

8.3.4.3 Offshore Extreme Wave and Wind Analysis

43. ERA5 hindcast wave and wind time series data (at approx. 10m above water surface) close to the wave model boundary has been downloaded from the European Centre for Medium-Range Weather Forecasts (ECMRWF) covering the time period between January 1979 and May 2023.

44. This time series data has been used in the extreme wave analysis and the results for the considered wave directions (due to their potential impact) are presented in **Table 8.3-8**. Based on these results it was decided that the model representing waves coming from a northerly direction (345degN) should be run due to representing the largest waves. In addition, waves from an easterly direction (90degN) were also chosen as they represent the shortest distance to the UK coastline.

45. The significant wave heights (Hs) for the three chosen probabilities, namely 50 percentile, and return periods 1 in 1 year and 1 in 100 years, and the two wave directions have been highlighted in red in **Table 8.3-8**.

Table 8.3-8: Extreme Offshore Wave Height at ERA5 Hindcast Point (for Relevant Wave Directions)

Return Period	Significant Wave Height (Hs,m) per Wave Direction Sector (degN)					
	N-NW (315-345)	N (345-15)	N-NE (15-45)	E-NE (45-75)	E (75-105)	E-SE (105-135)
50 percentile	**1.75**	1.48	1.16	1.19	**1.28**	1.27
1	**6.4**	5.62	3.44	3.42	**3.77**	3.34
5	8.24	7.37	4.62	4.88	5.18	4.35
10	9.02	8.13	5.13	5.51	5.78	4.82
25	10.05	9.16	5.8	6.36	6.56	5.48
50	10.82	9.94	6.3	7.01	7.15	6.01
100	**11.6**	10.74	6.81	7.66	**7.74**	6.58
200	12.37	11.54	7.31	8.32	8.32	7.19
500	13.38	12.62	7.97	9.20	9.08	8.06
1000	14.14	13.44	8.48	9.88	9.66	8.76

Note: highlighted wave conditions were chosen for assessing potential effects of the Project.

8.3.4.4 Sensitivity Model Runs

46. The sensitivity model runs were undertaken for a number of different wind farm layout options which are described below in order to identify the worst-case layout. These layouts are outlined in **Section 8.3.3** and **Section 8.3.1.1**.

47. **Table 8.3-3** shows the details of the four turbine layouts A to D and the three Offshore Platform options 1 to 3.

48. It should be noted that the number of turbines stated in **Table 8.3-3** excludes five 'spare' locations which have been removed from the location list; the 'spare' turbines were excluded from the north-east corner of each array based on advice given by engineers as this area being the most likely region to be used for spare locations.

49. **Table 8.3-9** summarises the wave model input parameters for the sensitivity runs, including wave height, wave period, wave direction, wind speed and wind direction. Each direction sector was run for the 'Baseline', the four turbine layouts and the three Offshore Platform options.

Table 8.3-9: Wave Model Input Parameters for Sensitivity Runs

Return Period	Direction Sector	Wave Height (Hs,m)	Wave Period (Tp,s)	Wave Direction (degN)	Wind Speed (m/s)	Wind Direction (degN)
50 percentile	Northerly	1.75	8.72	345	8.0	345
50 percentile	Easterly	1.28	5.8	90	7.3	90

50. **Figure 8.3-33** to **Figure 8.3-36** show the difference in significant wave height (Hs) between the 'Baseline' and turbine Layout A to D for Offshore Platform Options 1 to 3 for occurring probability of 50 percentile with waves coming from a northerly direction respectively.

51. **Figure 8.3-37** to **Figure 8.3-40** show the difference in significant wave height (Hs) between the 'Baseline' and turbine Layout A to D for Offshore Platform Options 1 to 3 for occurring probability of 50 percentile with waves coming from an easterly direction respectively.

52. The legend for **Figure 8.3-33** to **Figure 8.3-40,** showing the difference in significant wave height (Hs), is presented on **Figure 8.3-32**.

53. Any difference in significant wave height (Hs) smaller than +/- 0.01 are shown in white. Increases in significant wave height (Hs) greater than +0.01 are shown in yellow to orange to red. Decreases in significant wave height (Hs) smaller than -0.01 are shown in green to blue to purple.

54. It should be noted that the differences in significant wave height (Hs) are so small that in order to visualise the tiny change, the colour band intervals are set to +/- 1cm up to +/- 10cm. This colour scheme has only been used for the sensitivity runs to reveal the difference.

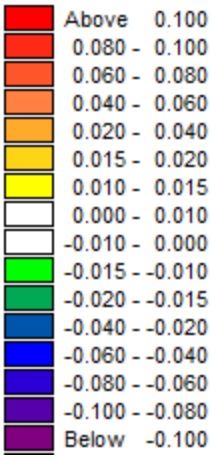

Figure 8.3-32: Legend showing Difference in Significant Wave Height (Hs)

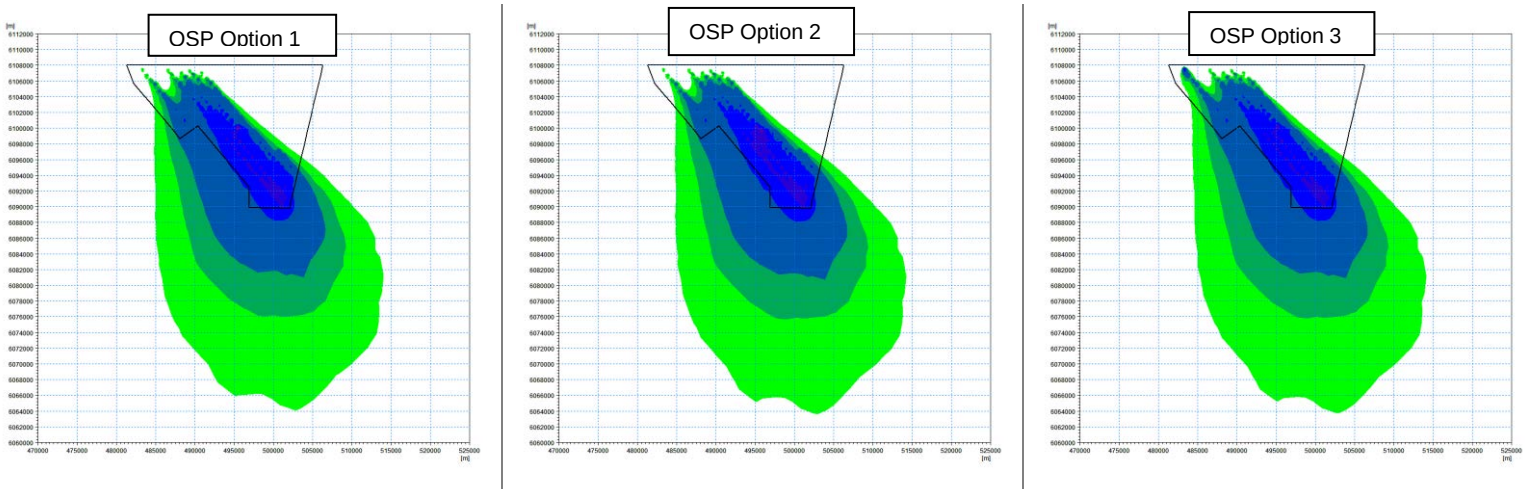

*Figure 8.3-33: Difference in Significant Wave Height (Hs) between 'Baseline' and Turbine **Layout A** - Offshore Platform Options 1-3 for Waves Coming from Northerly Direction with Occurring Probability of 50 Percentile*

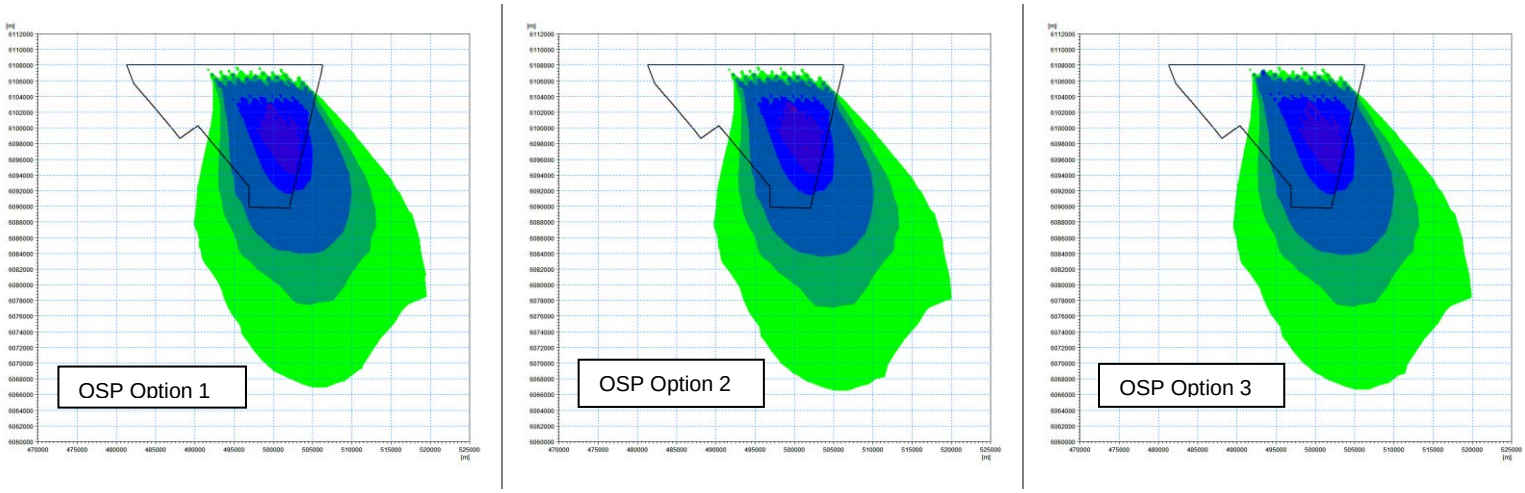

*Figure 8.3-34: Difference in Significant Wave Height (Hs) between 'Baseline' and Wind Farm **Layout B** - Offshore Platform Options 1 to 3 for Waves Coming from Northerly Direction with Occurring Probability of 50 Percentile*

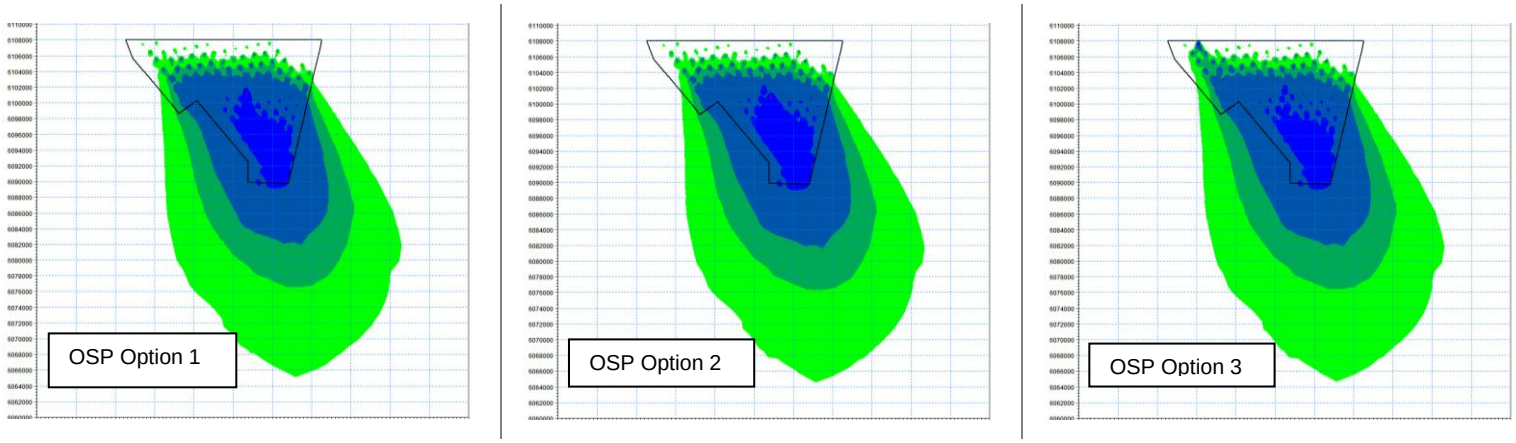

*Figure 8.3-35: Difference in Significant Wave Height (Hs) between 'Baseline' and Wind Farm **Layout C** - Offshore Platform Options 1 to 3 for Waves Coming from Northerly Direction with Occurring Probability of 50 Percentile*

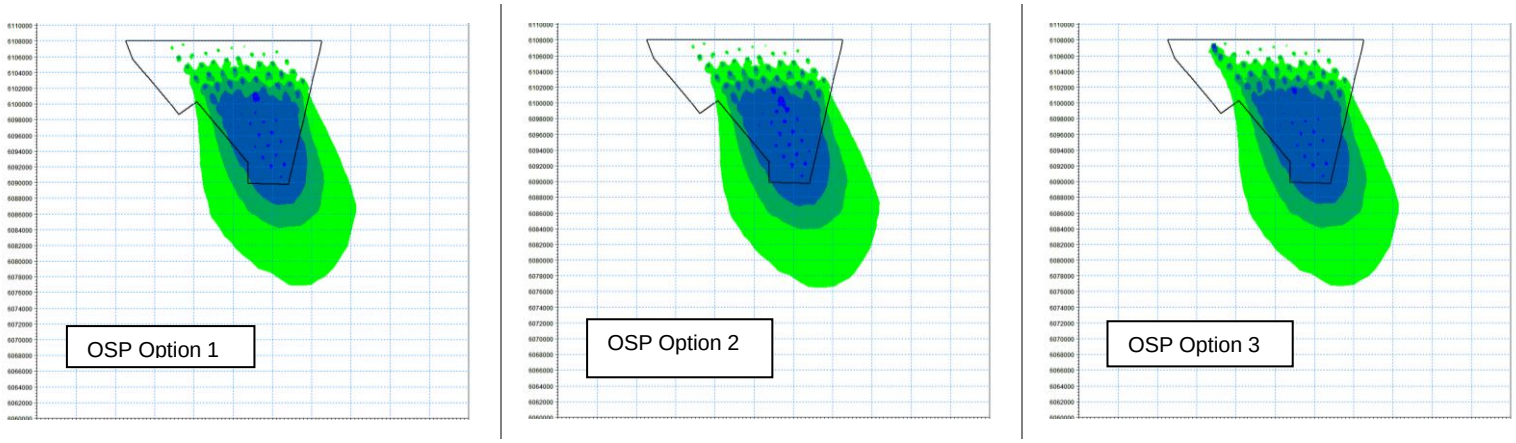

*Figure 8.3-36: Difference in Significant Wave Height (Hs) between 'Baseline' and Wind Farm **Layout D** – Offshore Platform Options 1-3 for Waves Coming from Northerly Direction with Occurring Probability of 50 Percentile*

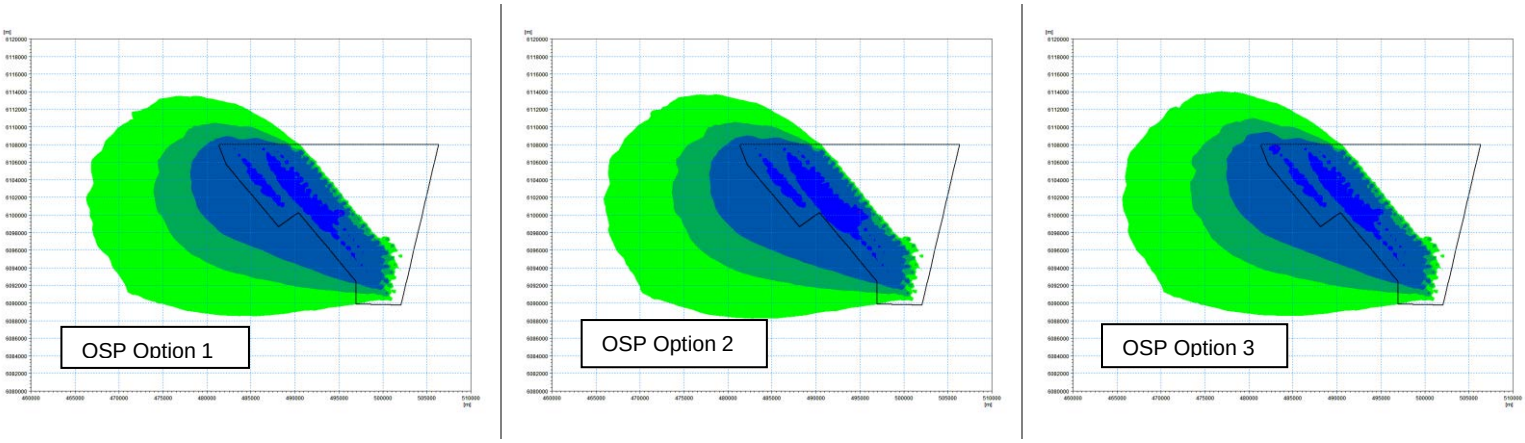

*Figure 8.3-37: Difference in Significant Wave Height (Hs) between 'Baseline' and Wind Farm **Layout A** - Offshore Platform Option 1 to 3 for Waves Coming from Easterly Direction with Occurring Probability of 50 Percentile*

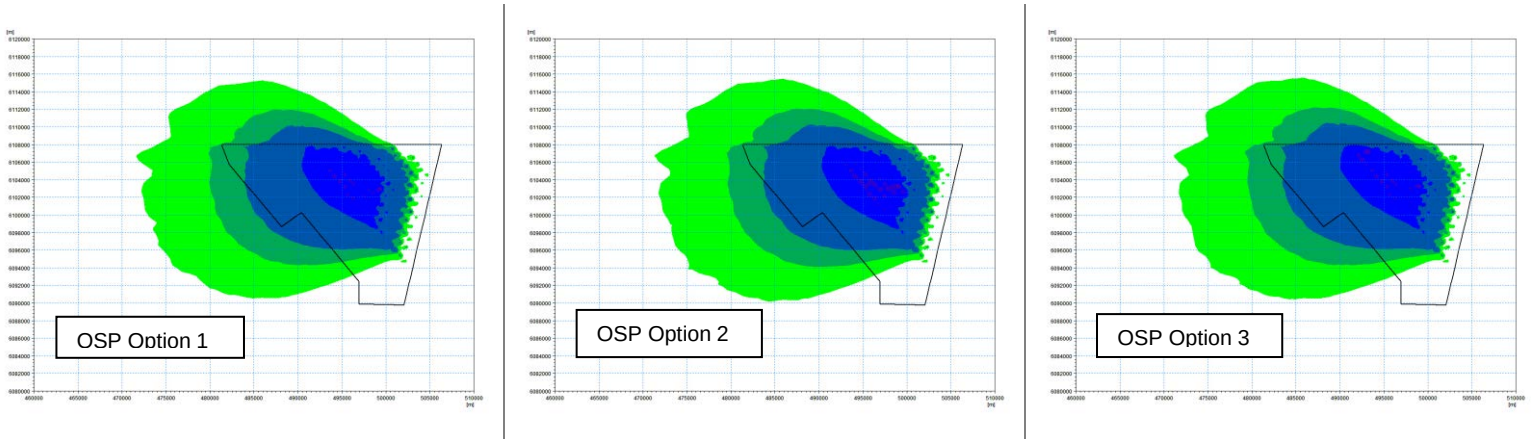

*Figure 8.3-38: Difference in Significant Wave Height (Hs) between 'Baseline' and Wind Farm **Layout B** - Offshore Platform Option 1 to 3 for Waves Coming from Easterly Direction with Occurring Probability of 50 Percentile*

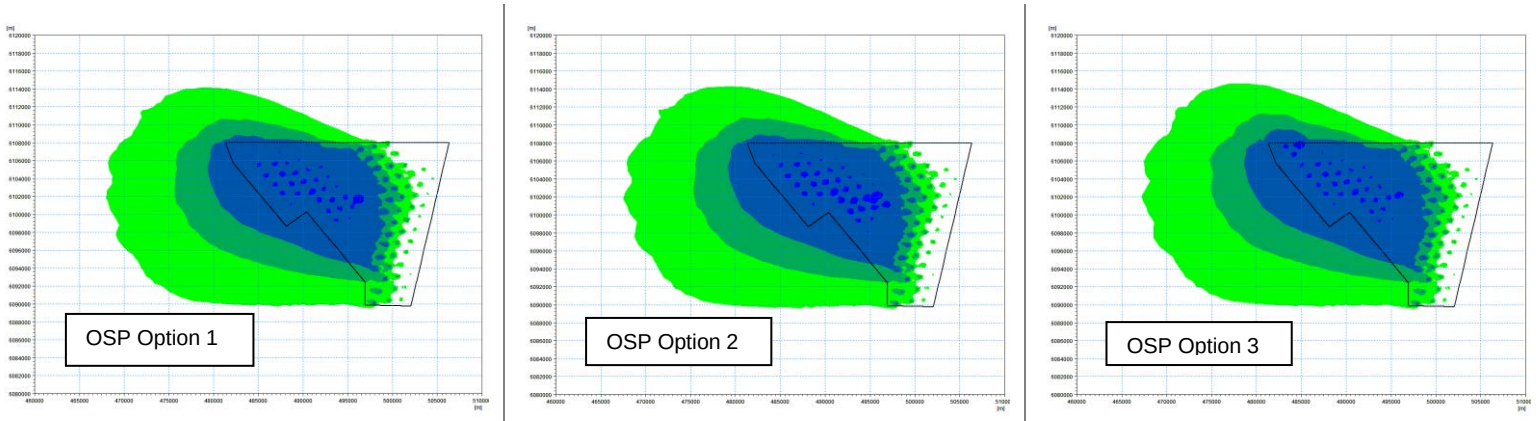

*Figure 8.3-39: Difference in Significant Wave Height (Hs) between 'Baseline' and Wind Farm **Layout C** - Offshore Platform Options 1 to 3 for Waves Coming from Easterly Direction with Occurring Probability of 50 Percentile*

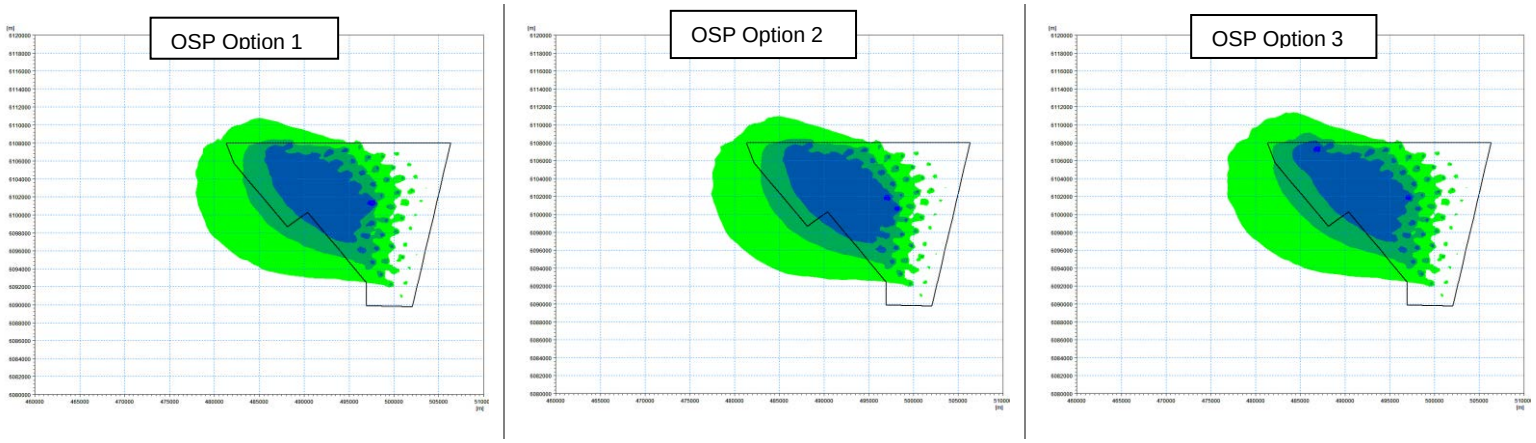

*Figure 8.3-40: Difference in Significant Wave Height (Hs) between 'Baseline' and Wind Farm **Layout D** - Offshore Platform Option 1 to 3 for Waves Coming from Easterly Direction with Occurring Probability of 50 Percentile*

8.3.4.4.1 Summary for model with waves coming from northerly direction

55. The wave reduction for waves from a northerly direction extends in a southerly direction.

56. Reduction of wave heights by -4cm to -6cm occurring mainly inside the Project array boundary, only extending by approximately 1.5km for Layout A and B, and by approximately 600m for Layout C.

57. The area of wave height reduction of the smallest magnitude of -0.01m extends for:

- Layout A by approximately 25km southwards;
- Layout B by approximately 23km southwards;
- Layout C by approximately 25km southwards; and
- Layout D by approximately 13km southwards.

8.3.4.4.2 Summary for model with waves coming from an easterly direction

58. The wave reduction for waves from an easterly direction extends in a westerly direction.

59. Reduction of wave heights by -4cm to -6cm occurring only inside the Project array boundary.

60. The area of wave height reduction of the smallest magnitude of -0.01m extends for

- Layout A by approximately 19km westwards;
- Layout B by approximately 13km westwards;
- Layout C by approximately 17km westwards; and
- Layout D by approximately 8km westwards.

8.3.4.4.3 Conclusion of Sensitivity Model Runs

61. When comparing the three Offshore Platform options for each turbine layout, it can be noted that the differences in significant wave height (Hs) are relatively small, with the Offshore Platform Option 2 (two small central Offshore Platforms) producing marginally larger impact.

62. For both wave directions the turbine Layout D has the smallest impact, and Layout A has the largest impact, being only marginally larger than Layout C.

63. Turbine Layout C with Offshore Platform Option 2 is chosen as the "worst-case" DBD layout for further assessment after identification that this is the most realistic worst case for assessment purposes, with minimal differences in layouts based on sensitivity testing.

64. Waves from a northerly direction have the biggest impact in terms of extent of wave reduction.

65. There is no increase in significant wave height (Hs) for any option.

66. The maximum reduction in wave height for all layouts is -0.1m which is localised around the Offshore Platform structures.

8.3.4.5 Model Simulations for Assessing Potential Impact

67. The wave model was run for the following four wind farm scenarios:

- 'Baseline' – without any wind farms;
- 'DBD Option' – shown on **Figure 8.3-12** with 113 turbines and two small Offshore Platform in the centre of the wind farm array;
- 'Scenario 1' – Includes proposed wind farm development 'DBD Option', and existing wind farms DBA, DBB, DBC and Sofia shown on **Figure 8.3-13** and in **Table 8.3-5**; and
- 'Scenario 2' – Includes proposed wind farm development 'DBD Option', and existing wind farms DBA, DBB, DBC and Sofia, as well as the planned wind farm DBS shown on **Figure 8.3-14** and in **Table 8.3-5**.

8.3.4.6 Baseline and Option Model Run Results

68. **Figure 8.3-41** to **Figure 8.3-46** show the significant wave height (Hs) for the 'Baseline' conditions for occurring probability of 50 percentile, return periods of 1 in 1 year and 1 in 100 years with waves coming from a northerly and easterly direction respectively.

69. **Figure 8.3-47** to **Figure 8.3-52** show the difference in significant wave height (Hs) in metres between the 'Baseline' and wind farm 'DBD Option' for occurring probability of 50 percentile, return periods of 1 in 1 year and 1 in 100 years with waves coming from a northerly and easterly direction respectively.

70. Any difference in significant wave height (Hs) smaller than +/- 0.02m are shown in white. Increases in significant wave height (Hs) are shown in light to dark red, whilst decreases in significant wave height (Hs) are shown in light to dark blue.

71. The plots of difference in significant wave height show that wave condition of 1 in 1 year return period produces the largest shadow areas comparing to other tested wave conditions.

72. **Figure 8.3-53** to **Figure 8.3-58** show the difference in significant wave height (Hs) in percent between the 'Baseline' and wind farm 'DBD Option' for occurring probability of 50 percentile, and return periods of 1 in 1 year and 1 in 100 years with waves coming from a northerly and easterly direction respectively.

73. Any difference in significant wave height (Hs) in percent smaller than +/- 2% are shown in white. Increases in significant wave height (Hs) are shown in light to dark red, whilst decreases in significant wave height (Hs) are shown in light to dark blue.

74. The plots of difference in percent of significant wave height show that wave condition of occurring probability of 50 percentile produces the largest shadow areas comparing to other tested wave conditions.

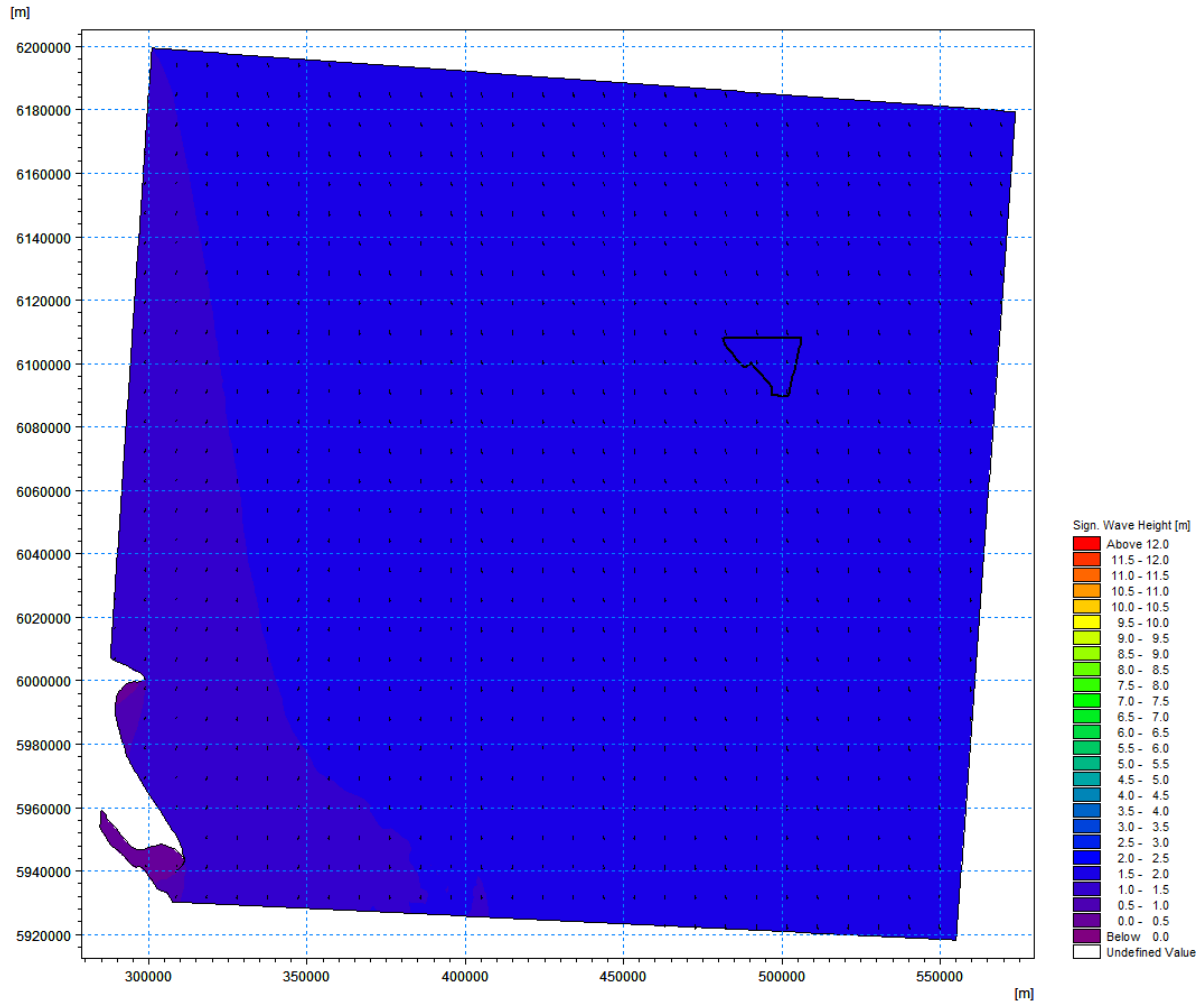

Figure 8.3-41: Significant Wave Height (Hs) for 'Baseline' for Waves Coming from Northerly Direction with Occurring Probability of 50 Percentile

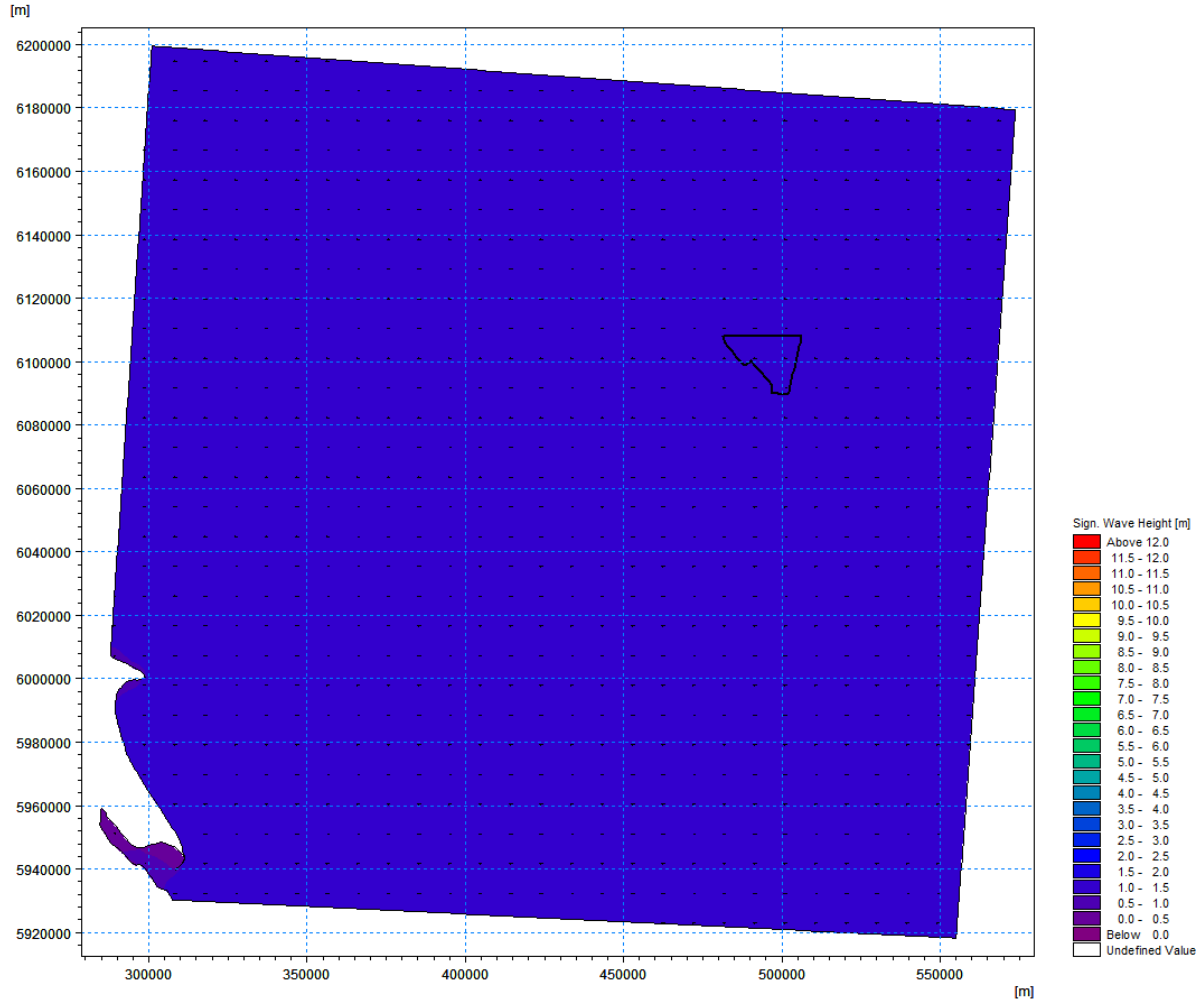

Figure 8.3-42: Significant Wave Height (Hs) for 'Baseline' for Waves Coming from Easterly Direction with Occurring Probability of 50 Percentile

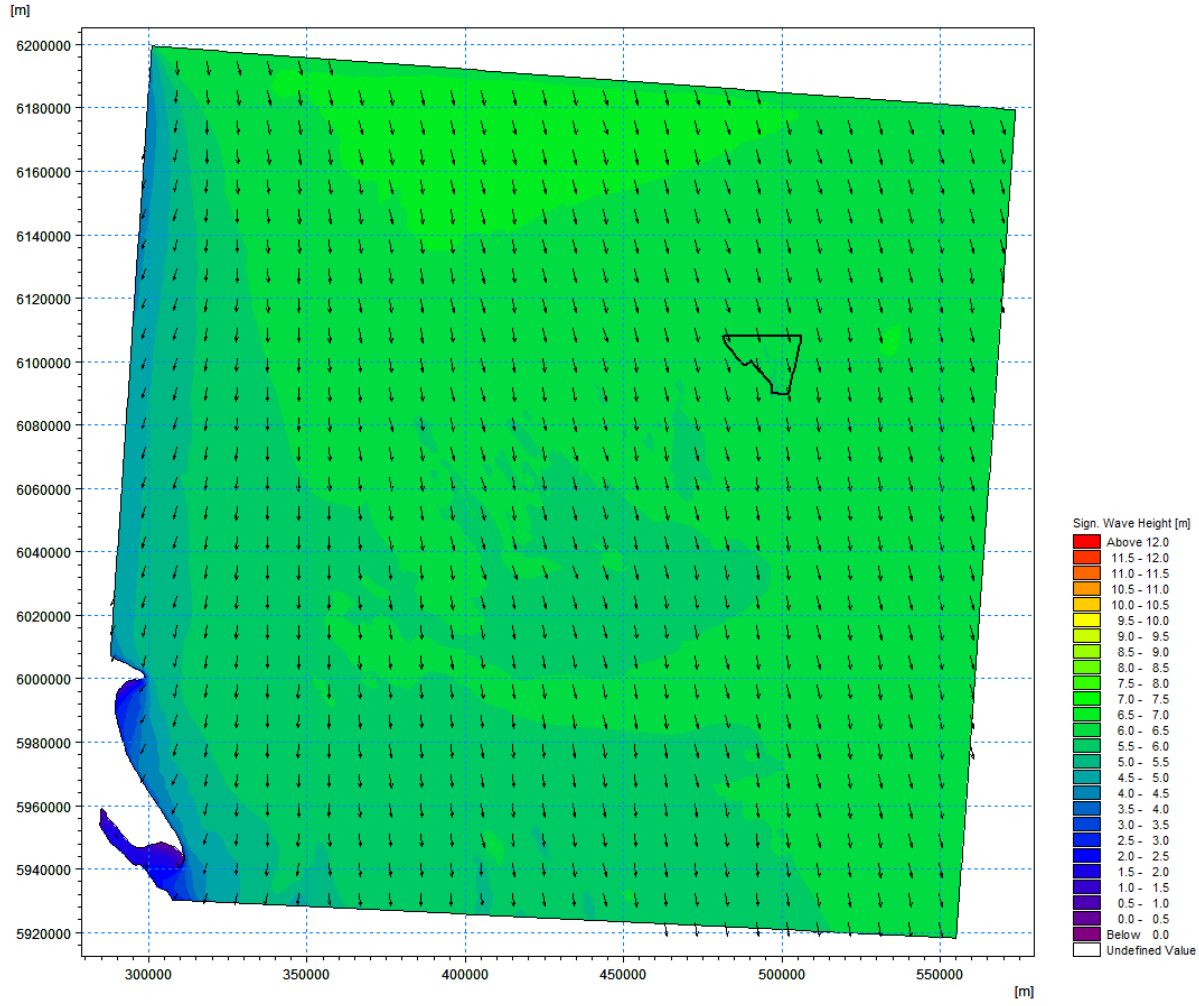

Figure 8.3-43: Significant Wave Height (Hs) for 'Baseline' for Waves Coming from Northerly Direction During 1 in 1 Year Return Period

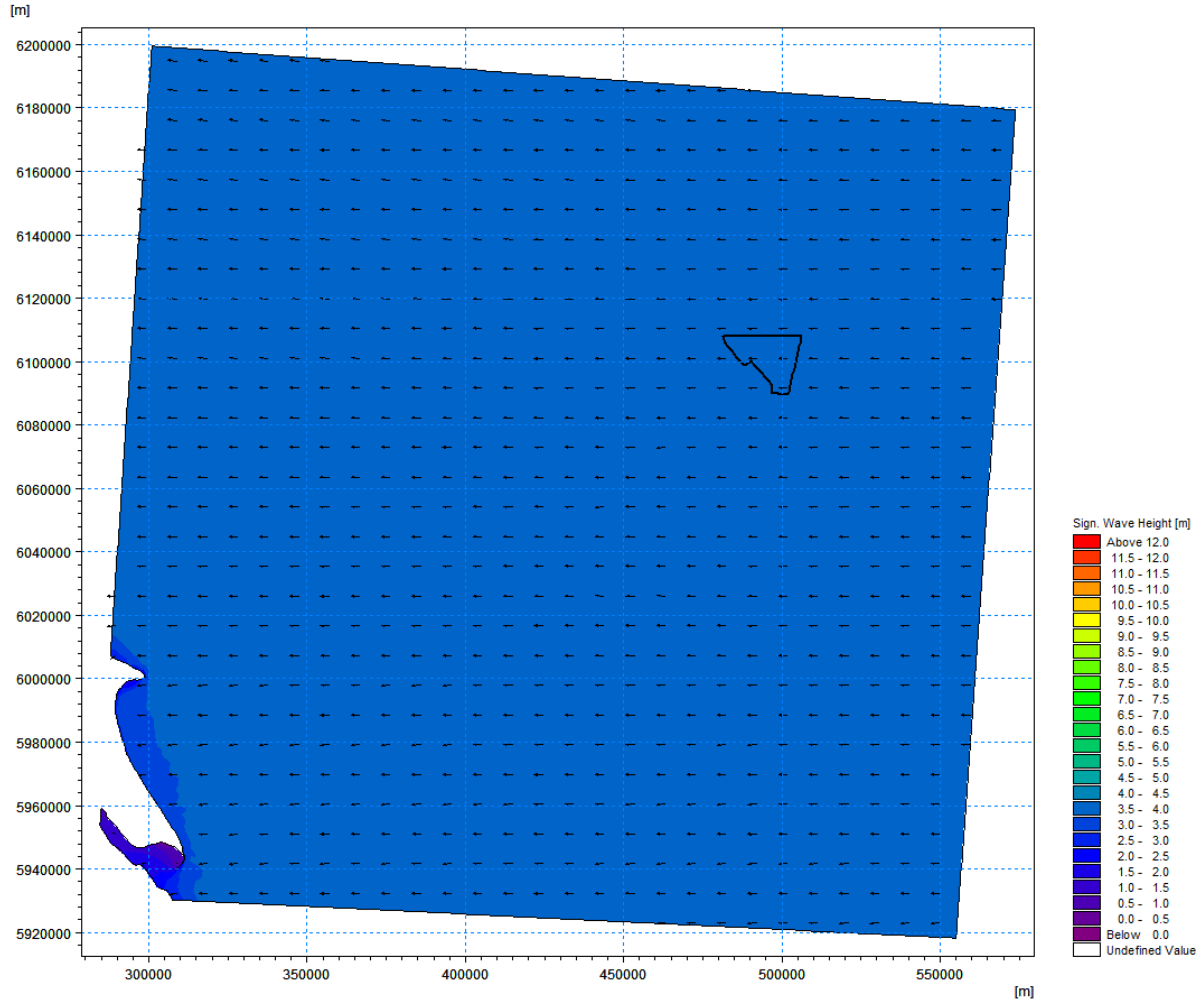

Figure 8.3-44: Significant Wave Height (Hs) for 'Baseline' for Waves Coming from Easterly Direction During 1 in 1 Year Return Period

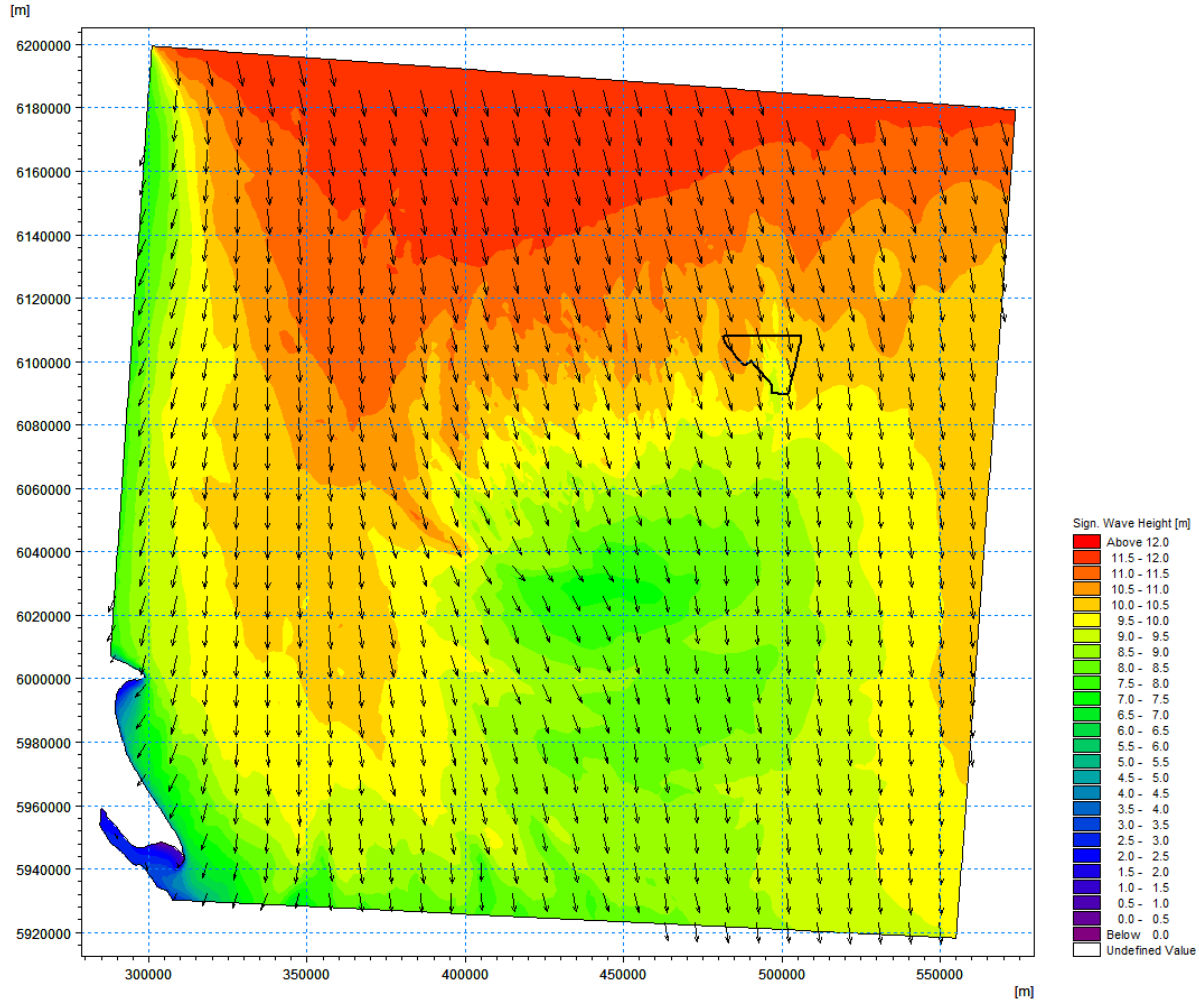

Figure 8.3-45: Significant Wave Height (Hs) for 'Baseline' for Waves Coming from Northerly Direction During 1 in 100 Year Return Period

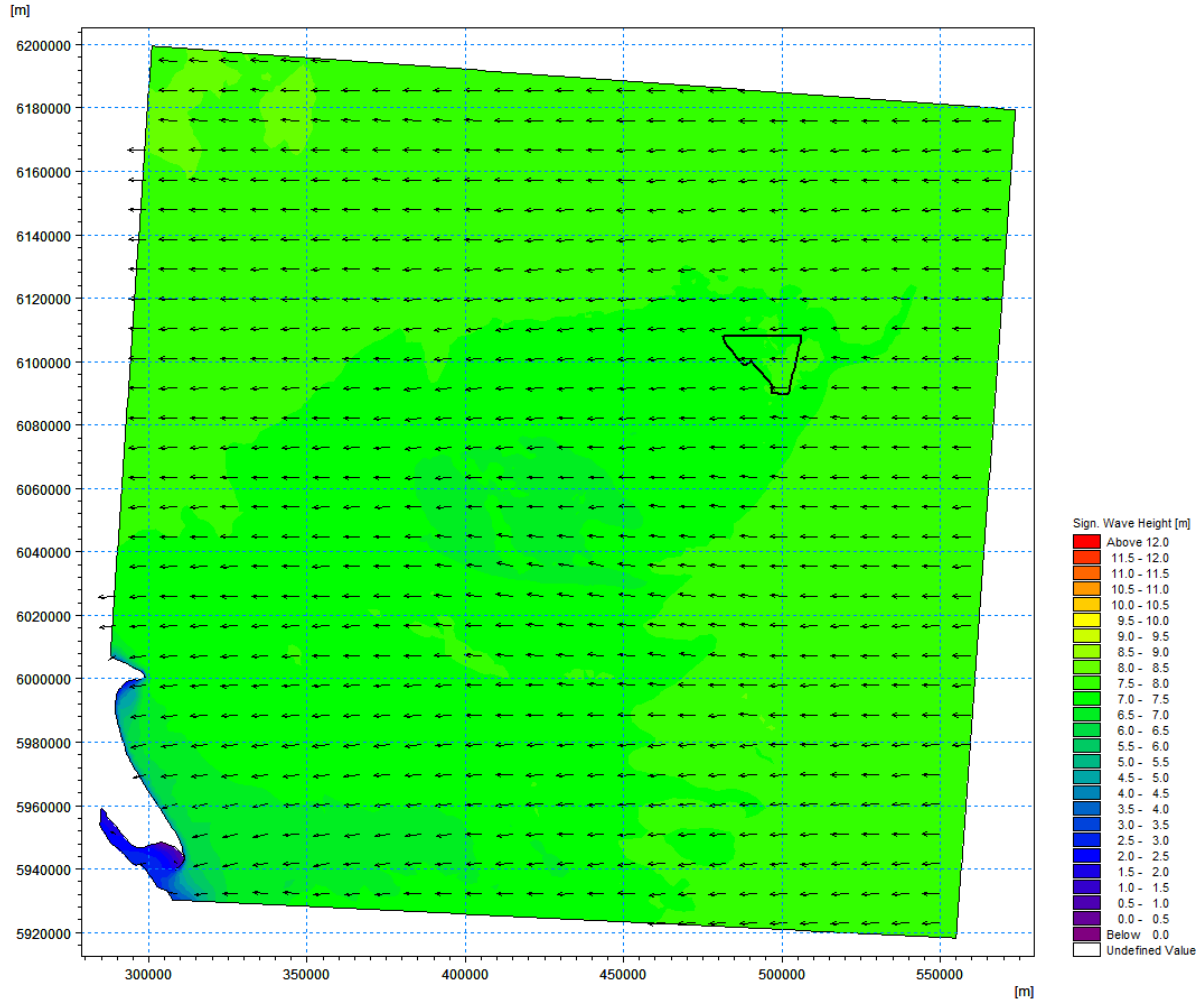

Figure 8.3-46: Significant Wave Height (Hs) for 'Baseline' for Waves Coming from Easterly Direction During 1 in 100 Year Return Period

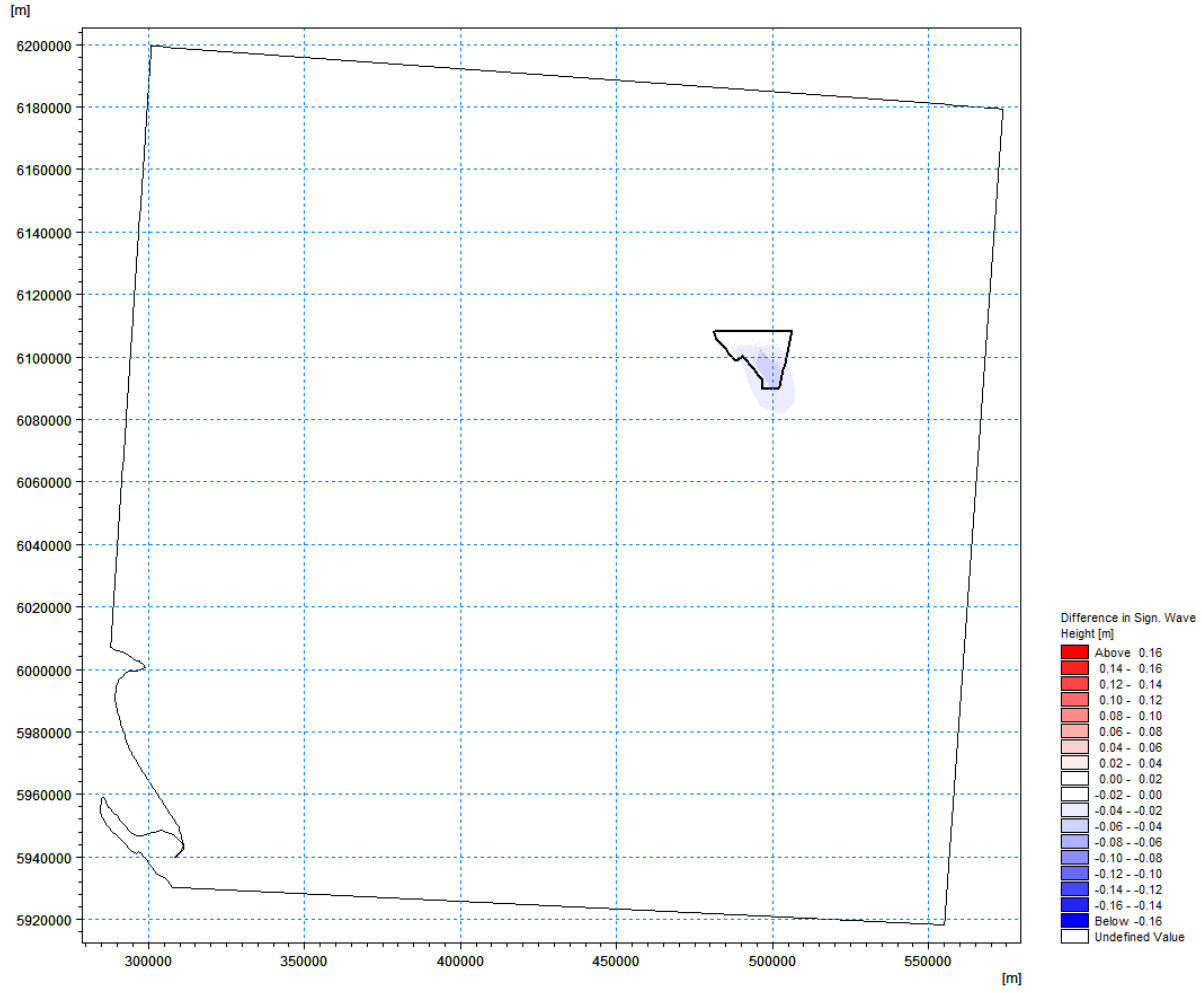

Figure 8.3-47: Difference in Significant Wave Height (Hs) in Metres between 'Baseline' and Wind Farm 'DBD Option' for Waves Coming from Northerly Direction with Occurring Probability of 50 Percentile

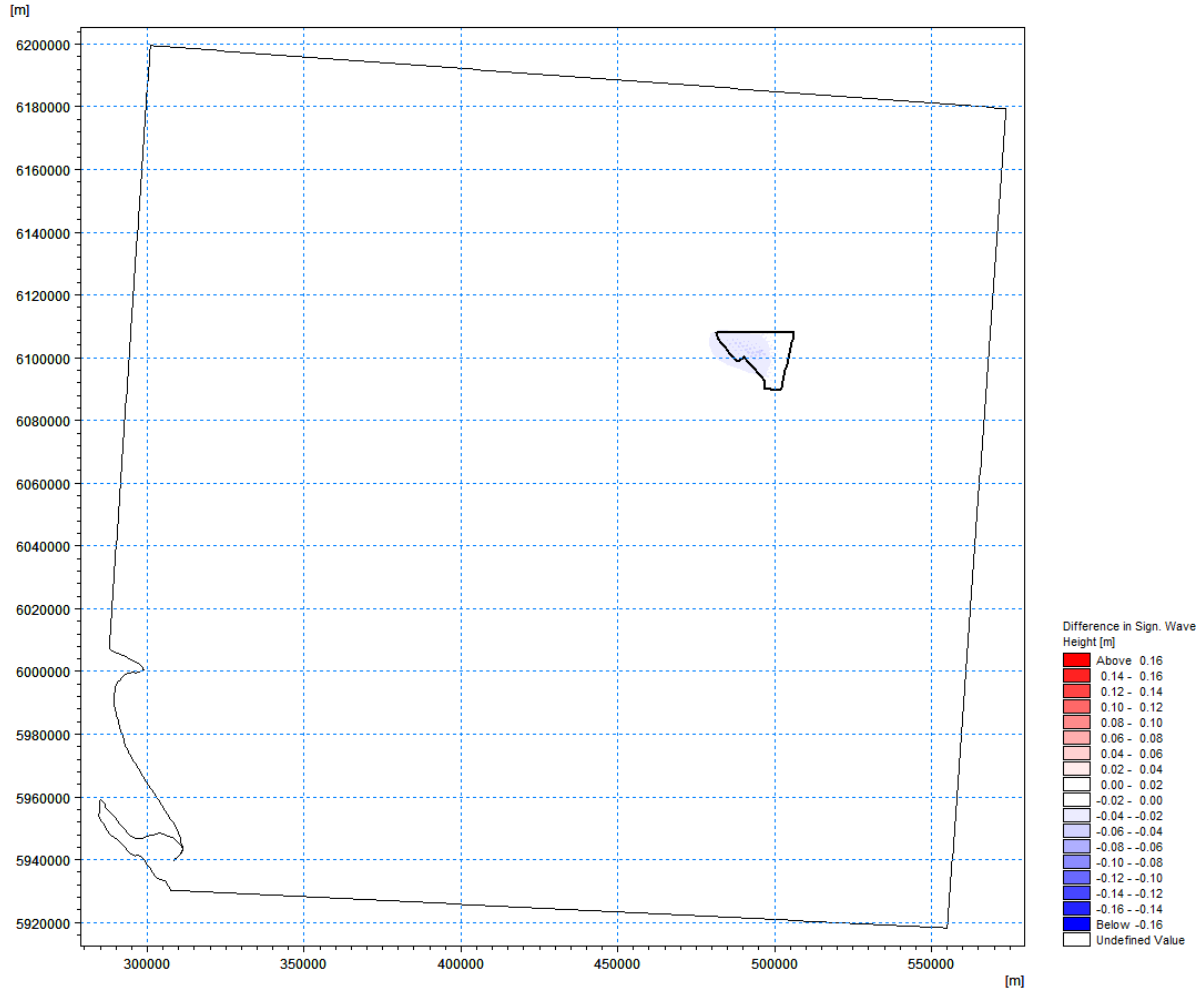

Figure 8.3-48: Difference in Significant Wave Height (Hs) in Metres between 'Baseline' and Wind Farm 'DBD Option' for Waves Coming from Easterly Direction with Occurring Probability of 50 Percentile

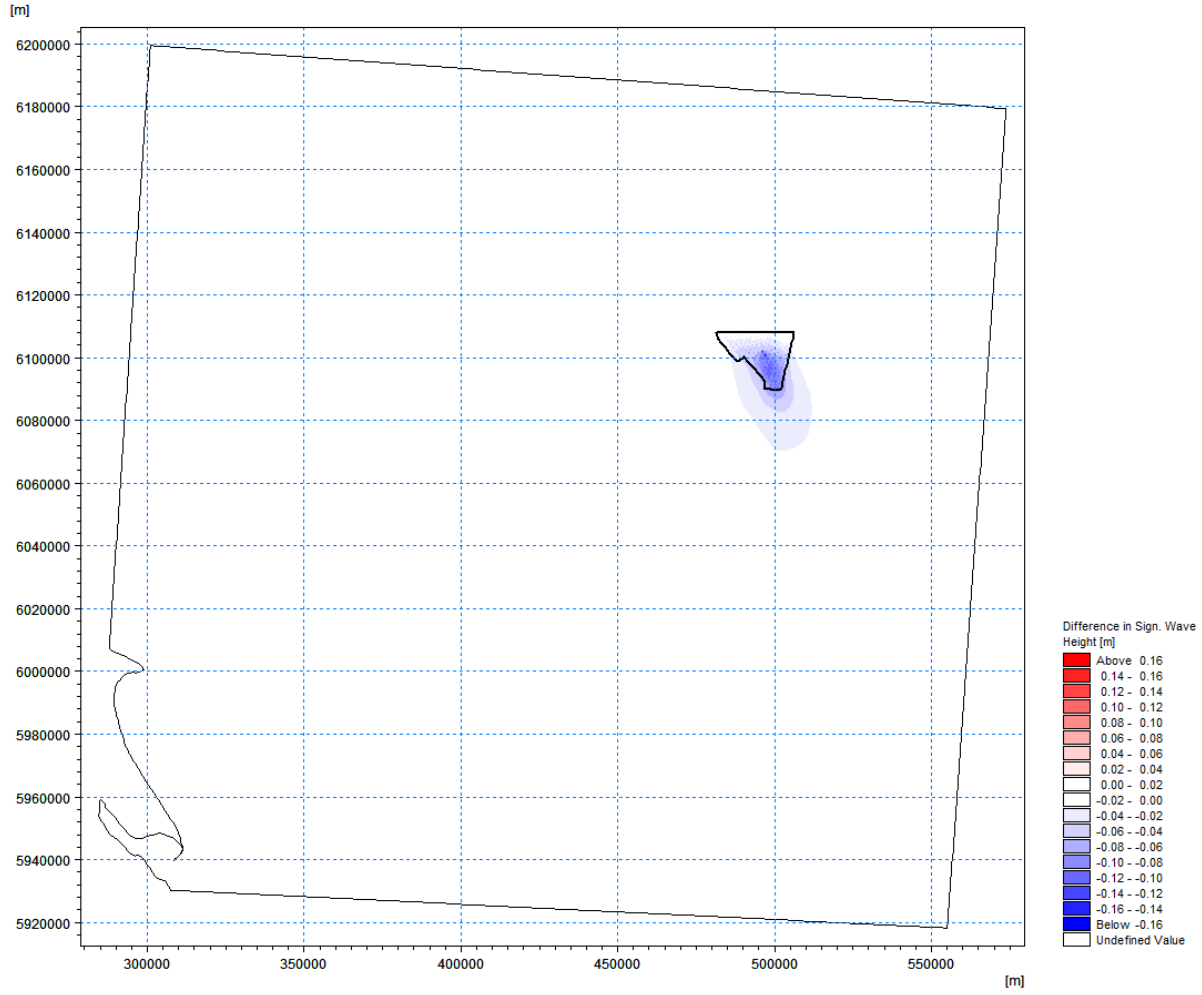

Figure 8.3-49: Difference in Significant Wave Height (Hs) in Metres between 'Baseline' and Wind Farm 'DBD Option' for 1 in 1 Year Waves Coming from Northerly Direction

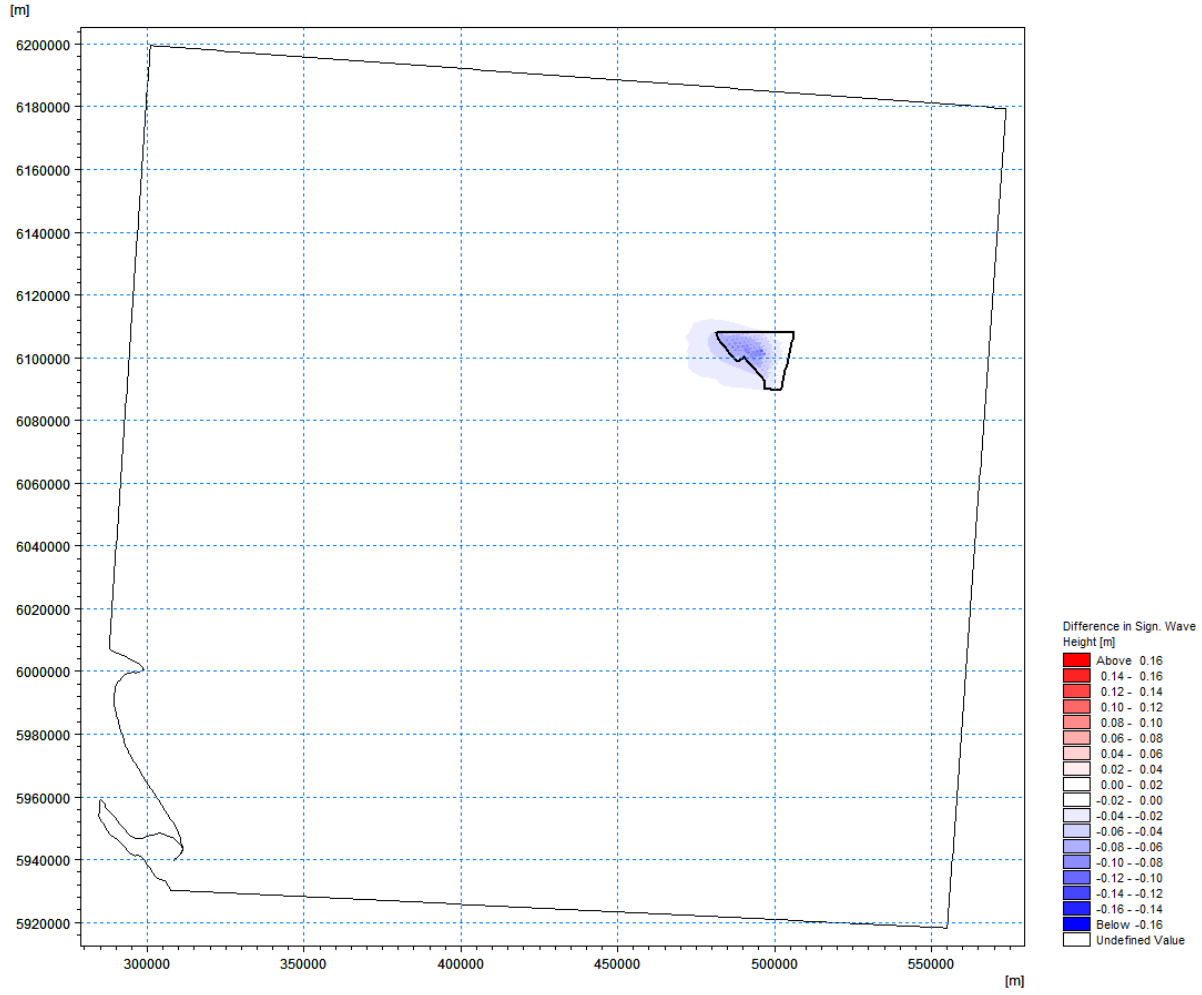

Figure 8.3-50: Difference in Significant Wave Height (Hs) in Metres between 'Baseline' and Wind Farm 'DBD Option' for 1 in 1 Year Waves Coming from Easterly Direction

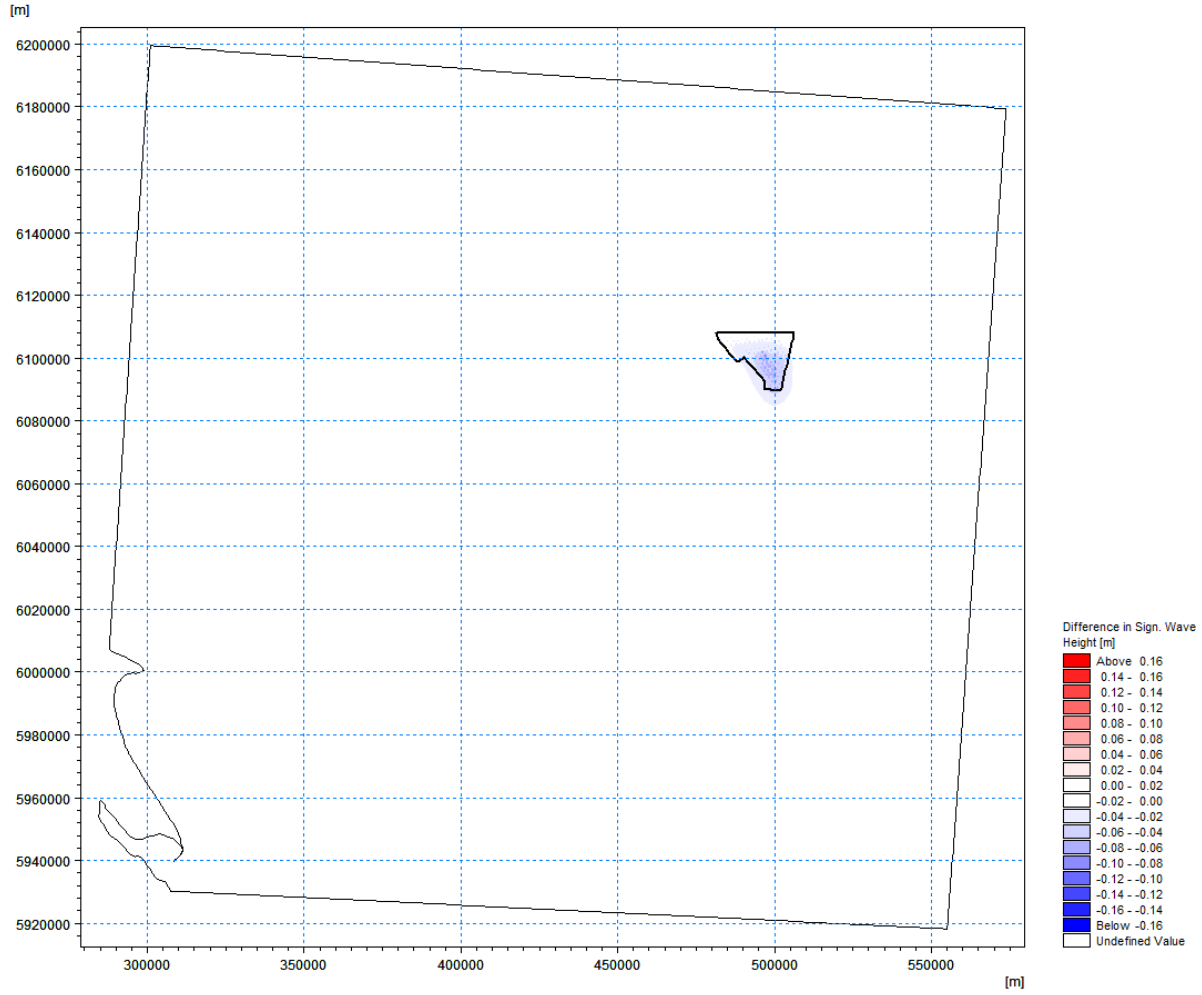

Figure 8.3-51: Difference in Significant Wave Height (Hs) in Metres between 'Baseline' and Wind Farm 'DBD Option' for 1 in 1 Year Waves Coming from Northerly Direction

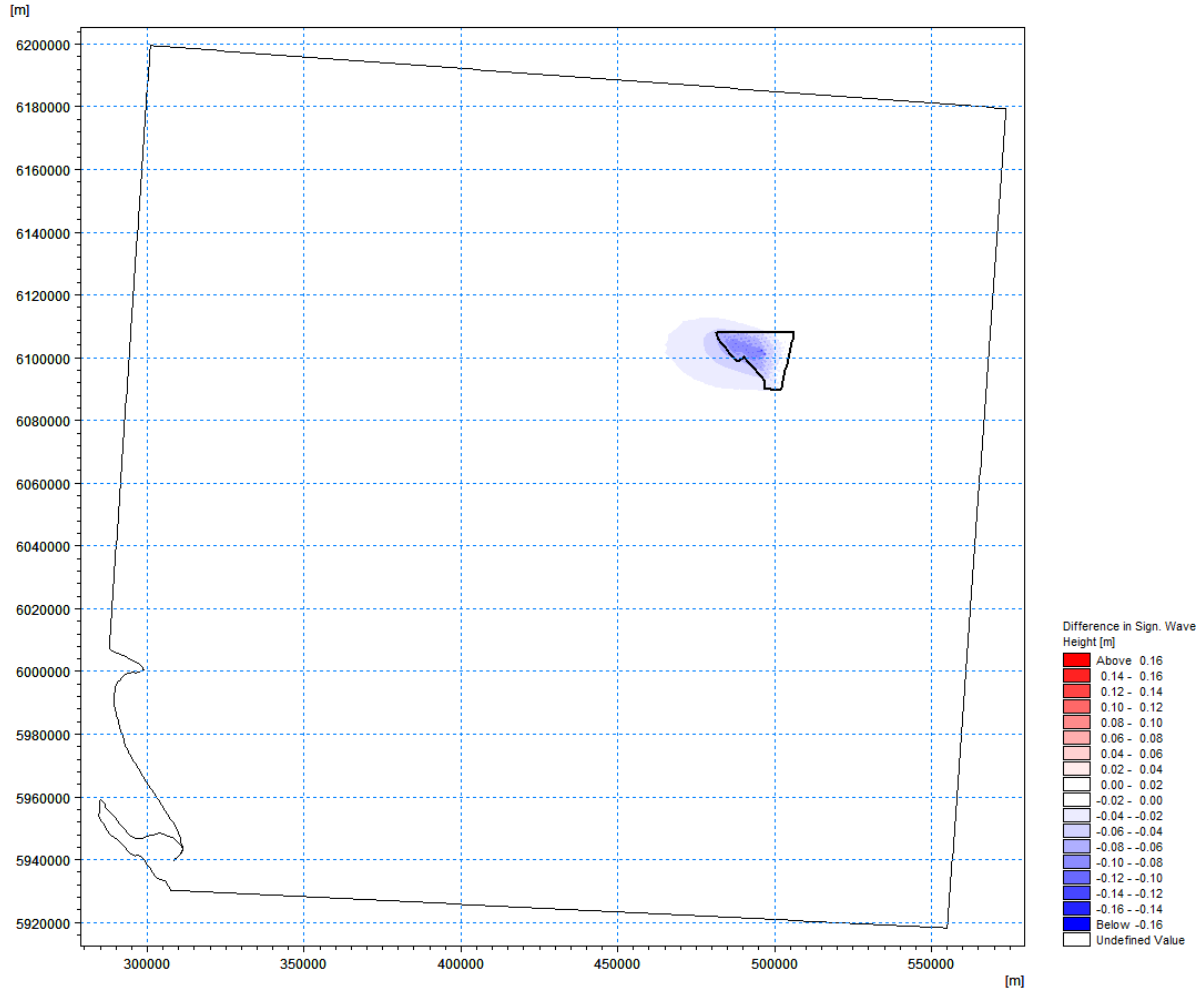

Figure 8.3-52: Difference in Significant Wave Height (Hs) in Metres between 'Baseline' and Wind Farm 'DBD Option' for 1 in 100 Year Waves Coming from Easterly Direction

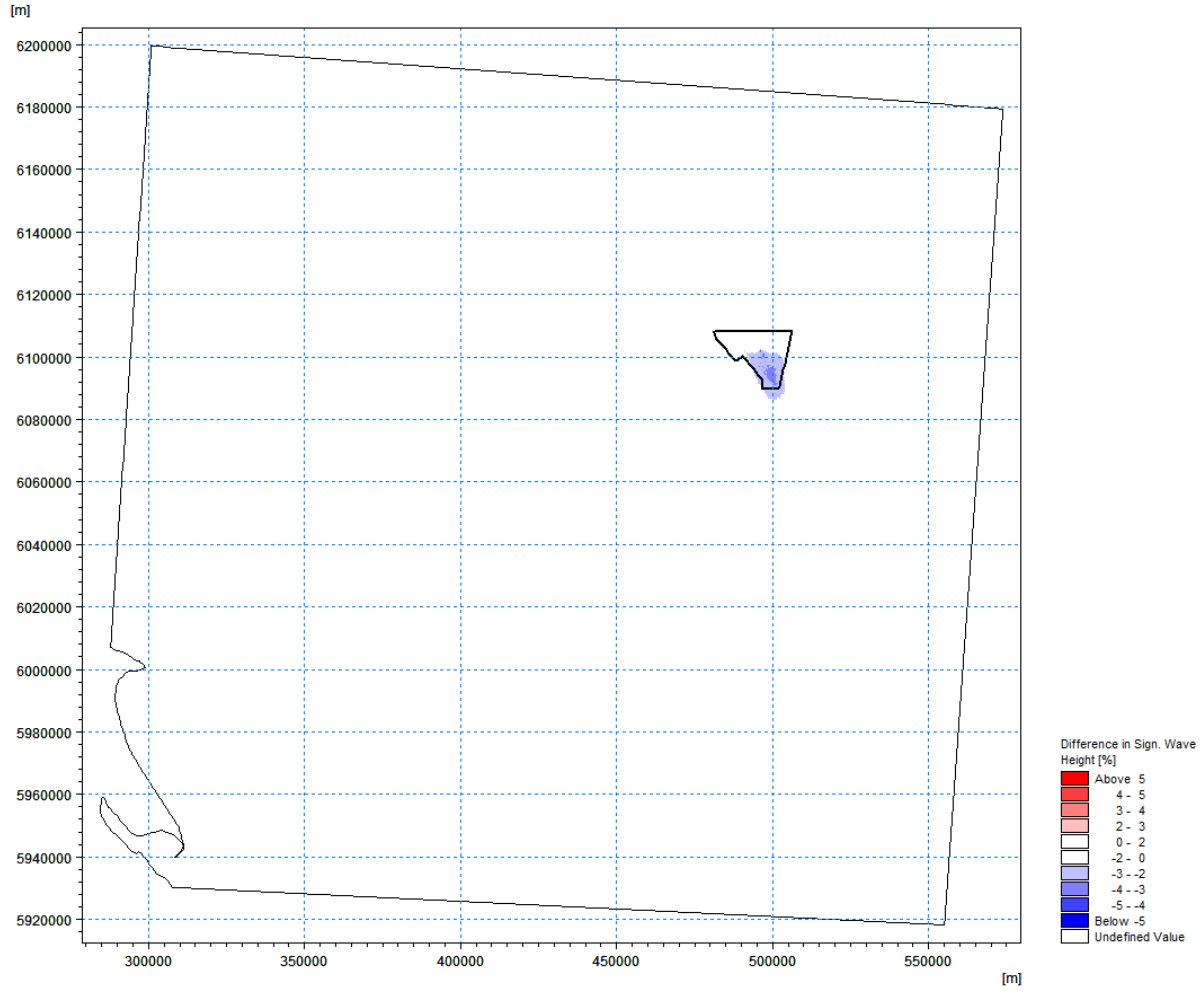

Figure 8.3-53: Difference in Significant Wave Height (Hs) in Percent between 'Baseline' and Wind Farm 'DBD Option' for Waves Coming from Northerly Direction with Occurring Probability of 50 Percentile

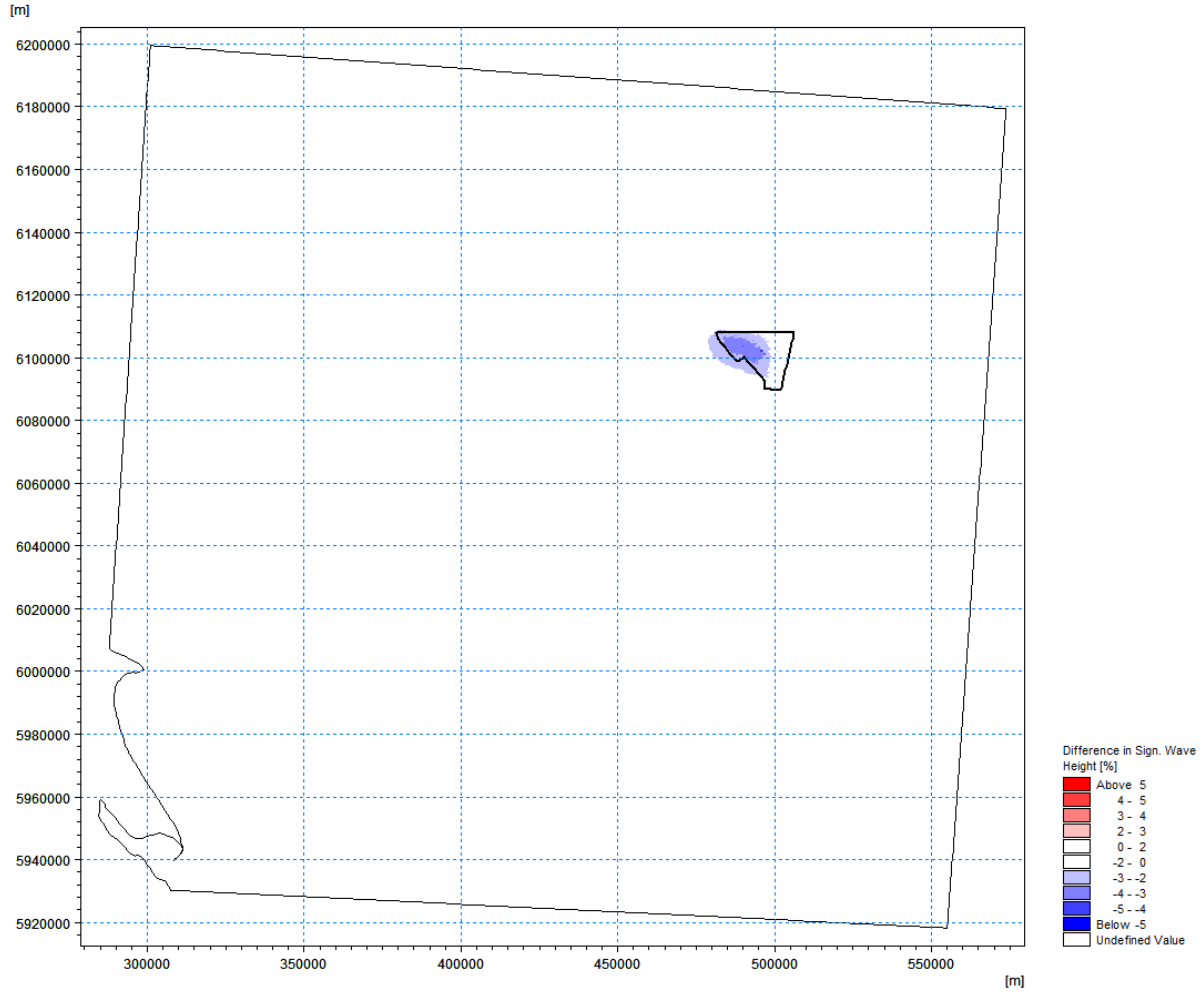

Figure 8.3-54: Difference in Significant Wave Height (Hs) in Percent between 'Baseline' and Wind Farm 'DBD Option' for Waves Coming from Easterly Direction with Occurring Probability of 50 Percentile

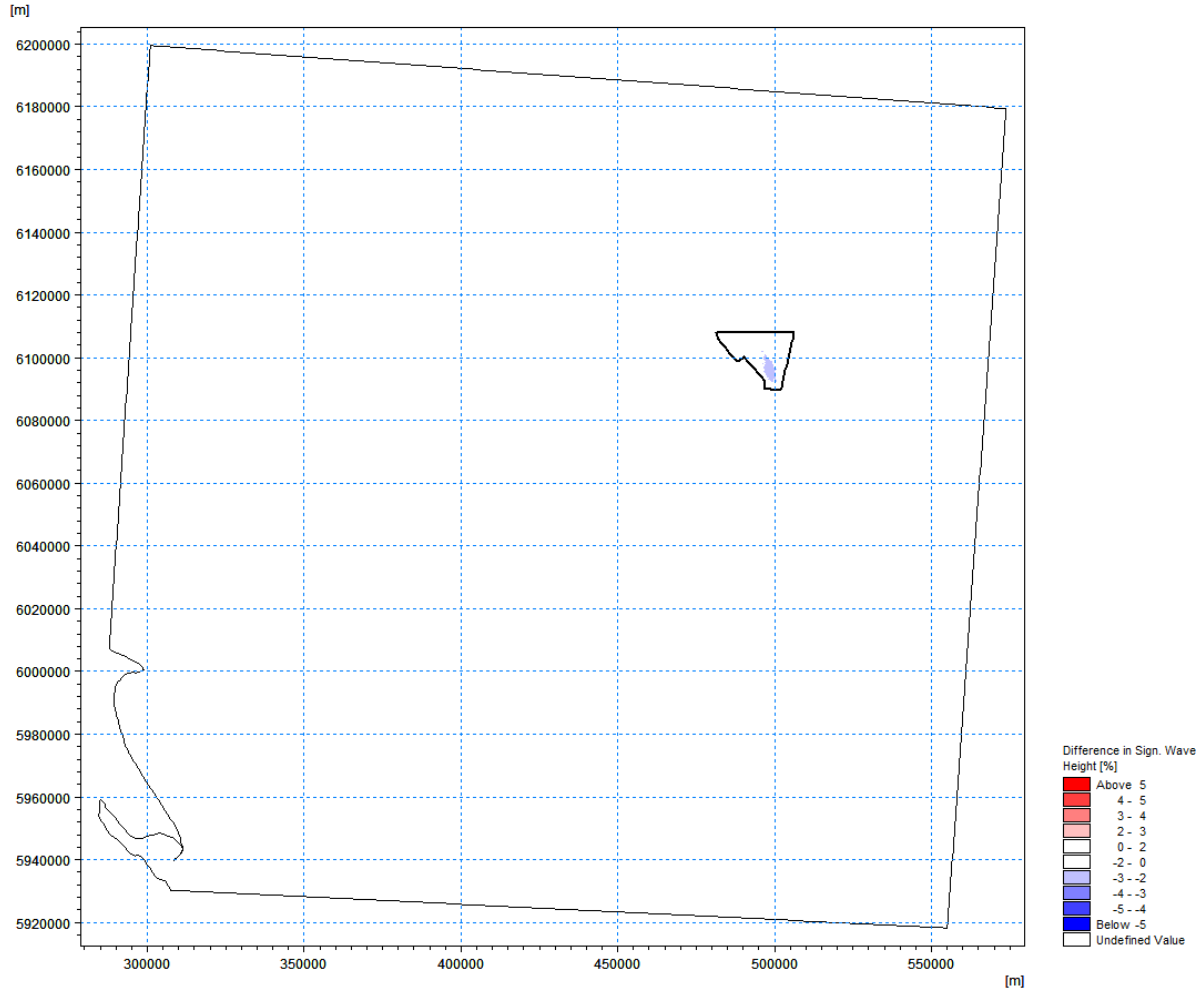

Figure 8.3-55: Difference in Significant Wave Height (Hs) in Percent between 'Baseline' and Wind Farm 'DBD Option' for 1 in 1 Year Waves Coming from Northerly Direction

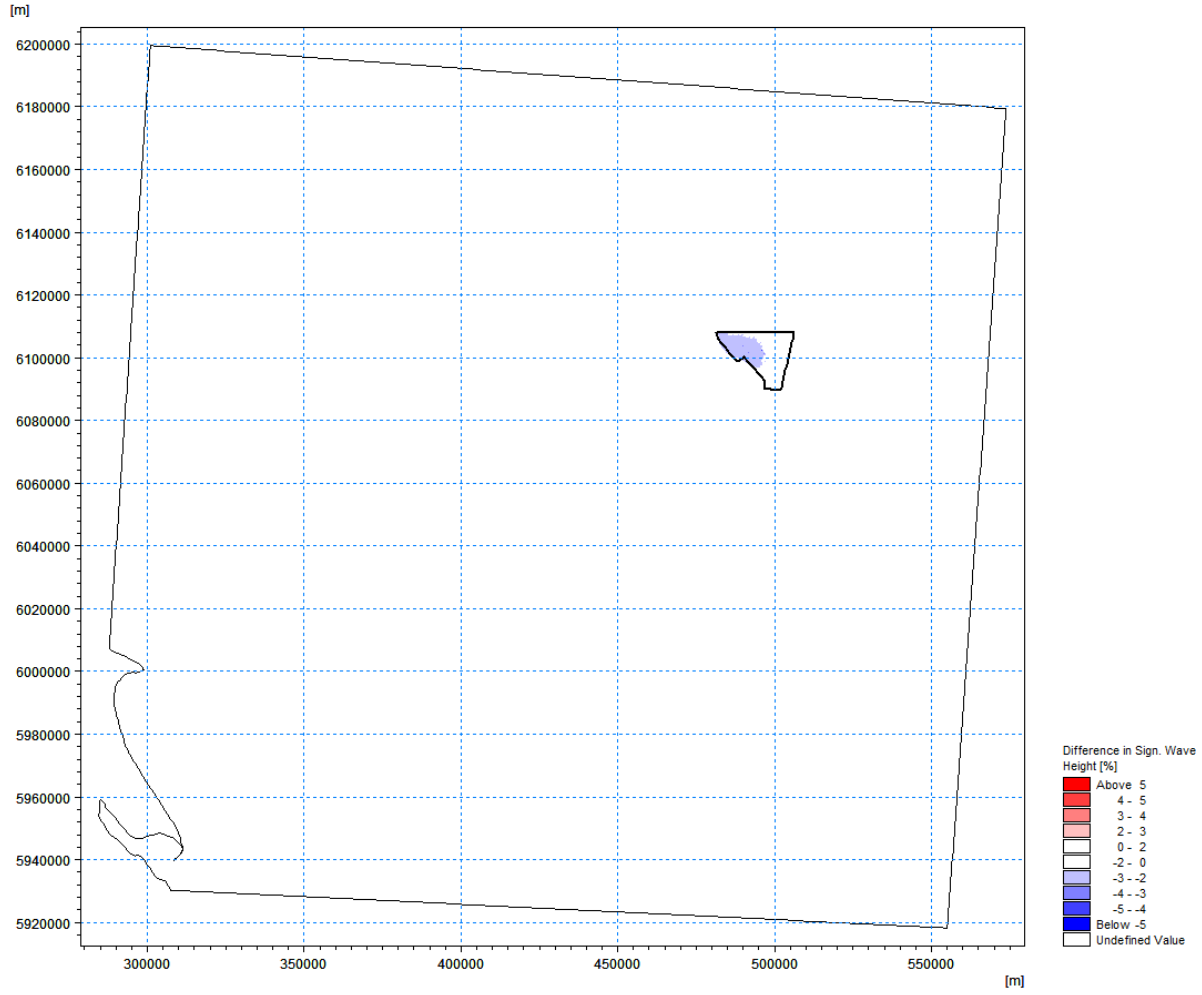

Figure 8.3-56: Difference in Significant Wave Height (Hs) in Percent between 'Baseline' and Wind Farm 'DBD Option' for 1 in 1 Year Waves Coming from Easterly Direction

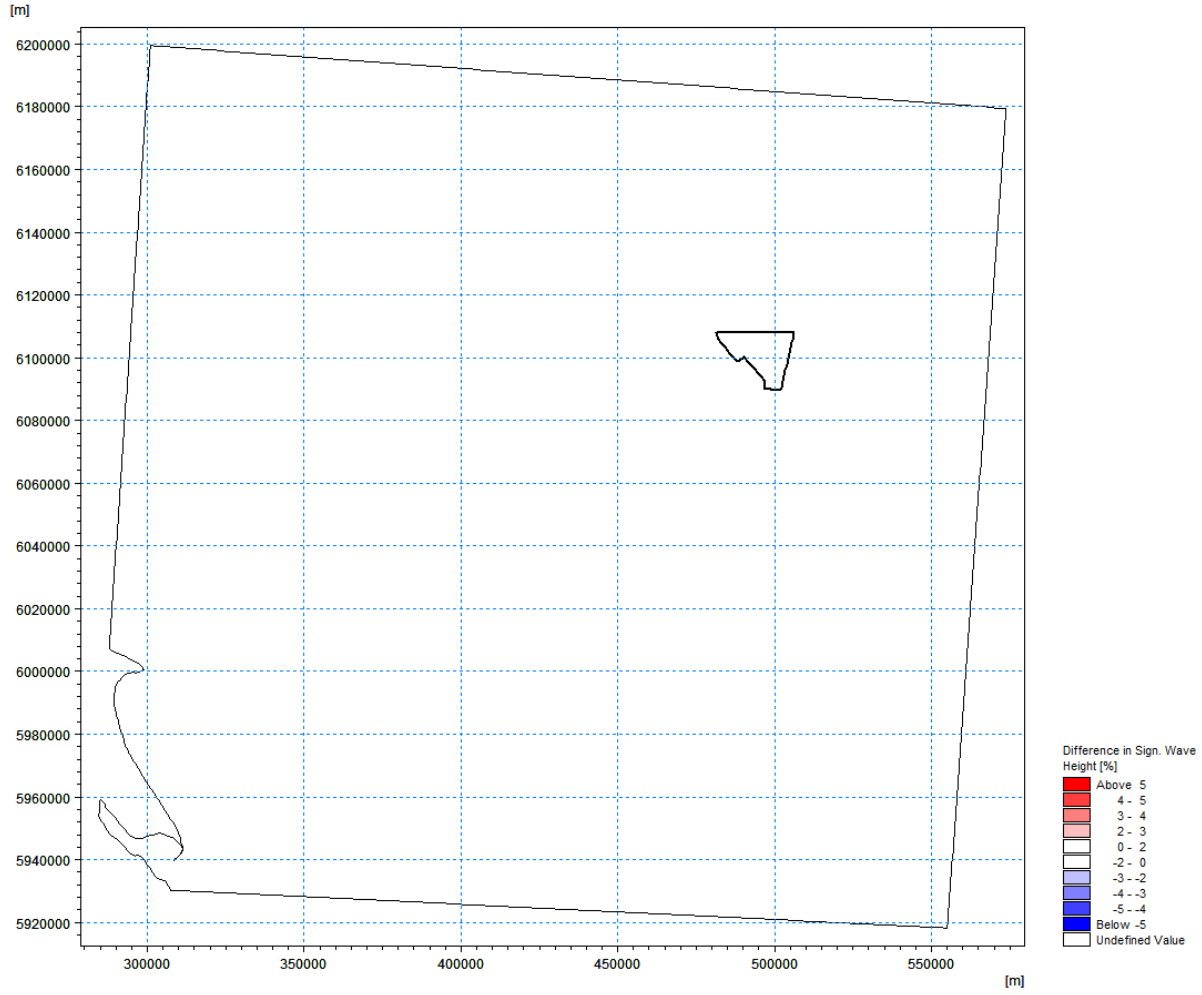

Figure 8.3-57: Difference in Significant Wave Height (Hs) in Percent between 'Baseline' and Wind Farm 'DBD Option' for 1 in 1 Year Waves Coming from Northerly Direction

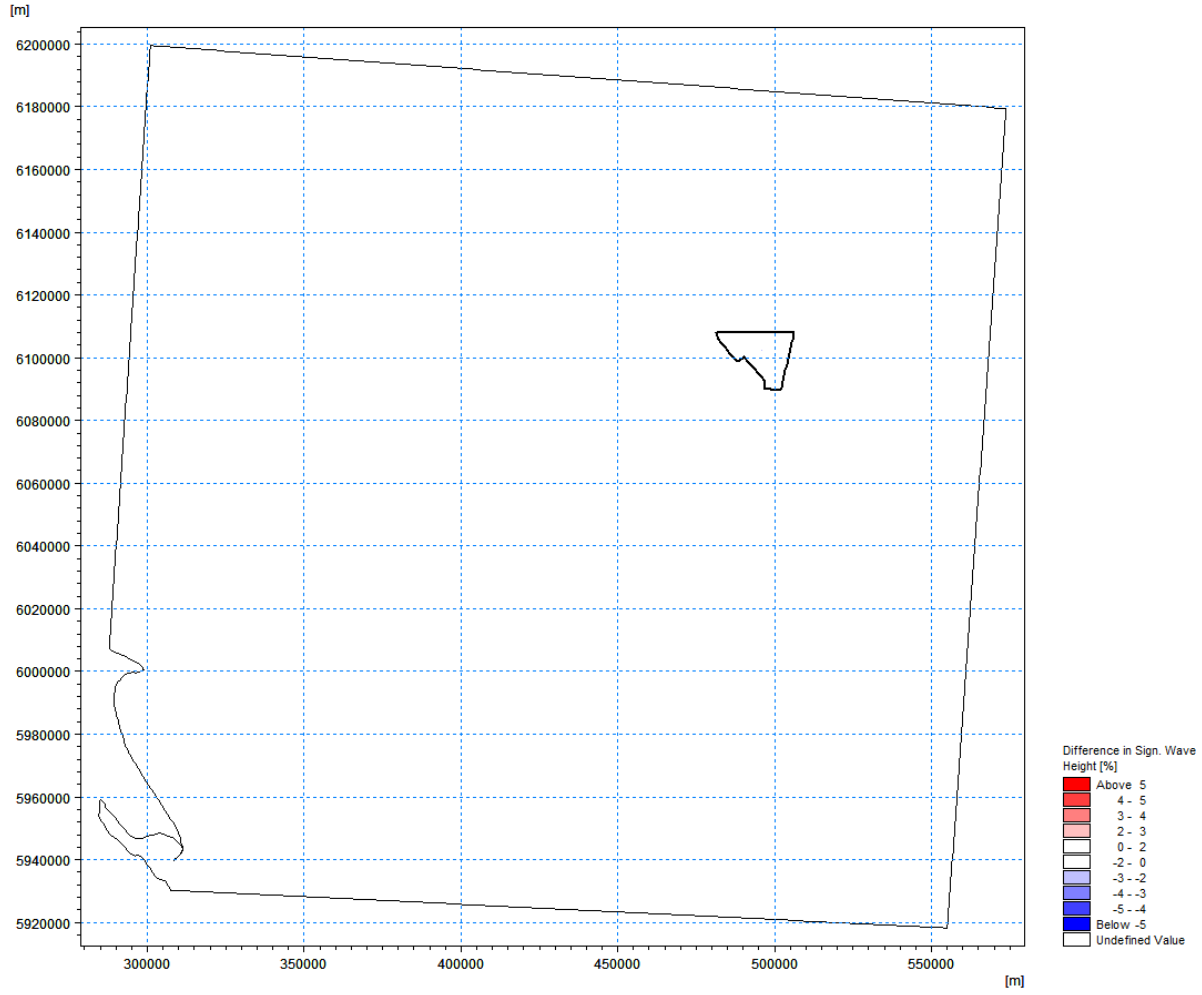

Figure 8.3-58: Difference in Significant Wave Height (Hs) in Percent between 'Baseline' and Wind Farm 'DBD Option' for 1 in 1 Year Waves Coming from Easterly Direction

75. For **Figure 8.3-41** to **Figure 8.3-46**, it can be seen that there is a higher significant wave height (Hs) coming from a northerly direction against coming from an easterly direction. While this can be seen in all of the return periods, it is less visible in the 50 percentile plots.

76. For **Figure 8.3-47** to **Figure 8.3-52**, there is a larger difference in significant wave height (Hs) in metres shown for the 1 in 1 year return period, with similar values of change occurring for waves coming from both a northerly and easterly direction (**Figure 8.3-49** and **Figure 8.3-50**).

77. For **Figure 8.3-53** to **Figure 8.3-58**, there is a larger difference in significant wave height (Hs) in percent shown for waves with occurring probability of 50 percentile, with a slightly larger change occurring for waves coming from easterly direction than northerly direction (**Figure 8.3-53** and **Figure 8.3-54)**.

8.3.4.7 Cumulative Model Run Results

78. For the cumulative effect, the model was run for both Scenario 1 and 2 using the 50 percentile probability wave conditions and 1 in 1 year return period. This is because the 50 percentile probability wave conditions produces the largest shadow areas with respect to percentage wave height change, and wave condition of 1 in 1 year return period produces the largest shadow areas with respect to change in wave height (see discussion in **Section 8.3.4.6**)

79. **Figure 8.3-59** to **Figure 8.3-62** show the difference in significant wave height (Hs) in metres between the 'Baseline' and model 'Scenario 1' and 'Scenario 2' for occurring probability of 50 percentile with waves coming from a northerly and easterly direction respectively.

80. For waves with occurring probability of 50 percentile, the predicted difference in significant wave height (Hs) in metres (**Figure 8.3-59** to **Figure 8.3-62**) shows that the 'DBD Option' has the largest detectable impact of all scenarios, and no cumulative effect between wind farms.

81. **Figure 8.3-63** to **Figure 8.3-66** show the difference in significant wave height (Hs) in percent between the 'Baseline' and model 'Scenario 1' and 'Scenario 2' for occurring probability of 50 percentile with waves coming from a northerly and easterly direction respectively.

82. For waves with occurring probability of 50 percentile, the predicted difference in significant wave height (Hs) in percent (**Figure 8.3-63** to **Figure 8.3-66**) shows that cumulative effect is limited between 'DBD Option' and DBC due to proximity between two wind farms.

83. **Figure 8.3-67** to **Figure 8.3-70** show the difference in significant wave height (Hs) in metres between the 'Baseline' and model 'Scenario 1' and 'Scenario 2' for 1 in 1 year waves coming from a northerly and easterly direction respectively.

84. Any difference in significant wave height (Hs) in metres smaller than +/- 0.02 are shown in white. Increases in significant wave height (Hs) are shown in light to dark red, whilst decreases in significant wave height (Hs) are shown in light to dark blue.

85. **Figure 8.3-71** to **Figure 8.3-74** show the difference in significant wave height (Hs) in percent between the 'Baseline' and model 'Scenario 1' and 'Scenario 2' for 1 in 1 year waves coming from a northerly and easterly direction respectively.

86. Any difference in significant wave height (Hs) in percent smaller than +/- 2% are shown in white. Increases in significant wave height (Hs) are shown in light to dark red, whilst decreases in significant wave height (Hs) are shown in light to dark blue.

87. For 1 in 1 year waves, the predicted difference in significant wave height (Hs) in both metres and percent (**Figure 8.3-67** to **Figure 8.3-74**) shows that the 'DBD Option' has the largest impact of all scenarios, and cumulative effect is limited between 'DBD Option' and DBC due to proximity between two wind farms.

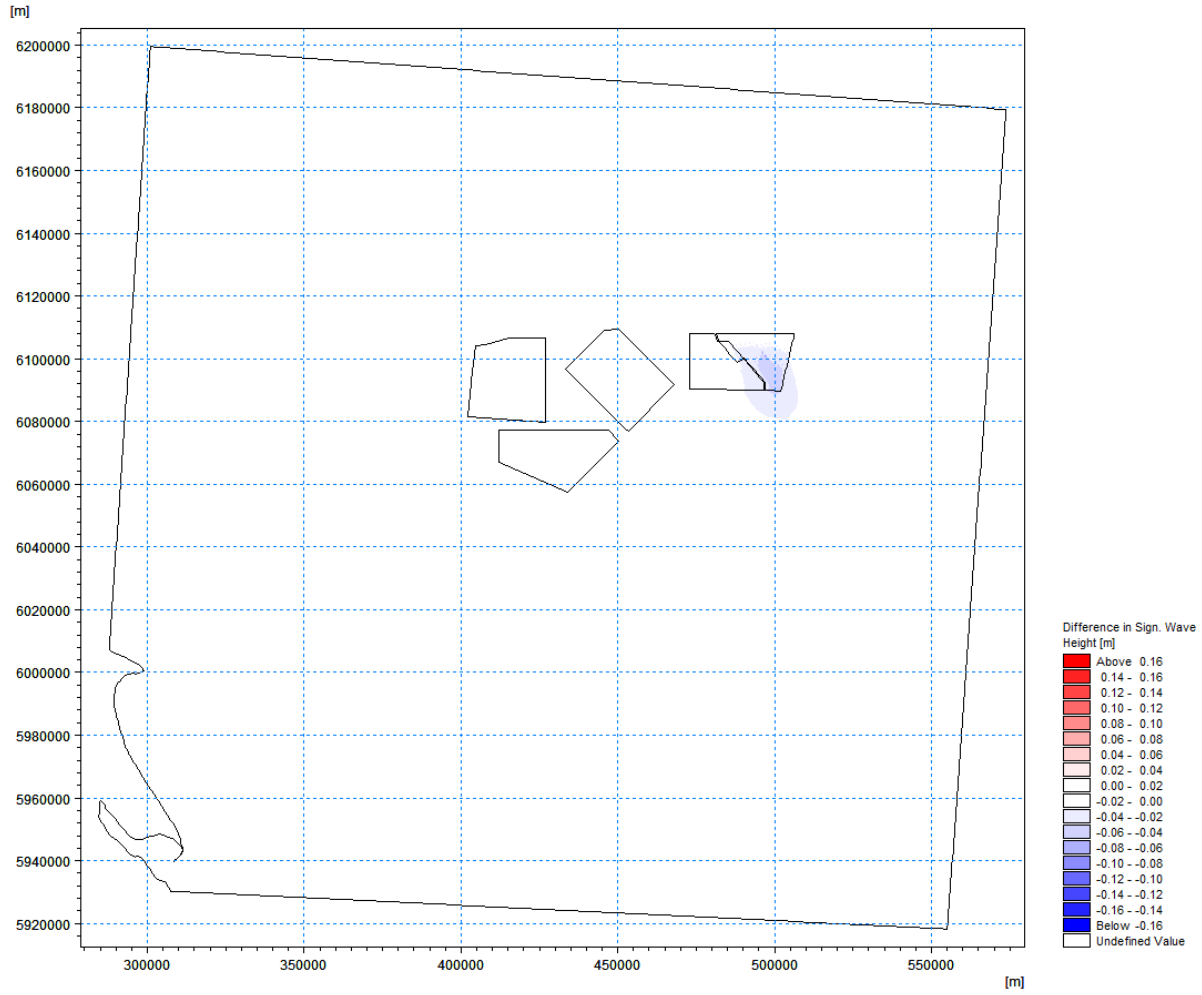

Figure 8.3-59: Difference in Significant Wave Height (Hs) in Metres between 'Baseline' and Wind Farm 'Scenario 1' for Waves Coming from Northerly Direction with Occurring Probability of 50 Percentile

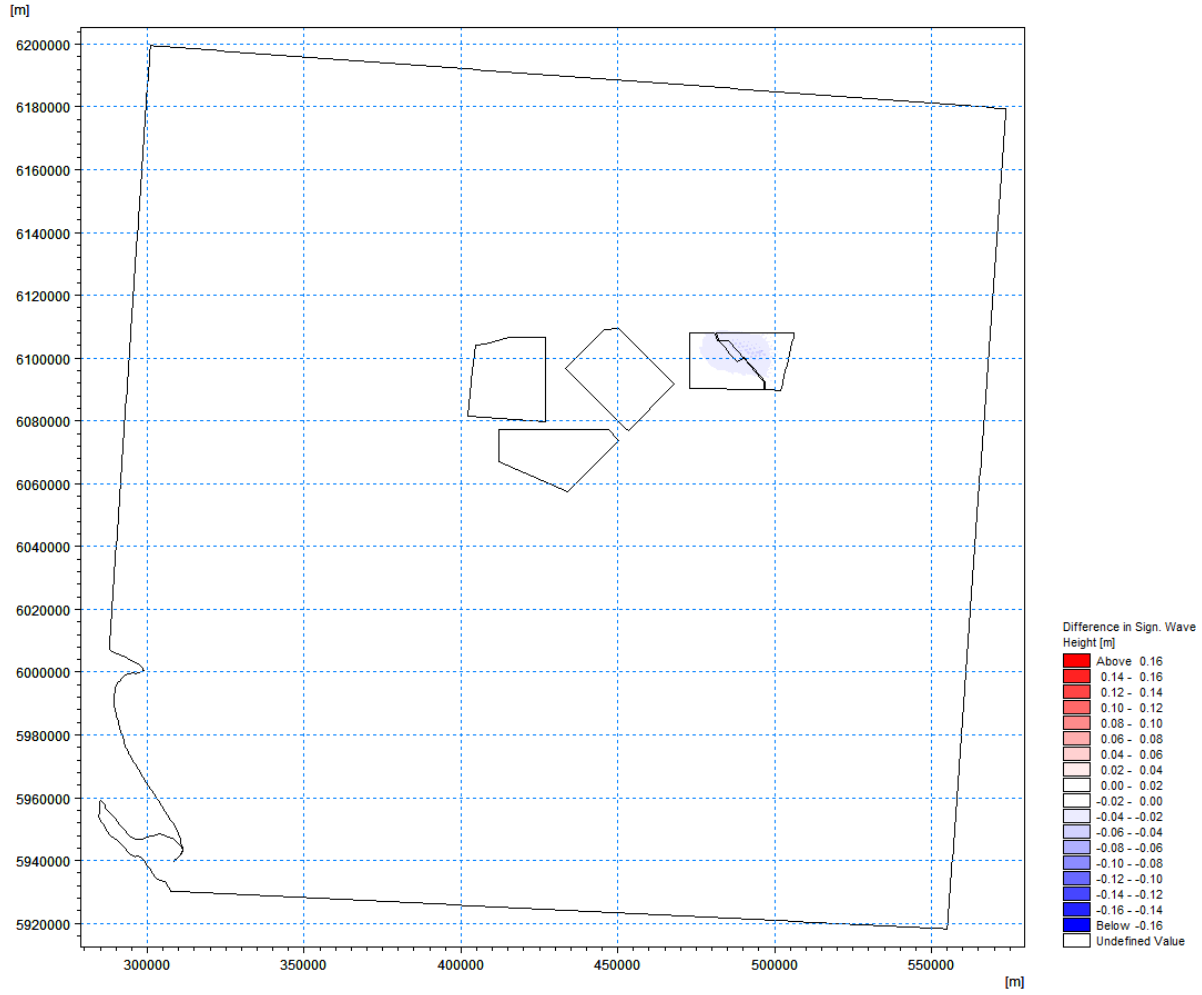

Figure 8.3-60: Difference in Significant Wave Height (Hs) in Metres between 'Baseline' and Wind Farm 'Scenario 1' for Waves Coming from Easterly Direction with Occurring Probability of 50 Percentile

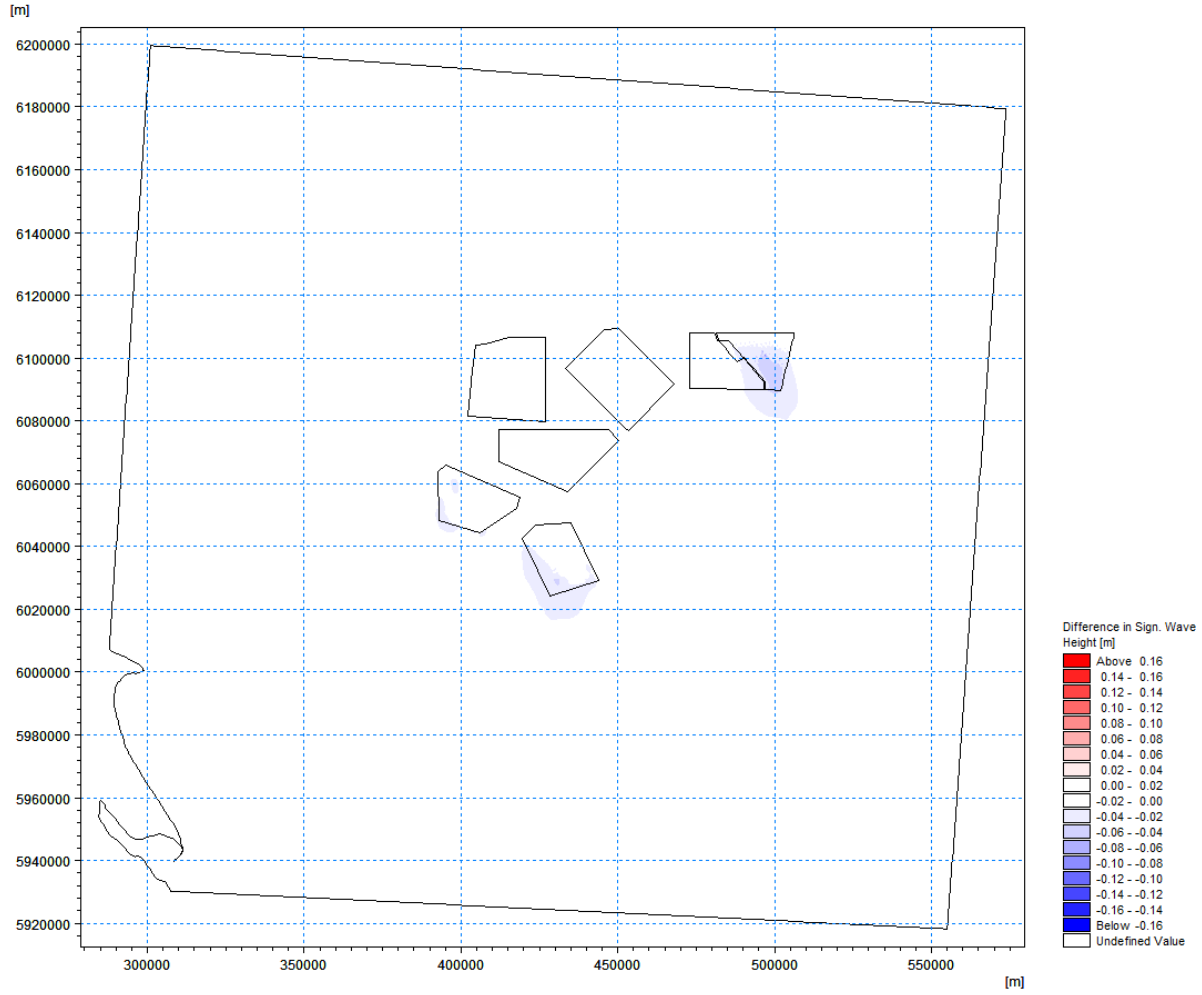

Figure 8.3-61: Difference in Significant Wave Height (Hs) in Metres between 'Baseline' and Wind Farm 'Scenario 2' for Waves Coming from Northerly Direction with Occurring Probability of 50 Percentile

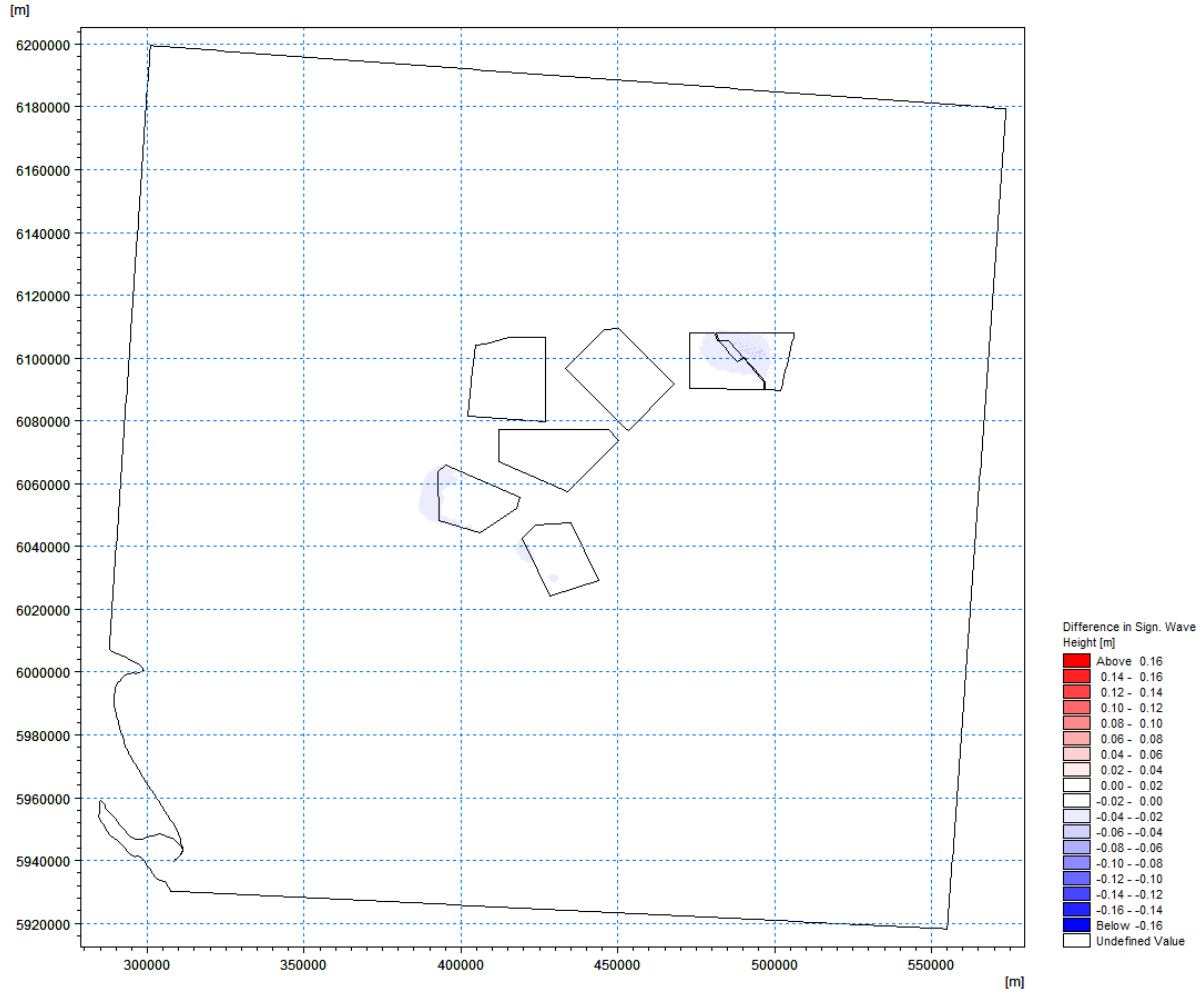

Figure 8.3-62: Difference in Significant Wave Height (Hs) in Metres between 'Baseline' and Wind Farm 'Scenario 2' for Waves Coming from Easterly Direction with Occurring Probability of 50 Percentile

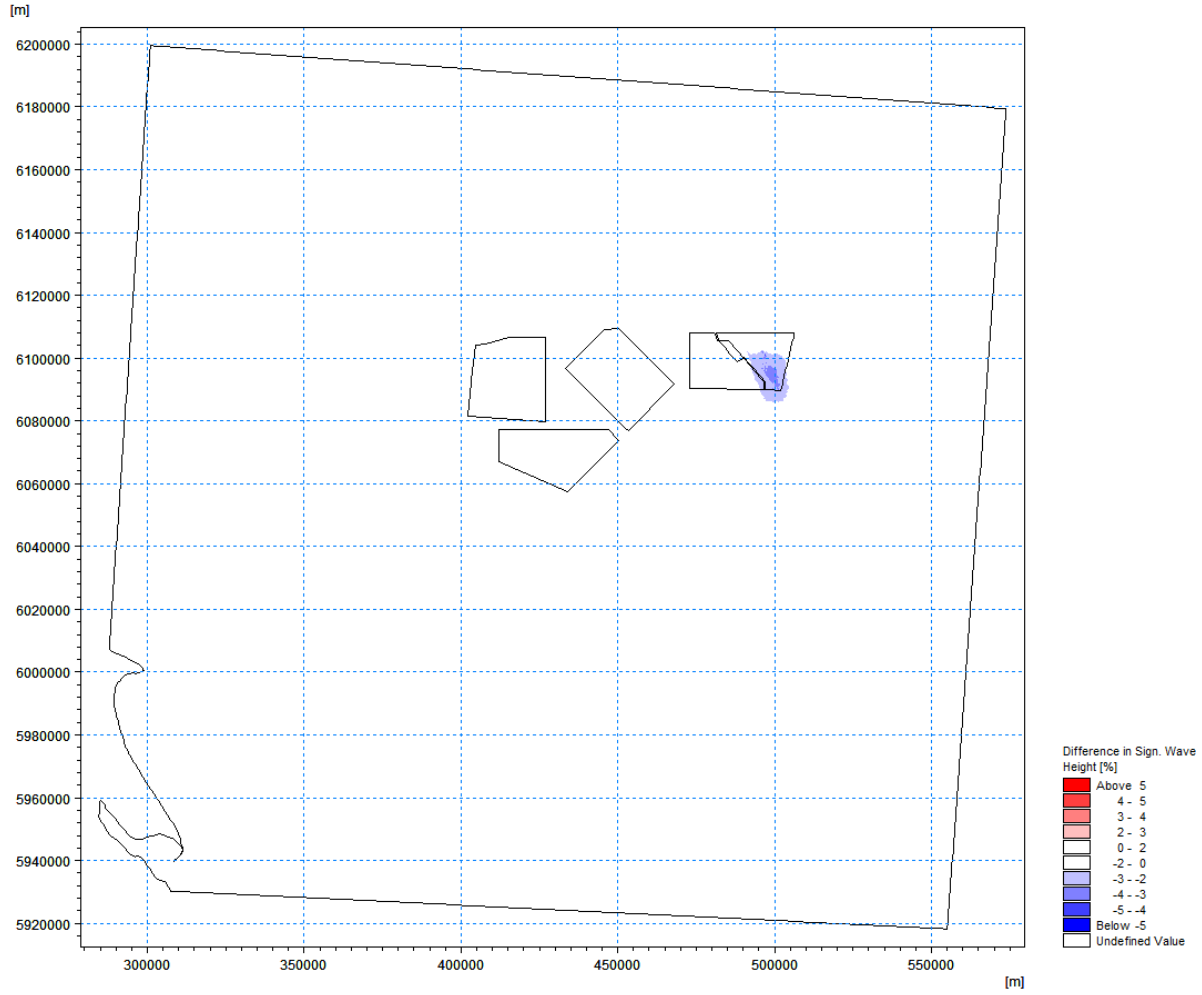

Figure 8.3-63: Difference in Significant Wave Height (Hs) in Percent between 'Baseline' and Wind Farm 'Scenario 1' for Waves Coming from Northerly Direction with Occurring Probability of 50 Percentile

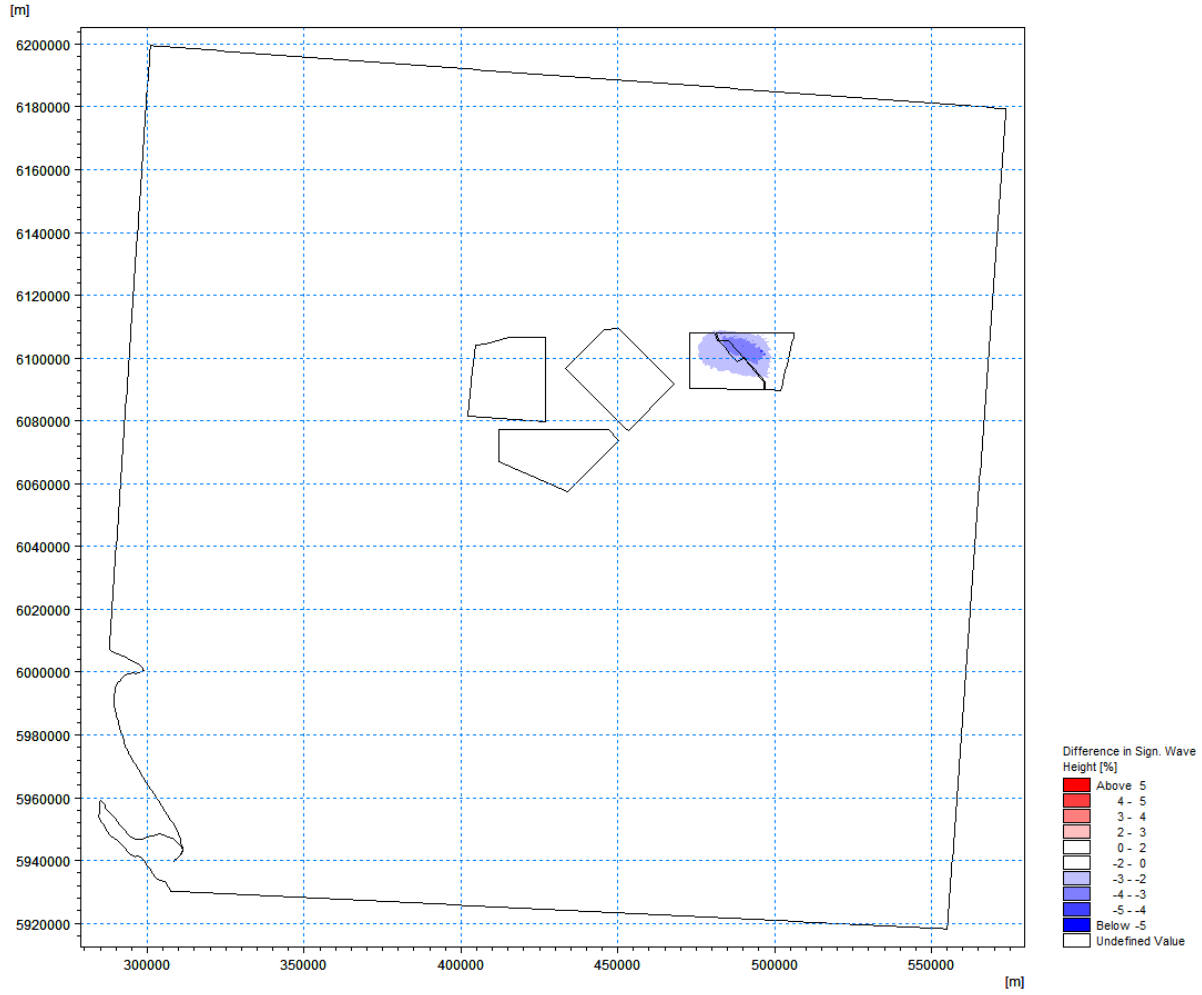

Figure 8.3-64: Difference in Significant Wave Height (Hs) in Percent between 'Baseline' and Wind Farm 'Scenario 1' for Waves Coming from Easterly Direction with Occurring Probability of 50 Percentile

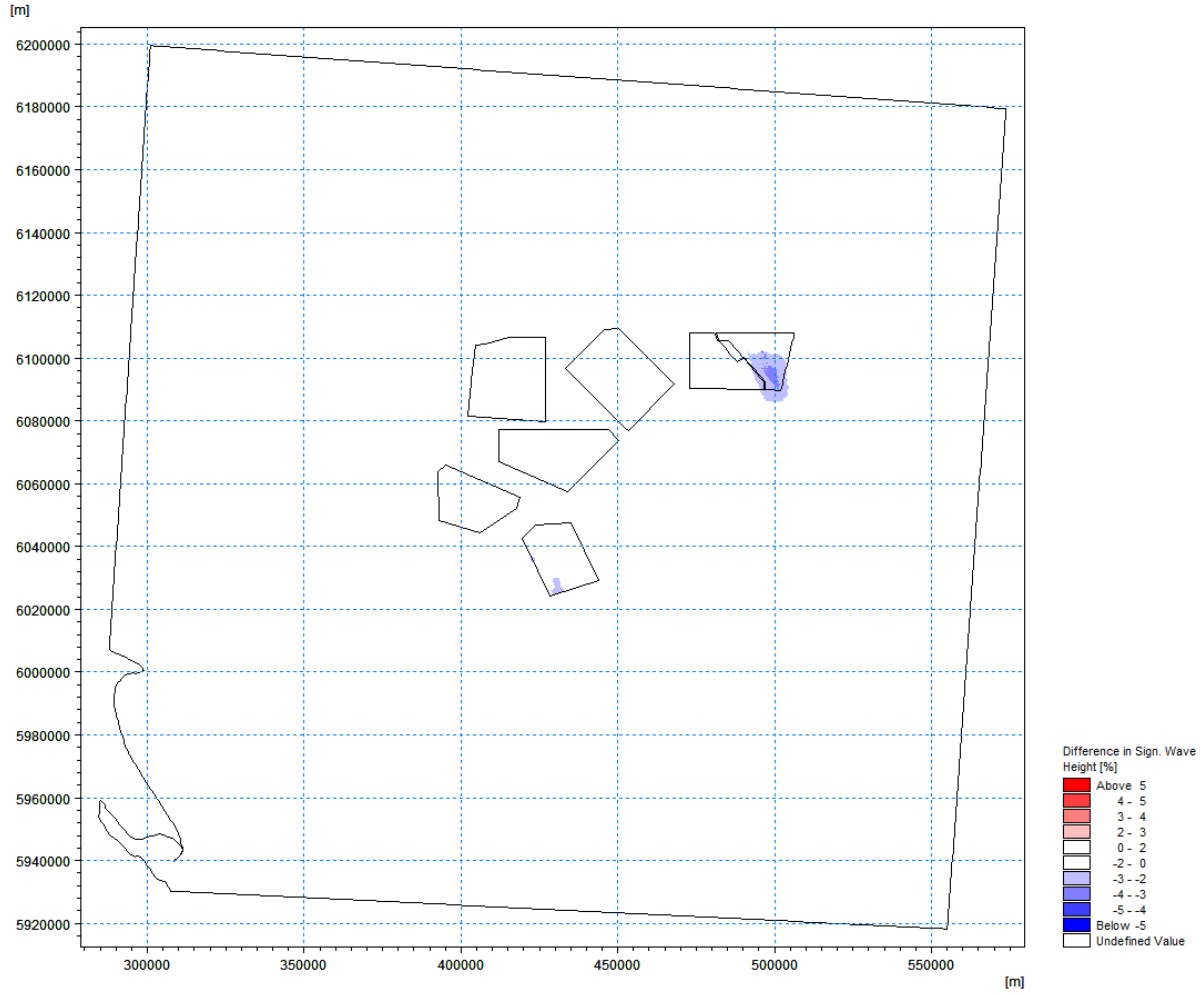

Figure 8.3-65: Difference in Significant Wave Height (Hs) in Percent between 'Baseline' and Wind Farm 'Scenario 2' for Waves Coming from Northerly Direction with Occurring Probability of 50 Percentile

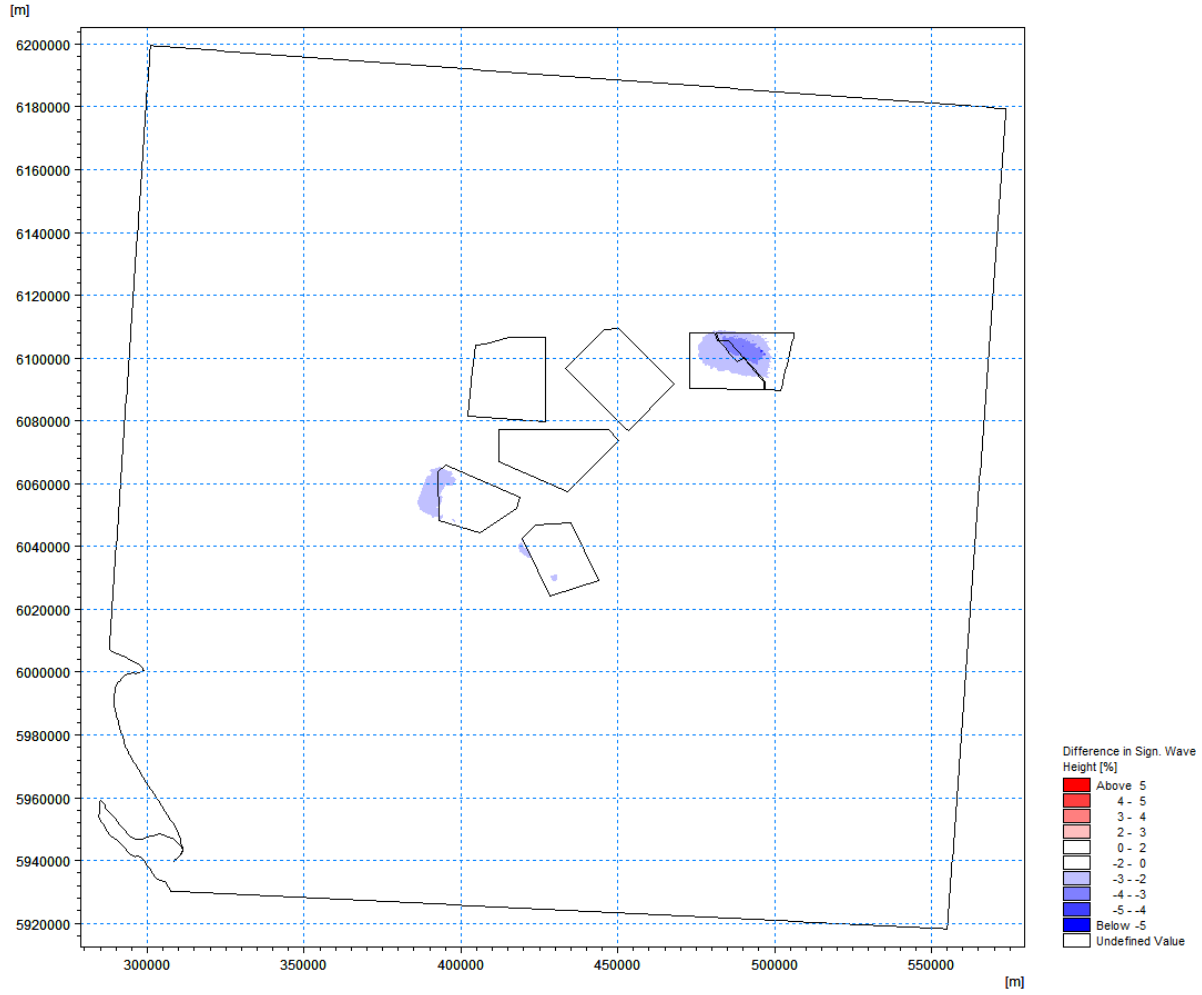

Figure 8.3-66: Difference in Significant Wave Height (Hs) in Percent between 'Baseline' and Wind Farm 'Scenario 2' for Waves Coming from Easterly Direction with Occurring Probability of 50 Percentile

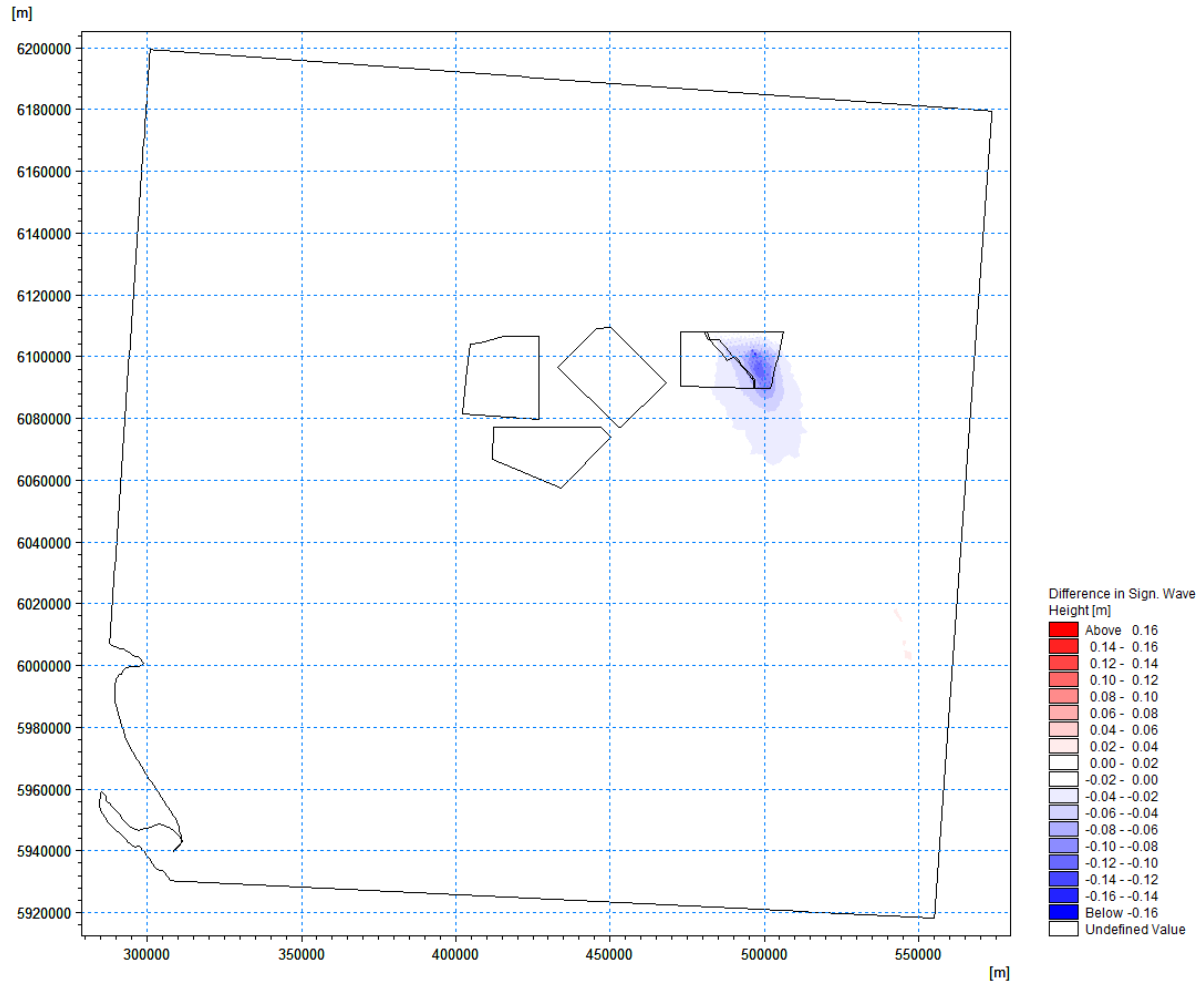

Figure 8.3-67: Difference in Significant Wave Height (Hs) in Metres between 'Baseline' and Wind Farm 'Scenario 1' for 1 in 1 Year Waves Coming from Northerly Direction

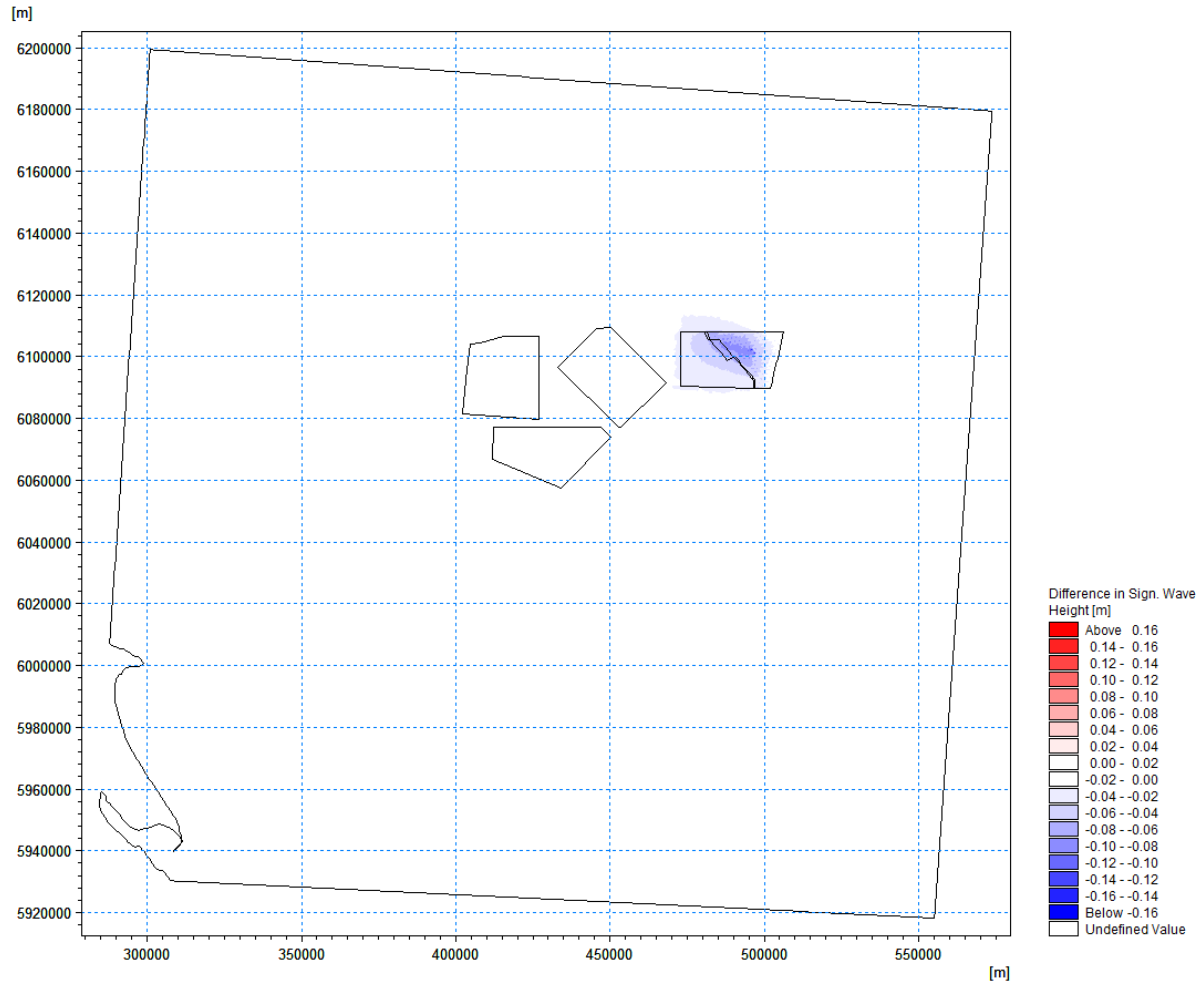

Figure 8.3-68: Difference in Significant Wave Height (Hs) in Metres between 'Baseline' and Wind Farm 'Scenario 1' for 1 in 1 Year Waves Coming from Easterly Direction

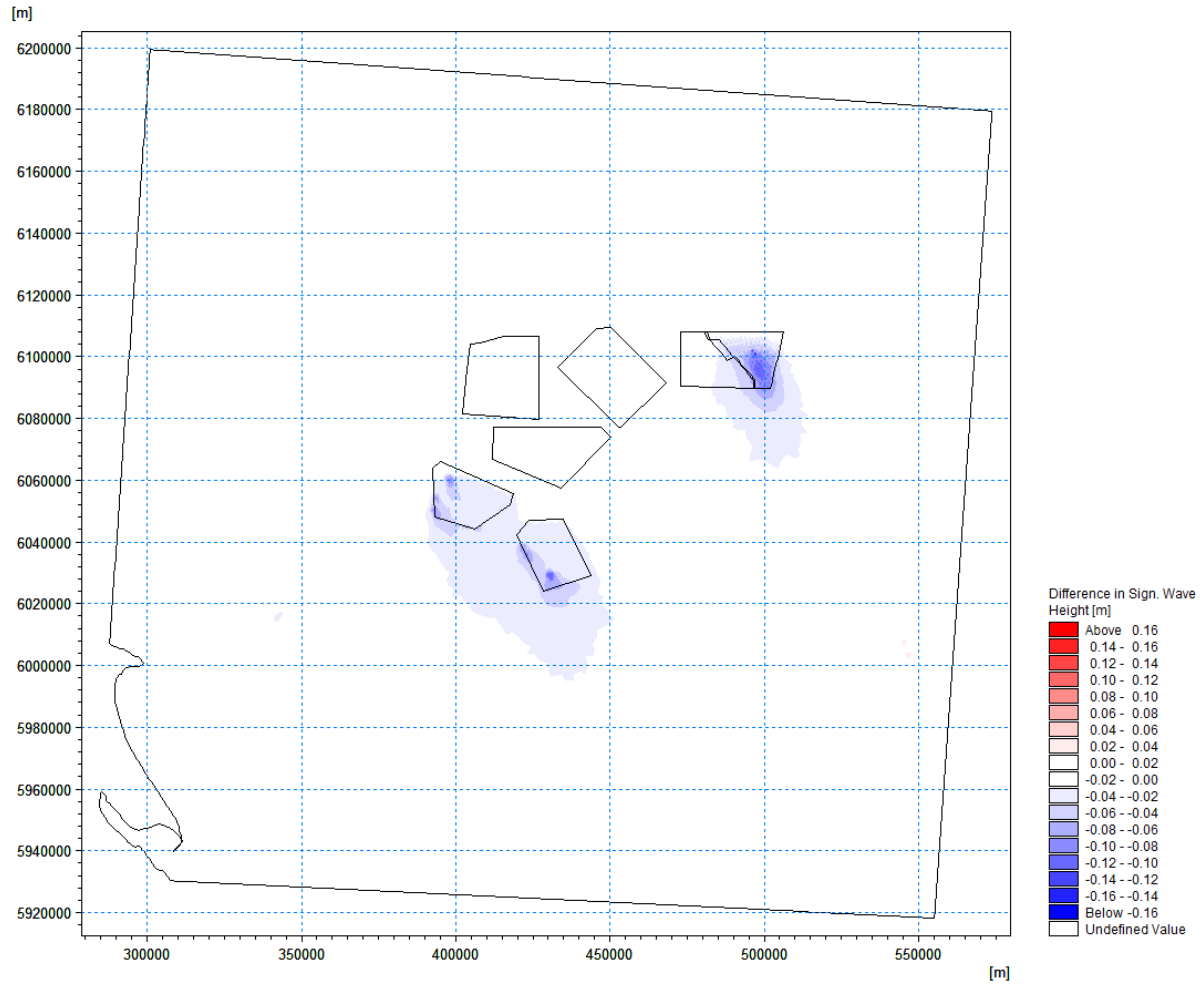

Figure 8.3-69: Difference in Significant Wave Height (Hs) in Metres between 'Baseline' and Wind Farm 'Scenario 2' for 1 in 1 Year Waves Coming from Northerly Direction

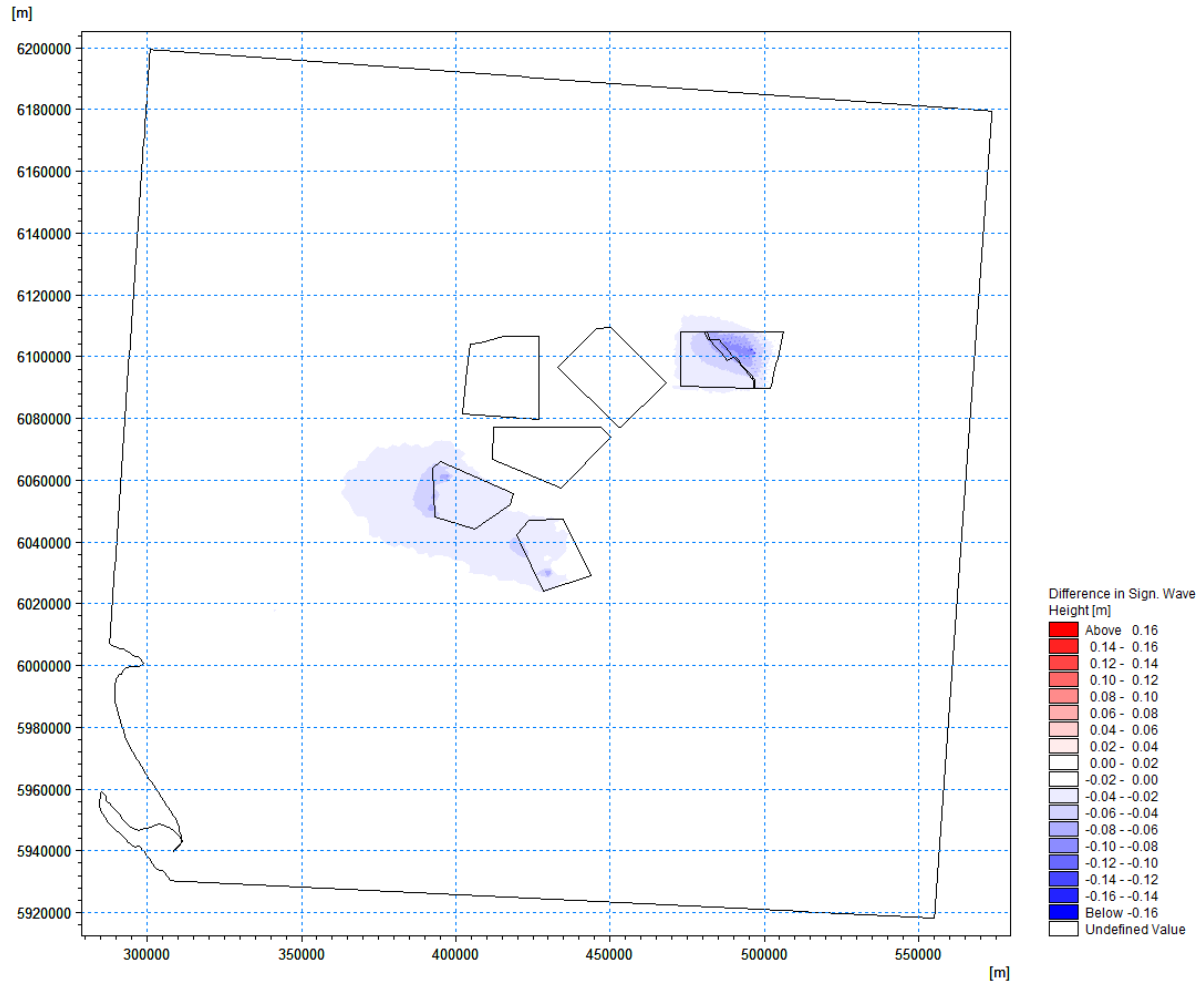

Figure 8.3-70: Difference in Significant Wave Height (Hs) in Metres between 'Baseline' and Wind Farm 'Scenario 2' for 1 in 1 Year Waves Coming from Easterly Direction

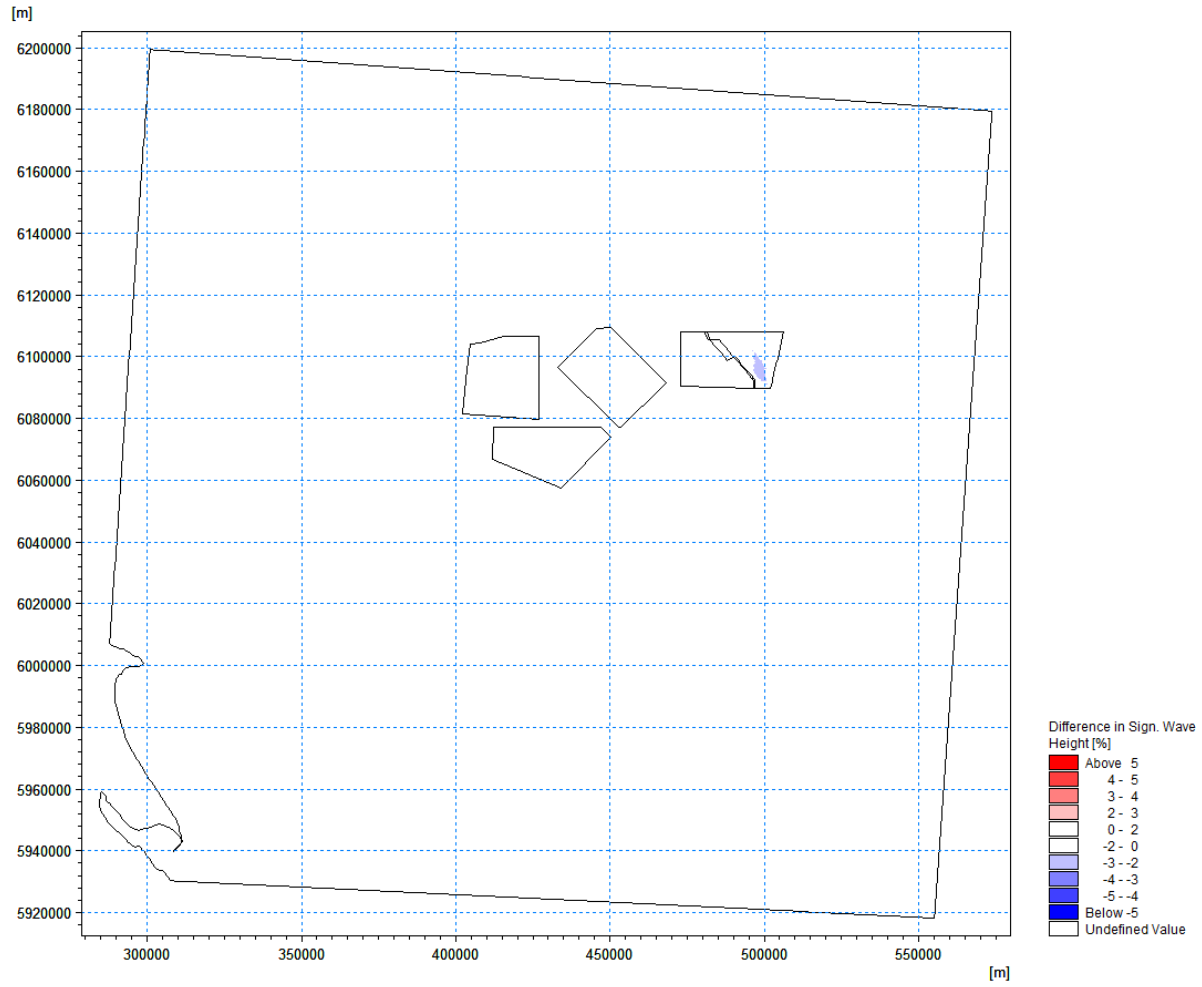

Figure 8.3-71: Difference in Significant Wave Height (Hs) in Percent between 'Baseline' and Wind Farm 'Scenario 1' for 1 in 1 Year Waves Coming from Northerly Direction

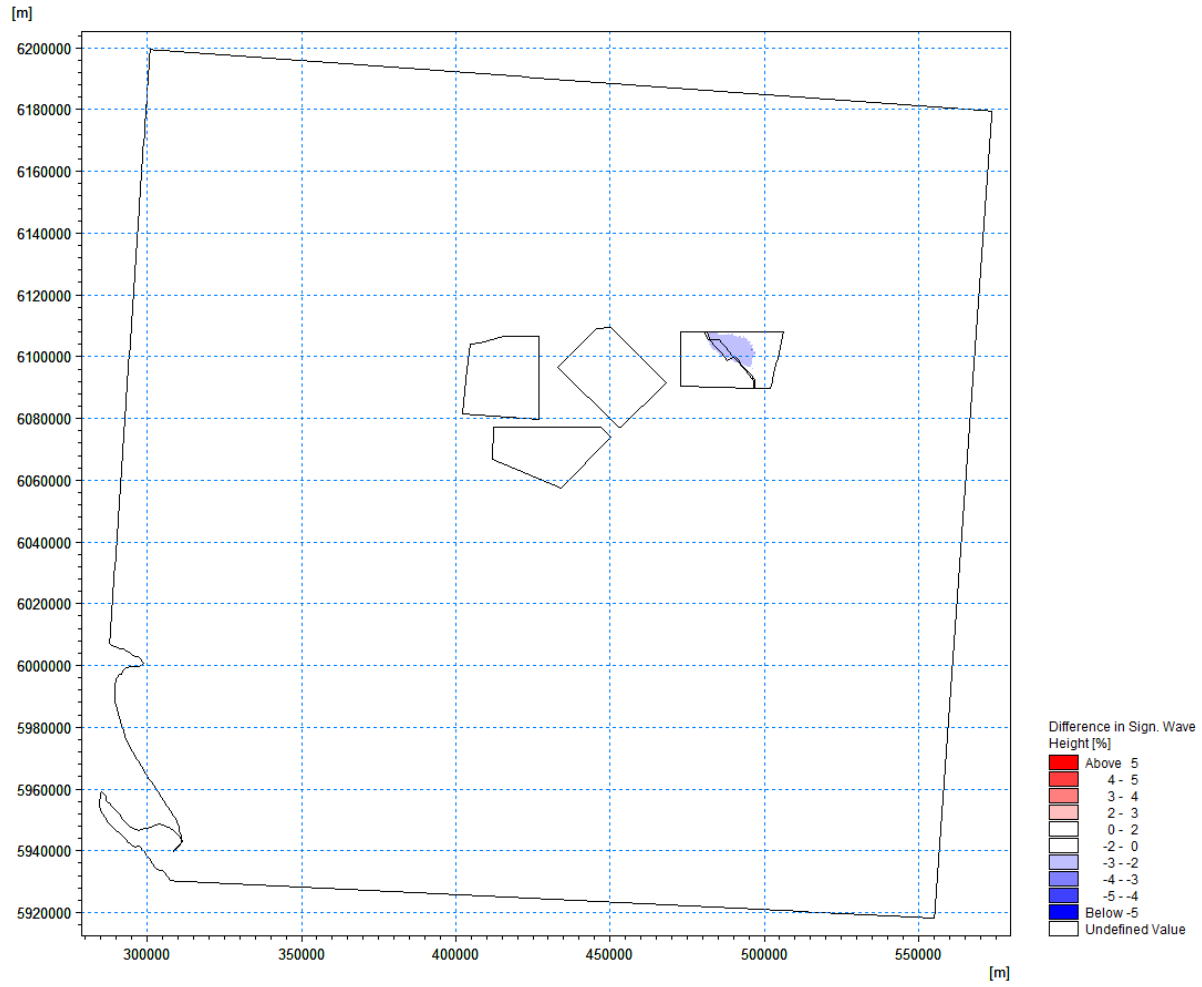

Figure 8.3-72: Difference in Significant Wave Height (Hs) in Percent between 'Baseline' and Wind Farm 'Scenario 1' for 1 in 1 Year Waves Coming from Easterly Direction

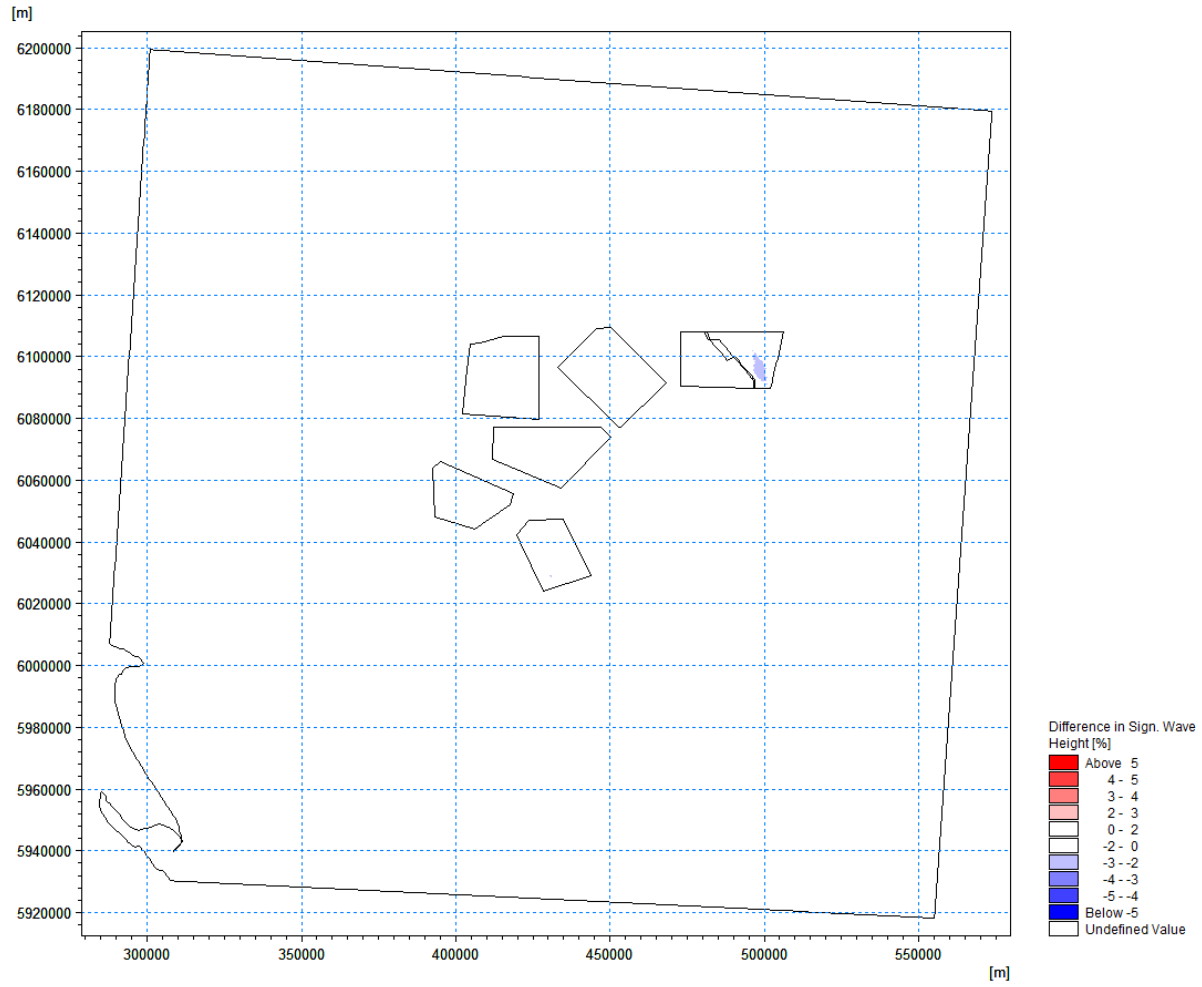

Figure 8.3-73: Difference in Significant Wave Height (Hs) in Percent between 'Baseline' and Wind Farm 'Scenario 2' for 1 in 1 Year Waves Coming from Northerly Direction

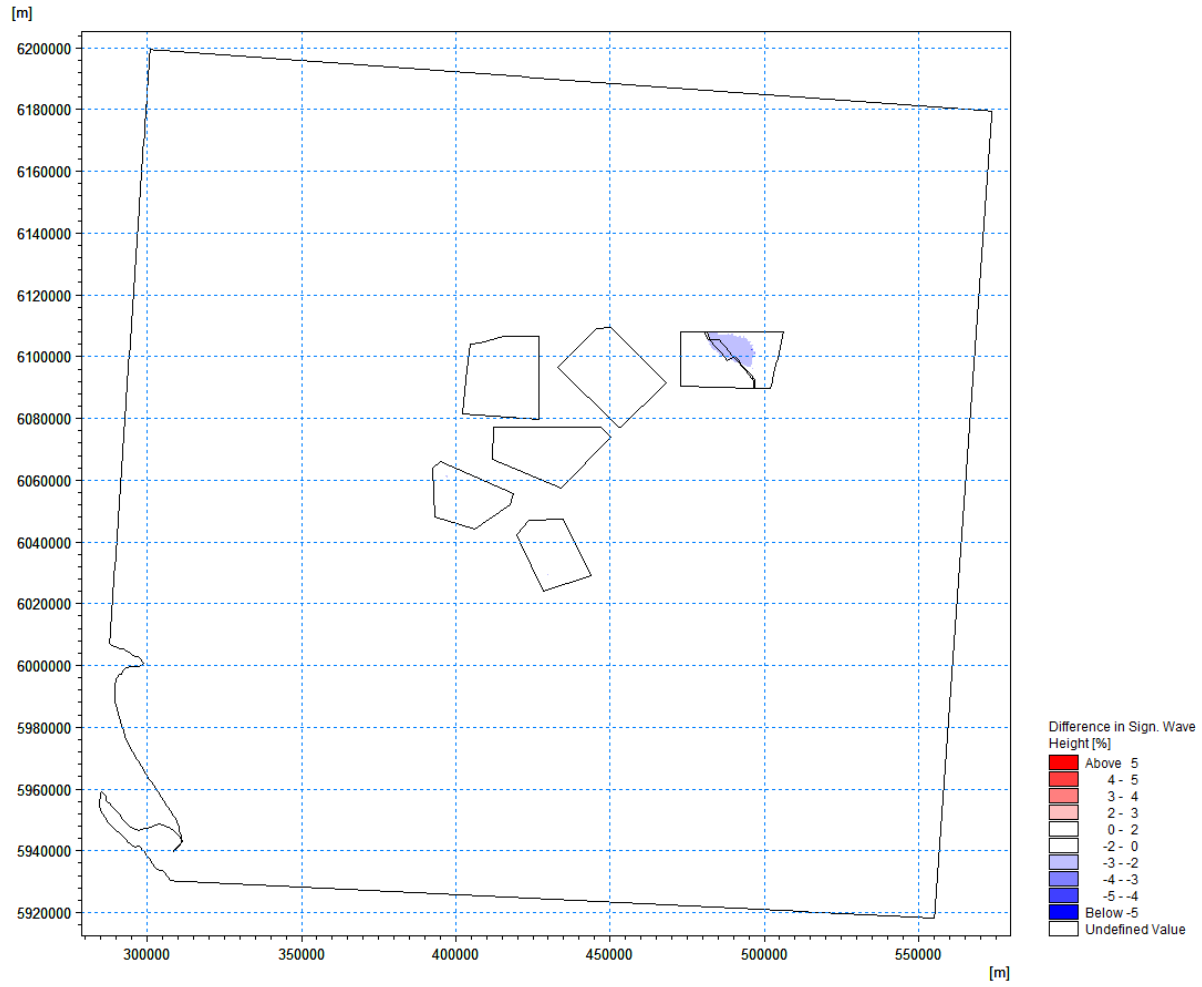

Figure 8.3-74: Difference in Significant Wave Height (Hs) in Percent between 'Baseline' and Wind Farm 'Scenario 2' for 1 in 1 Year Waves Coming from Easterly Direction

8.3.4.8 Discussions of Wave Model Results

88. The wave model exercise can be summarised as follows:

- Waves from a northerly direction have the biggest impact in terms of extent of wave reduction.
- There is no increase in significant wave height (Hs).
- The wave reduction for waves from a northerly direction extends in a southerly direction.
- The wave reduction for waves from an easterly direction extends in a westerly direction.
- When comparing the three Offshore Platform options for each DBD wind farm array layout, it can be noted that the differences in significant wave height (Hs) are relatively small, with the Offshore Platform Option 2 (two small central Offshore Platform) producing marginally larger impact.
- For both wave directions the DBD array area Layout D has the smallest impact, and Layout A has the largest impact, being only marginally larger than Layout C. The maximum reduction in wave height for all DBD layouts is -0.1 m which is localised around the Offshore Platform structures.
- Reduction of wave heights by -4cm to -6cm occurring only inside the Project array boundary.
- The DBD wind farm array Layout C (with two small Offshore Platform in centre) has been chosen as a realistic worst-case for the Project. Noting that engagement at future ETGs and PEIR consultation along with ongoing array design may result in change to this between the PEIR and ES stage. Hereafter this will be called ‘DBD Option’.
- For the chosen worst-case ‘DBD Option’ the area of wave height reduction of the smallest (0.01m) magnitude extends for waves coming from a northerly direction for approximately 25km southwards, and for waves coming from an easterly direction by approximately 17km.
- The affected area is largest under the 50th percentile wave condition (with the shortest wave length) in terms of percentage of ‘Baseline’ wave height. The affected area is largest under 1 in 1 year wave condition in terms of change in wave height.
- The cumulative ‘Scenario 1’ run shows that the DBD Option’ has the largest detectable impact of all scenarios, whilst only recording a maximum reduction of 4% (**Figure 8.3-63** and **Figure 8.3-64**) in wave height.

- The cumulative 'Scenario 2' run shows that both DBD and DBS offshore wind farms have a small detectable impact, with a maximum reduction of 2% in wave height (**Figure 8.3-65** and **Figure 8.3-66**). It is to be expected that the wind farm layouts with potentially larger turbine and platform diameters (DBD & DBS) will result in a greater impact, although still relatively small.
- The wind farm layouts with smaller turbine and platform diameter (DBA, DBB, DBC, Sofia) have no notable impact on the wave climate.
- The model results of both Scenarios 1 and 2 show no cumulative effect between DBD, existing wind farms and also the planned DBS wind farm. For waves from a northerly direction (actual direction of 345^{0}N, see explanation in paragraph 44), the model results showed no cumulative effect extending eastwards into Dutch waters.

8.3.5 Hydrodynamic Modelling

8.3.5.1 Model Description

89. Royal HaskoningDHV's established regional hydrodynamic model was used to provide boundary conditions for a local hydrodynamic model which was set up for investigating potential impact on hydrodynamics by the proposed wind farm. The local hydrodynamic model was also used to drive a suspended sediment dispersion model which is presented in **Section 8.3.6**.

8.3.5.1.1 Regional Model

90. The regional model was built in MIKE21-HD modelling software developed by DHI. The computational mesh consists of 292,000 elements and 143,000 nodes. As the regional model was developed for simulation of the large scale circulation patterns, the mesh resolution is relatively coarse, ranging from 1km to 5km. In general, the grid resolution increases towards the coastline in order to capture the nearshore shallow water (**Figure 8.3-75**).

91. The model bathymetry and grid were constructed based on C-Map dataset and Admiralty Maritime Data Solutions' data with coastline positions digitised from Google Earth. The model bathymetry, shown on **Figure 8.3-76** has then been generated by the combined bathymetric data.

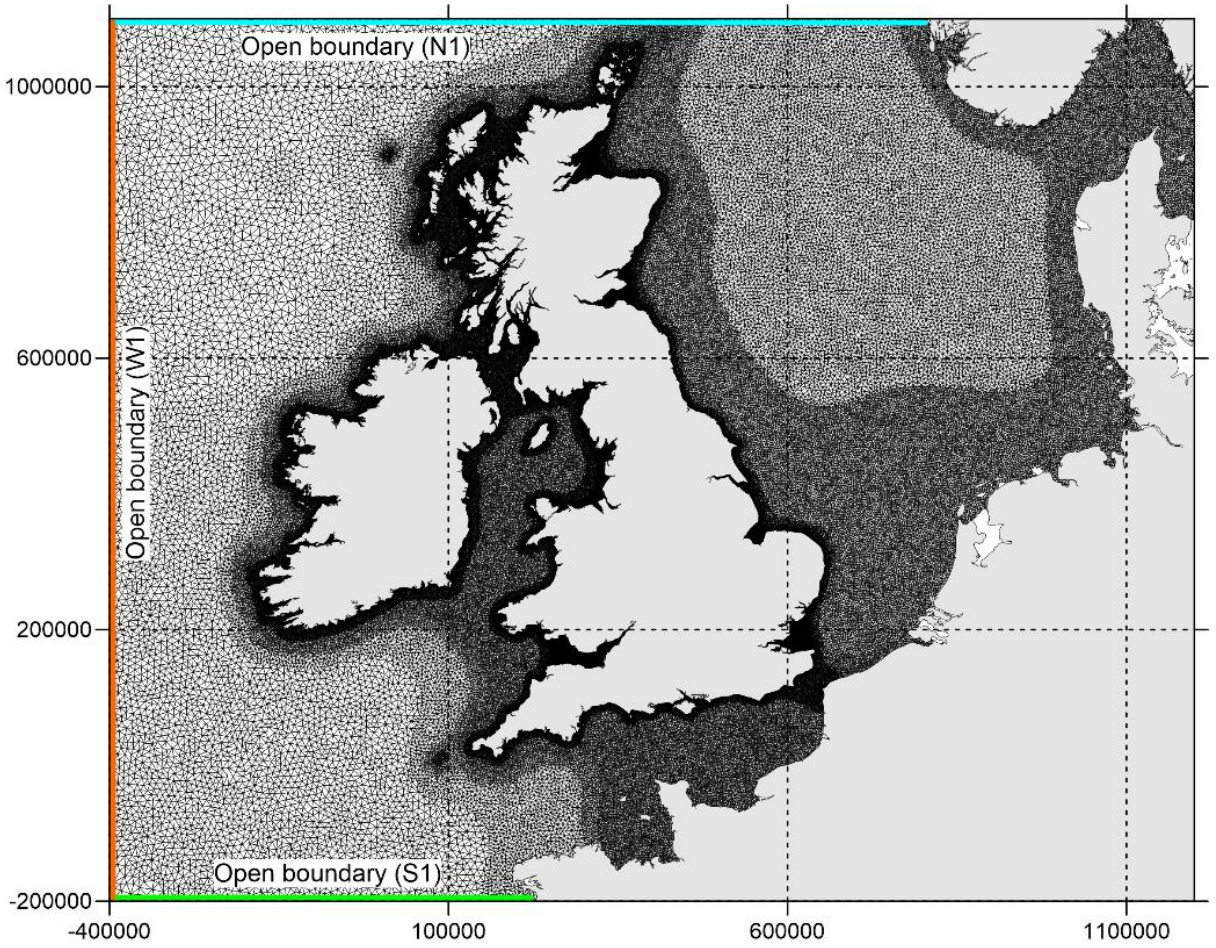

Figure 8.3-75: Computational Mesh of the Regional HD Model

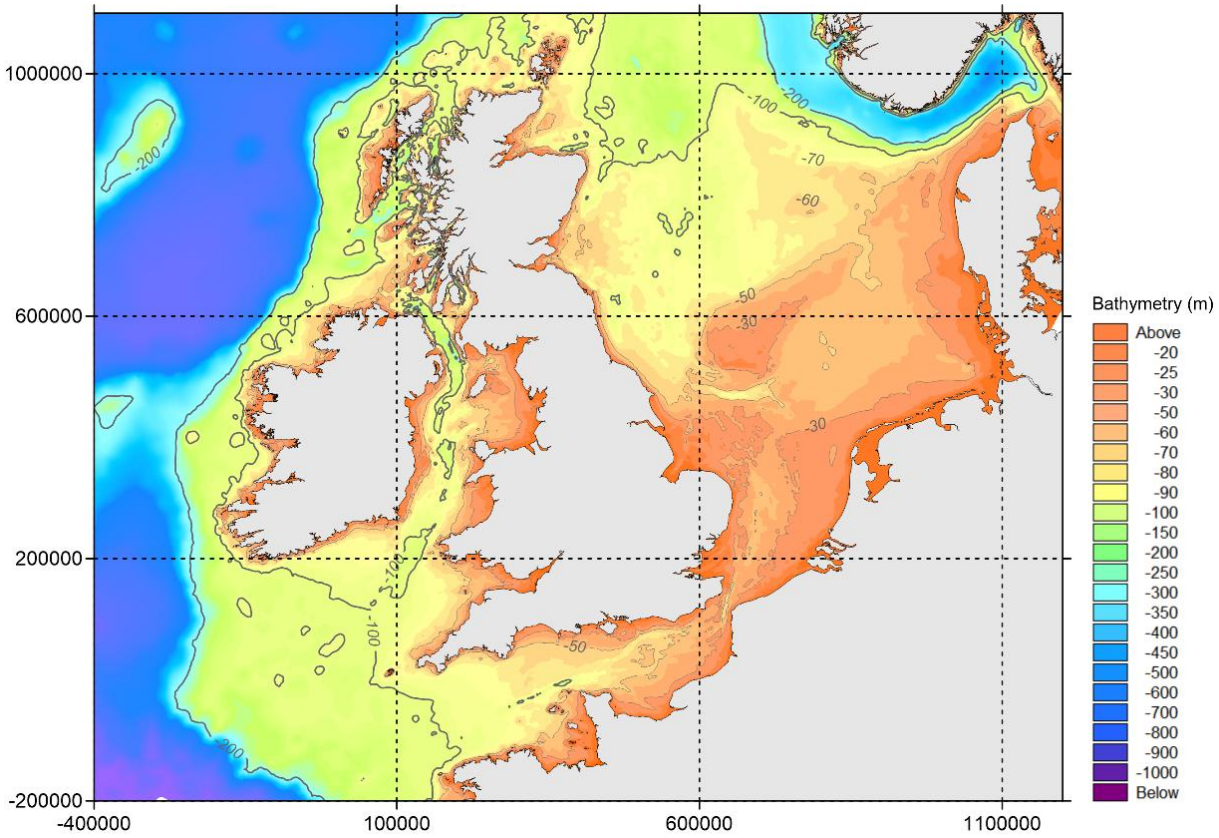

Figure 8.3-76: Regional HD Model Bathymetry

8.3.5.1.2 Local Model

92. Like the regional model, the flexible mesh was adopted in the local model. A coarser grid (1,000-2,000m) was used in remote areas and a finer grid (200-300m) in the areas of interest. For later model application runs for assessing the potential impact, mesh will be further refined around the Project site.

93. The computational mesh for the model calibration consists of 52,516 elements and 26,799 nodes (see **Figure 8.3-77**). The local model bathymetry is shown on **Figure 8.3-78**.

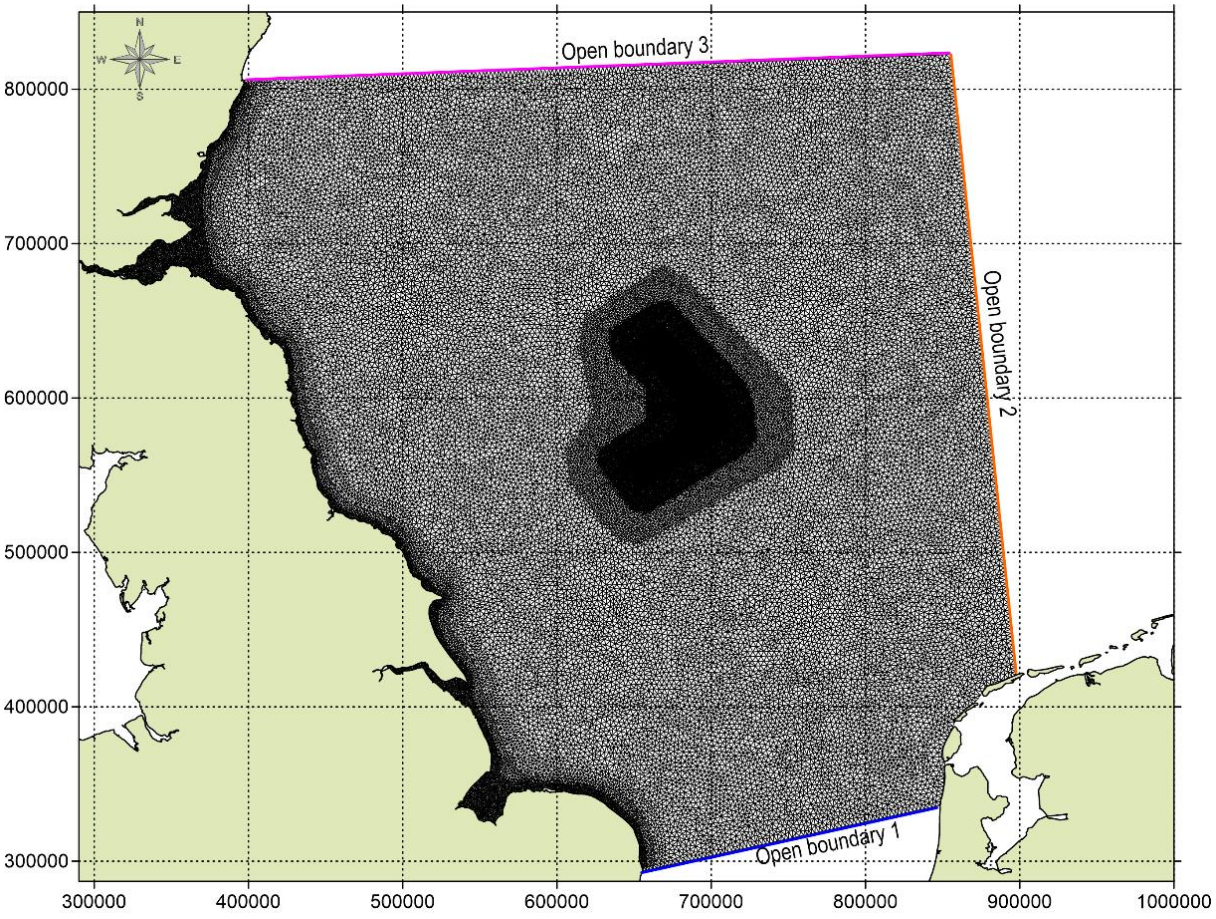

Figure 8.3-77: Local Model Computational Mesh

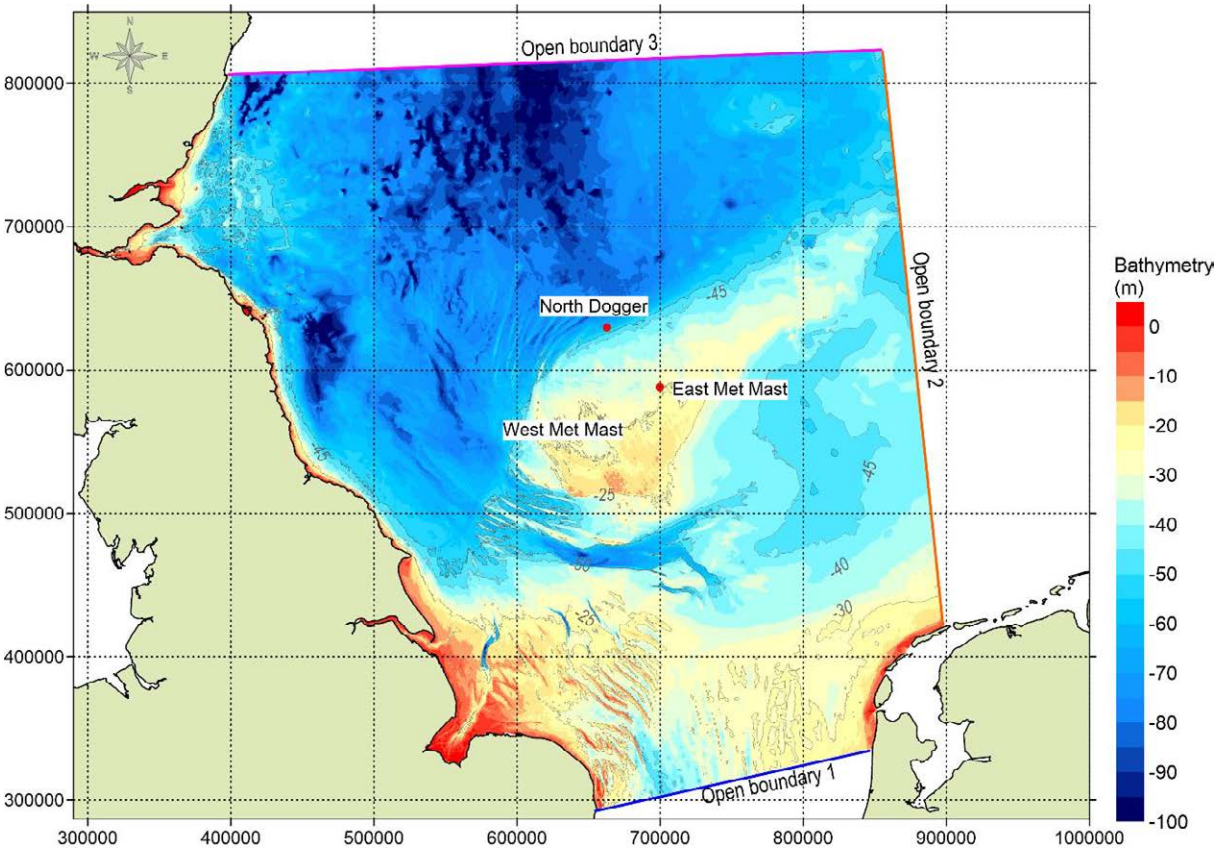

Figure 8.3-78: Bathymetry of Local Model Domain (with Tidal Gauges and Current Stations Marked)

8.3.5.2 Model Boundary Conditions

94. At the open boundaries of the regional model, water levels were used, which vary in time and along the boundaries. The input data for these boundaries were extracted (at locations N1, S1 and W1 as on **Figure 8.3-75**) from the Global Tidal Model of DHI with a spatial resolution of 0.25° × 0.25°. The data represents the major diurnal (K1, O1, P1 and Q1) and semidiurnal tidal constituents (M2, S2, N2 and K2) based on OPEX / POSEIDON altimetry data.

95. **Figure 8.3-77** shows the boundaries of the local model. The open boundaries 1 and 3 are set as velocity boundaries varying in time, and open boundaries 2 is set to water level boundary varying in time along the boundary. The velocity and water level along these boundaries were extracted from the regional model.

8.3.5.3 Model Calibration

8.3.5.3.1 Regional Model Calibration (water levels)

96. For this study, the regional model has been re-calibrated using measured water levels recorded at North Shields, Whitby, Cromer, West Met Mast and East Met Mast for two periods (June 2012 and December 2012) and at North Dogger for June 2012 (measured data at North Dogger does not cover December 2012). Re-calibration performance is assessed by both visual comparison and quantifying errors using statistical parameters including Correlation Coefficient and Mean Absolute Error. **Figure 8.3-78** to **Figure 8.3-89** show the modelled and measured water levels, and **Table 8.3-10** presents quantified errors. The model errors in predicted water level are low, no more than 0.15m in Mean Absolute Error. Both visual comparison and error statistics show reasonably good agreement between the measured and modelled water levels.

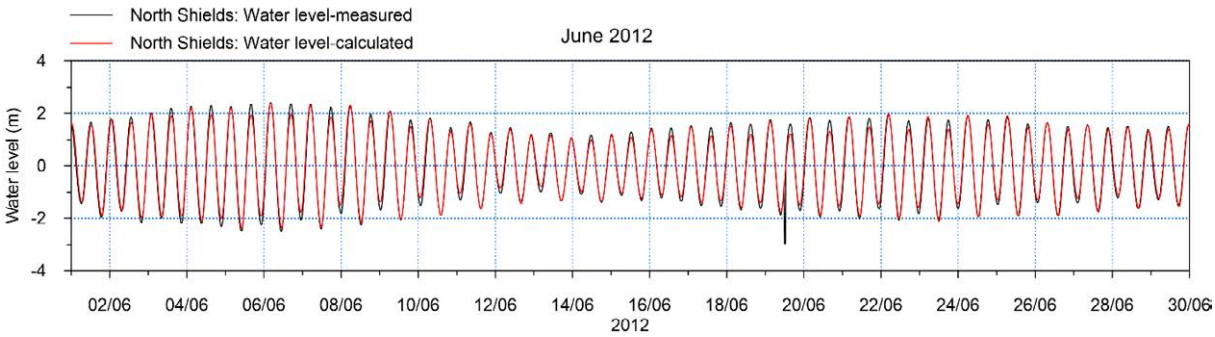

Figure 8.3-79: Time Series Comparison between Simulated and Observed Water Levels at North Shields in June 2012 (Regional Model)

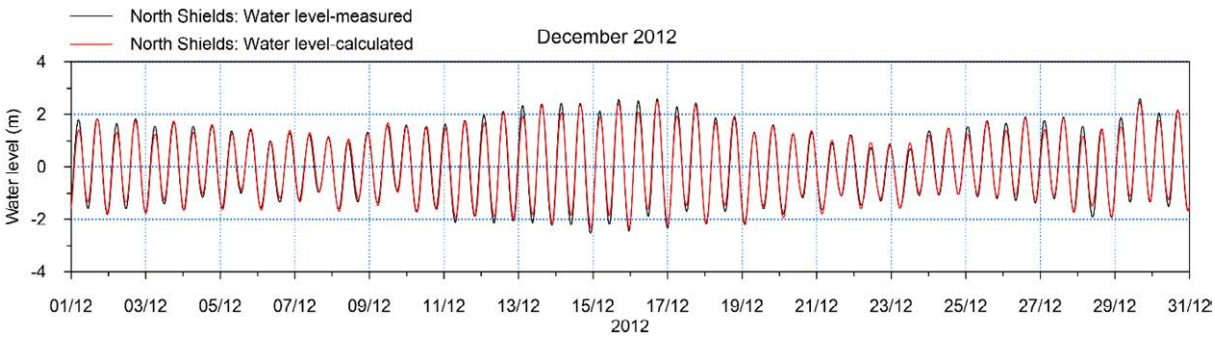

Figure 8.3-80: Time Series Comparison between Simulated and Observed Water Levels at North Shields in December 2012 (Regional Model)

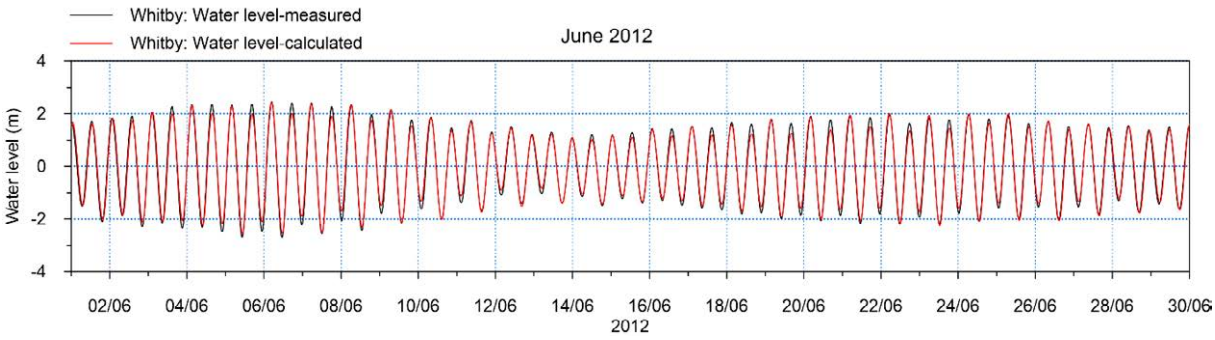

Figure 8.3-81: Time Series Comparison between Simulated and Observed Water Levels at Whitby in June 2012 (Regional Model)

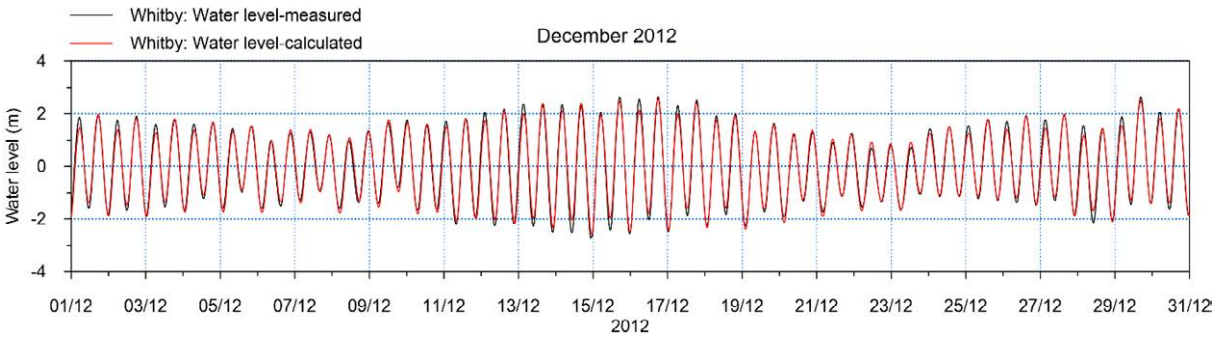

Figure 8.3-82: Time Series Comparison between Simulated and Observed Water Levels at Whitby in December 2012 (Regional Model)

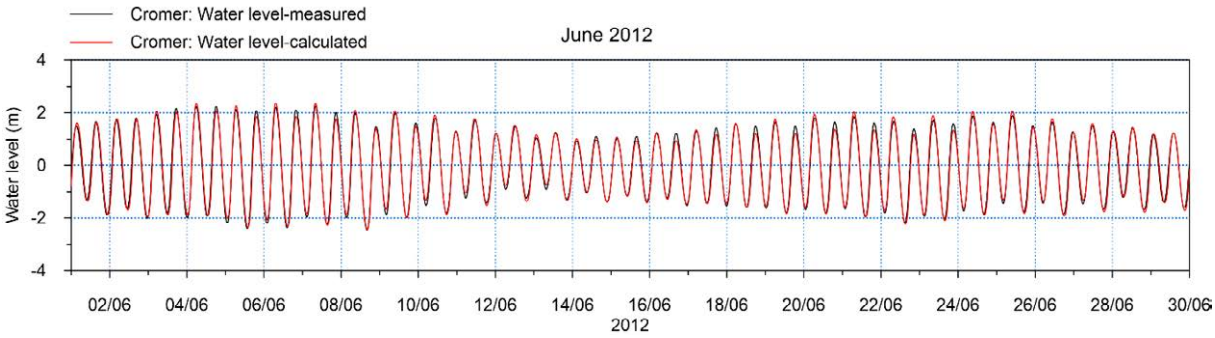

Figure 8.3-83: Time Series Comparison between Simulated and Observed Water Levels at Cromer in June 2012 (Regional Model)

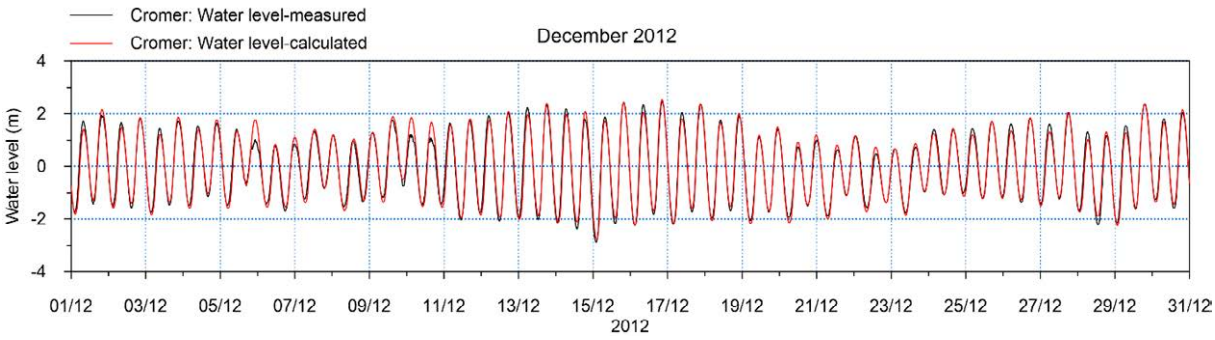

Figure 8.3-84: Time Series Comparison between Simulated and Observed Water Levels at Cromer in December 2012 (Regional Model)

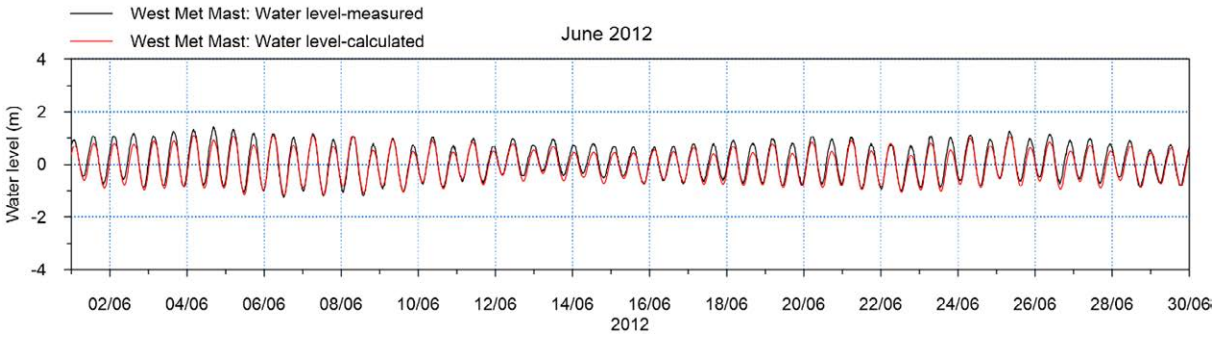

Figure 8.3-85: Time Series Comparison between Simulated and Observed Water Levels at West Met Mast in June 2012 (Regional Model)

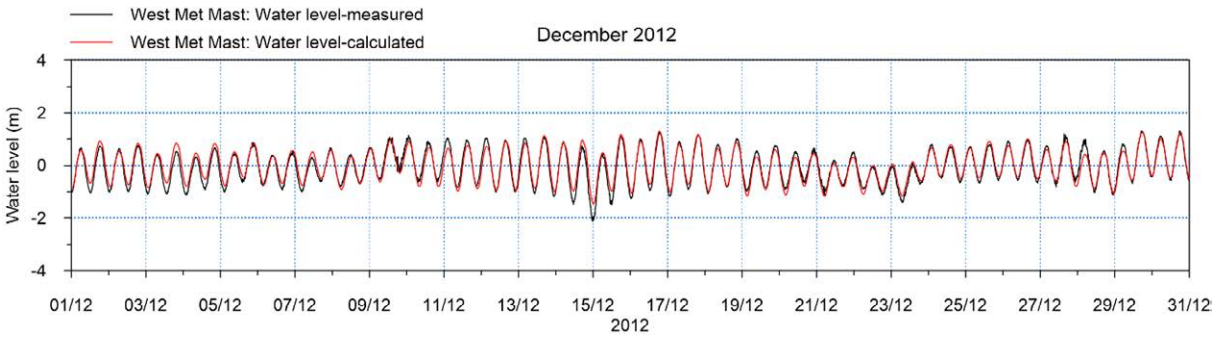

Figure 8.3-86: Time Series Comparison between Simulated and Observed Water Levels at West Met Mast in December 2012 (Regional Model)

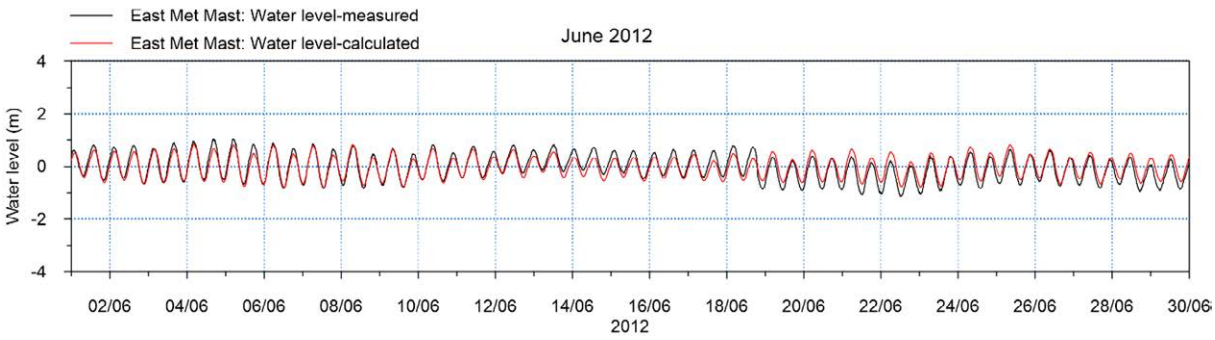

Figure 8.3-87: Time Series Comparison between Simulated and Observed Water Levels at East Met Mast in June 2012 (Regional Model)

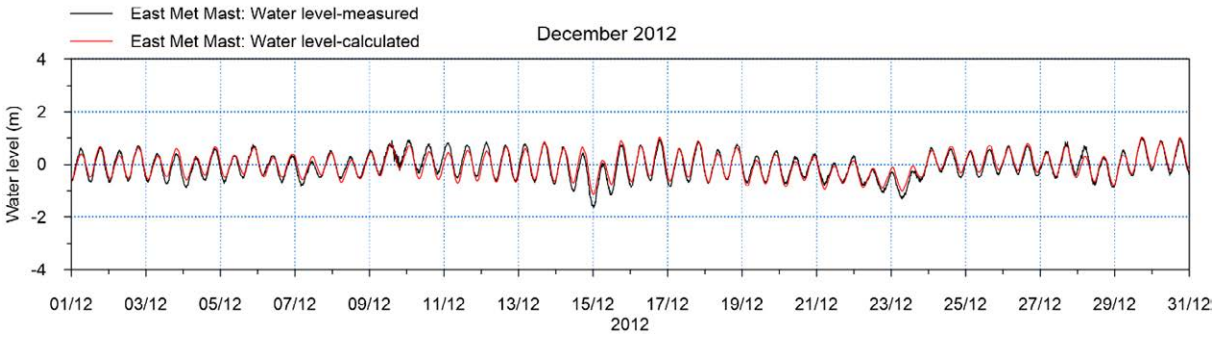

Figure 8.3-88: Time Series Comparison between Simulated and Observed Water Levels at East Met Mast in December 2012 (Regional Model)

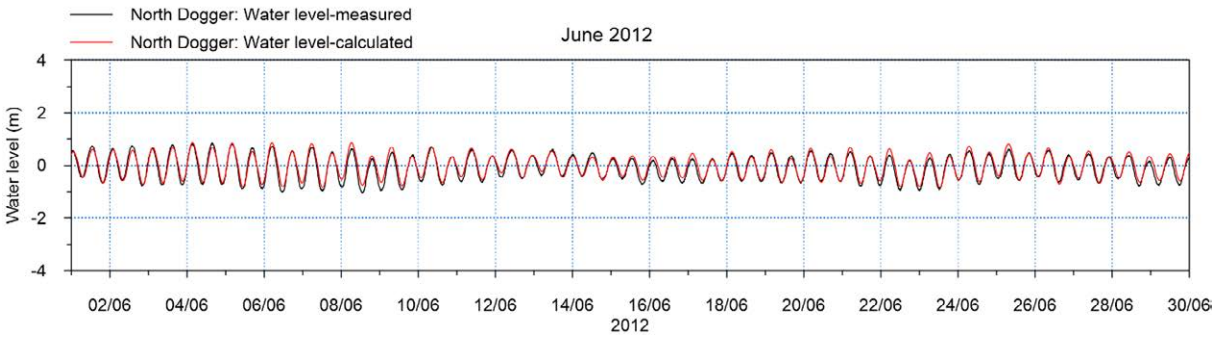

Figure 8.3-89: Time Series Comparison between Simulated and Observed Water Levels at North Dogger in June 2012 (Regional Model)

Table 8.3-10: Model Errors in Water Level (Regional Model)

Name of station	ME (m)	MAE (m)	Std (m)	R
North Shields	-0.02	0.13	0.18	0.98
Whitby	-0.02	0.13	0.17	0.98
Cromer	0.01	0.13	0.16	0.98
West Met Mast	0.13	0.15	0.13	0.95
East Met Mast	-0.02	0.13	0.15	0.89
North Dogger	-0.10	0.11	0.11	0.93

Note: ME: Mean Error; MAE: Mean Absolute Error; Std: Std. dev of Residuals; R: Coefficient of Determination

8.3.5.3.2 Local Model Calibration (water levels)

97. The local model has been calibrated using measured water levels recorded at North Dogger, West Met Mast and East Met Mast for June 2012 when measured data was available at all three stations and for December 2012 when measured data was recorded at both West Met Mast and East Met Mast. Model calibration performance is assessed by both visual comparison and quantifying errors using statistical parameters including Correlation Coefficient and Mean Absolute Error. **Figure 8.3-90** to **Figure 8.3-94** show the modelled and measured water levels, and **Table 8.3-11** presents quantified errors. The model errors in predicted water level are low, no more than 0.15m in Mean Absolute Error. Both visual comparison and error statistics show reasonably good agreement between measured and modelled water levels.

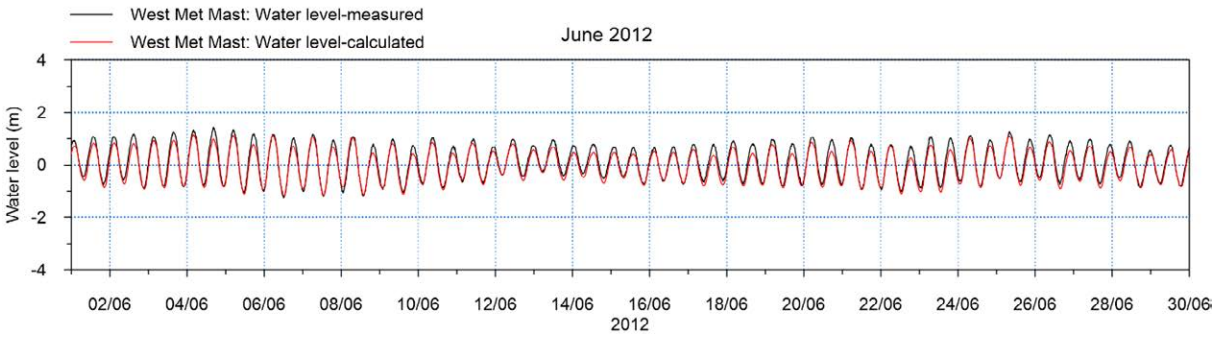

Figure 8.3-90: Time Series Comparison between Simulated and Observed Water Levels at West Met Mast in June 2012 (Local Model)

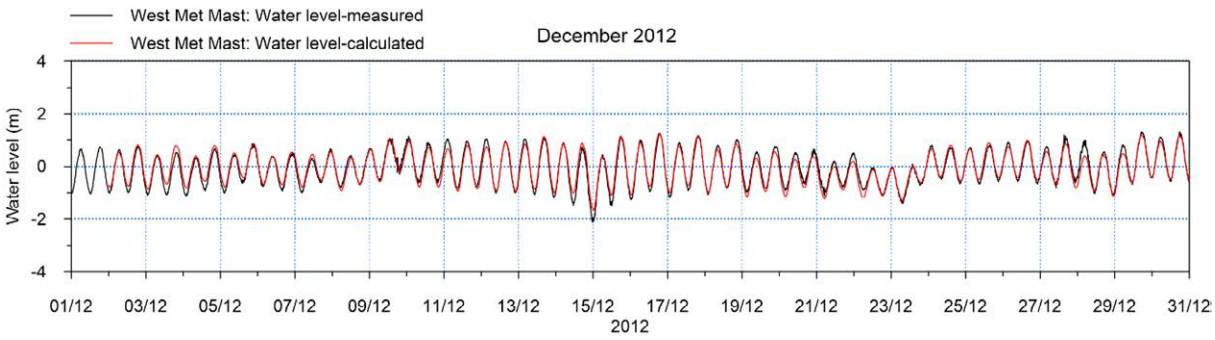

Figure 8.3-91: Time Series Comparison between Simulated and Observed Water Levels at West Met Mast in December 2012 (Local Model)

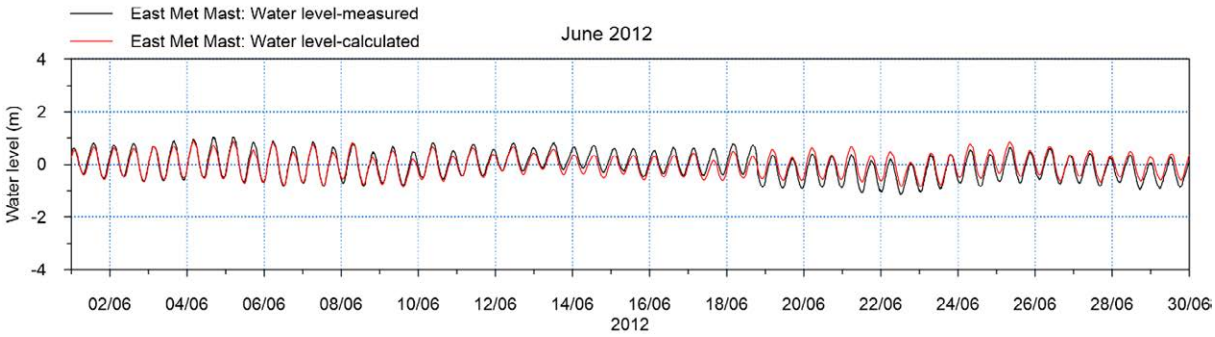

Figure 8.3-92: Time Series Comparison between Simulated and Observed Water Levels at East Met Mast in June 2012 (Local Model)

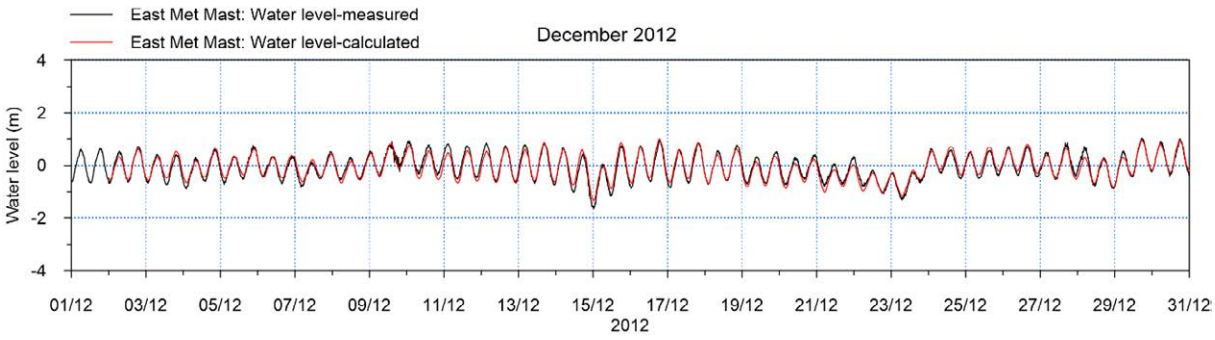

Figure 8.3-93: Time Series Comparison between Simulated and Observed Water Levels at East Met Mast in December 2012 (Local Model)

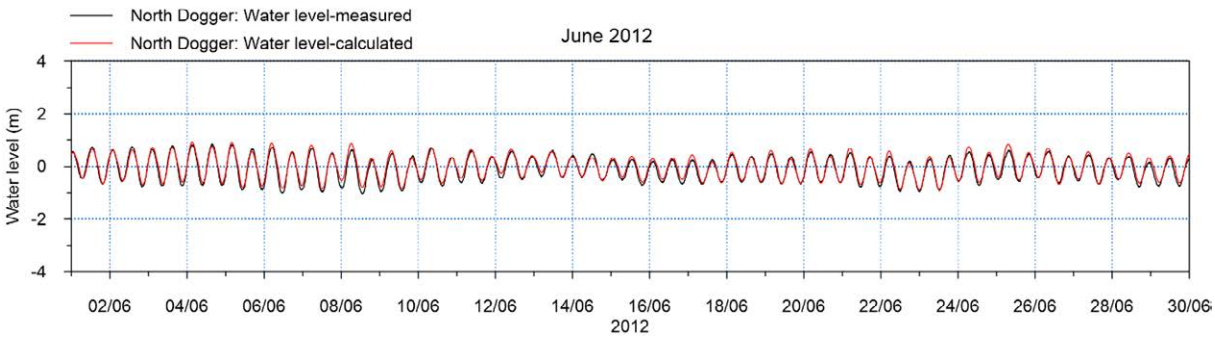

Figure 8.3-94: Time Series Comparison between Simulated and Observed Water Levels at North Dogger in June 2012 (Local Model)

Table 8.3-11: Model Errors in Water Level (Local Model)

Name of station	ME (m)	MAE (m)	Std (m)	R
West Met Mast	0.13	0.15	0.13	0.95
East Met Mast	-0.02	0.13	0.15	0.89
North Dogger	-0.10	0.11	0.11	0.93

Note: ME: Mean Error; MAE: Mean Absolute Error; Std: Std. dev of Residuals; R: Coefficient of Determination

8.3.5.3.3 Local Model Calibration (currents)

98. The local model has been also calibrated using measured current data recorded at West Met Mast and East Met Mast for two periods (June 2022 and December 2022) and at North Dogger for June 2012. Model calibration performance is assessed by both visual comparison and quantifying errors using statistical parameters including Correlation Coefficient and Mean Absolute Error. **Figure 8.3-95** to **Figure 8.3-104** show the modelled and measured current speed and direction, and **Table 8.3-12** presents quantified errors.

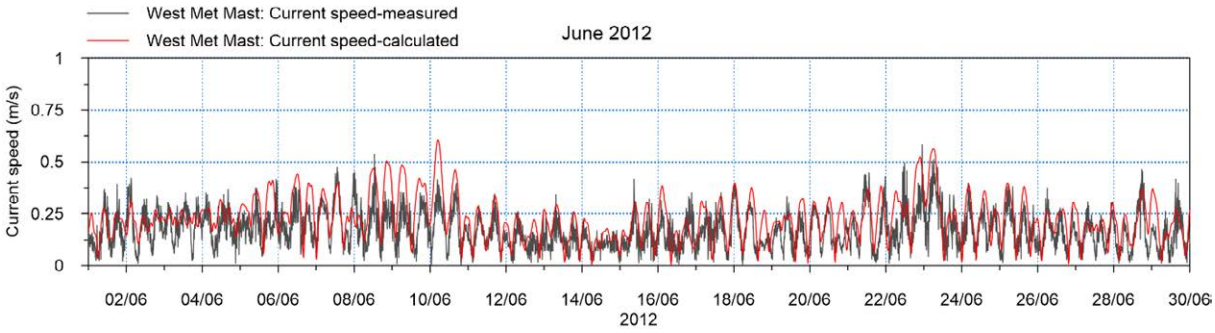

Figure 8.3-95: Time Series Comparison between Simulated and Observed Current Speeds at West Met Mast in June 2012 (Local Model)

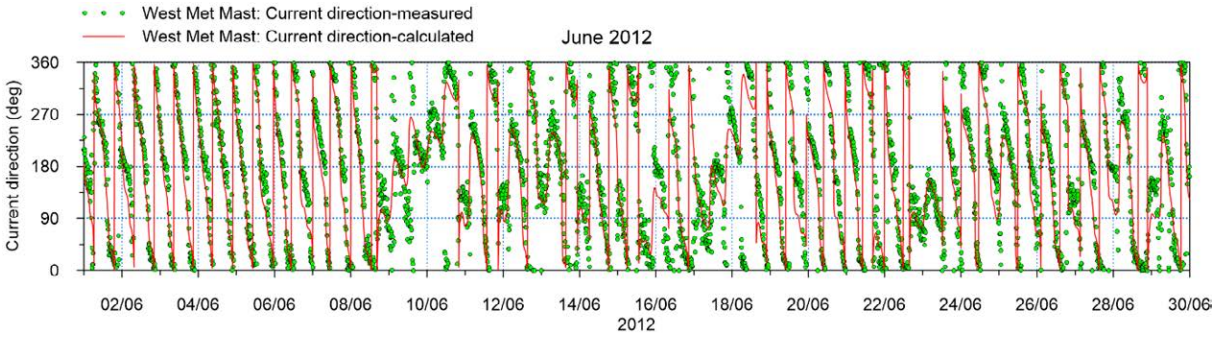

Figure 8.3-96: Time Series Comparison between Simulated and Observed Current Directions at West Met Mast in June 2012 (Local Model)

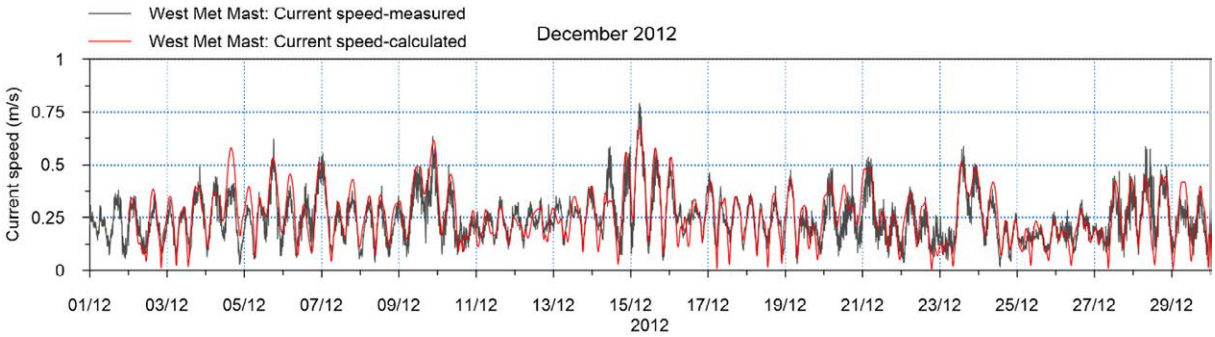

Figure 8.3-97: Time Series Comparison between Simulated and Observed Current Speeds at West Met Mast in December 2012 (Local Model)

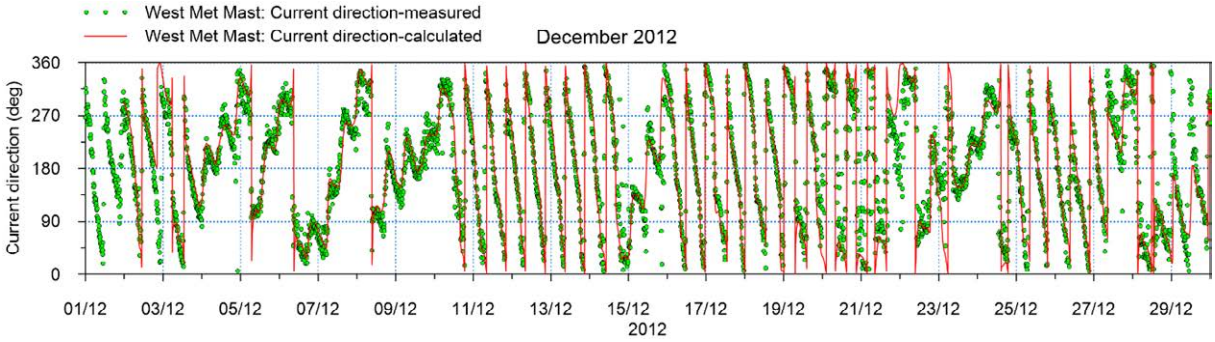

Figure 8.3-98: Time Series Comparison between Simulated and Observed Current Directions at West Met Mast in December 2012 (Local Model)

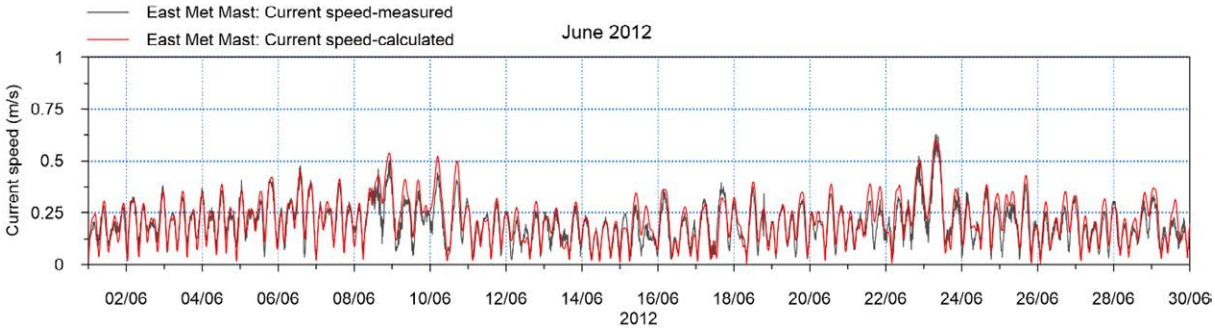

Figure 8.3-99: Time Series Comparison between Simulated and Observed Current Speeds at East Met Mast in June 2012 (Local Model)

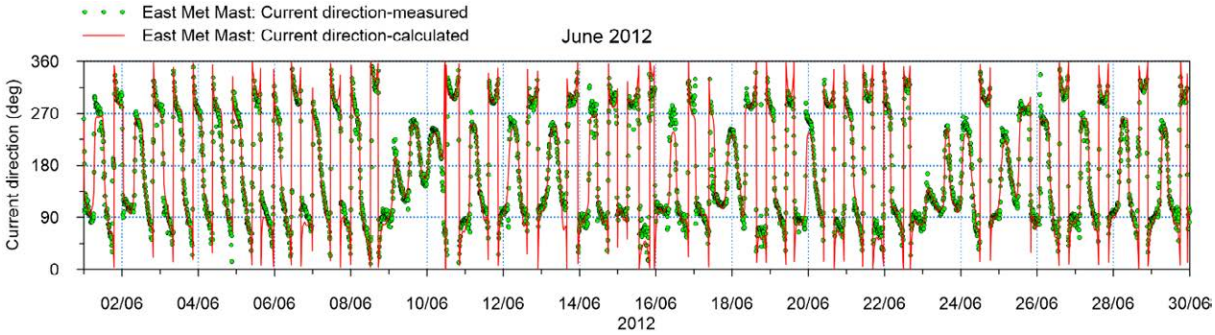

Figure 8.3-100: Time Series Comparison between Simulated and Observed Current Directions at East Met Mast in June 2012 (Local Model)

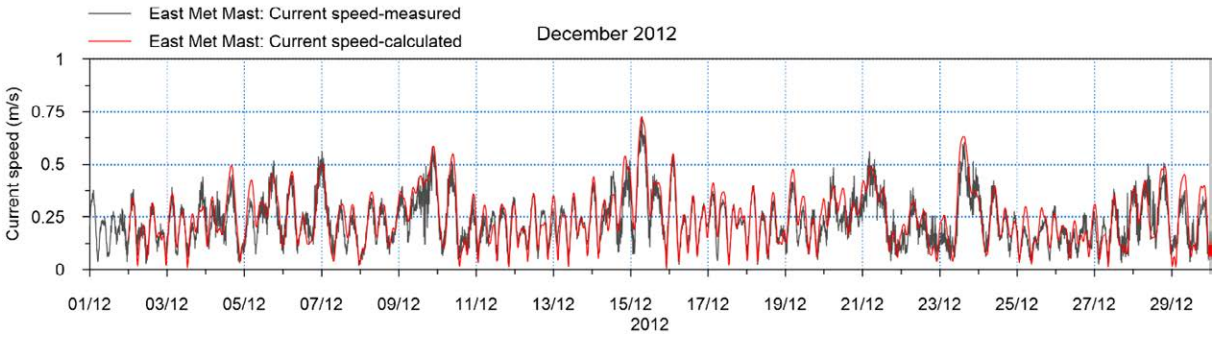

Figure 8.3-101: Time Series Comparison between Simulated and Observed Current Speeds at East Met Mast in December 2012 (Local Model)

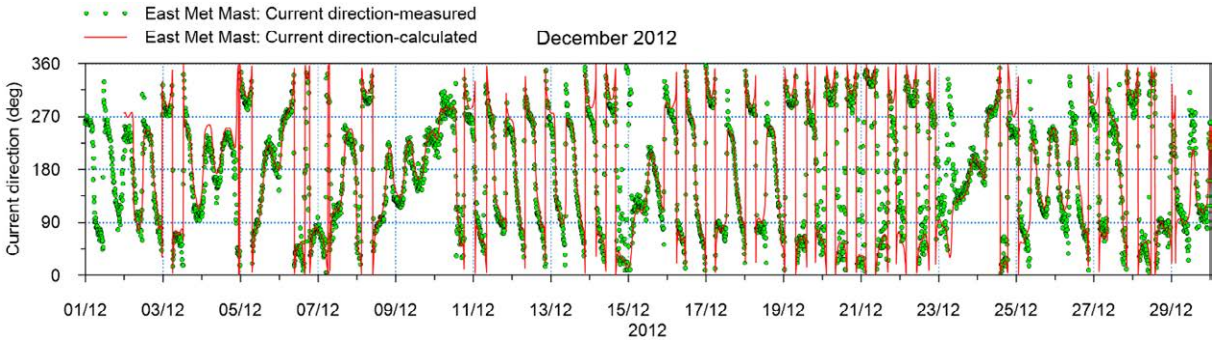

Figure 8.3-102: Time Series Comparison between Simulated and Observed Current Directions at East Met Mast in December 2012 (Local Model)

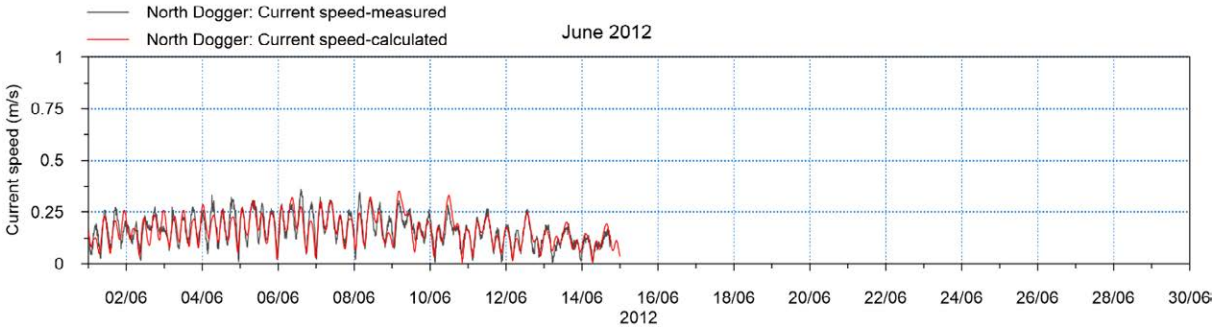

Figure 8.3-103: Time Series Comparison between Simulated and Observed Current Speeds at North Dogger in June 2012 (Local Model)

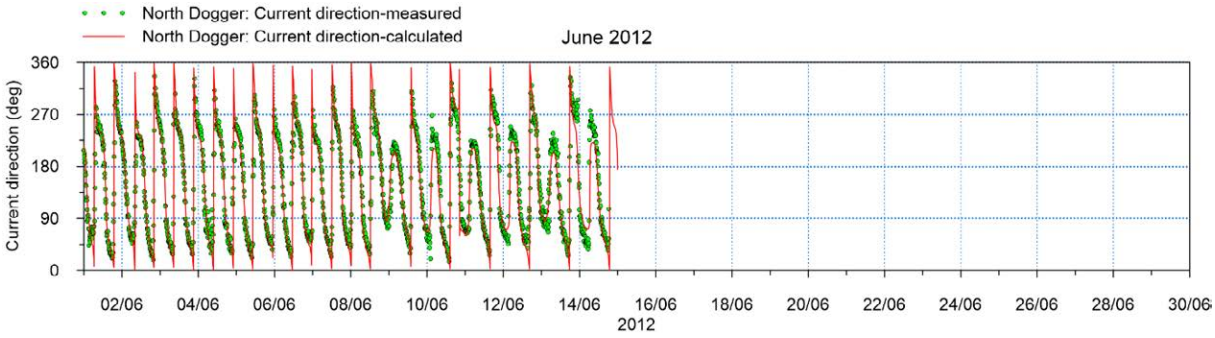

Figure 8.3-104: Time Series Comparison between Simulated and Observed Current Directions at North Dogger in June 2012 (Local Model)

Table 8.3-12: Model Errors in Current Speed (Local Model)

Name of station	ME (m)	MAE (m)	Std (m)	R
West Met Mast	-0.01	0.05	0.06	0.70
East Met Mast	-0.01	0.04	0.05	0.81
North Dogger	0.01	0.02	0.02	0.80

Note: ME: Mean Error; MAE: Mean Absolute Error; Std: Std. dev of Residuals; R: Coefficient of Determination

8.3.5.4 Hydrodynamic Model Production Runs

99. The calibrated hydrodynamic model has been run for a period of 30 days to assess the potential impact by the proposed DBD offshore wind farm (including four turbine layout options and three Offshore Platform options). These are outlined in **Section 8.3.3** and **Section 8.3.1.1**.

100. **Table 8.3-3** shows the details of the four turbine layouts A to D and the three Offshore Platform Options 1 to 3.

101. It should be noted that the number of turbines stated in **Table 8.3-3** excludes five 'spare' locations which have been removed from the location list; the 'spare' turbines were excluded from the north-east corner of each array based on advice given by engineers as being the most likely region to be used for spare locations.

102. The tidal level variation in the simulation period at the location of East Met Mast wave buoy (location is illustrated on **Figure 8.3-6**) is shown on **Figure 8.3-105**.

103. Following model runs for Baseline and DBD options (A-D), the "worst case" scenario of DBD options was identified, which was taken forward to be run with two scenarios investigating potential cumulative impact outlined in **Section 8.3.3.4** and **Section 8.3.3.5.**

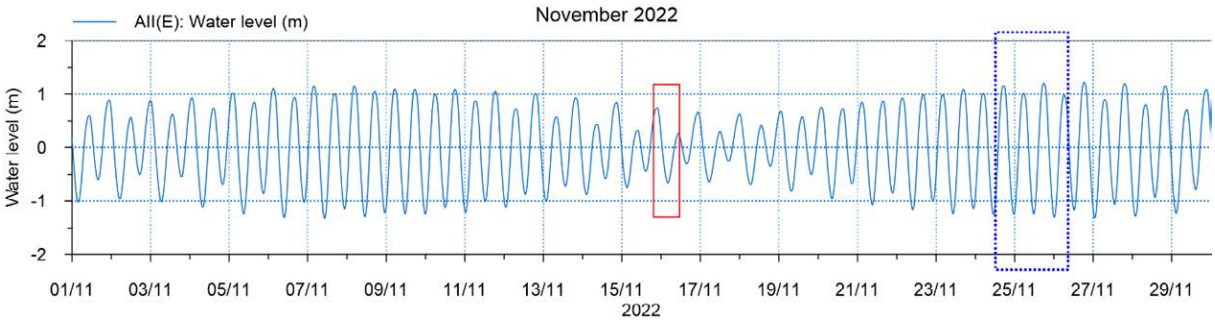

Figure 8.3-105: Modelled Water Levels at East Met Mast Adcp for A Period of 30 Days (Blue Frame Indicates Spring Tides and Red Frame Indicates Neap Tides)

8.3.5.5 Hydrodynamic Model Results and Discussions

104. The model results from the baseline model runs are presented as contour plots in **Appendix A**, and include:

- Spatial variation of modelled peak south-east and north-west going tidal currents at a spring tide and neap tide over the 30-day simulation for Baseline, Layout A to D;
- Spatial variation of modelled maximum tidal current speed over the 30-day simulation;
- Difference of modelled peak south-east and north-west going tidal currents at a spring tide over the 30-day simulation; and
- Difference of modelled maximum tidal current speed over the 30-day simulation.

105. **Table 8.3-13** shows the maximum tidal currents registered in the array location for the Baseline.

Table 8.3-13: Maximum Tidal Currents Measured Around Array for Baseline (All Values in M/S)

Spring Tides		Neap Tides		Maximum Current
South-east-going	North-west-going	South-east-going	North-west-going	
0.37	0.42	0.2	0.27	0.45

106. **Table 8.3-14** shows the maximum tidal currents registered in the array location for Layouts A-D with 3 different Offshore Platform configurations.

Table 8.3-14: Maximum Tidal Currents Measured around Array for Layouts A-D, Offshore Platform 1-3 (All Values in m/s)

		Spring Tides		Neap Tides		Maximum Current
		South-east-going	North-west-going	South-east-going	North-west-going	
Layout A	Offshore Platform 1	0.37	0.41	0.20	0.27	0.44
	Offshore Platform 2	0.36	0.42	0.20	0.27	0.44
	Offshore Platform 3	0.37	0.42	0.20	0.27	0.44

		Spring Tides		Neap Tides		Maximum Current
		South-east-going	North-west-going	South-east-going	North-west-going	
Layout B	Offshore Platform 1	0.35	0.40	0.19	0.26	0.43
	Offshore Platform 2	0.36	0.41	0.19	0.25	0.43
	Offshore Platform 3	0.36	0.40	0.19	0.27	0.43
Layout C	Offshore Platform 1	0.37	0.42	0.20	0.27	0.44
	Offshore Platform 2	0.37	0.42	0.20	0.27	0.45
	Offshore Platform 3	0.37	0.42	0.20	0.27	0.45
Layout D	Offshore Platform 1	0.36	0.40	0.20	0.27	0.45
	Offshore Platform 2	0.36	0.42	0.20	0.27	0.45
	Offshore Platform 3	0.36	0.42	0.20	0.27	0.45

107. Upon review of the comparison graphs from **Appendix A** (*Figures A.131* to *A.190*), the change of maximum current speed graphs were used to determine the "worst case" scenario to be carried forward for the cumulative model runs.

108. For all four layouts, A to D, it was seen (shown in **Appendix A,** *Figures A.131* to *A.190*) that the "worst case" was Offshore Platform 2, followed by Offshore Platform 1 and then Offshore Platform 3.

109. For all Offshore Platforms, the "worst case" was deemed to be Layout B, followed closely by Layout A, with Layouts C and D being similar to each other but significantly less than Layouts A and B.

110. The "worst case" scenario, following on the above review, was chosen to be Layout B, Offshore Platform 2. This was carried forward to the cumulative runs for the two scenarios.

111. It is important to note that Layout C, Offshore Platform 2 was also carried forward to be run for the cumulative runs following the wave modelling to allow for conjunction between the two modelling processes.

112. **Figure 8.3-106** and **Figure 8.3-107** shows the maximum current speed graphs for Layout B, Offshore Platform 2 and Layout C, Offshore Platform 2 respectively.

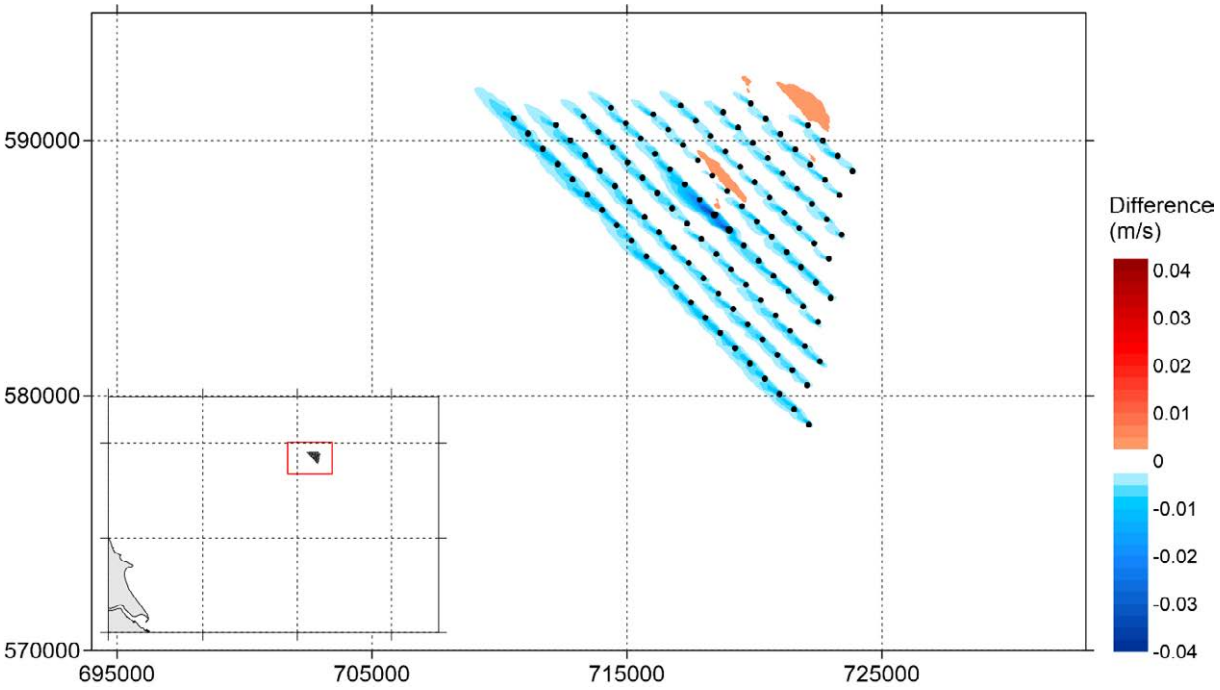

Figure 8.3-106: Change in Maximum Current Speed over 30 Days (Layout B - Offshore Platform 2 - Baseline)

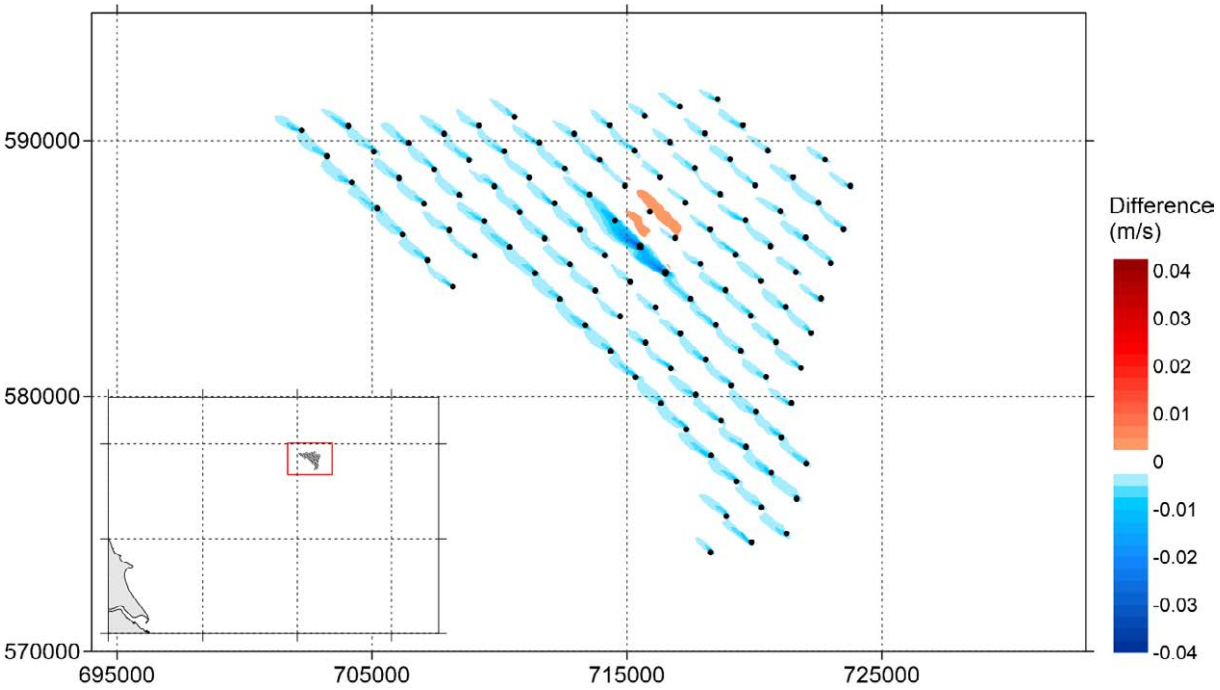

Figure 8.3-107: Change of Maximum Current Speed over 30 Days (Layout C- Offshore Platform 2 - Baseline)

113. **Appendix B** supplies the results from the cumulative set of model runs for Layout C Offshore Platform Layout 2, and they include:

- Spatial variation of modelled peak south-east and north-west going tidal currents at a spring tide and neap tide over the 30-day simulation for Scenario 1 and Scenario 2;
- Spatial variation of modelled maximum tidal current speed over the 30-day simulation;
- Difference of modelled peak south-east and north-west going tidal currents at a spring tide over the 30-day simulation in comparison to the baseline; and
- Difference of modelled maximum tidal current speed over the 30-day simulation in comparison to the baseline.

114. For Scenario 1, the model predicts that there are higher current speeds viewed around DBD and DBC for both neap and spring tides. These values are approximately 0.05m/s to 0.2m/s higher than those viewed around DBA, DBB and Sofia. As was shown with the baseline model results, the values predicted for neap tide is less than that determined for spring tide, with the spring tide values being double that neap tide values. When looking at the maximum current speeds, not only are higher speeds found around DBD and DBC, at approximately 0.4m/s, but the same speeds are found around the south of both DBA and DBB. The only offshore wind farm that doesn't increase in speed is Sofia.

115. For Scenario 1, the model predicts there will be minimal change in tidal current speeds DBA, DBB and Sofia for all spring and neap tides. A change occurs during the maximum current speeds registered, where DBB and DBA experience slightly elevated differences in current speeds. For DBC and DBD, the model predicts a higher level of change of tidal speed than for the rest of the wind farm locations. This appears to be between 0.002m/s and 0.004m/s for all tide changes, and the same is true for the change in maximum current speed. It is also clear that most of this change occurs in the location of DBD, with the furthest extent of the change stretching into DBC (see **Figure 8.3-108**).

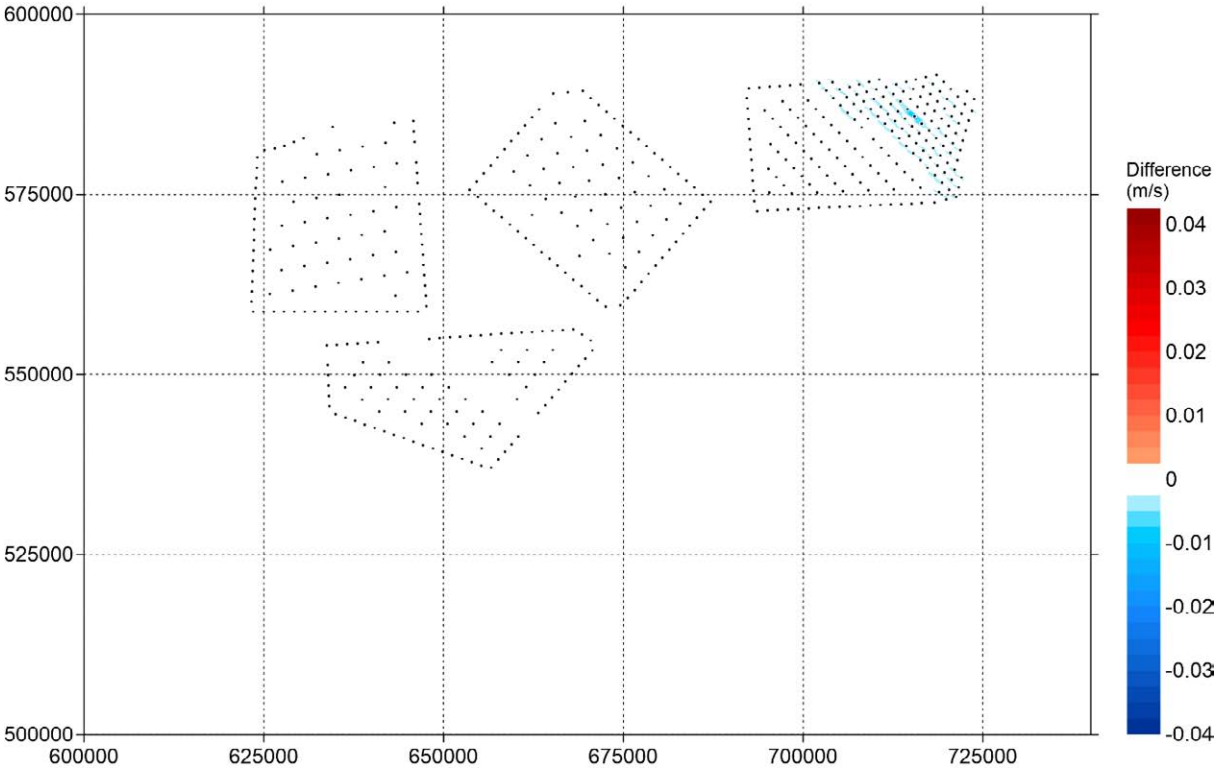

Figure 8.3-108: Change of Maximum Current Speed over 30 Days (DBD Layout C / Offshore Platform Layout 2 with Cumulative Layout Scenario 1)

116. For Scenario 2, the model predicts that the currents will be higher at the proposed site for DBS (both East and West) than anywhere else in the layout. For peak south-east -going currents during the spring tide, both DBS West and East show a current speed of ~0.4m/s, 0.1m/s higher than the current speed at DBD. When observing the predicted currents for both peak south-east-going and north-west-going currents for neap tides, the currents predicted around DBS East is higher than that shown around West Met Mast, by 0.1m/s and 0.05m/s respectively. During the maximum current speeds, DBS West shows a slightly higher current that East Met Mast, with speeds of 0.6m/s and 0.5m/s respectively. Finally, during the peak south-east-going currents for spring tide, both DBS areas shows a current of ~0.4m/s. Despite these changes, the currents around the other layouts including DBD are similar to those shown in Scenario 1.

117. For Scenario 2, the model predicts the changes in current speed will be similar to those seen in Scenario 1 for DBA, DBB, DBC, DBD and Sofia for all tidal patterns. As for DBS East and West, large changes in speed occur for all tidal patterns, with a change in excess of 0.001m/s observed on *Figures B.26 to B.29* in **Appendix B**, and between 0.002 and 0.004m/s for the change in maximum current speed. Greater changes in speed appear to occur at DBS West (see **Figure 8.3-109**).

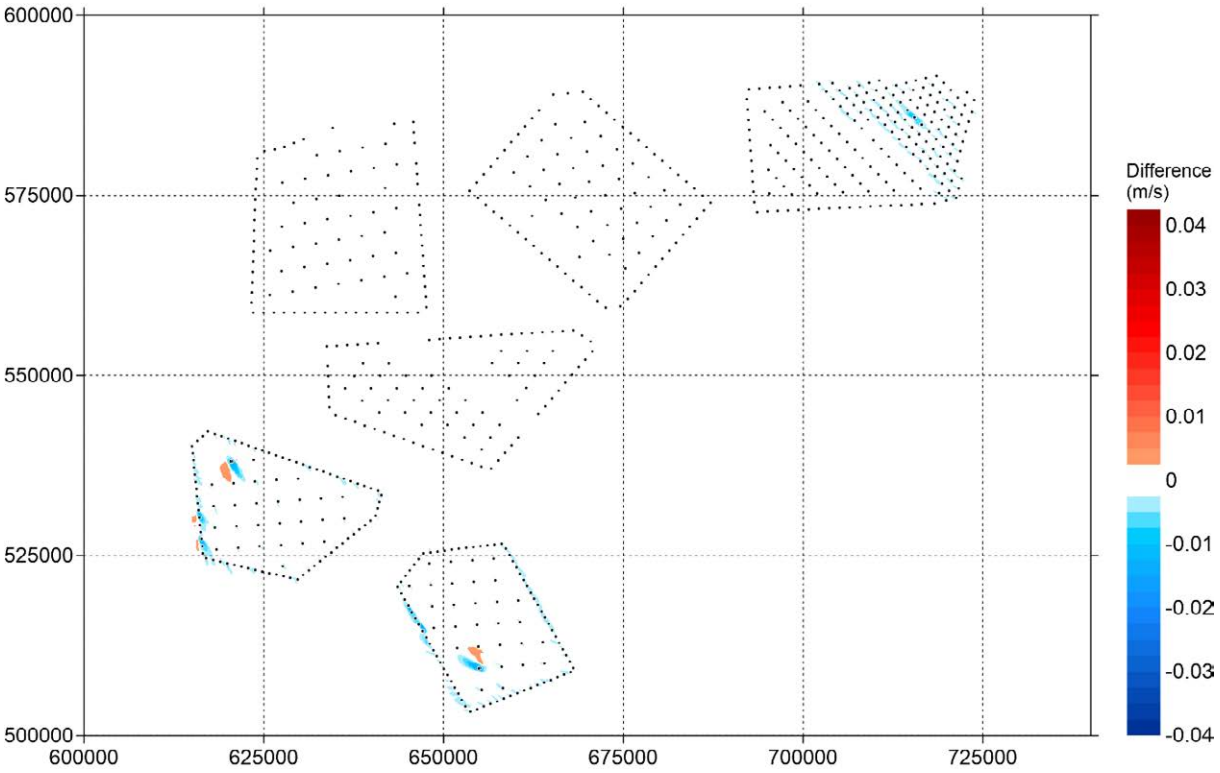

Figure 8.3-109: Change of Maximum Current Speed over 30 Days (DBD Layout C / Offshore Platform Layout 2 with cumulative layout Scenario 2)

118. Overall in Scenario 2 where both DBD and DBS are included a larger impact on currents is observed in the model. This is due to the much larger foundations being considered at these sites, along with them sitting in higher velocity areas than the existing wind farms.

119. The model results show no overlaps of shadow areas between the modelled wind farms except between DBD and DBC, whereby DBD is being developed immediately adjacent to DBC and therefore this is expected.

120. **Appendix C** supplies the results for the cumulative set of model runs for Layout B Offshore Platform Layout 2, and they include:

- Spatial variation of modelled peak south-east and north-west going tidal currents at a spring tide and neap tide over the 30-day simulation for Scenario 1 and Scenario 2;

- Spatial variation of modelled maximum tidal current speed over the 30-day simulation;
- Difference of modelled peak south-east and north-west going tidal currents at a spring tide over the 30-day simulation in comparison to the baseline; and
- Difference of modelled maximum tidal current speed over the 30-day simulation in comparison to the baseline.

121. For Scenario 1, the model predicts that DBD and DBC will be experiencing similar tidal currents to those experienced by all previous offshore wind farm locations, with the closest to being directly comparable being DBA. As was shown with the baseline model, there are significantly higher tidal currents experienced during spring tide than during neap tide, with a reduction of ~0.15m/s between the two different tide times. When looking at the maximum current speeds, a peak maximum tidal current speed of ~0.4m/s viewed at the edges of DBD, DBC, DBA and DBB, with Sofia experiencing peak maximum tidal current speeds of 0.3m/s.

122. For Scenario 1, the model predicts that there is minimal change of speed, with regard to the baseline, for all wind farm layouts other than DBD, where greater change occurs. For example, when looking at the change in speed in comparison to the baseline for spring tide, south-east-going tides, there is a maximum change of 0.003m/s around DBD, in comparison to a change of <0.001m/s for all other wind farms. This is also true for all other tidal options until the maximum current speed change, where DBD, DBC and DBB all experience higher changes than DBA and Sofia. The largest changes still occur within DBD, but changes of ~0.001m/s occur around both DBC and DBB.

123. For Scenario 2, the model predicts that there will consistently be higher tidal current speeds for DBS East than for the rest of the wind farm locations. There are some tidal patterns that cause DBS West to have higher tidal current speeds, but there are also some where there is minimal change. For example, during the spring tide north-west going currents, DBS East has the highest current speed of all at approximately 0.4m/s, whereas DBS West has one of the lower current speeds of 0.2m/s, with the only location lower being DBB. Conversely, all other tide patterns show DBS East and West having the same, high current speeds, culminating in the maximum current speed, where both DBS East and West show levels of 0.5m/s to 0.6m/s, where all other wind farm locations including DBD have currents <0.4m/s.

124. For Scenario 2, the model predicts that, similarly to Scenario 1, DBD has a larger difference in current speed than DBC, DBB and DBA. This is also true for DBS East and West. While DBD, DBC, DBB, DBA and Sofia show similar changes in tidal current to those shown by Scenario 1, DBS East and West both have higher changes in peak current, in excess of 0.008m/s around the borders for spring tides and maximum current speeds, and >0.002m/s for neap tides.

125. Overall, as with Layout B Offshore Platform 2, there appears to be a larger impact on currents when DBD and DBS are incorporated though the absolute change of tidal currents, as expected with the larger foundations proposed for both of these projects, however the change is still very small.

126. The model results show no overlaps of shadow areas between the modelled wind farms (see **Figure 8.3-110, Figure 8.3-111** and *Figure C.21 – Figure C.30* in **Appendix C**).

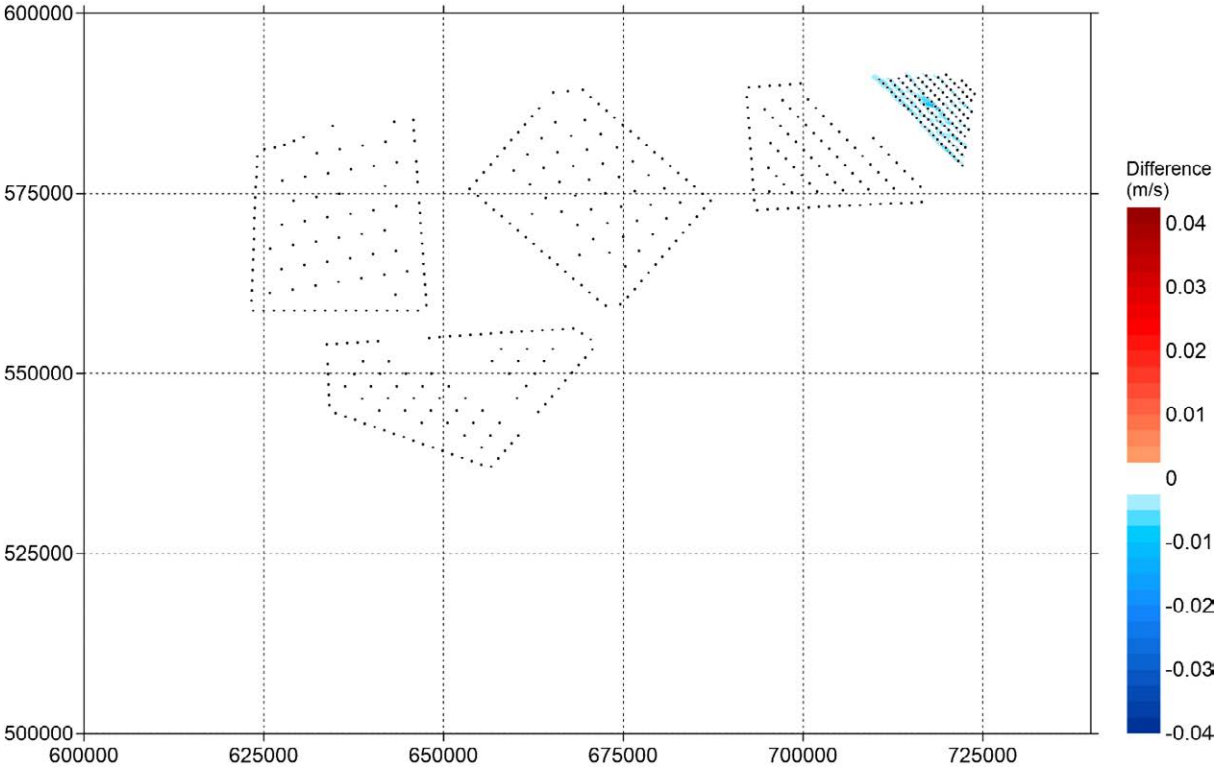

Figure 8.3-110: Change of Maximum Current Speed over 30 Days (DBD Layout B / Offshore Platform Layout 2 with cumulative layout Scenario 1)

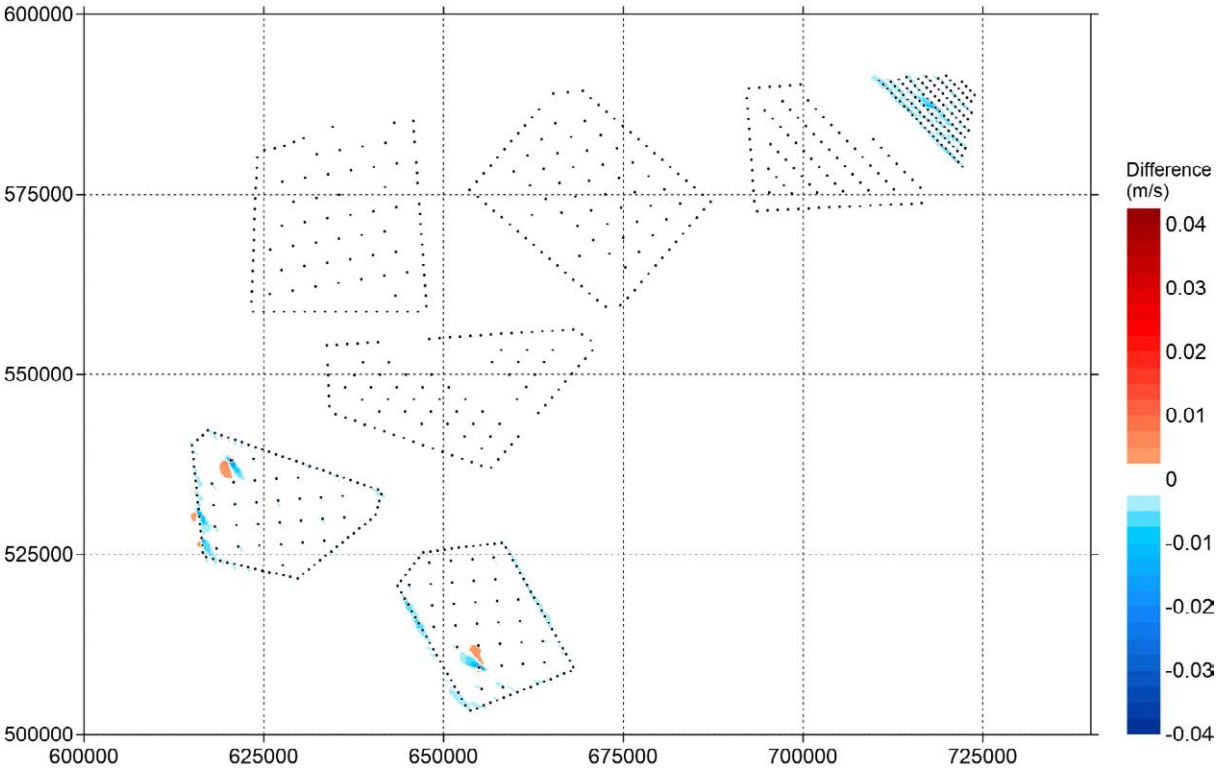

Figure 8.3-111: Change of Maximum Current Speed over 30 Days (DBD Layout B / Offshore Platform Layout 2 with cumulative layout Scenario 2)

8.3.6 Suspended Sediment Dispersion Modelling

8.3.6.1 Model Configuration

127. Over the construction period installation of foundations and cables will generate suspended sediment into the water column, which may result in the formation of sediment plumes. The mobilised sediment may then be transported away from the disturbance source by tidal currents. The magnitude of the plume will be a function of seabed type, the installation method and the hydrodynamic conditions in which dispersion takes place.

128. The simulation of the release and spreading of fine sediments due to foundation and cable installation activities have been modelled using the 3D model MIKE3-MT. The MIKE3-MT model is coupled with the local 3D MIKE3-HD hydrodynamic model described in **Section 8.3.5** and uses the same mesh. The number of vertical mesh was set to five in the suspended sediment dispersion simulations.

129. This dispersion model considers:

- The release of sediments as a function of time, location and sediment characteristics;
- Advection and dispersion of the suspended sediment in the water column as a function of the 3D hydrodynamics predicted by MIKE3-HD;

- No stratification is assumed in the model simulation considering the location is far away from any major rivers and relatively shallow water of North Sea;
- Settling and deposition of the dispersed sediment; and
- The effect of waves in keeping sediment in suspension for a longer period.

130. In the suspended sediment dispersion modelling, it is assumed that the initial suspended concentration in the model domain is zero and flow entering the model domain at the open boundaries contains no sediments. The suspended sediment dispersion model predicts excess suspended sediments induced by the proposed construction activities only.

131. In this modelling exercise, sediment re-suspension is not considered. Therefore, the predicted sediment deposition is a result of the proposed construction.

132. For the entire simulation periods, a wave condition of Hs=1m and Ts=6s were applied. This condition represents upper limit of dredging operation.

8.3.6.2 Construction Activities and Sediment Release

133. The proposed construction involves the following activities which will cause suspended sediment release into the water column:

- Export cable routes (locations shown on **Figure 8.3-112** and **Figure 8.3-113**) - note that two were selected within the characterisation area, one presenting the worst case in the event of an extension to the Marine Protected Area, the other being the preferred option currently;
  - Levelling through sand waves;
  - Trenching;
- Inter-array cable routes are currently not sufficiently defined to progress sediment dispersion modelling from construction at PEIR, however inter-array cable modelling will be presented for DCO submission;
- Installing turbines and platforms (locations shown on Figure 8.3-12);
  - Seabed preparation; and
  - Drilling for foundations (turbines and platforms).

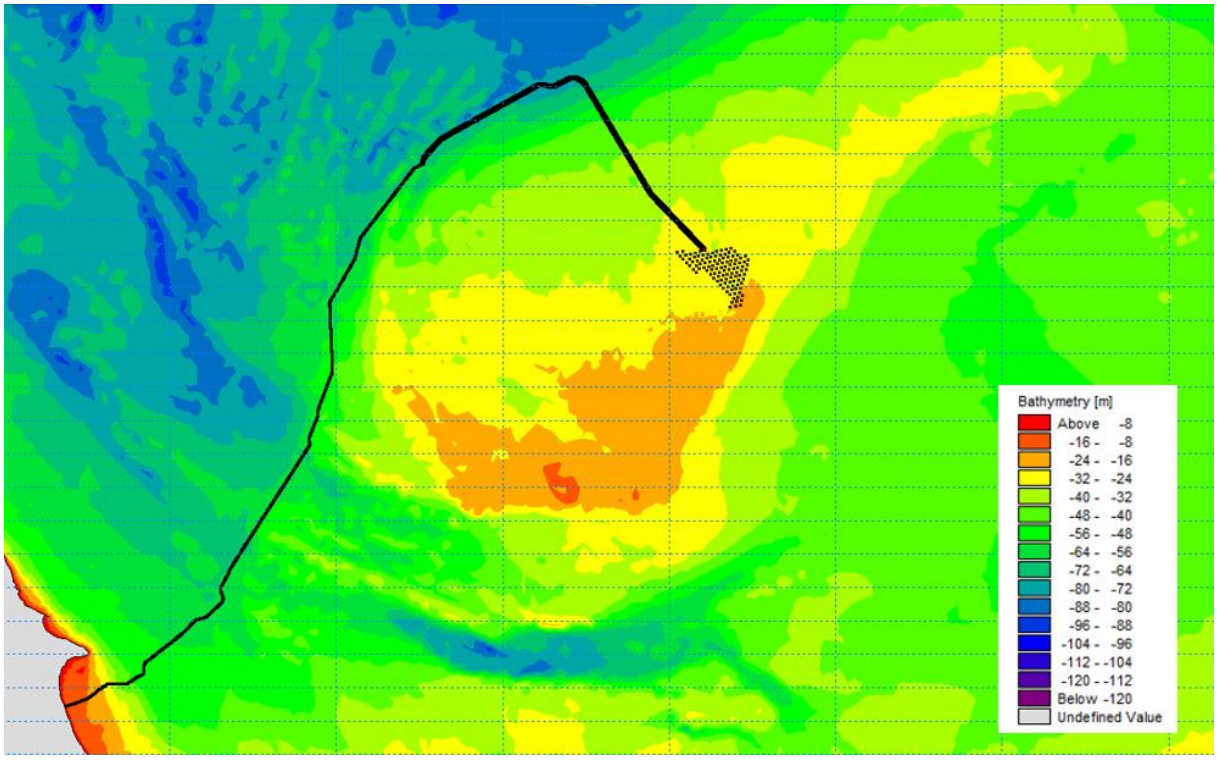

Figure 8.3-112: Offshore Export Cable Route (Option 1) (thick line shows where levelling is required)

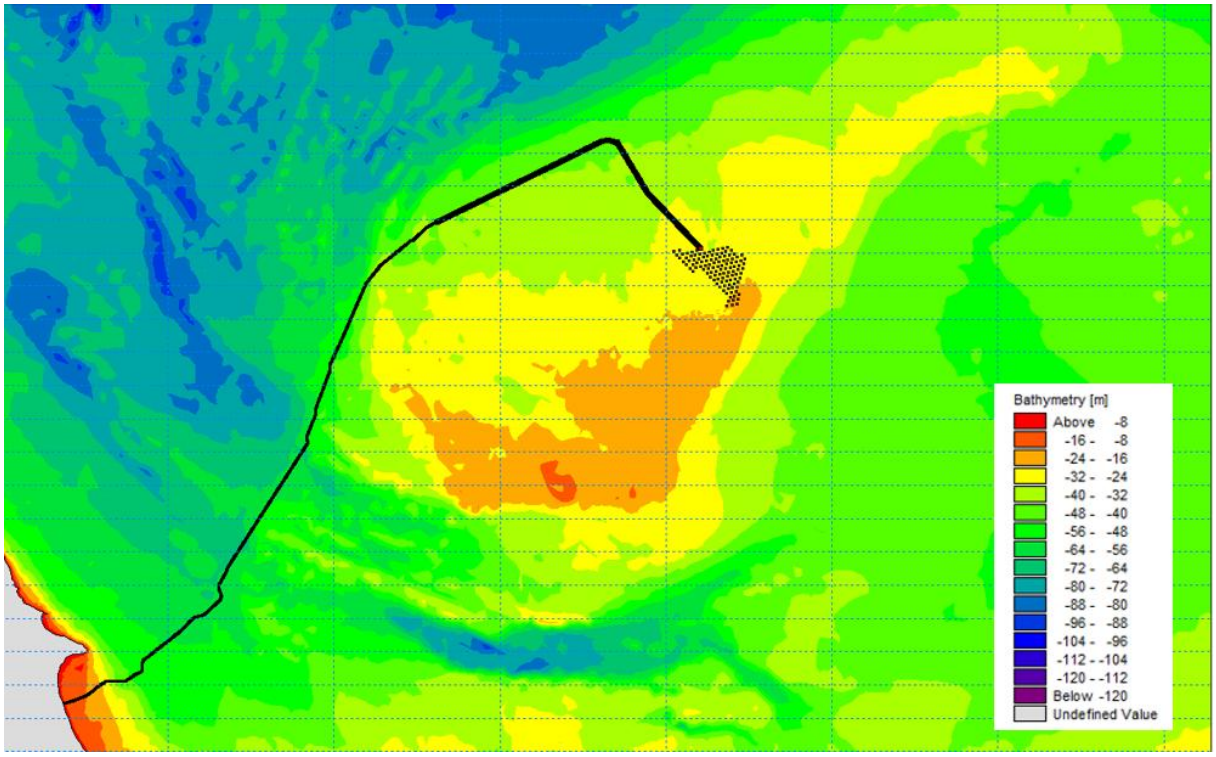

Figure 8.3-113: Offshore Export Cable Route (Option 2) (thick line shows where levelling is required)

134. In the dispersion modelling, Turbine Layout C with 113 turbines and two Offshore Platforms in the centre of the Array Area was chosen as the "worst-case" DBD layout (Figure 8.3-12). The "worst-case" layout is discussed further in **Section 8.3.4.4** and **Section 8.3.5.5**.

135. The construction activities set out in **paragraph 133**, have been simulated with **Table 8.3-15** and **Table 8.3-16** listing the relevant construction method, duration and sediment release rates. The sediment release rate of 15kg/s for levelling cable routes through sand waves is estimated by using an 'S-Factor' of 15kg/m^3 for trailing suction hopper dredger (TSHD) and a production rate of 1m^3/s. The sediment release rate of 6kg/s for seabed preparation and drilling is based on an 'S-Factor' of 6kg/m^3 for CSD and a production rate of 1m^3/s. These 'S-Factor' values are taken from CIRIA guidance (CIRIA, 1999).

136. Following running the model for PEIR, minor changes to the worse case scenarios in relation to the total lengths and volumes of export cables for levelling and trenching arose (see **Table 8.3-15**). Small changes in total length and volume would make little difference in predicted maximum suspended sediment concentration which is governed by tidal hydrodynamics, production rate and sediment size. A small change in dredging or trenching volume would increase or decrease deposition depth slightly and proportionally, which is unlikely to be distinguishable and will not impact on the conclusions of the assessments made on the basis of the model outputs presented below.

Table 8.3-15: Construction Activities for Export Cables

Activities	Modelled (per cable)		Latest at PEIR Submission (per cable)		Method	Production Rate (m^3/s)	Duration (days)	Sediment Release rate (kg/s)
	Length (km)	Volume (million m^3)	Length (km)	Volume (million m^3)				
Export Cable (Option 1) - levelling	119	16.7	115.2	16.13	TSHD	1.00	193	15
Export Cable (Option 2) - levelling	101	14.1	n/a	n/a	TSHD	1.00	164	15
Export Cable (Option 1) - trenching	329	5.8	400.0	7.0	Cable Plough	0.97	68	1,604*
Export Cable (Option 2) - trenching	296	5.1	n/a	n/a	Cable Plough	0.97	62	1,604*

Note *: 100% sediment is released in the bottom layer during trenching by cable plough.

Table 8.3-16: Construction Activities for Turbine and Platform Foundations

Activities	Volume (m^3 per)	Production Rate (m^3/s)	Duration (hours per)	Sediment Release Rate (kg/s)
Drill Turbine Foundation	15,268	1	4.2	6
Drill Platform Foundation	17,671	1	4.9	6

8.3.6.3 Seabed Sediment Properties

137. **Table 8.3-17** presents the sediment composition in percentages within the DBD Array Area and Export Cable Corridor. The Array Area characterisation is based on the average composition of 47 seabed sediment samples collected across it by Fugro in August 2023 (Fugro, 2023c). Due to changes in the location of the Project offshore ECC post the Fugro (2023) survey, it was not appropriate to use the sediment data collected along the previously surveyed cable route. Seabed sediment samples were collected in September 2024 (post the completion of the modelling) within the Offshore ECC and will be updated at the DCO application stage. Therefore, the values for the Offshore ECC for PEIR were derived from sediment data from the Dogger Bank South offshore ECC as the most recent data available across a similar geographical area.

Table 8.3-17: Sediment Composition (in percentages) for Dispersion Simulation

Sediment size	Export Cable Route (%)	DBD Array Area (%)
Silt / Clay	4.1	0.0
Fine Sand	46.9	85.4
Medium Sand	30.4	4.2
Coarse Sand	9.6	8.0
Gravel / Cobble	9.1	2.0

138. **Table 8.3-18** presents sediment settling velocities and critical bed shear stress for different sediment size factions used in the suspended sediment dispersion modelling. These values were calculated using the Soulsby method (Soulsby, 1998).

Table 8.3-18: Sediment Settling Velocities and Critical Bed Shear Stresses

Sediment size	Sediment Size (mm)	Settling Velocity (m/s)	Critical Bed Shear Stress (N/m^2)
Silt / Clay	0.031	0.000554	0.0847
Fine Sand	0.13	0.00935	0.1548
Medium Sand	0.3	0.0372	0.2025
Coarse Sand	1.3	0.135	0.657
Gravel / Cobble	2.0	0.1734	1.166

8.3.6.4 Model Simulations

139. The coupled 3D MIKE3-MT and MIKE3-HD model has been run for the entire period of each relevant construction activity (described in **Table 8.3-15** and **Table 8.3-16)** in which sediment will be released into water column. The model results are presented as contour plots of maximum suspended sediment concentrations for bottom, middle and surface layers of the water column, and total sediment deposition thickness as a result of each construction activity. These contour plots are provided in **Appendix D** (for laying export cables) and **Appendix E** (for drilling turbine and platform foundations) of this report.

140. The model results presented in this report are all excess suspended sediment concentration and excess sediment deposition caused by the proposed construction activities for the Project (i.e. excluding any background). The suspended sediment concentration and deposition caused by natural morphological processes are not modelled and included.

141. Time series plots of predicted suspended sediment concentrations are presented at selected points (shown on **Figure 8.3-114**) during trenching the offshore export cable route. The plots are presented only for the periods and locations that predicted suspended sediment concentrations are measurable (exceeding 0.5mg/l). The time series plots are provided in **Appendix F** of this report.

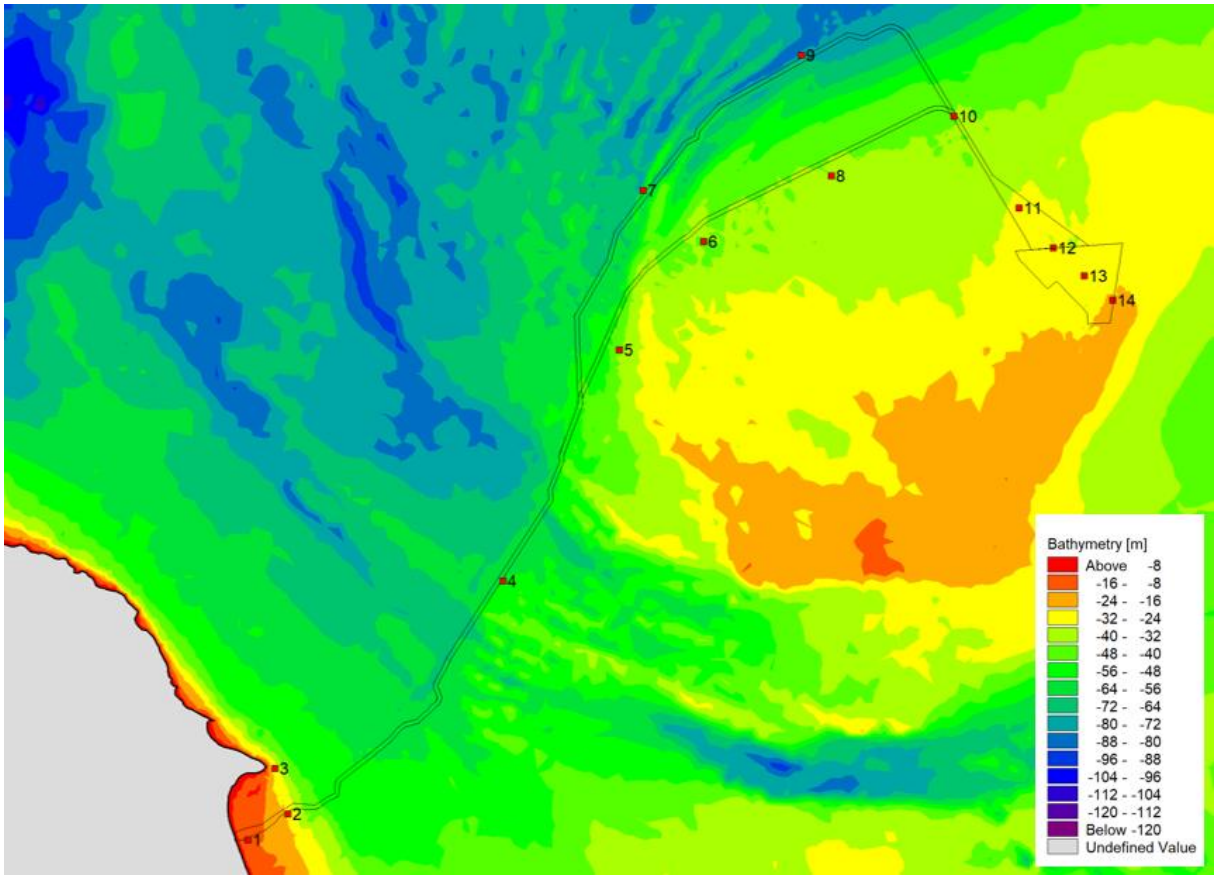

Figure 8.3-114: Locations of Time Series Plots of Predicted Suspended Sediment Concentration

8.3.6.5 Discussion of Suspended Sediment Dispersion Model Results

8.3.6.5.1 Offshore Export Cable Corridor

142. The maximum suspended sediment concentration caused by the levelling processes through sand waves is less than 10mg/l in the bottom layer and less than 5mg/l in the surface layer. This is due to relatively low sediment release rate by TSHD compared to cable ploughing for trenching.

143. The model results from trenching predict higher near-bed maximum suspended sediment concentrations (up to 1,690mg/l in the bottom layer) along the Offshore Export Cable Corridor. This is because the cable plough method would disturb 100% of the sediments into the bottom layer of the water column. The maximum suspended sediment concentration by trenching is much lower in the surface layer (below 26mg/l).

144. Sediment plumes are larger in the nearshore area due to faster tidal currents, and much smaller in offshore areas. Table 8.3-19 and

145. **Table 8.3-20** present estimated sediment 'plume' size (using the threshold value of 0.5mg/l) in the nearshore and offshore along the ECC Option 1 and Option 2 respectively by trenching. The 'plume' size is based on the modelled maximum suspended sediment concentration over the entire simulation. Therefore, the 'plume' size is the maximum extent of modelled maximum suspended sediment concentrations exceeding 0.5mg/l and does not represent the spatial extent of the plume at any single point in time.

Table 8.3-19: Estimated Sediment 'Plume' Size Based on Modelled Maximum Suspended Sediment Concentrations Exceeding 0.5mg/l During Trenching for Offshore Export Cables (Option 1)

Location	Bottom Layer	Middle Layer	Surface Layer
Nearshore (near Point 3 shown on **Figure 8.3-115**)	35.3km	33.4km	30.6km
Offshore (near Point 4 shown on **Figure 8.3-115**)	17.6km	16.8km	15.1km
Offshore (near Point 5 shown on **Figure 8.3-115**)	7.7km	7.1km	5.8km
Offshore (near Point 10 shown on **Figure 8.3-115**)	8.4km	8.1km	6.2km

Table 8.3-20: Estimated Sediment 'Plume' Size Based on Modelled Maximum Suspended Sediment Concentrations Exceeding 0.5mg/l During Trenching for Offshore Export Cables (Option 2)

Location	Bottom Layer	Middle Layer	Surface Layer
Nearshore (near Point 3 shown on **Figure 8.3-116**)	35.3km	33.3km	30.6km
Offshore (near Point 4 shown on **Figure 8.3-116**)	17.6km	16.8km	15.1km
Offshore (near Point 5 shown on **Figure 8.3-116**)	9.8km	9.6km	8.8km
Offshore (near Point 10 shown on **Figure 8.3-116**)	9.1km	8.9km	7.8km

146. The time series plots show that modelled excess suspended sediment concentrations greater than 5mg/l at any locations only last no more than 4 hours.

147. The time series plots show small or little excess suspended sediment concentration at Points 3, 5, 6, 7, 8, 13 and 14 due to their distance away from the modelled trench location.

148. The model results predict local sediment deposition along the ECC after both levelling and trenching processes.

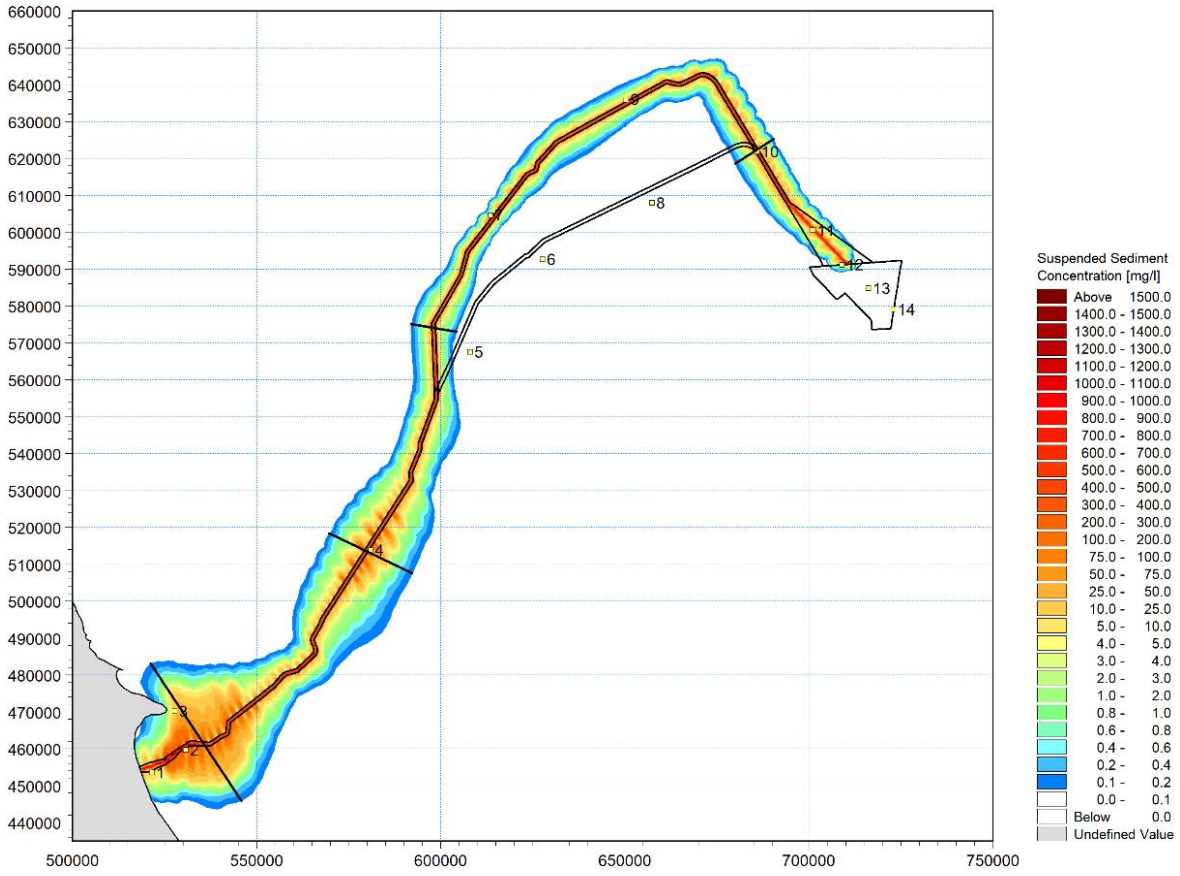

Figure 8.3-115: Locations where Plume Size Estimated (Contours are Maximum Suspended Sediment Concentration in Bottom Layer – Export Cable Route Option 1 – Trenching)

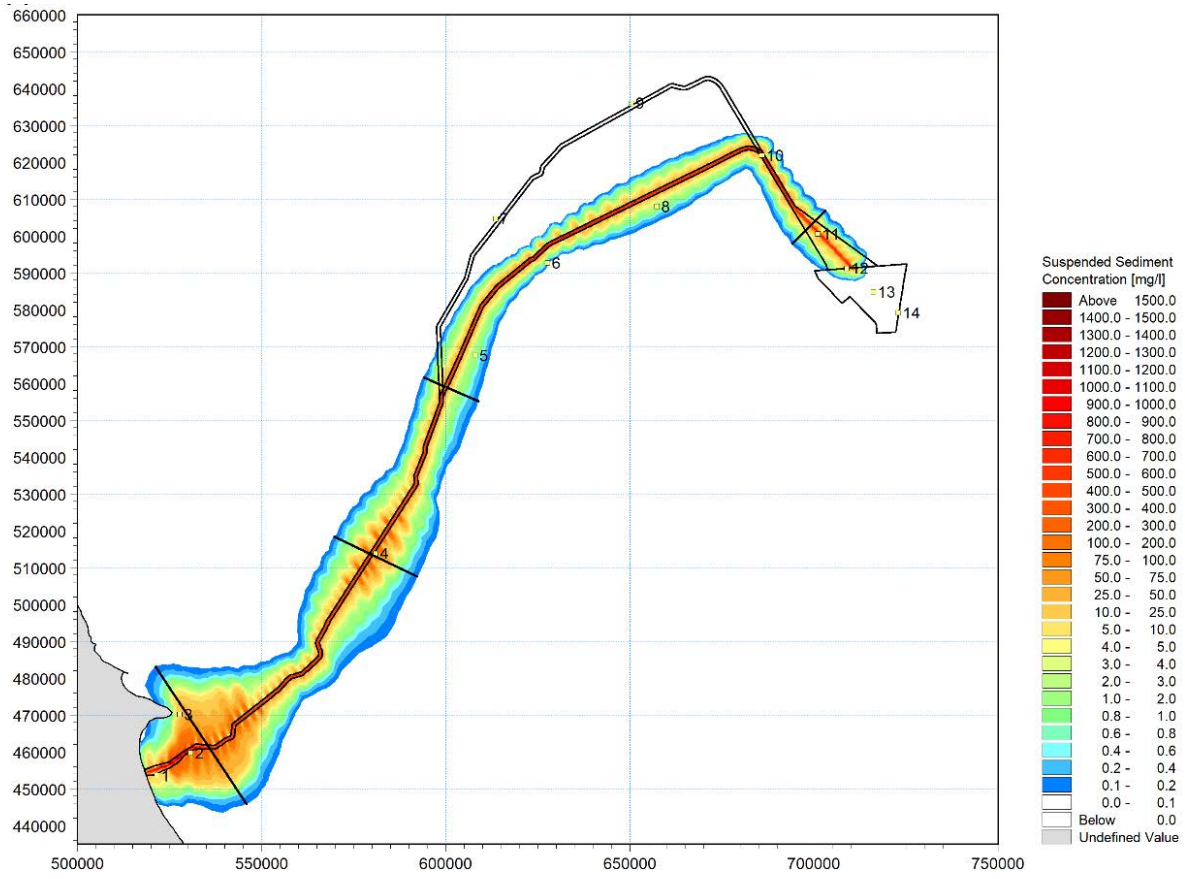

Figure 8.3-116: Locations where Plume Size Estimated (Contours are Maximum Suspended Sediment Concentration in Bottom Layer – Export Cable Route Option 2 – Trenching)

8.3.6.5.2 Turbine and Platform Foundations

149. The model predicts low suspended sediment concentrations caused by the drilling of turbine and platform foundations. The model results show that the maximum suspended sediment concentrations are less than 1mg/l and 2mg/l in the surface and bottom layers of the water column, respectively. The predicted sediment deposition from the drilling is less than 1mm. The contour plots of maximum suspended sediment concentrations and sediment deposition are presented in **Appendix F**.

References

Fugro (2023a). DBS WPM1 Array Area Seafloor Results. Report 004267910.

Fugro (2023b). DBS WPM2 WPM3 ECR Seafloor and Shallow Geological Results. Report 004267912.

Fugro, (2023c). Dogger Bank D 2023 Benthic Surveys Dogger Bank D UK, North Sea Benthic Characterisation Report. Report 221061-R-002 01.

Fugro (2023d). DBS Preliminary Environmental Information Report. Appendix 9-2: Draft Benthic Ecology Characterisation Report. Document reference: 004300116.

CIRIA (1999). Scoping the assessment of sediment plumes arising from dredging.

List of Figures, Tables and Plates

List of Tables

Table 8.3-1: Locations of the Measured Water Levels 11
Table 8.3-2: Locations of the Measured Currents 12
Table 8.3-3: Details of Array Layouts A to D and Offshore Platform Options 1 to 3 14
Table 8.3-4: Dimensions of Large and Small Offshore Platform 15
Table 8.3-5: Details of Wind Farm Layouts for Cumulative Scenarios 18
Table 8.3-6: MIKE21-SW Model Settings 22
Table 8.3-7: Summary of Calibration Storm Events 32
Table 8.3-8: Extreme Offshore Wave Height at ERA5 Hindcast Point (for Relevant Wave Directions) 34
Table 8.3-9: Wave Model Input Parameters for Sensitivity Runs 35
Table 8.3-10: Model Errors in Water Level (Regional Model) 86
Table 8.3-11: Model Errors in Water Level (Local Model) 88
Table 8.3-12: Model Errors in Current Speed (Local Model) 92
Table 8.3-13: Maximum Tidal Currents Measured Around Array for Baseline (All Values in M/S) 93
Table 8.3-14: Maximum Tidal Currents Measured around Array for Layouts A-D, Offshore Platform 1-3 (All Values in m/s) 93
Table 8.3-15: Construction Activities for Export Cables 104
Table 8.3-16: Construction Activities for Turbine and Platform Foundations 105
Table 8.3-17: Sediment Composition (in percentages) for Dispersion Simulation 105
Table 8.3-18: Sediment Settling Velocities and Critical Bed Shear Stresses 106
Table 8.3-19: Estimated Sediment 'Plume' Size Based on Modelled Maximum Suspended Sediment Concentrations Exceeding 0.5mg/l During Trenching for Offshore Export Cables (Option 1) 108
Table 8.3-20: Estimated Sediment 'Plume' Size Based on Modelled Maximum Suspended Sediment Concentrations Exceeding 0.5mg/l During Trenching for Offshore Export Cables (Option 2) 109

List of Figures

Figure 8.3-1: Detailed Bathymetry of DBD Wind Farm Area 7
Figure 8.3-2: Detailed Bathymetry of Dogger Bank Tranche A and Tranche B Wind Farm Areas 7
Figure 8.3-3: Detailed Bathymetry of Areas DBS West and DBS East 8
Figure 8.3-4: Coverage of Detailed Bathymetry Data used in the Wave and Local Hydrodynamic Model 8
Figure 8.3-5: C-map and Admiralty Maritime Data Solutions Data used in the Regional Hydrodynamic Model 9
Figure 8.3-6: Locations of wave buoys North and South and ERA5 Hindcast Data Points 10

Figure 8.3-7: Locations of Tidal Gauges and Current Stations (Gauge and Station Detailed are Given in Table 8.3-1 and Table 8.3-2)..... 11
Figure 8.3-8: Wind Farm Array **Layout A** with Offshore Platform Options 1 to 3 13
Figure 8.3-9: Wind Farm Array **Layout B** with Offshore Platform Options 1 to 3 13
Figure 8.3-10: DBD Turbine **Layout C** with Offshore Platform Options 1 to 3..... 15
Figure 8.3-11: DBD Turbine **Layout D** with Offshore Platform Options 1 to 3..... 15
Figure 8.3-12: DBD Option 16
Figure 8.3-13: Wind Farm Layouts included in 'Scenario 1' 17
Figure 8.3-14: Wind Farm Layouts included in 'Scenario 2' 19
Figure 8.3-15: Extent of MIKE21-SW-FM Model Domain and Bathymetry used for Model Verification 20
Figure 8.3-16: Wave Model Mesh Resolution 21
Figure 8.3-17: Partrac Wave Buoy Locations and ERA5 Hindcast Model Points Used for Wave Model Verification 24
Figure 8.3-18: Comparison of Measured and Modelled Wave Height for Waves Coming from Northerly Direction - Event 1..... 25
Figure 8.3-19: Comparison of Measured and Modelled Wave Height for Waves Coming from Northerly Direction - Event 2..... 25
Figure 8.3-20: Comparison of Measured and Modelled Wave Height for Waves Coming from Northerly Direction - Event 3..... 26
Figure 8.3-21: Comparison of Measured and Modelled Wave Height for Waves Coming from Northerly Direction - Event 4 (please note that there was no measured data available for wave buoy 'North' for this storm event) 26
Figure 8.3-22: Comparison of Measured and Modelled Wave Height for Waves Coming from the Northerly Direction at Dogger Bank "North" and "South" - Event 5..... 27
Figure 8.3-23: Comparison of Measured and Modelled Wave Height for Waves Coming from Northerly Direction at Dogger Bank B Wave Buoy - Event 5..... 27
Figure 8.3-24: Comparison of Measured and Modelled Wave Height for Waves Coming from Northerly Direction - Event 6..... 28
Figure 8.3-25: Comparison of Measured and Modelled Wave Height for Waves Coming from Northerly Direction - Event 7..... 28
Figure 8.3-26: Comparison of Measured and Modelled Wave Height for Waves Coming from North-easterly Direction - Event 8 29
Figure 8.3-27: Comparison of Measured and Modelled Wave Height for Waves Coming from Easterly Direction - Event 9..... 29
Figure 8.3-28: Comparison of Measured and Modelled Wave Height for Waves Coming from Easterly Direction at Dogger Bank "North" and "South" - Event 10 30
Figure 8.3-29: Comparison of Measured and Modelled Wave Height for Waves Coming from Easterly Direction at Dogger Bank B Wave Buoy - Event 10..... 30
Figure 8.3-30: Comparison of Measured and Modelled Wave Height for Waves Coming from Easterly Direction - Event 11..... 31
Figure 8.3-31: Comparison of Measured and Modelled Wave Height for Waves Coming from Southerly Direction - Event 12 31
Figure 8.3-32: Legend showing Difference in Significant Wave Height (Hs)..... 36

Figure 8.3-33: Difference in Significant Wave Height (Hs) between 'Baseline' and Turbine **Layout A** - Offshore Platform Options 1-3 for Waves Coming from Northerly Direction with Occurring Probability of 50 Percentile 36
Figure 8.3-34: Difference in Significant Wave Height (Hs) between 'Baseline' and Wind Farm **Layout B** - Offshore Platform Options 1 to 3 for Waves Coming from Northerly Direction with Occurring Probability of 50 Percentile 36
Figure 8.3-35: Difference in Significant Wave Height (Hs) between 'Baseline' and Wind Farm **Layout C** - Offshore Platform Options 1 to 3 for Waves Coming from Northerly Direction with Occurring Probability of 50 Percentile 37
Figure 8.3-36: Difference in Significant Wave Height (Hs) between 'Baseline' and Wind Farm **Layout D** – Offshore Platform Options 1-3 for Waves Coming from Northerly Direction with Occurring Probability of 50 Percentile 37
Figure 8.3-37: Difference in Significant Wave Height (Hs) between 'Baseline' and Wind Farm **Layout A** - Offshore Platform Option 1 to 3 for Waves Coming from Easterly Direction with Occurring Probability of 50 Percentile 37
Figure 8.3-38: Difference in Significant Wave Height (Hs) between 'Baseline' and Wind Farm **Layout B** - Offshore Platform Option 1 to 3 for Waves Coming from Easterly Direction with Occurring Probability of 50 Percentile 38
Figure 8.3-39: Difference in Significant Wave Height (Hs) between 'Baseline' and Wind Farm **Layout C** - Offshore Platform Options 1 to 3 for Waves Coming from Easterly Direction with Occurring Probability of 50 Percentile 38
Figure 8.3-40: Difference in Significant Wave Height (Hs) between 'Baseline' and Wind Farm **Layout D** - Offshore Platform Option 1 to 3 for Waves Coming from Easterly Direction with Occurring Probability of 50 Percentile 38
Figure 8.3-41: Significant Wave Height (Hs) for 'Baseline' for Waves Coming from Northerly Direction with Occurring Probability of 50 Percentile 41
Figure 8.3-42: Significant Wave Height (Hs) for 'Baseline' for Waves Coming from Easterly Direction with Occurring Probability of 50 Percentile 42
Figure 8.3-43: Significant Wave Height (Hs) for 'Baseline' for Waves Coming from Northerly Direction During 1 in 1 Year Return Period 43
Figure 8.3-44: Significant Wave Height (Hs) for 'Baseline' for Waves Coming from Easterly Direction During 1 in 1 Year Return Period 44
Figure 8.3-45: Significant Wave Height (Hs) for 'Baseline' for Waves Coming from Northerly Direction During 1 in 100 Year Return Period 45
Figure 8.3-46: Significant Wave Height (Hs) for 'Baseline' for Waves Coming from Easterly Direction During 1 in 100 Year Return Period 46
Figure 8.3-47: Difference in Significant Wave Height (Hs) in Metres between 'Baseline' and Wind Farm 'DBD Option' for Waves Coming from Northerly Direction with Occurring Probability of 50 Percentile 47
Figure 8.3-48: Difference in Significant Wave Height (Hs) in Metres between 'Baseline' and Wind Farm 'DBD Option' for Waves Coming from Easterly Direction with Occurring Probability of 50 Percentile 48
Figure 8.3-49: Difference in Significant Wave Height (Hs) in Metres between 'Baseline' and Wind Farm 'DBD Option' for 1 in 1 Year Waves Coming from Northerly Direction .. 49

Figure 8.3-50: Difference in Significant Wave Height (Hs) in Metres between 'Baseline' and Wind Farm 'DBD Option' for 1 in 1 Year Waves Coming from Easterly Direction 50
Figure 8.3-51: Difference in Significant Wave Height (Hs) in Metres between 'Baseline' and Wind Farm 'DBD Option' for 1 in 1 Year Waves Coming from Northerly Direction .. 51
Figure 8.3-52: Difference in Significant Wave Height (Hs) in Metres between 'Baseline' and Wind Farm 'DBD Option' for 1 in 100 Year Waves Coming from Easterly Direction. 52
Figure 8.3-53: Difference in Significant Wave Height (Hs) in Percent between 'Baseline' and Wind Farm 'DBD Option' for Waves Coming from Northerly Direction with Occurring Probability of 50 Percentile 53
Figure 8.3-54: Difference in Significant Wave Height (Hs) in Percent between 'Baseline' and Wind Farm 'DBD Option' for Waves Coming from Easterly Direction with Occurring Probability of 50 Percentile 54
Figure 8.3-55: Difference in Significant Wave Height (Hs) in Percent between 'Baseline' and Wind Farm 'DBD Option' for 1 in 1 Year Waves Coming from Northerly Direction .. 55
Figure 8.3-56: Difference in Significant Wave Height (Hs) in Percent between 'Baseline' and Wind Farm 'DBD Option' for 1 in 1 Year Waves Coming from Easterly Direction 56
Figure 8.3-57: Difference in Significant Wave Height (Hs) in Percent between 'Baseline' and Wind Farm 'DBD Option' for 1 in 1 Year Waves Coming from Northerly Direction .. 57
Figure 8.3-58: Difference in Significant Wave Height (Hs) in Percent between 'Baseline' and Wind Farm 'DBD Option' for 1 in 1 Year Waves Coming from Easterly Direction 58
Figure 8.3-59: Difference in Significant Wave Height (Hs) in Metres between 'Baseline' and Wind Farm 'Scenario 1' for Waves Coming from Northerly Direction with Occurring Probability of 50 Percentile 60
Figure 8.3-60: Difference in Significant Wave Height (Hs) in Metres between 'Baseline' and Wind Farm 'Scenario 1' for Waves Coming from Easterly Direction with Occurring Probability of 50 Percentile 61
Figure 8.3-61: Difference in Significant Wave Height (Hs) in Metres between 'Baseline' and Wind Farm 'Scenario 2' for Waves Coming from Northerly Direction with Occurring Probability of 50 Percentile 62
Figure 8.3-62: Difference in Significant Wave Height (Hs) in Metres between 'Baseline' and Wind Farm 'Scenario 2' for Waves Coming from Easterly Direction with Occurring Probability of 50 Percentile 63
Figure 8.3-63: Difference in Significant Wave Height (Hs) in Percent between 'Baseline' and Wind Farm 'Scenario 1' for Waves Coming from Northerly Direction with Occurring Probability of 50 Percentile 64
Figure 8.3-64: Difference in Significant Wave Height (Hs) in Percent between 'Baseline' and Wind Farm 'Scenario 1' for Waves Coming from Easterly Direction with Occurring Probability of 50 Percentile 65
Figure 8.3-65: Difference in Significant Wave Height (Hs) in Percent between 'Baseline' and Wind Farm 'Scenario 2' for Waves Coming from Northerly Direction with Occurring Probability of 50 Percentile 66
Figure 8.3-66: Difference in Significant Wave Height (Hs) in Percent between 'Baseline' and Wind Farm 'Scenario 2' for Waves Coming from Easterly Direction with Occurring Probability of 50 Percentile 67

Figure 8.3-67: Difference in Significant Wave Height (Hs) in Metres between 'Baseline' and Wind Farm 'Scenario 1' for 1 in 1 Year Waves Coming from Northerly Direction 68
Figure 8.3-68: Difference in Significant Wave Height (Hs) in Metres between 'Baseline' and Wind Farm 'Scenario 1' for 1 in 1 Year Waves Coming from Easterly Direction 69
Figure 8.3-69: Difference in Significant Wave Height (Hs) in Metres between 'Baseline' and Wind Farm 'Scenario 2' for 1 in 1 Year Waves Coming from Northerly Direction 70
Figure 8.3-70: Difference in Significant Wave Height (Hs) in Metres between 'Baseline' and Wind Farm 'Scenario 2' for 1 in 1 Year Waves Coming from Easterly Direction 71
Figure 8.3-71: Difference in Significant Wave Height (Hs) in Percent between 'Baseline' and Wind Farm 'Scenario 1' for 1 in 1 Year Waves Coming from Northerly Direction 72
Figure 8.3-72: Difference in Significant Wave Height (Hs) in Percent between 'Baseline' and Wind Farm 'Scenario 1' for 1 in 1 Year Waves Coming from Easterly Direction 73
Figure 8.3-73: Difference in Significant Wave Height (Hs) in Percent between 'Baseline' and Wind Farm 'Scenario 2' for 1 in 1 Year Waves Coming from Northerly Direction 74
Figure 8.3-74: Difference in Significant Wave Height (Hs) in Percent between 'Baseline' and Wind Farm 'Scenario 2' for 1 in 1 Year Waves Coming from Easterly Direction 75
Figure 8.3-75: Computational Mesh of the Regional HD Model 78
Figure 8.3-76: Regional HD Model Bathymetry 79
Figure 8.3-77: Local Model Computational Mesh 80
Figure 8.3-78: Bathymetry of Local Model Domain (with Tidal Gauges and Current Stations Marked) 81
Figure 8.3-79: Time Series Comparison between Simulated and Observed Water Levels at North Shields in June 2012 (Regional Model) 82
Figure 8.3-80: Time Series Comparison between Simulated and Observed Water Levels at North Shields in December 2012 (Regional Model) 82
Figure 8.3-81: Time Series Comparison between Simulated and Observed Water Levels at Whitby in June 2012 (Regional Model) 83
Figure 8.3-82: Time Series Comparison between Simulated and Observed Water Levels at Whitby in December 2012 (Regional Model) 83
Figure 8.3-83: Time Series Comparison between Simulated and Observed Water Levels at Cromer in June 2012 (Regional Model) 83
Figure 8.3-84: Time Series Comparison between Simulated and Observed Water Levels at Cromer in December 2012 (Regional Model) 84
Figure 8.3-85: Time Series Comparison between Simulated and Observed Water Levels at West Met Mast in June 2012 (Regional Model) 84
Figure 8.3-86: Time Series Comparison between Simulated and Observed Water Levels at West Met Mast in December 2012 (Regional Model) 84
Figure 8.3-87: Time Series Comparison between Simulated and Observed Water Levels at East Met Mast in June 2012 (Regional Model) 85
Figure 8.3-88: Time Series Comparison between Simulated and Observed Water Levels at East Met Mast in December 2012 (Regional Model) 85
Figure 8.3-89: Time Series Comparison between Simulated and Observed Water Levels at North Dogger in June 2012 (Regional Model) 85
Figure 8.3-90: Time Series Comparison between Simulated and Observed Water Levels at West Met Mast in June 2012 (Local Model) 86

Figure 8.3-91: Time Series Comparison between Simulated and Observed Water Levels at West Met Mast in December 2012 (Local Model) 87
Figure 8.3-92: Time Series Comparison between Simulated and Observed Water Levels at East Met Mast in June 2012 (Local Model) 87
Figure 8.3-93: Time Series Comparison between Simulated and Observed Water Levels at East Met Mast in December 2012 (Local Model) 87
Figure 8.3-94: Time Series Comparison between Simulated and Observed Water Levels at North Dogger in June 2012 (Local Model) 88
Figure 8.3-95: Time Series Comparison between Simulated and Observed Current Speeds at West Met Mast in June 2012 (Local Model) 88
Figure 8.3-96: Time Series Comparison between Simulated and Observed Current Directions at West Met Mast in June 2012 (Local Model) 89
Figure 8.3-97: Time Series Comparison between Simulated and Observed Current Speeds at West Met Mast in December 2012 (Local Model) 89
Figure 8.3-98: Time Series Comparison between Simulated and Observed Current Directions at West Met Mast in December 2012 (Local Model) 89
Figure 8.3-99: Time Series Comparison between Simulated and Observed Current Speeds at East Met Mast in June 2012 (Local Model) 90
Figure 8.3-100: Time Series Comparison between Simulated and Observed Current Directions at East Met Mast in June 2012 (Local Model) 90
Figure 8.3-101: Time Series Comparison between Simulated and Observed Current Speeds at East Met Mast in December 2012 (Local Model) 90
Figure 8.3-102: Time Series Comparison between Simulated and Observed Current Directions at East Met Mast in December 2012 (Local Model) 91
Figure 8.3-103: Time Series Comparison between Simulated and Observed Current Speeds at North Dogger in June 2012 (Local Model) 91
Figure 8.3-104: Time Series Comparison between Simulated and Observed Current Directions at North Dogger in June 2012 (Local Model) 91
Figure 8.3-105: Modelled Water Levels at East Met Mast Adcp for A Period of 30 Days (Blue Frame Indicates Spring Tides and Red Frame Indicates Neap Tides) 92
Figure 8.3-106: Change in Maximum Current Speed over 30 Days (Layout B - Offshore Platform 2 - Baseline) 95
Figure 8.3-107: Change of Maximum Current Speed over 30 Days (Layout C- Offshore Platform 2 - Baseline) 96
Figure 8.3-108: Change of Maximum Current Speed over 30 Days (DBD Layout C / Offshore Platform Layout 2 with Cumulative Layout Scenario 1) 97
Figure 8.3-109: Change of Maximum Current Speed over 30 Days (DBD Layout C / Offshore Platform Layout 2 with cumulative layout Scenario 2) 98
Figure 8.3-110: Change of Maximum Current Speed over 30 Days (DBD Layout B / Offshore Platform Layout 2 with cumulative layout Scenario 1) 100
Figure 8.3-111: Change of Maximum Current Speed over 30 Days (DBD Layout B / Offshore Platform Layout 2 with cumulative layout Scenario 2) 101
Figure 8.3-112: Offshore Export Cable Route (Option 1) (thick line shows where levelling is required) 103

Figure 8.3-113: Offshore Export Cable Route (Option 2) (thick line shows where levelling is required) 103
Figure 8.3-114: Locations of Time Series Plots of Predicted Suspended Sediment Concentration.....107
Figure 8.3-115: Locations where Plume Size Estimated (Contours are Maximum Suspended Sediment Concentration in Bottom Layer – Export Cable Route Option 1 – Trenching) 110
Figure 8.3-116: Locations where Plume Size Estimated (Contours are Maximum Suspended Sediment Concentration in Bottom Layer – Export Cable Route Option 2 – Trenching) 111

List of Acronyms

Acronym	Definition
3D	Three Dimensional
ADCP	Acoustic Doppler Current Profiler
BODC	British Oceanographic Data Centre
CD (or mCD)	Chart Datum (or meter above Chart Datum)
CIRIA	Construction Industry Research and Information Association
cm	Centimetre
CSD	Cutter Suction Dredger
Danish Hydraulic Institute	DHI
DBA	Dogger Bank A
DBB	Dogger Bank B
DBC	Dogger Bank C
DBD	Dogger Bank D
DBS	Dogger Bank South
DCO	Development Consent Order
^{0}	Degrees
degN	Degrees North
DHI	Danish Hydraulic Institute
DSD	Directional Standard Deviation
ECMRWF	European Centre for Medium-Range Weather Forecasts
ECC	Export Cable Corridor
ES	Environmental Statement
Hs	Significant Wave Height
km	Kilometre

Acronym	Definition
m	Metre
MAE	Mean Absolute Error
ME	Mean Error
mg/l	Milligrams per litre
MHWS	Mean High Water Spring
mm	Millimetre
m/s	Metres per second
MWD	Mean Wave Direction
N	North
NE	North-East
NW	North-West
OSP	Offshore Substation Platform
%	Percent
PEIR	Preliminary Environmental Information Report
R	Coefficient of Determination
SE	South-East
Std	Standard deviation of Residuals
SW	South-West
Tp	Spectral Peak Period
TSHD	Trailer Suction Hopper Dredger

Appendix A: Hydrodynamic Modelling Baseline Run Results

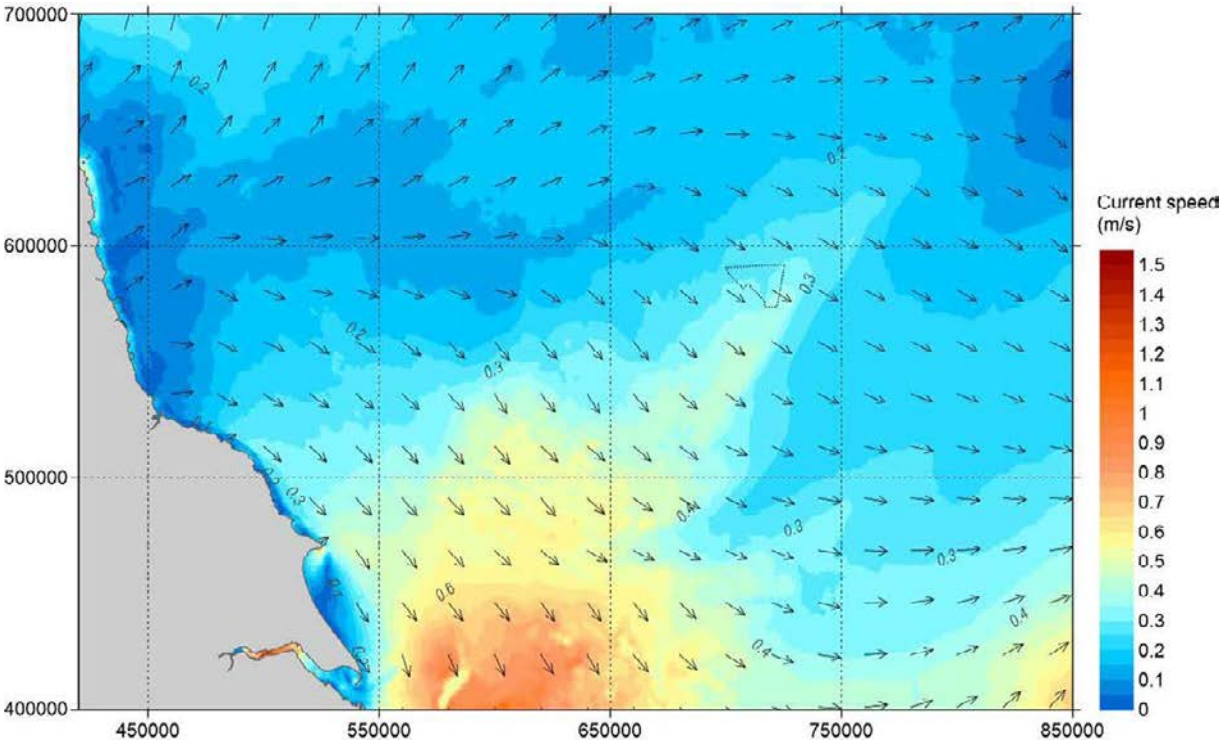

Figure A.1 Overview of Spatial Variation of Peak South-east-going Currents in a Spring Tide – Baseline

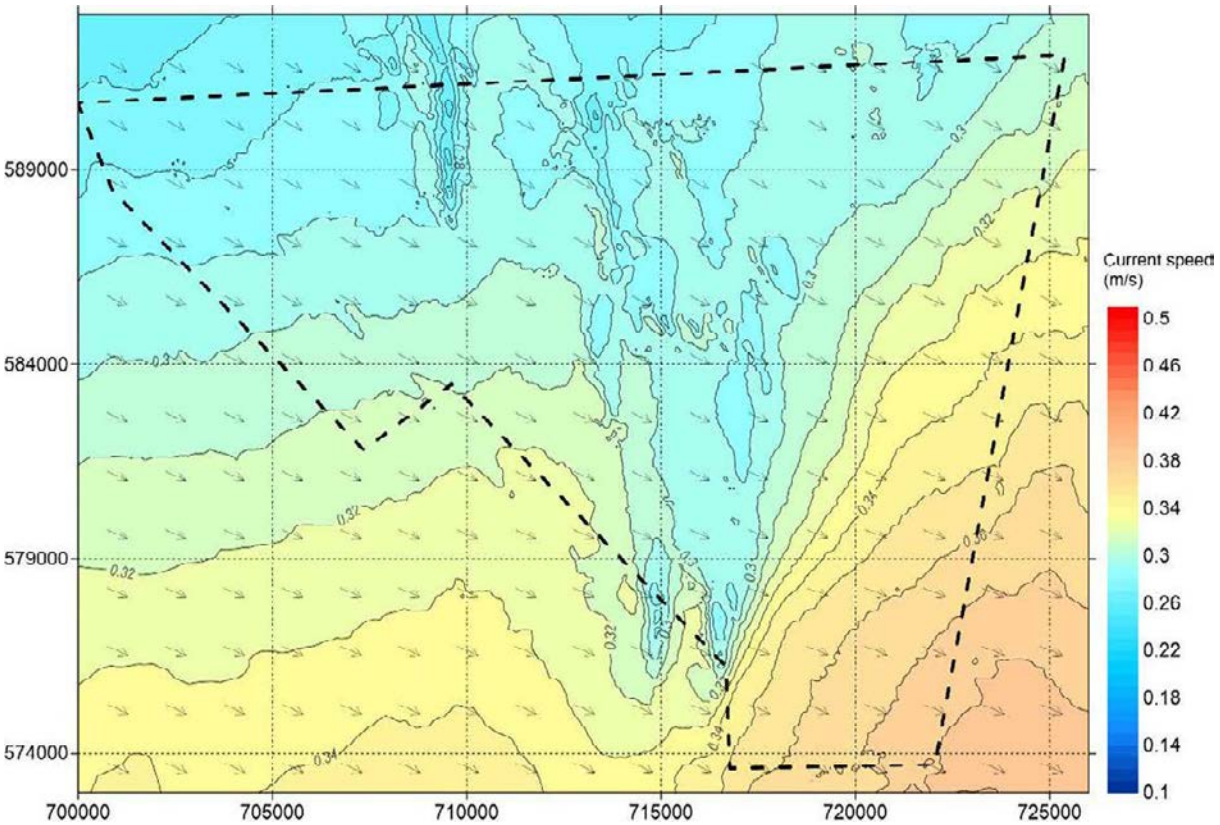

Figure A.2 A Closer View of Spatial Variation of Peak South-east-going Currents in a Spring Tide - Baseline

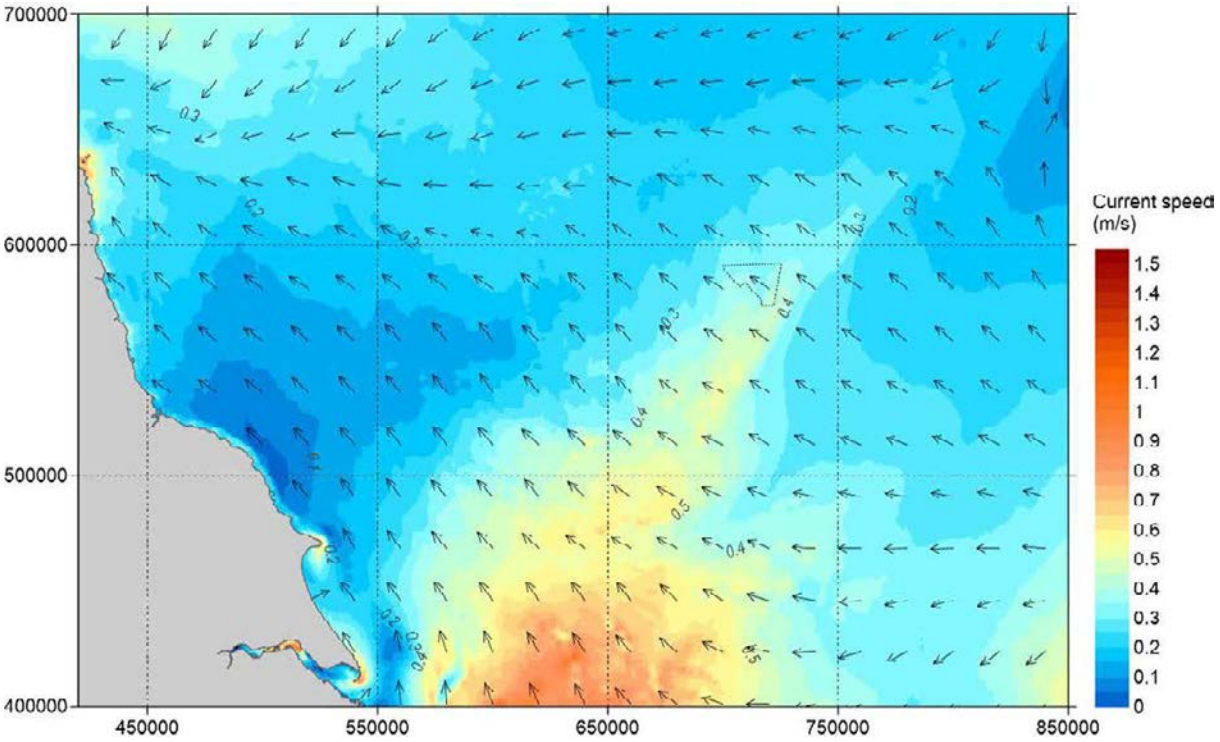

Figure A.3 Overview of Spatial Variation of Peak South-east-going Currents in a Spring Tide - Baseline (Dotted Line Indicates DBD Layout C Which is Not Included in Baseline)

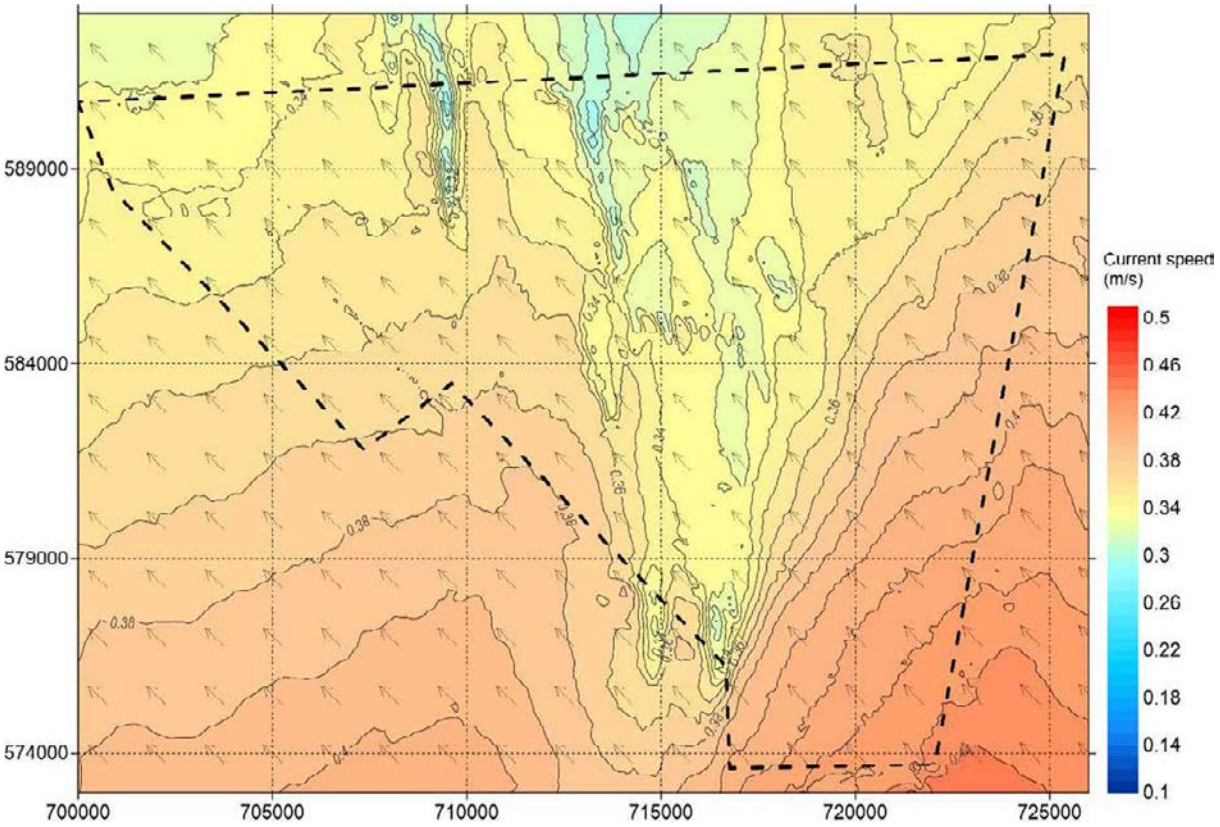

Figure A.4 A Closer View of Spatial Variation of Peak North-west-going Currents in a Spring Tide – Baseline (Dotted Line Indicates DBD Layout C Which is Not Included in Baseline)

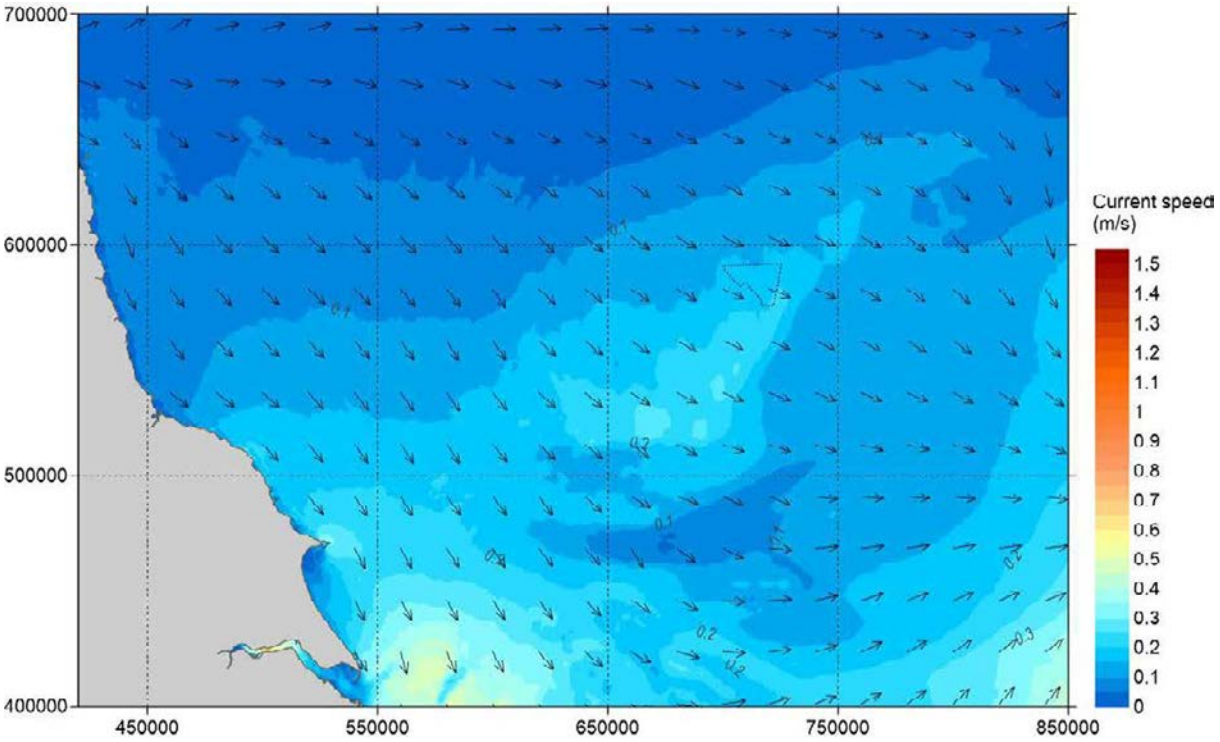

Figure A.5 Overview of Spatial Variation of Peak South-east-going Currents in a Neap Tide – Baseline (Dotted Line Indicates DBD Layout C Which is Not Included in Baseline)

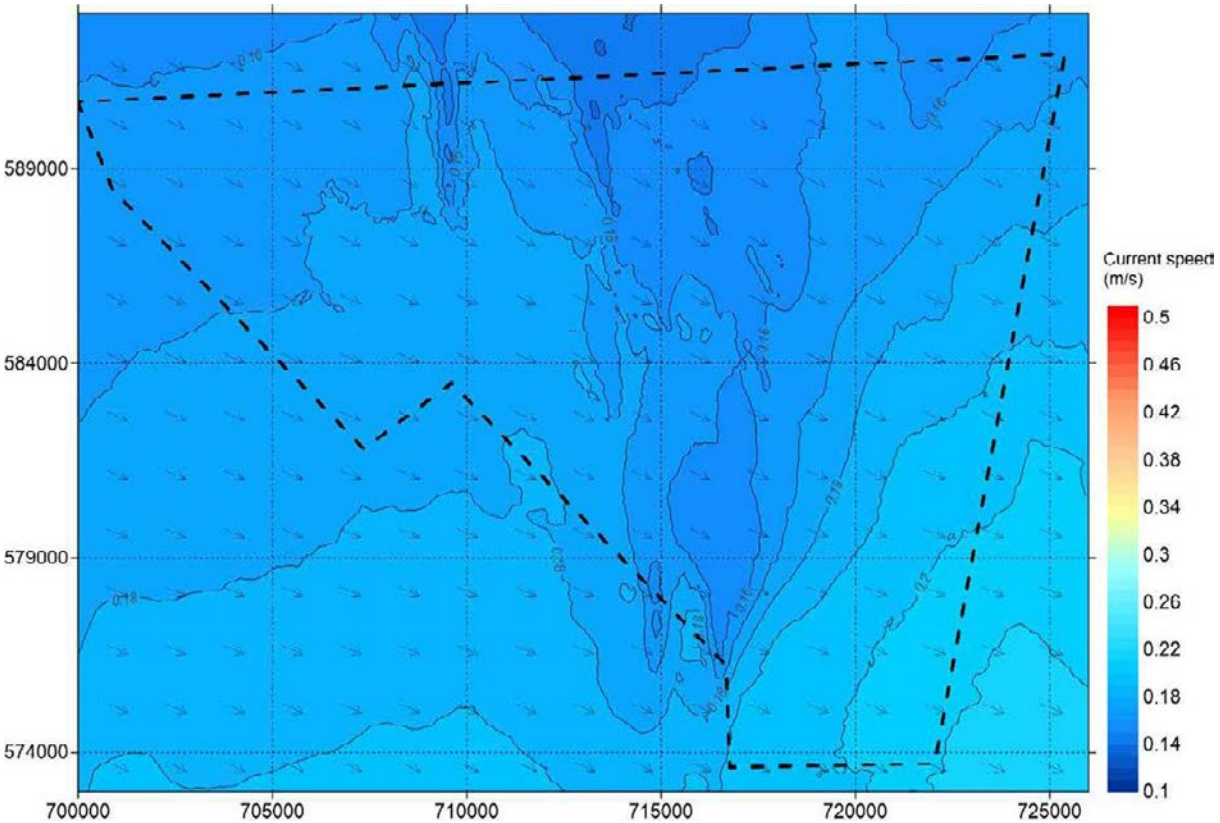

Figure A.6 A Closer View of Spatial Variation of Peak South-east-going Currents in a Neap Tide – Baseline (Dotted Line Indicates DBD Layout C Which is Not Included in Baseline)

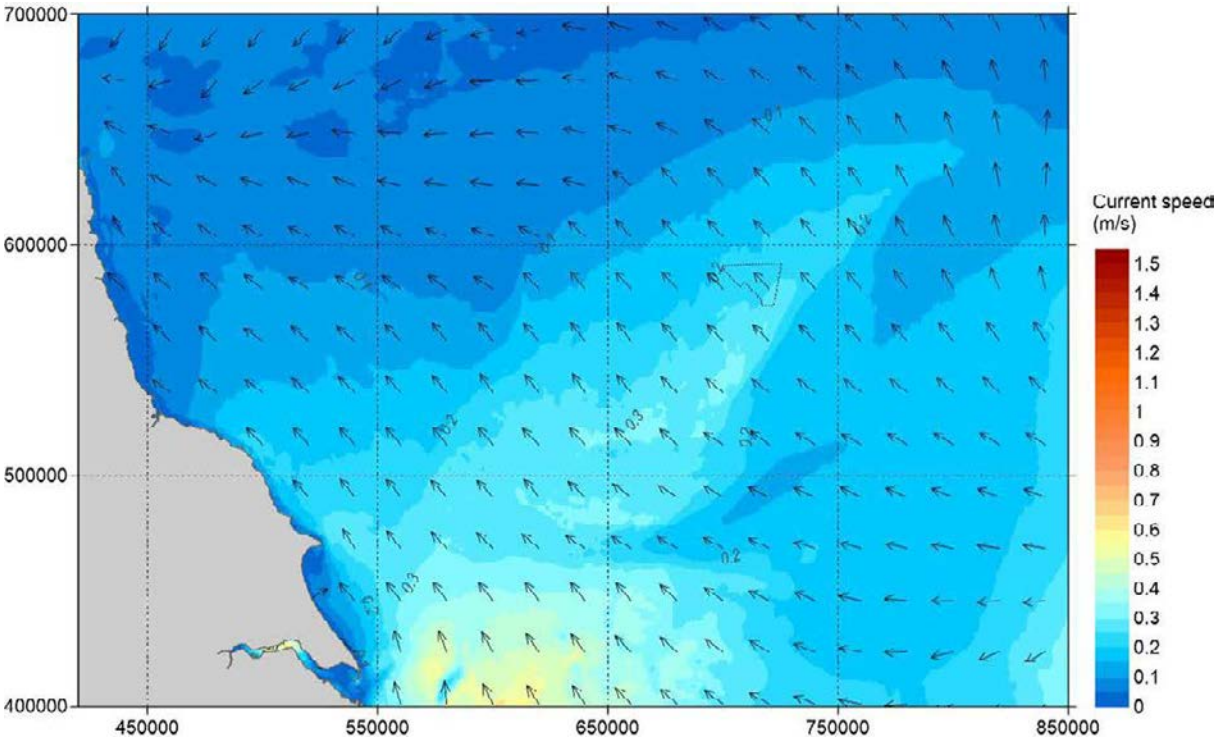

Figure A.7 Overview of Spatial Variation of Peak North-west-going Currents in a Neap Tide – Baseline (Dotted Line Indicates DBD Layout C Which is Not Included in Baseline)

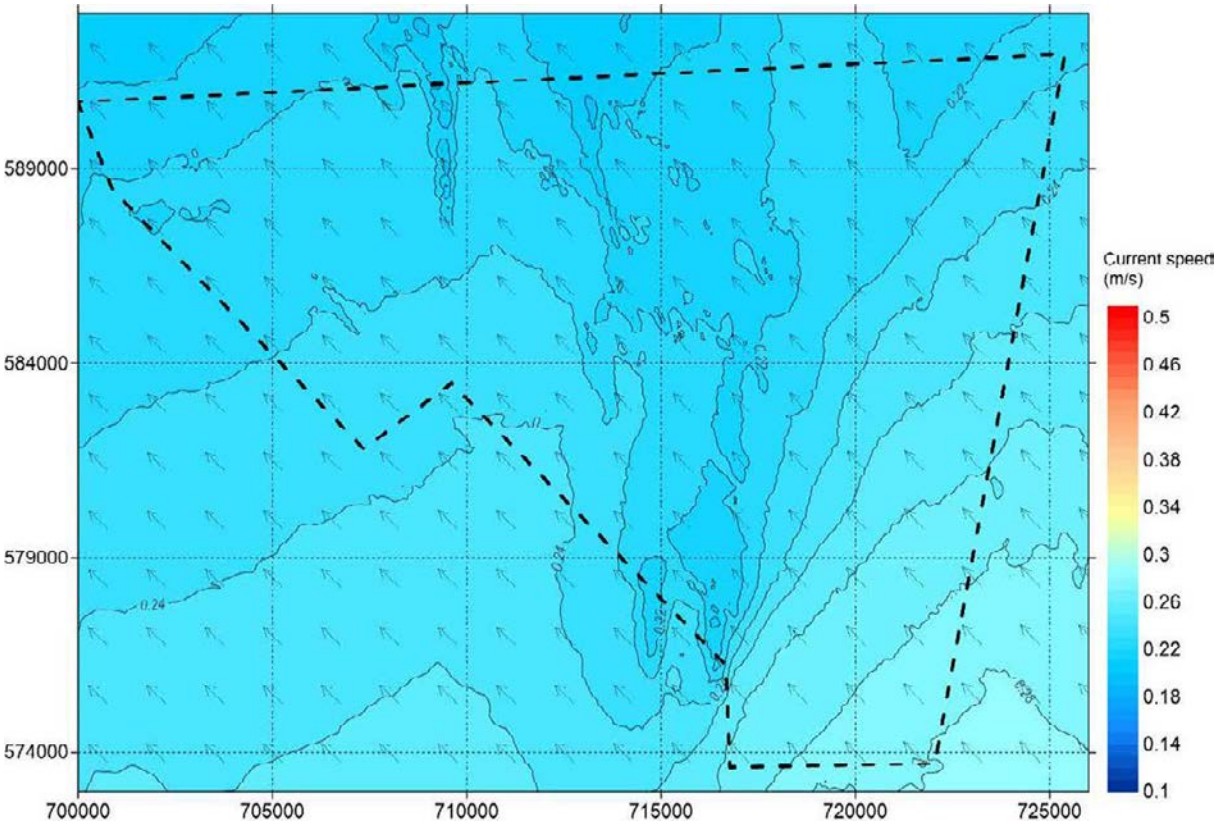

Figure A.8 A Closer View of Spatial Variation of Peak North-west-going Currents in a Neap Tide – Baseline (Dotted Line Indicates DBD Layout C Which is Not Included in Baseline)

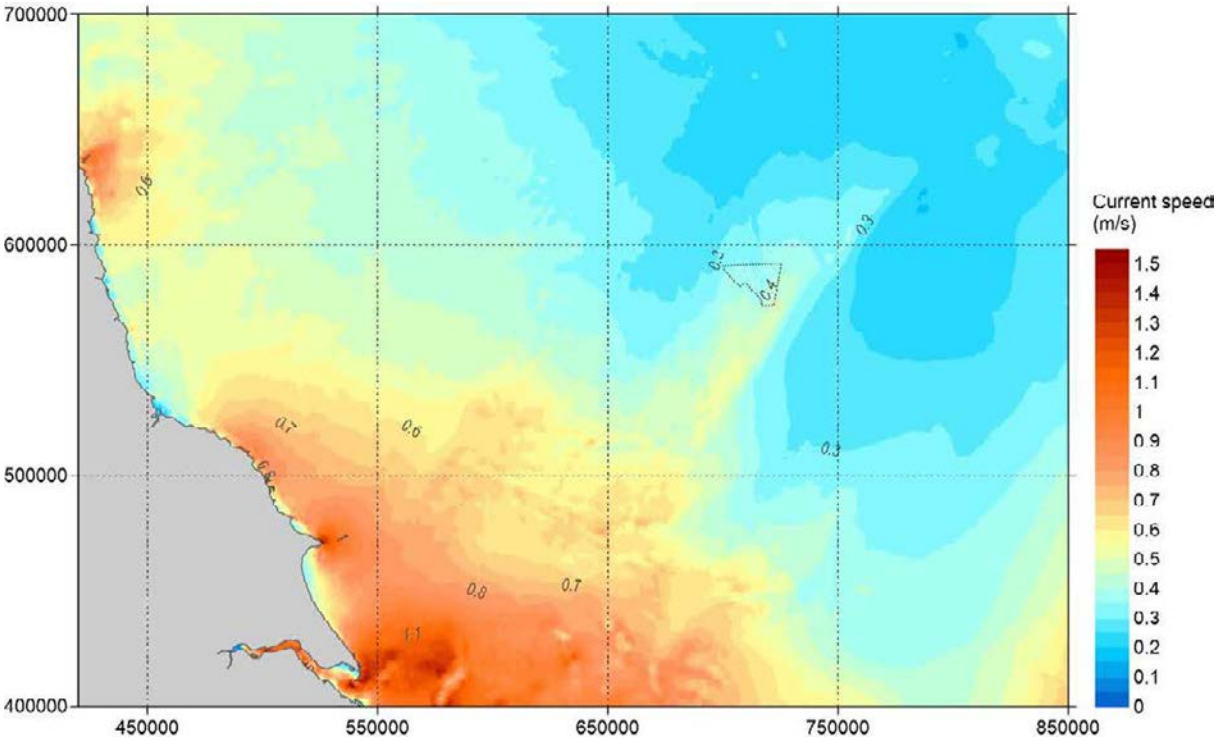

Figure A.9 Overview of Spatial Variation of Maximum current Speed Over 30 days- Baseline (Dotted Line Indicates DBD Layout C Which is Not Included in Baseline)

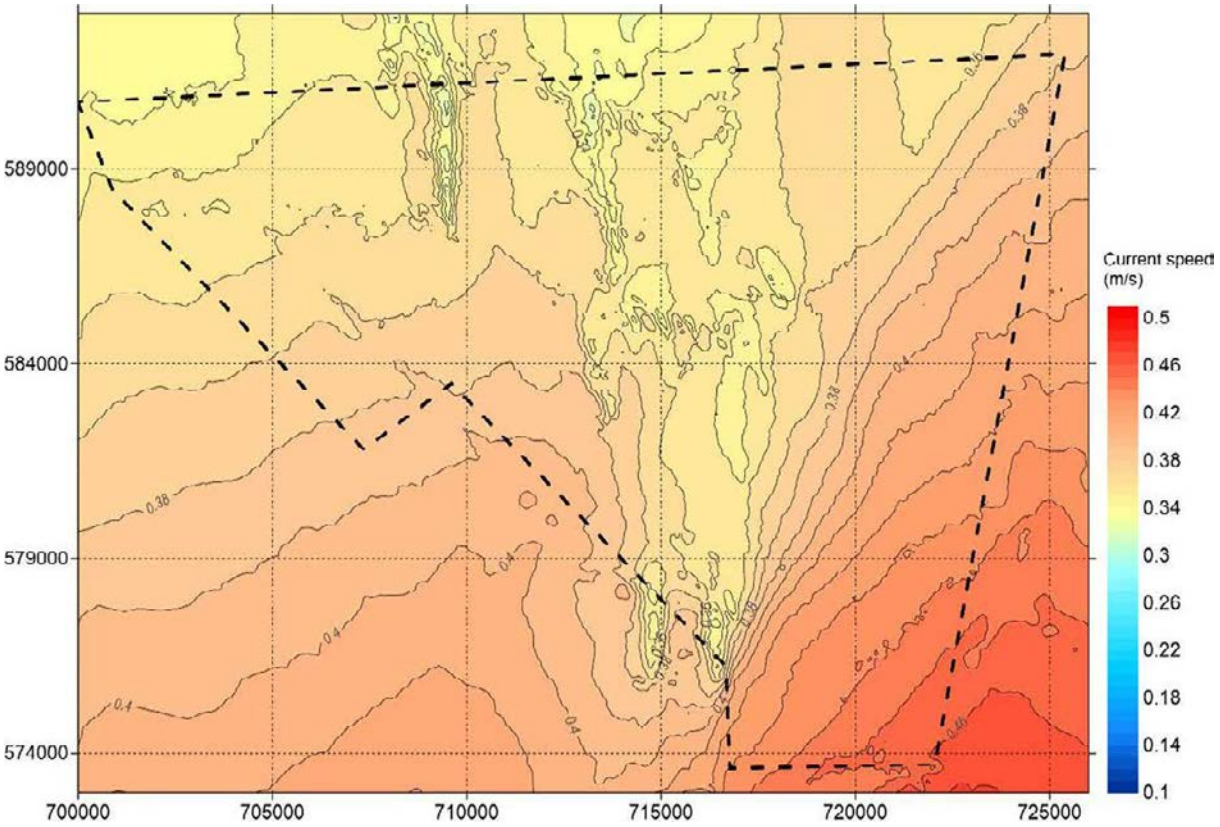

Figure A.10 A Closer View of Spatial Variation of Maximum Current Speed Over 30 days- Baseline (Dotted Line Indicates DBD Layout C Which is Not Included in Baseline)

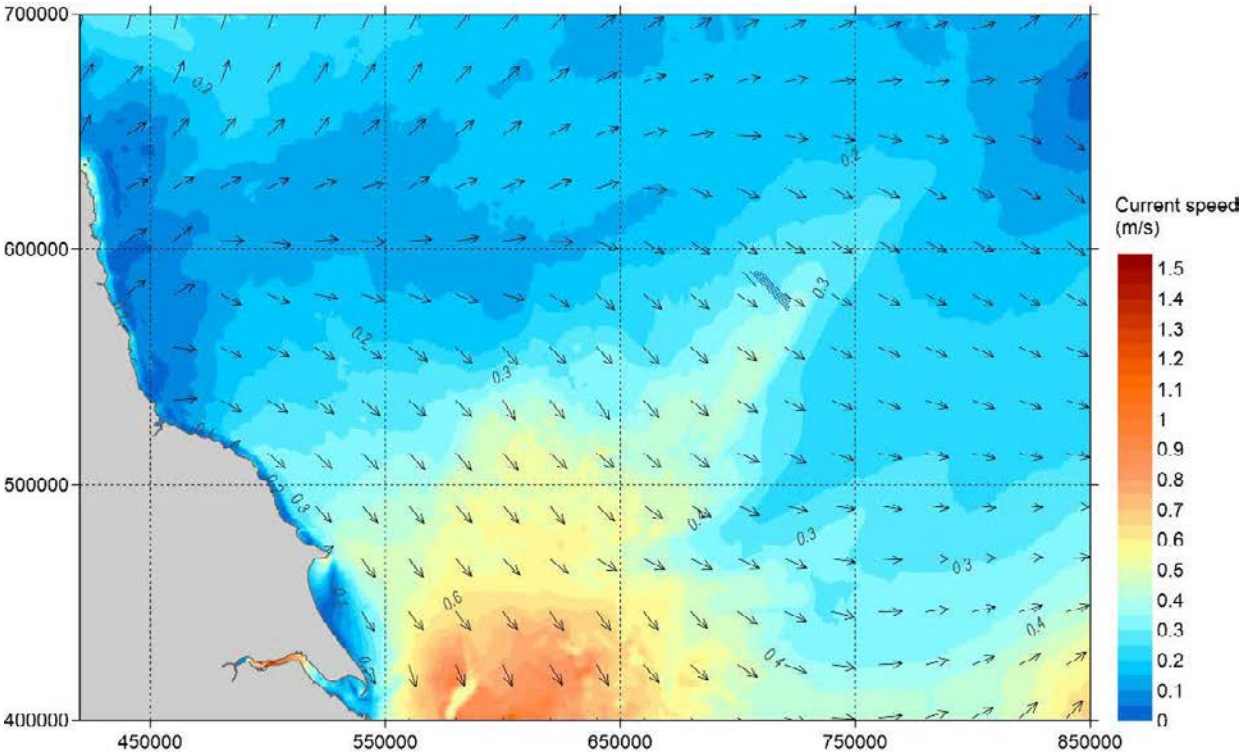

Figure A.11 Overview of Spatial Variation of Peak South-east-going Currents in a Spring Tide – Layout A – OSP 1

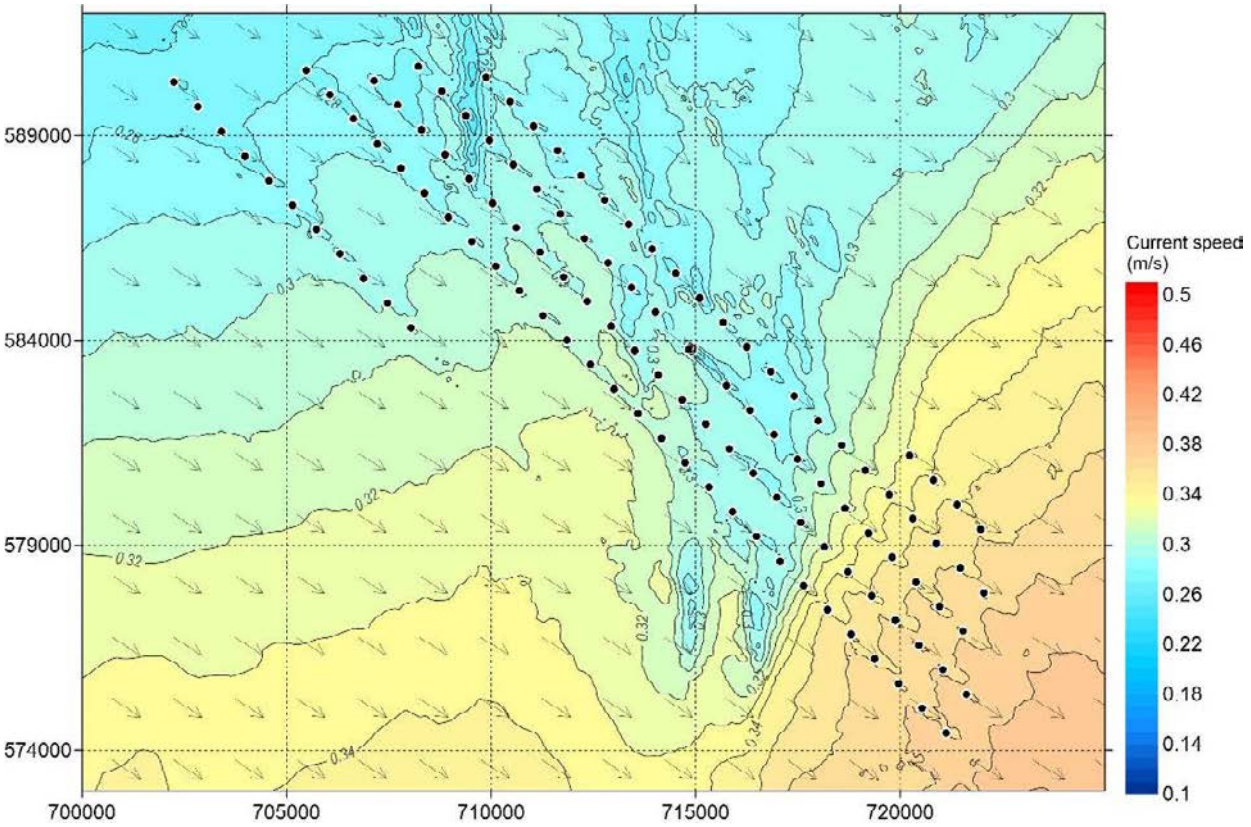

Figure A.12 A Closer View of Spatial Variation of Peak South-east-going Currents in a Spring Tide – Layout A – OSP 1

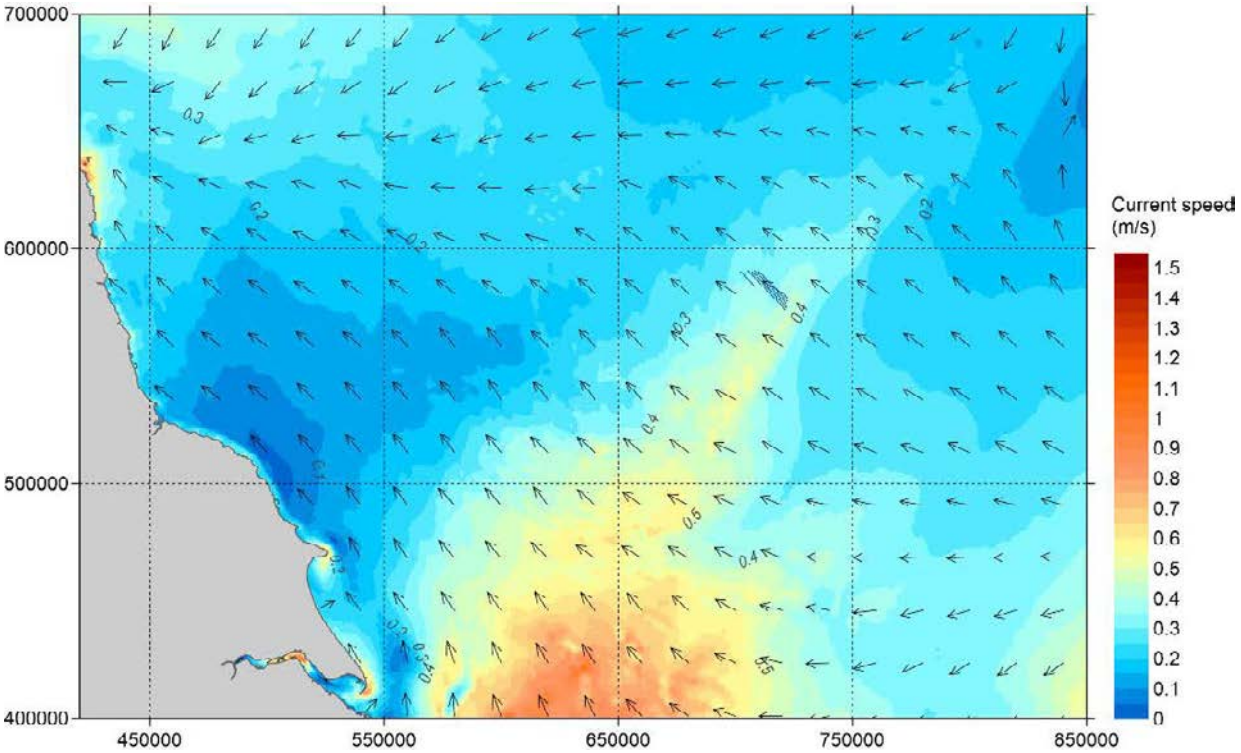

Figure A.13 Overview of Spatial Variation of Peak North-west-going Currents in a Spring Tide – Layout A – OSP 1

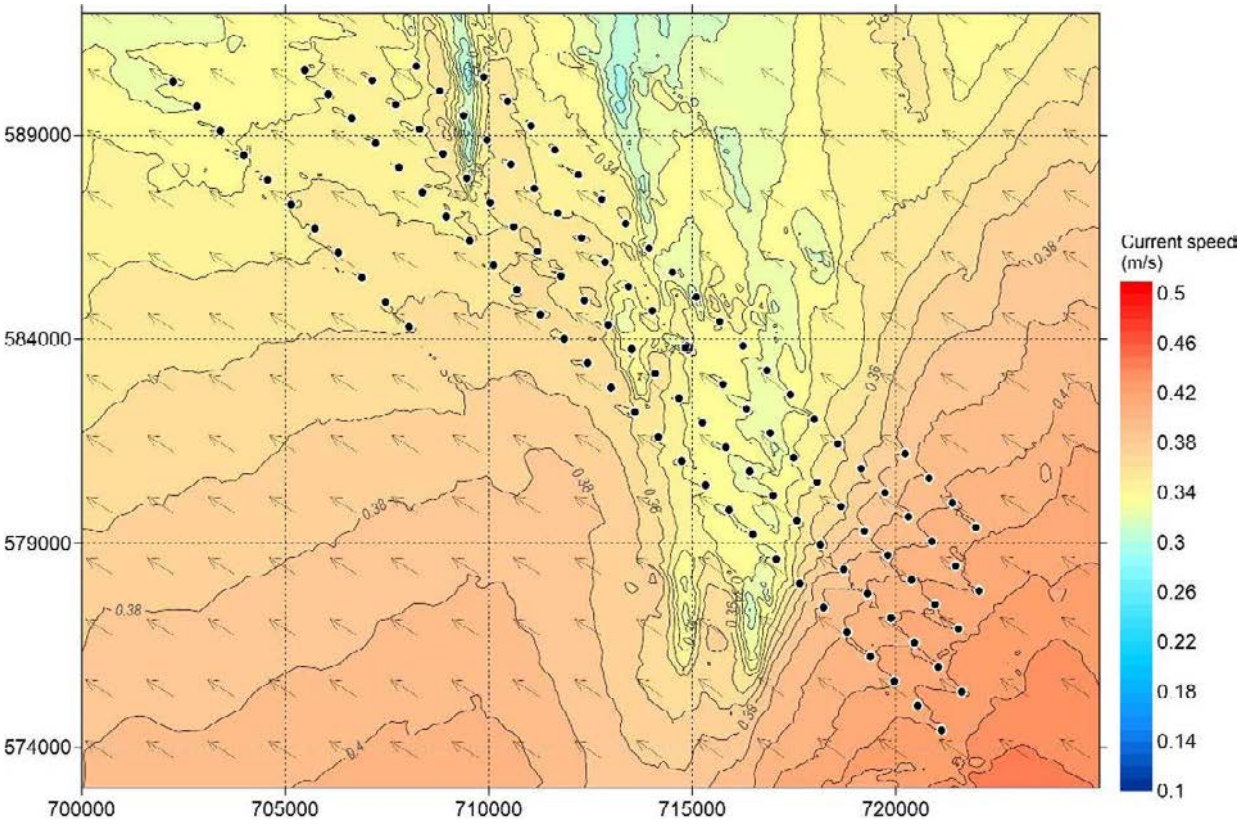

Figure A.14 A Closer View of Spatial Variation of Peak North-west-going Currents in a Spring Tide – Layout A – OSP 1

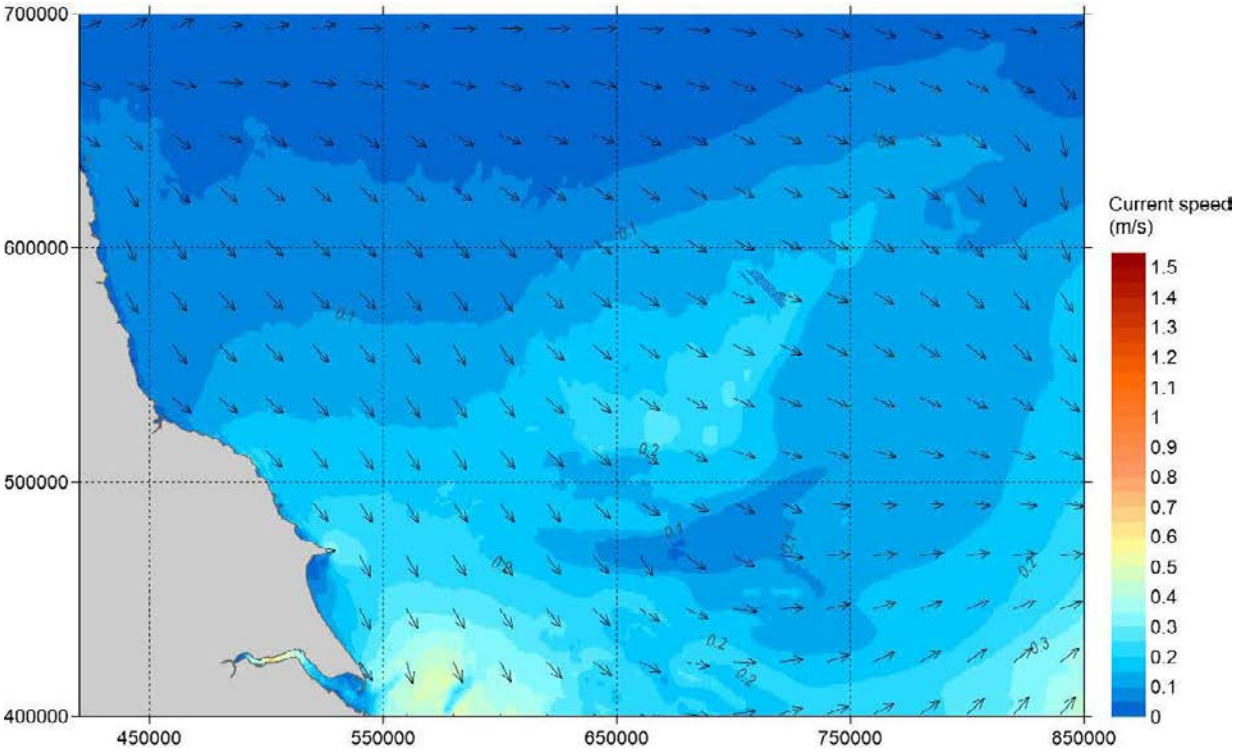

Figure A.15 Overview of Spatial Variation of Peak South-east-going Currents in a Neap Tide – Layout A – OSP 1

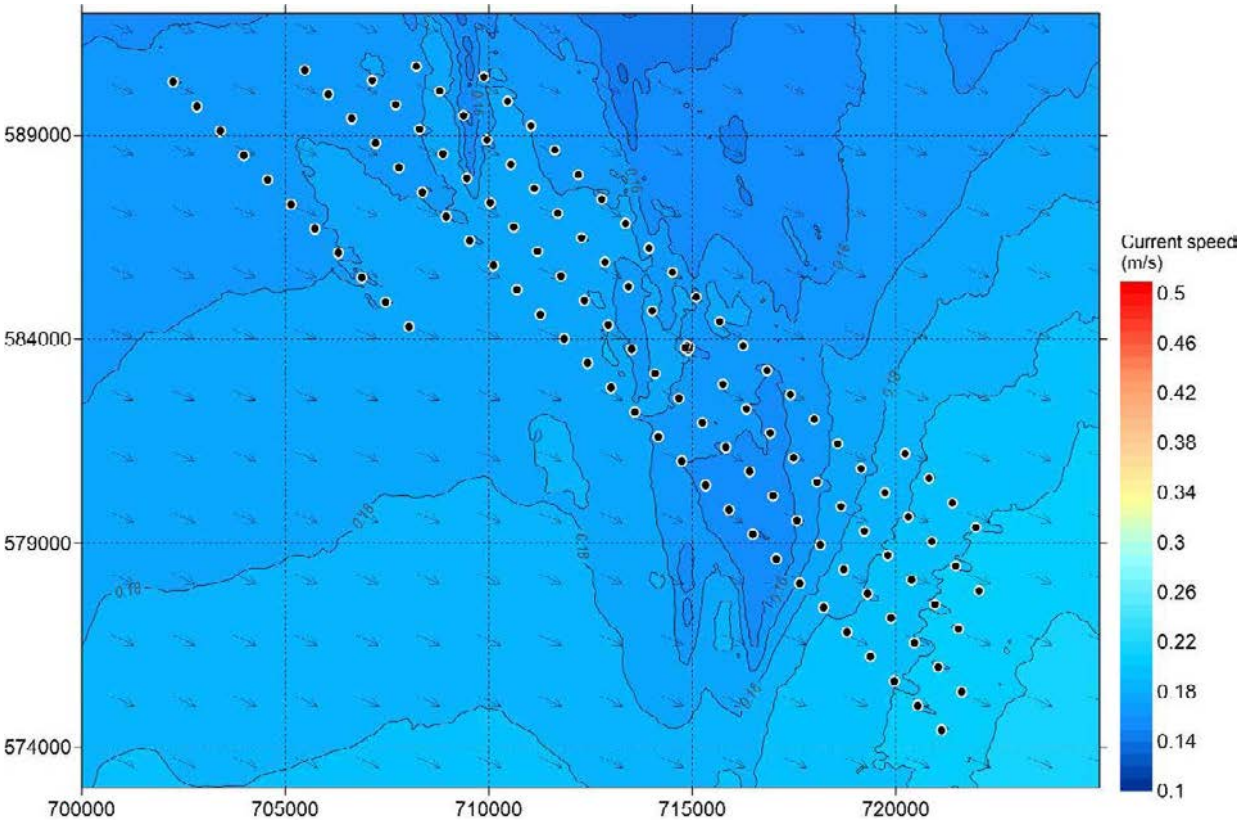

Figure A.16 Overview of Spatial Variation of Peak South-east-going Currents in a Neap Tide – Layout A – OSP 1

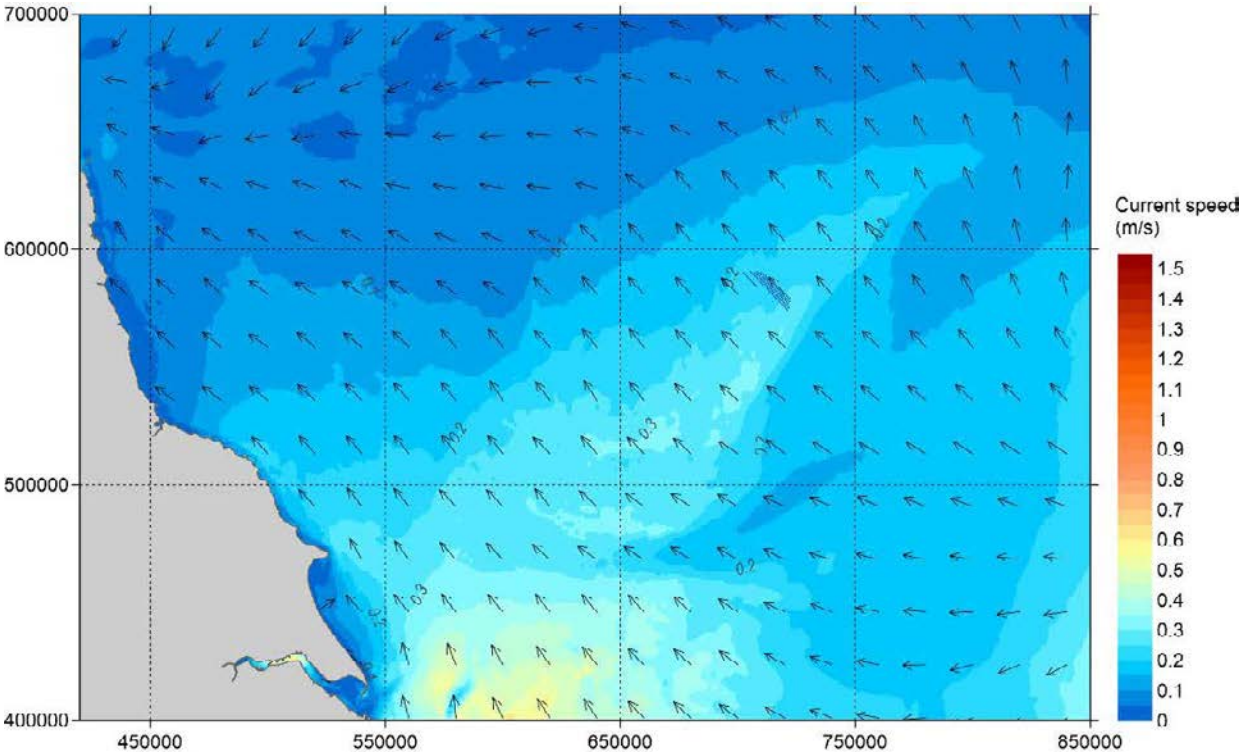

Figure A.17 Overview of Spatial Variation of Peak North-west-going Currents in a Neap Tide – Layout A – OSP 1

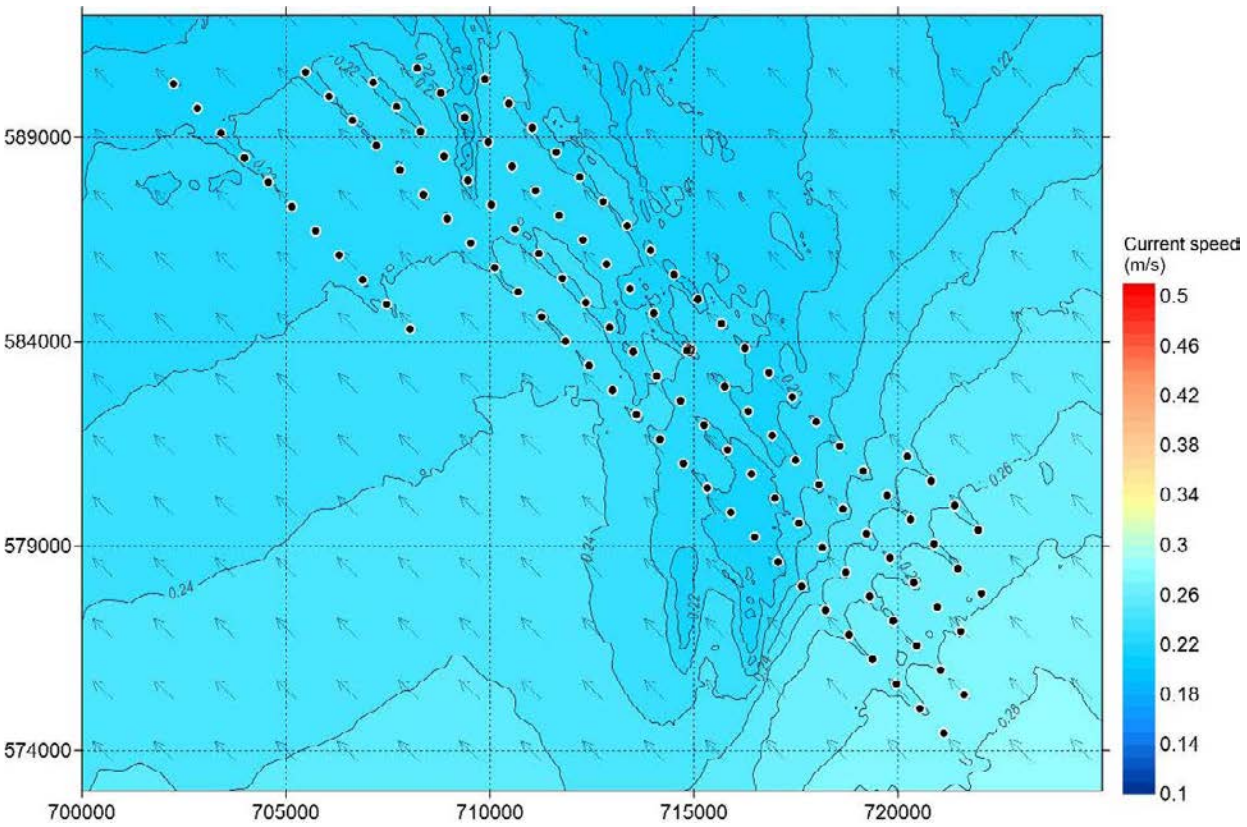

Figure A.18 Overview of Spatial Variation of Peak South-east-going Currents in a Neap Tide – Layout A – OSP 1

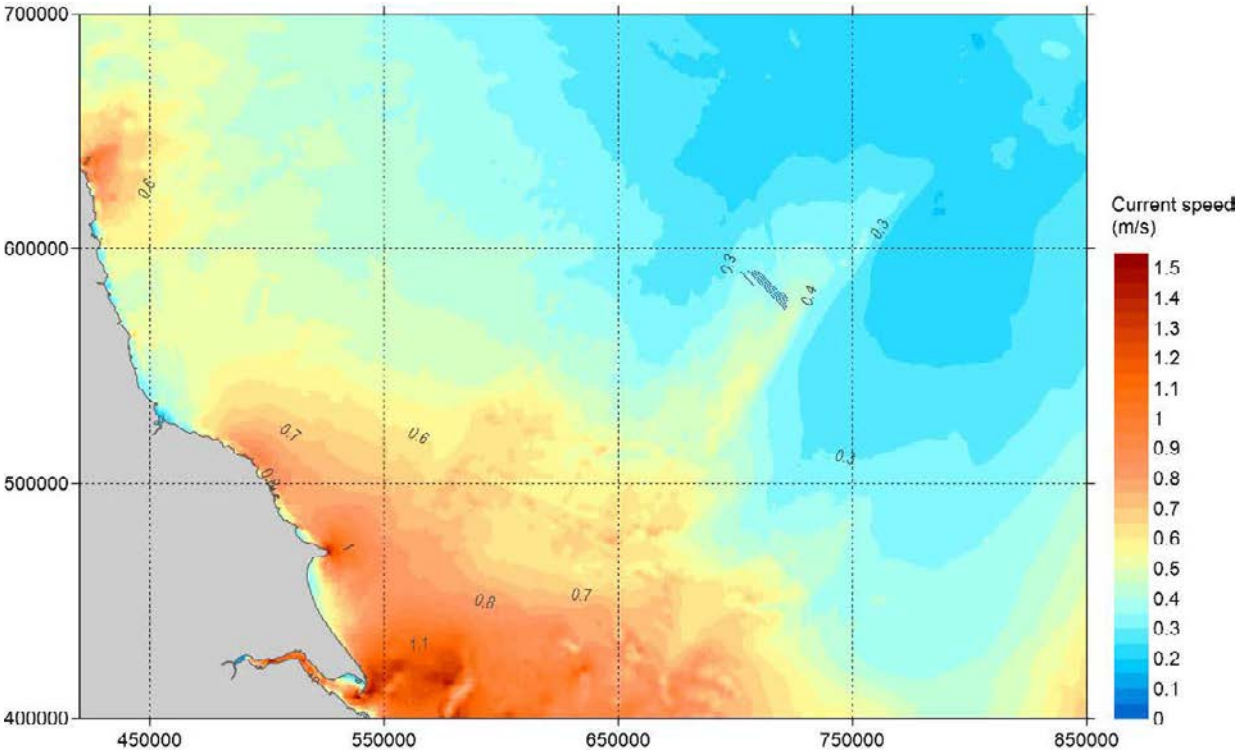

Figure A.19 Overview of Spatial Variation of Maximum Current Speed Over 30 days- Layout A – OSP 1

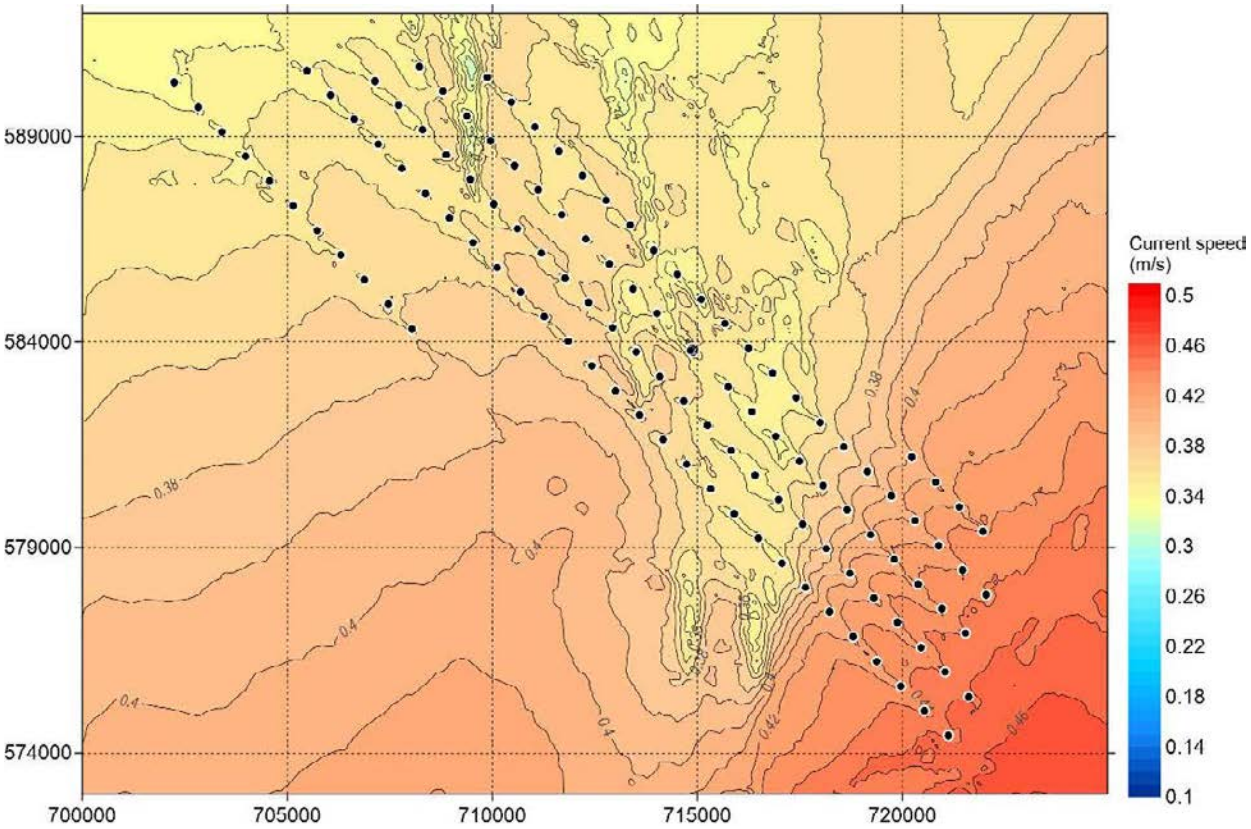

Figure A.20 Overview of Spatial Variation of Maximum Current Speed Over 30 days- Layout A – OSP 1

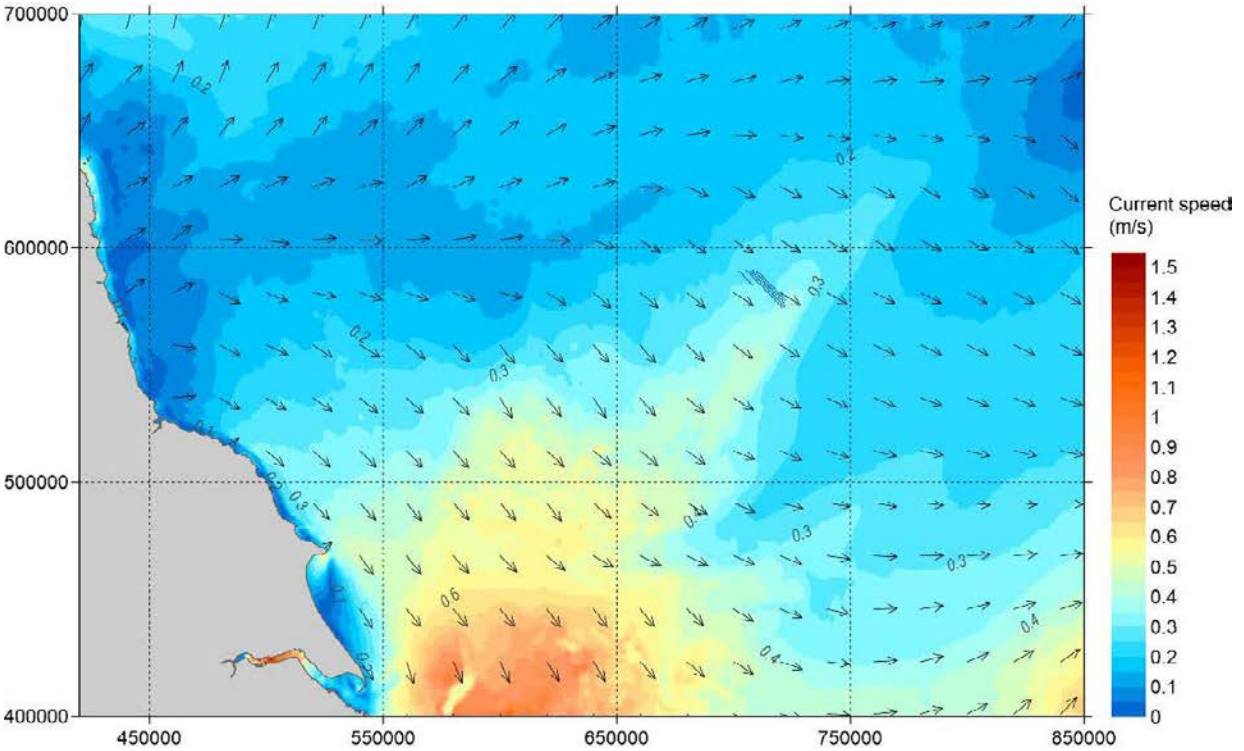

Figure A.21 Overview of Spatial Variation of Peak South-east-going Currents in a Spring Tide – Layout A – OSP 2

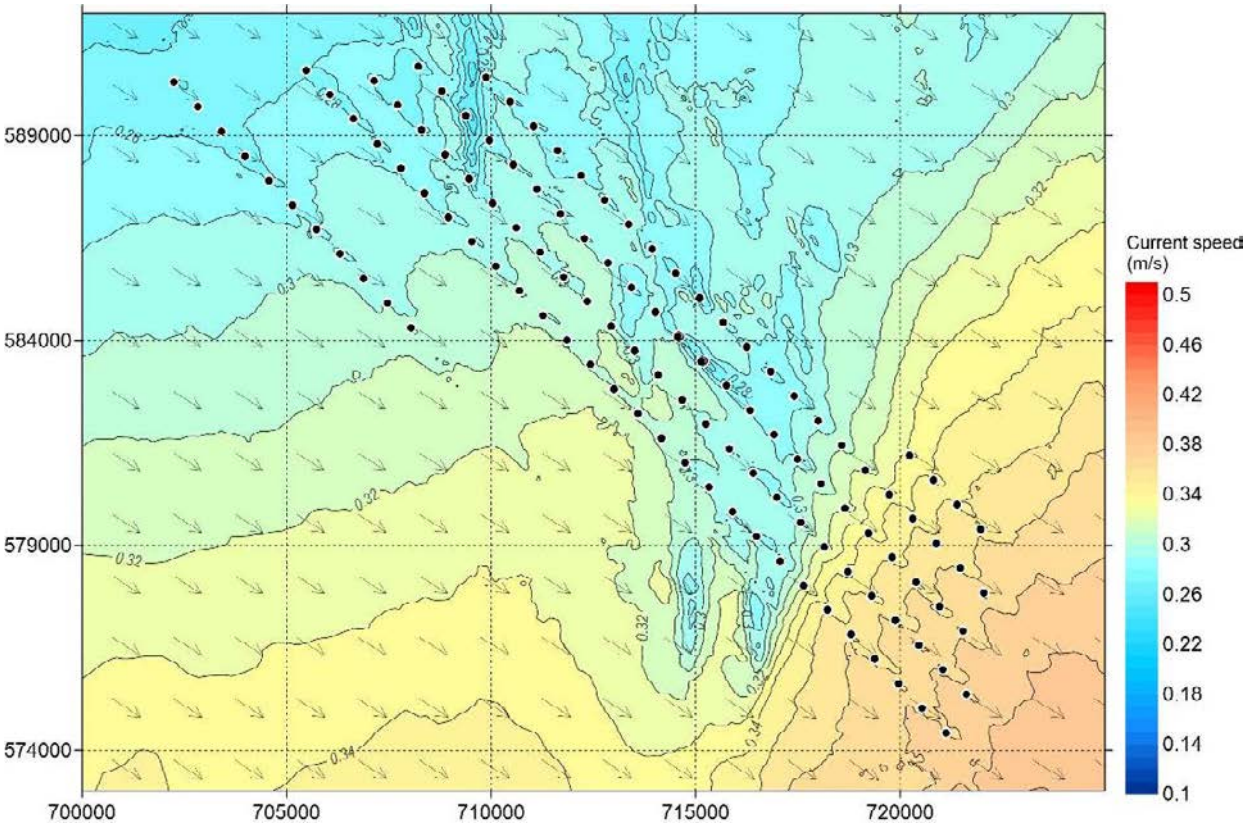

Figure A.22 A Closer View of Spatial Variation of Peak South-east-going Currents in a Spring Tide – Layout A – OSP 2

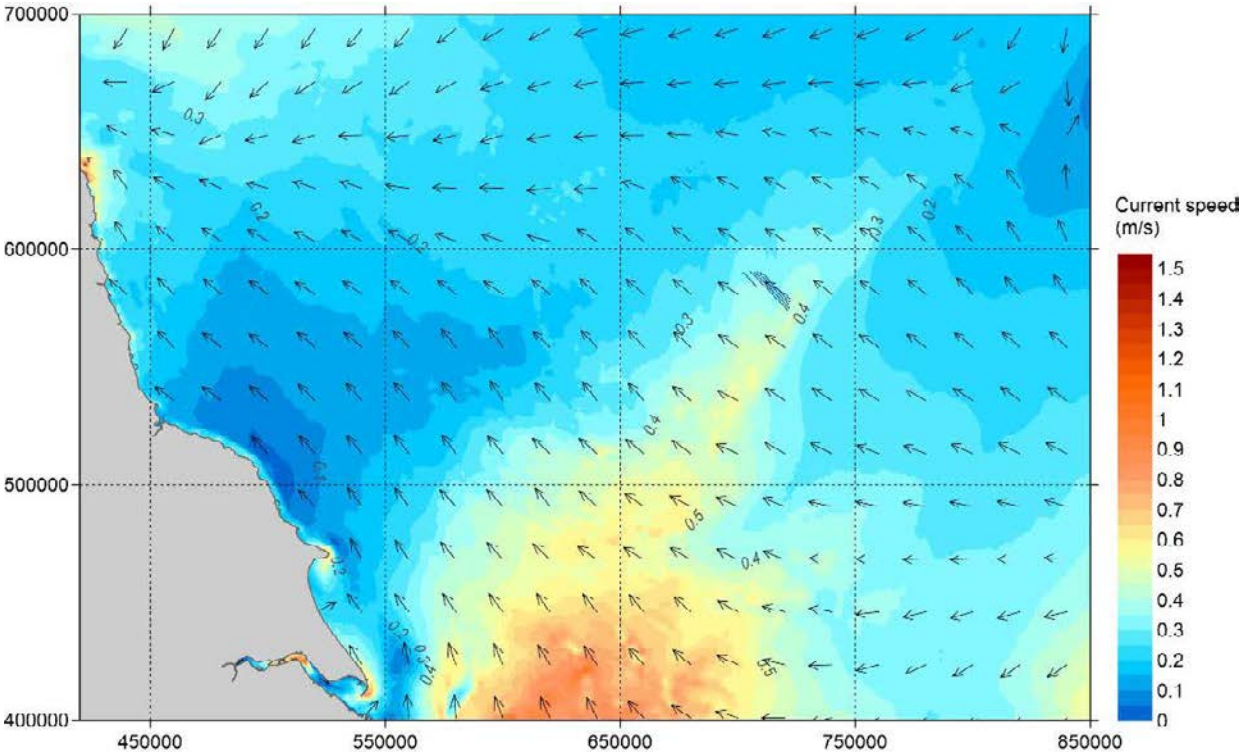

Figure A.23 Overview of Spatial Variation of Peak North-west-going Currents in a Spring Tide – Layout A – OSP 2

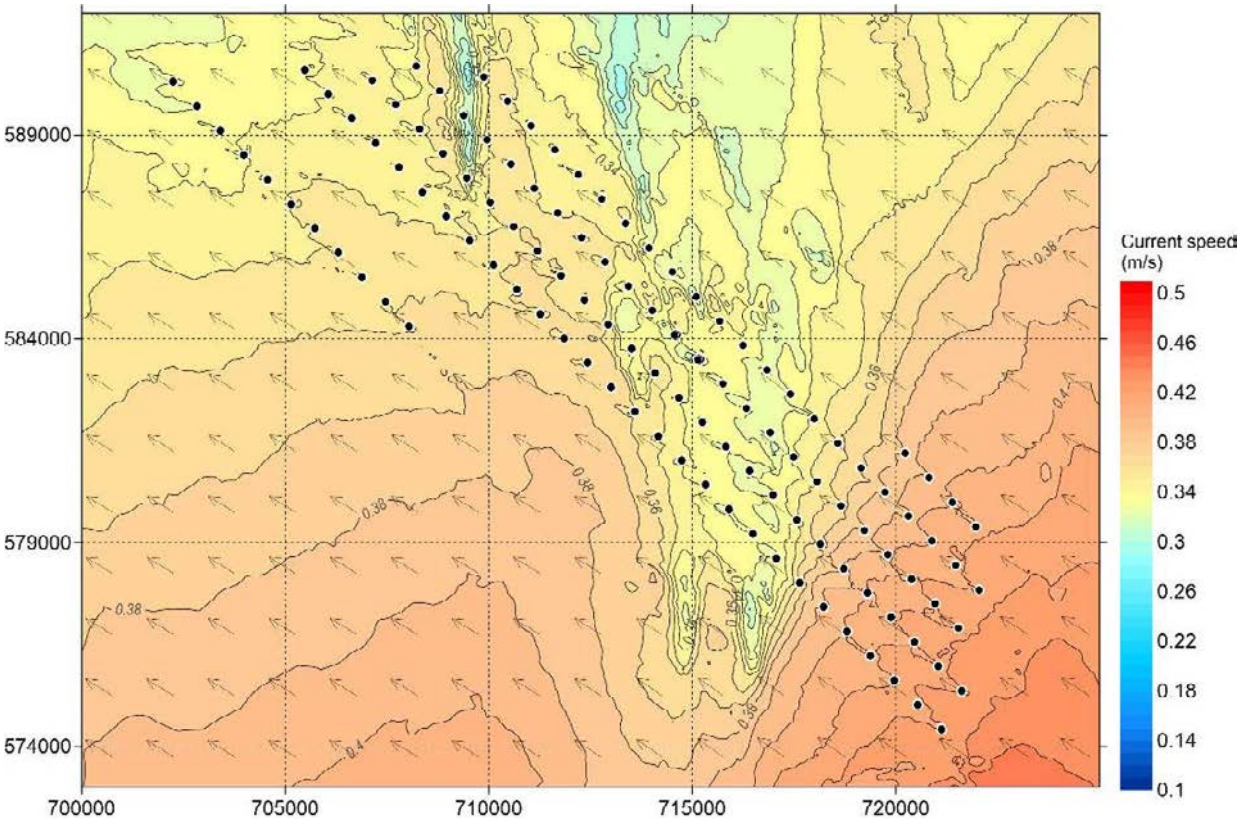

Figure A.24 A Closer View of Spatial Variation of Peak North-west-going Currents in a Spring Tide – Layout A – OSP 2

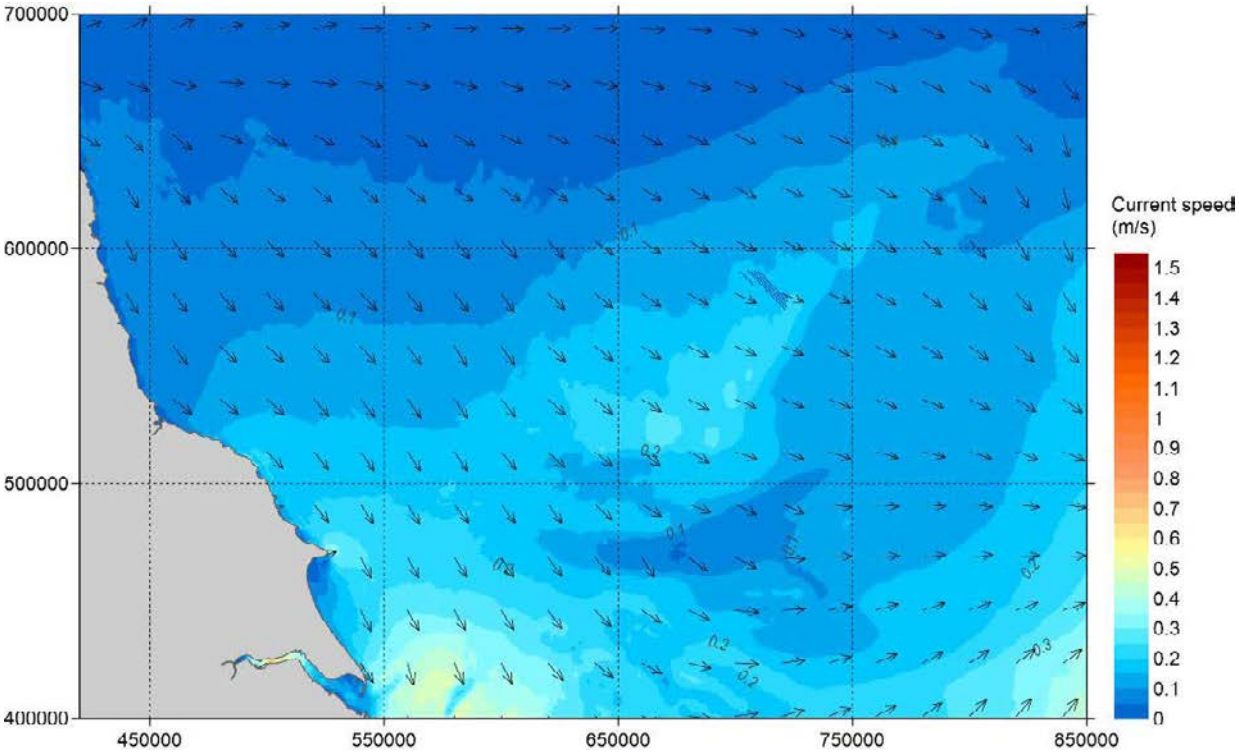

Figure A.25 Overview of Spatial Variation of Peak South-east-going Currents in a Neap Tide – Layout A – OSP 2

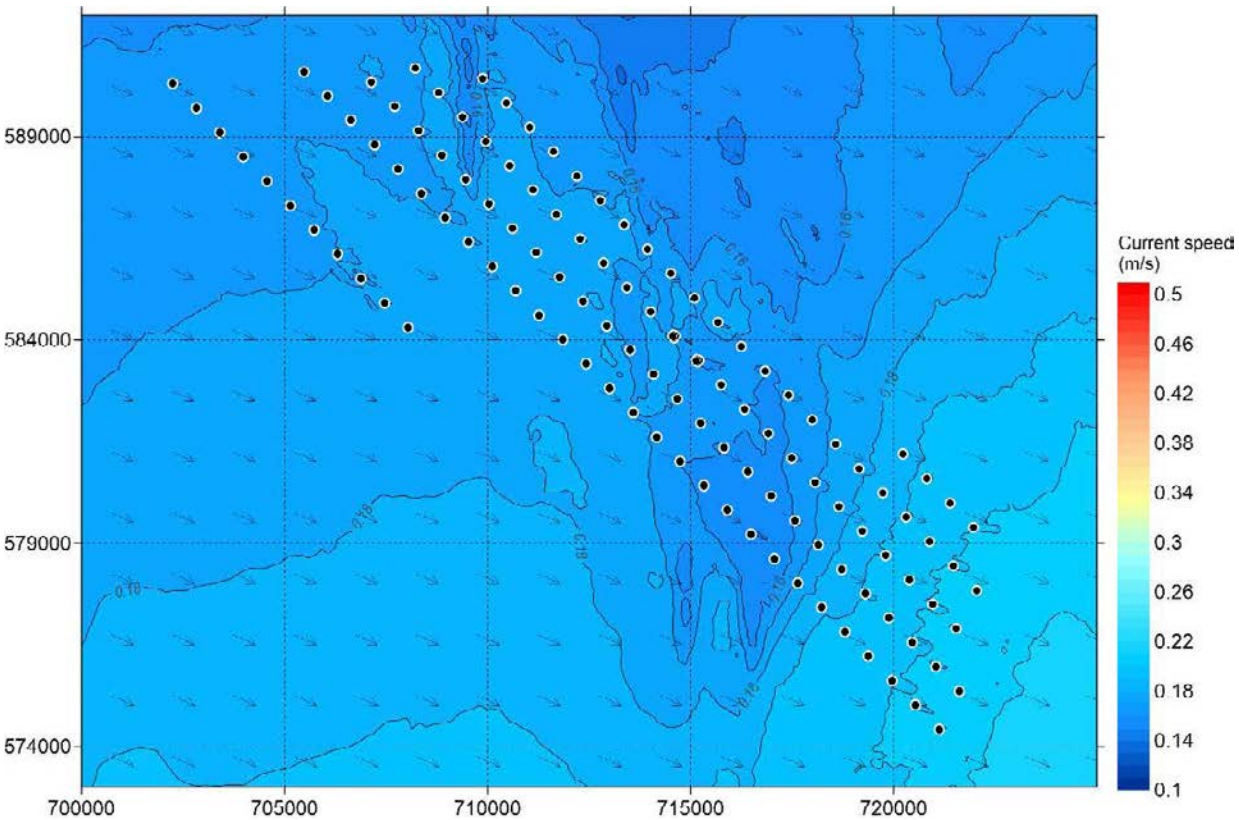

Figure A.26 Overview of Spatial Variation of Peak South-east-going Currents in a Neap Tide – Layout A – OSP 2

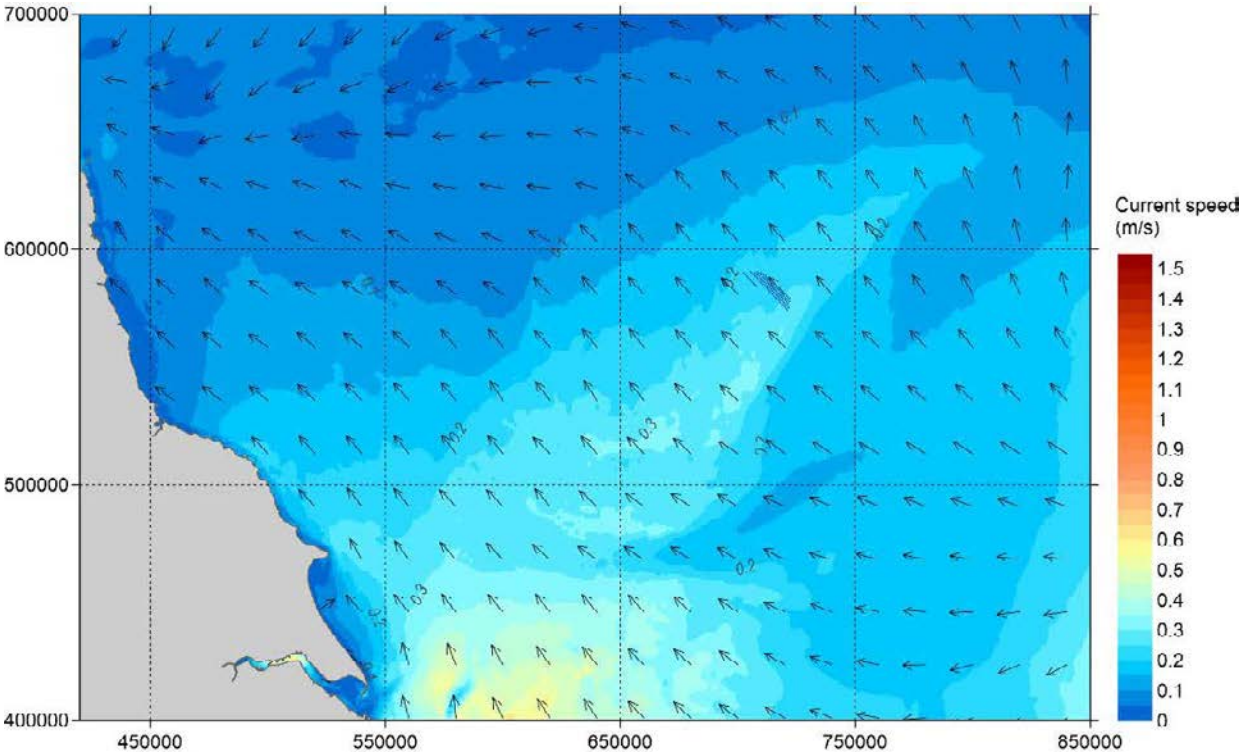

Figure A.27 Overview of Spatial Variation of Peak North-west-going Currents in a Neap Tide – Layout A – OSP 2

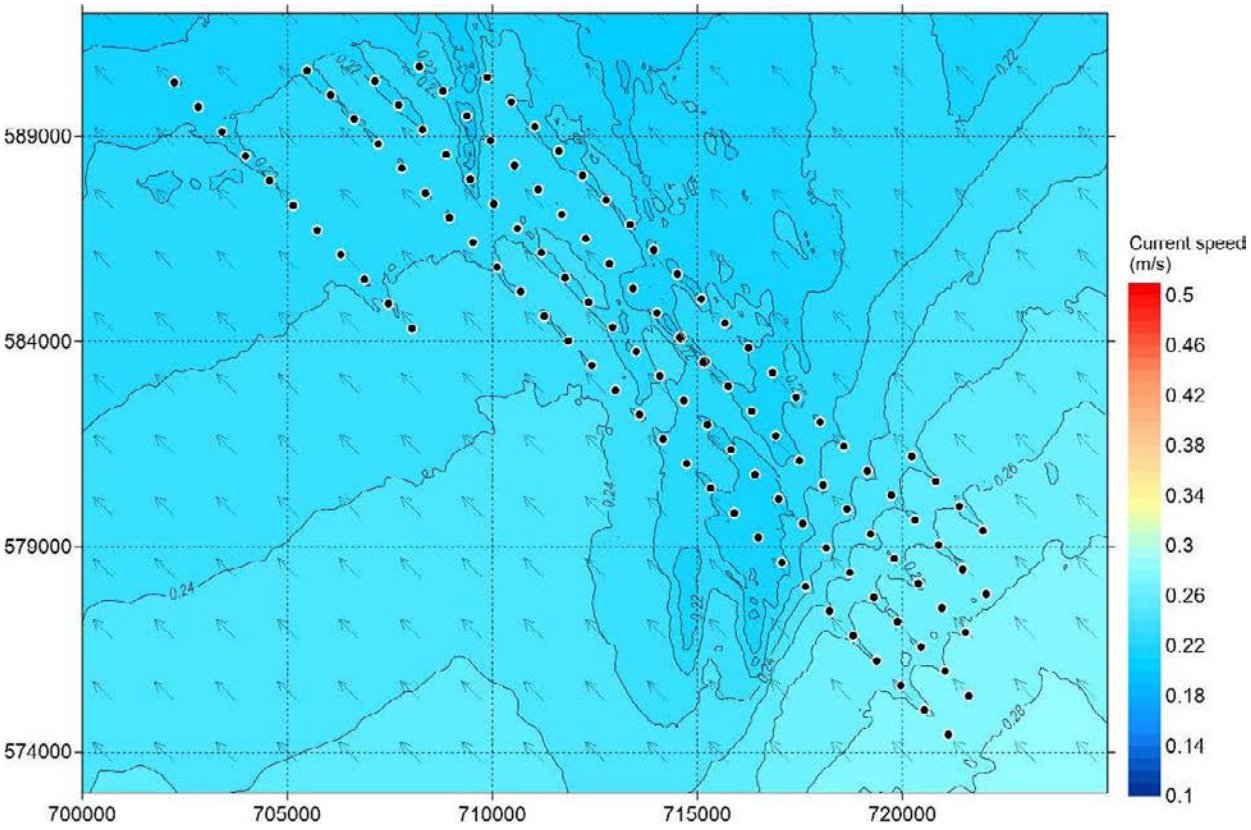

Figure A.28 Overview of Spatial Variation of Peak South-east-going Currents in a Neap Tide – Layout A – OSP 2

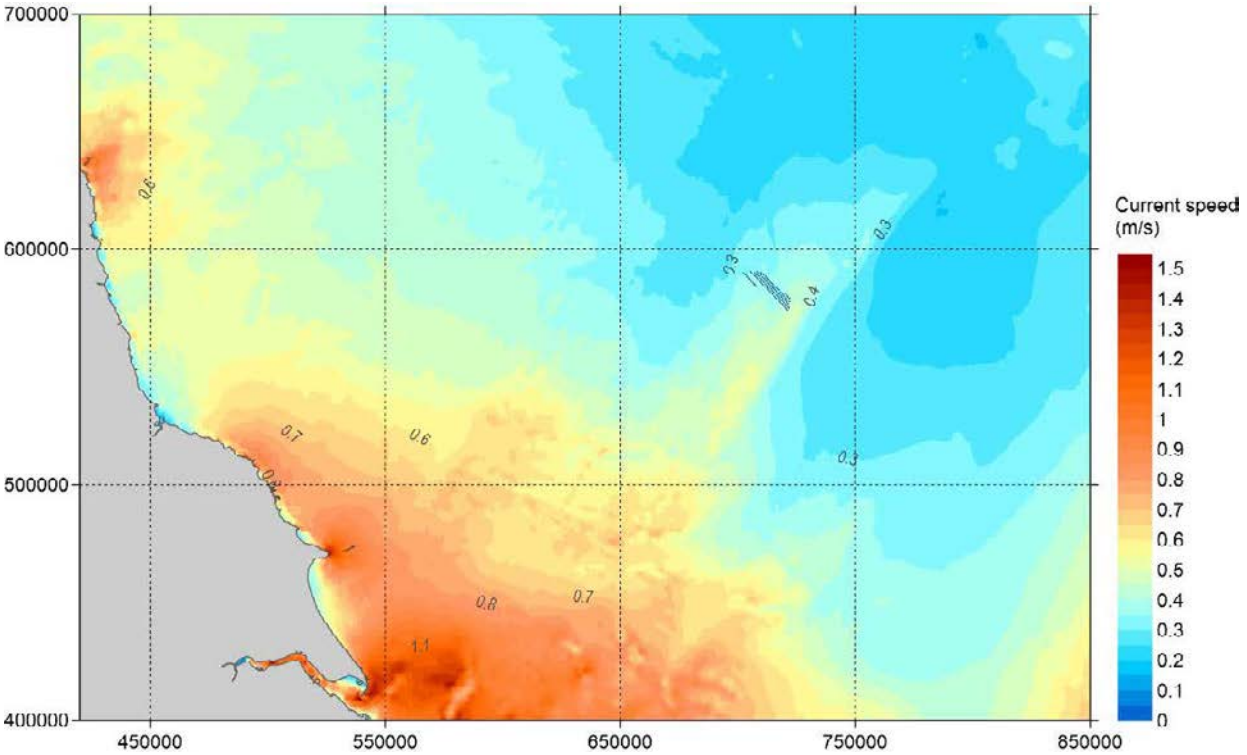

Figure A.29 Overview of Spatial Variation of Maximum Current Speed Over 30 days- Layout A – OSP 2

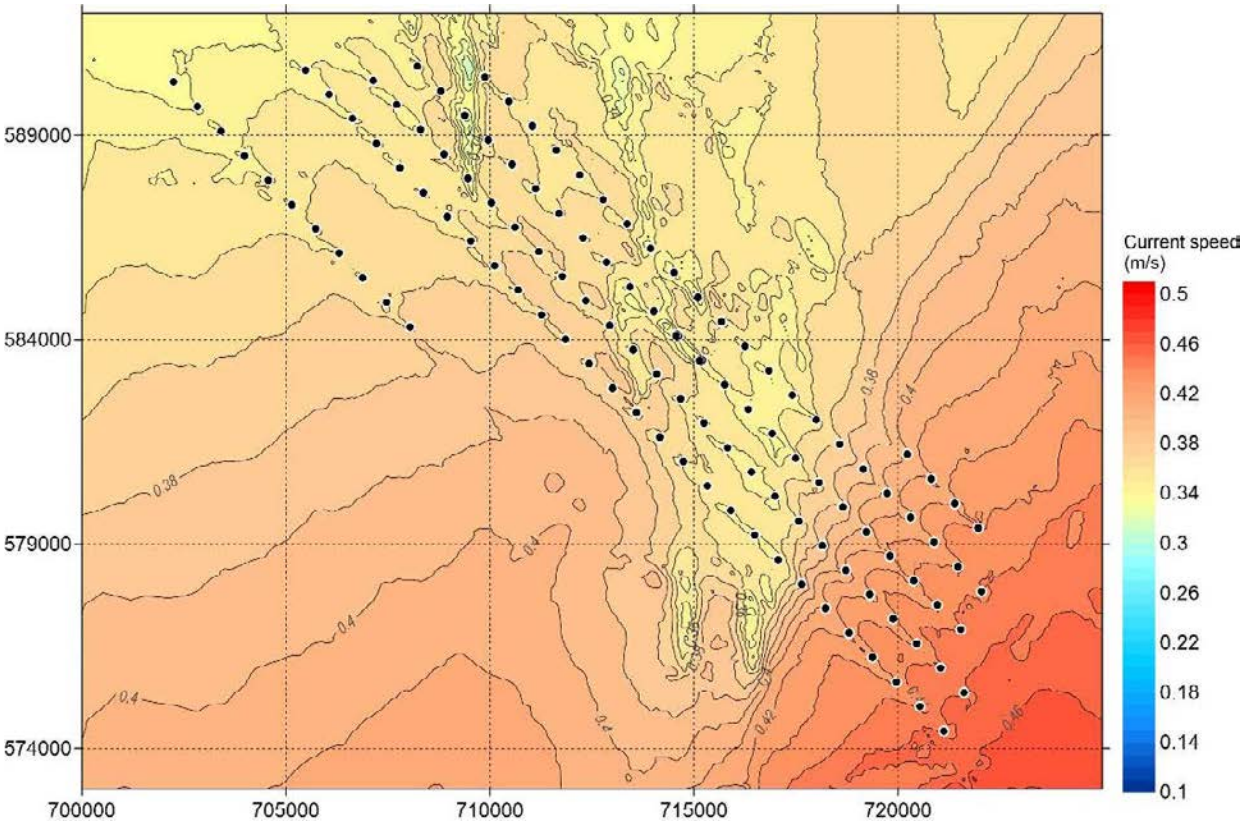

Figure A.30 Overview of Spatial Variation of Maximum Current Speed Over 30 days- Layout A – OSP 2

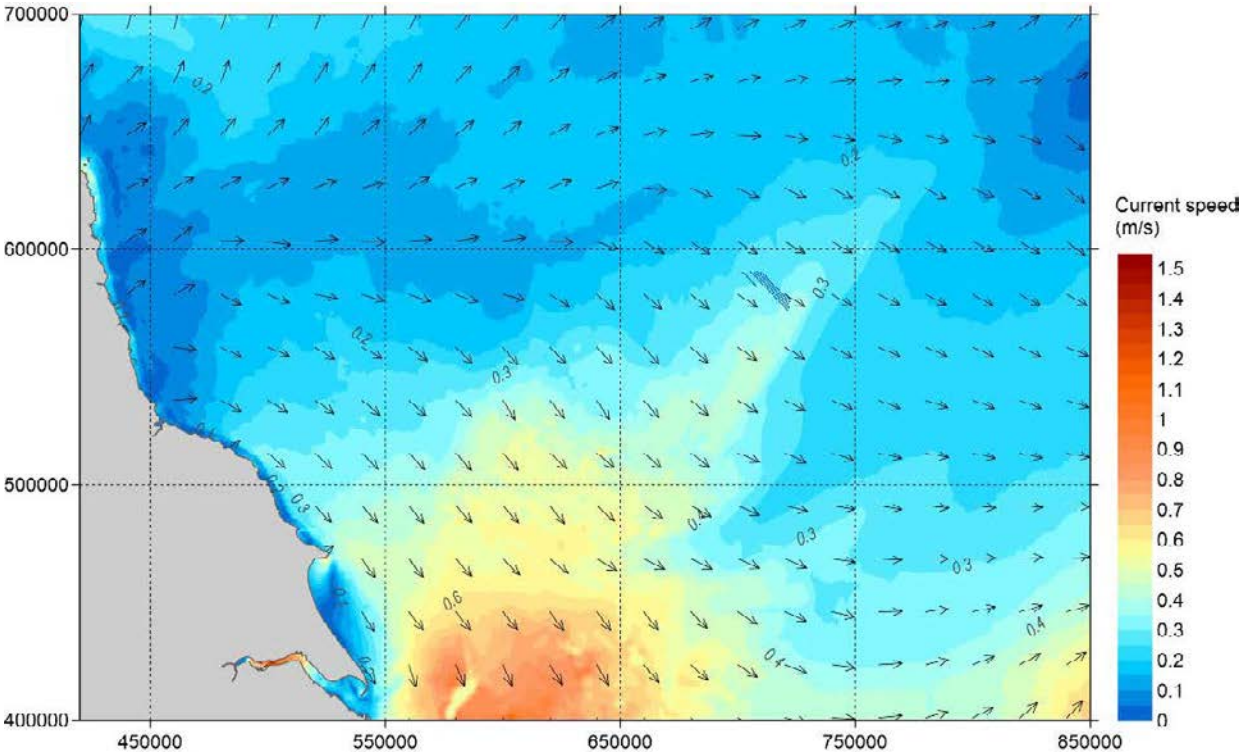

Figure A.31 Overview of Spatial Variation of Peak South-east-going Currents in a Spring Tide – Layout A – OSP 3

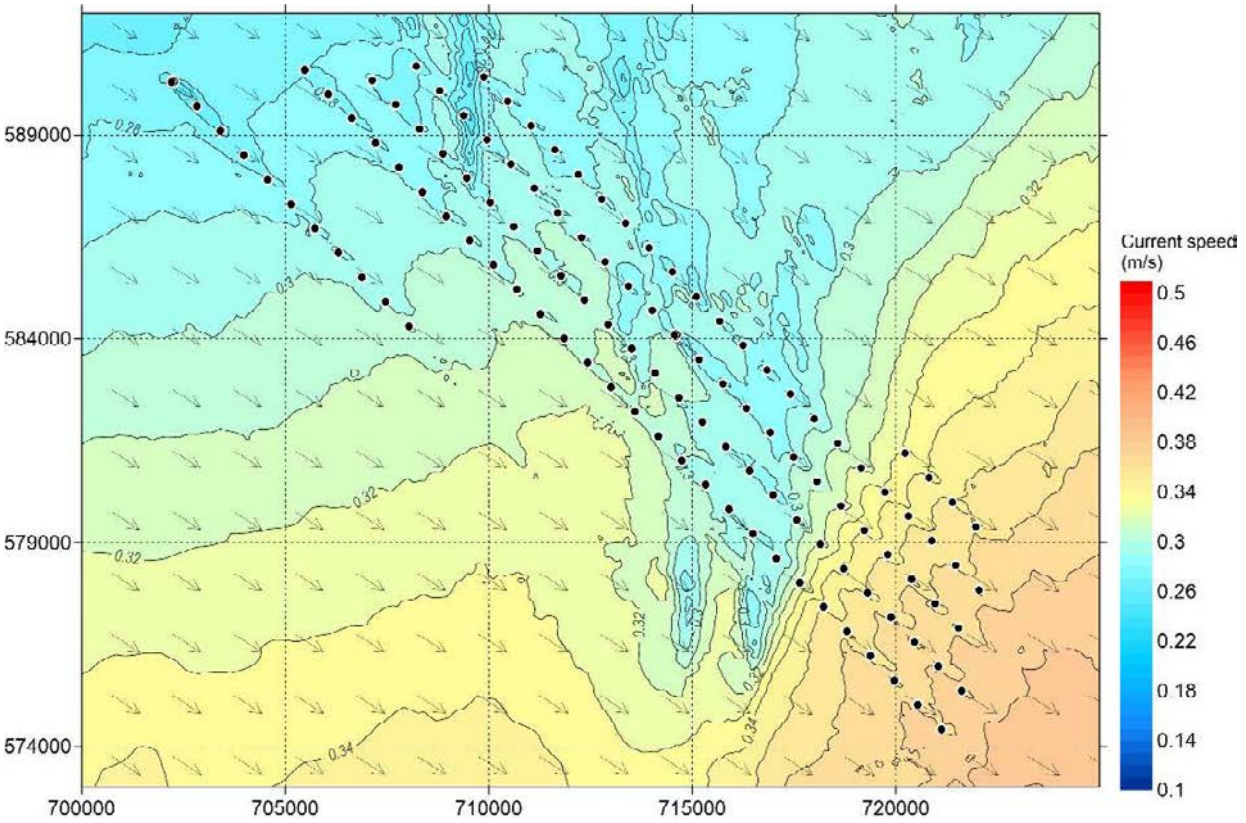

Figure A.32 A Closer View of Spatial Variation of Peak South-east-going Currents in a Spring Tide – Layout A – OSP 3

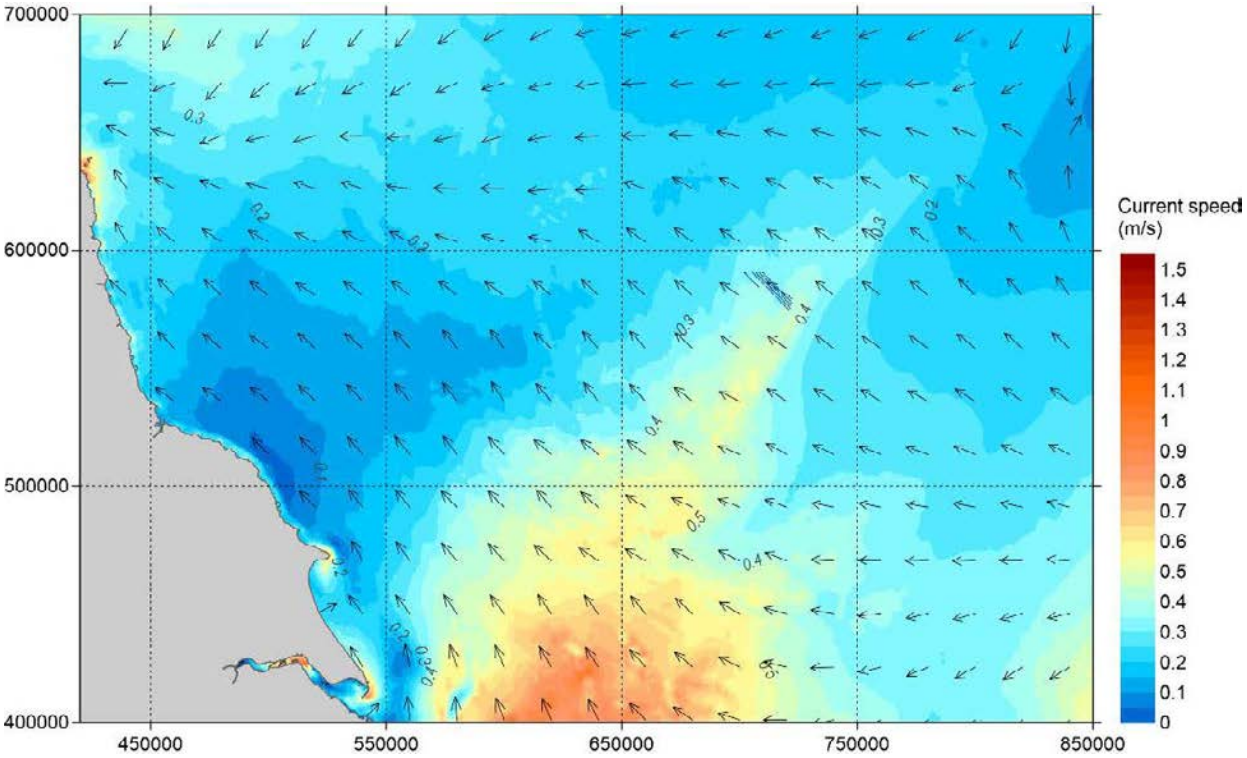

Figure A.33 Overview of Spatial Variation of Peak North-west-going Currents in a Spring Tide – Layout A – OSP 3

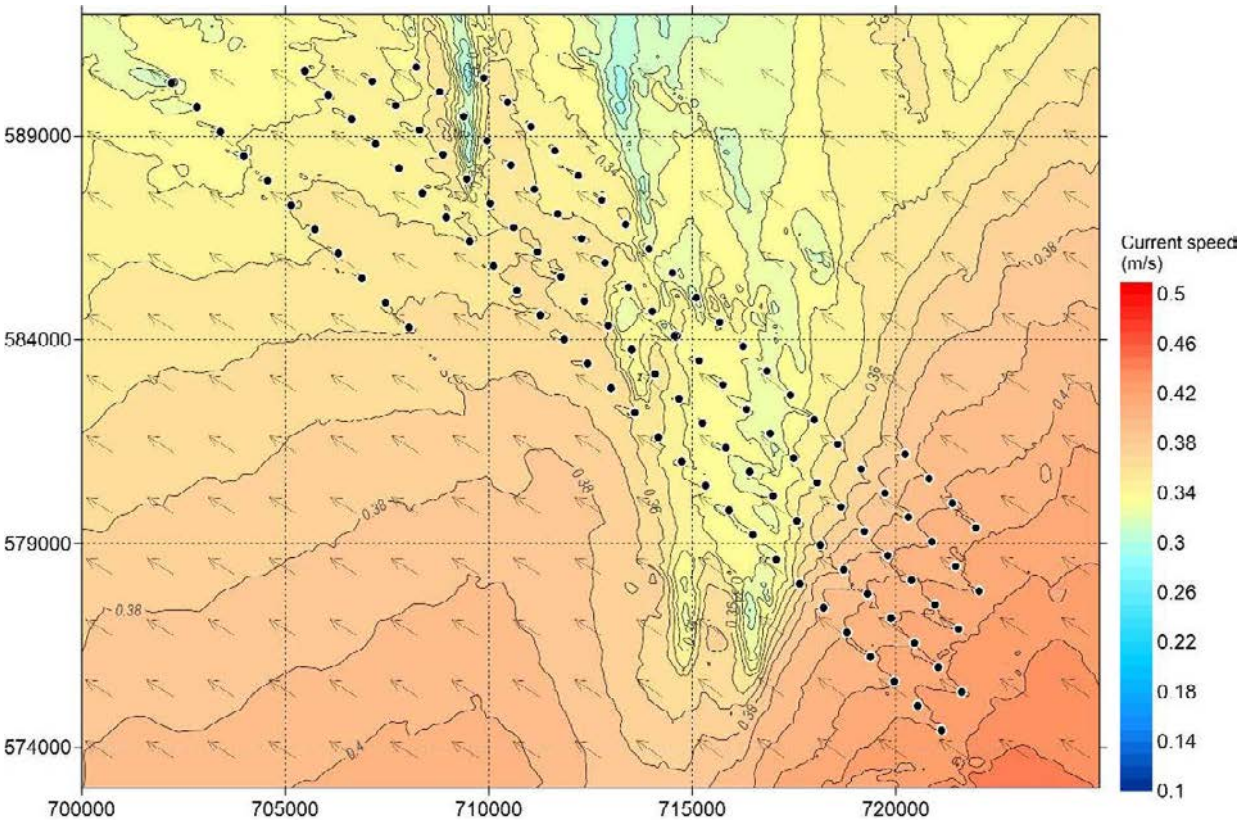

Figure A.34 A Closer View of Spatial Variation of Peak North-west-going Currents in a Spring Tide – Layout A – OSP 3

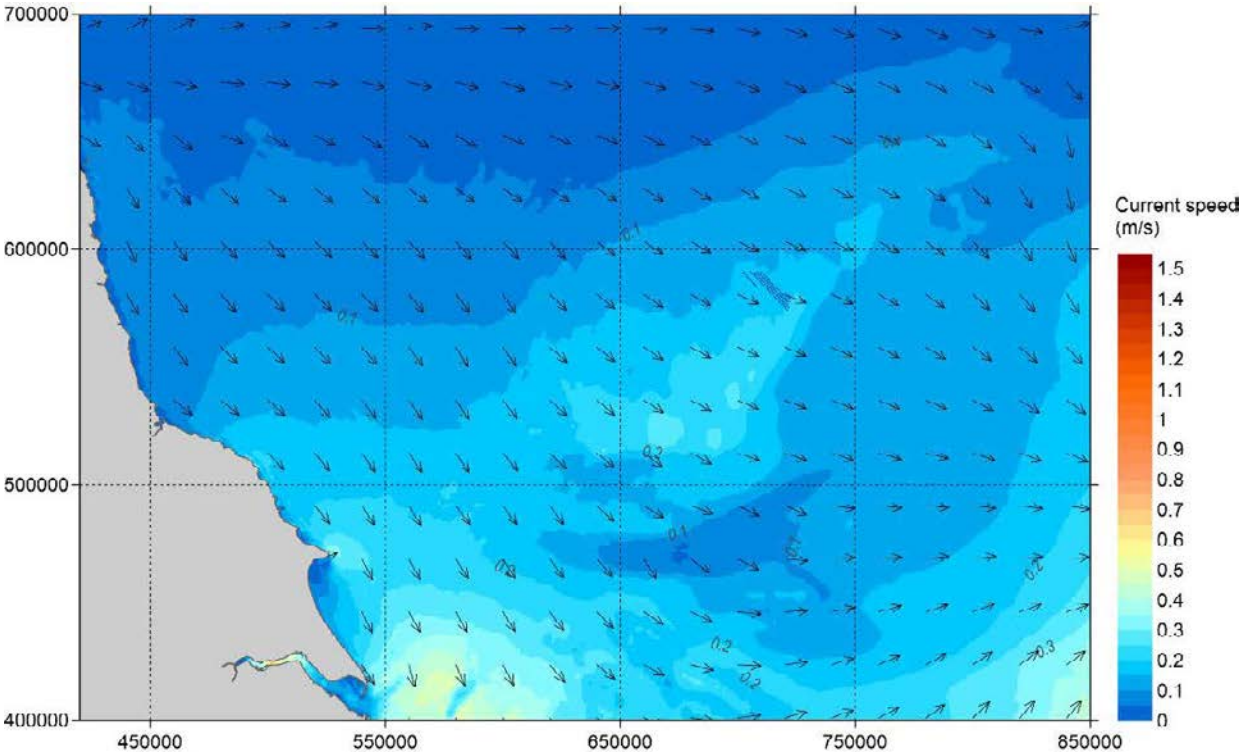

Figure A.35 Overview of Spatial Variation of Peak South-east-going Currents in a Neap Tide – Layout A – OSP 3

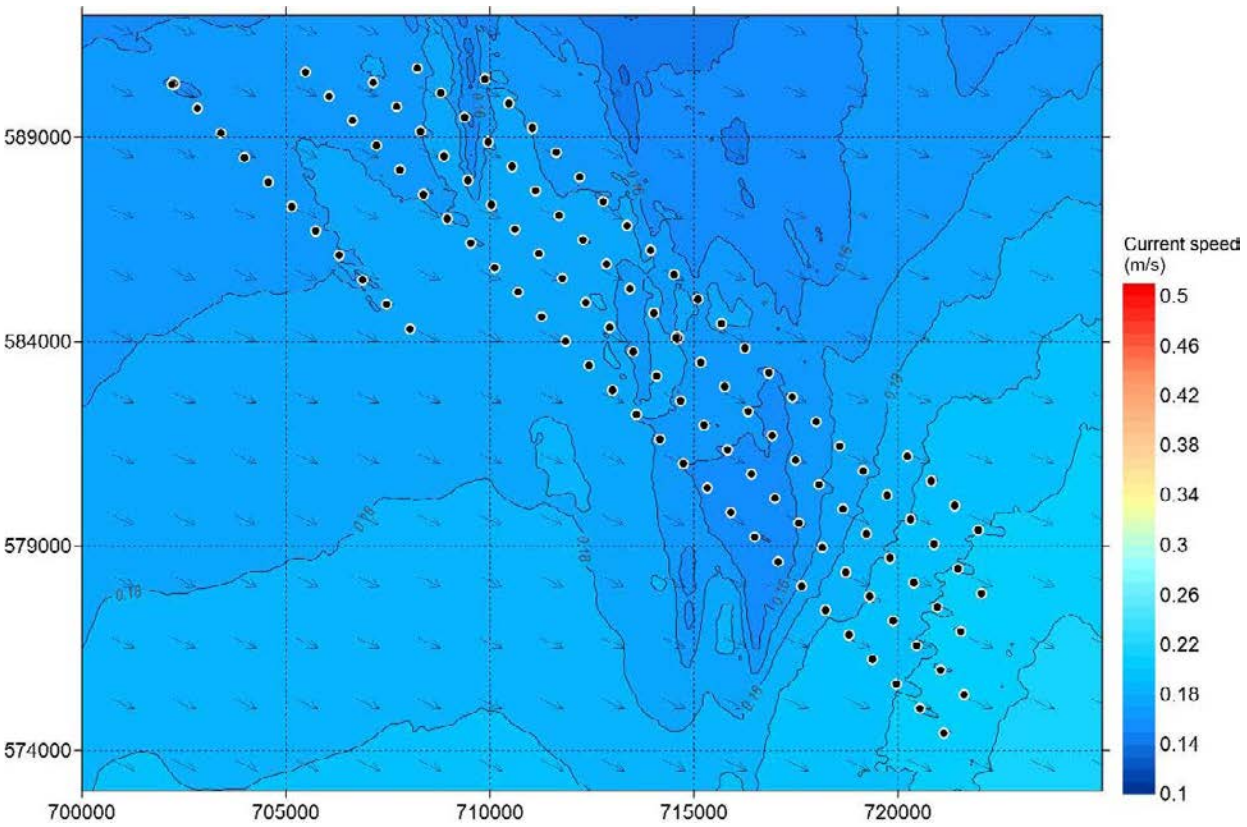

Figure A.36 Overview of Spatial Variation of Peak South-east-going Currents in a Neap Tide – Layout A – OSP 3

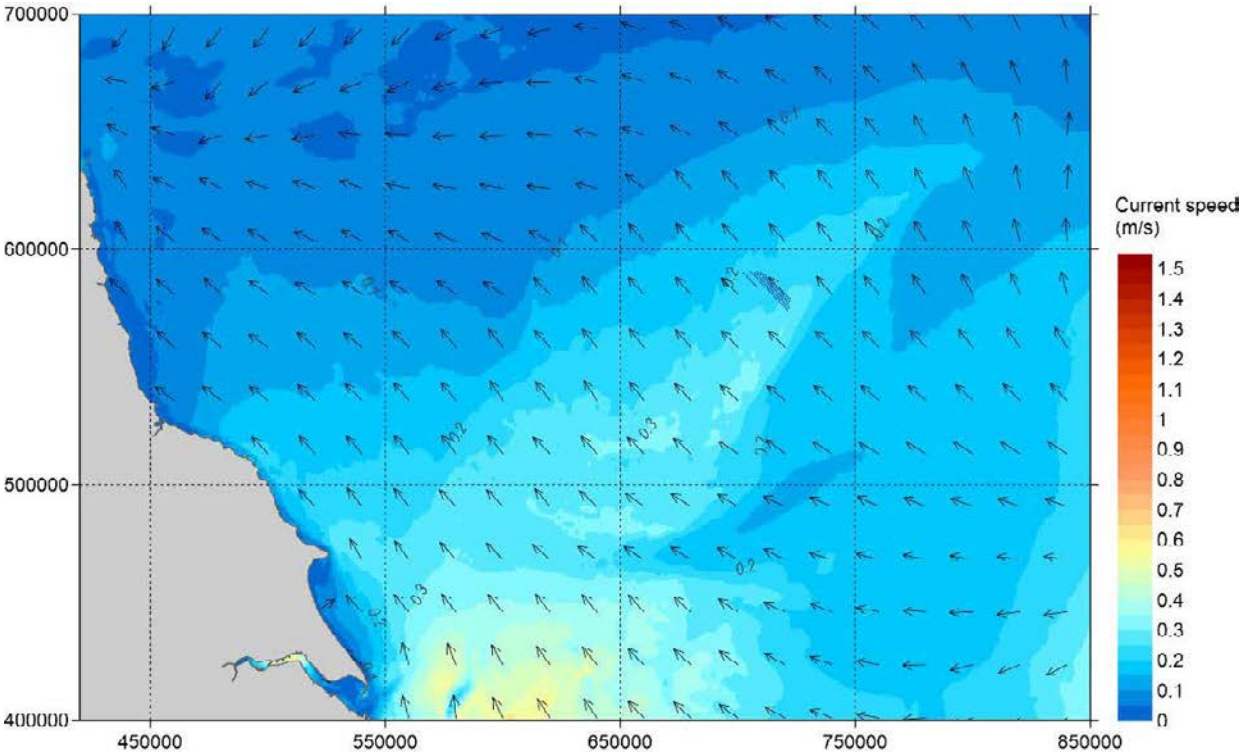

Figure A.37 Overview of Spatial Variation of Peak North-west-going Currents in a Neap Tide – Layout A – OSP 3

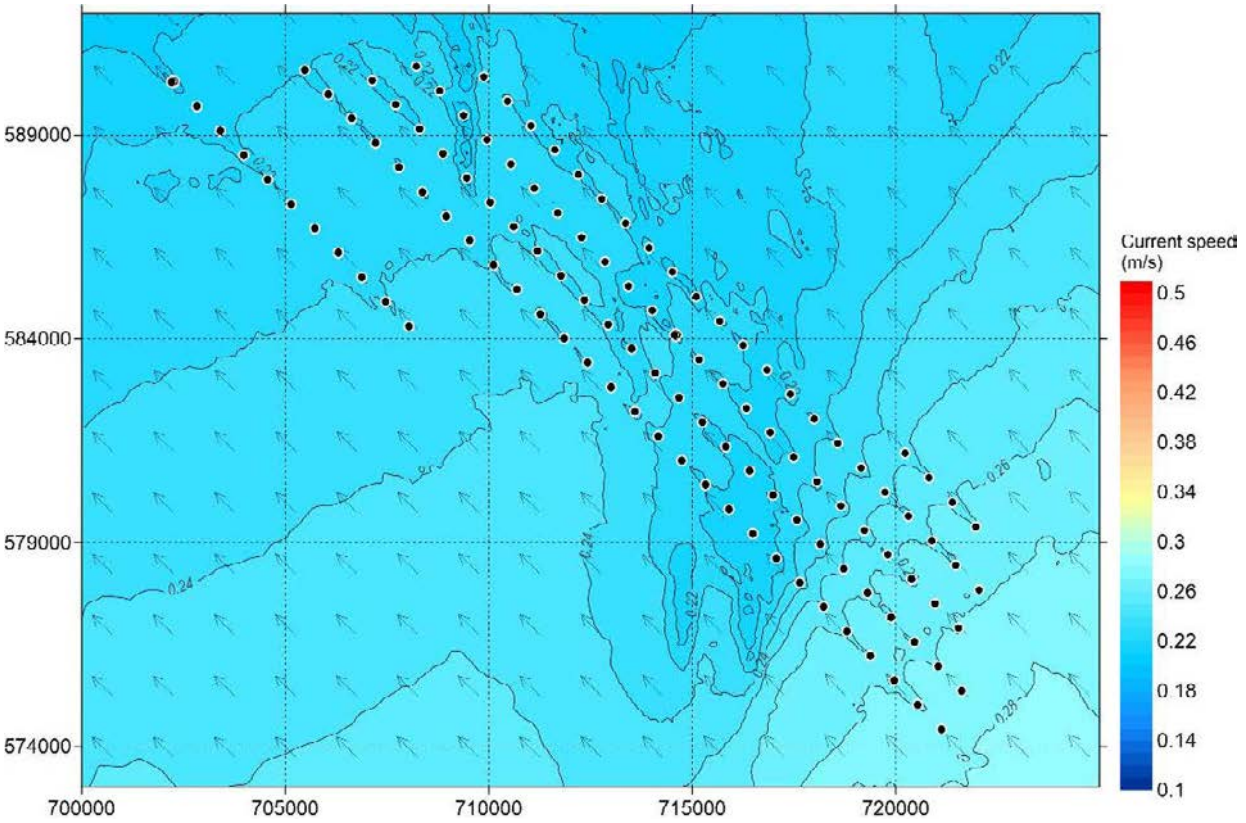

Figure A.38 Overview of Spatial Variation of Peak South-east-going Currents in a Neap Tide – Layout A – OSP 3

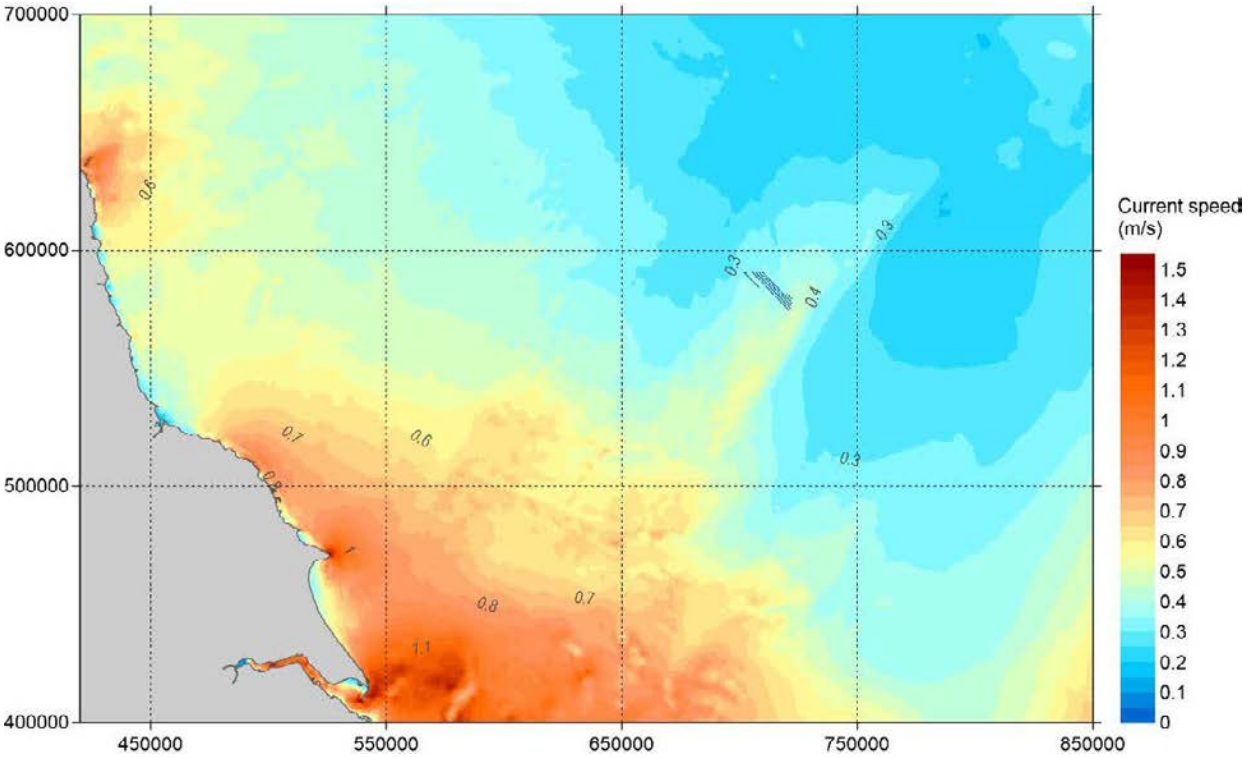

Figure A.39 Overview of Spatial Variation of Maximum Current Speed Over 30 days- Layout A – OSP 3

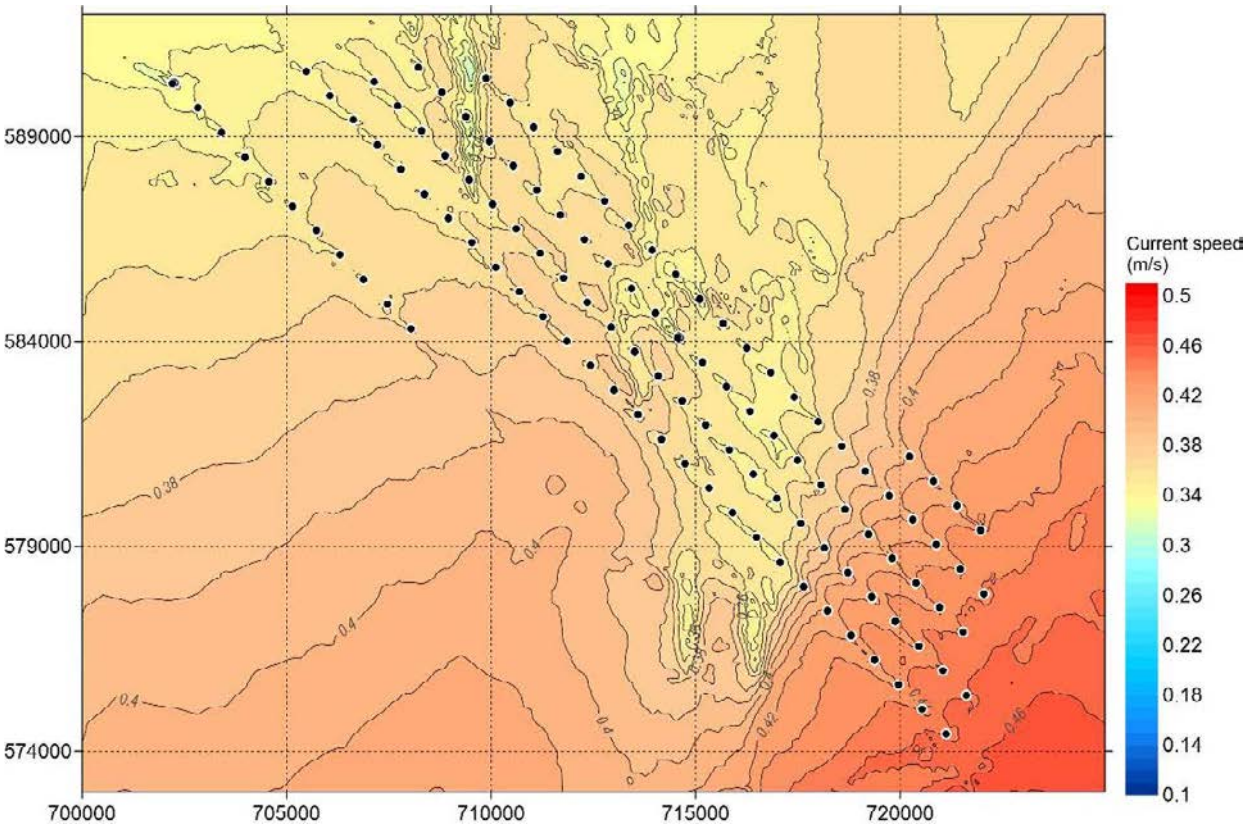

Figure A.40 Overview of Spatial Variation of Maximum Current Speed Over 30 days- Layout A – OSP 3

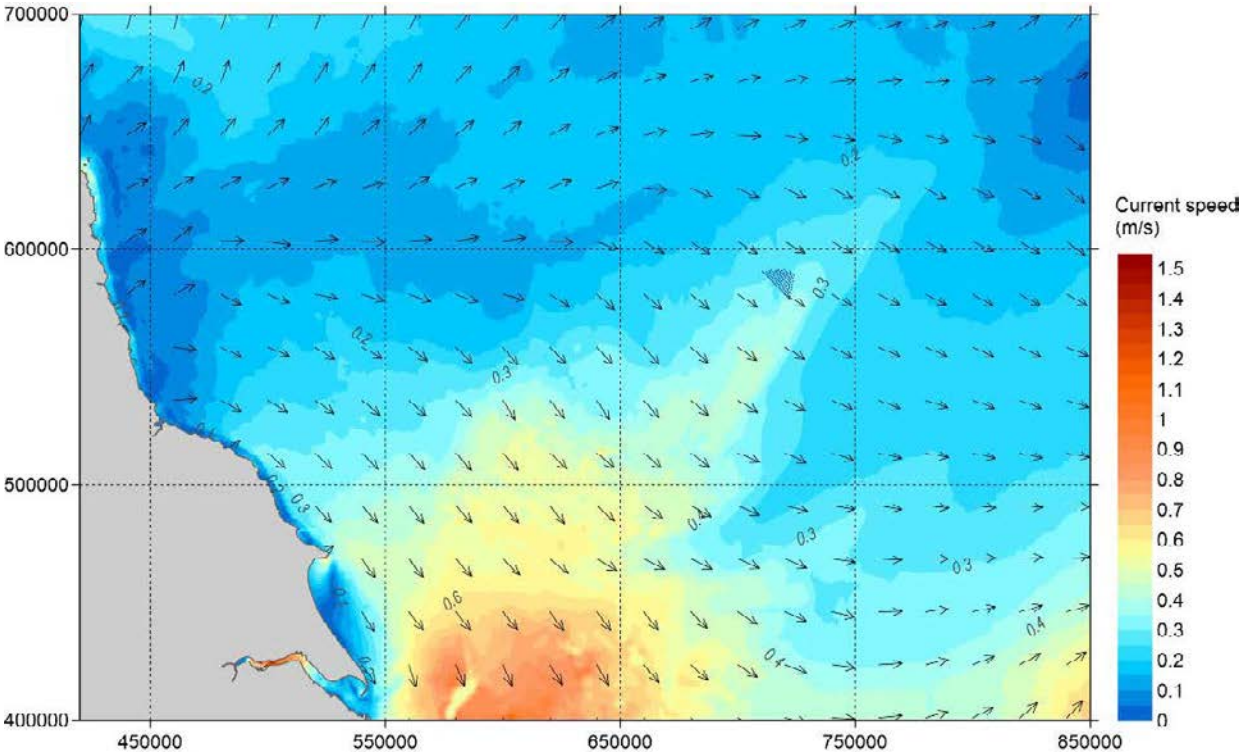

Figure A.41 Overview of Spatial Variation of Peak South-east-going Currents in a Spring Tide – Layout B – OSP 1

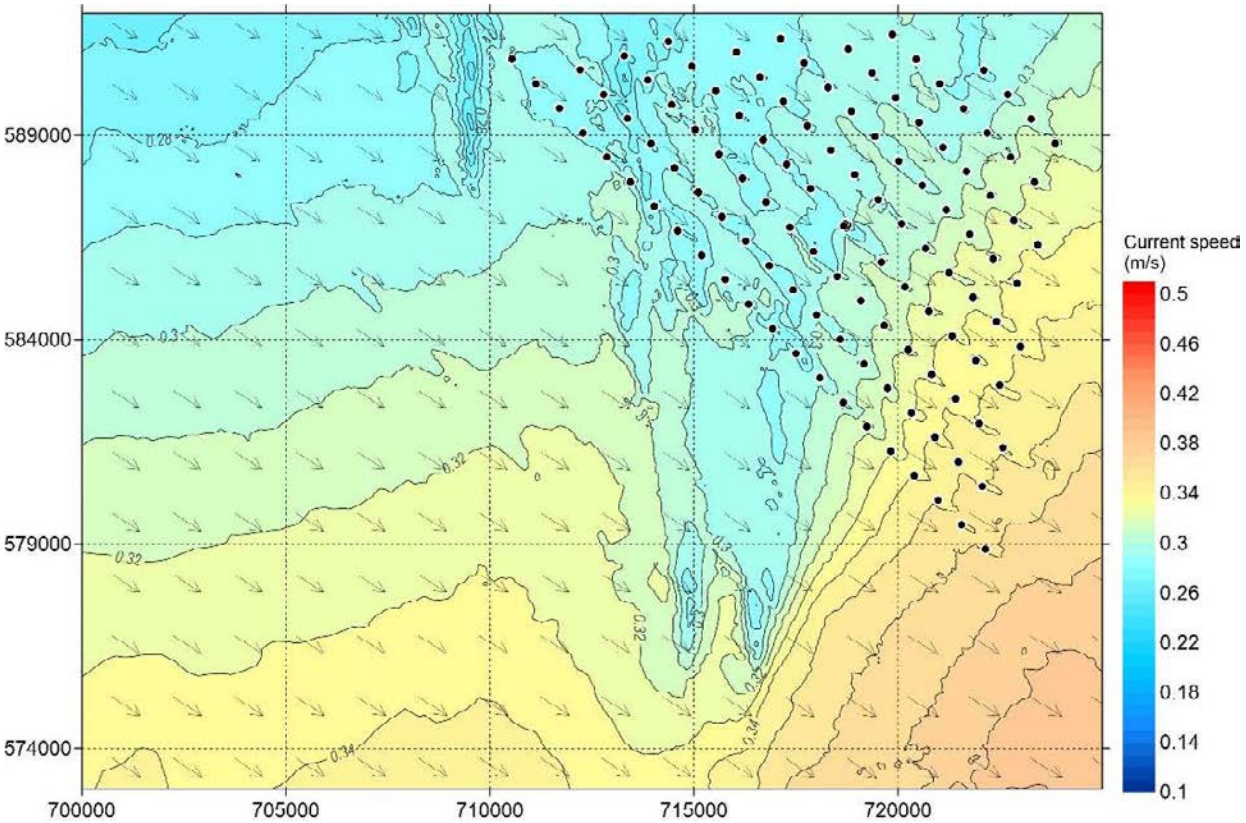

Figure A.42 A Closer View of Spatial Variation of Peak South-east-going Currents in a Spring Tide – Layout B – OSP 1

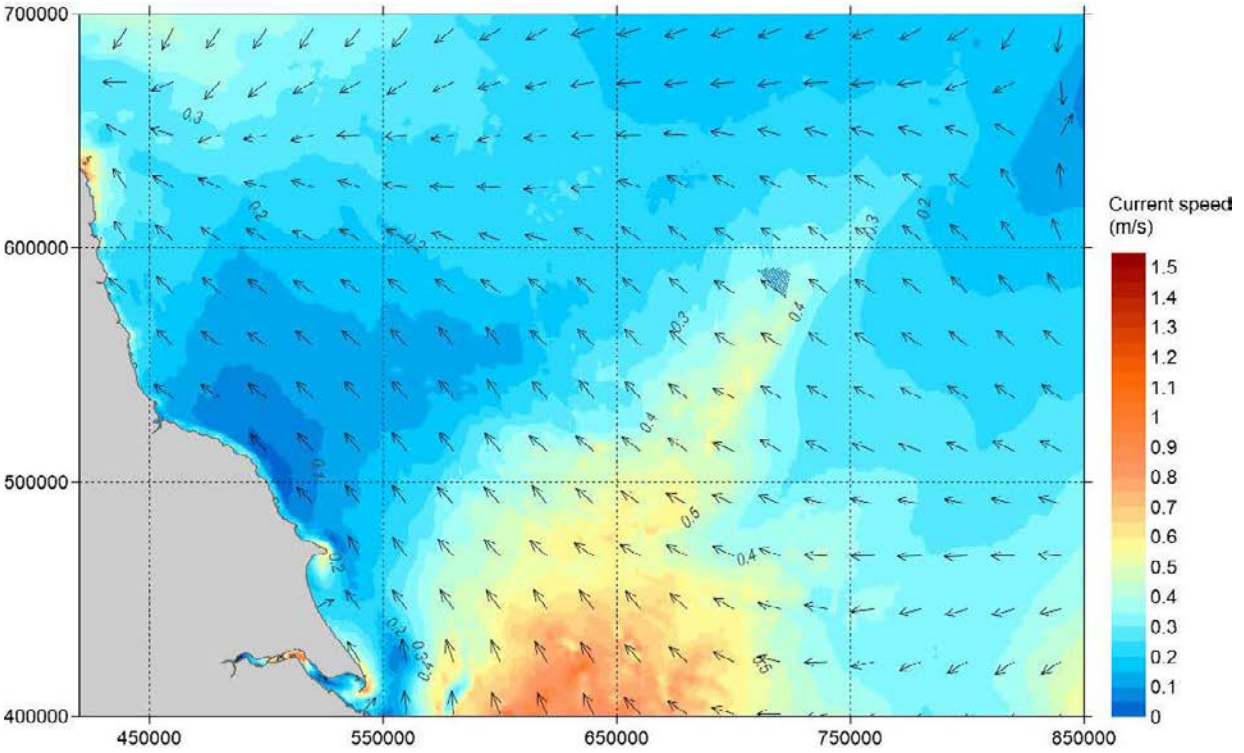

Figure A.43 Overview of Spatial Variation of Peak North-west-going Currents in a Spring Tide – Layout B – OSP 1

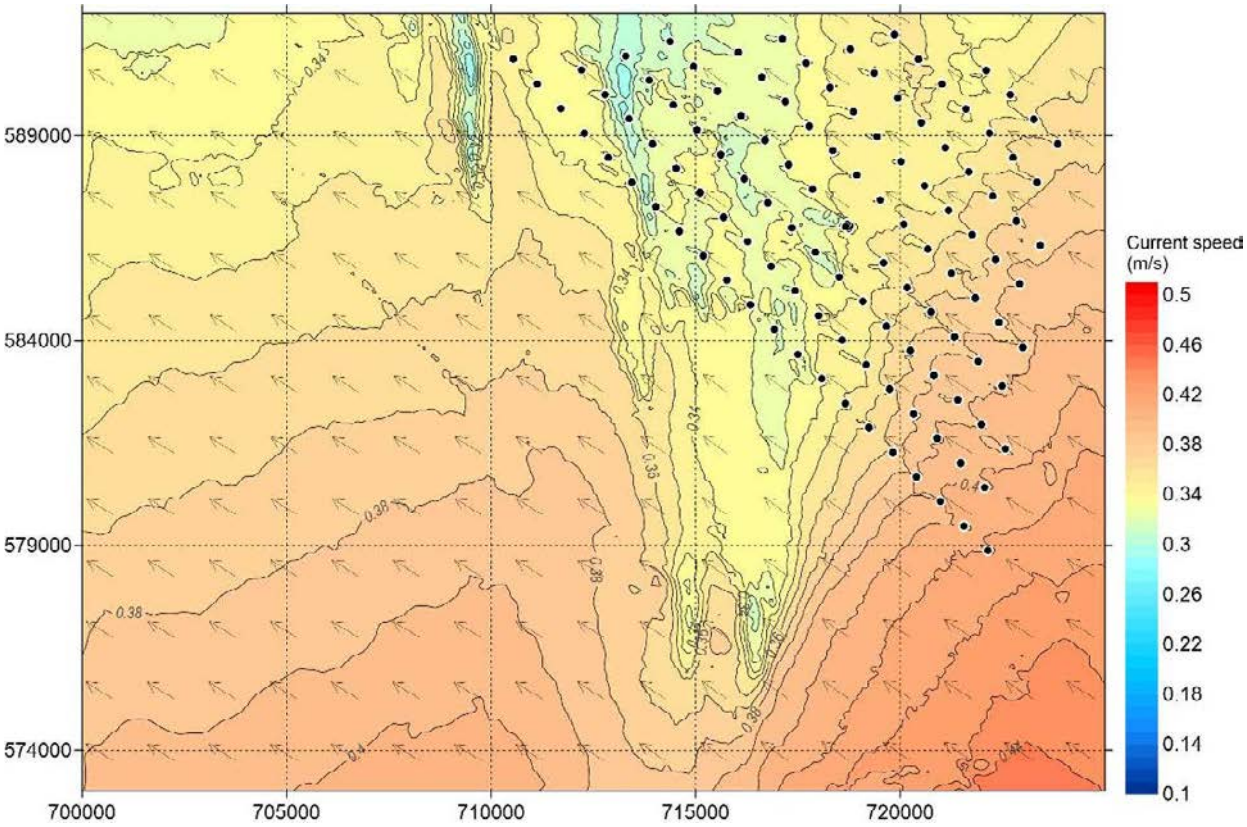

Figure A.44 A Closer View of Spatial Variation of Peak North-west-going Currents in a Spring Tide – Layout B – OSP 1

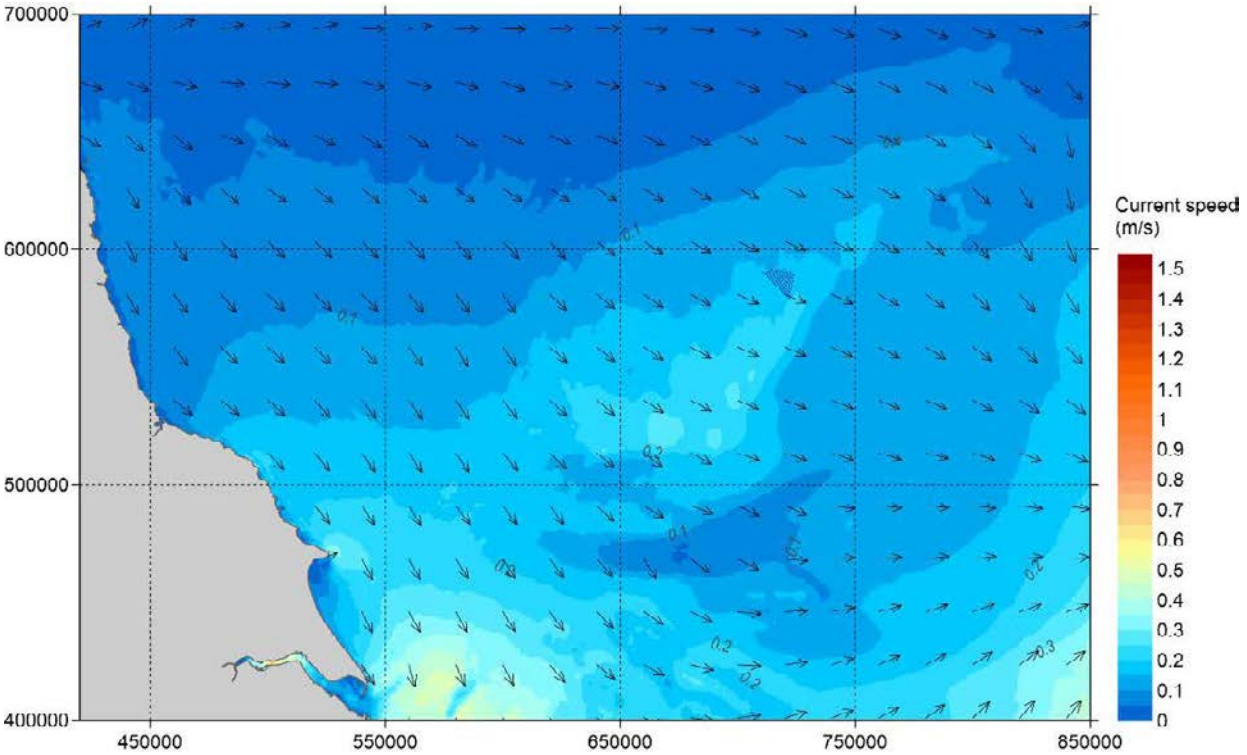

Figure A.45 Overview of Spatial Variation of Peak South-east-going Currents in a Neap Tide – Layout B – OSP 1

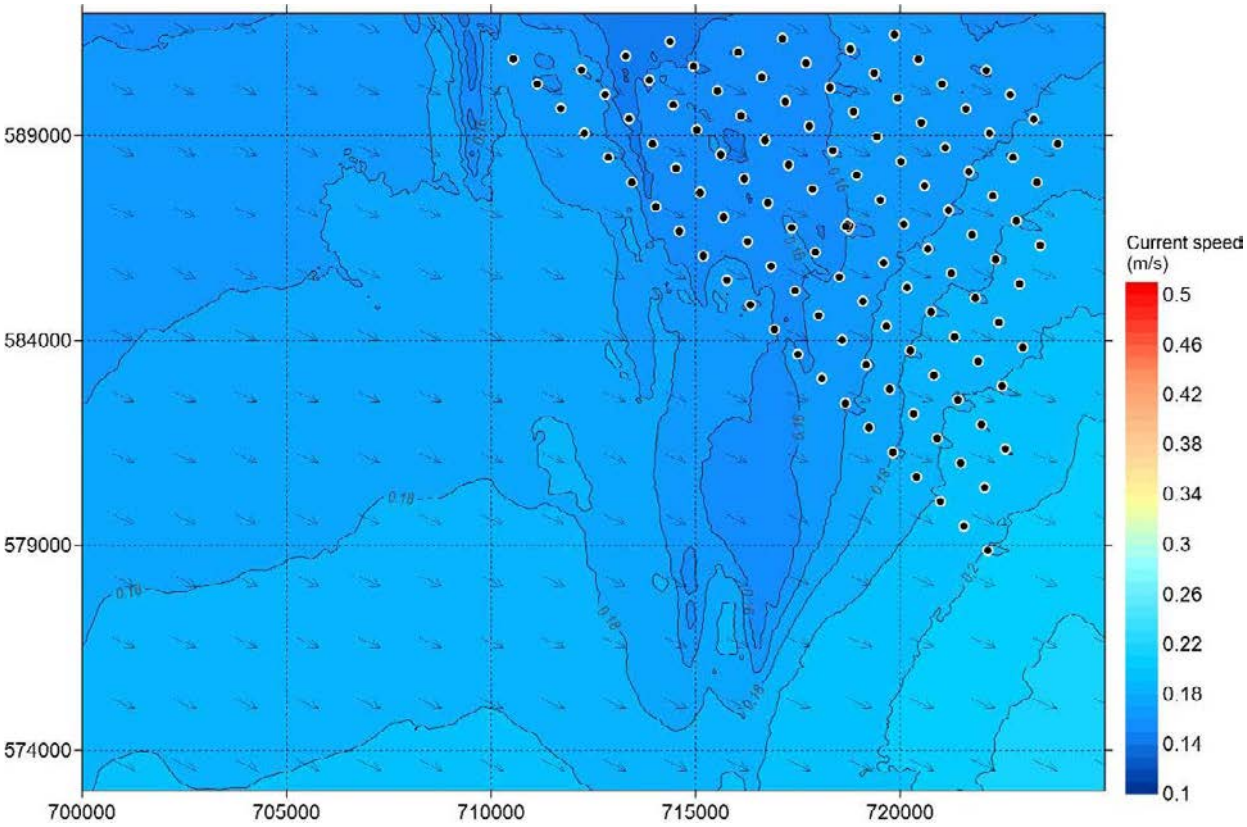

Figure A.46 Overview of Spatial Variation of Peak South-east-going Currents in a Neap tide – Layout B – OSP 1

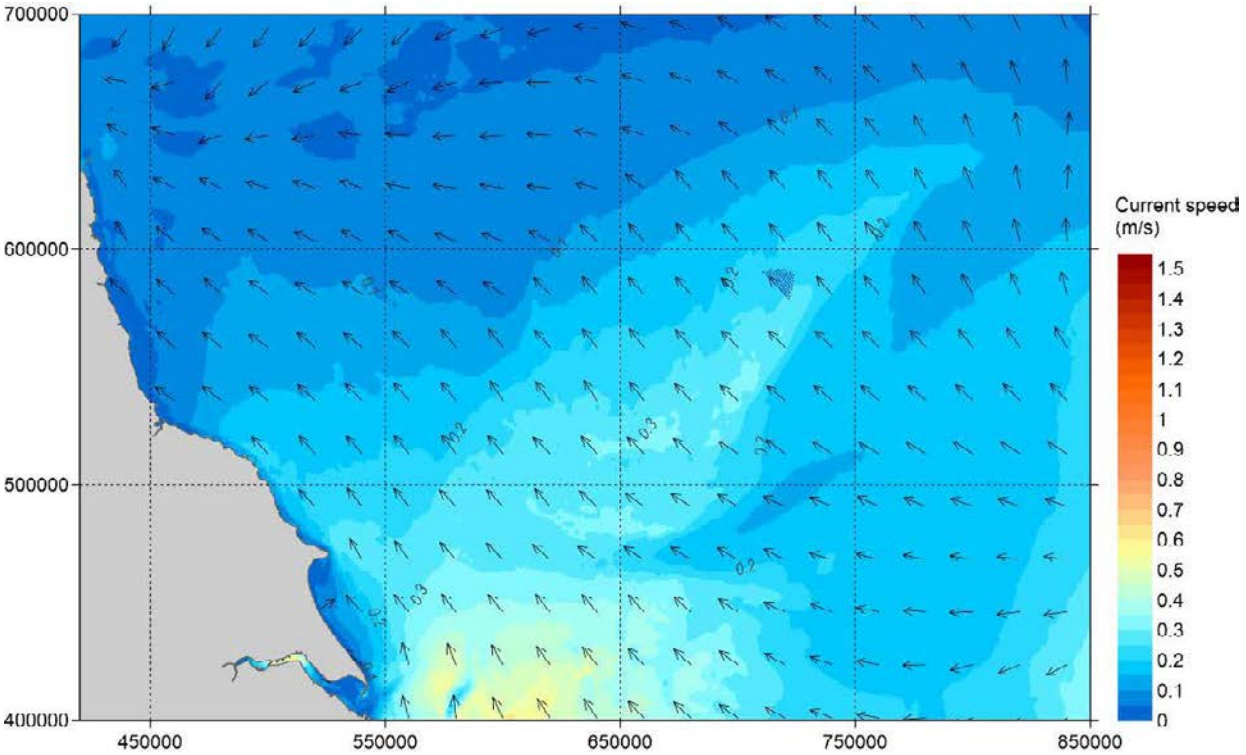

Figure A.47 Overview of Spatial Variation of Peak North-west-going Currents in a Neap tide – Layout B – OSP 1

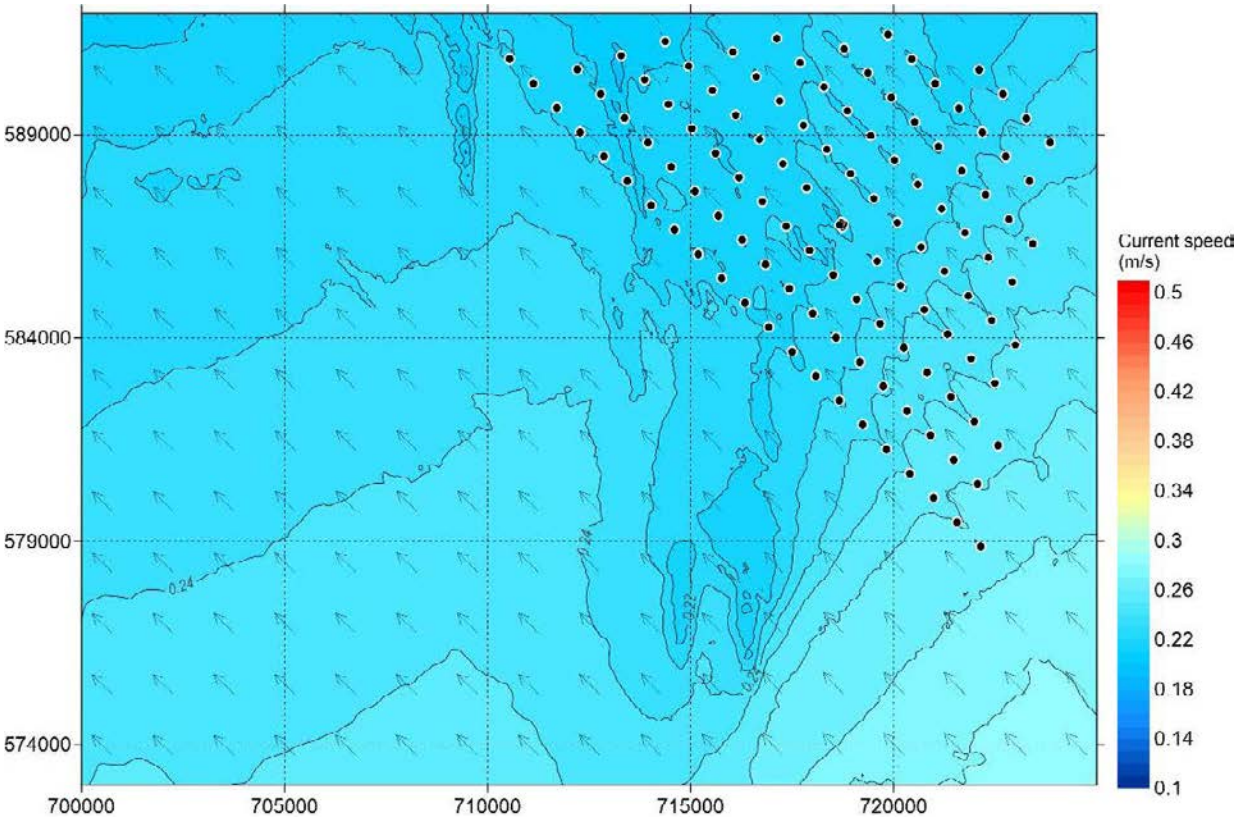

Figure A.48 Overview of Spatial Variation of Peak South-east-going Currents in a Neap tide – Layout B – OSP 1

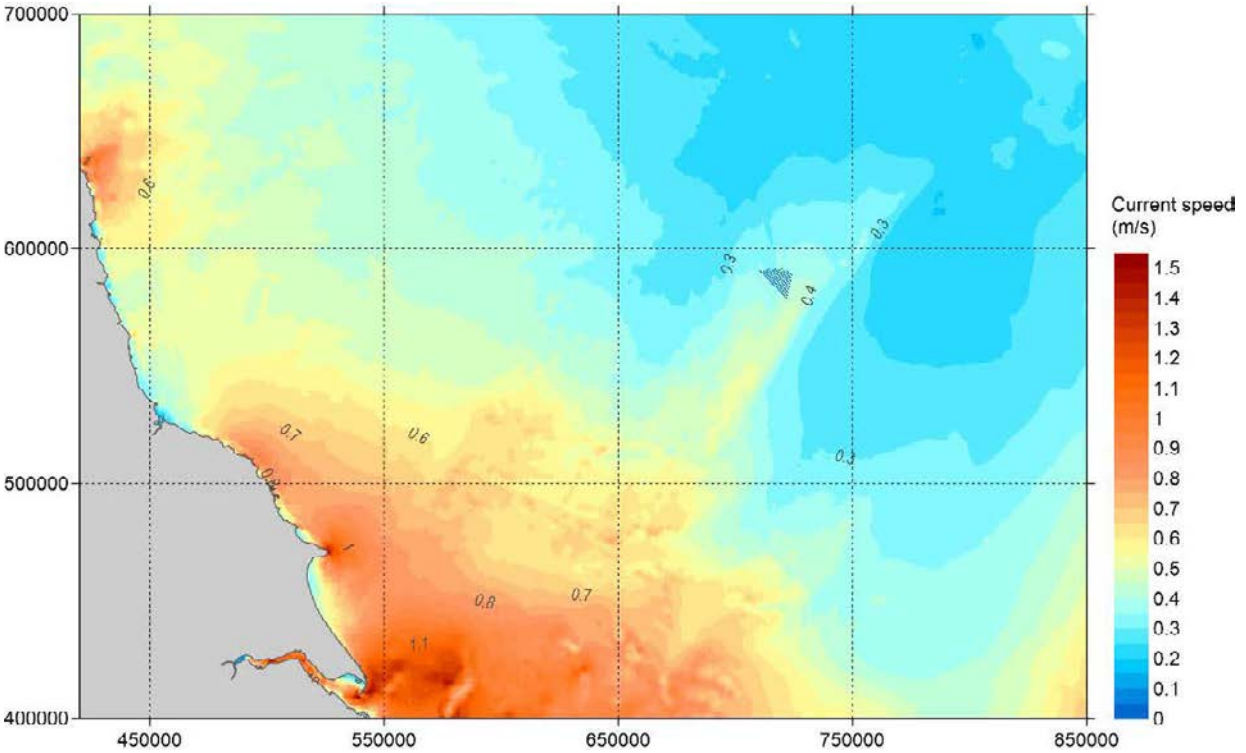

Figure A.49 Overview of Spatial Variation of Maximum Current Speed Over 30 days- Layout B – OSP 1

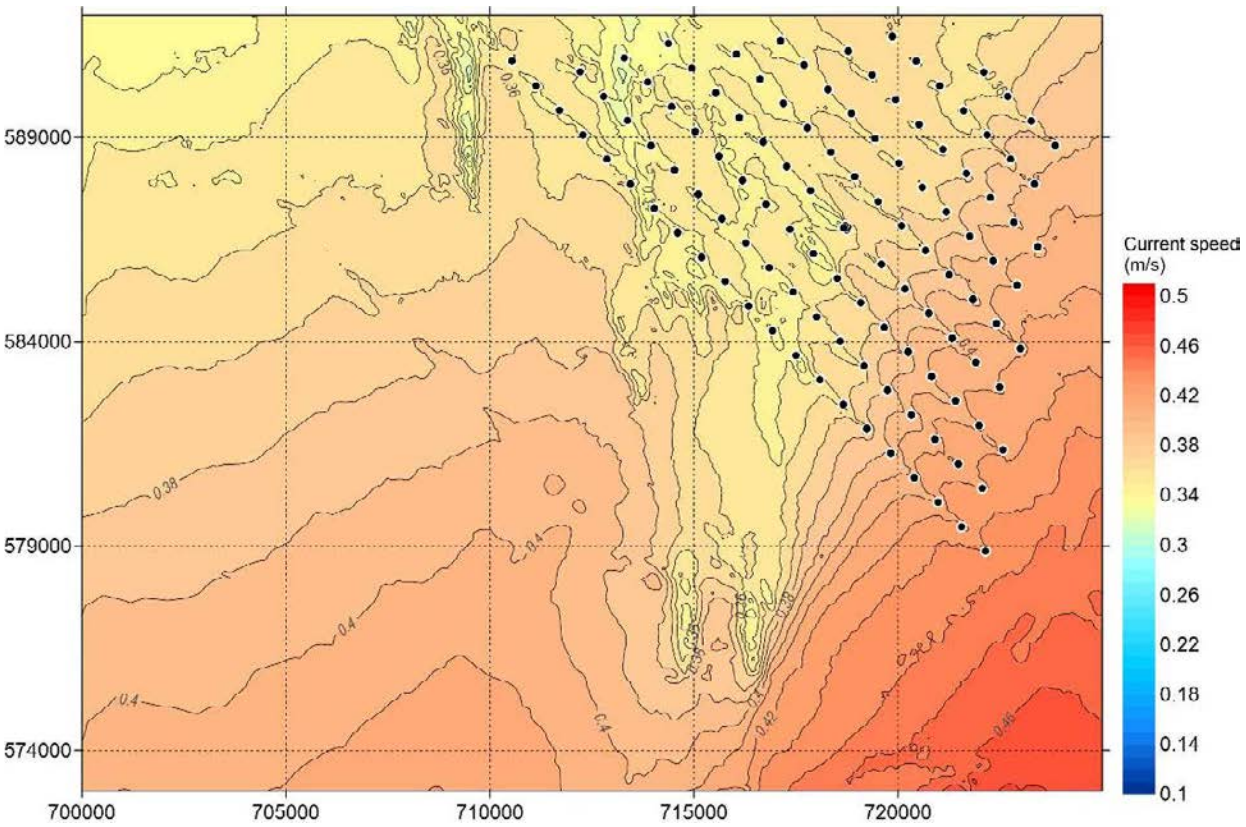

Figure A.50 Overview of Spatial Variation of Maximum Current Speed Over 30 days- Layout B – OSP 1

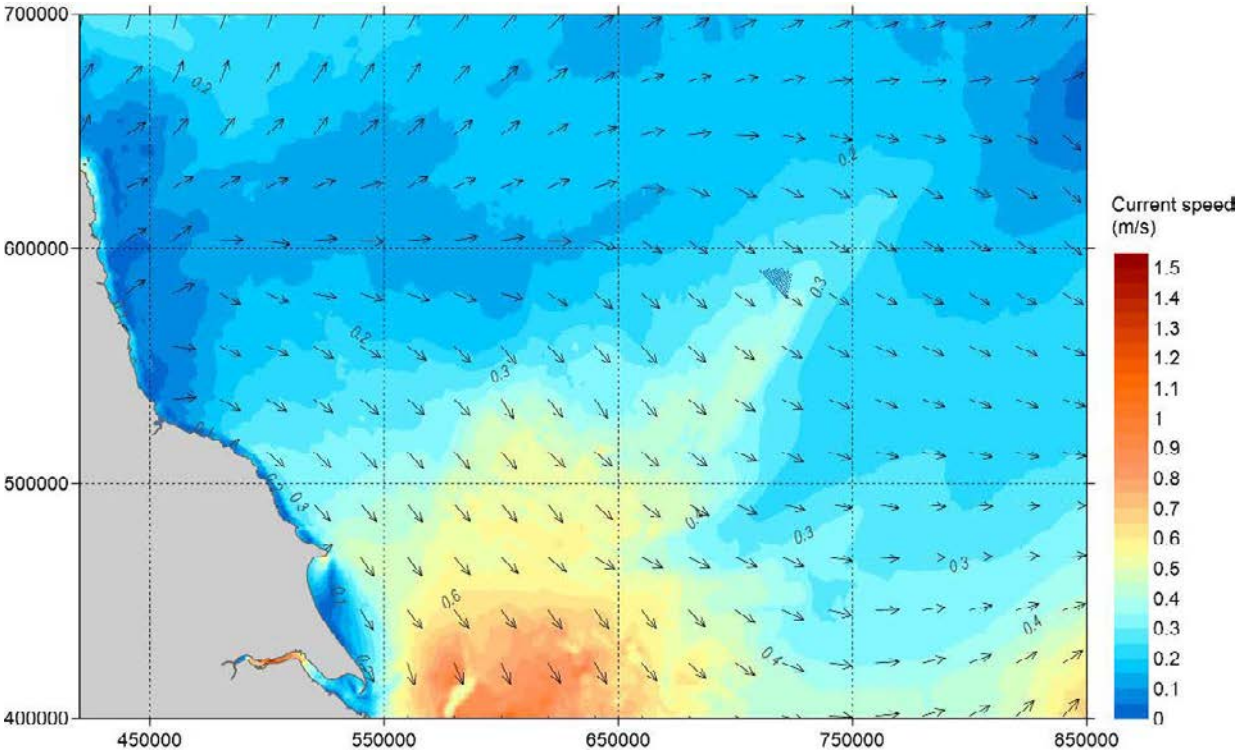

Figure A.51 Overview of Spatial Variation of Peak South-east-going Currents in a Spring Tide – Layout B – OSP 2

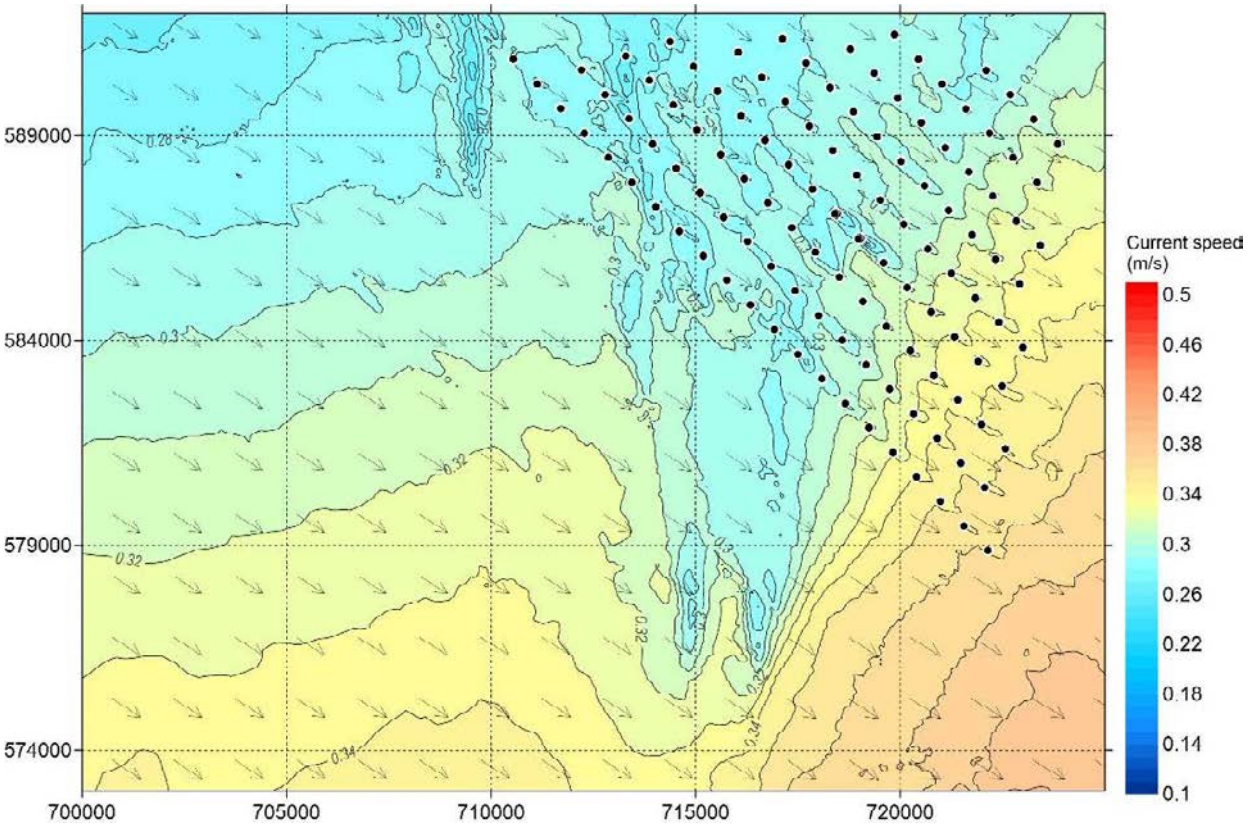

Figure A.52 A Closer View of Spatial Variation of Peak South-east-going Currents in a Spring Tide – Layout B – OSP 2

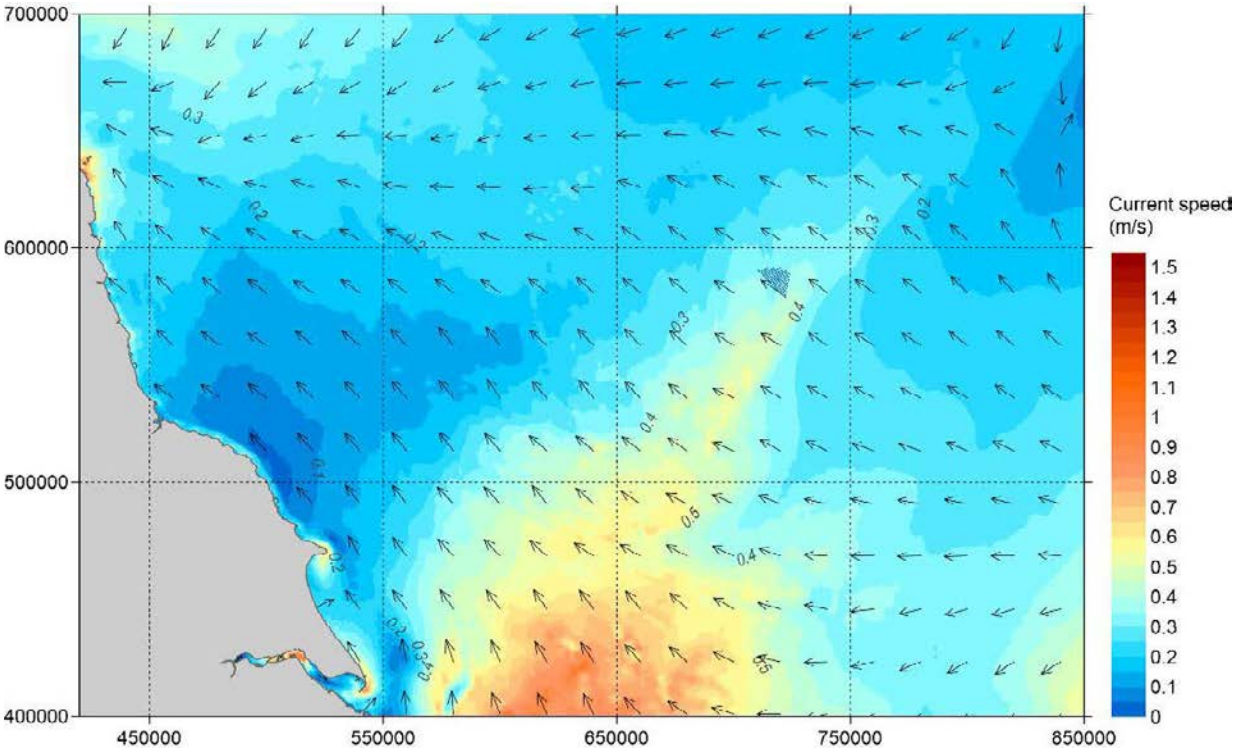

Figure A.53 Overview of Spatial Variation of Peak North-west-going Currents in a Spring Tide – Layout B – OSP 2

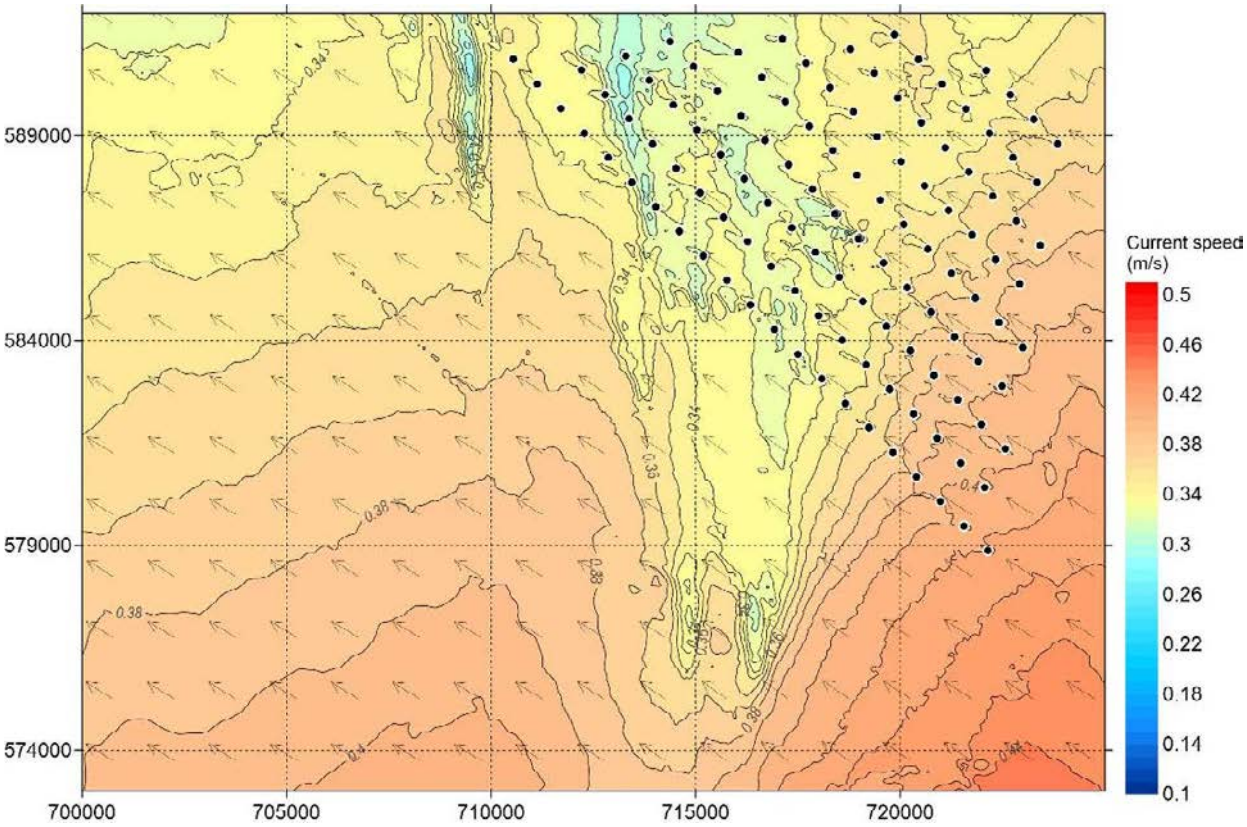

Figure A.54 A Closer View of Spatial Variation of Peak North-west-going Currents in a Spring Tide – Layout B – OSP 2

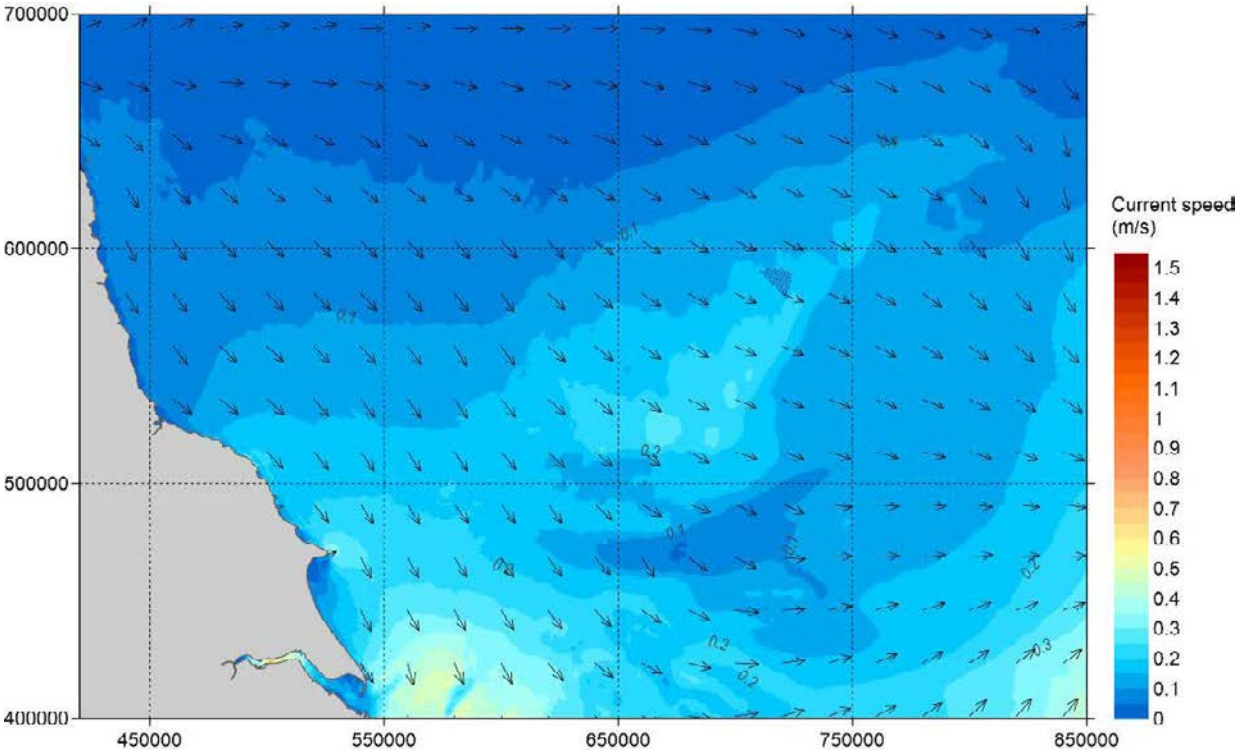

Figure A.55 Overview of Spatial Variation of Peak South-east-going Currents in a Neap tide – Layout B – OSP 2

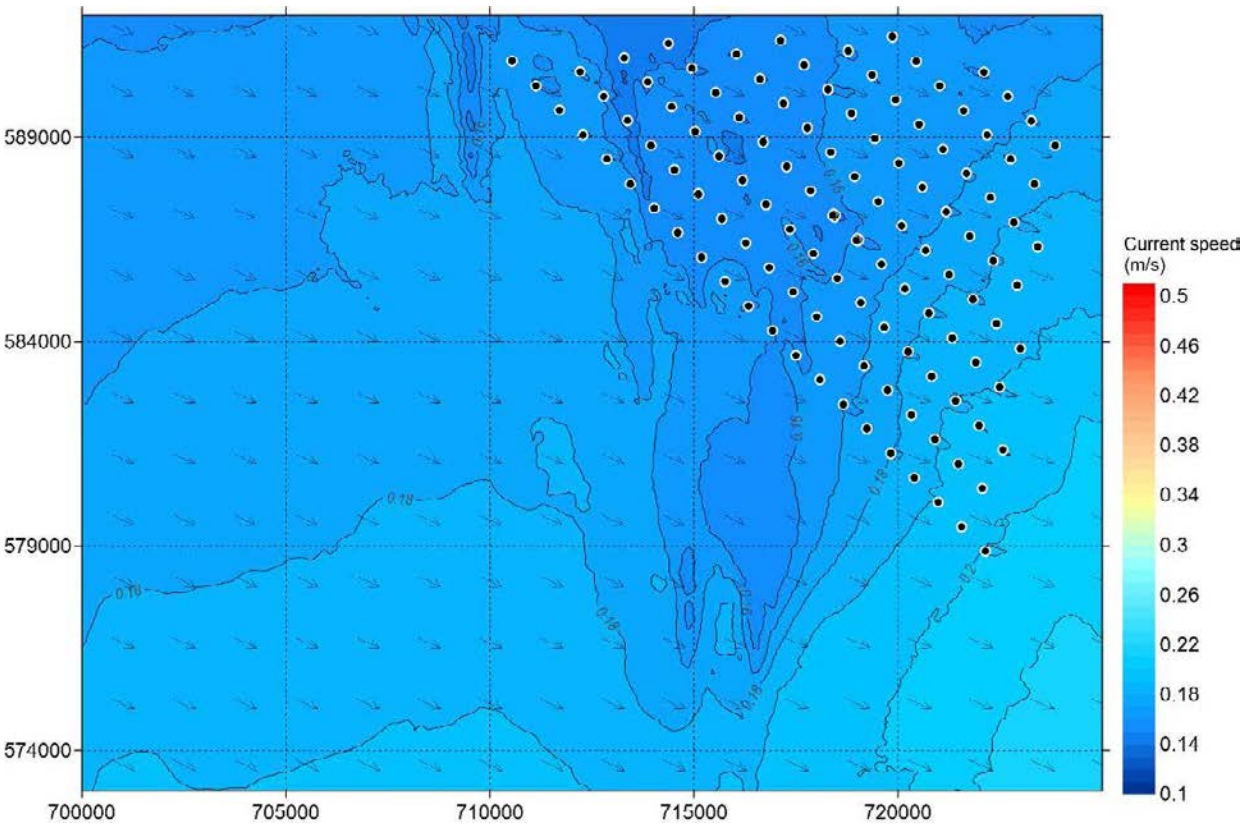

Figure A.56 Overview of Spatial Variation of Peak South-east-going Currents in a Neap tide – Layout B – OSP 2

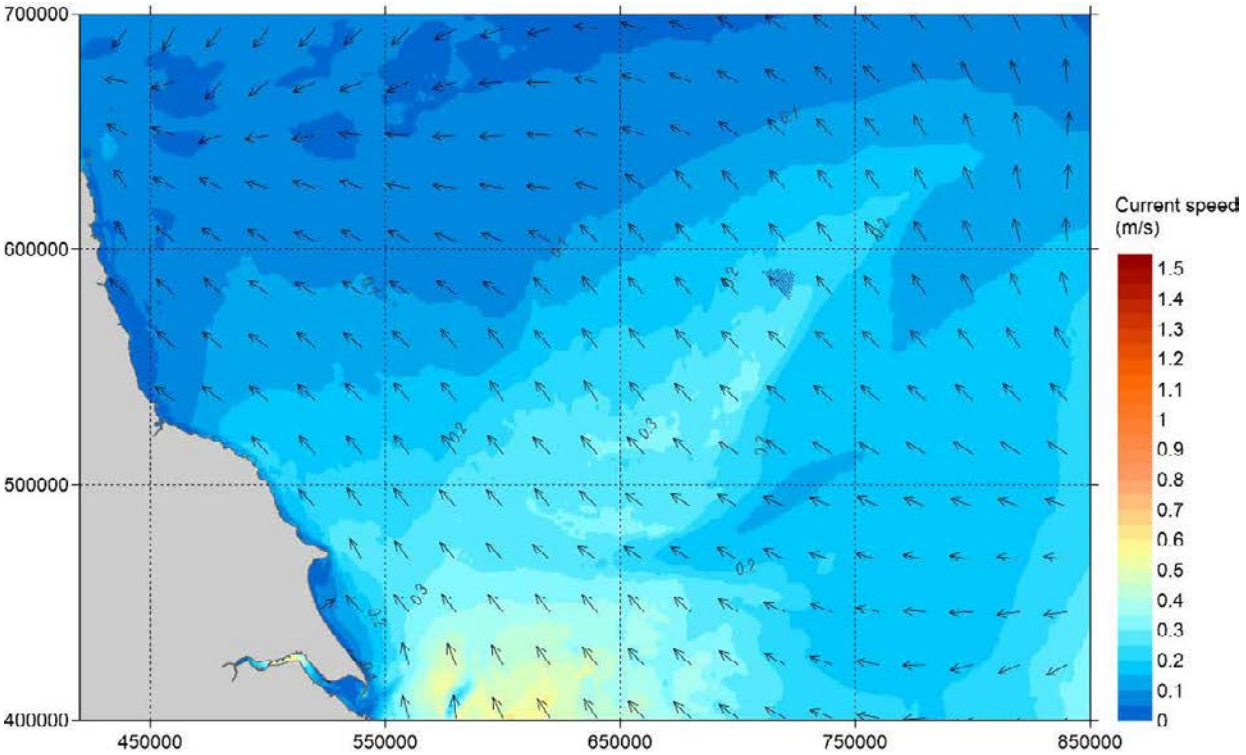

Figure A.57 Overview of Spatial Variation of Peak North-west-going Currents in a Neap tide – Layout B – OSP 2

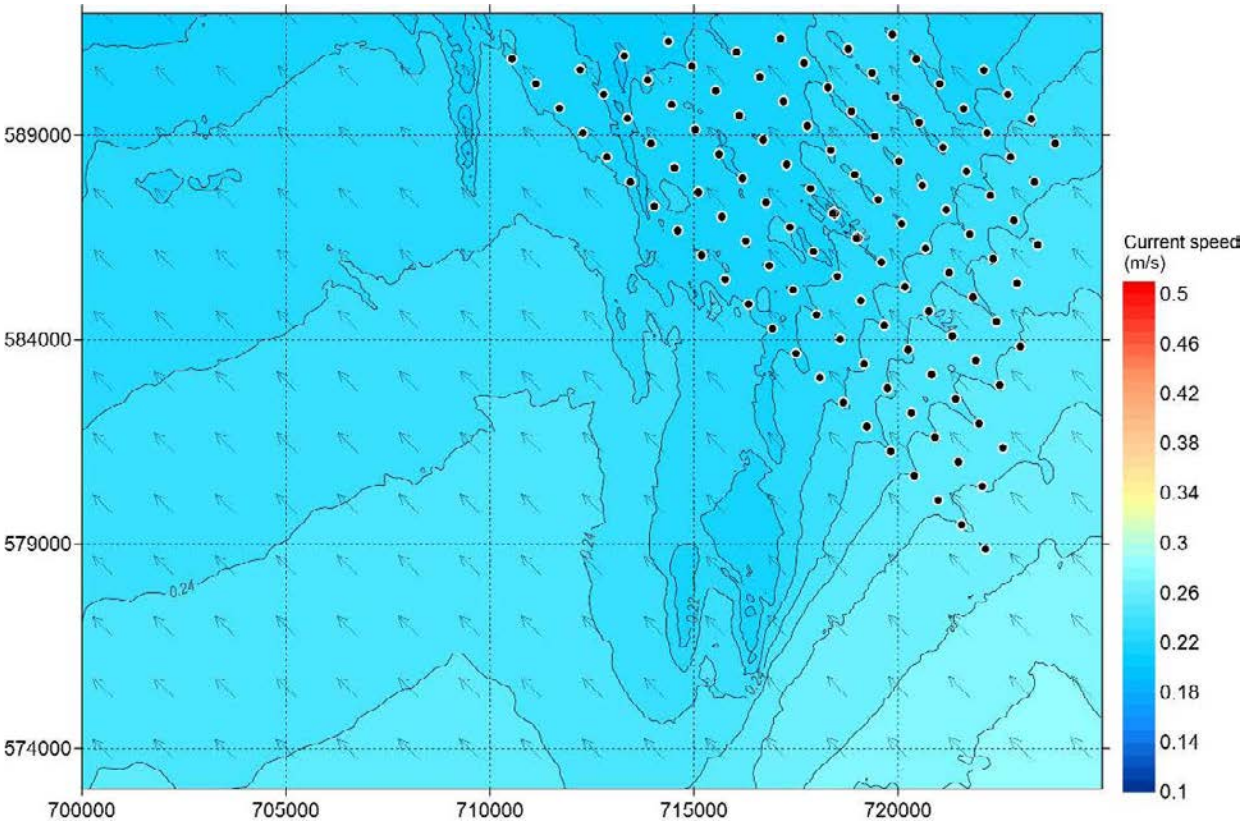

Figure A.58 Overview of Spatial Variation of Peak South-east-going Currents in a Neap tide – Layout B – OSP 2

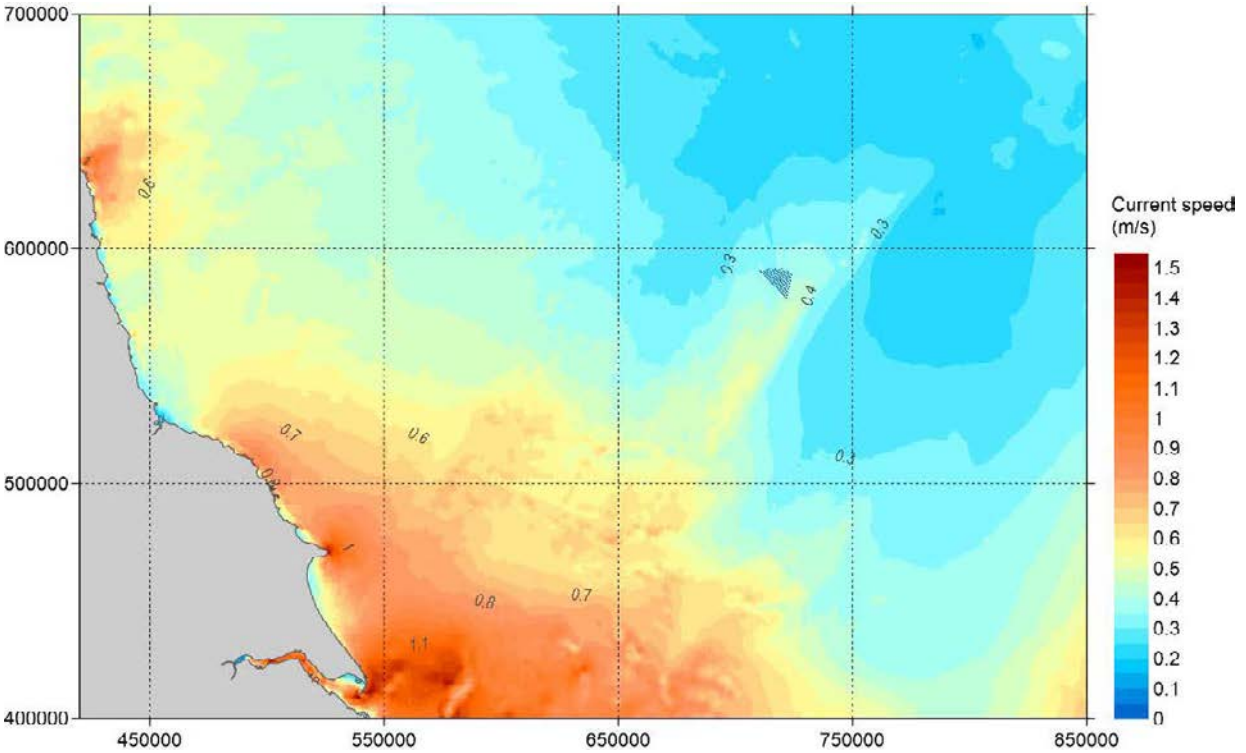

Figure A.59 Overview of Spatial Variation of Maximum Current Speed Over 30 days- Layout B – OSP 2

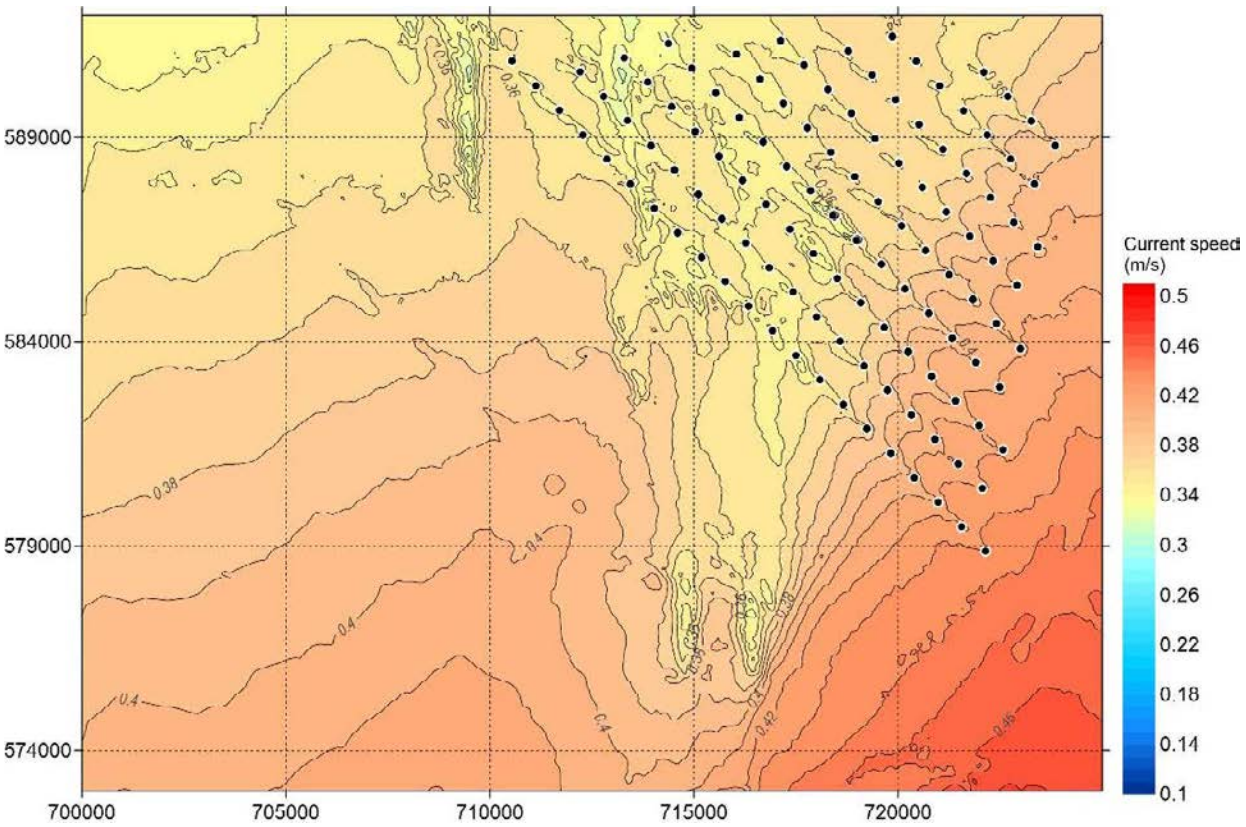

Figure A.60 Overview of Spatial Variation of Maximum Current Speed Over 30 days- Layout B – OSP 2

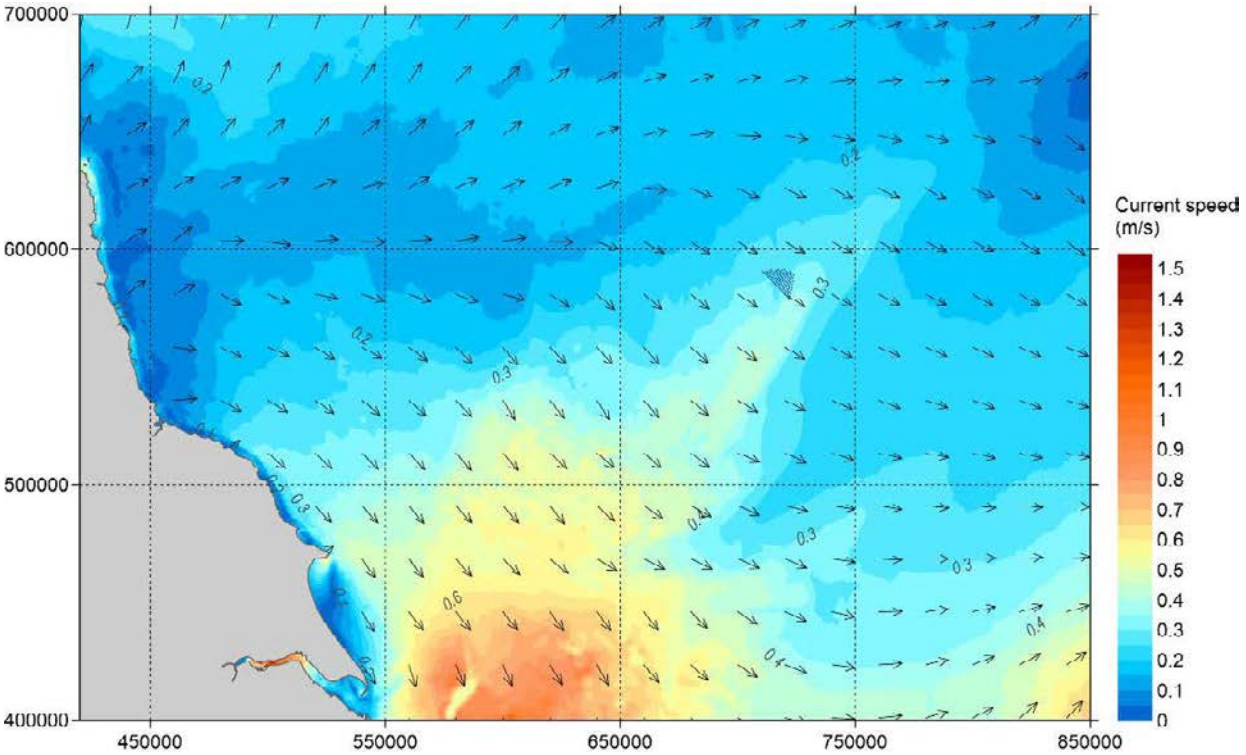

Figure A.61 Overview of Spatial Variation of Peak South-east-going Currents in a Spring Tide – Layout B – OSP 3

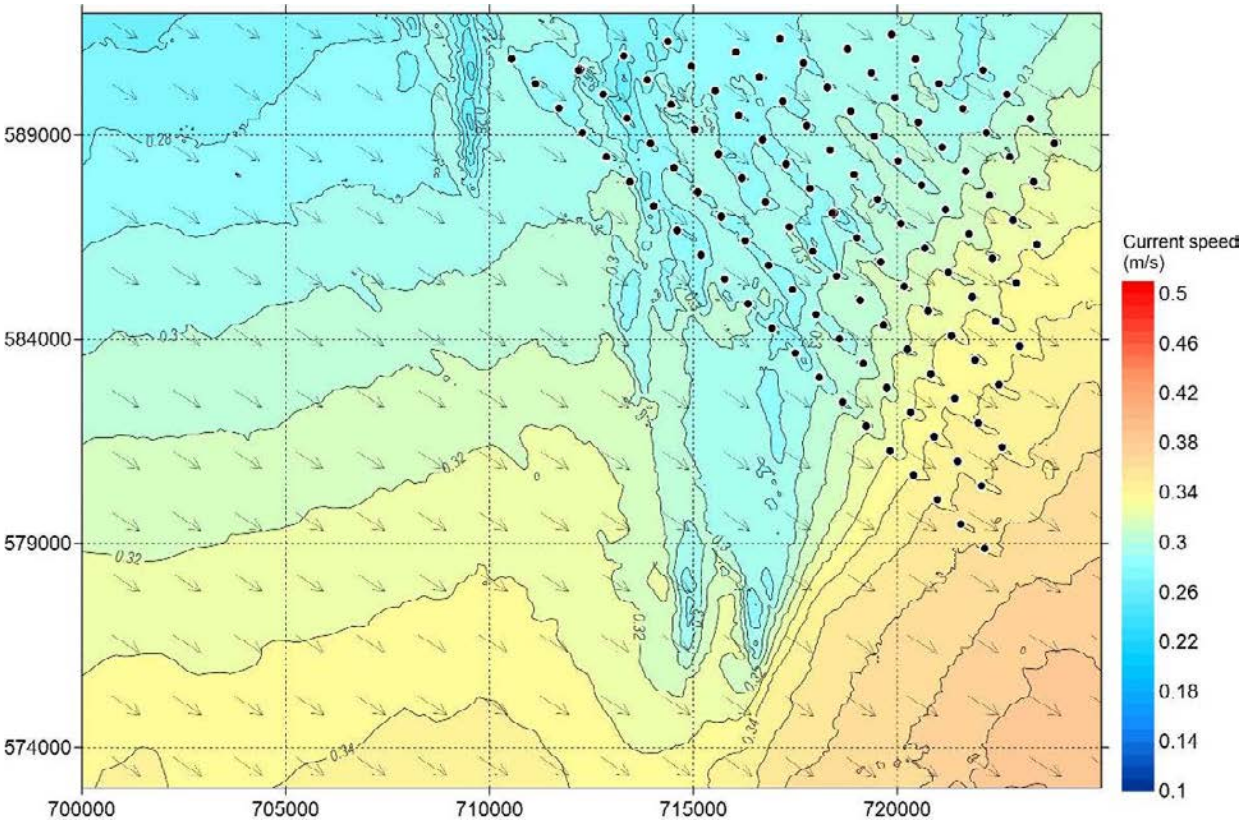

Figure A.62 A Closer View of Spatial Variation of Peak South-east-going Currents in a Spring Tide – Layout B – OSP 3

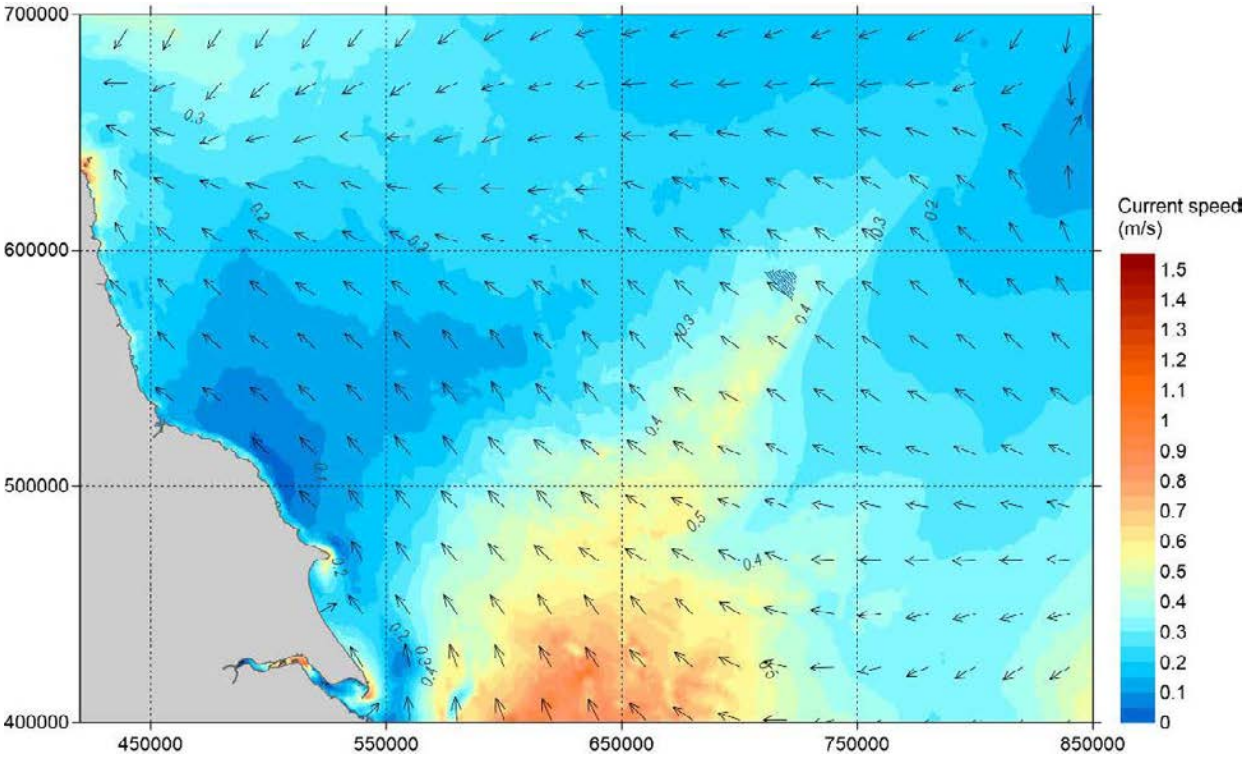

Figure A.63 Overview of Spatial Variation of Peak North-west-going Currents in a Spring Tide – Layout B – OSP 3

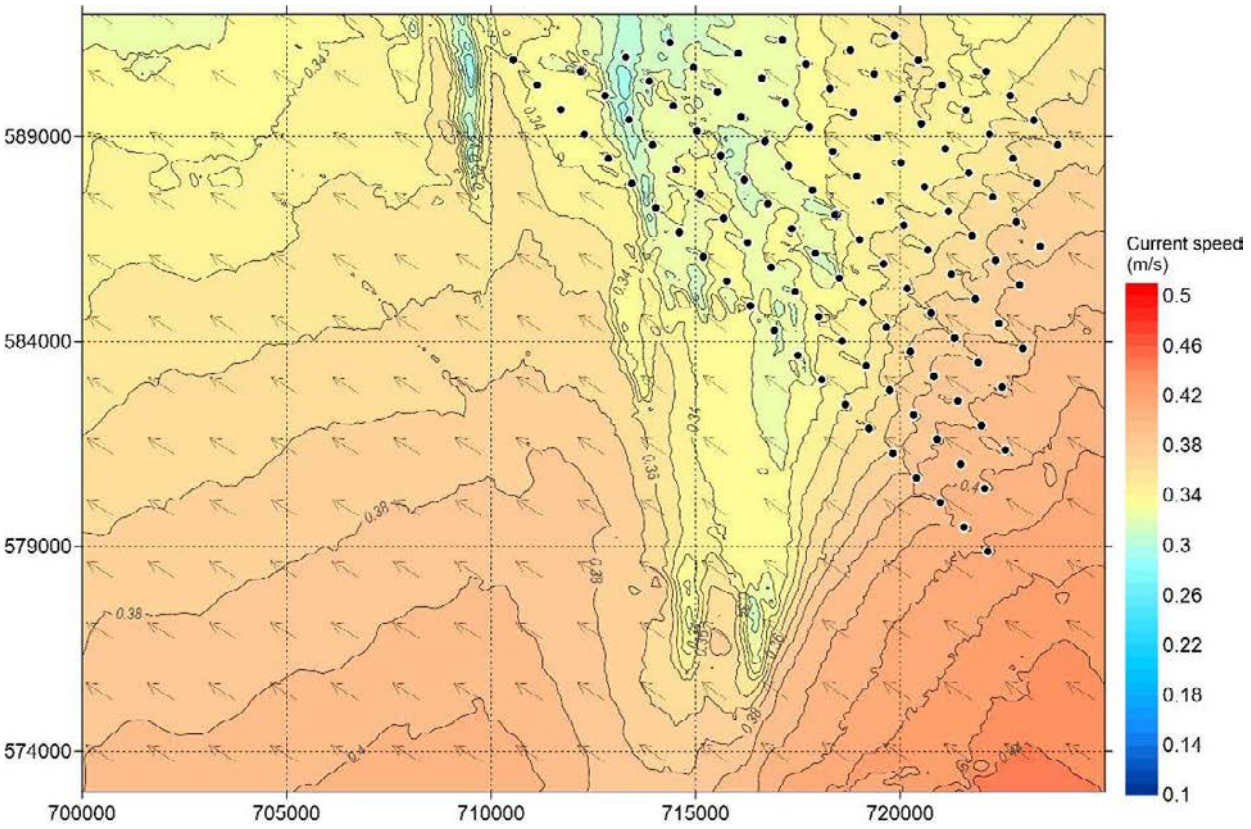

Figure A.64 A Closer View of Spatial Variation of Peak North-west-going Currents in a Spring Tide – Layout B – OSP 3

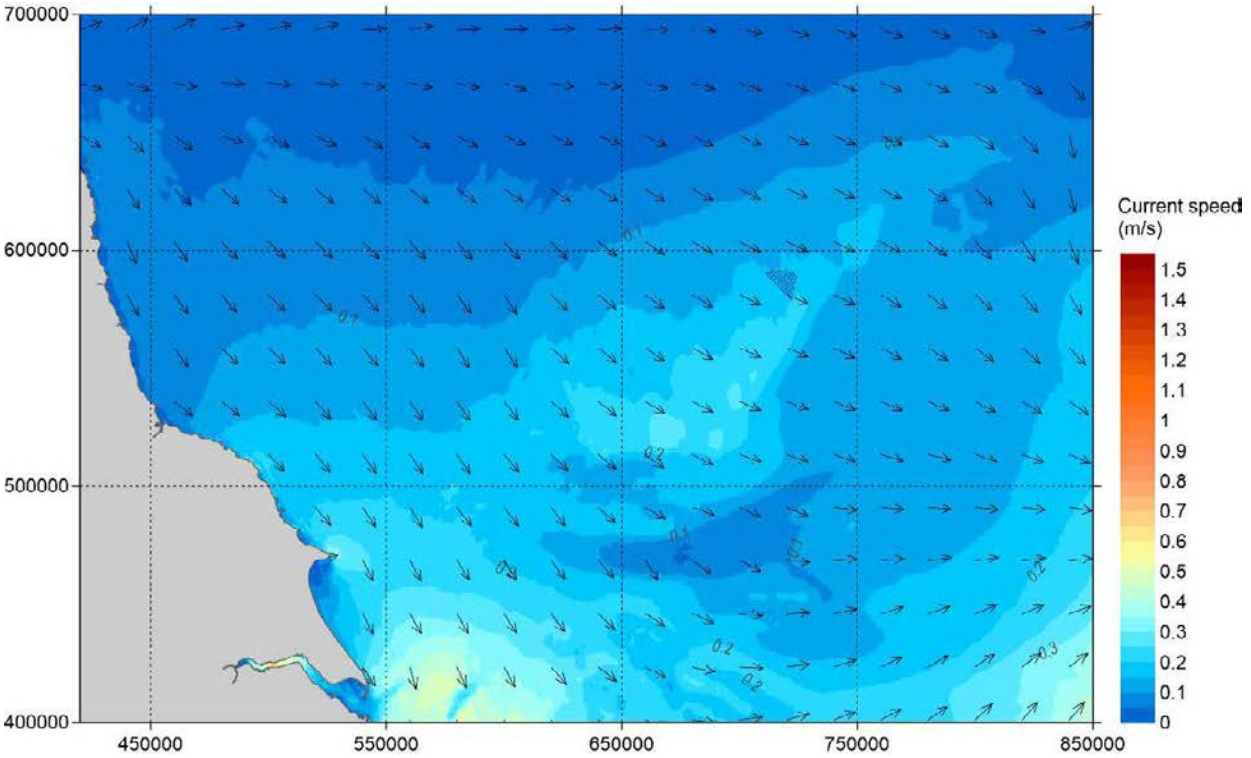

Figure A.65 Overview of Spatial Variation of Peak South-east-going Currents in a Neap tide – Layout B – OSP 3

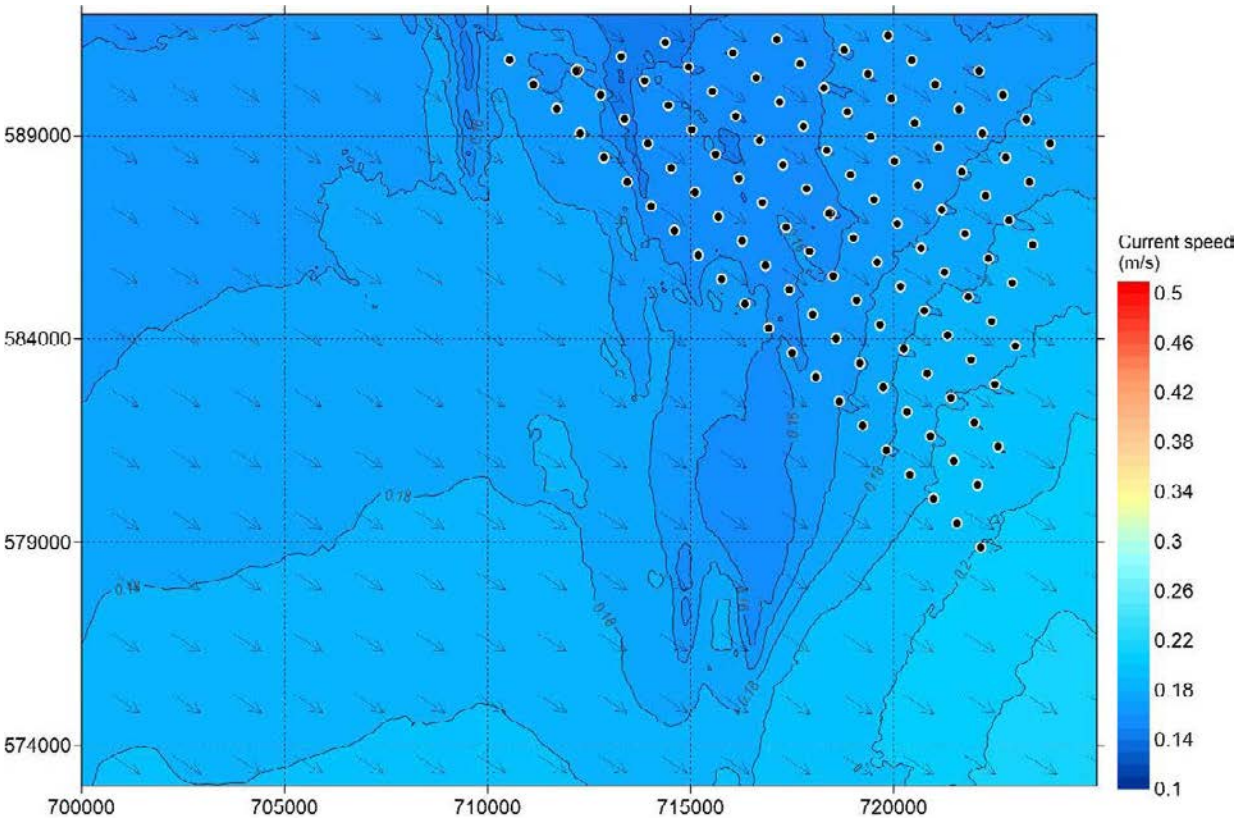

Figure A.66 Overview of Spatial Variation of Peak South-east-going Currents in a Neap tide – Layout B – OSP 3

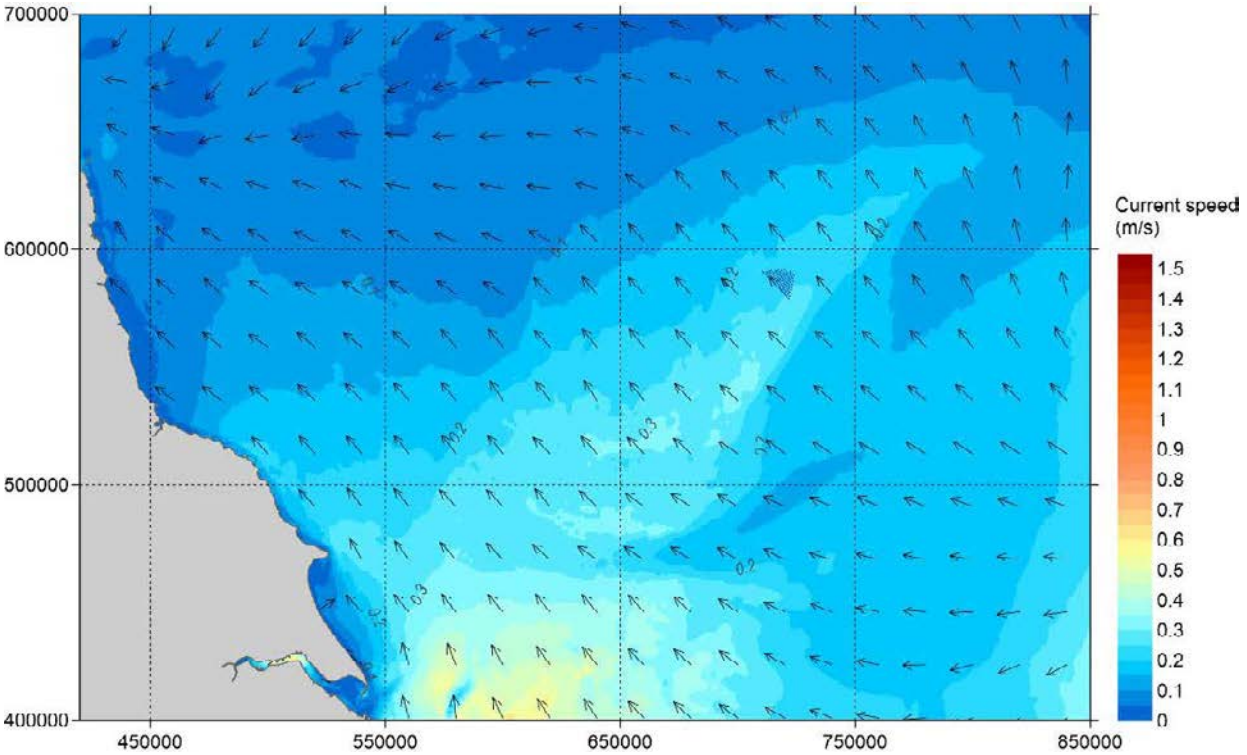

Figure A.67 Overview of Spatial Variation of Peak North-west-going Currents in a Neap tide – Layout B – OSP 3

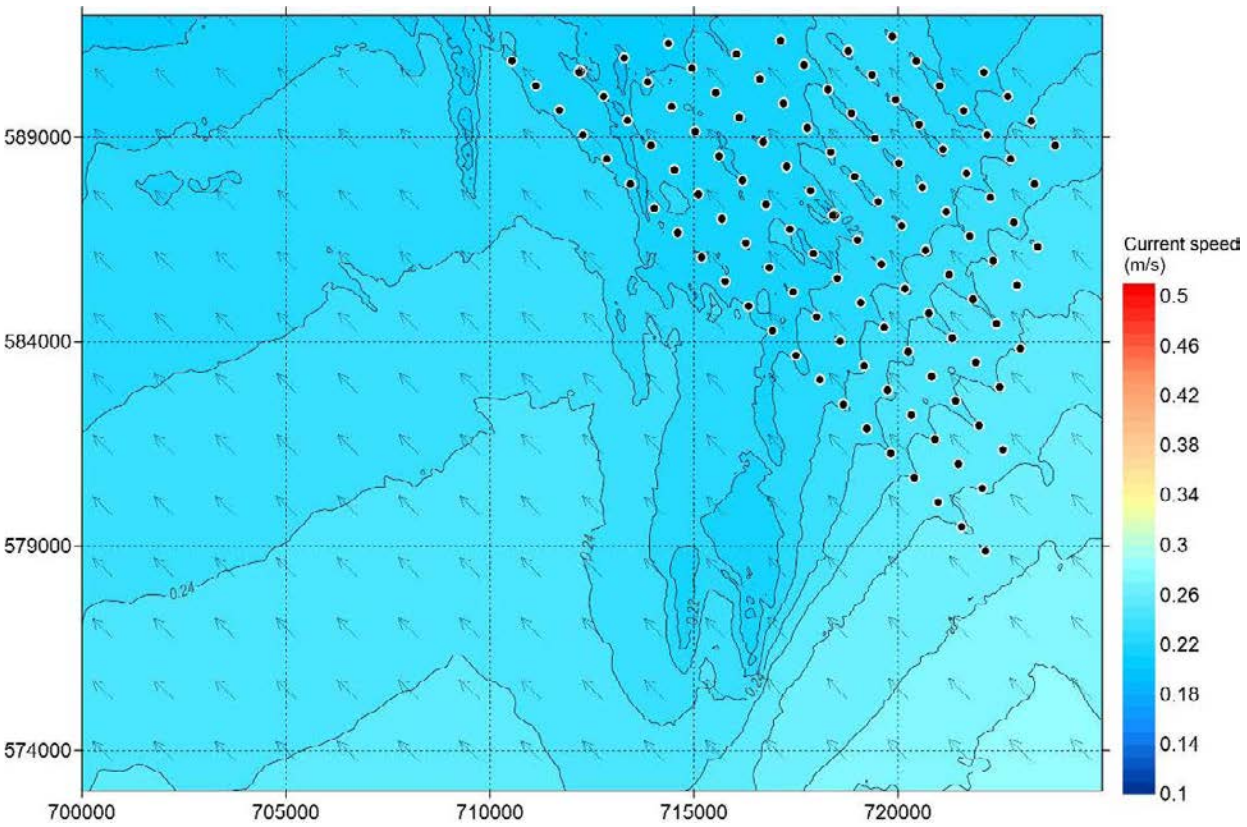

Figure A.68 Overview of Spatial Variation of Peak South-east-going Currents in a Neap tide – Layout B – OSP 3

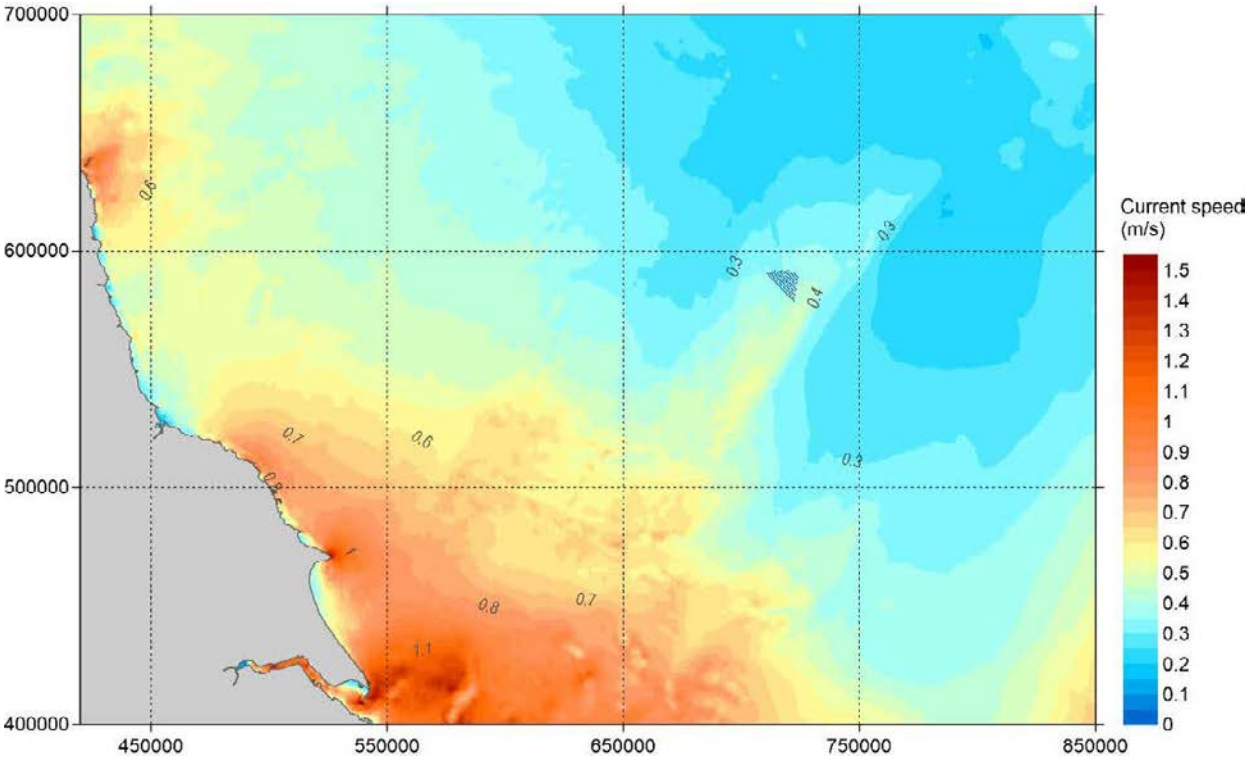

Figure A.69 Overview of Spatial Variation of Maximum Current Speed Over 30 days- Layout B – OSP 3

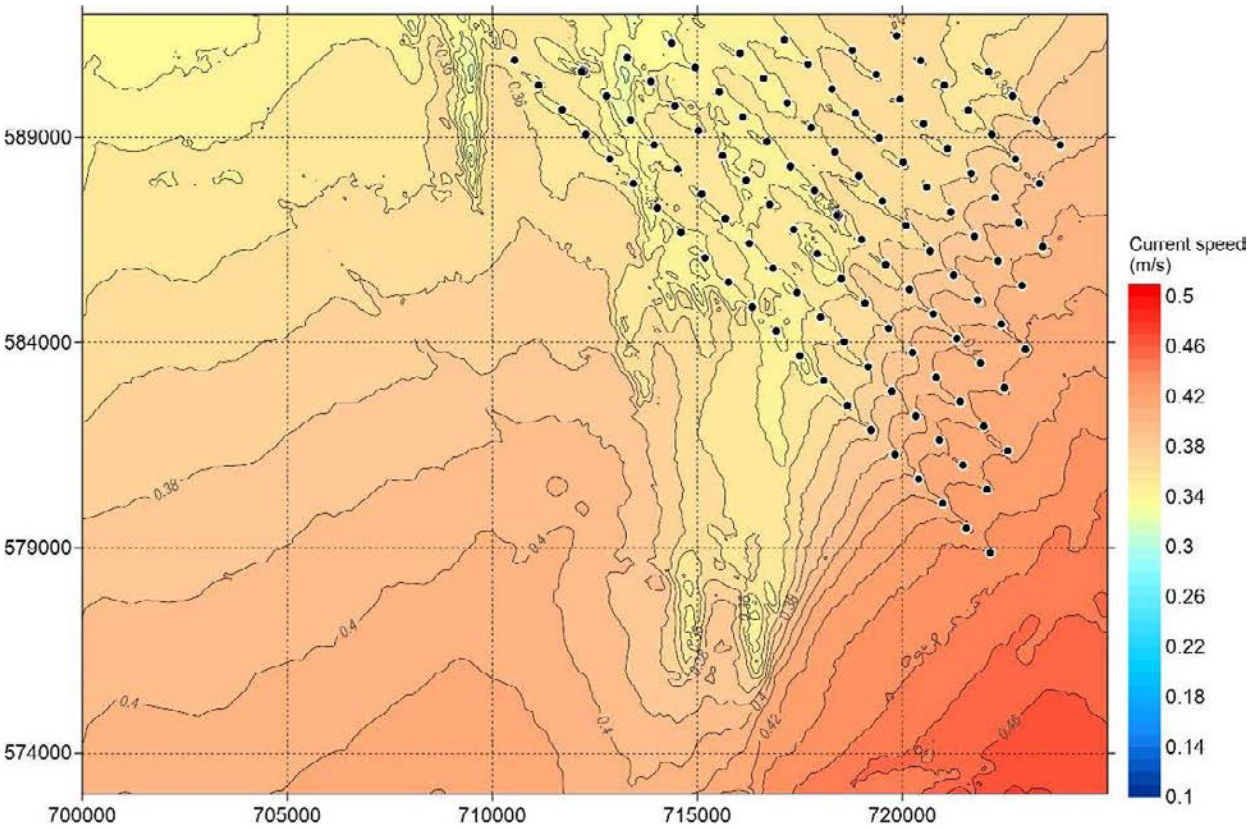

Figure A.70 Overview of Spatial Variation of Maximum Current Speed Over 30 days- Layout B – OSP 3

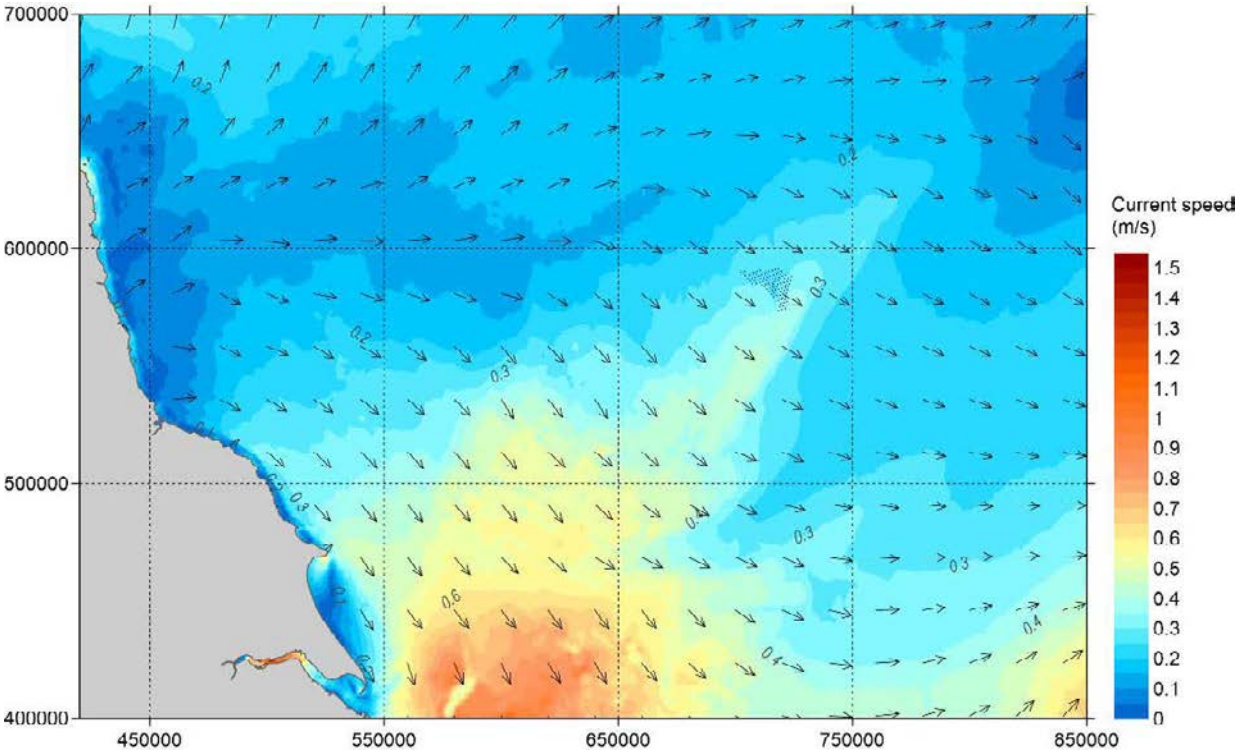

Figure A.71 Overview of Spatial Variation of Peak South-east-going Currents in a Spring Tide – Layout C – OSP 1

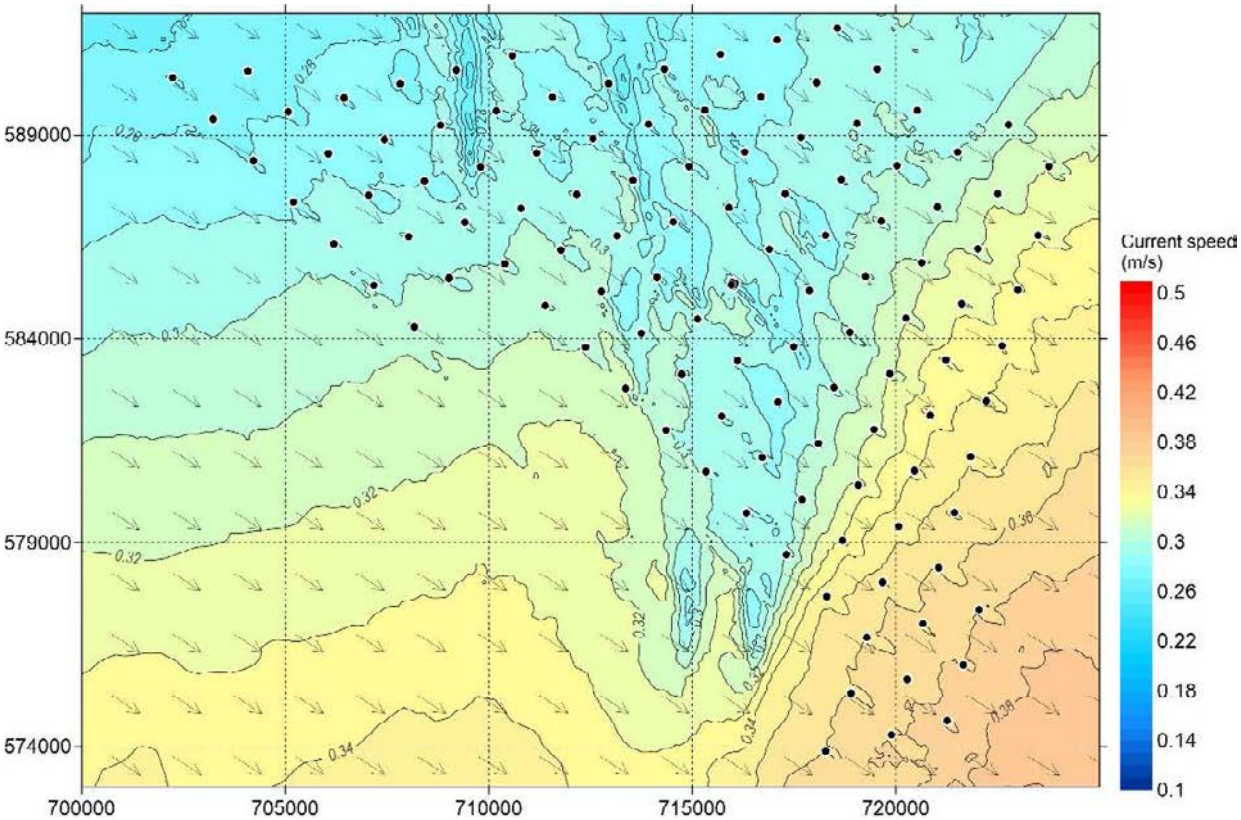

Figure A.72 A Closer View of Spatial Variation of Peak South-east-going Currents in a Spring Tide – Layout C – OSP 1

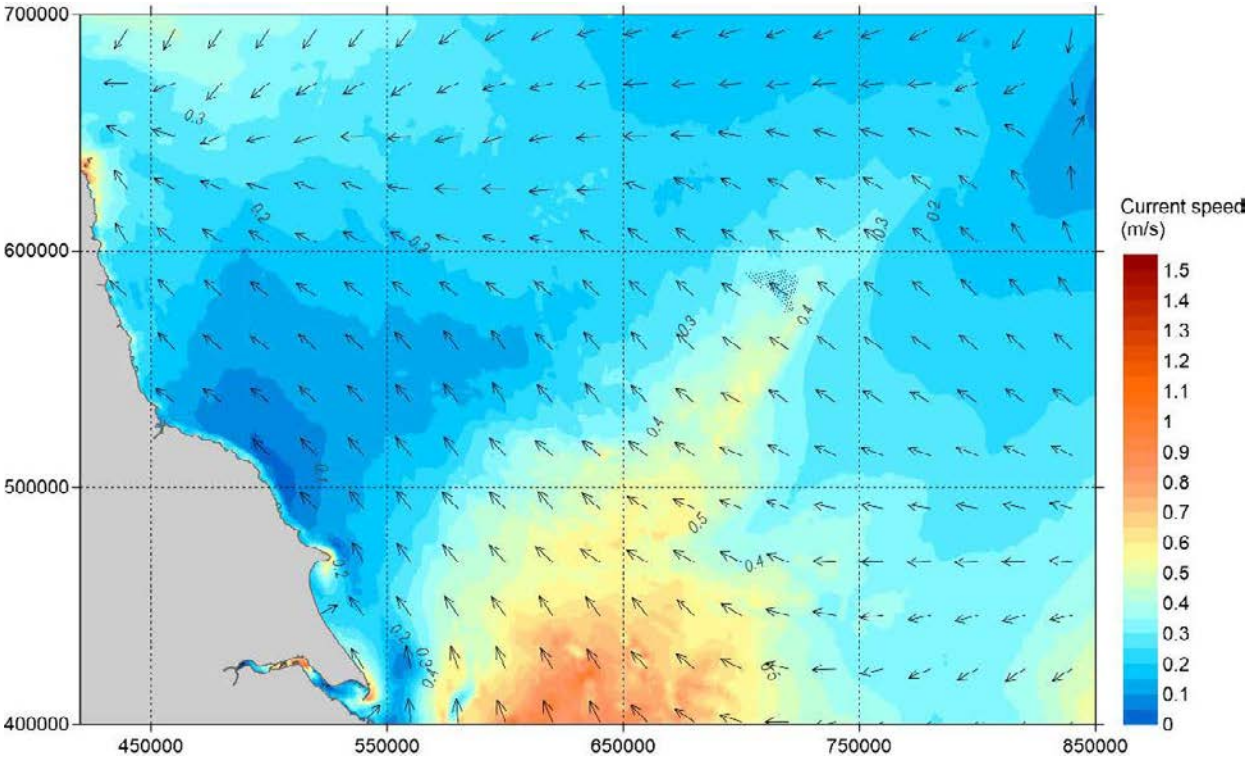

Figure A.73 Overview of Spatial Variation of Peak North-west-going Currents in a Spring Tide – Layout C – OSP 1

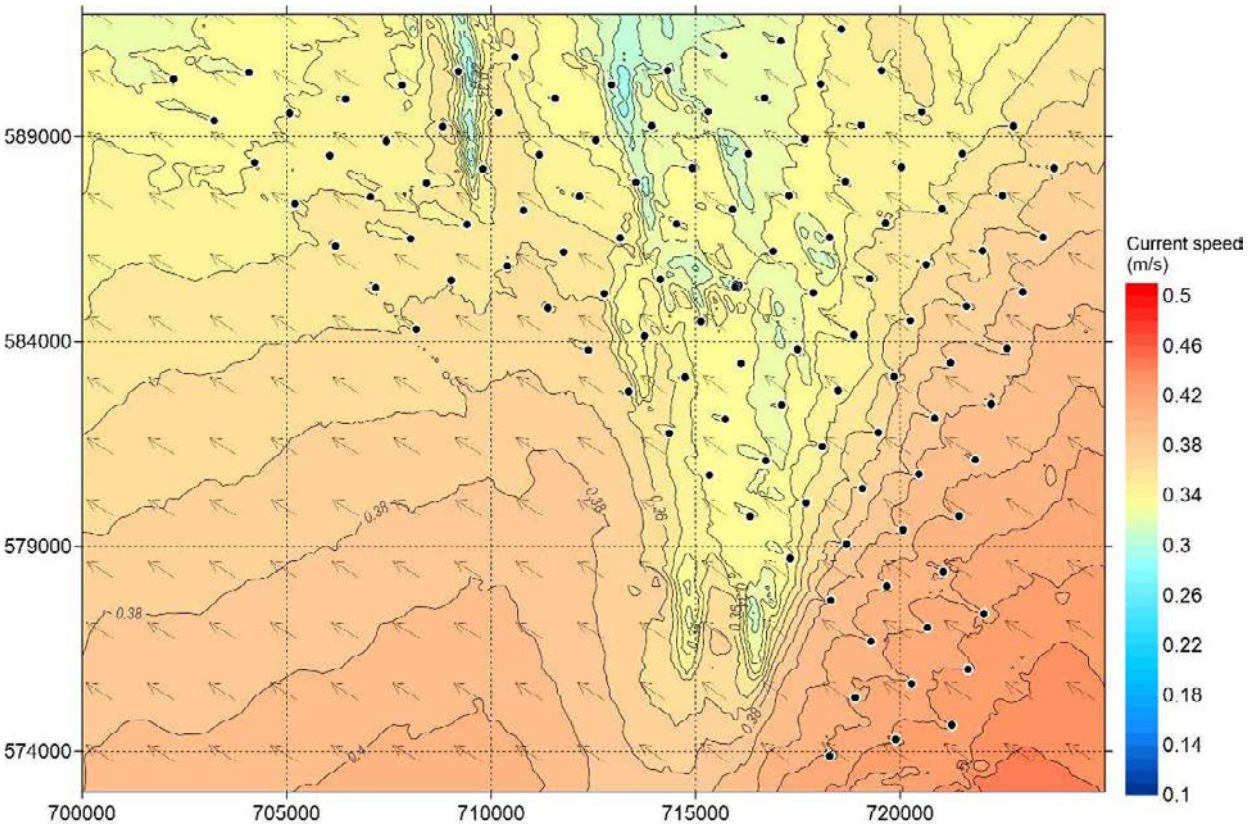

Figure A.74 A Closer View of Spatial Variation of Peak North-west-going Currents in a Spring Tide – Layout C – OSP 1

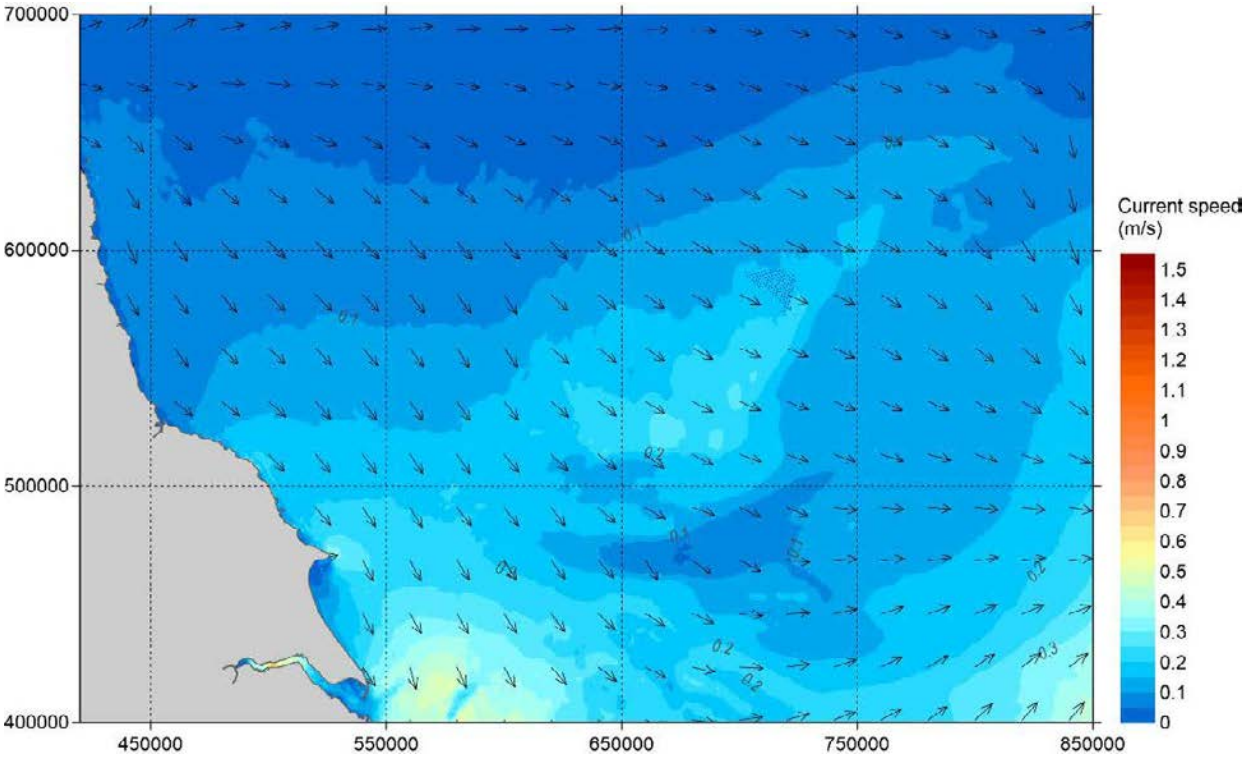

Figure A.75 Overview of Spatial Variation of Peak South-east-going Currents in a Neap tide – Layout C – OSP 1

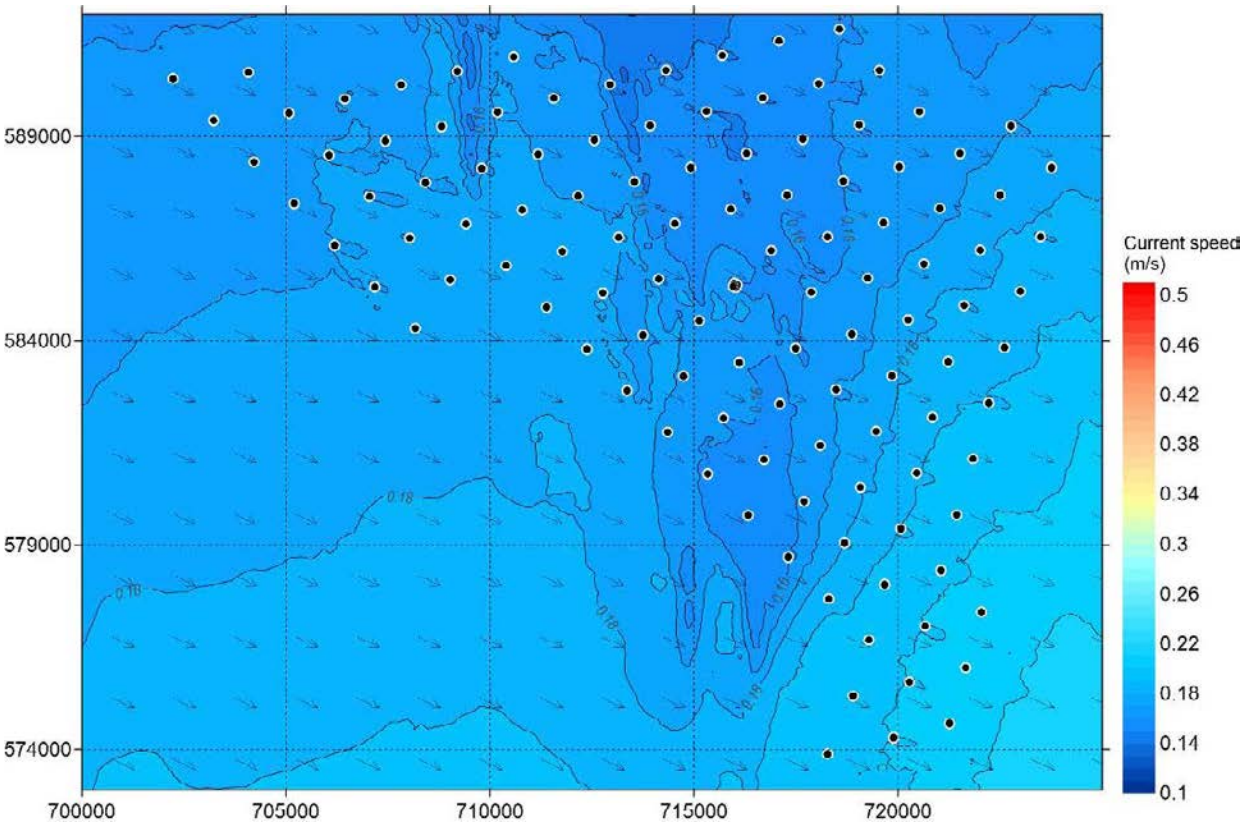

Figure A.76 Overview of Spatial Variation of Peak South-east-going Currents in a Neap tide – Layout C – OSP 1

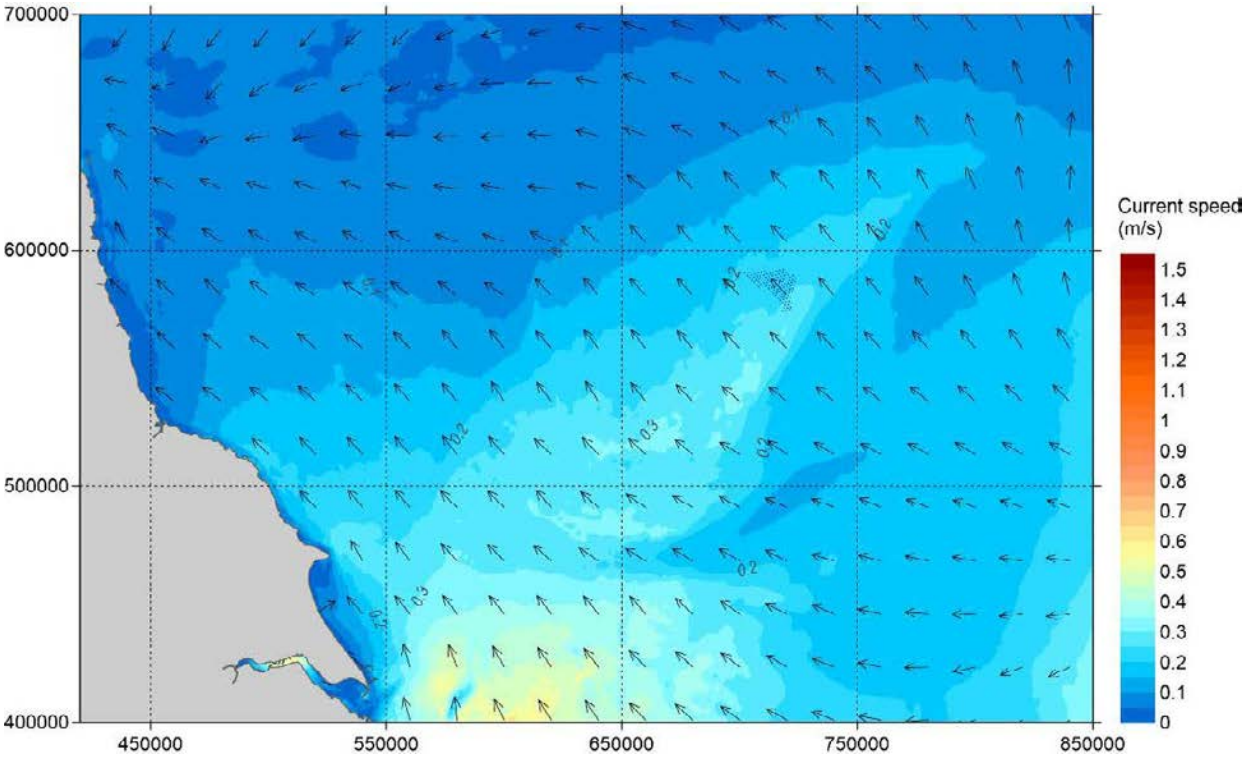

Figure A.77 Overview of Spatial Variation of Peak North-west-going Currents in a Neap tide – Layout C – OSP 1

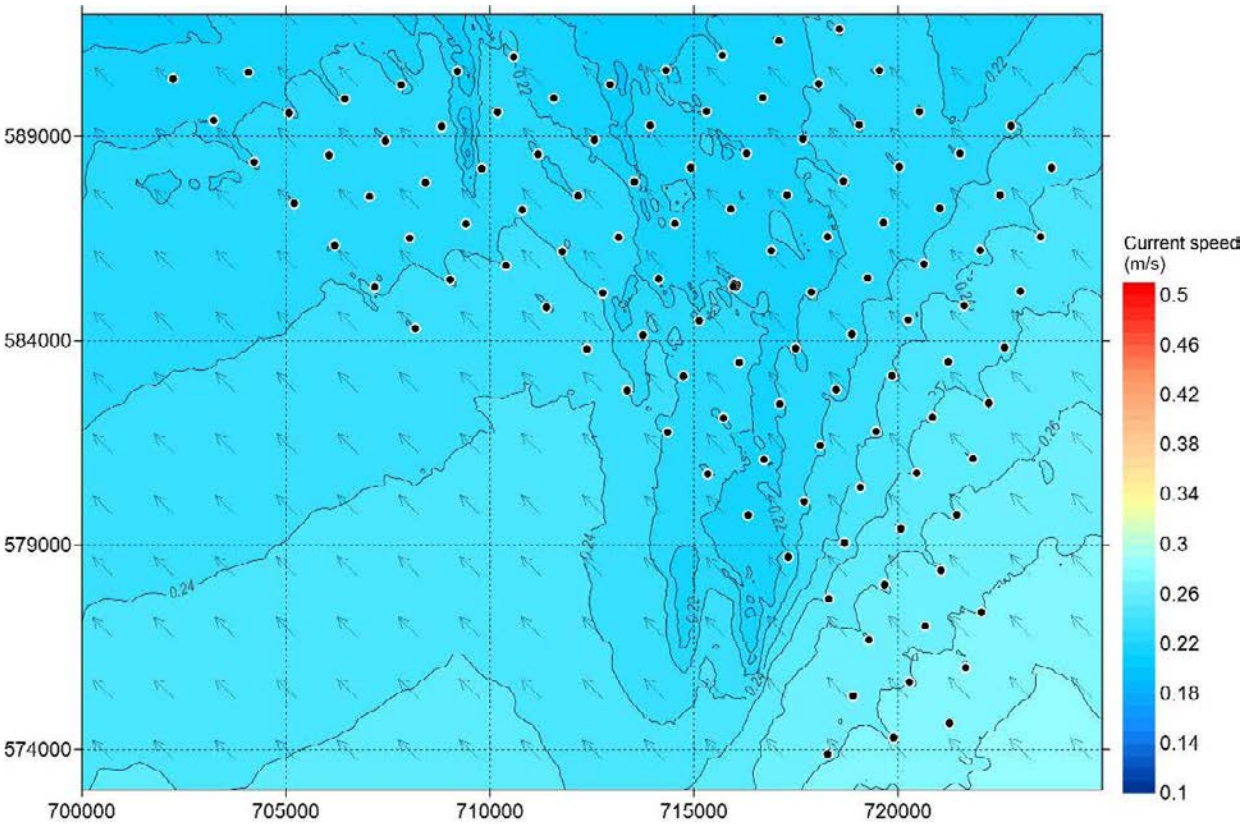

Figure A.78 Overview of Spatial Variation of Peak South-east-going Currents in a Neap tide – Layout C – OSP 1

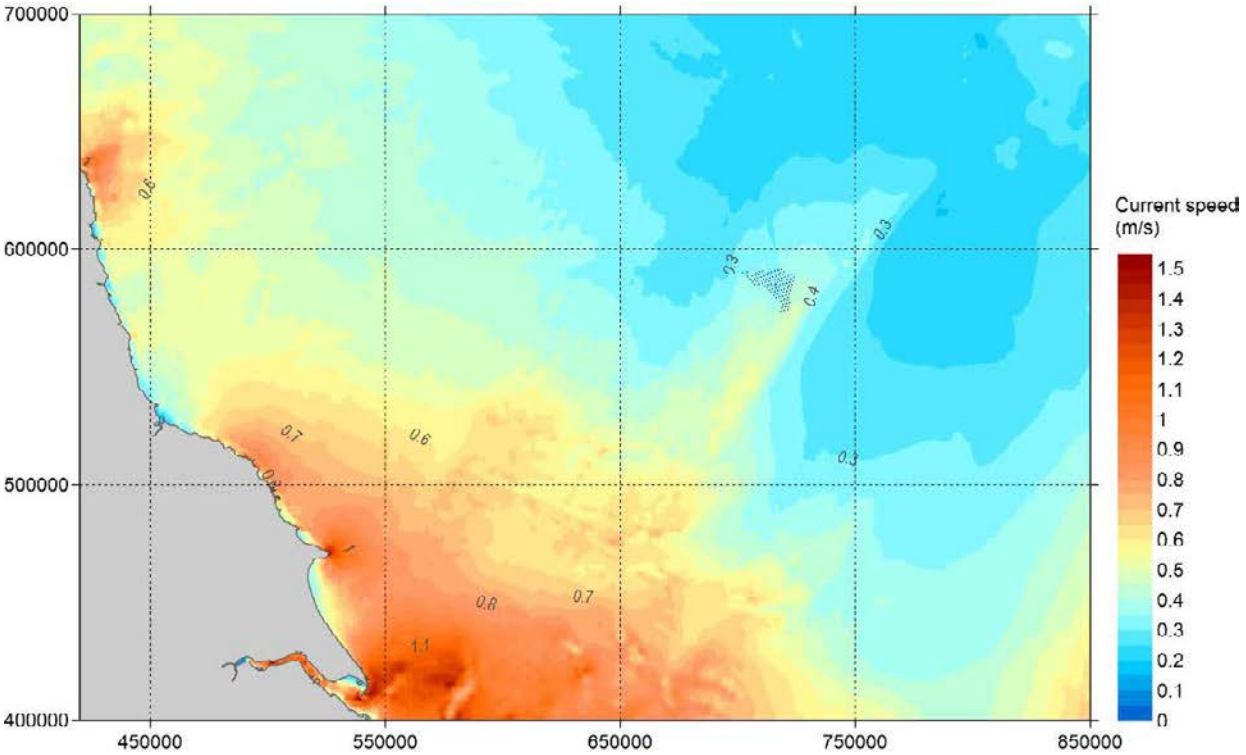

Figure A.79 Overview of Spatial Variation of Maximum Current Speed Over 30 days- Layout C – OSP 1

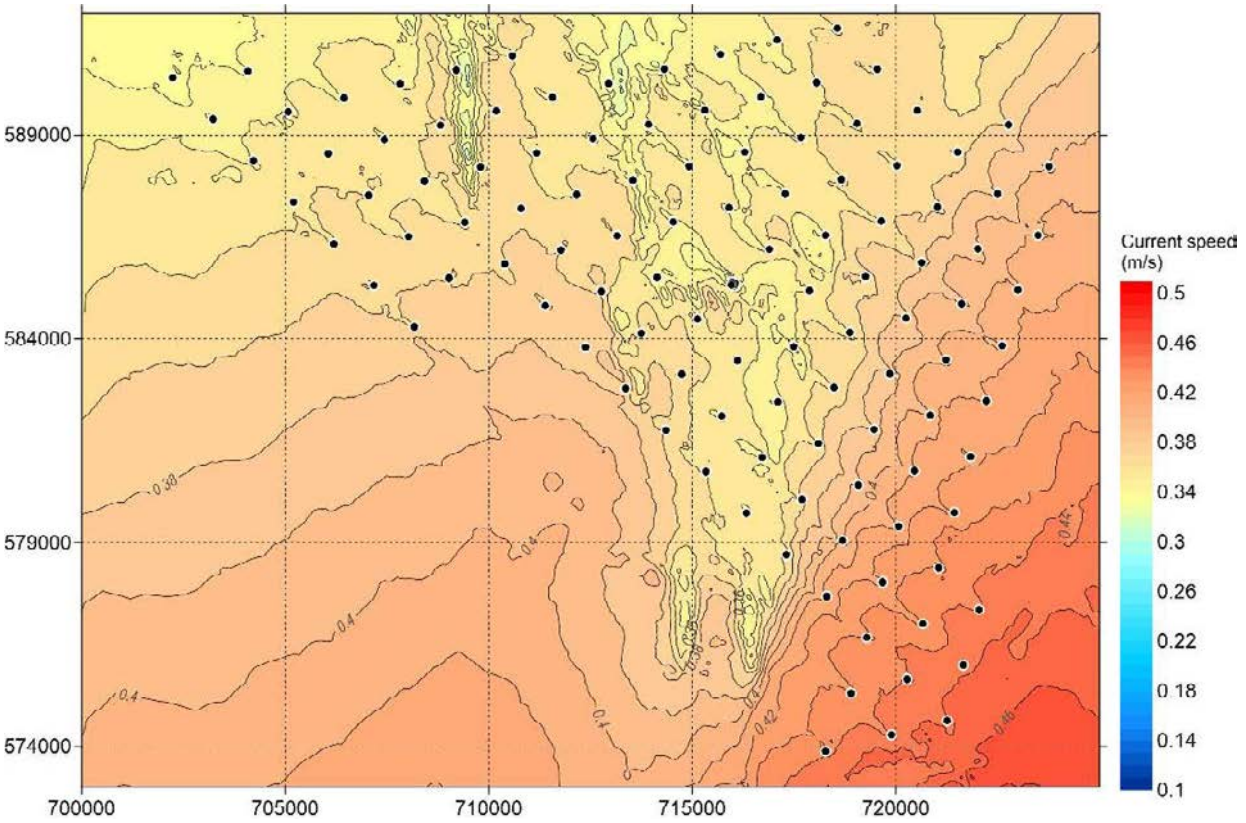

Figure A.80 Overview of Spatial Variation of Maximum Current Speed Over 30 days- Layout C – OSP 1

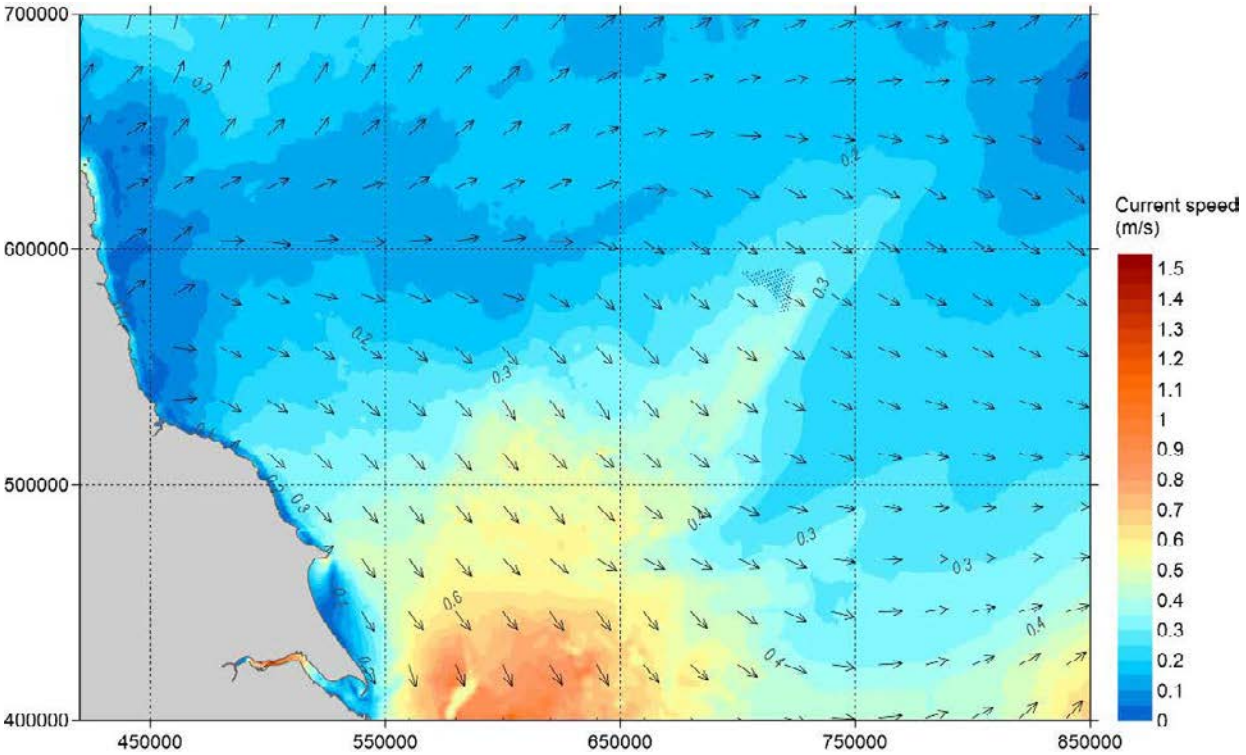

Figure A.81 Overview of Spatial Variation of Peak South-east-going Currents in a Spring Tide – Layout C – OSP 2

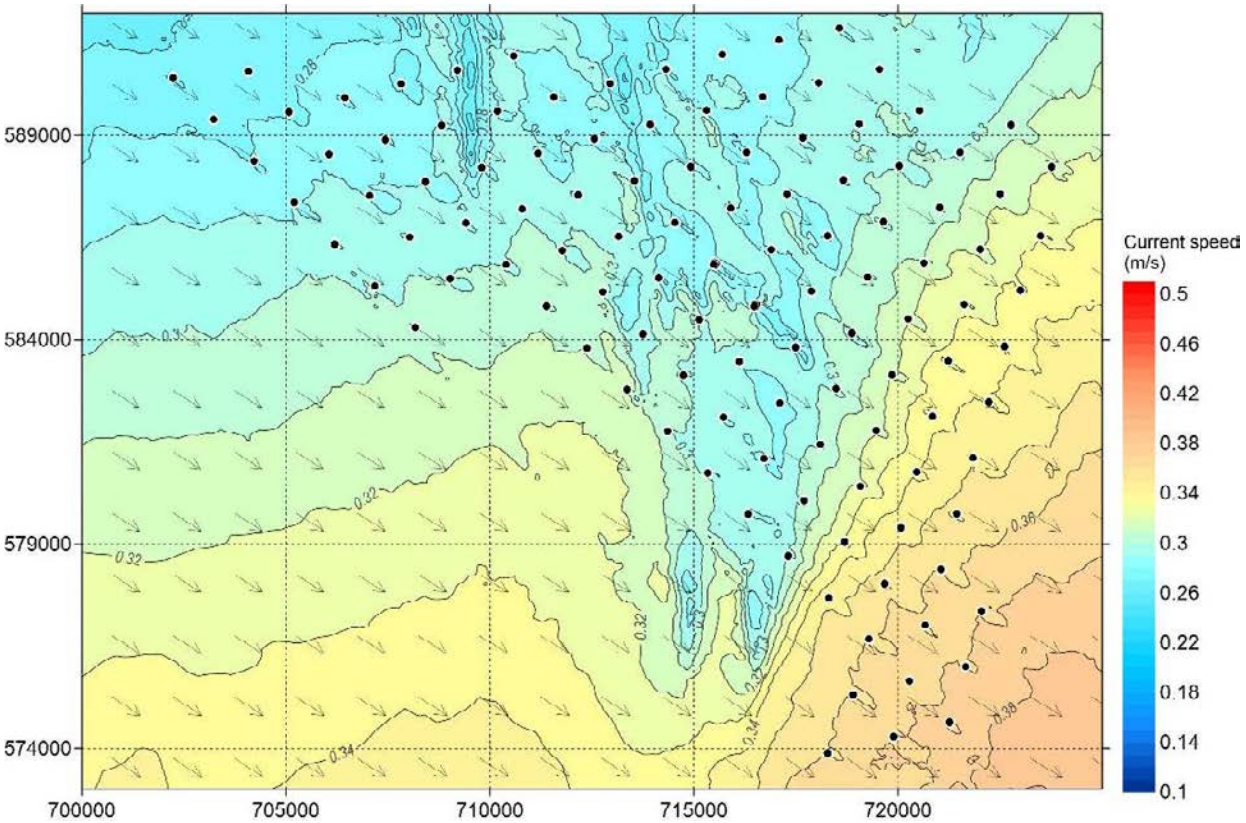

Figure A.82 A Closer View of Spatial Variation of Peak South-east-going Currents in a Spring Tide – Layout C – OSP 2

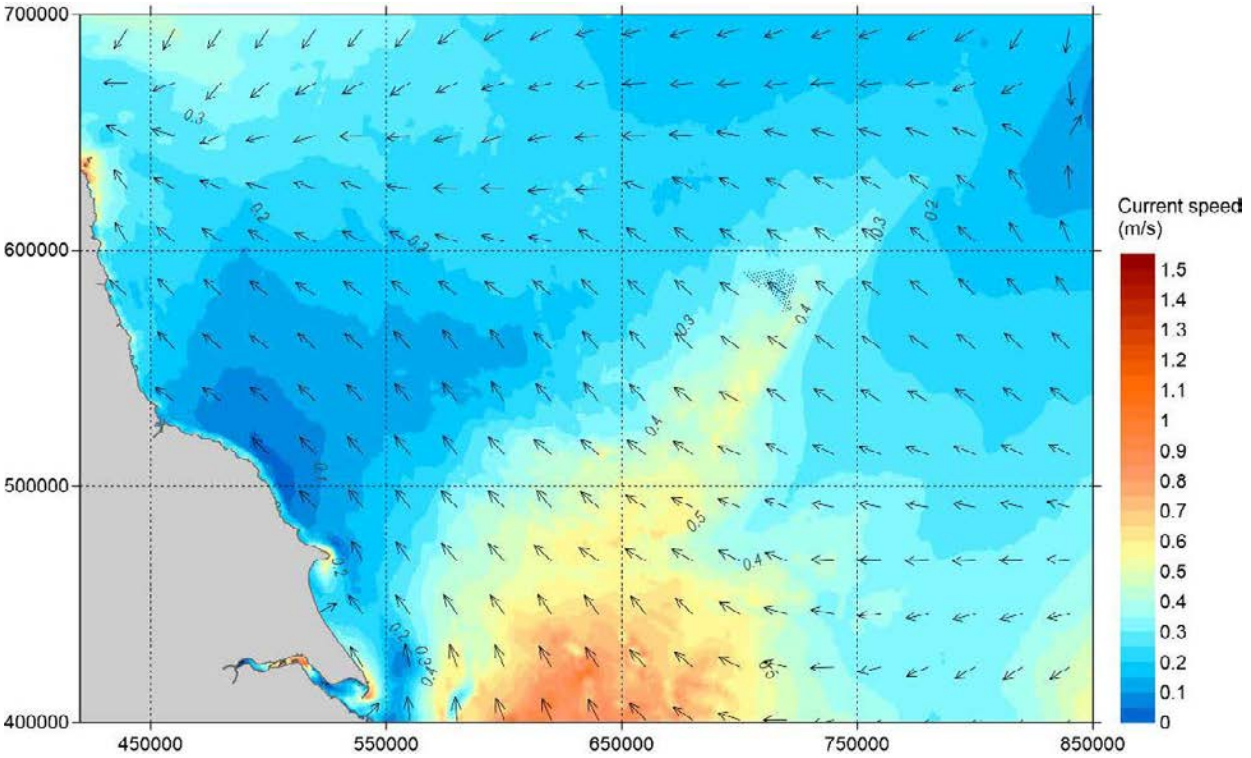

Figure A.83 Overview of Spatial Variation of Peak North-west-going Currents in a Spring Tide – Layout C – OSP 2

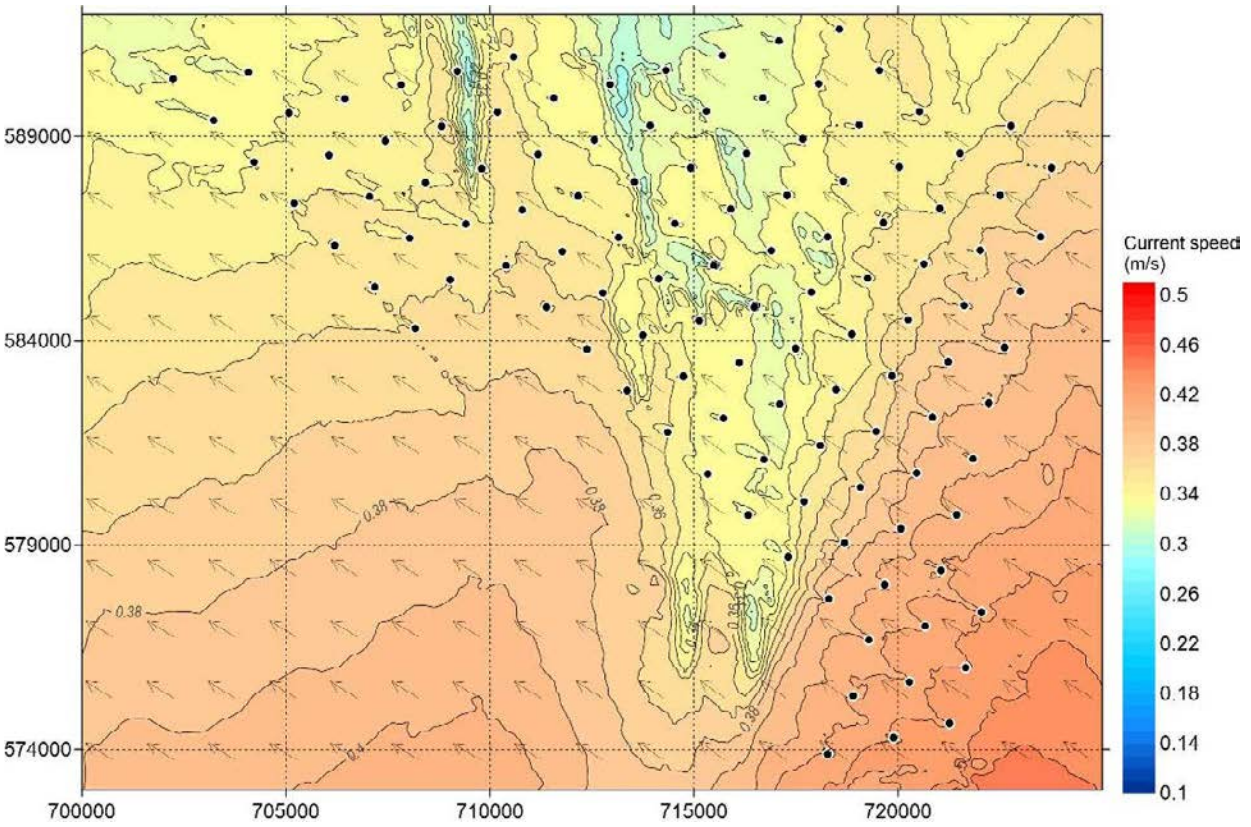

Figure A.84 A Closer View of Spatial Variation of Peak North-west-going Currents in a Spring Tide – Layout C – OSP 2

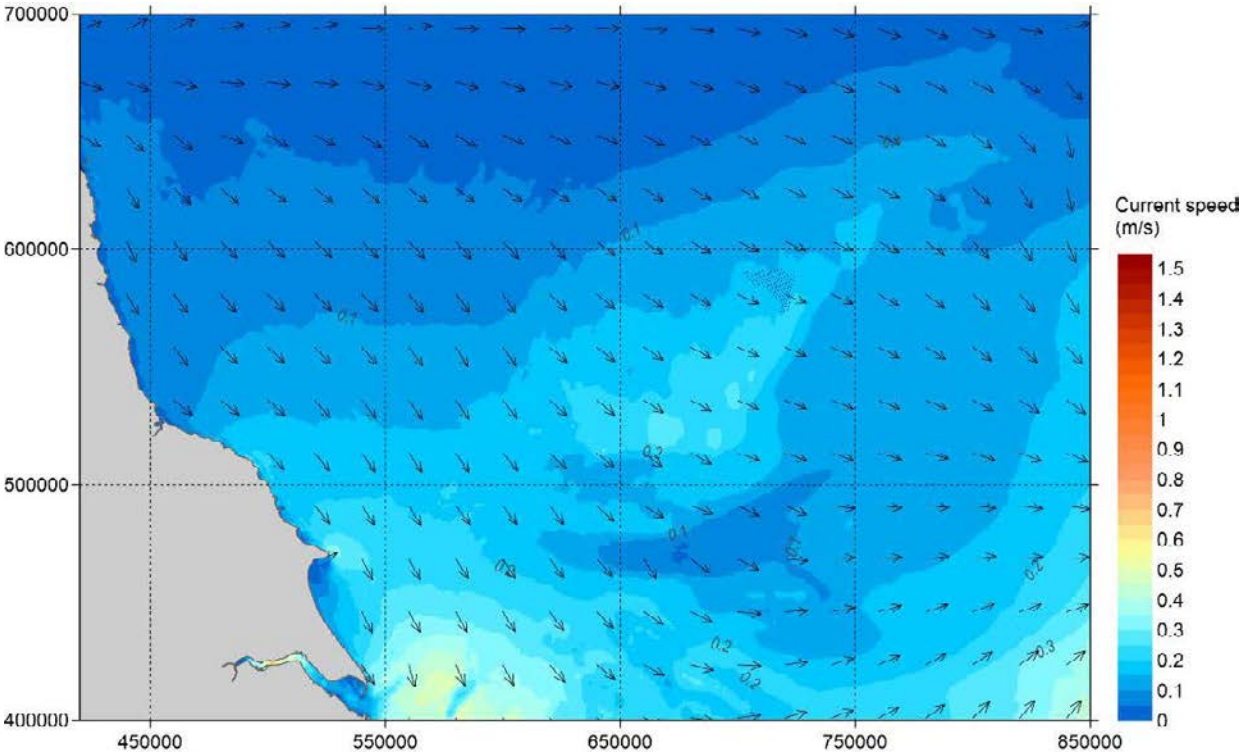

Figure A.85 Overview of Spatial Variation of Peak South-east-going Currents in a Neap tide – Layout C – OSP 2

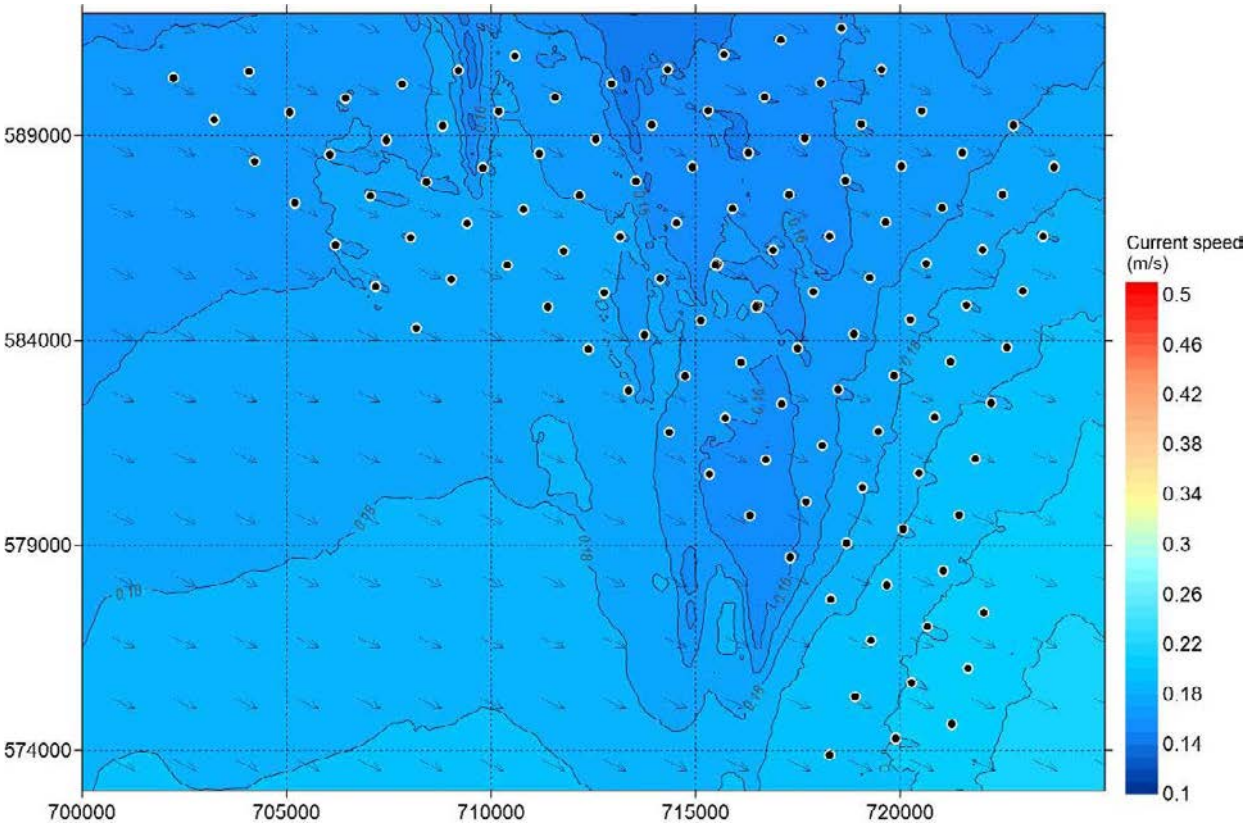

Figure A.86 Overview of Spatial Variation of Peak South-east-going Currents in a Neap tide – Layout C – OSP 2

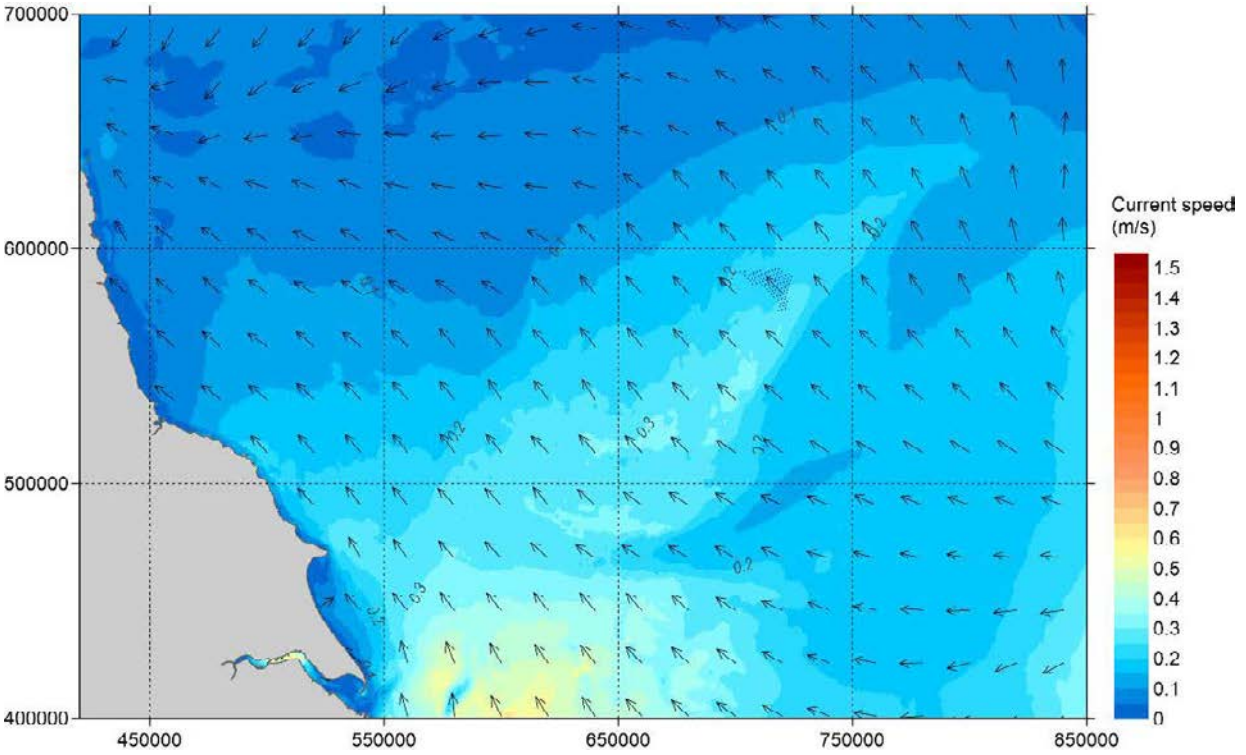

Figure A.87 Overview of Spatial Variation of Peak North-west-going Currents in a Neap tide – Layout C – OSP 2

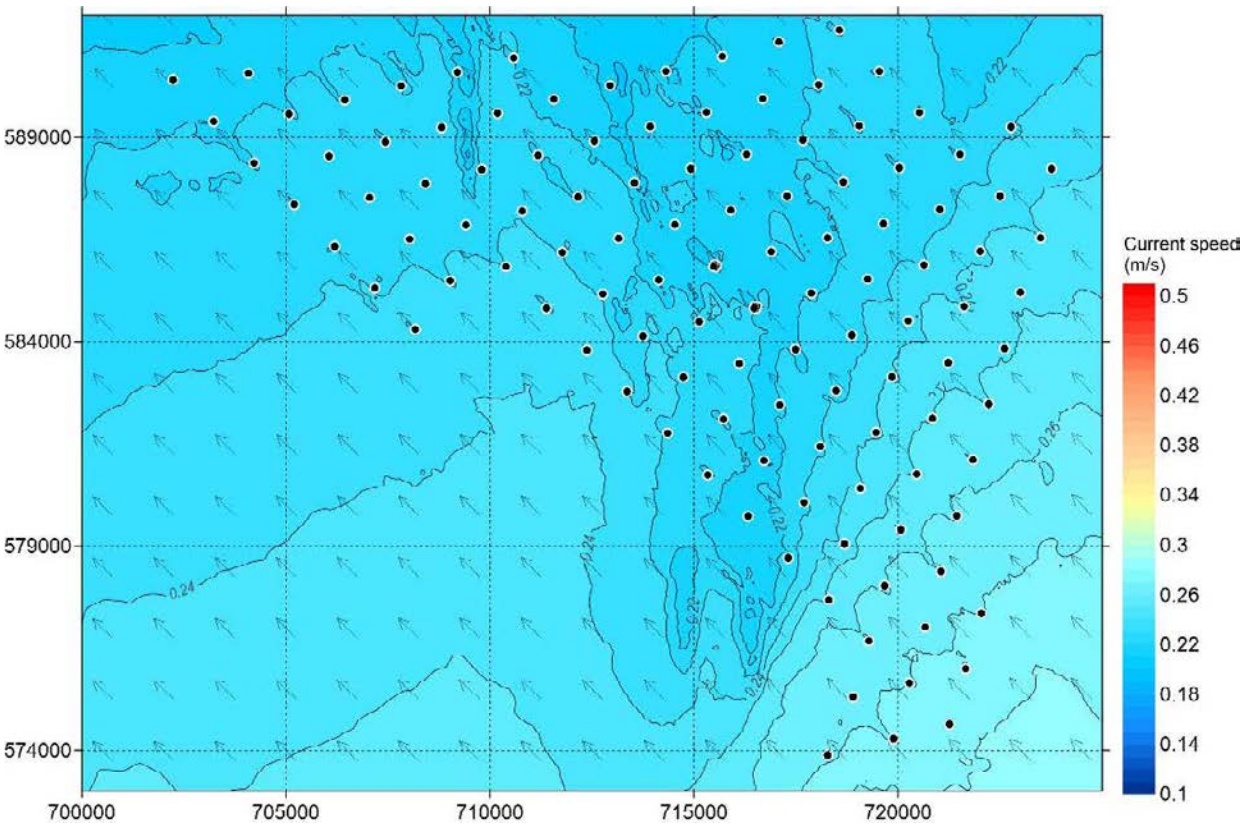

Figure A.88 Overview of Spatial Variation of Peak South-east-going Currents in a Neap tide – Layout C – OSP 2

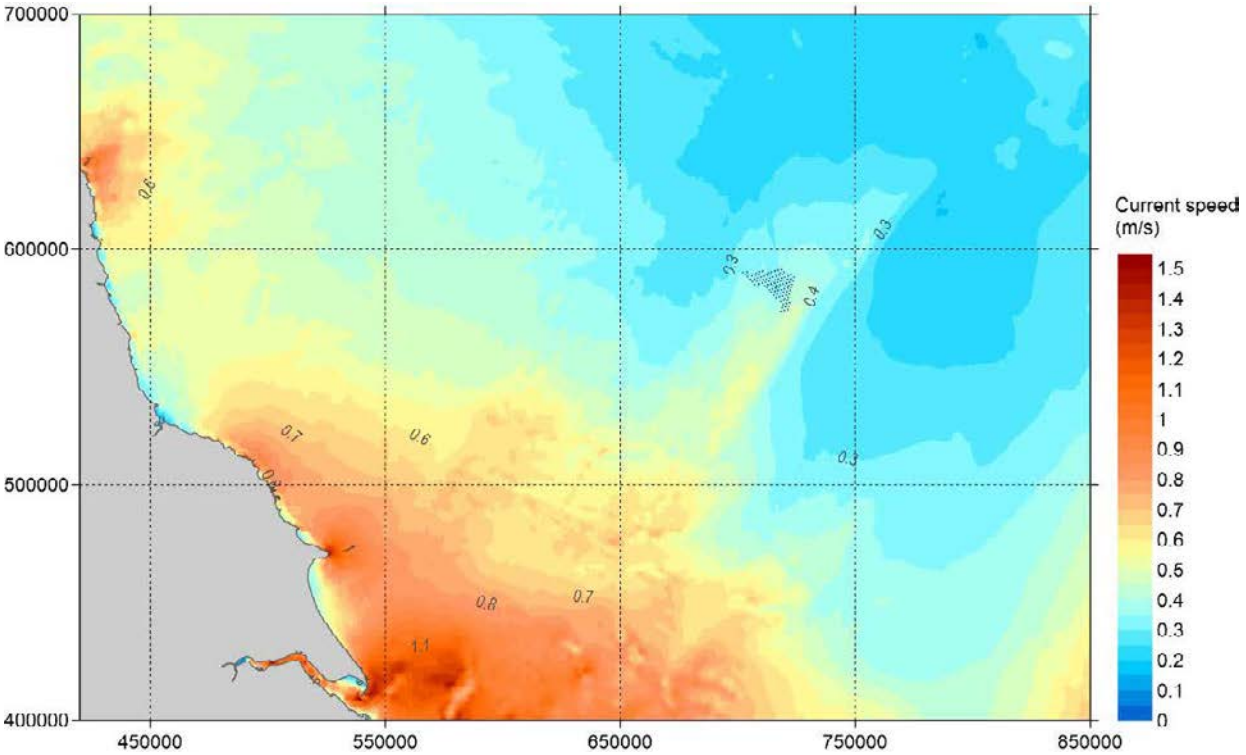

Figure A.89 Overview of Spatial Variation of Maximum Current Speed Over 30 days- Layout C – OSP 2

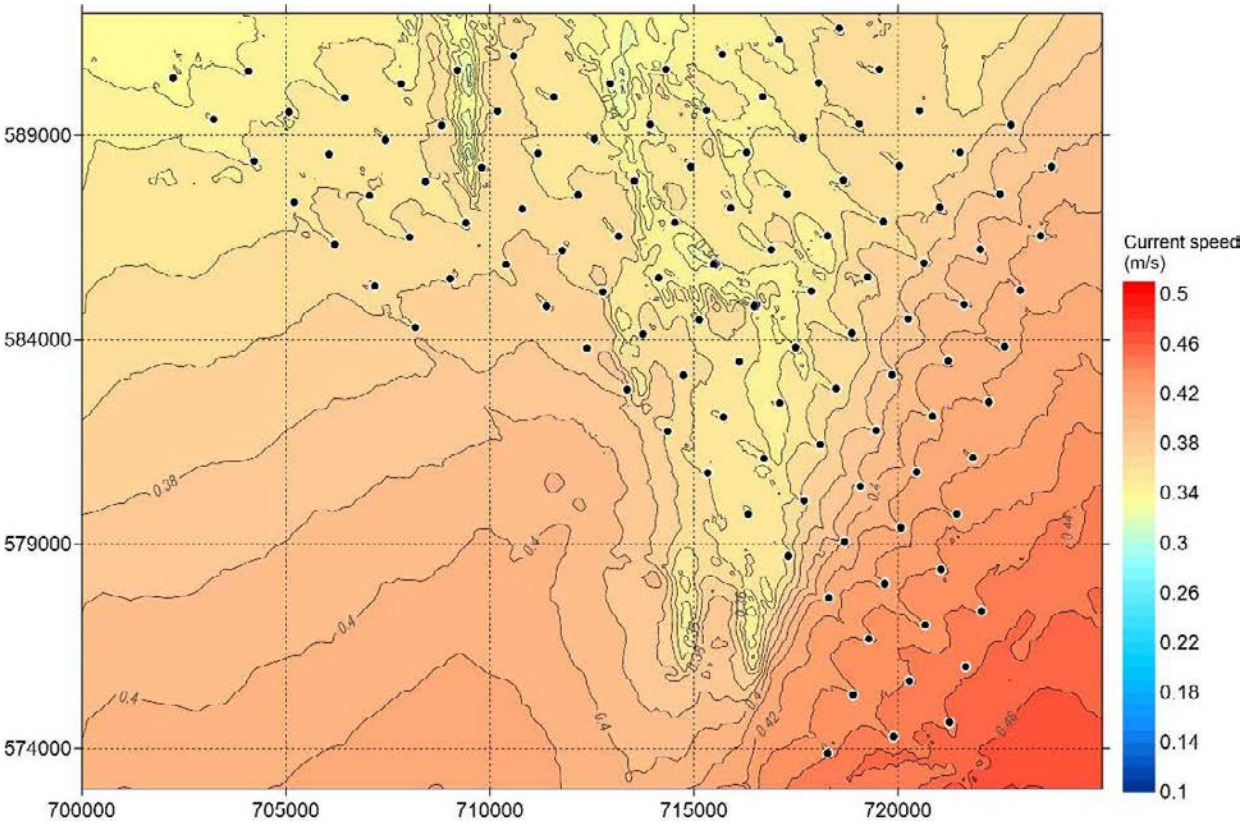

Figure A.90 Overview of Spatial Variation of Maximum Current Speed Over 30 days- Layout C – OSP 2

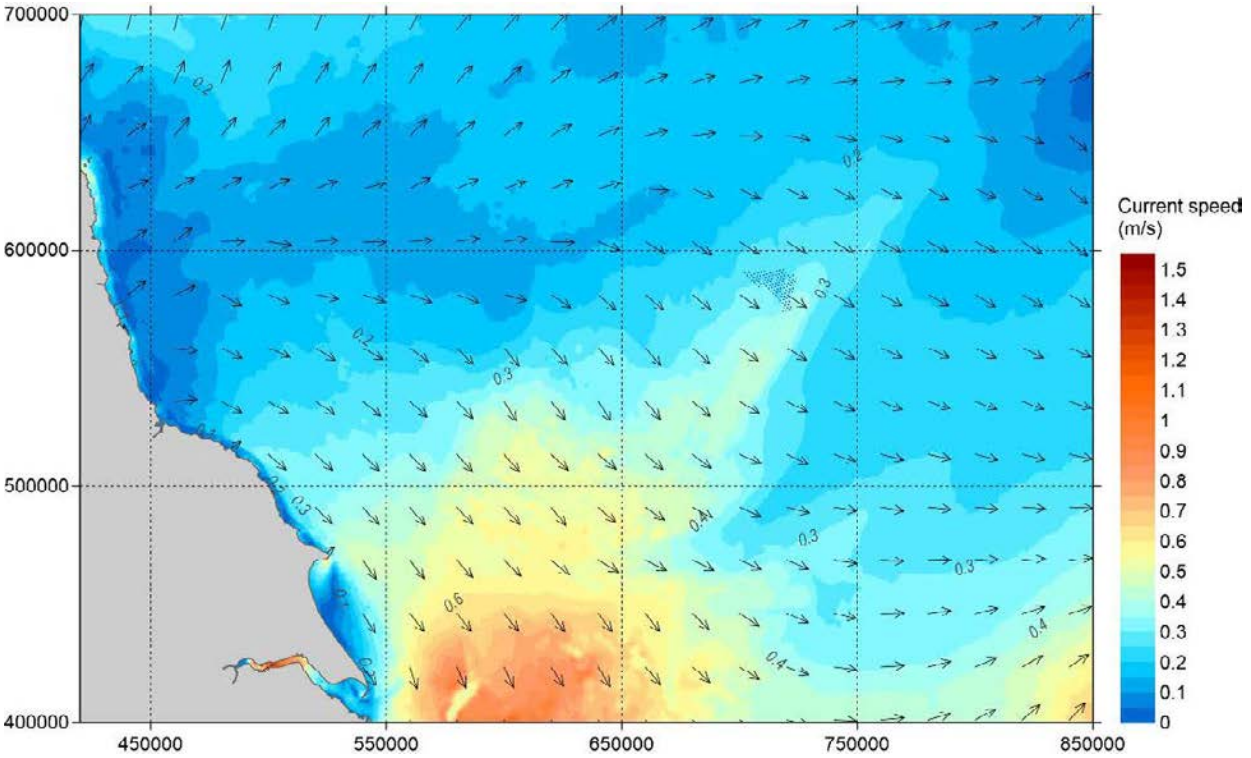

Figure A.91 Overview of Spatial Variation of Peak South-east-going Currents in a Spring Tide – Layout C – OSP 3

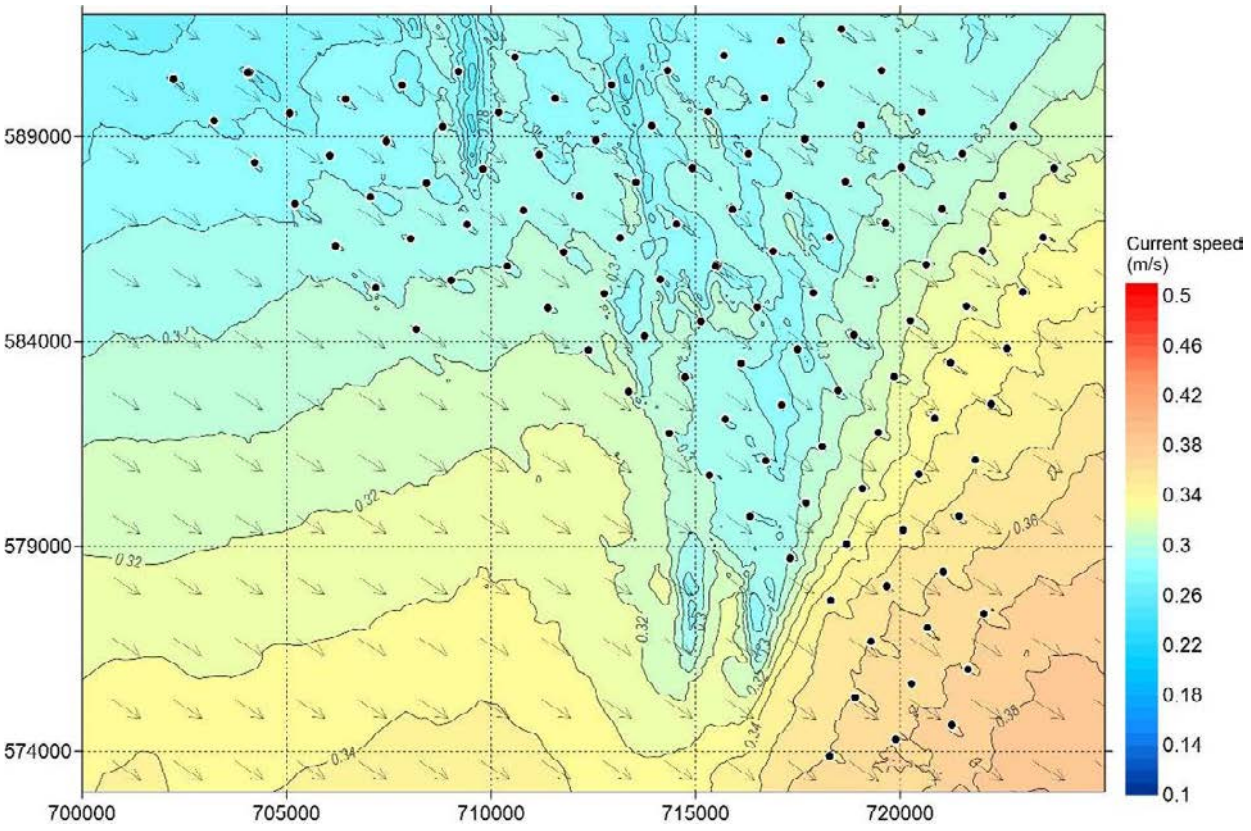

Figure A.92 A Closer View of Spatial Variation of Peak South-east-going Currents in a Spring Tide – Layout C – OSP 3

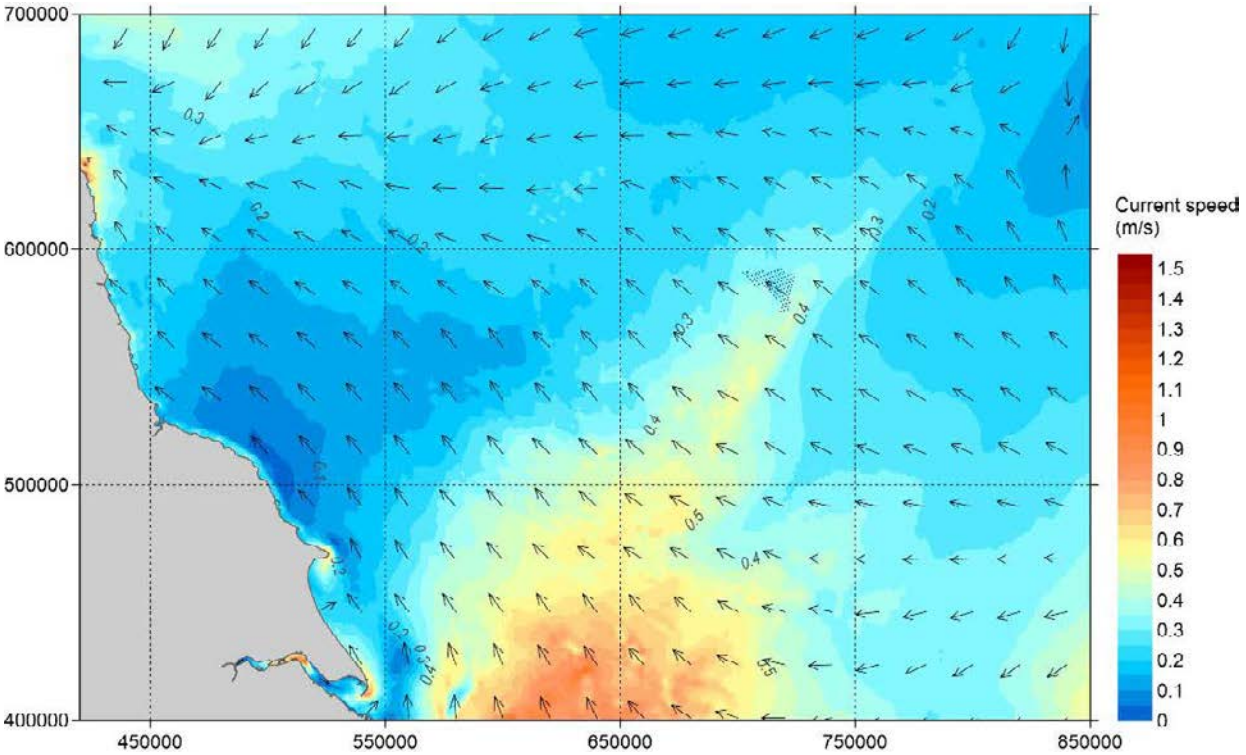

Figure A.93 Overview of Spatial Variation of Peak North-west-going Currents in a Spring Tide – Layout C – OSP 3

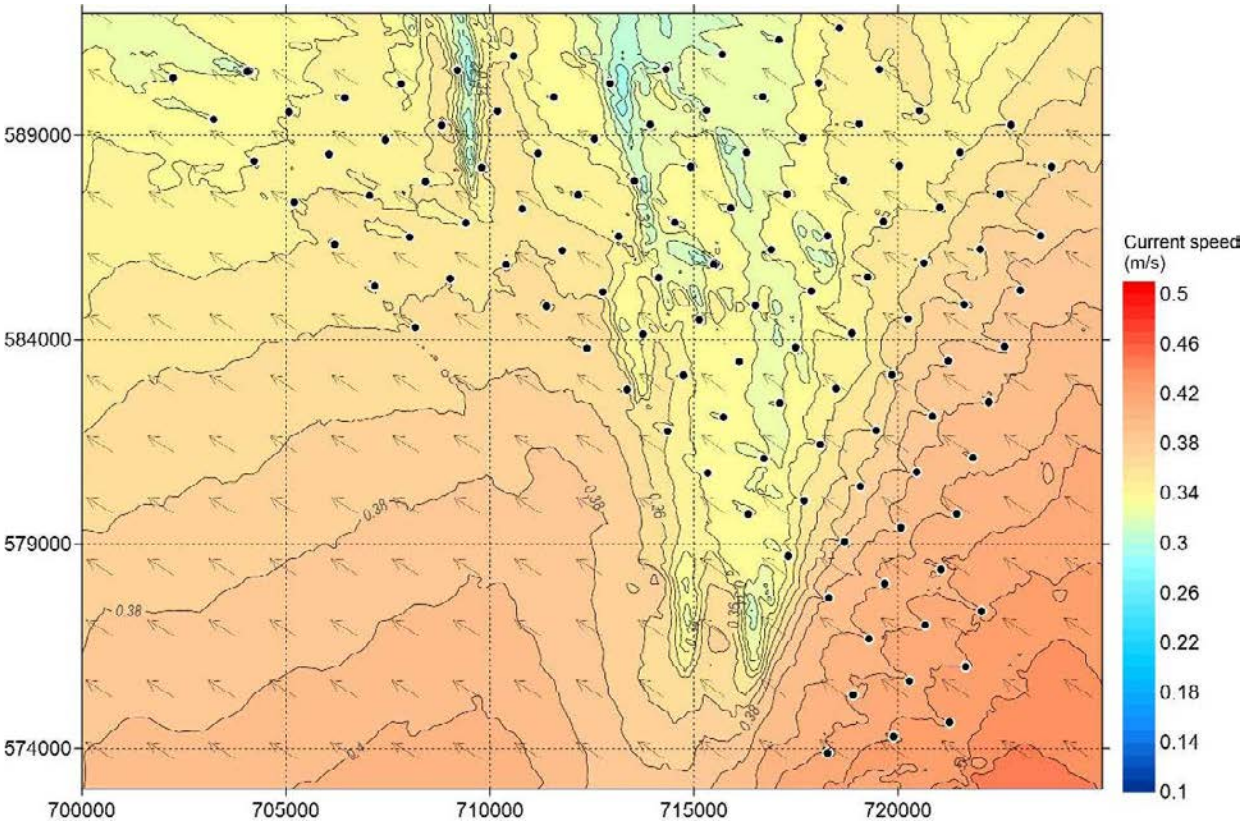

Figure A.94 A Closer View of Spatial Variation of Peak North-west-going Currents in a Spring Tide – Layout C – OSP 3

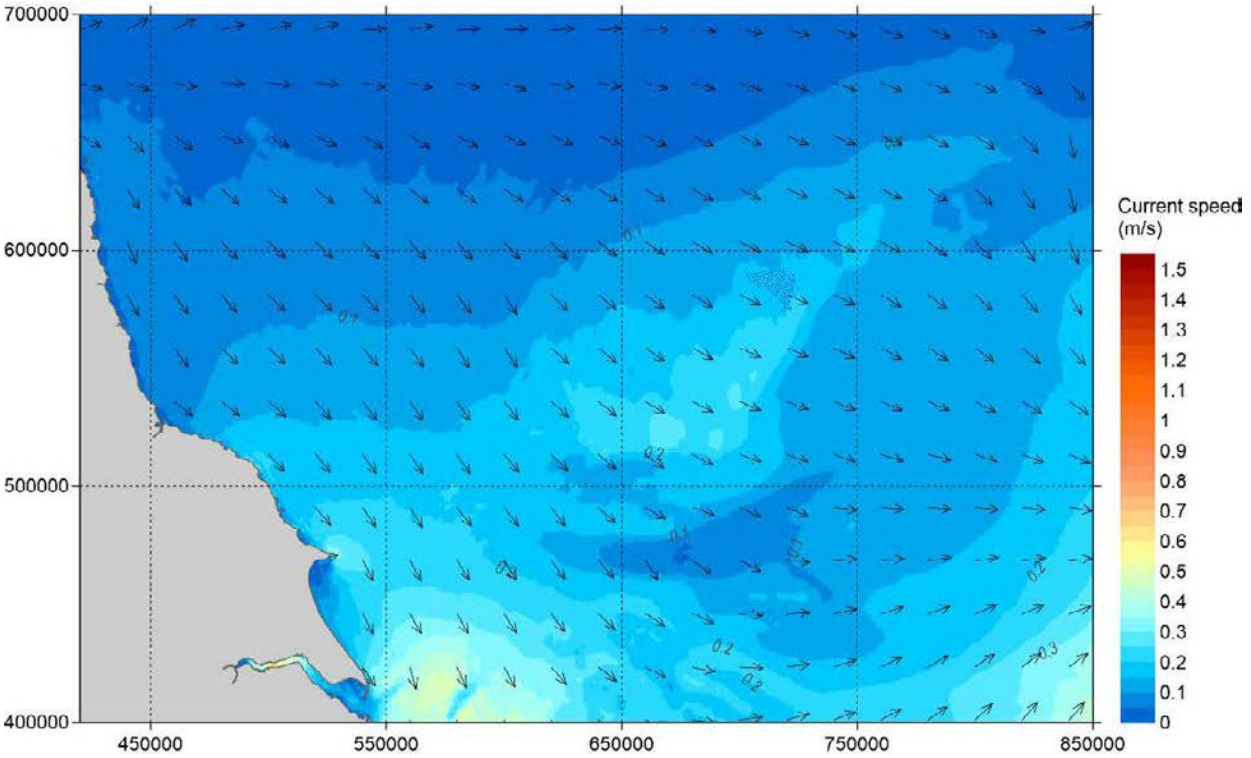

Figure A.95 Overview of Spatial Variation of Peak South-east-going Currents in a Neap tide – Layout C – OSP 3

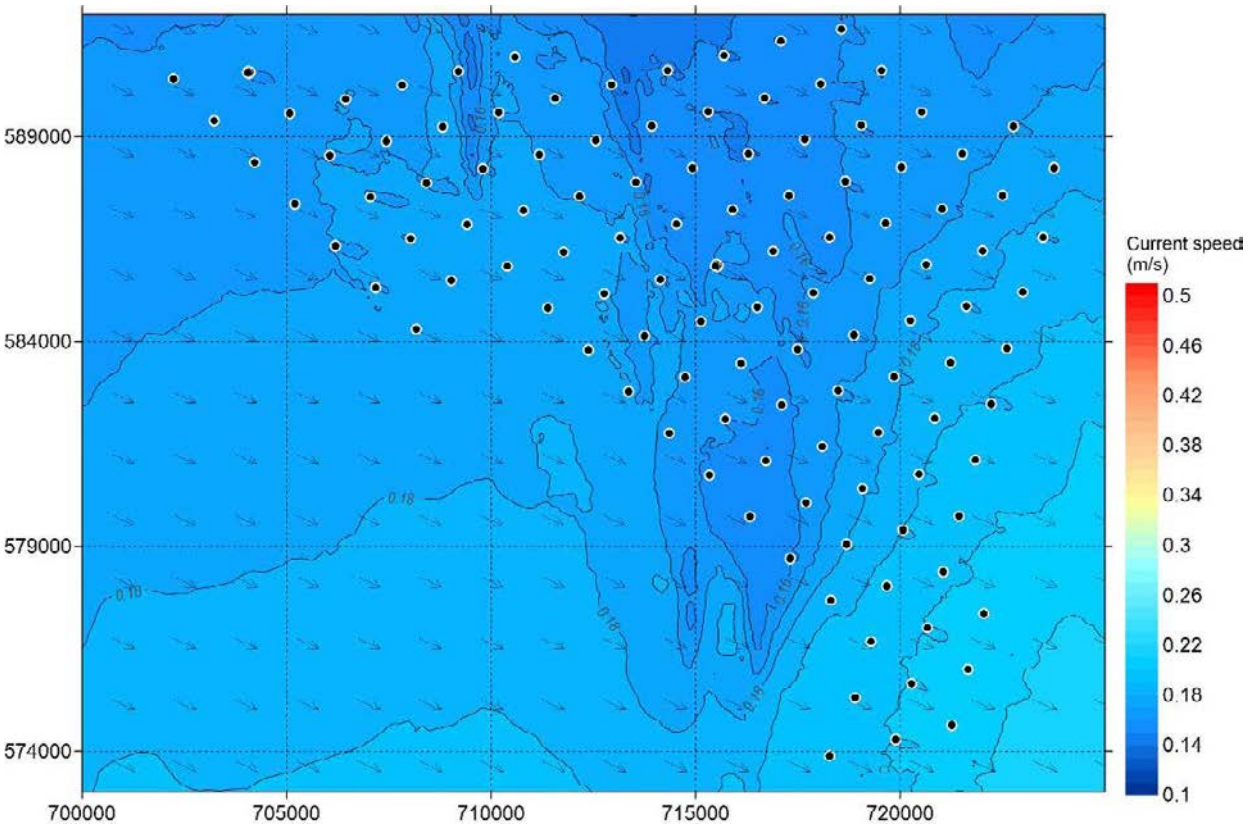

Figure A.96 Overview of Spatial Variation of Peak South-east-going Currents in a Neap tide – Layout C – OSP 3

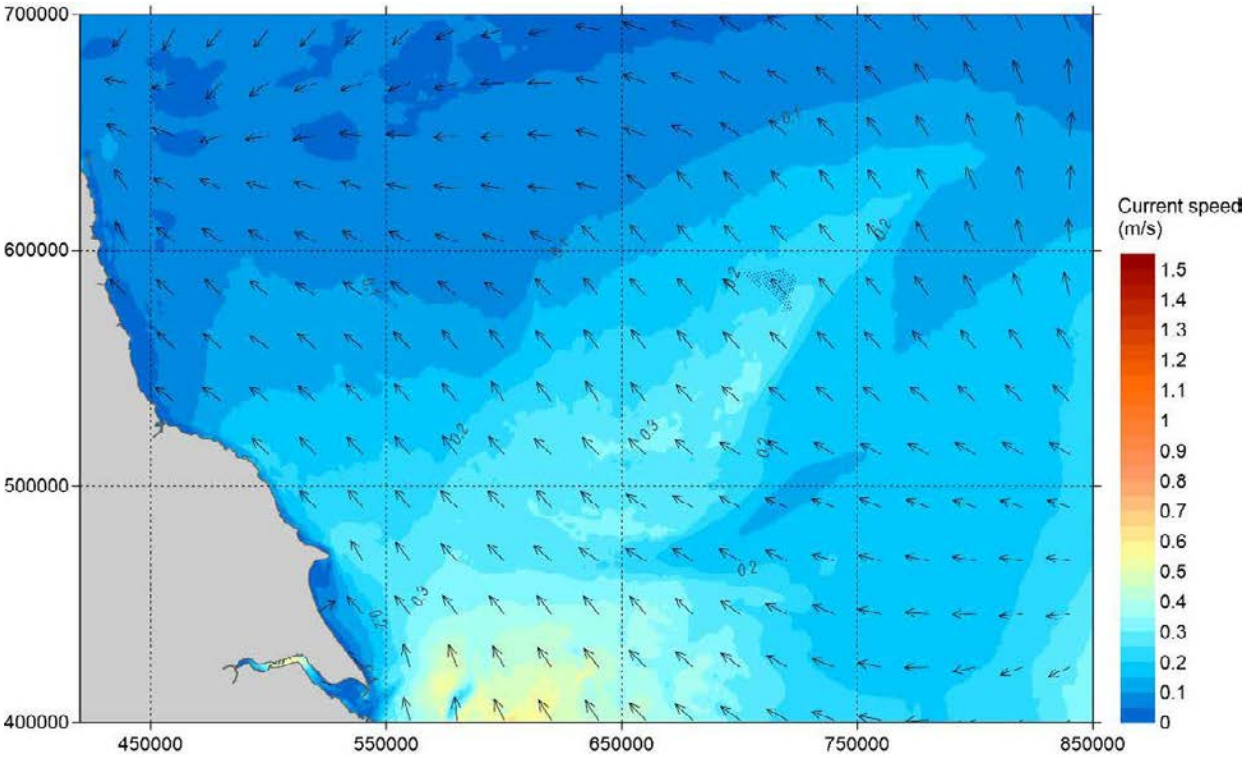

Figure A.97 Overview of Spatial Variation of Peak North-west-going Currents in a Neap tide – Layout C – OSP 3

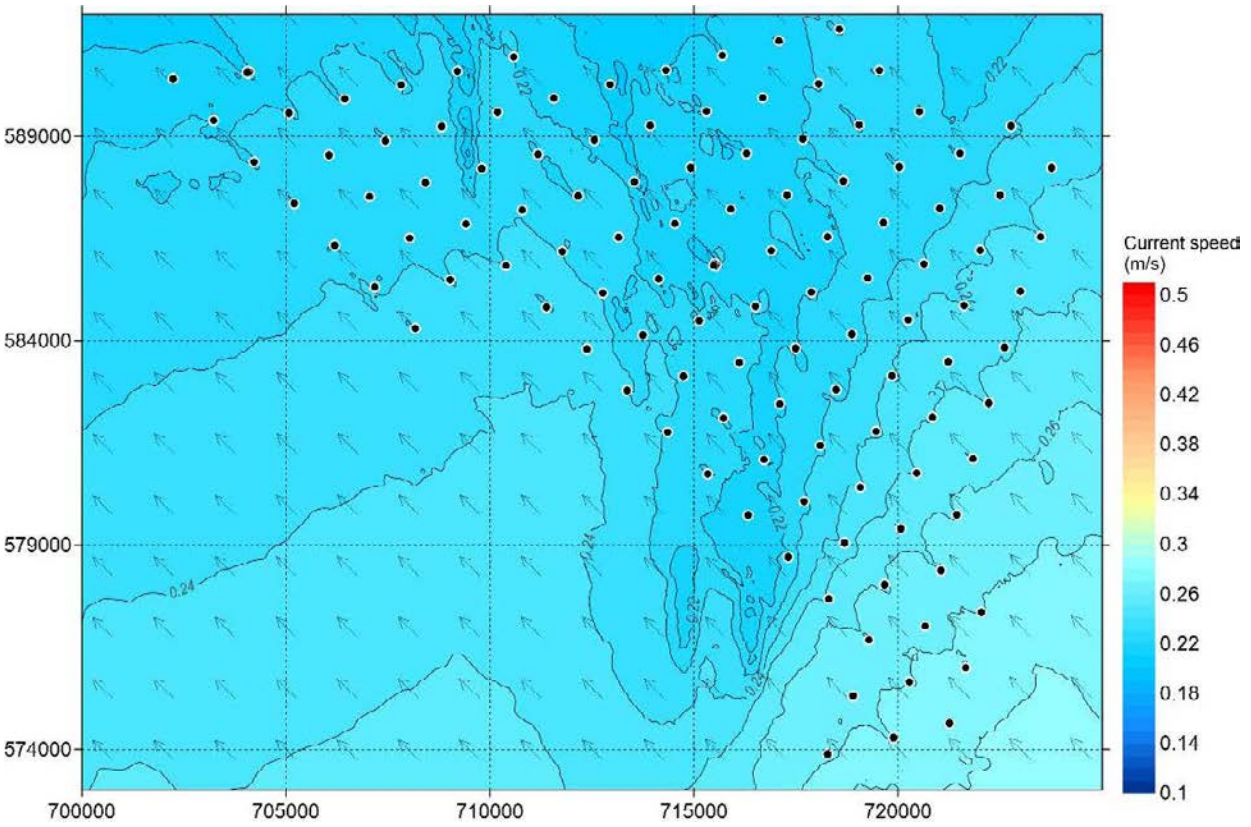

Figure A.98 Overview of Spatial Variation of Peak South-east-going Currents in a Neap tide – Layout C – OSP 3

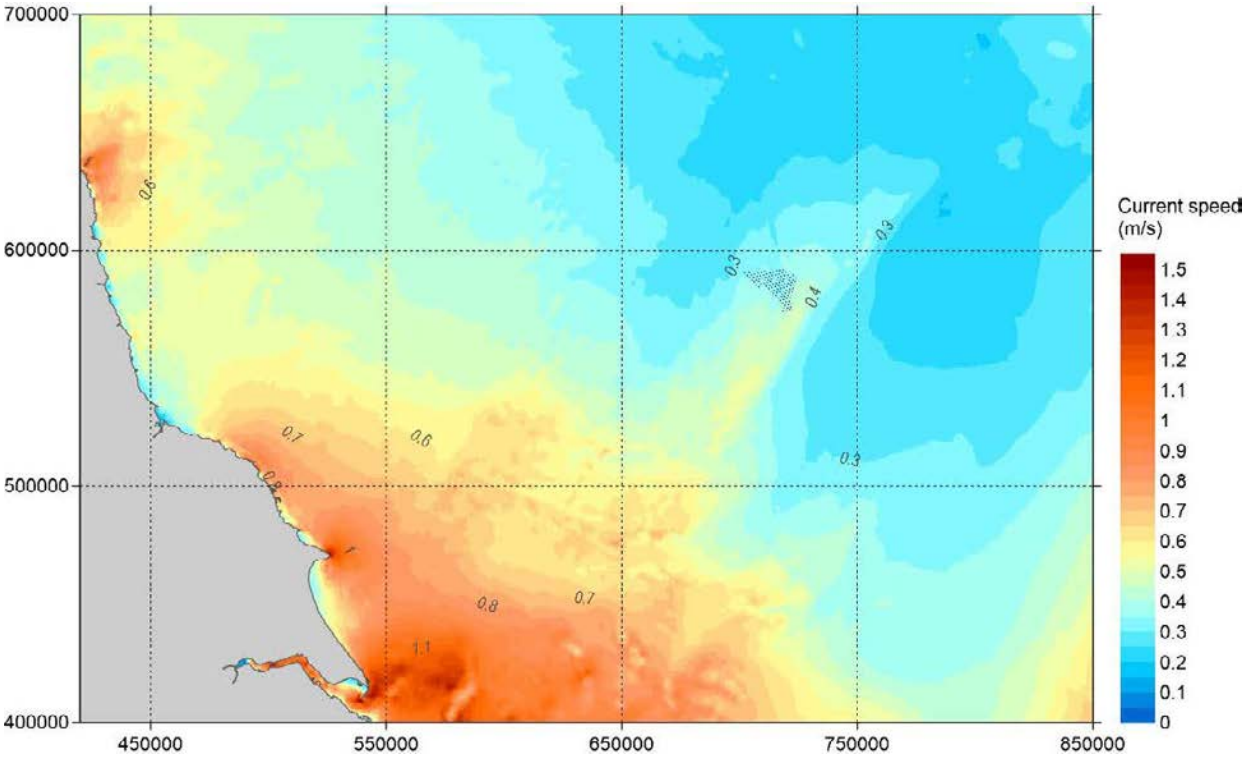

Figure A.99 Overview of Spatial Variation of Maximum Current Speed Over 30 days- Layout C – OSP 3

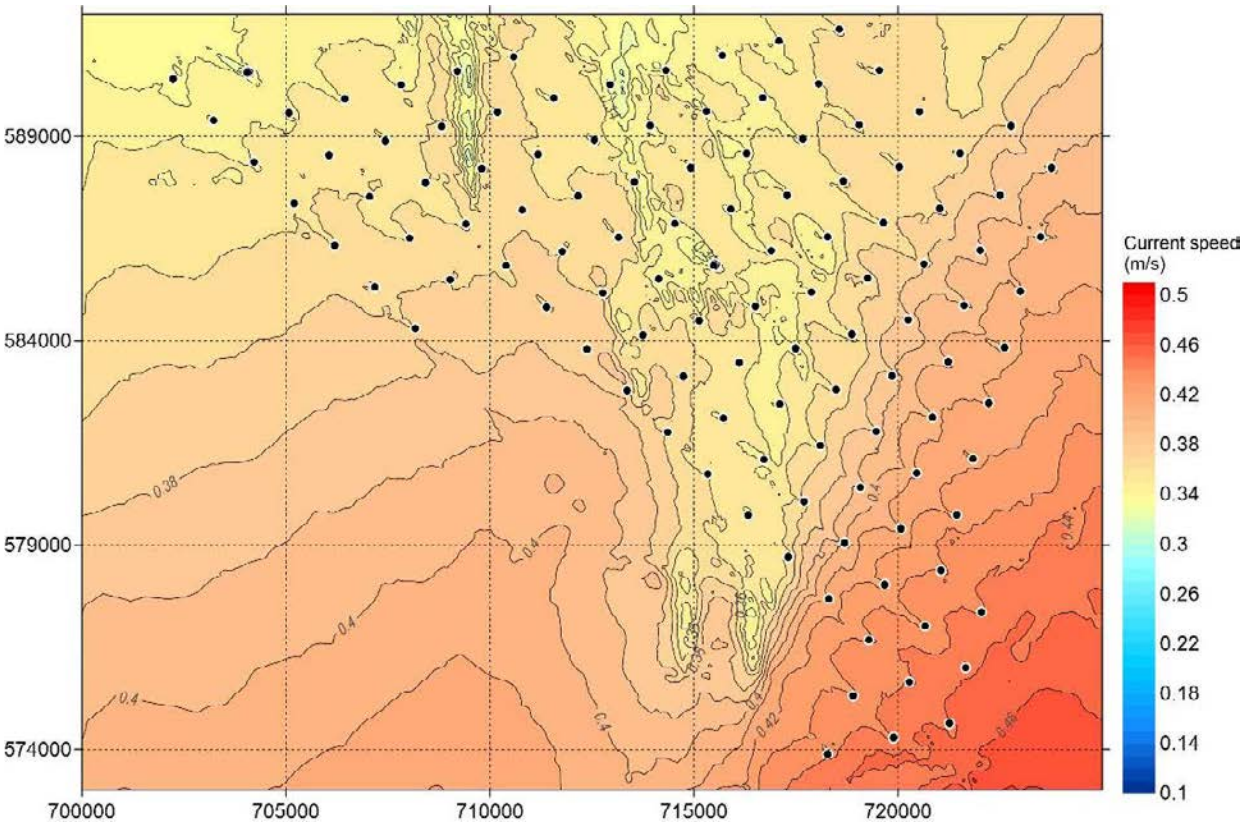

Figure A.100 Overview of Spatial Variation of Maximum Current Speed Over 30 days- Layout C – OSP 3

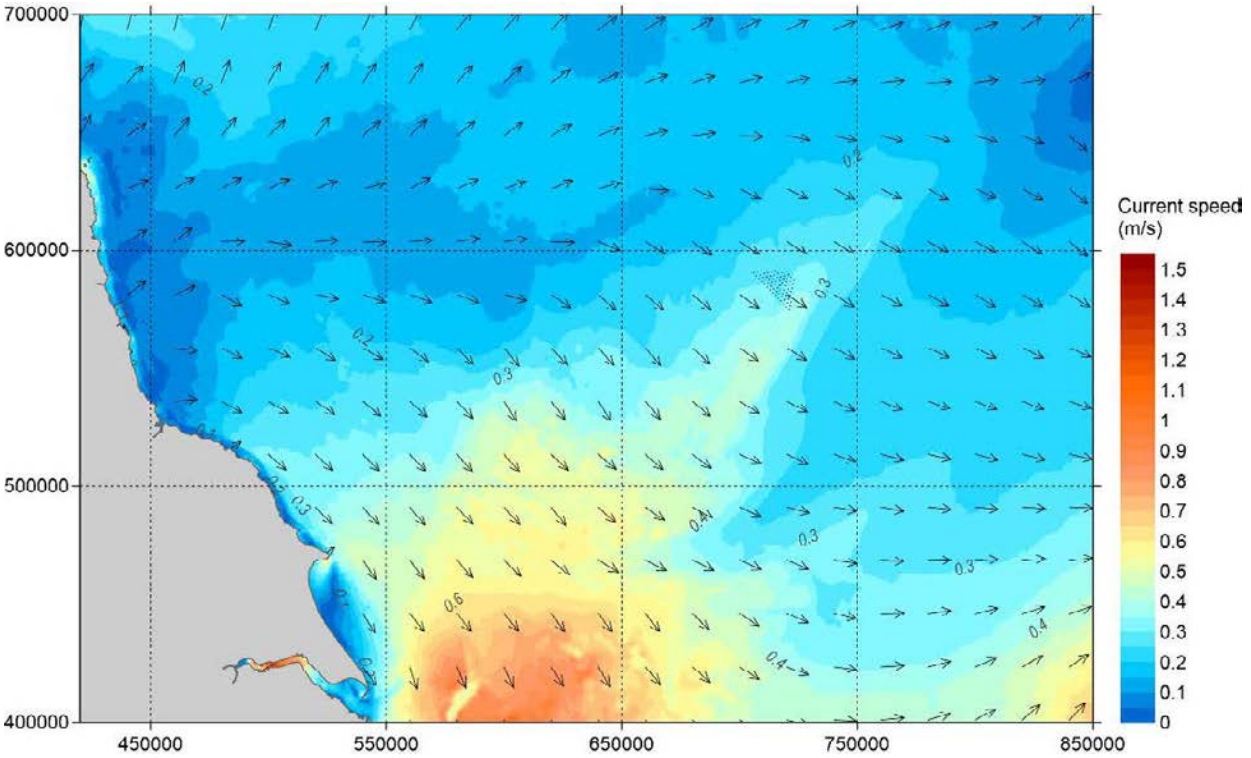

Figure A.101 Overview of Spatial Variation of Peak South-east-going Currents in a Spring Tide – Layout D – OSP 1

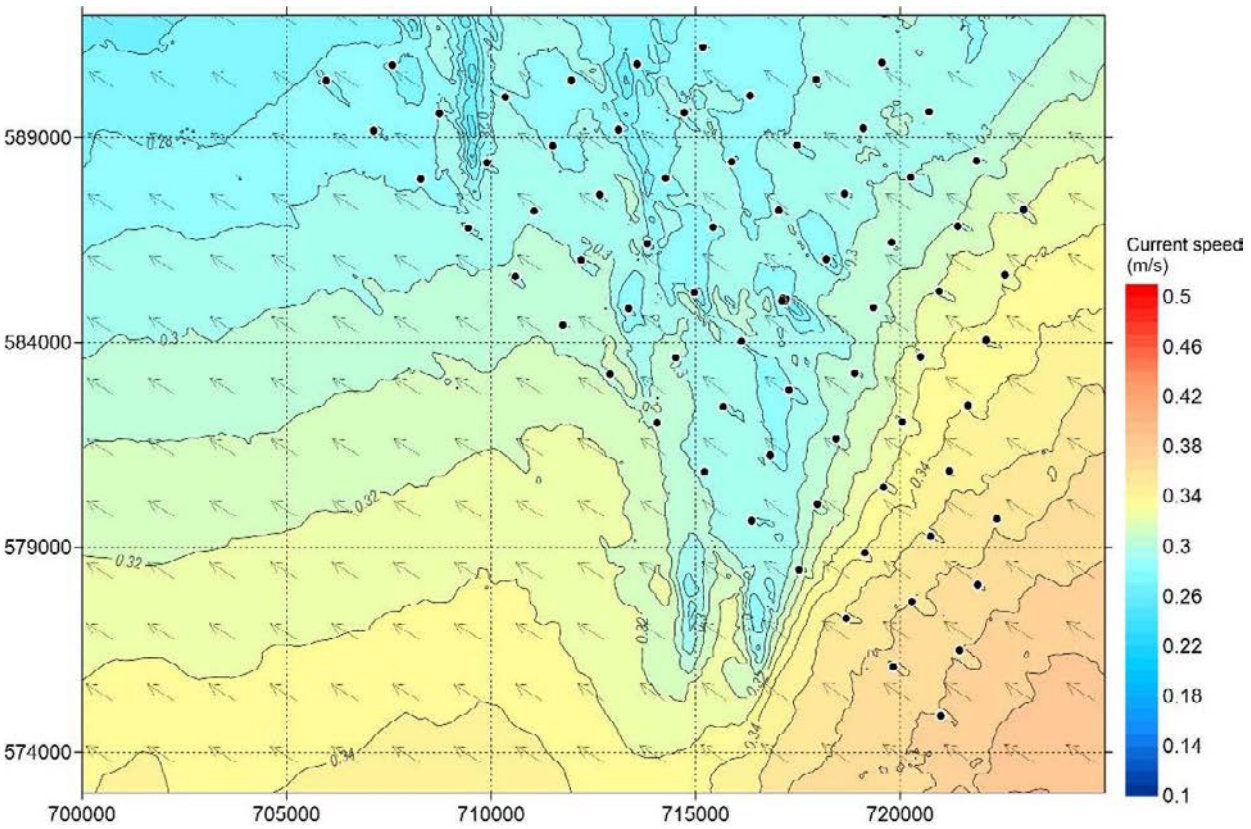

Figure A.102 A Closer View of Spatial Variation of Peak South-east-going Currents in a Spring Tide – Layout D – OSP 1

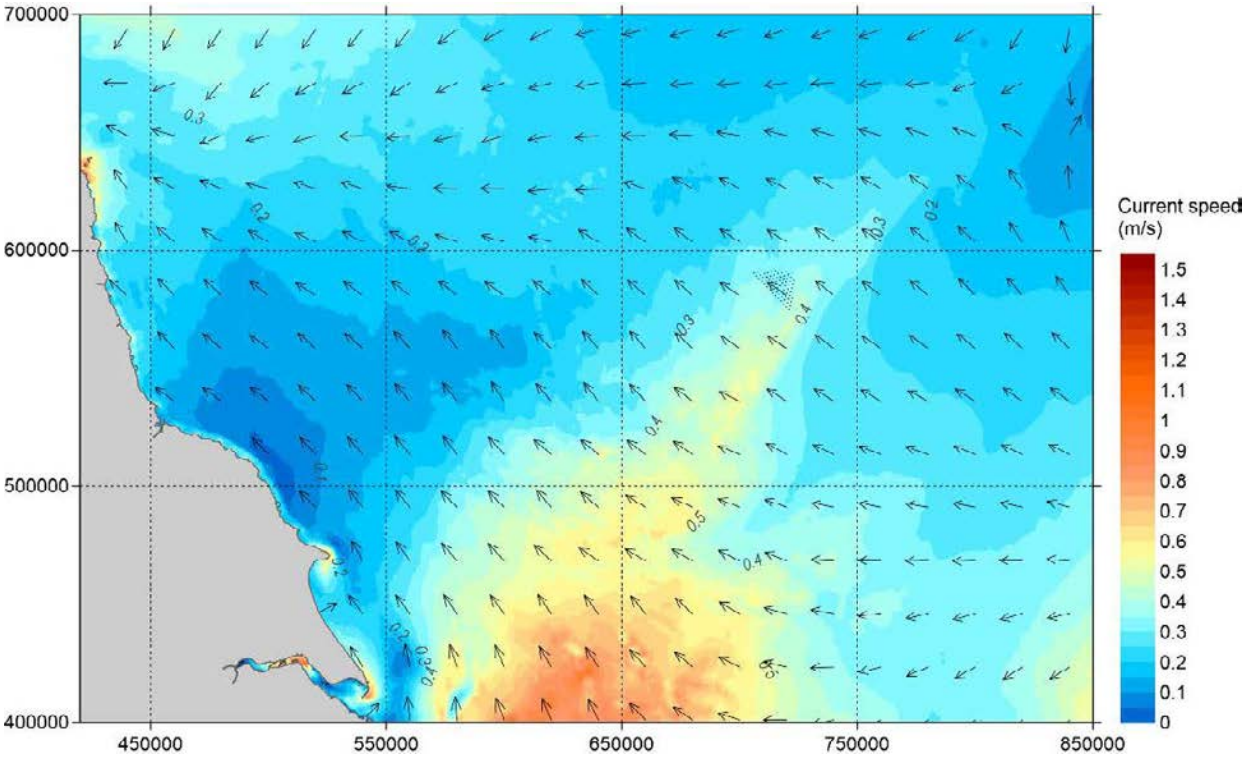

Figure A.103 Overview of Spatial Variation of Peak North-west-going Currents in a Spring Tide – Layout D – OSP 1

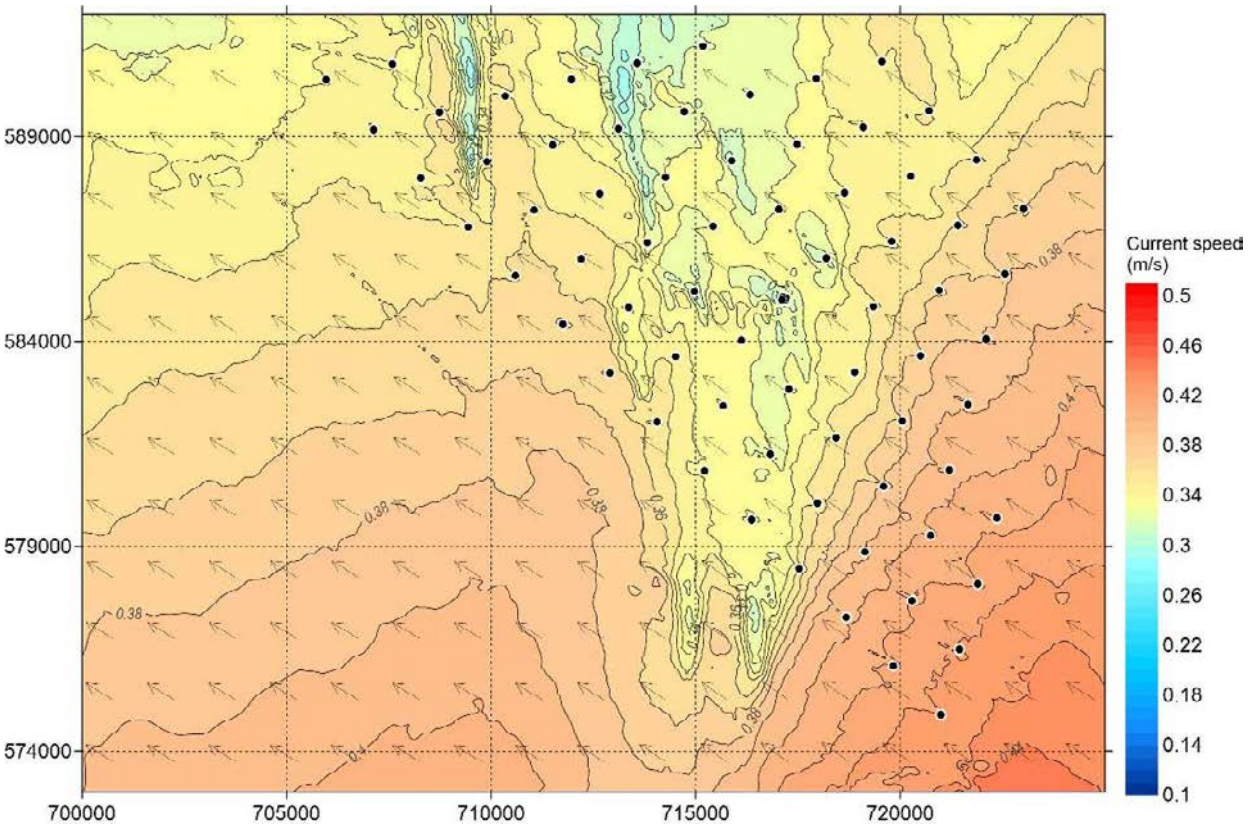

Figure A.104 A Closer View of Spatial Variation of Peak North-west-going Currents in a Spring Tide – Layout D – OSP 1

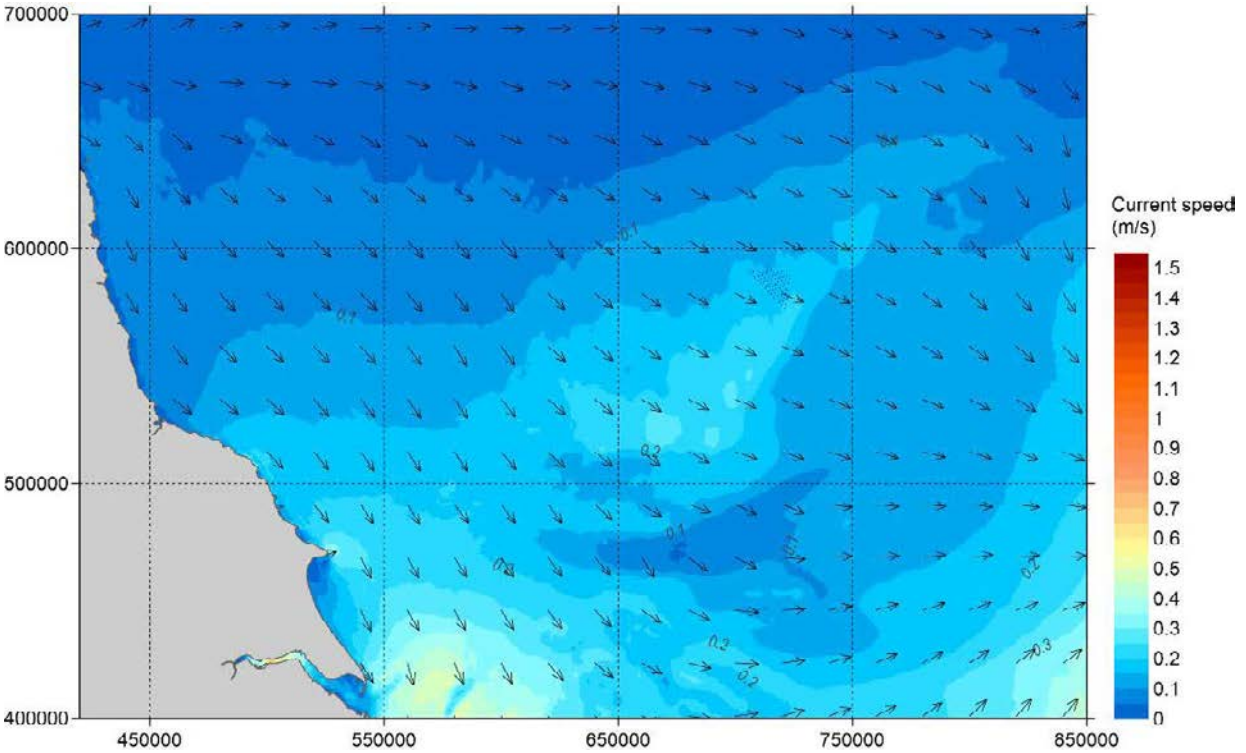

Figure A.105 Overview of Spatial Variation of Peak South-east-going Currents in a Neap tide – Layout D – OSP 1

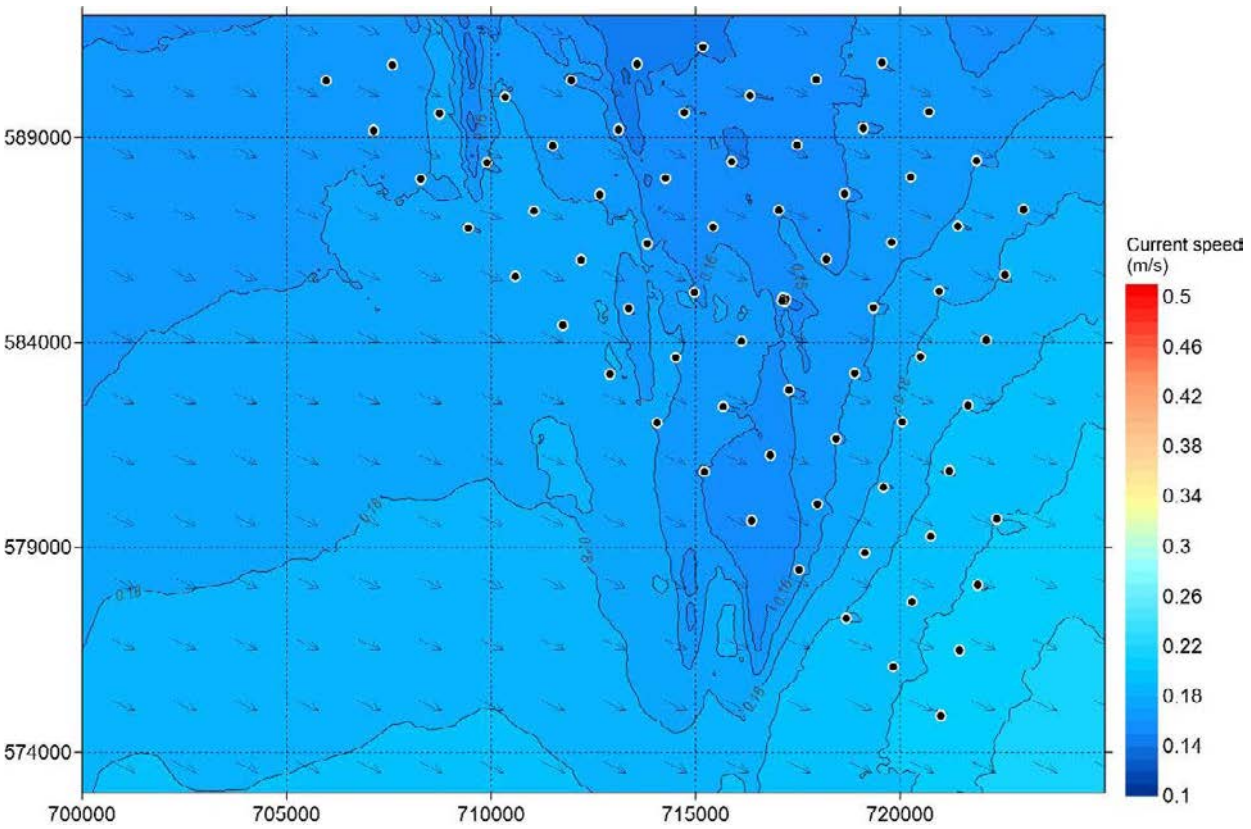

Figure A.106 Overview of Spatial Variation of Peak South-east-going Currents in a Neap tide – Layout D – OSP 1

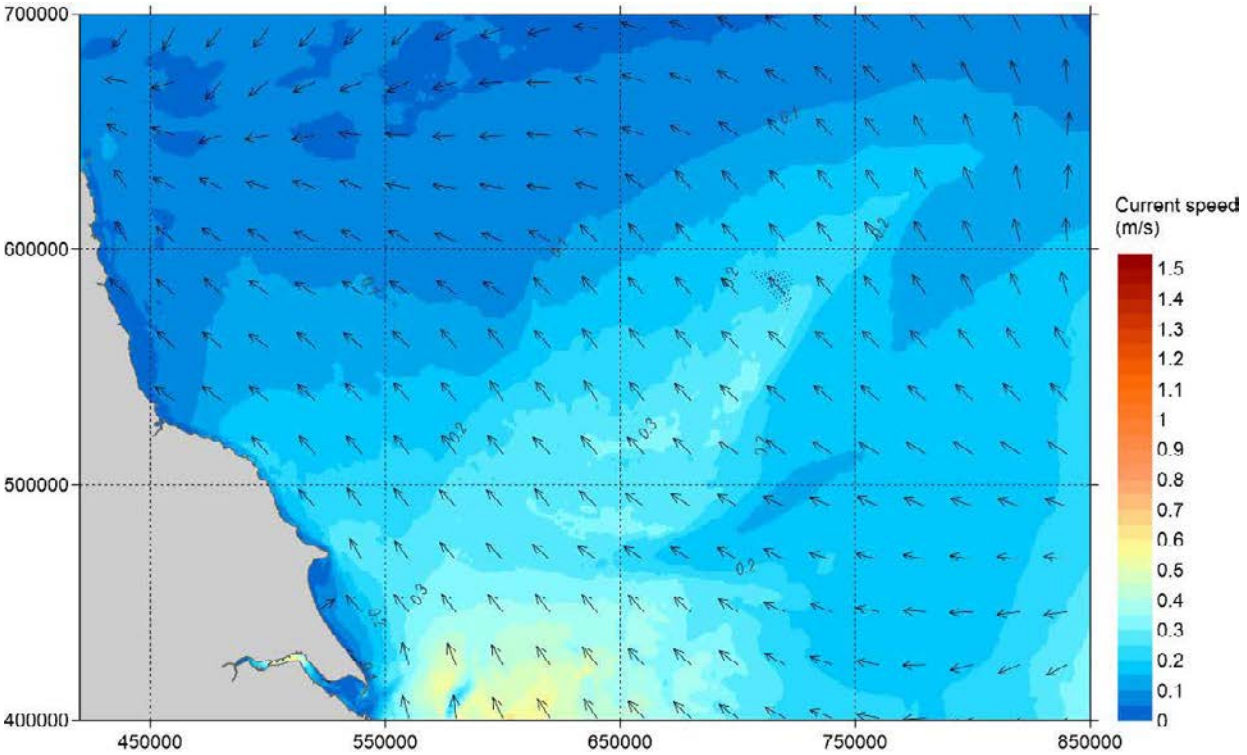

Figure A.107 Overview of Spatial Variation of Peak North-west-going Currents in a Neap tide – Layout D – OSP 1

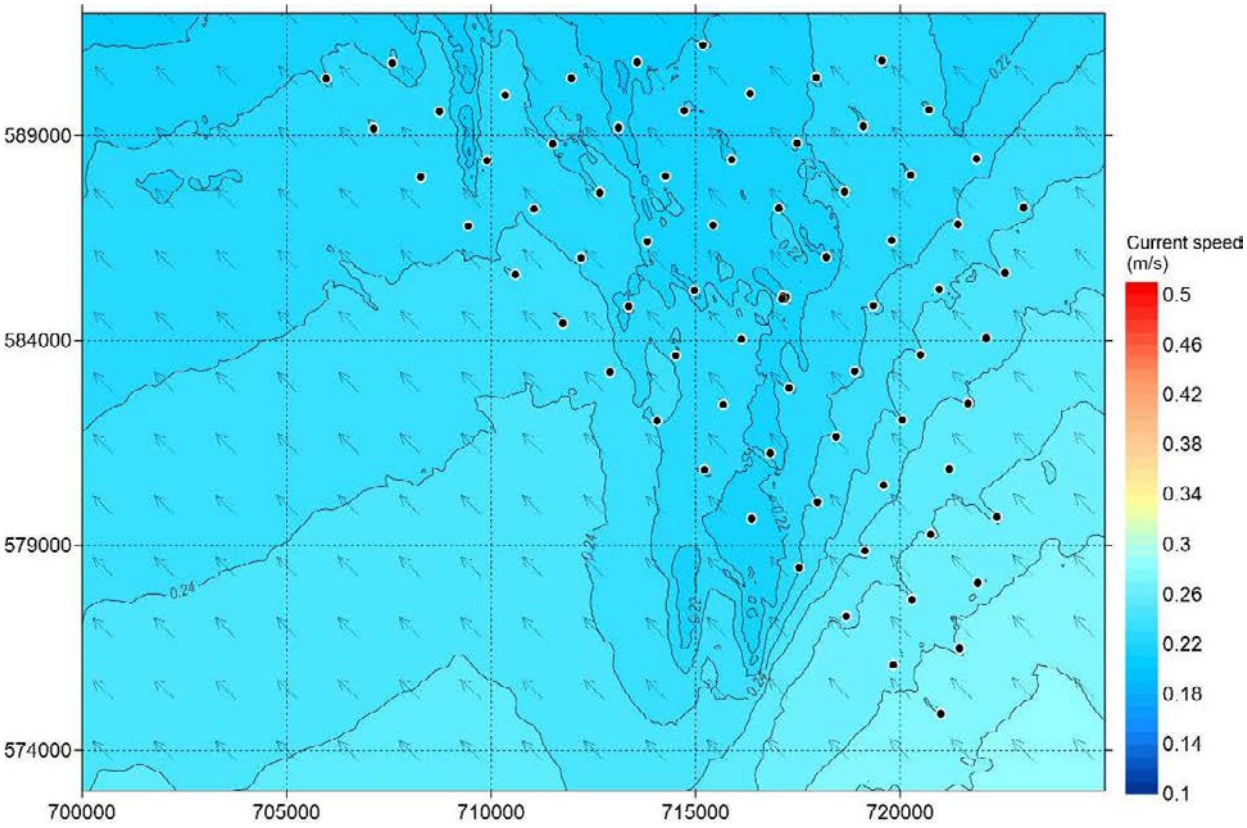

Figure A.108 Overview of Spatial Variation of Peak South-east-going Currents in a Neap tide – Layout D – OSP 1

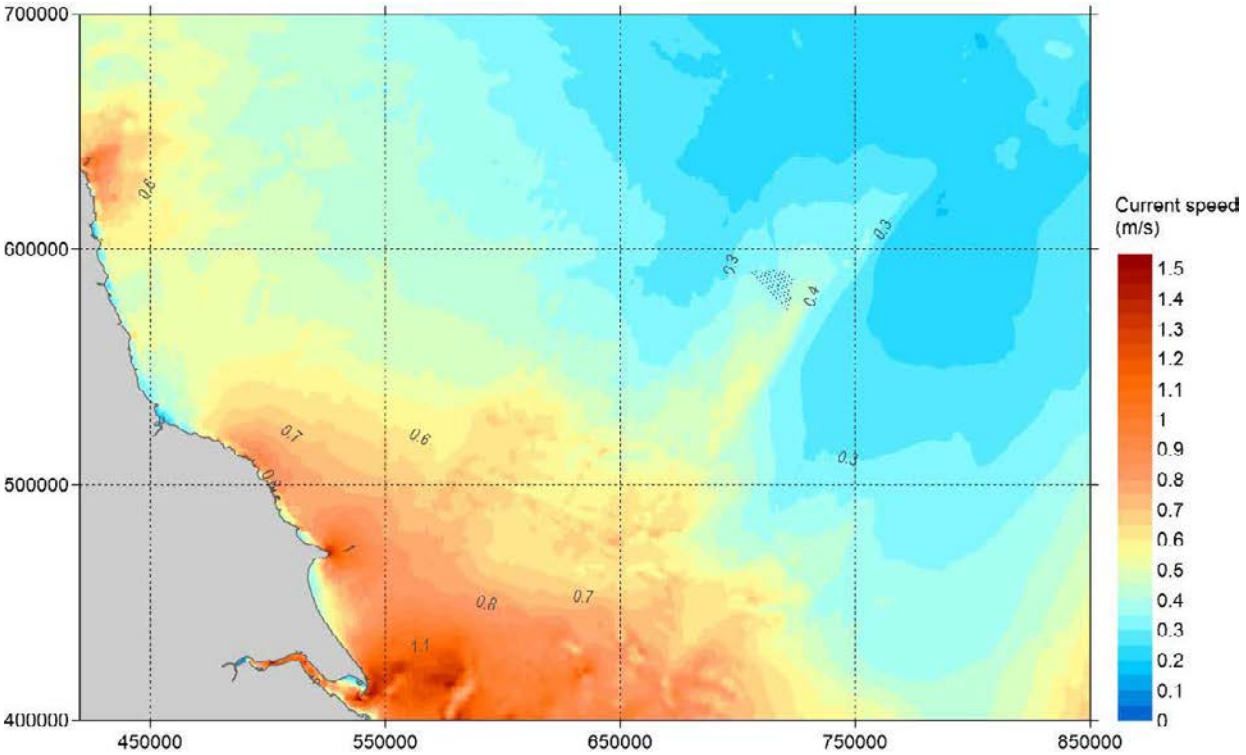

Figure A.109 Overview of Spatial Variation of Maximum Current Speed Over 30 days- Layout D – OSP 1

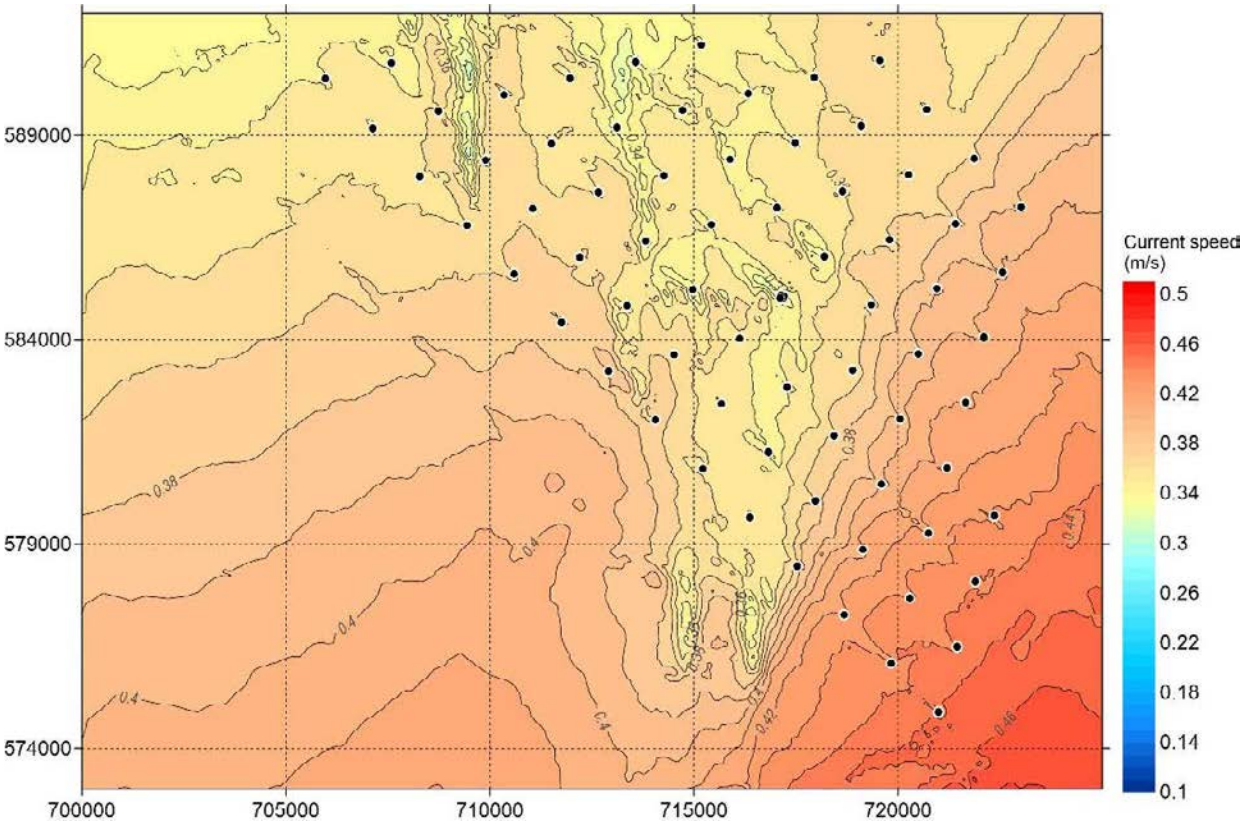

Figure A.110 Overview of Spatial Variation of Maximum Current Speed Over 30 days- Layout D – OSP 1

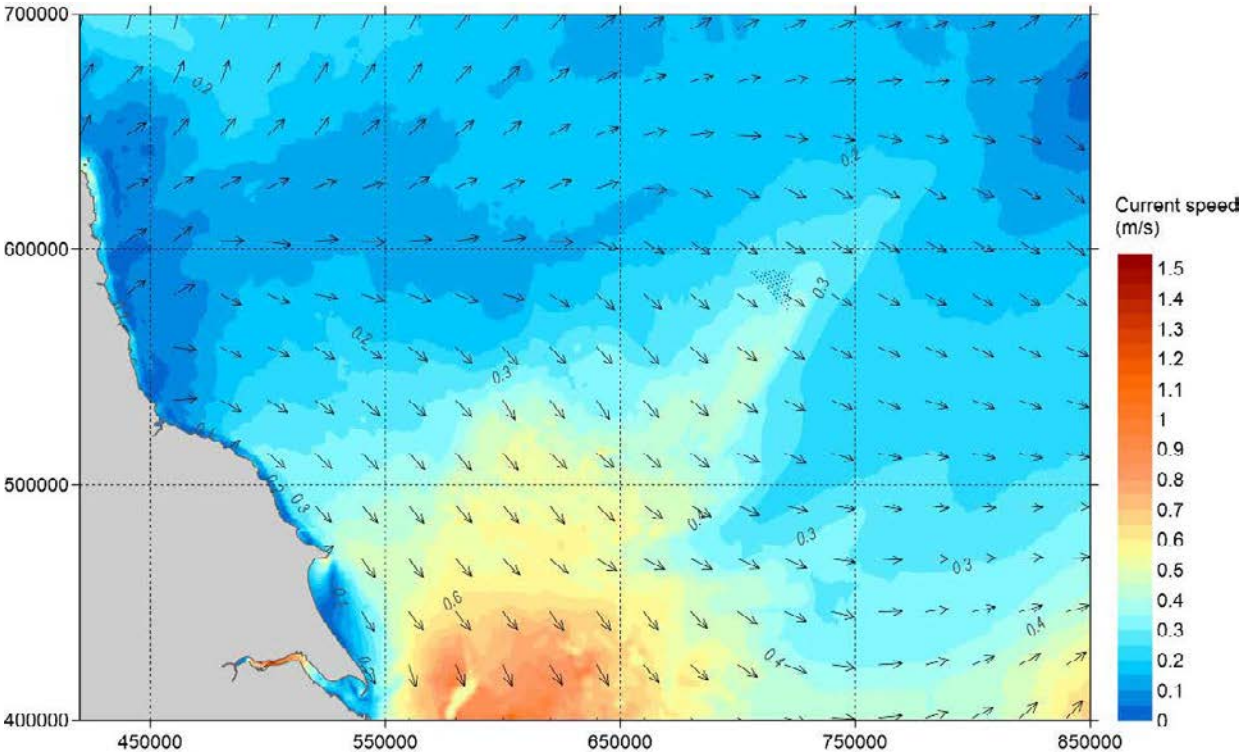

Figure A.111 Overview of Spatial Variation of Peak South-east-going Currents in a Spring Tide – Layout D – OSP 2

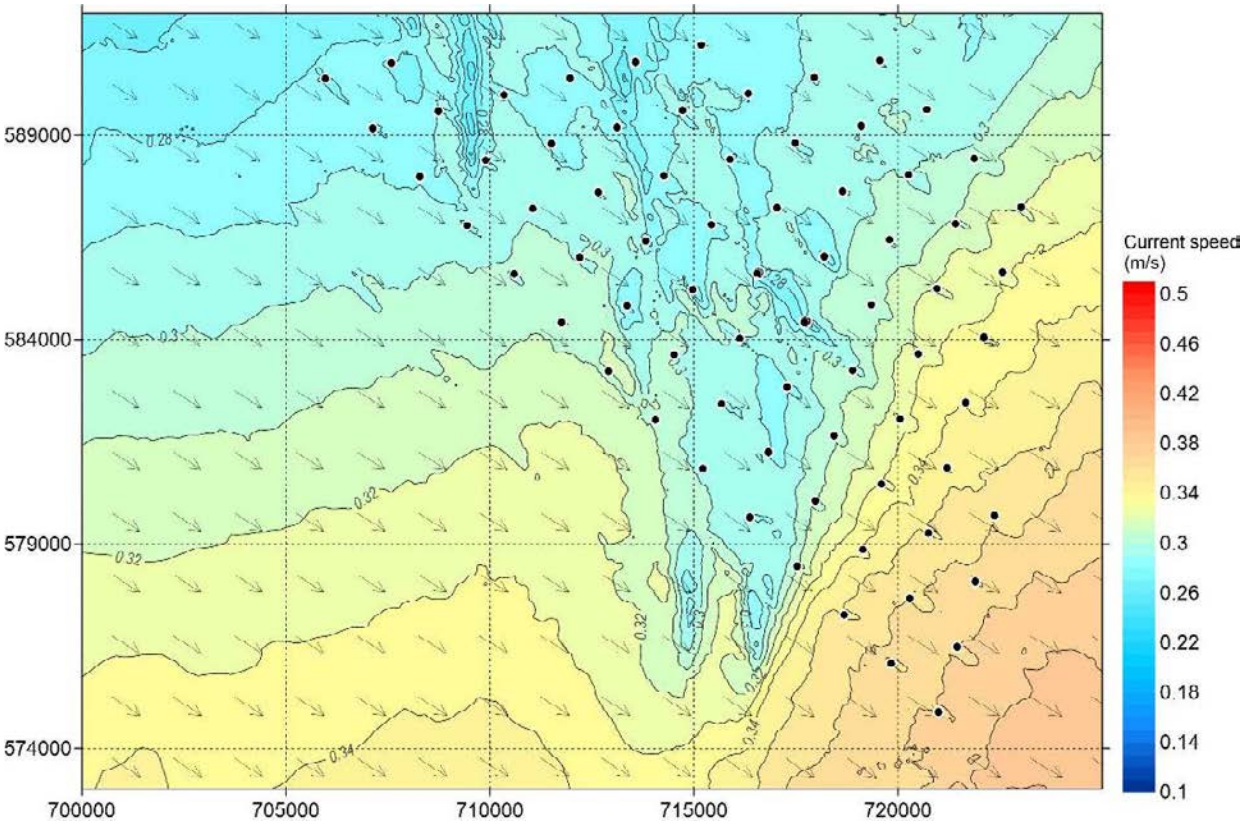

Figure A.112 A Closer View of Spatial Variation of Peak South-east-going Currents in a Spring Tide – Layout D – OSP 2

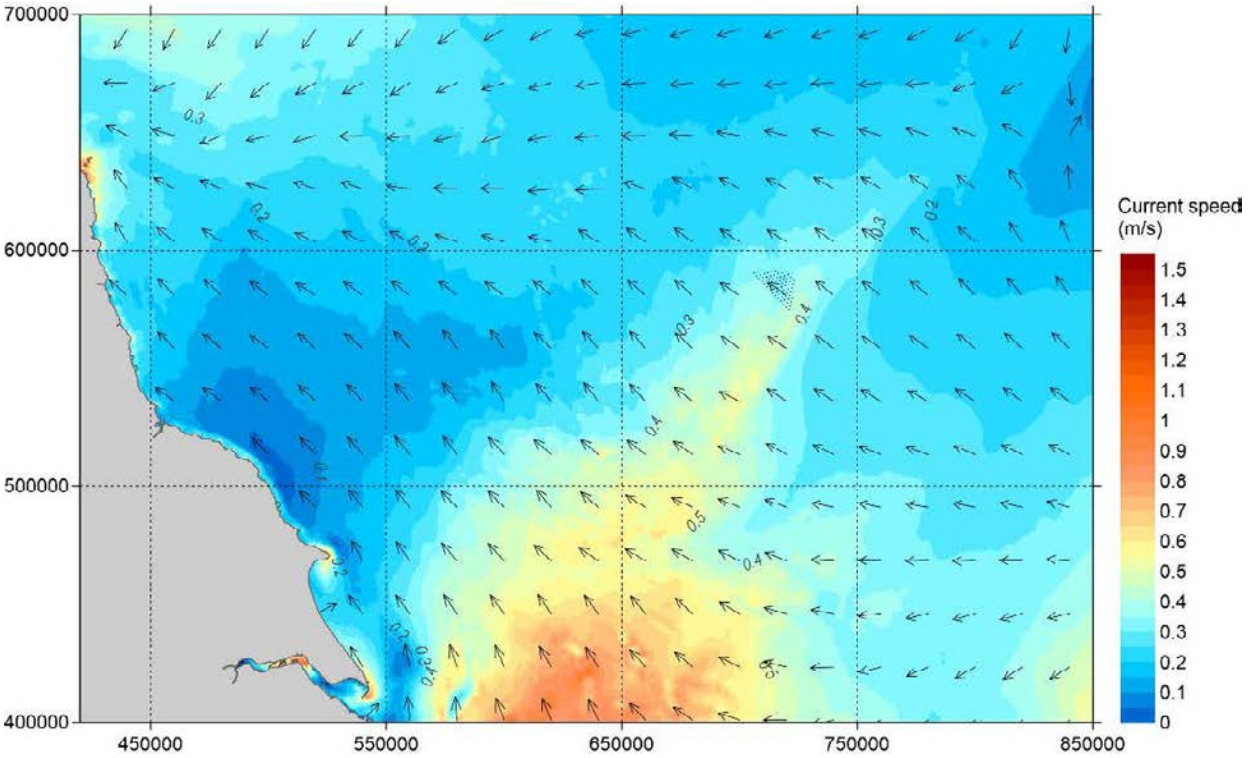

Figure A.113 Overview of Spatial Variation of Peak North-west-going Currents in a Spring Tide – Layout D – OSP 2

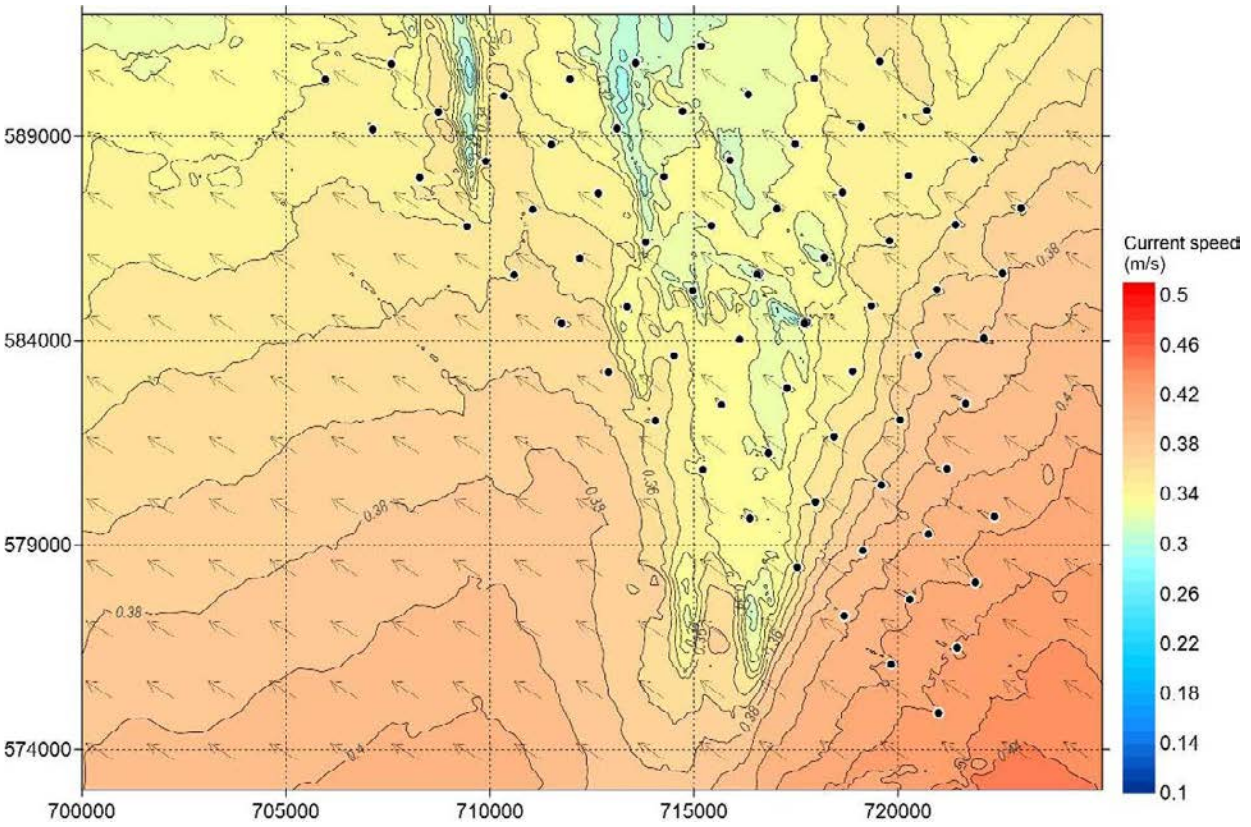

Figure A.114 A Closer View of Spatial Variation of Peak North-west-going Currents in a Spring Tide – Layout D – OSP 2

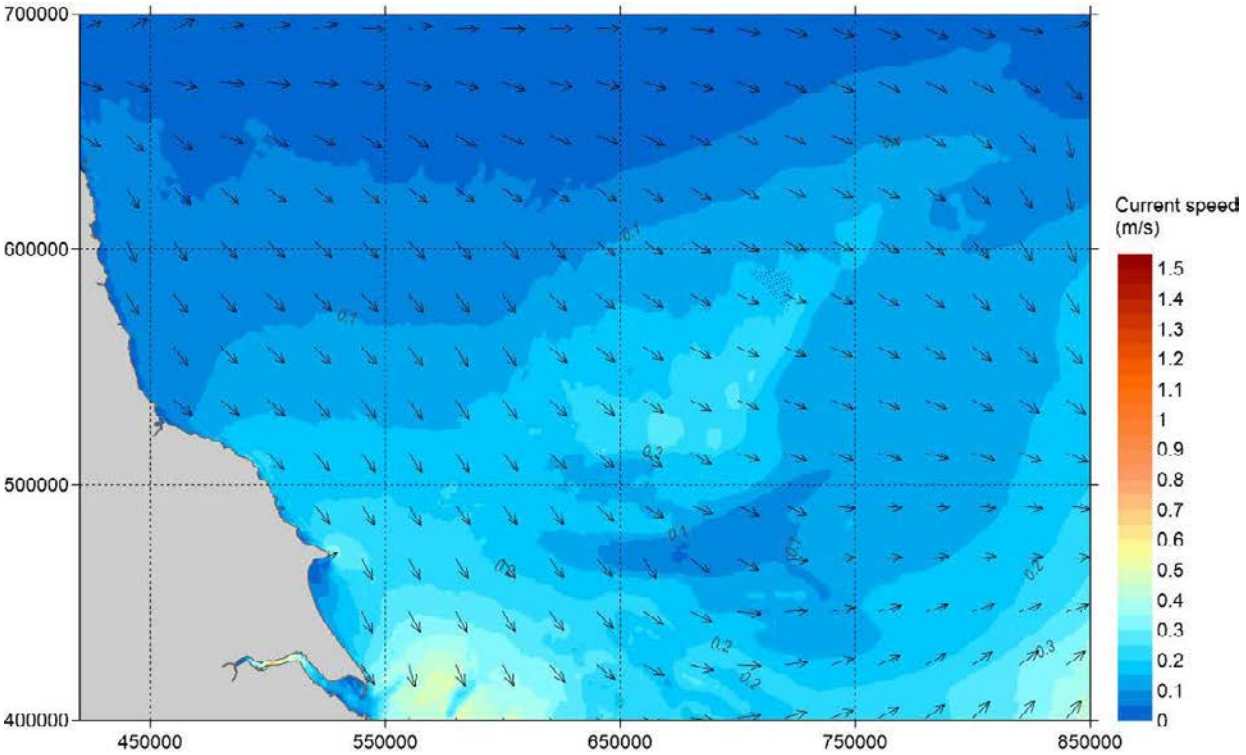

Figure A.115 Overview of Spatial Variation of Peak South-east-going Currents in a Neap tide – Layout D – OSP 2

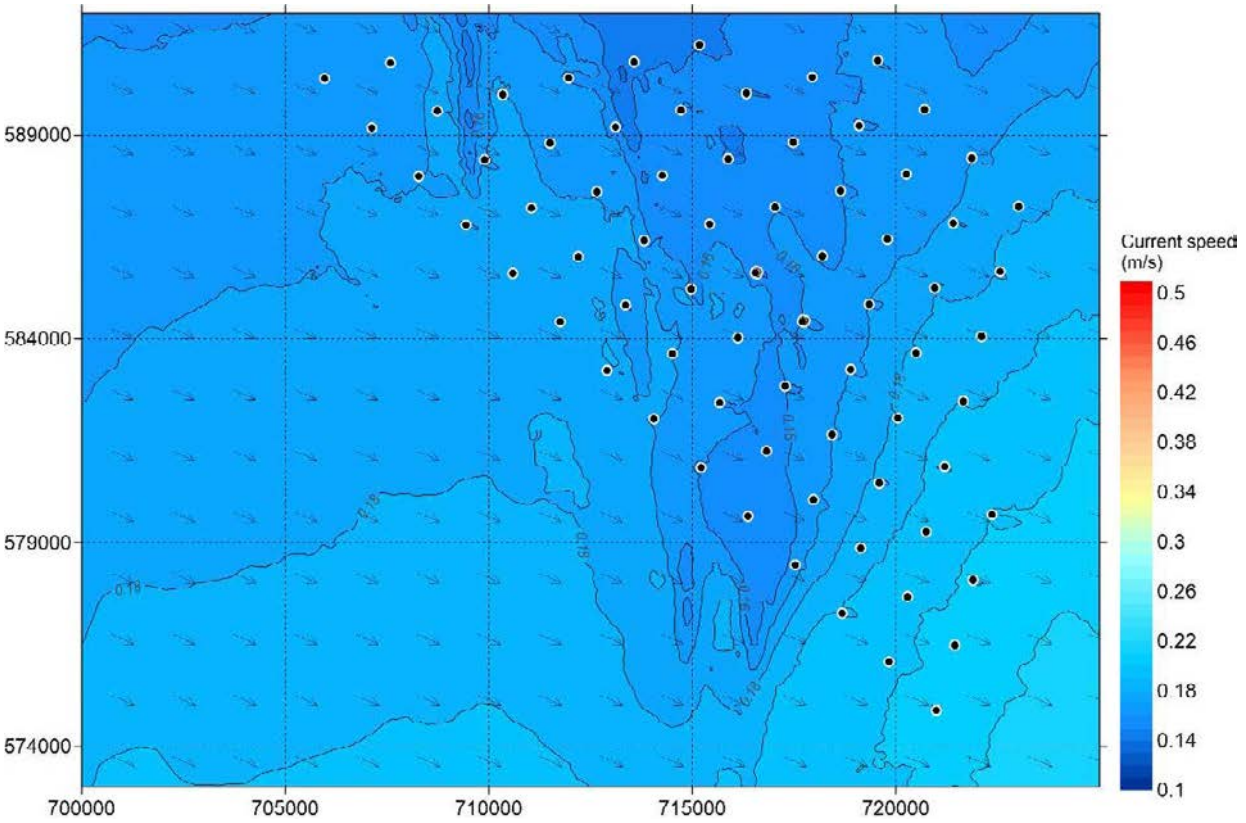

Figure A.116 Overview of Spatial Variation of Peak South-east-going Currents in a Neap tide – Layout D – OSP 2

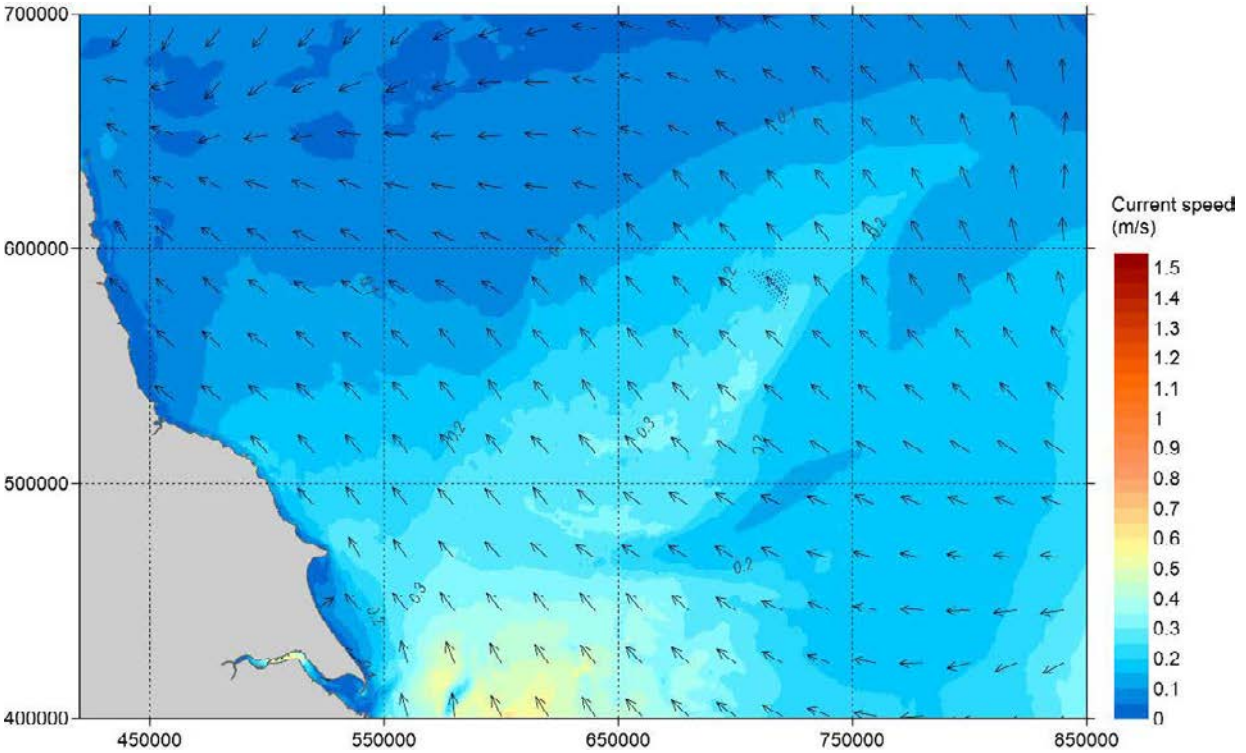

Figure A.117 Overview of Spatial Variation of Peak North-west-going Currents in a Neap tide – Layout D – OSP 2

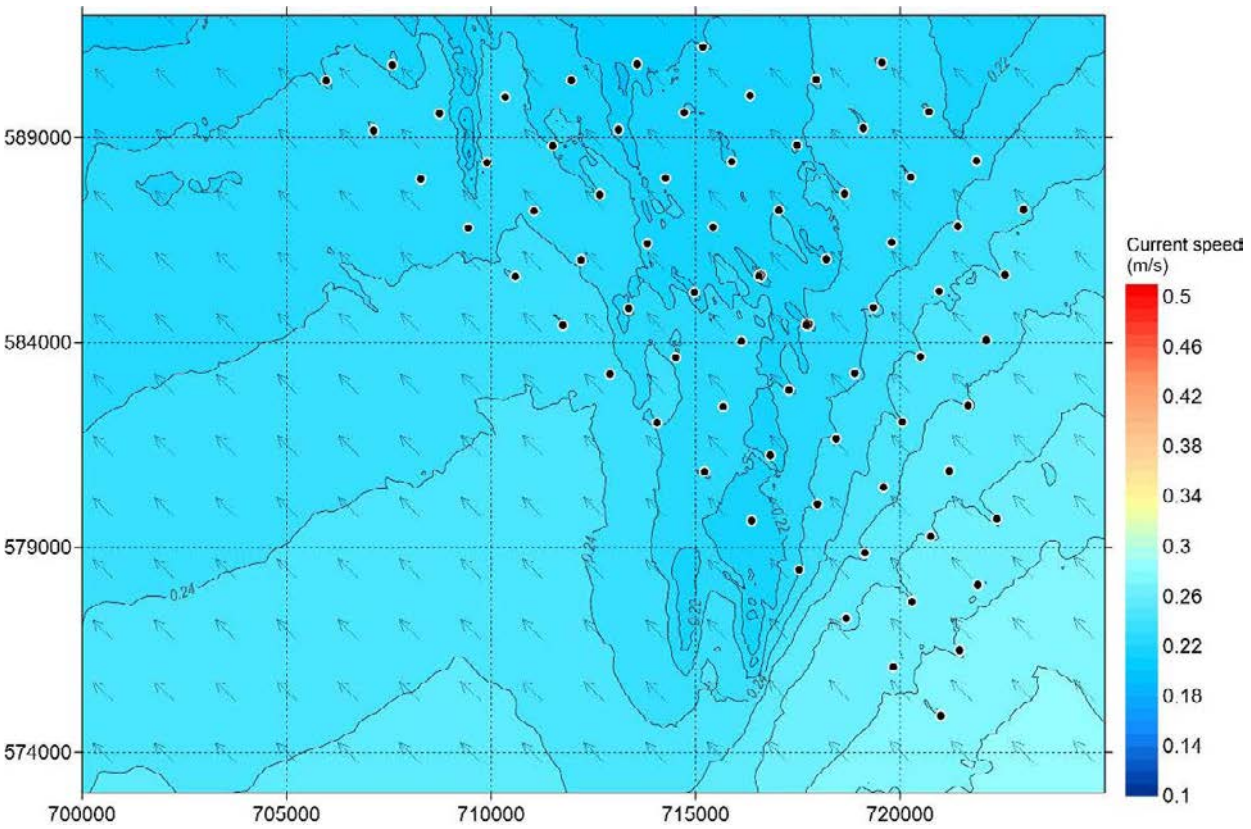

Figure A.118 Overview of Spatial Variation of Peak South-east-going Currents in a Neap tide – Layout D – OSP 2

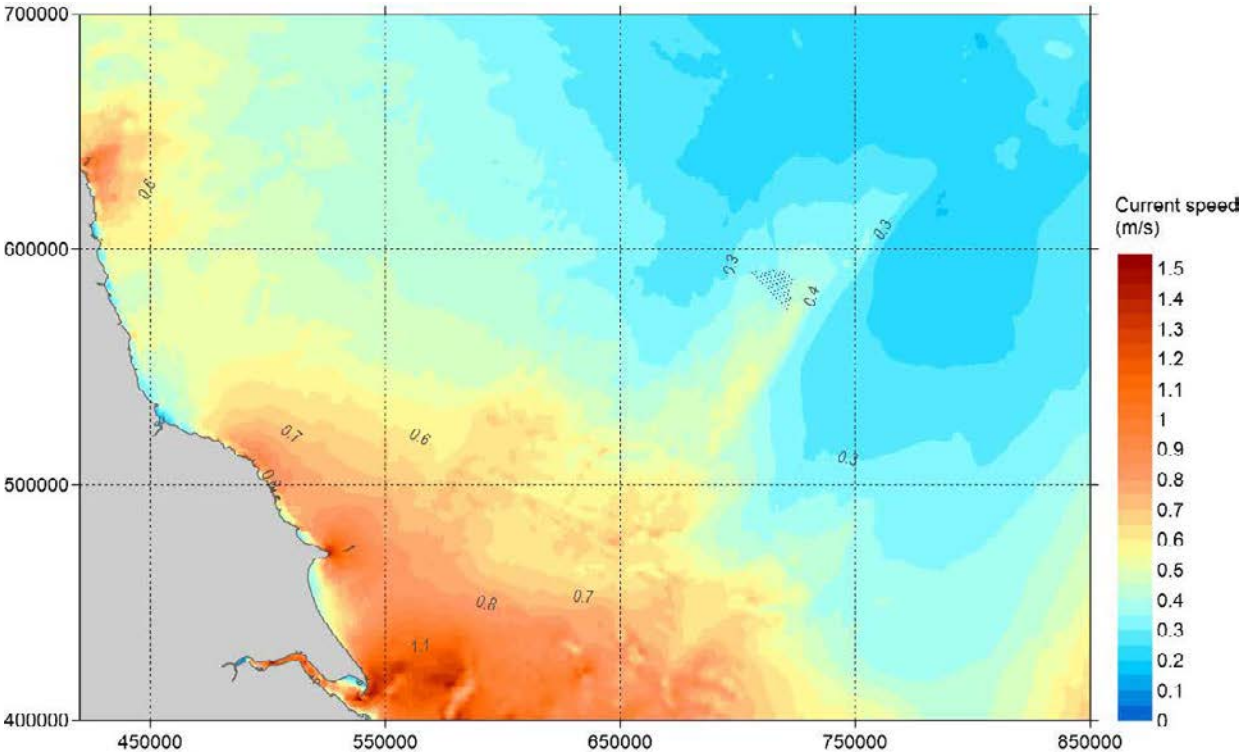

Figure A.119 Overview of Spatial Variation of Maximum Current Speed Over 30 days- Layout D – OSP 2

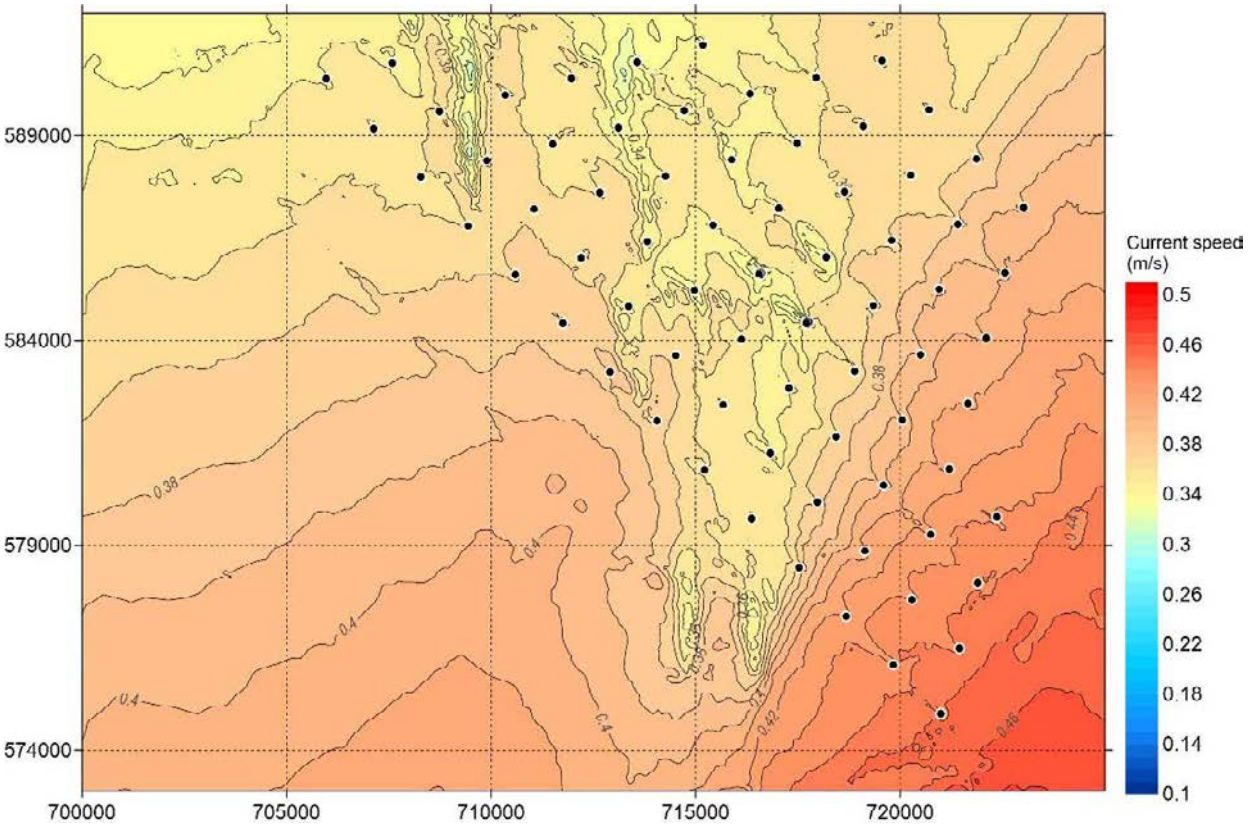

Figure A.120 Overview of Spatial Variation of Maximum Current Speed Over 30 days- Layout D – OSP 2

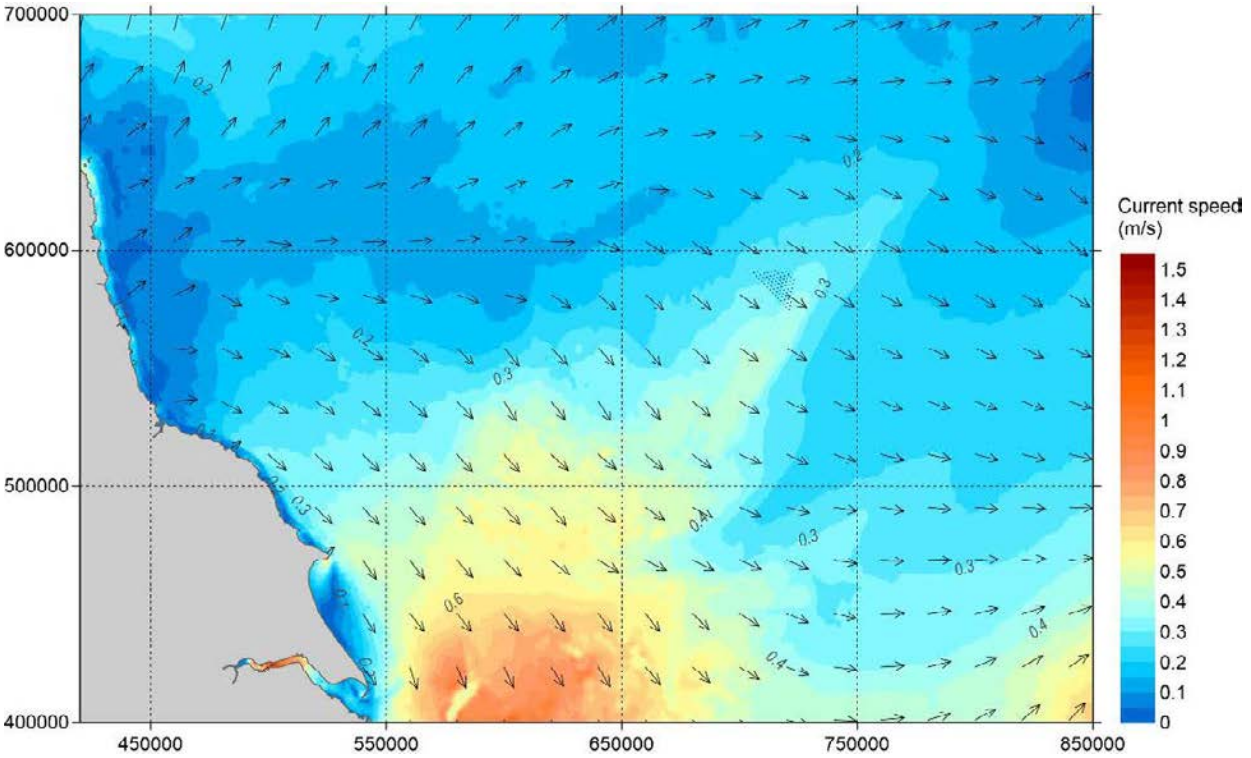

Figure A.121 Overview of Spatial Variation of Peak South-east-going Currents in a Spring Tide – Layout D – OSP 3

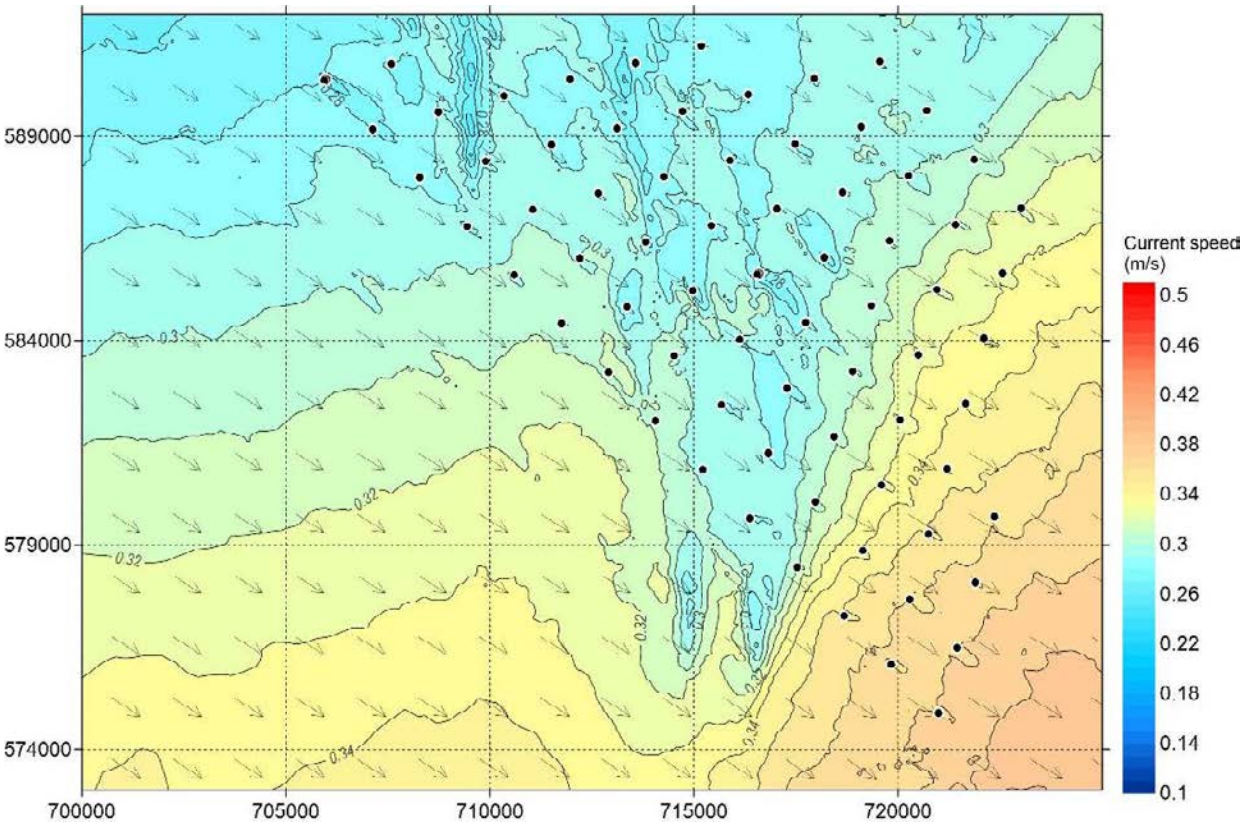

Figure A.122 A Closer View of Spatial Variation of Peak South-east-going Currents in a Spring Tide – Layout D – OSP 3

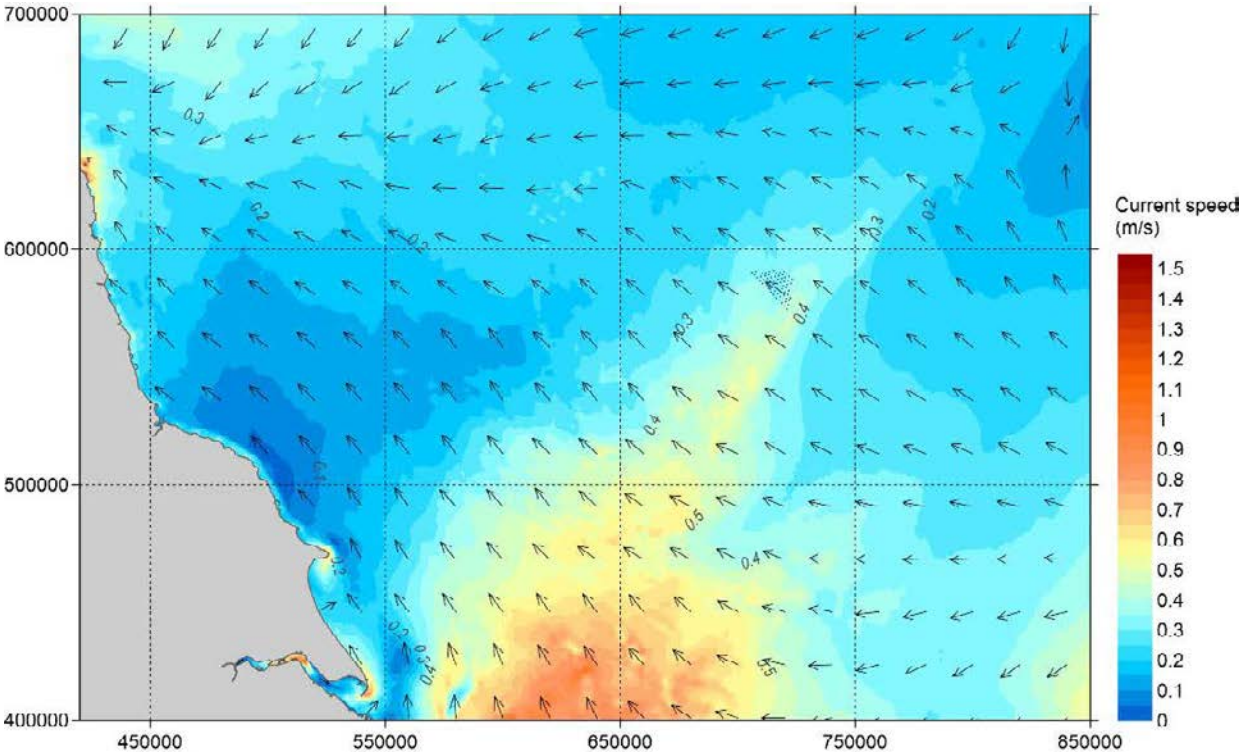

Figure A.123 Overview of Spatial Variation of Peak North-west-going Currents in a Spring Tide – Layout D – OSP 3

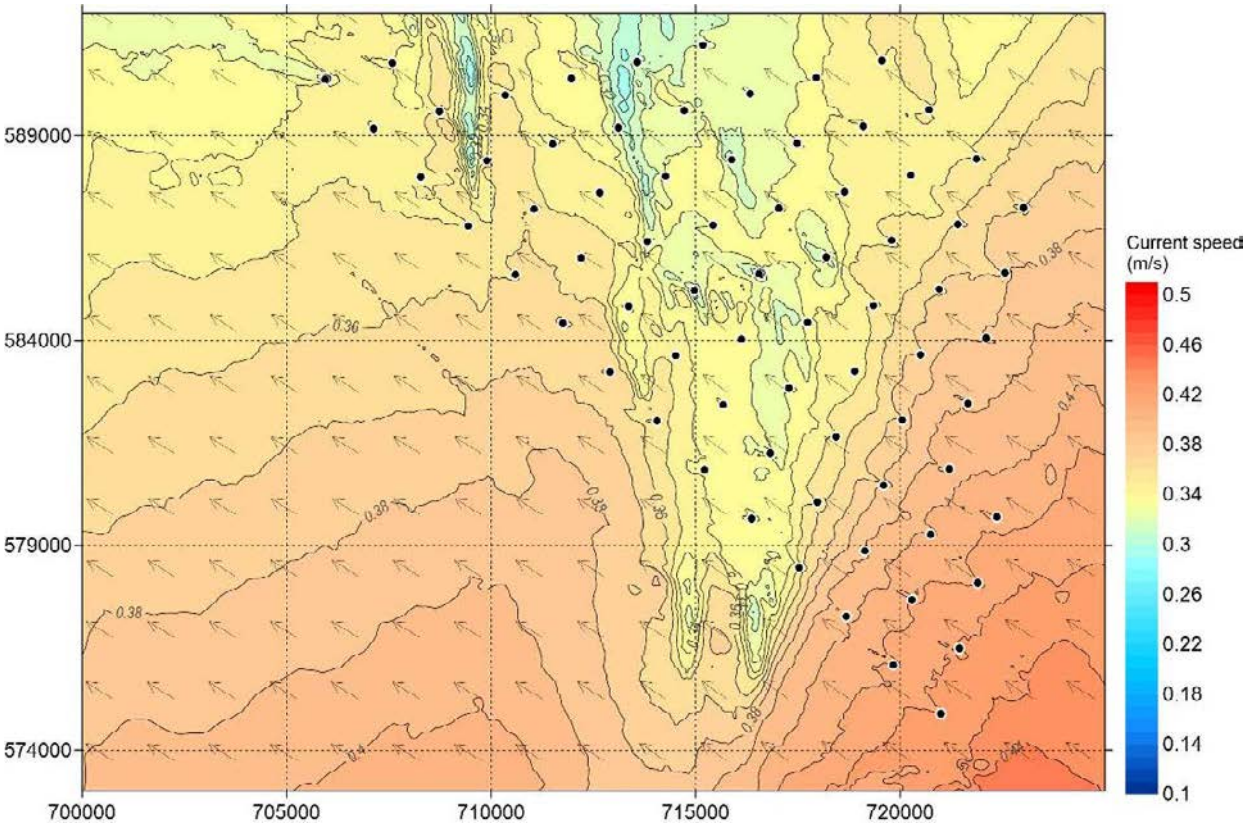

Figure A.124 A Closer View of Spatial Variation of Peak North-west-going Currents in a Spring Tide – Layout D – OSP 3

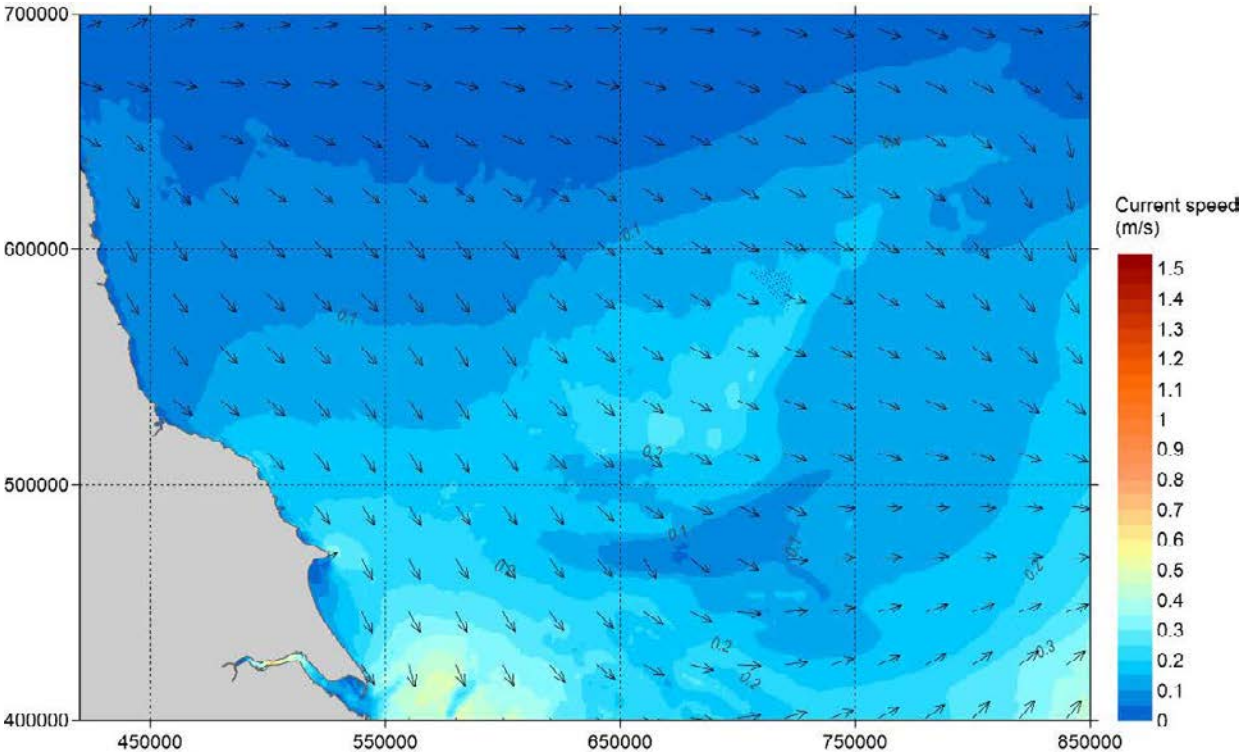

Figure A.125 Overview of Spatial Variation of Peak South-east-going Currents in a Neap tide – Layout D – OSP 3

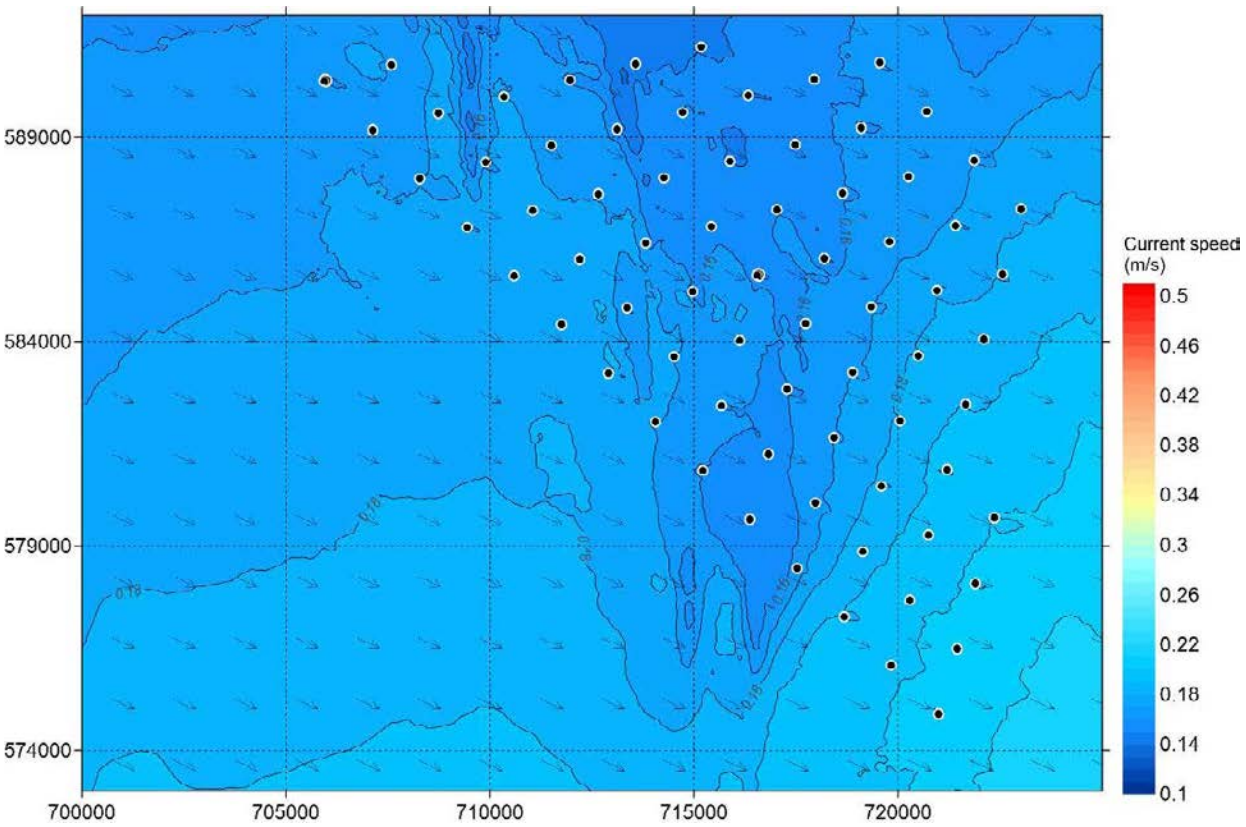

Figure A.126 Overview of Spatial Variation of Peak South-east-going Currents in a Neap tide – Layout D – OSP 3

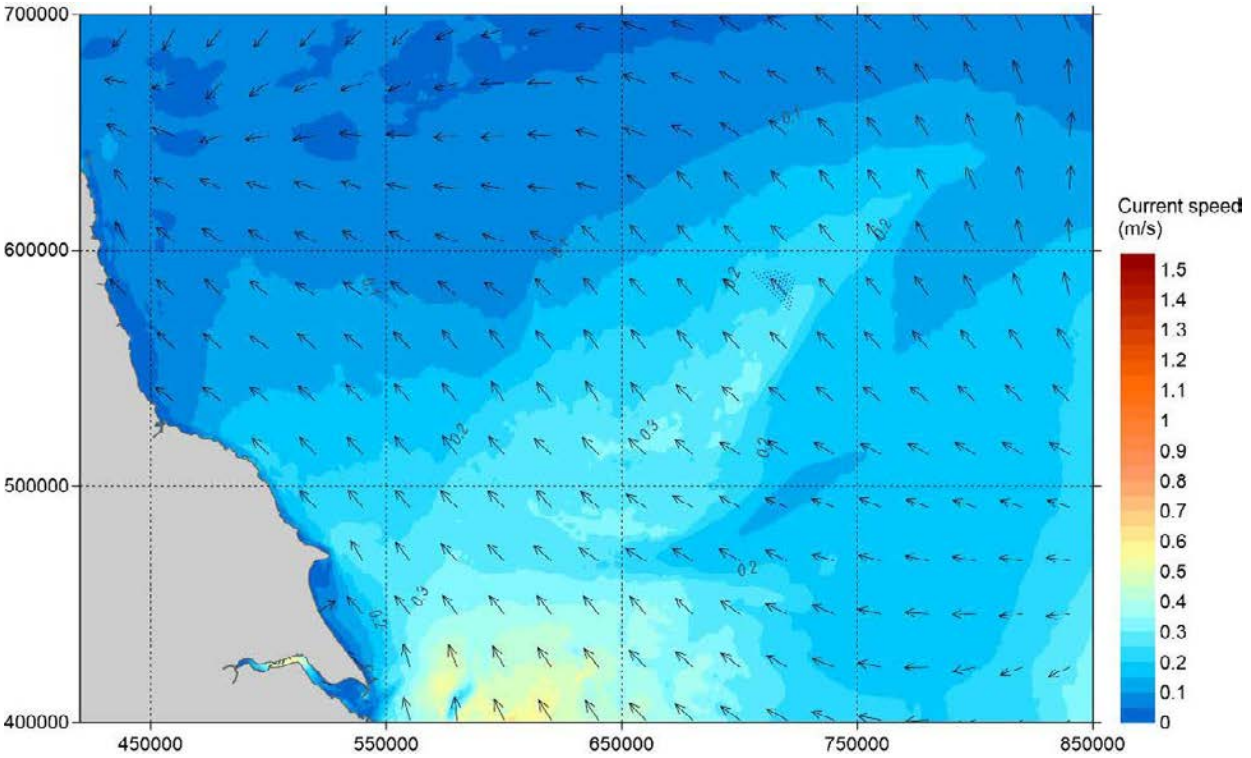

Figure A.127 Overview of Spatial Variation of Peak North-west-going Currents in a Neap tide – Layout D – OSP 3

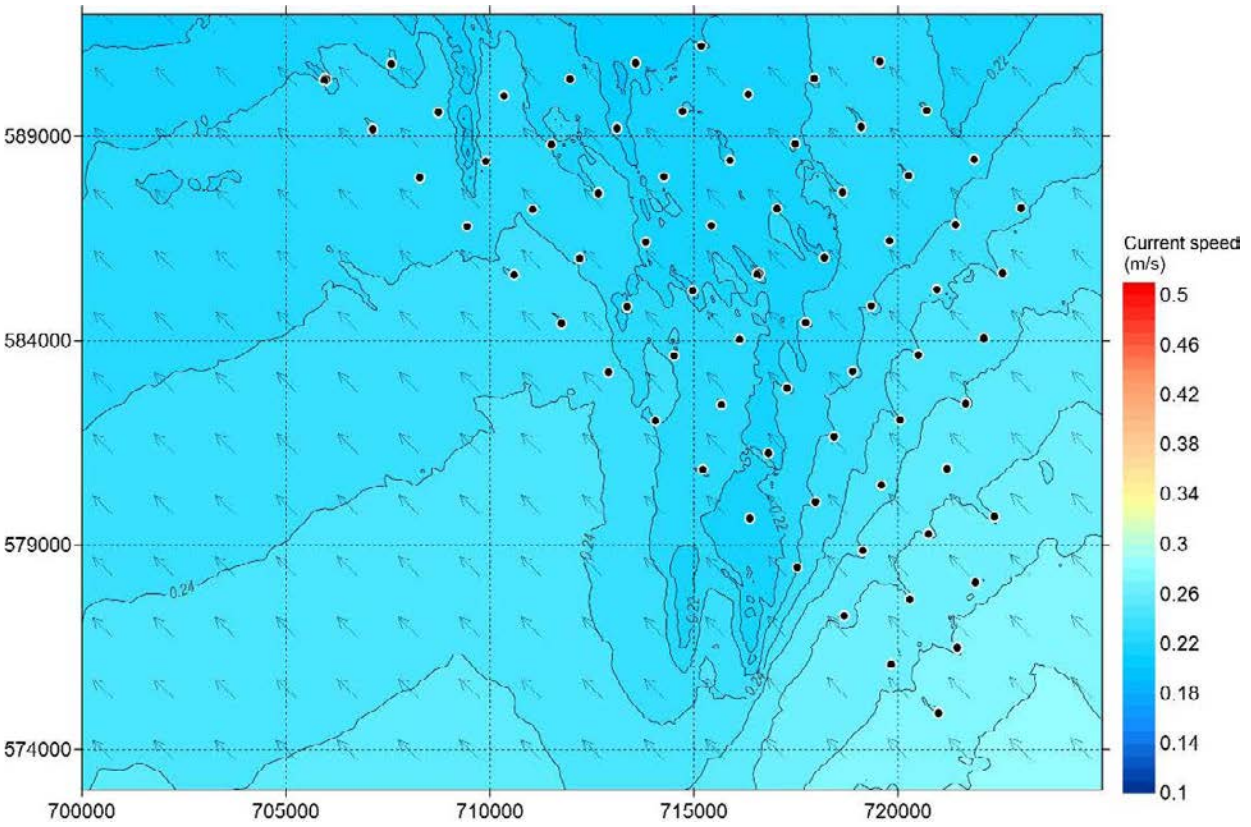

Figure A.128 Overview of Spatial Variation of Peak South-east-going Currents in a Neap tide – Layout D – OSP 3

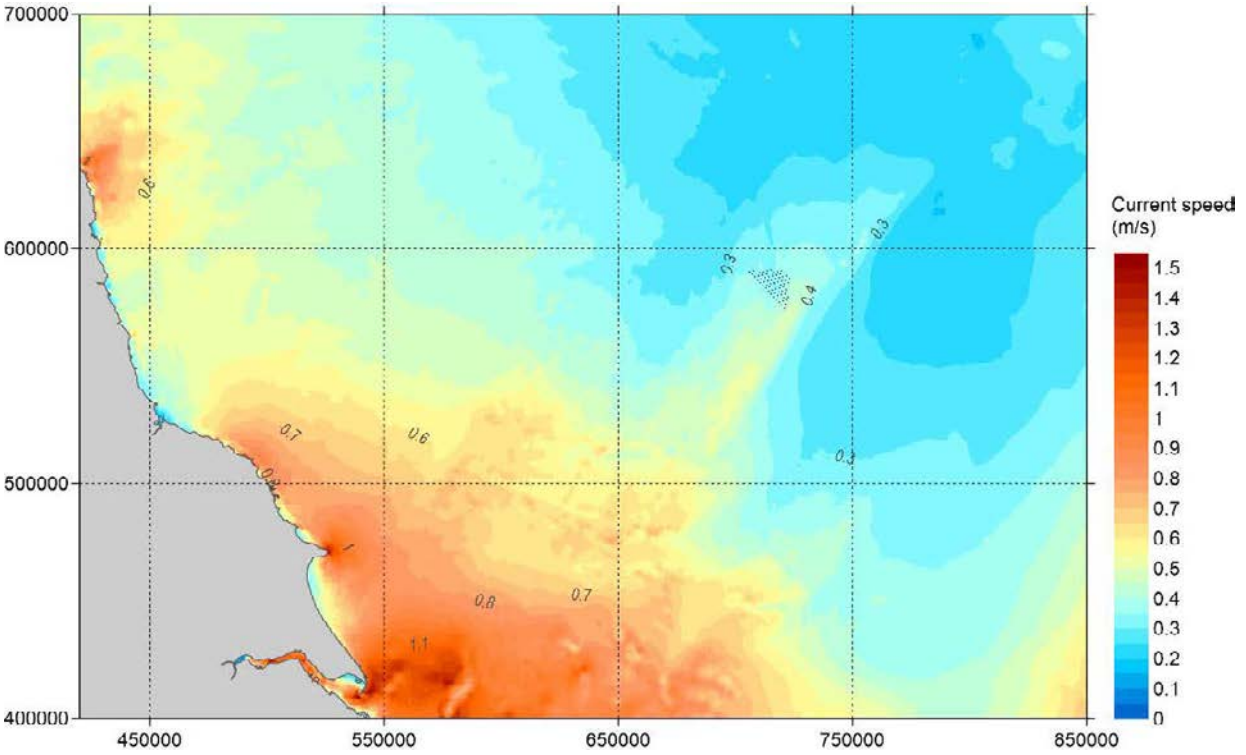

Figure A.129 Overview of Spatial Variation of Maximum Current Speed Over 30 days- Layout D – OSP 3

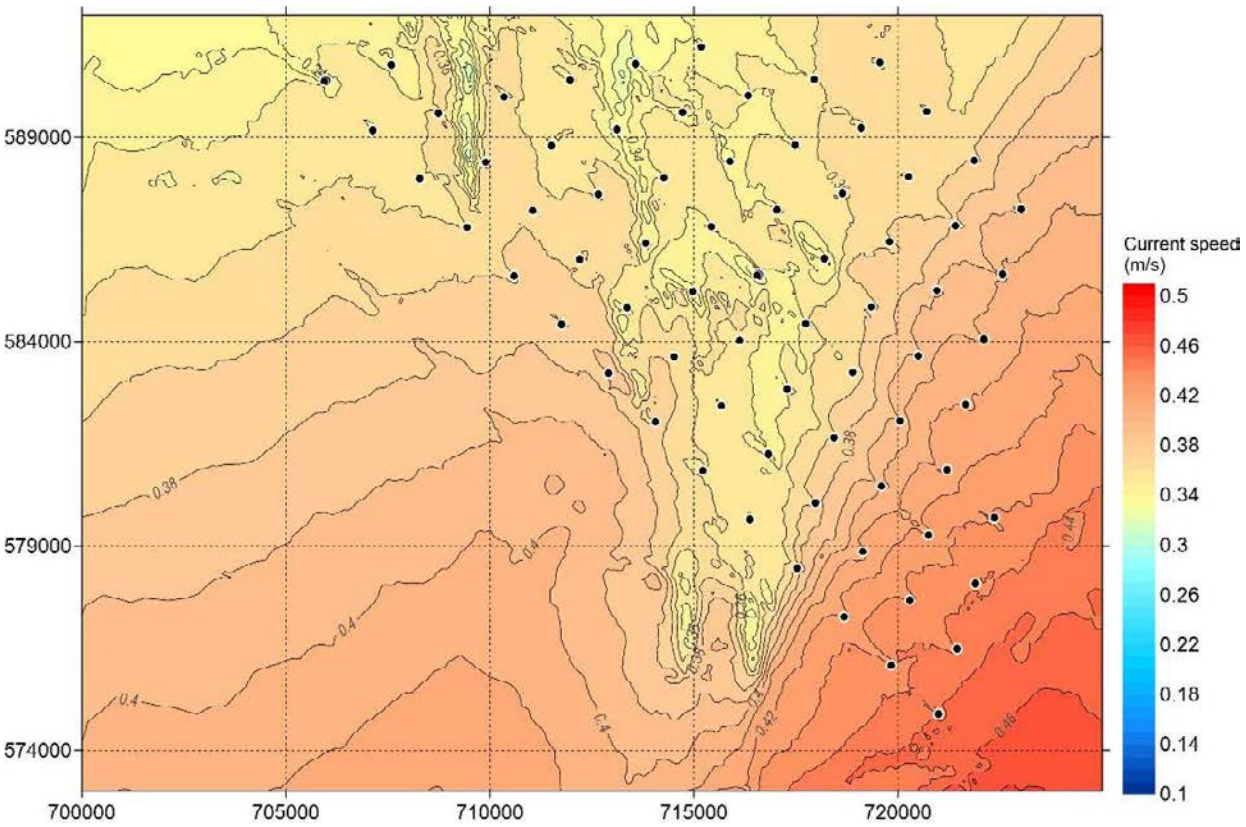

Figure A.130 Overview of Spatial Variation of Maximum Current Speed Over 30 days- Layout D – OSP 3

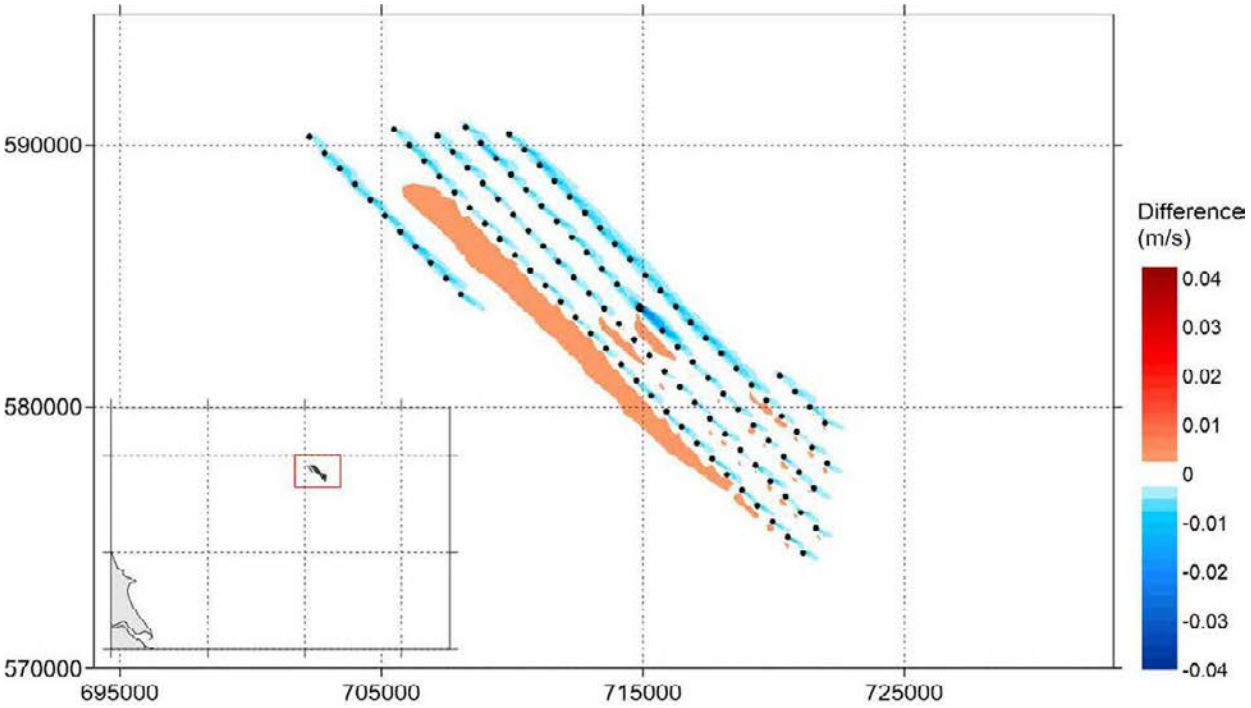

Figure A.131 Change of Speed of Peak South-east-going Currents in a Spring Tide (Layout A-OSP1 – Baseline)

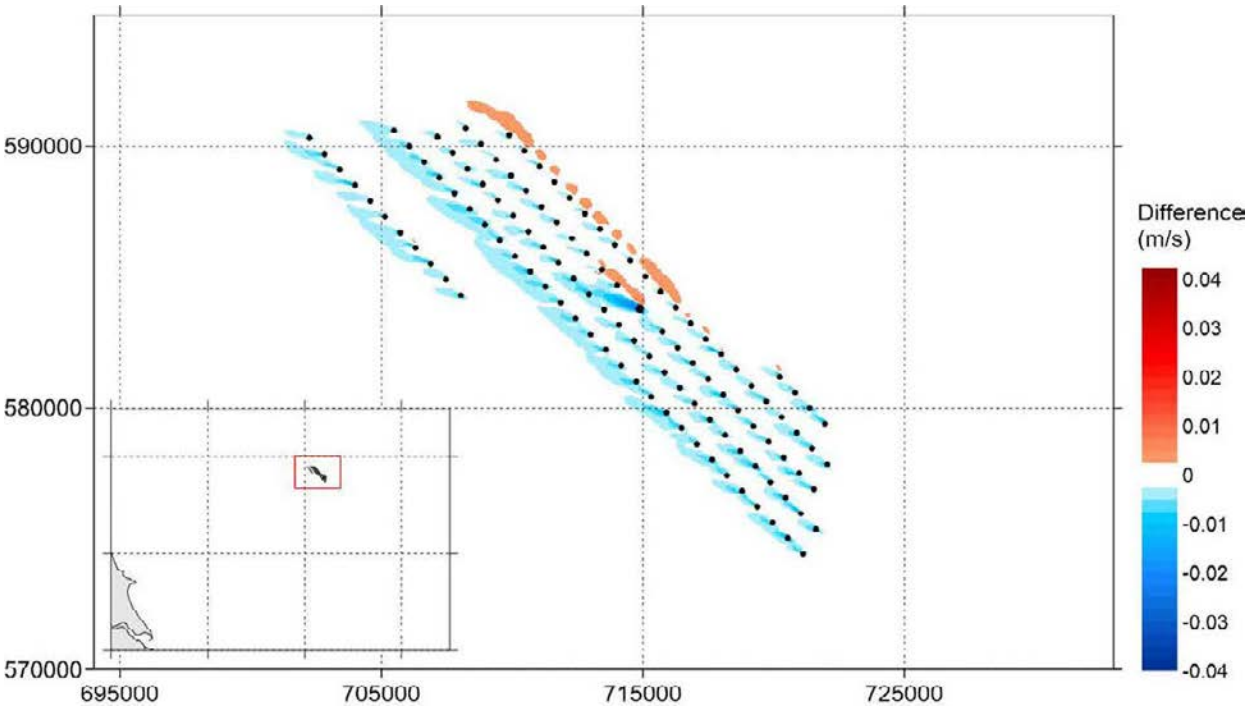

Figure A.132 Change of Speed of Peak North-west-going Currents in a Spring Tide (Layout A-OSP1 – Baseline)

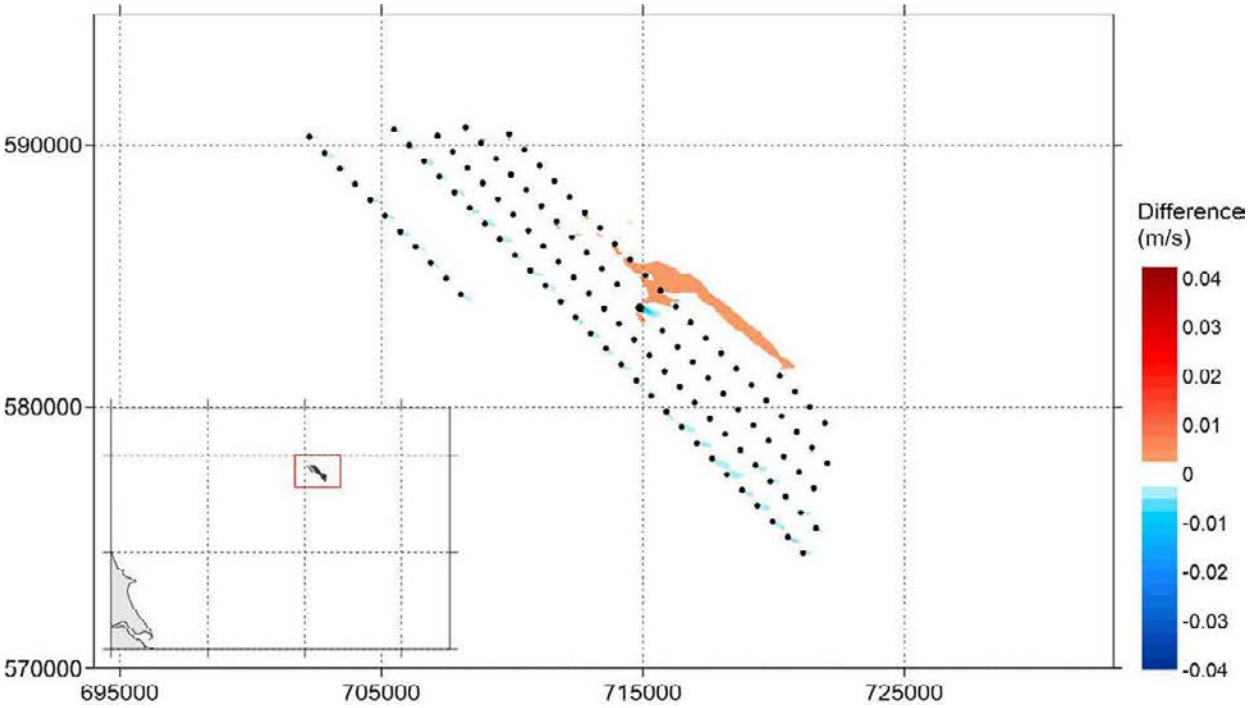

Figure A.133 Change of Speed of Peak South-east-going Currents in a Neap tide (Layout A-OSP1 – Baseline)

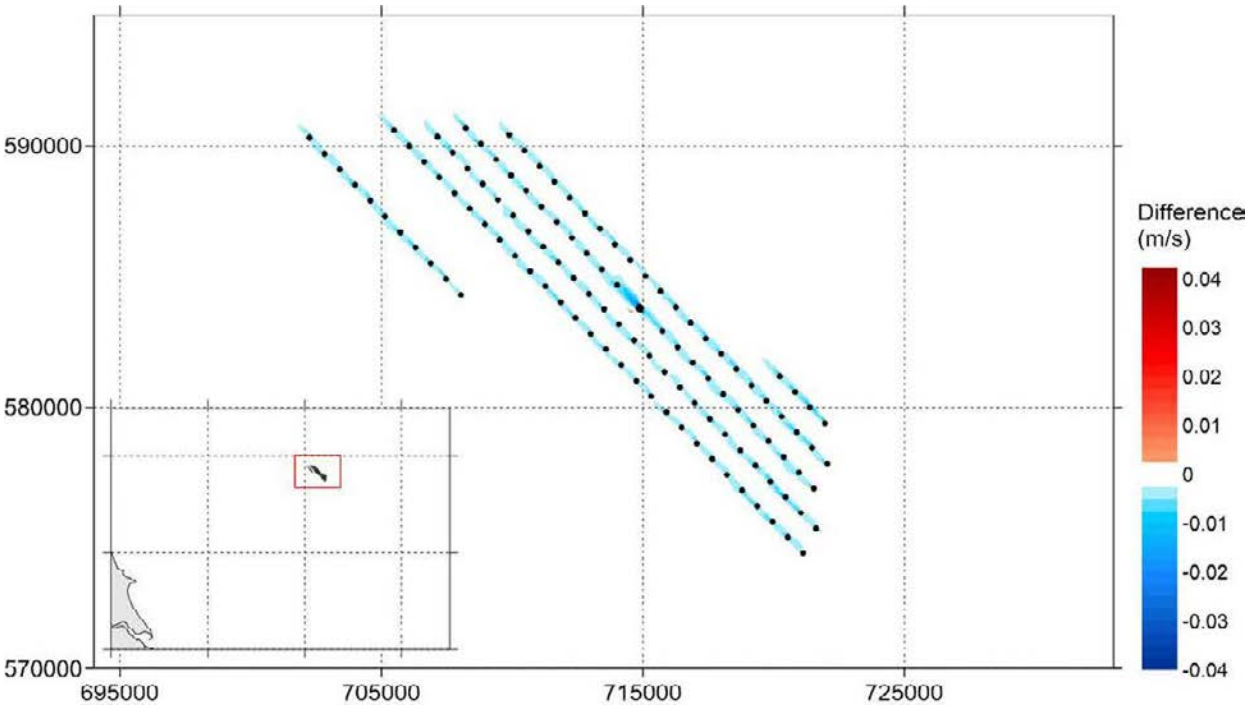

Figure A.134 Change of Speed of Peak North-west-going Currents in a Neap tide (Layout A-OSP1 – Baseline)

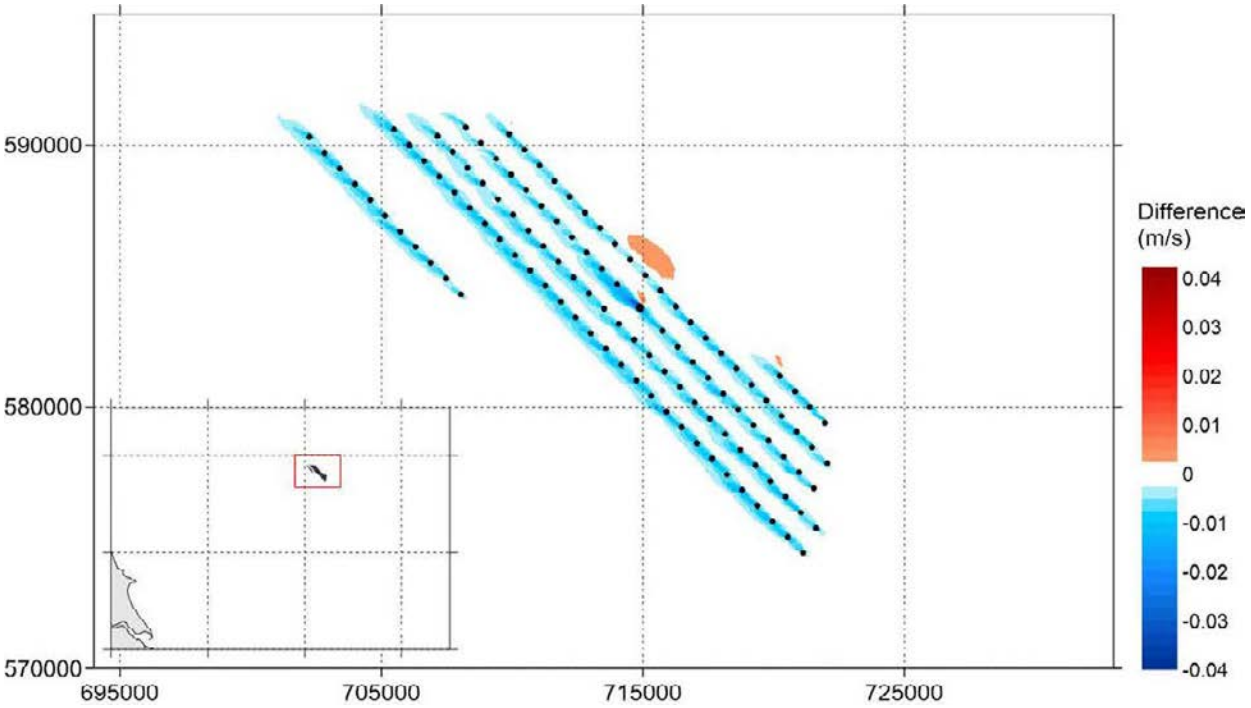

Figure A.135 Change of Maximum Current Speed Over 30 days (Layout A-OSP1 – Baseline)

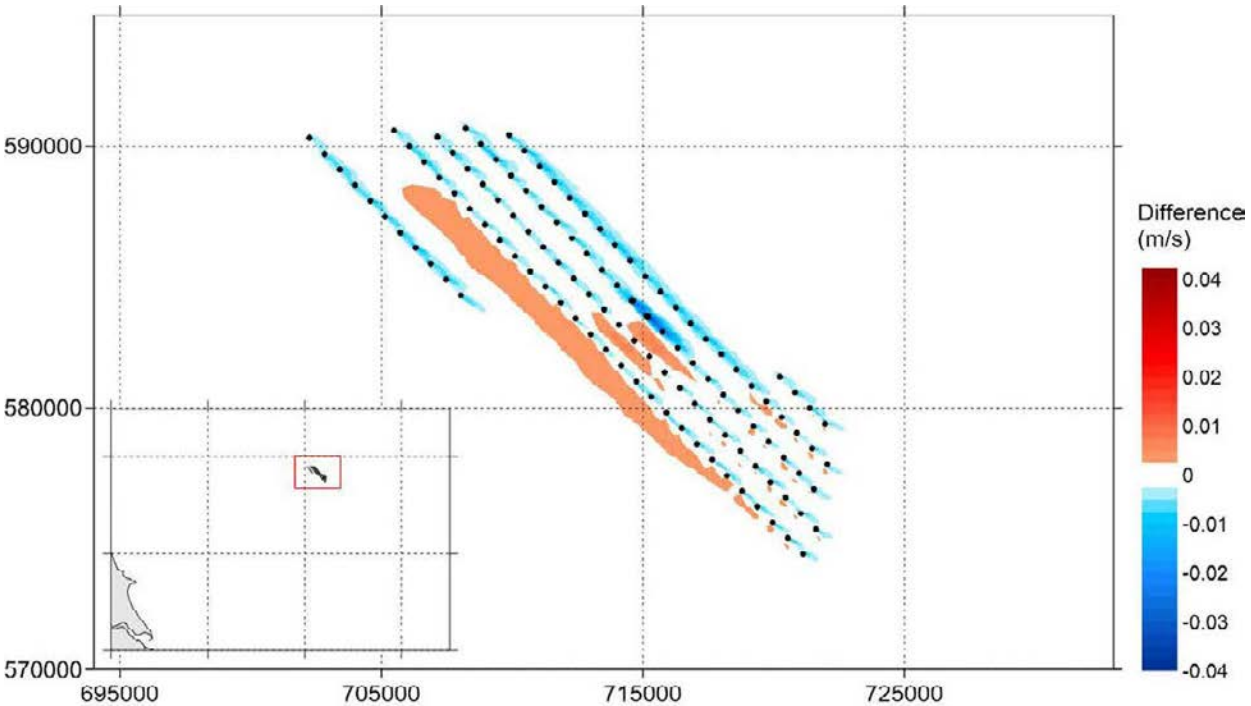

Figure A.136 Change of Speed of Peak South-east-going Currents in a Spring Tide (Layout A-OSP2 – Baseline)

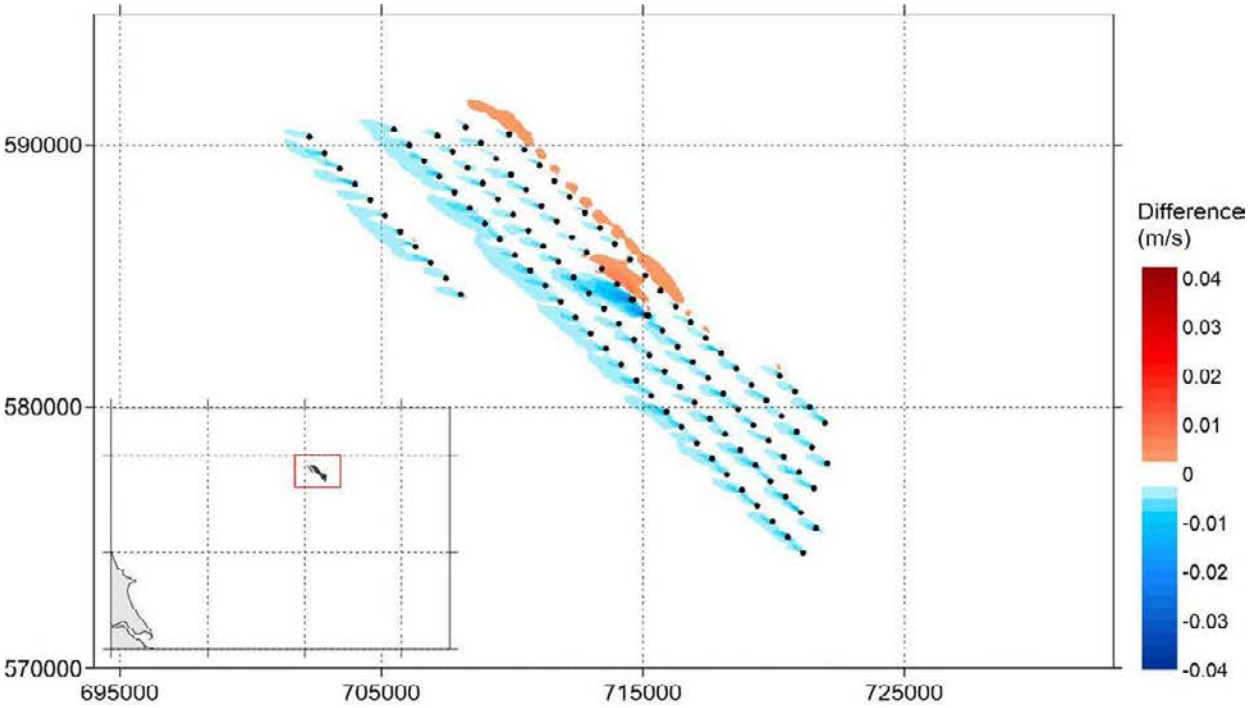

Figure A.137 Change of Speed of Peak North-west-going Currents in a Spring Tide (Layout A-OSP2 – Baseline)

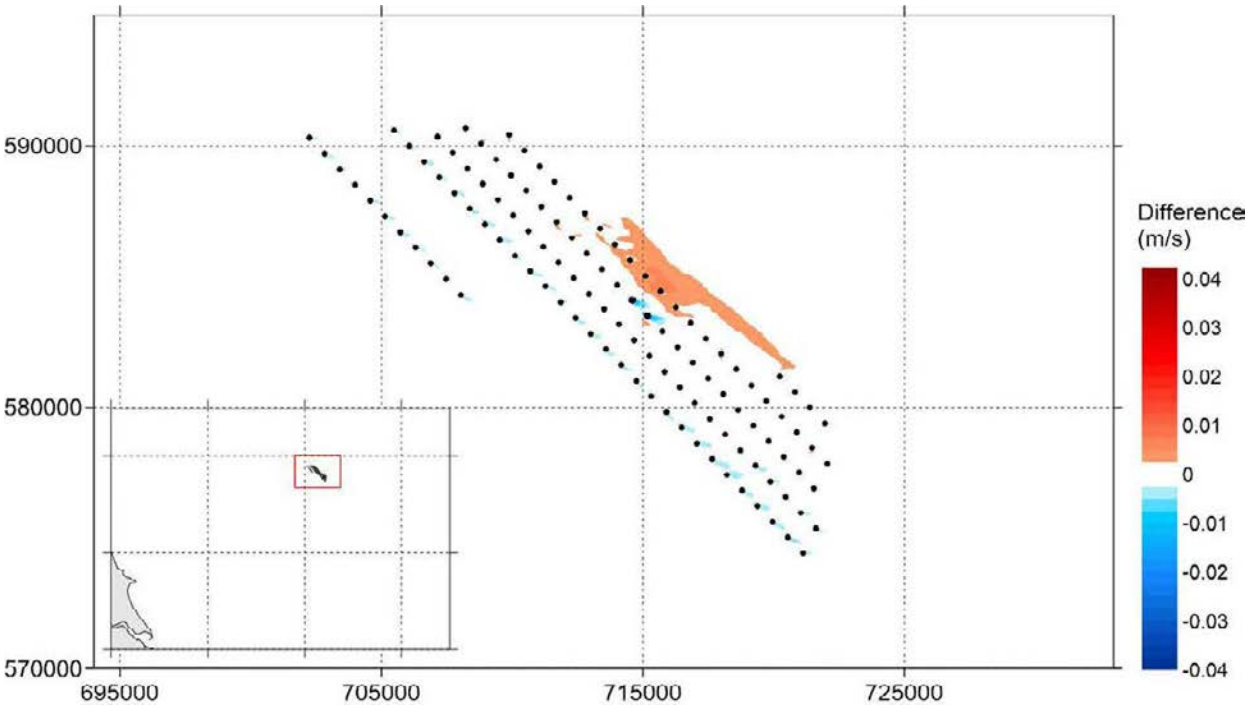

Figure A.138 Change of Speed of Peak South-east-going Currents in a Neap tide (Layout A-OSP2 – Baseline)

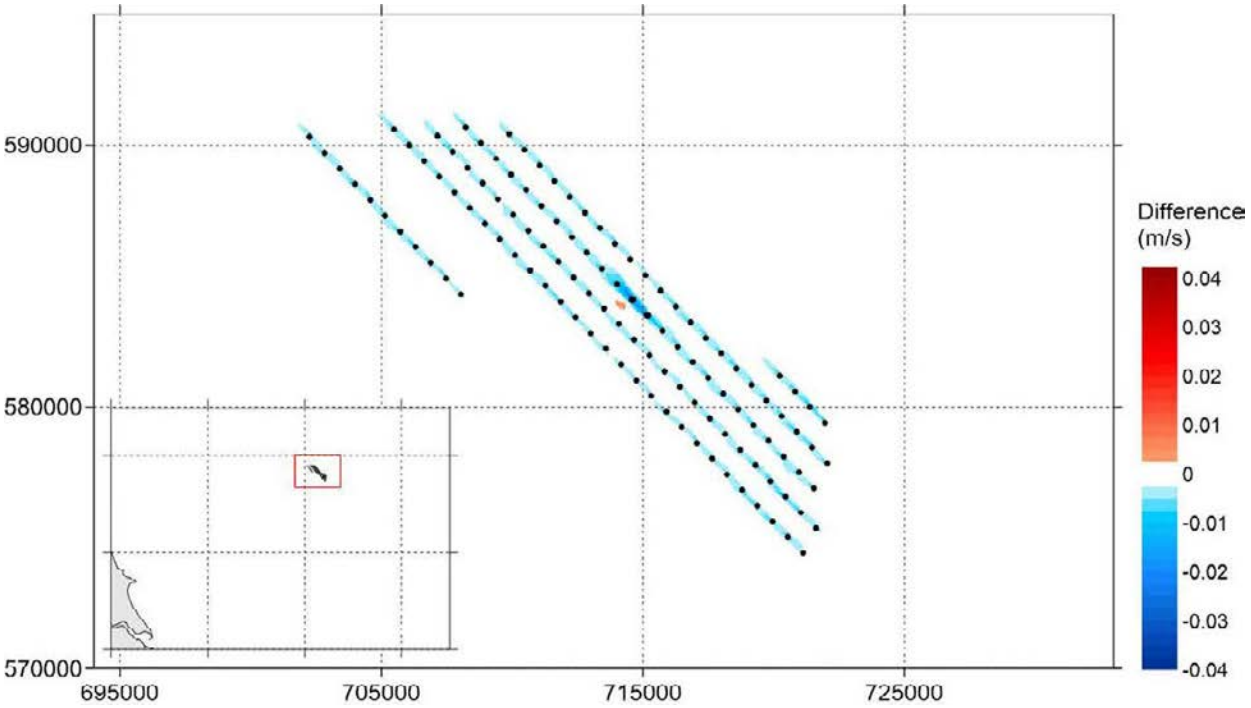

Figure A.139 Change of Speed of Peak North-west-going Currents in a Neap tide (Layout A-OSP2 – Baseline)

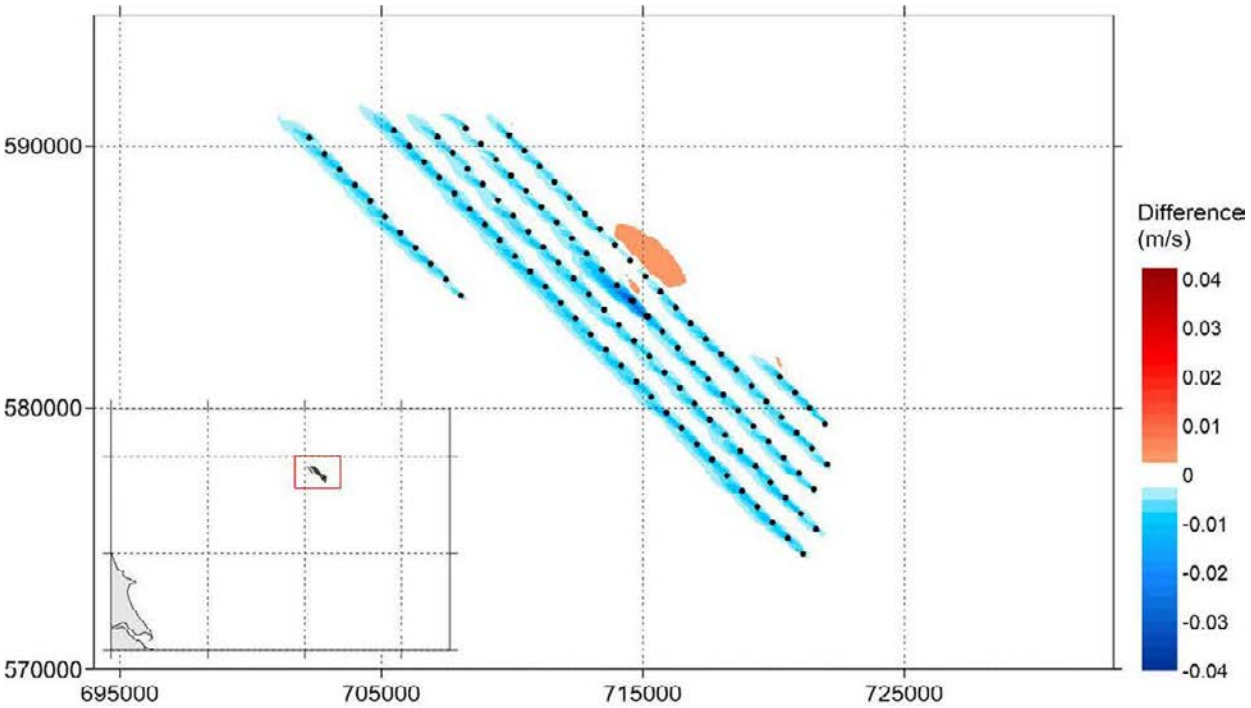

Figure A.140 Change of Maximum Current Speed Over 30 days (Layout A-OSP2 – Baseline)

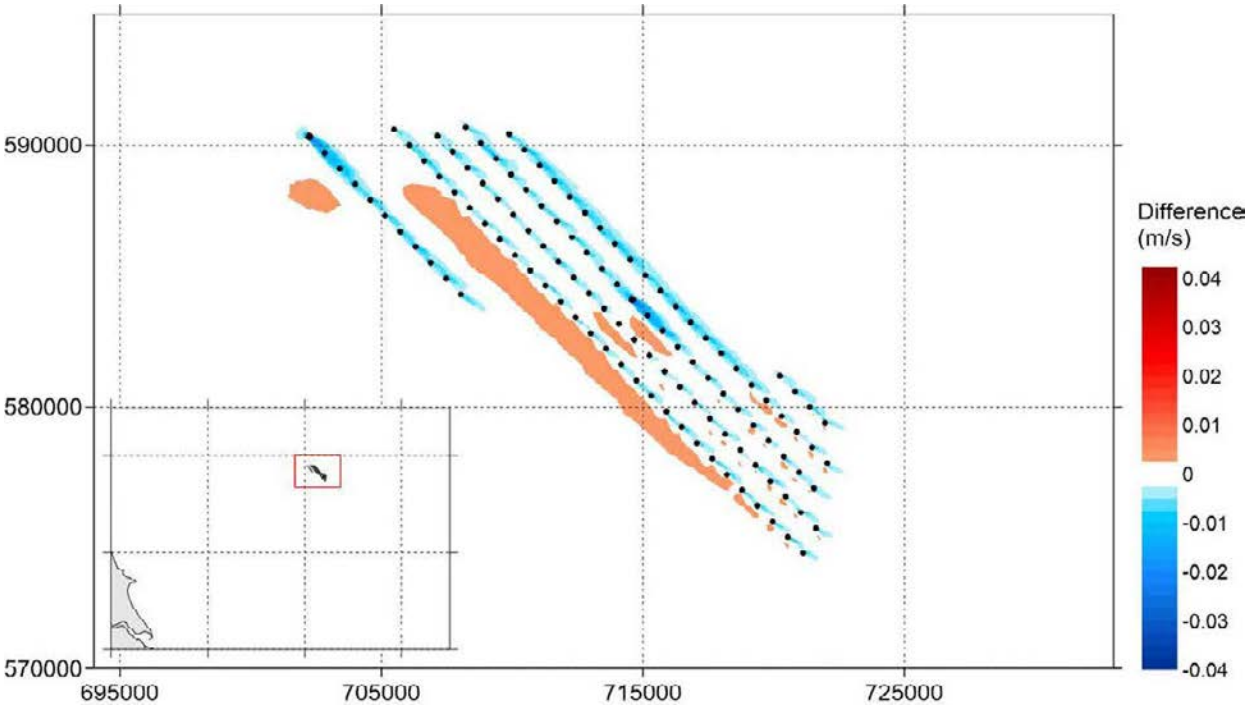

Figure A.141 Change of Speed of Peak South-east-going Currents in a Spring Tide (Layout A-OSP3 – Baseline)

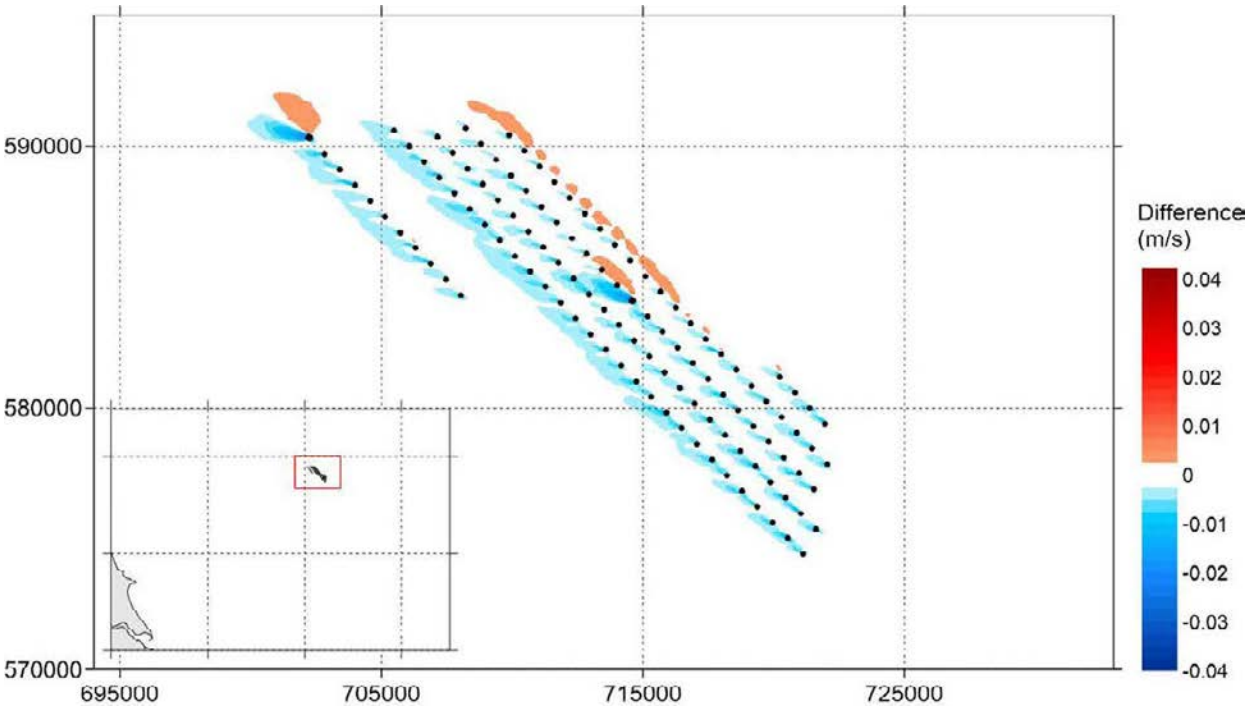

Figure A.142 Change of Speed of Peak North-west-going Currents in a Spring Tide (Layout A-OSP3 – Baseline)

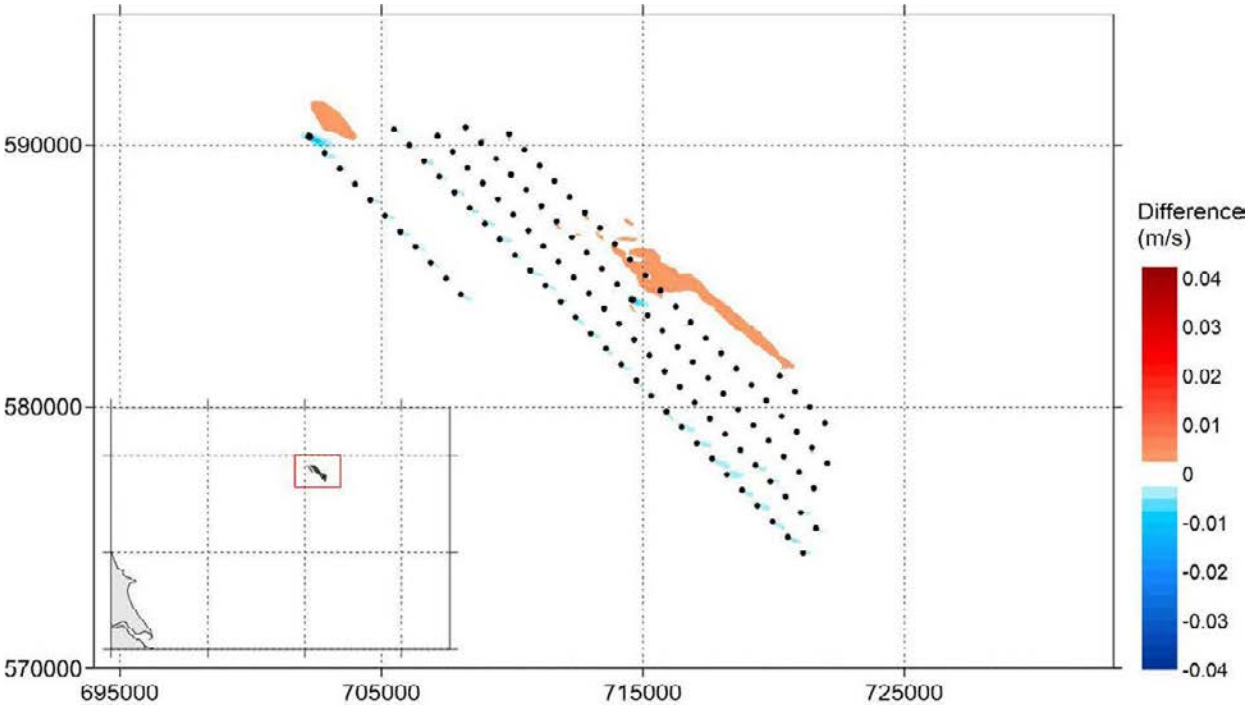

Figure A.143 Change of Speed of Peak South-east-going Currents in a Neap tide (Layout A-OSP3 – Baseline)

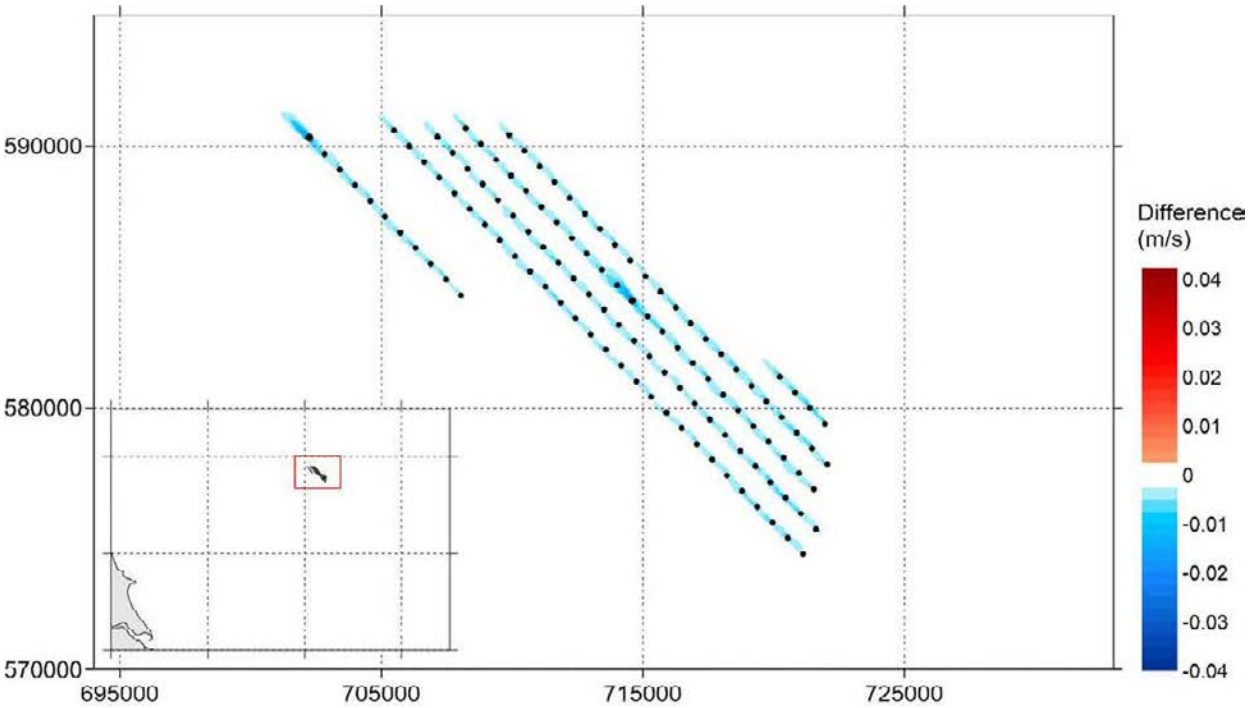

Figure A.144 Change of Speed of Peak North-west-going Currents in a Neap tide (Layout A-OSP3 – Baseline)

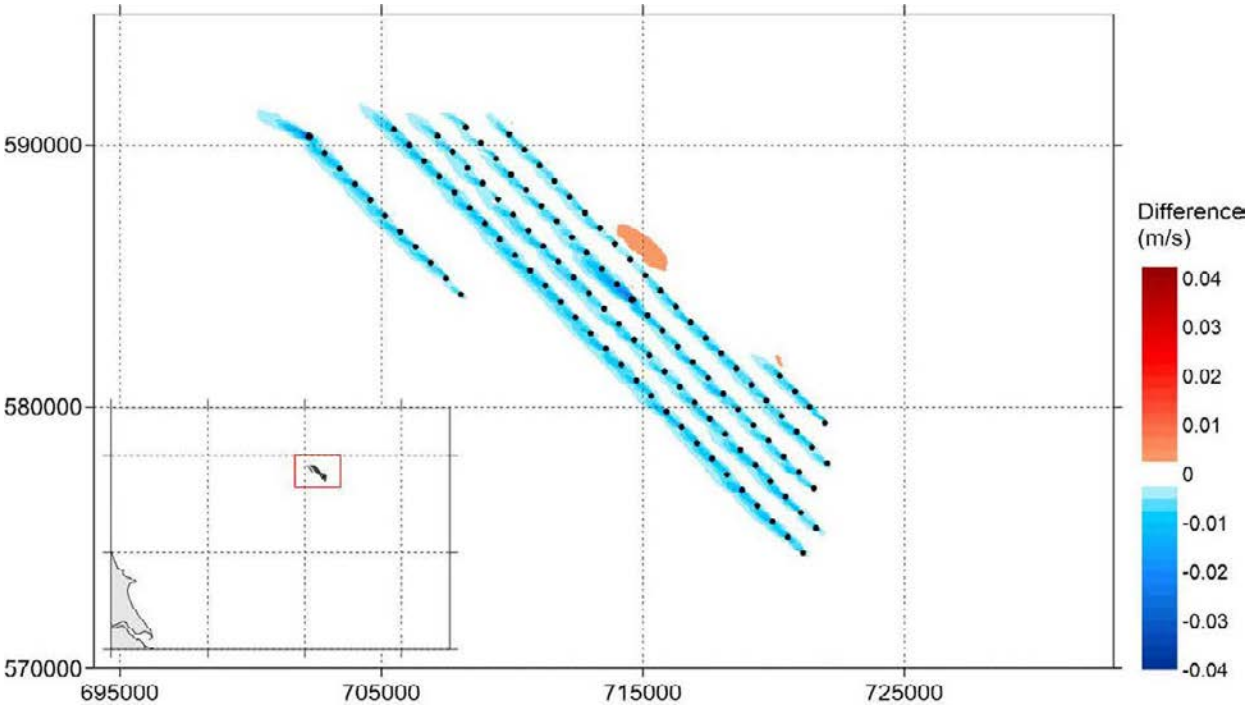

Figure A.145 Change of Maximum Current Speed Over 30 days (Layout A-OSP3 – Baseline)

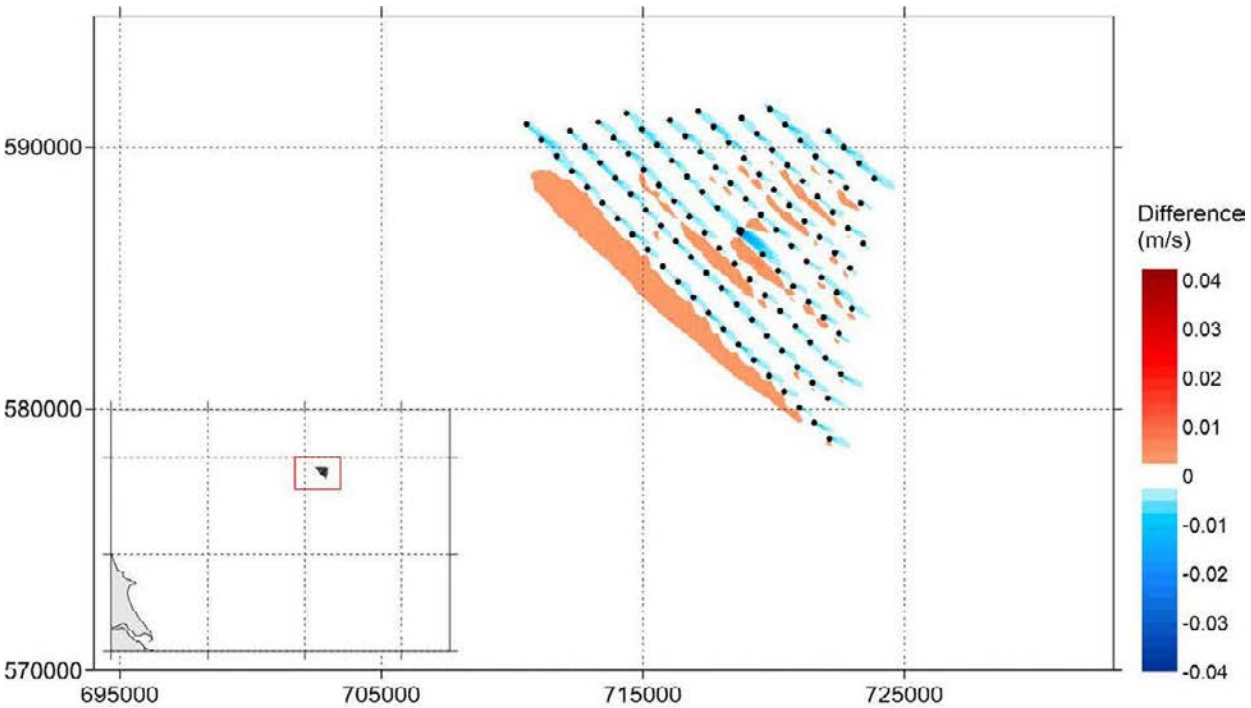

Figure A.146 Change of Speed of Peak South-east-going Currents in a Spring Tide (Layout B-OSP1 – Baseline)

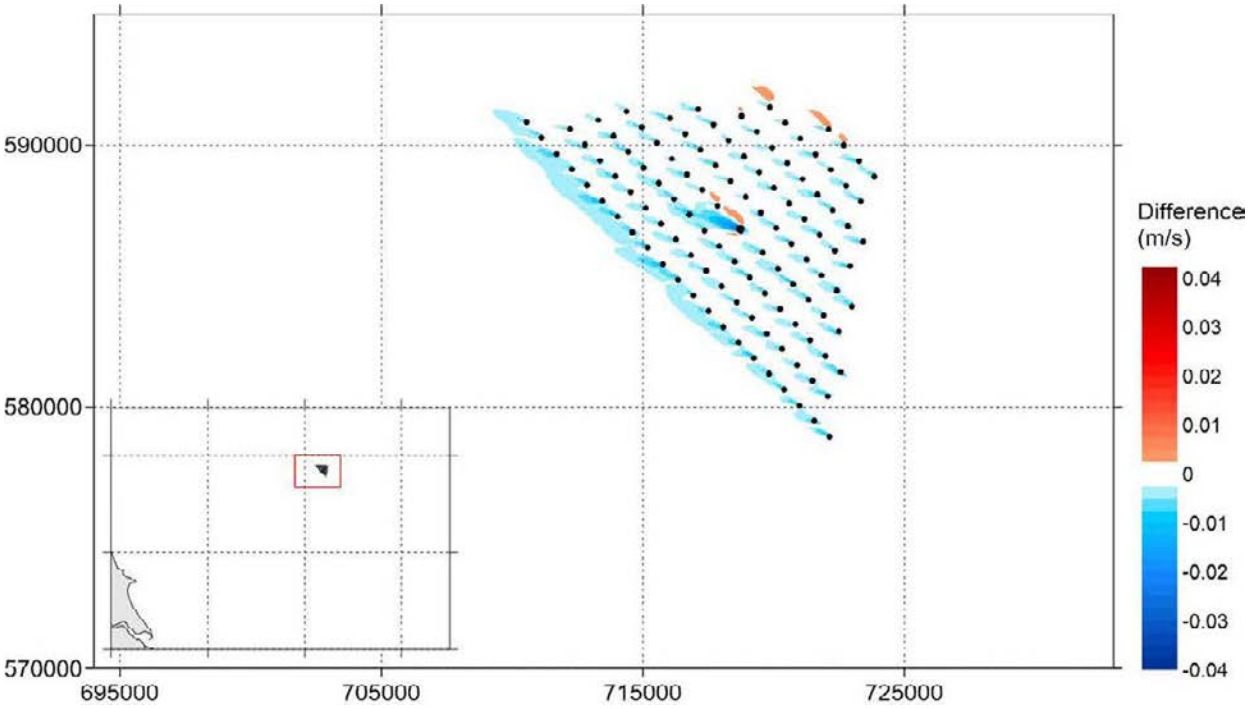

Figure A.147 Change of Speed of Peak North-west-going Currents in a Spring Tide (Layout B-OSP1 – Baseline)

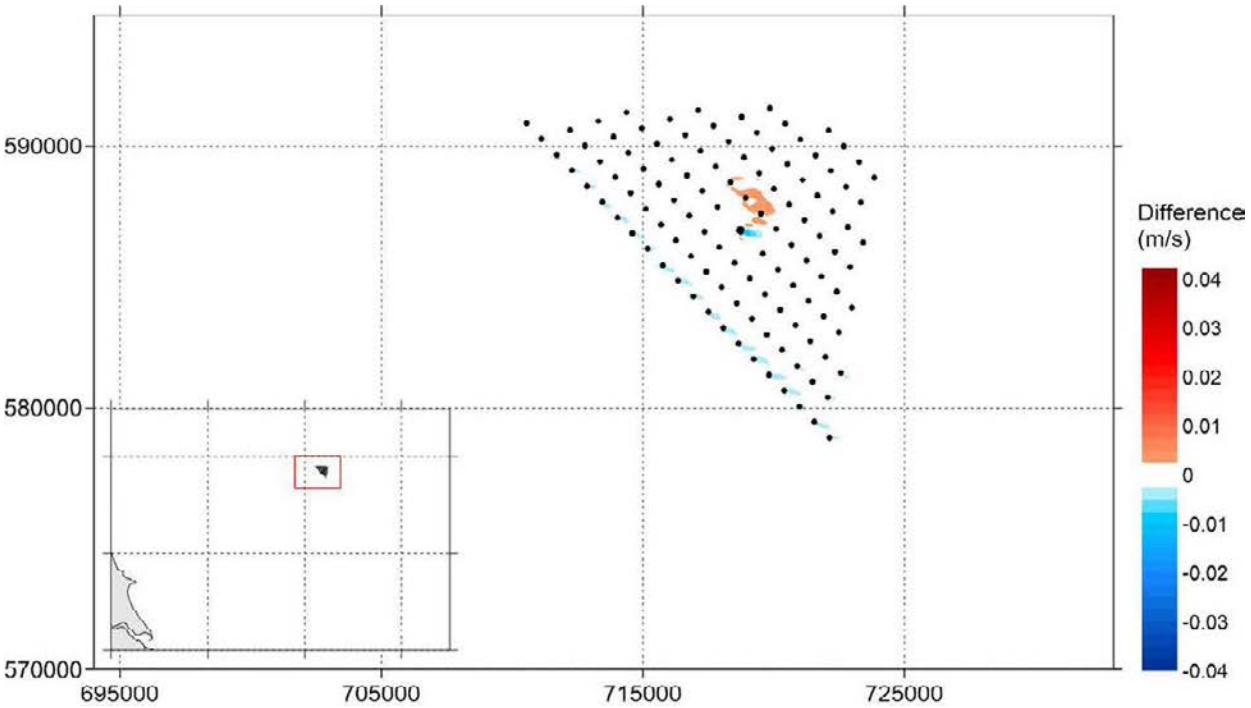

Figure A.148 Change of Speed of Peak South-east-going Currents in a Neap tide (Layout B-OSP1 – Baseline)

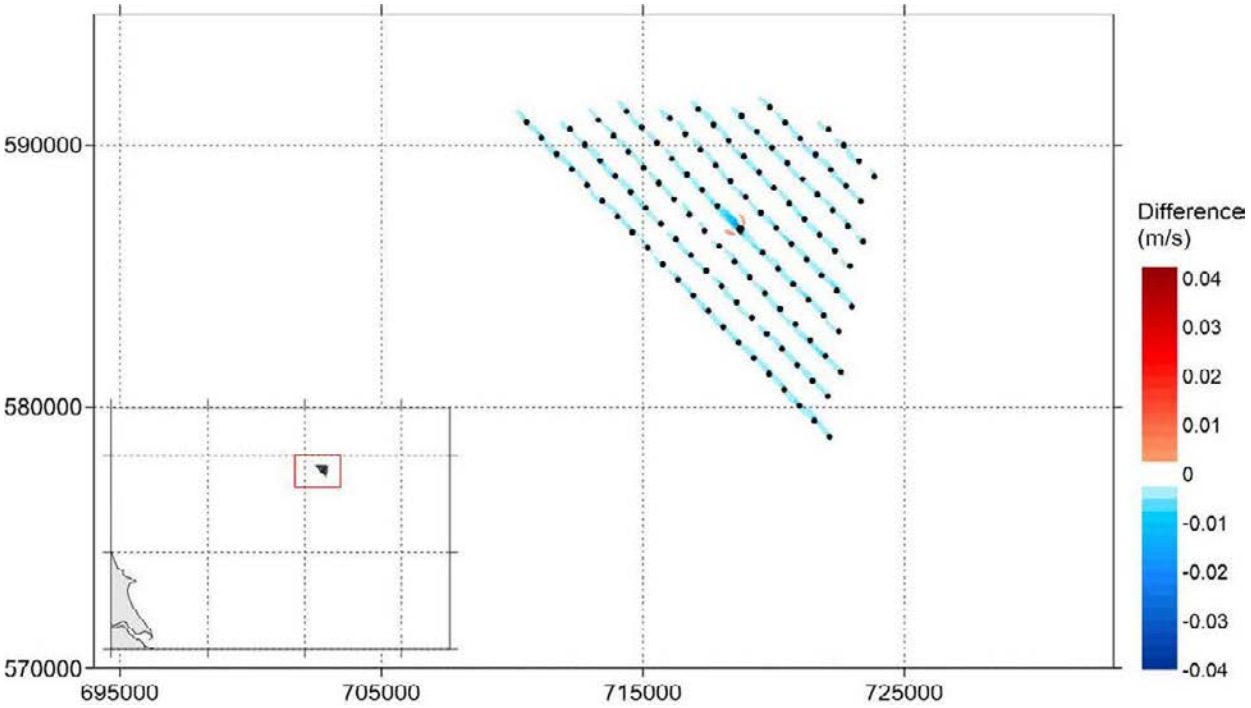

Figure A.149 Change of Speed of Peak North-west-going Currents in a Neap tide (Layout B-OSP1 – Baseline)

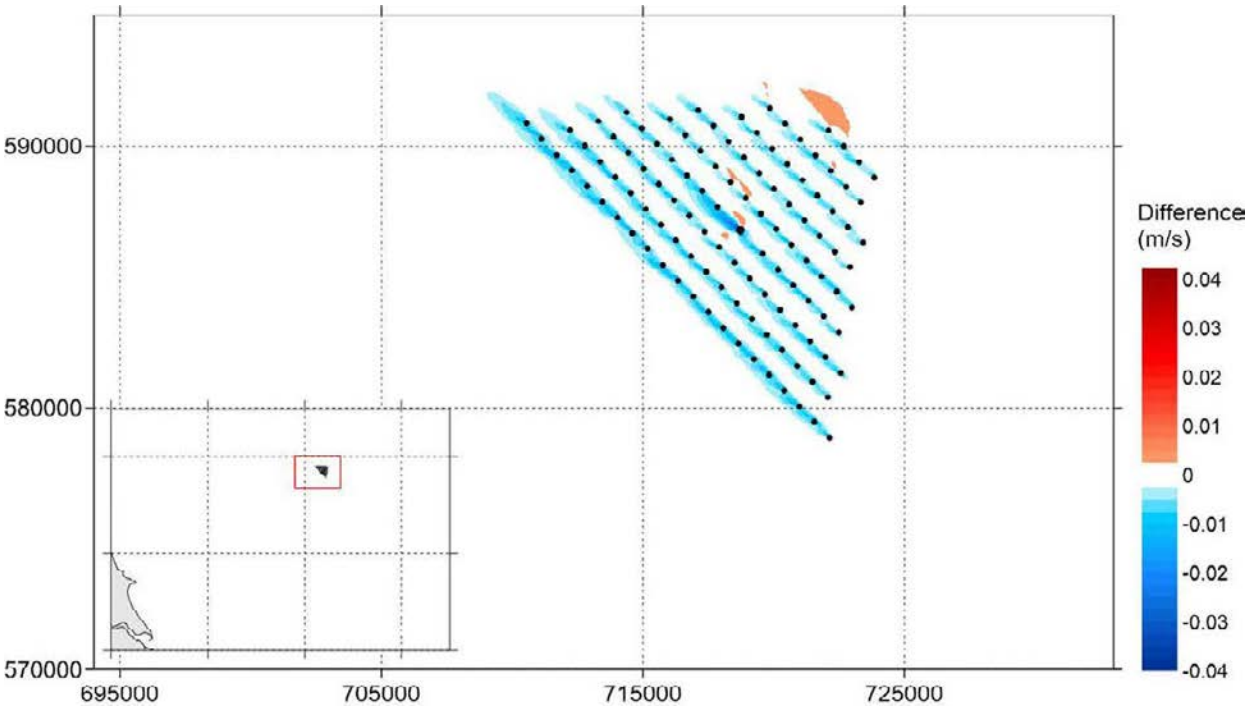

Figure A.150 Change of Maximum Current Speed Over 30 days (Layout B-OSP1 – Baseline)

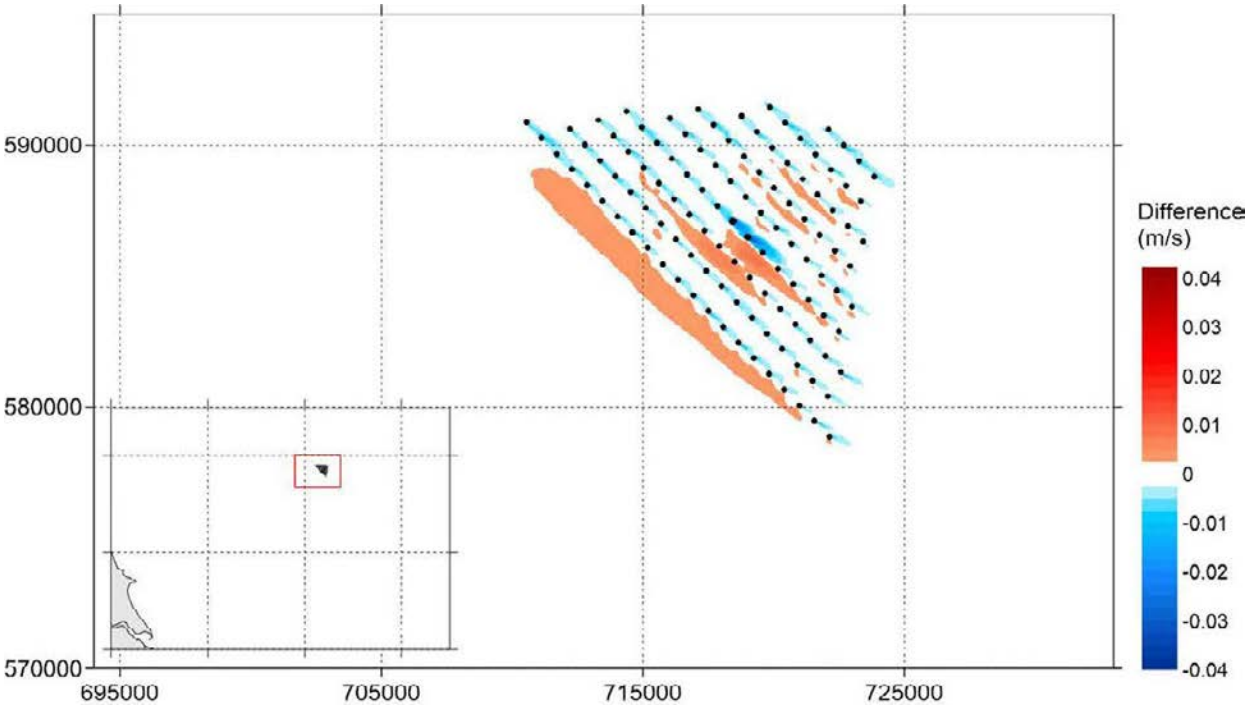

Figure A.151 Change of Speed of Peak South-east-going Currents in a Spring Tide (Layout B-OSP2 – Baseline)

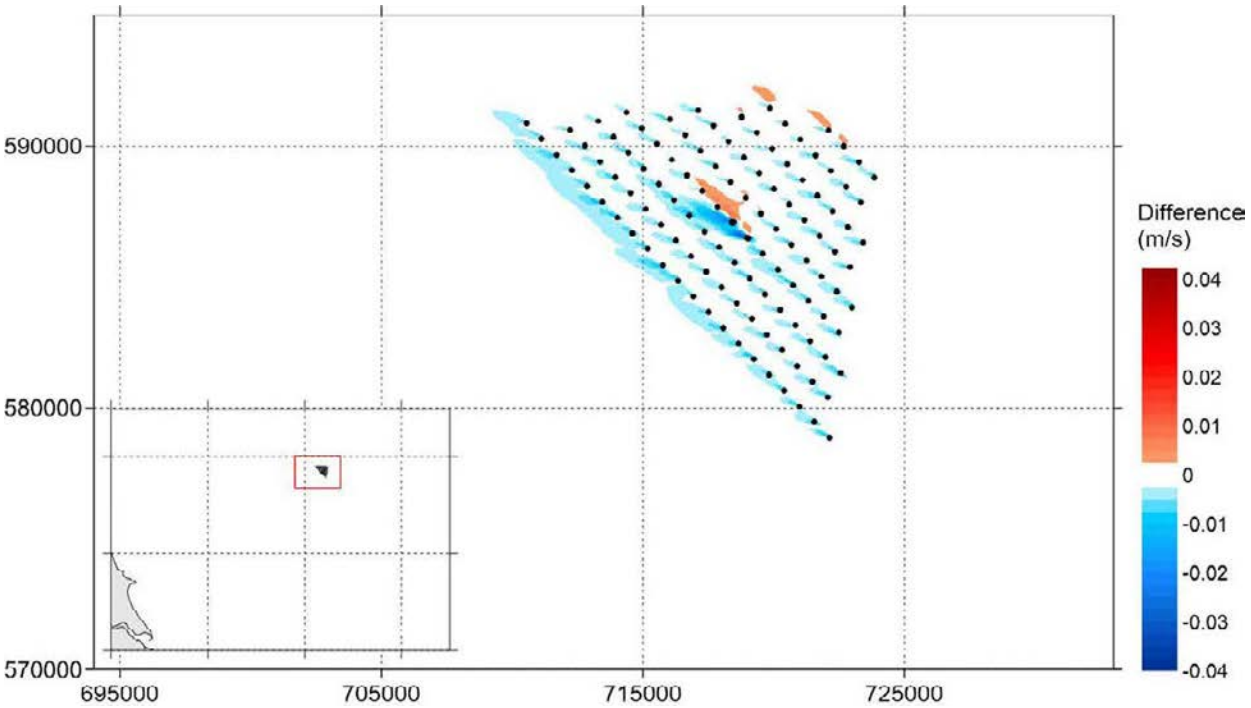

Figure A.152 Change of Speed of Peak North-west-going Currents in a Spring Tide (Layout B-OSP2 – Baseline)

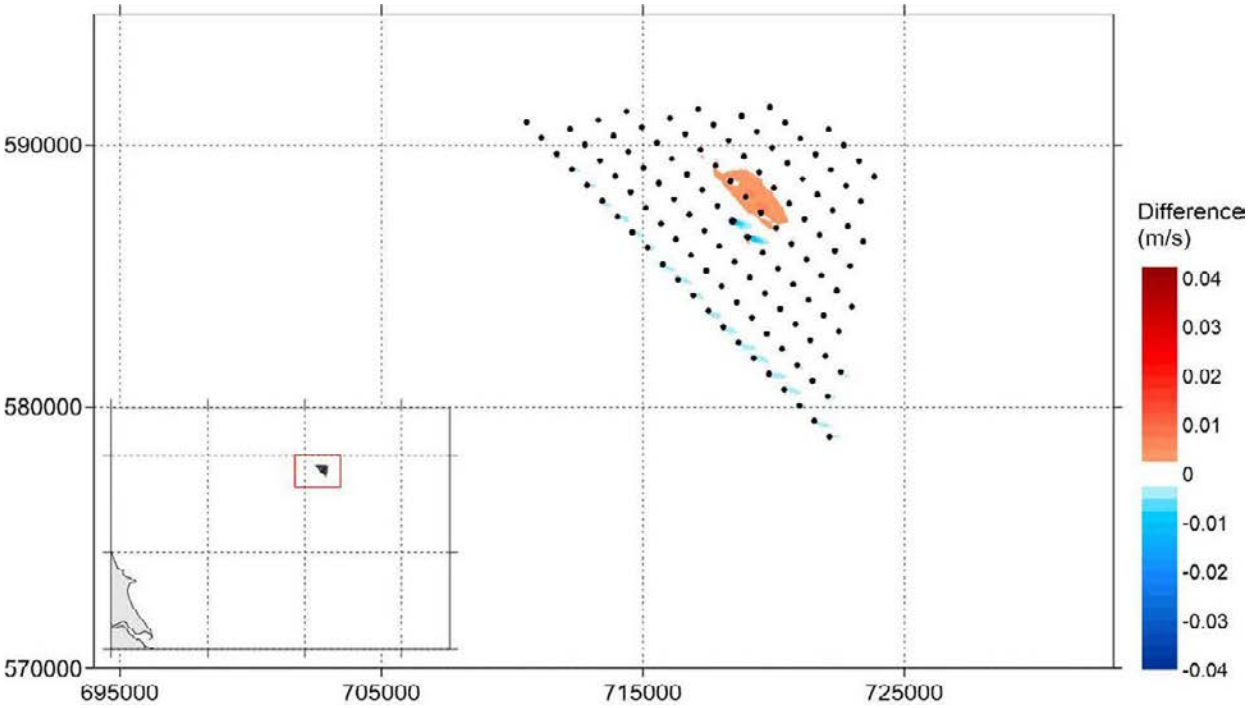

Figure A.153 Change of Speed of Peak South-east-going Currents in a Neap tide (Layout B-OSP2 – Baseline)

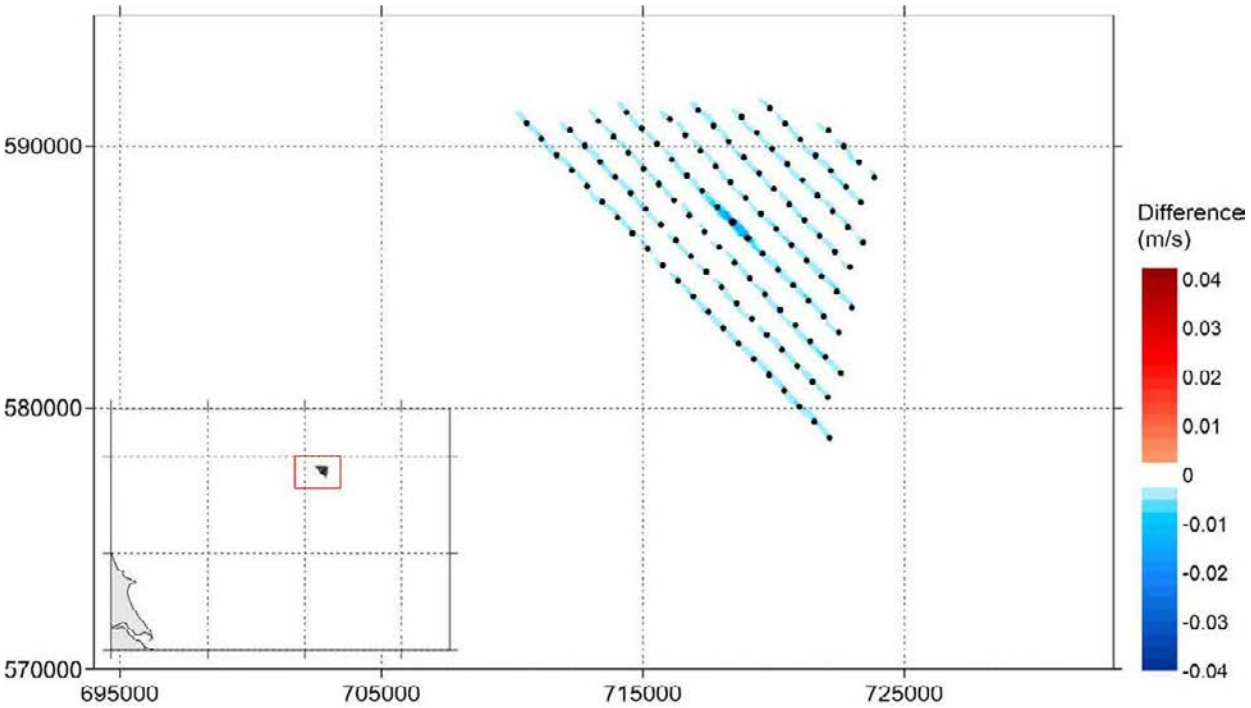

Figure A.154 Change of Speed of Peak North-west-going Currents in a Neap tide (Layout B-OSP2 – Baseline)

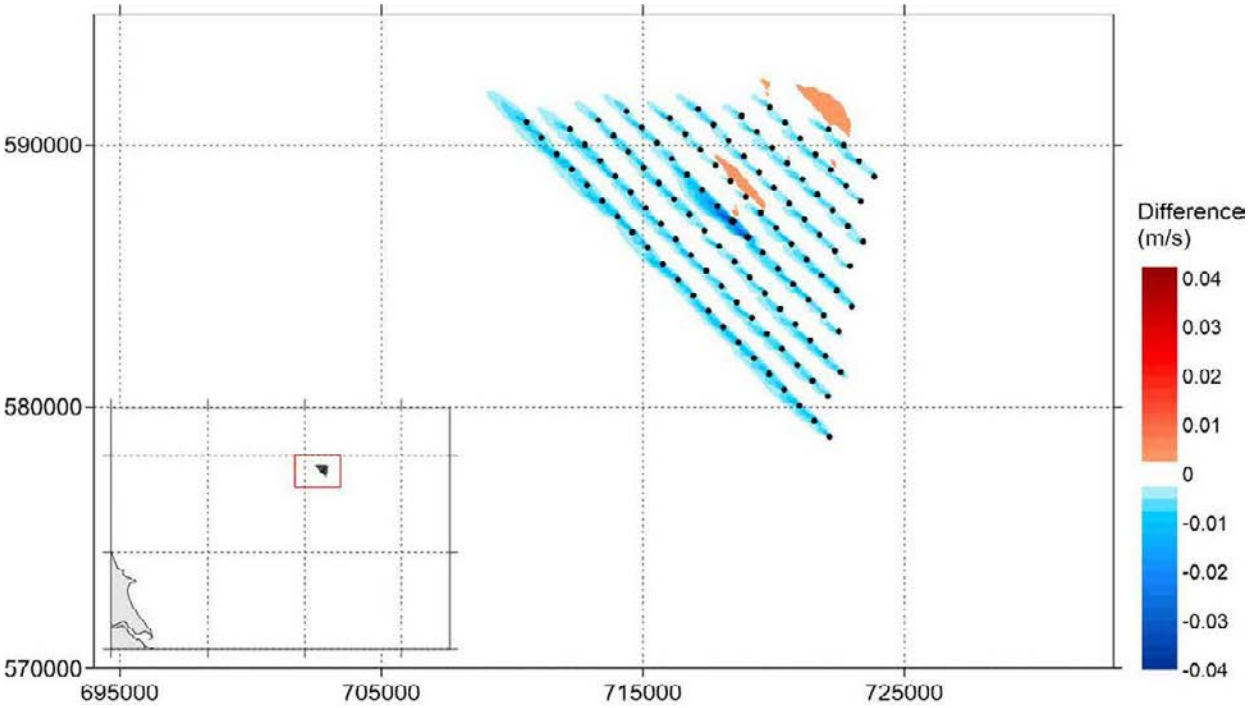

Figure A.155 Change of Maximum Current Speed Over 30 days (Layout B-OSP2 – Baseline)

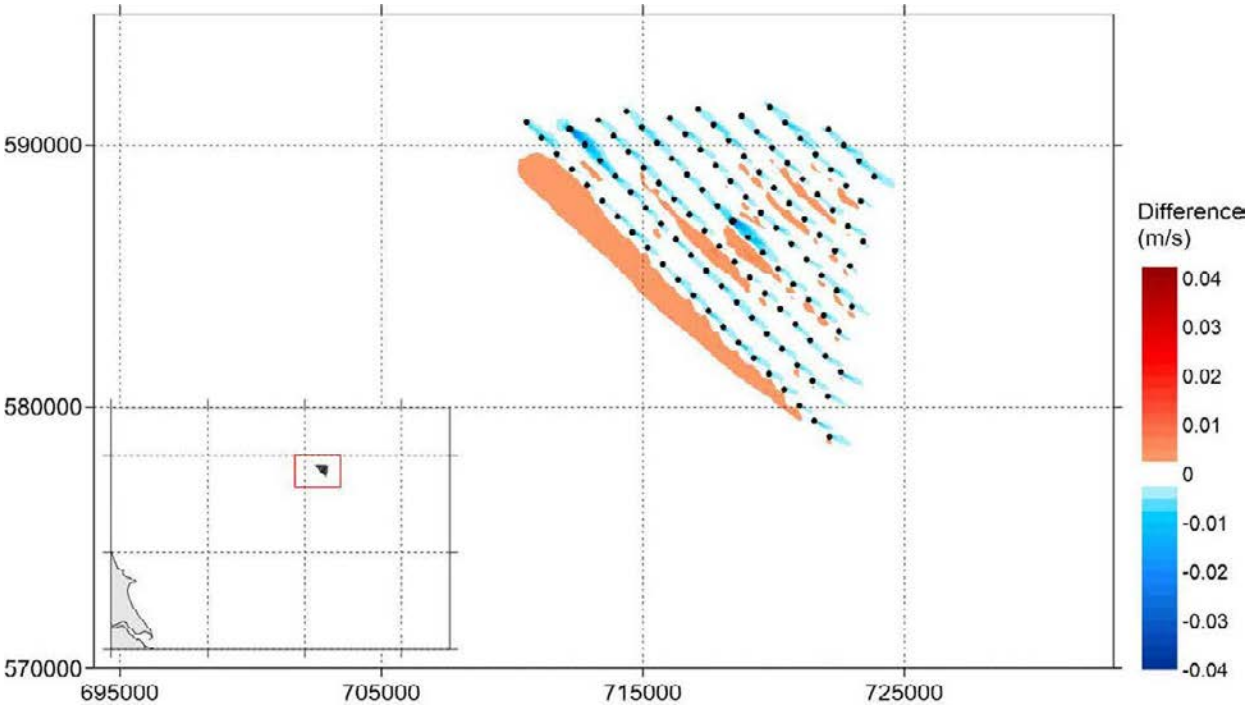

Figure A.156 Change of Speed of Peak South-east-going Currents in a Spring Tide (Layout B-OSP3 – Baseline)

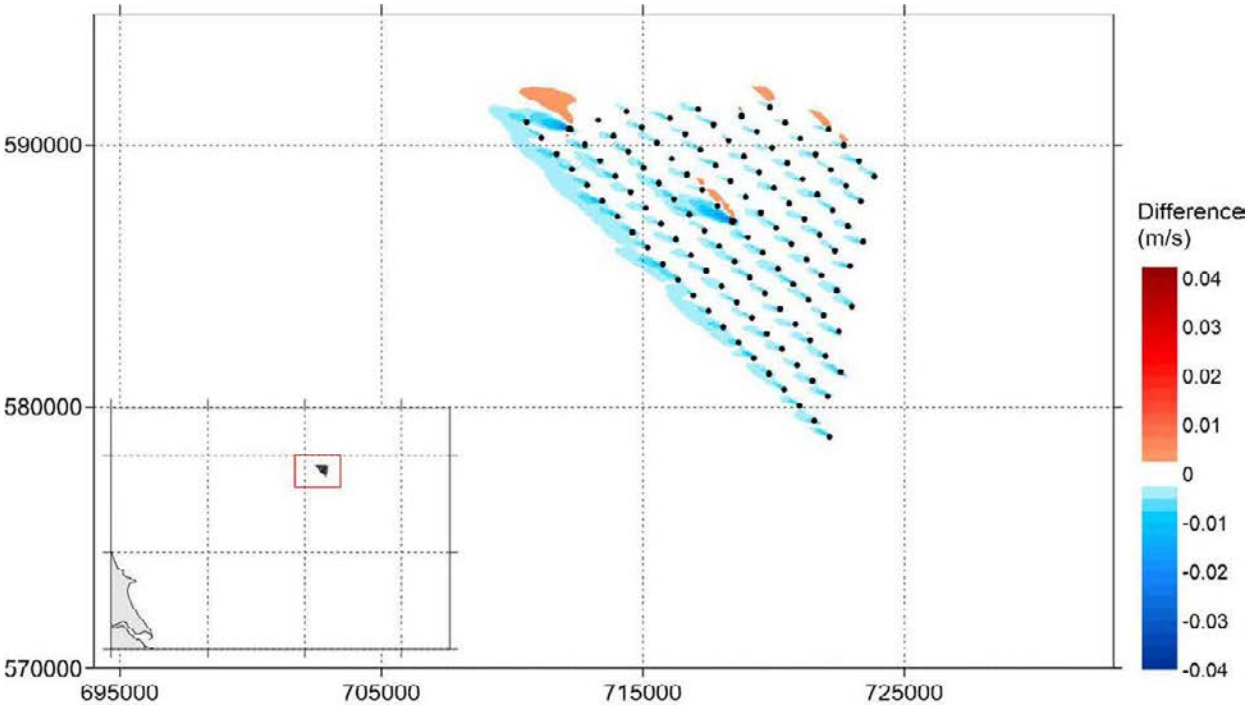

Figure A.157 Change of Speed of Peak North-west-going Currents in a Spring Tide (Layout B-OSP3 – Baseline)

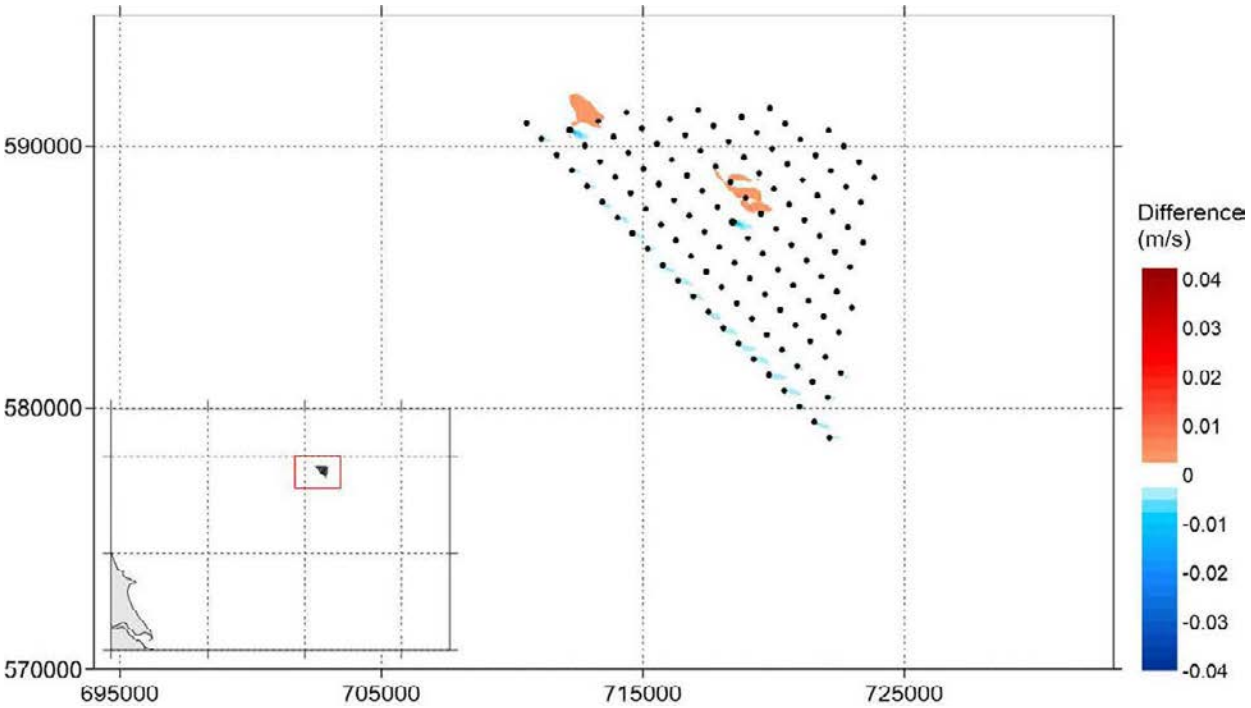

Figure A.158 Change of Speed of Peak South-east-going Currents in a Neap tide (Layout B-OSP3 – Baseline)

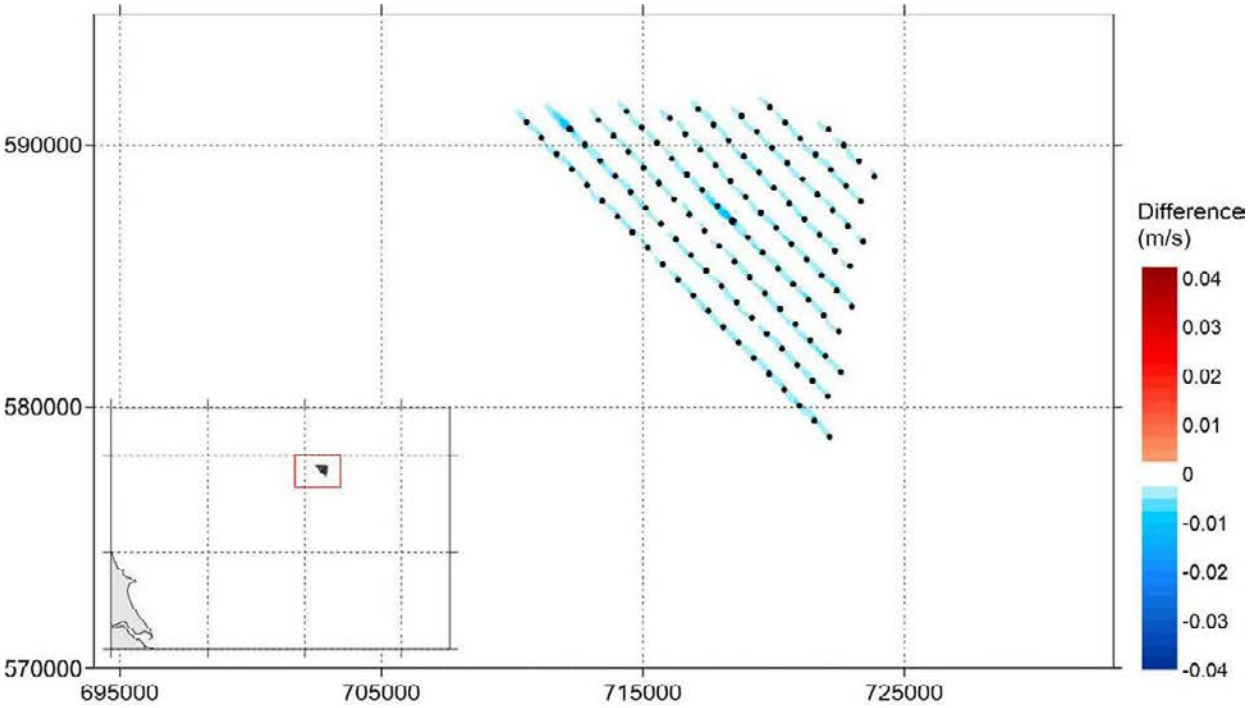

Figure A.159 Change of Speed of Peak North-west-going Currents in a Neap tide (Layout B-OSP3 – Baseline)

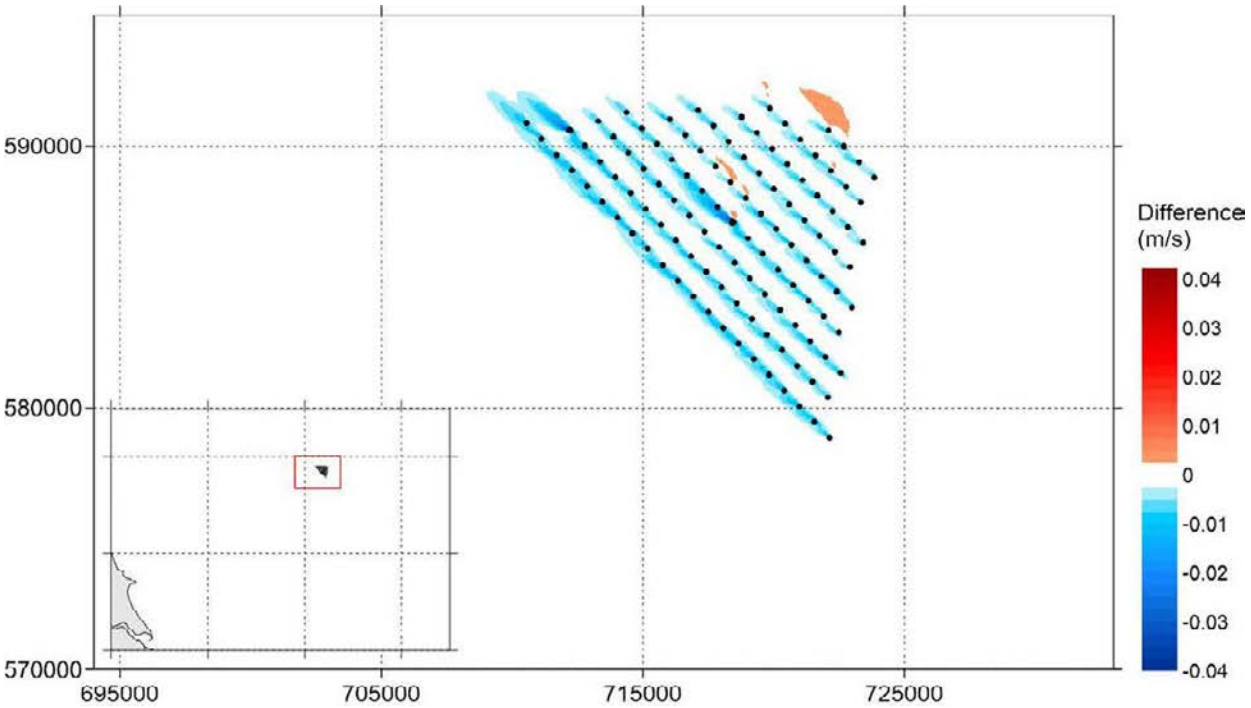

Figure A.160 Change of Maximum Current Speed Over 30 days (Layout B-OSP3 – Baseline)

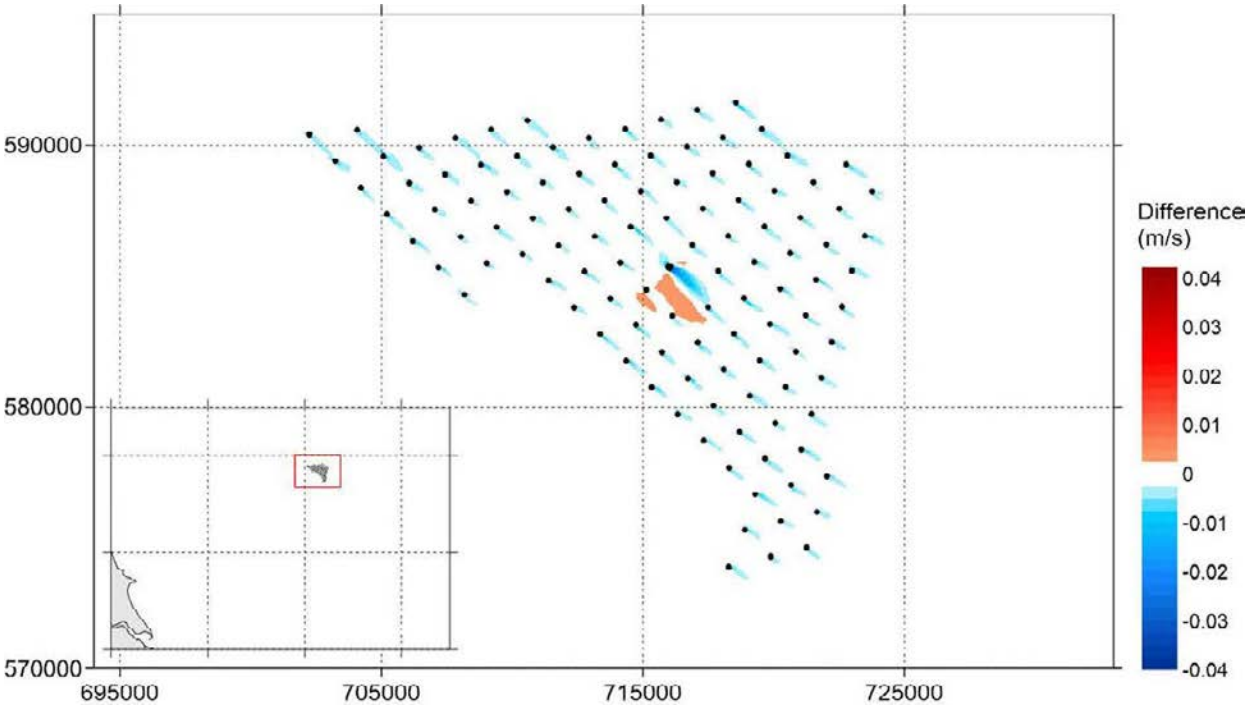

Figure A.161 Change of Speed of Peak South-east-going Currents in a Spring Tide (Layout C-OSP1 – Baseline)

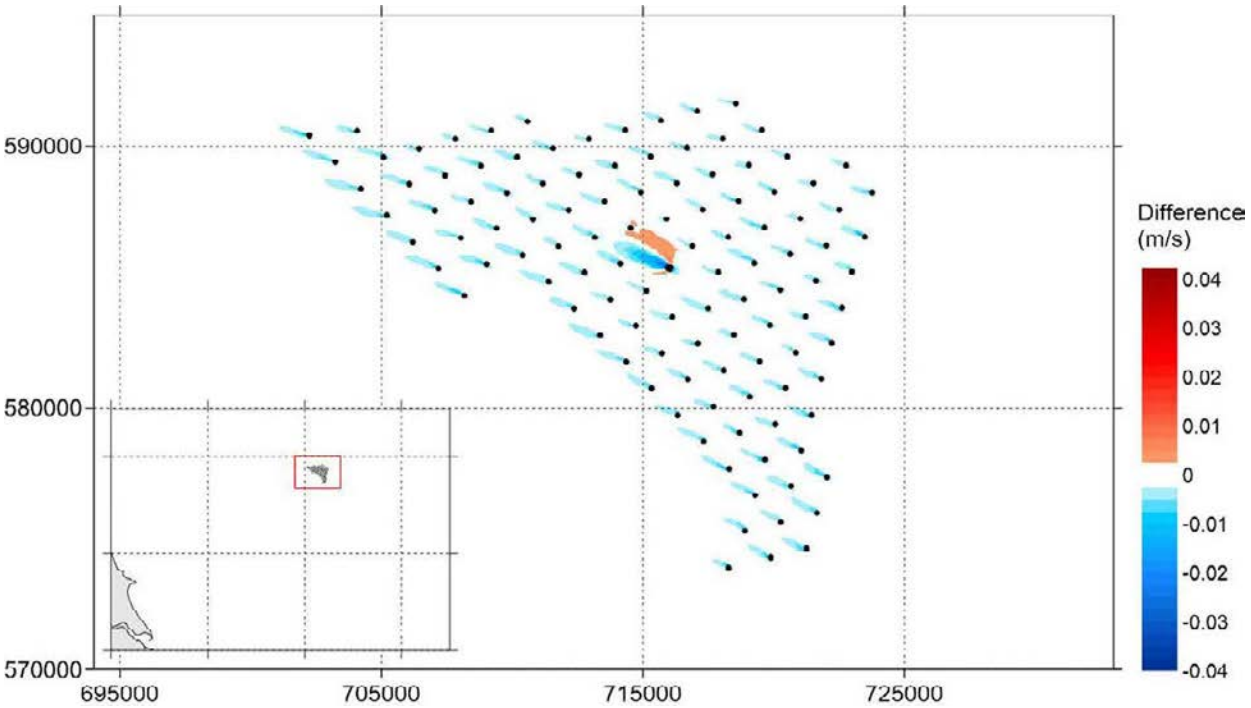

Figure A.162 Change of Speed of Peak North-west-going Currents in a Spring Tide (Layout C-OSP1 – Baseline)

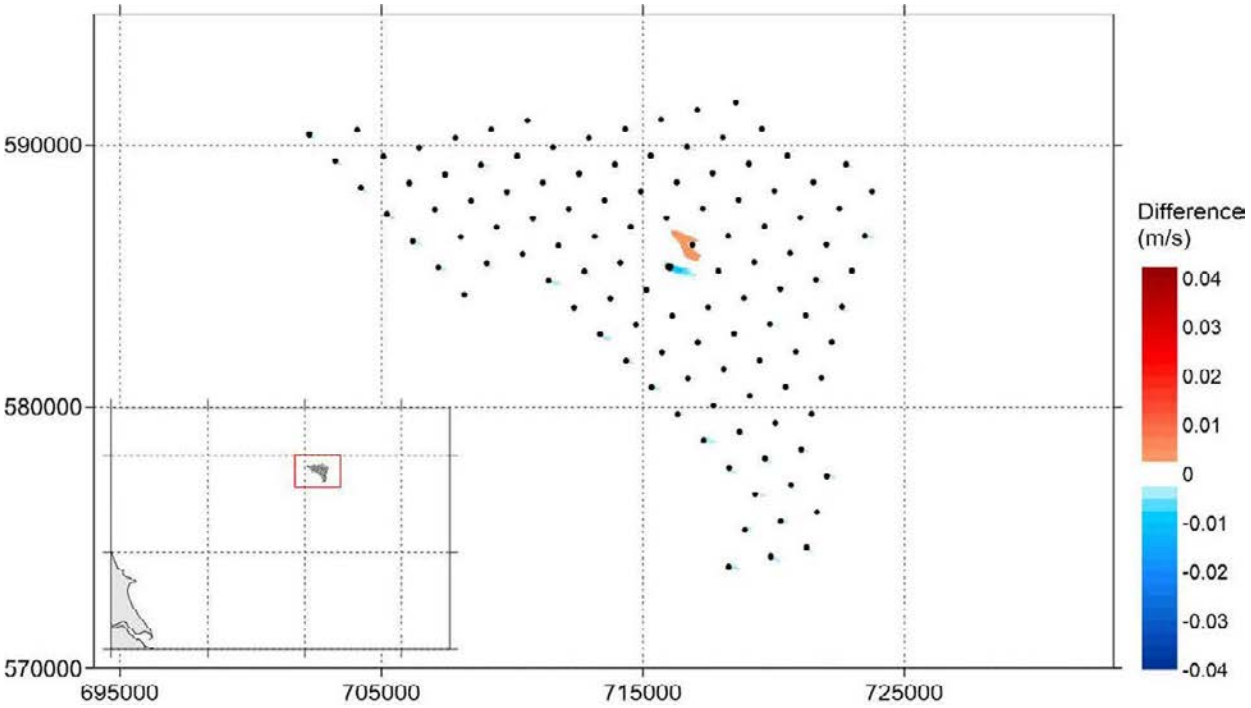

Figure A.163 Change of Speed of Peak South-east-going Currents in a Neap tide (Layout C-OSP1 – Baseline)

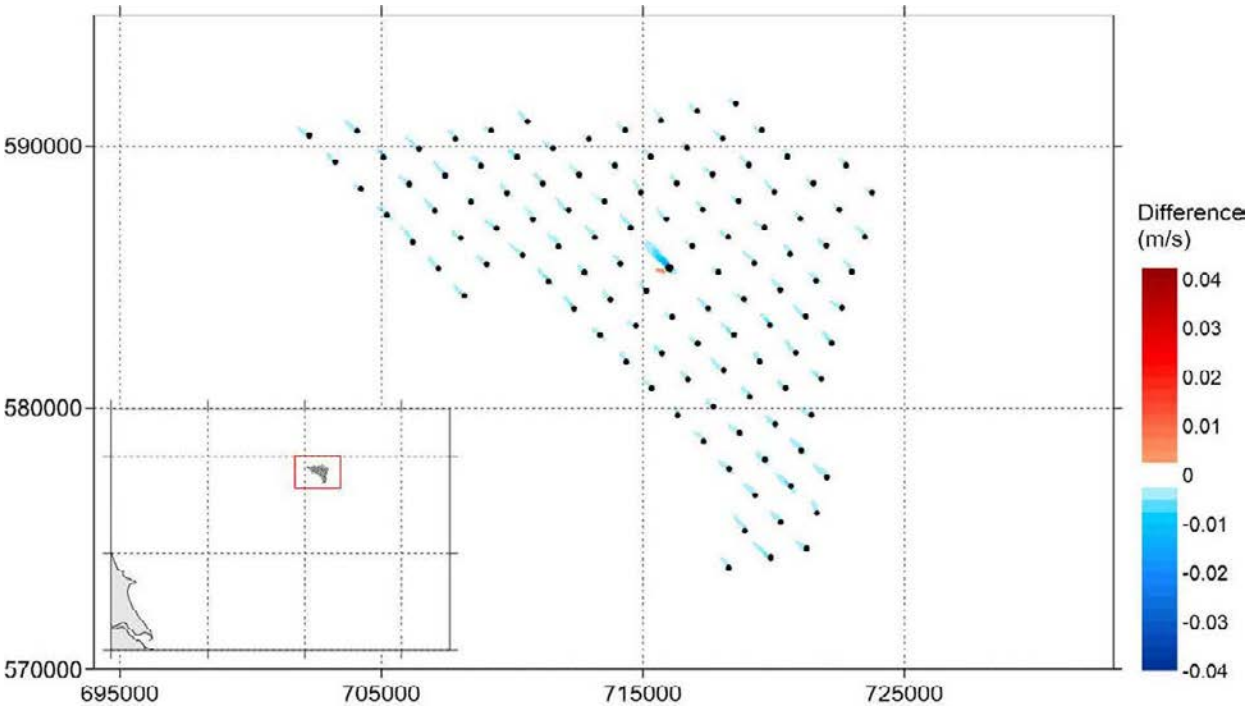

Figure A.164 Change of Speed of Peak North-west-going Currents in a Neap tide (Layout C-OSP1 – Baseline)

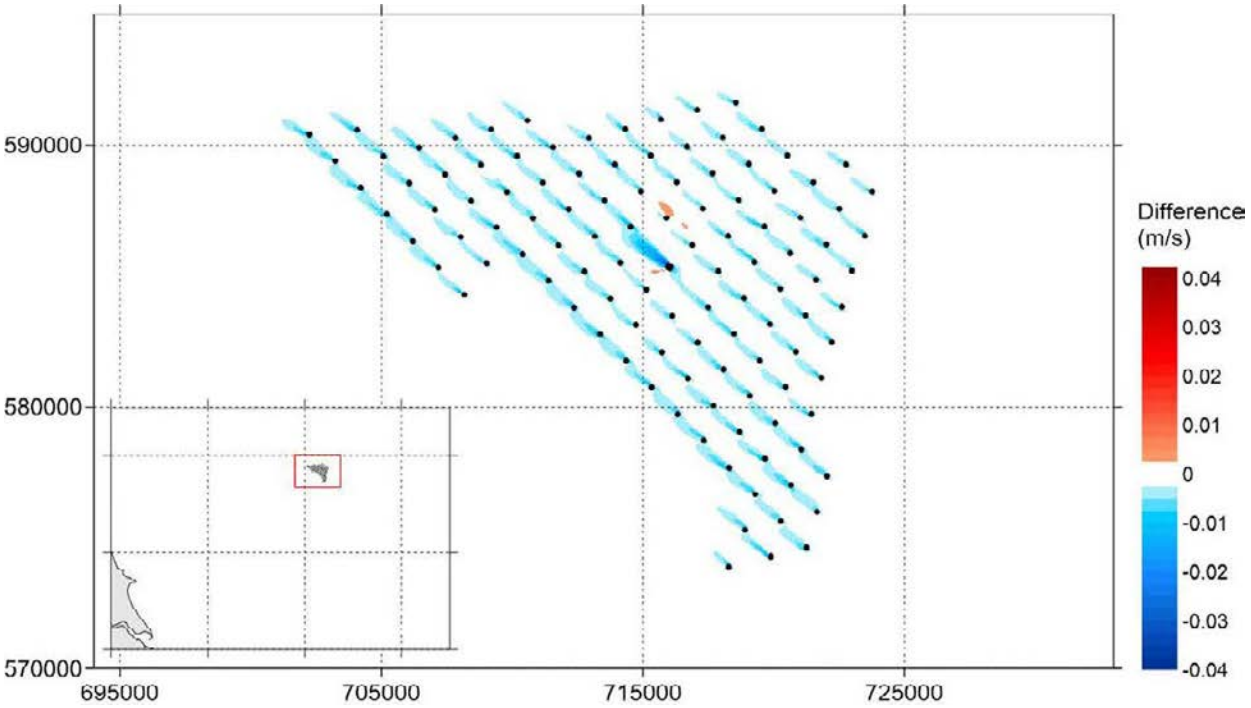

Figure A.165 Change of Maximum Current Speed Over 30 days (Layout C-OSP1 – Baseline)

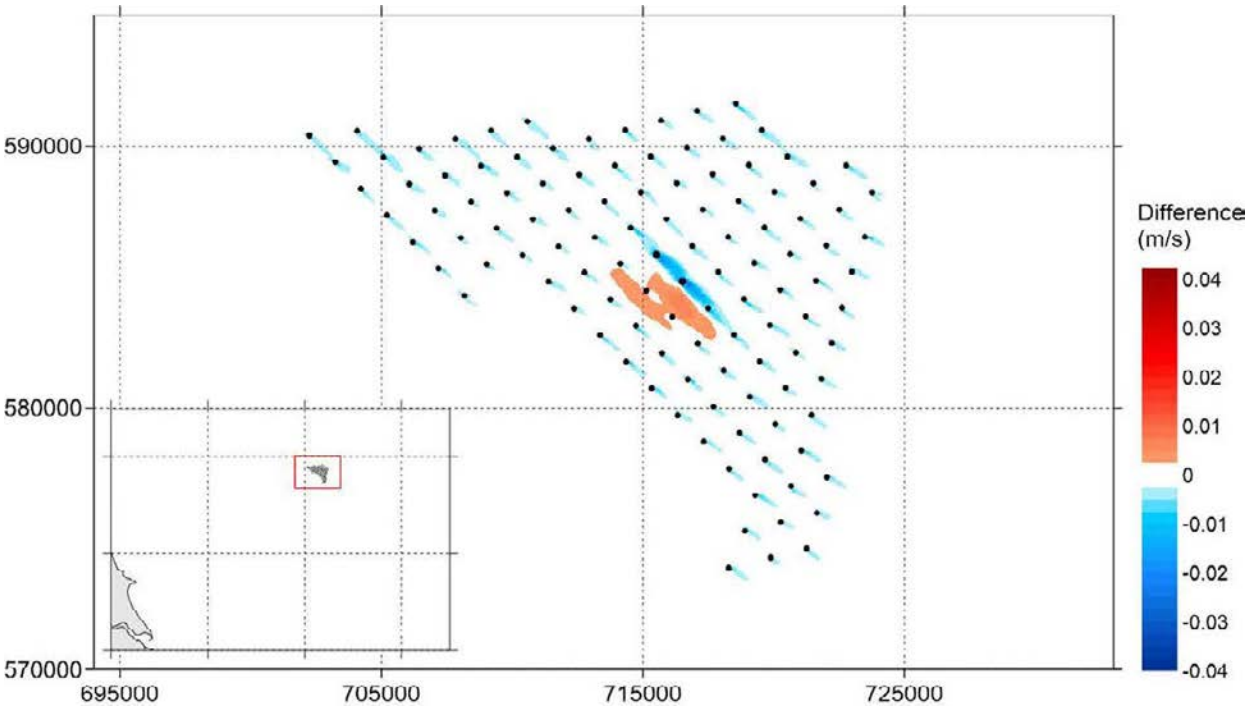

Figure A.166 Change of Speed of Peak South-east-going Currents in a Spring Tide (Layout C-OSP2 – Baseline)

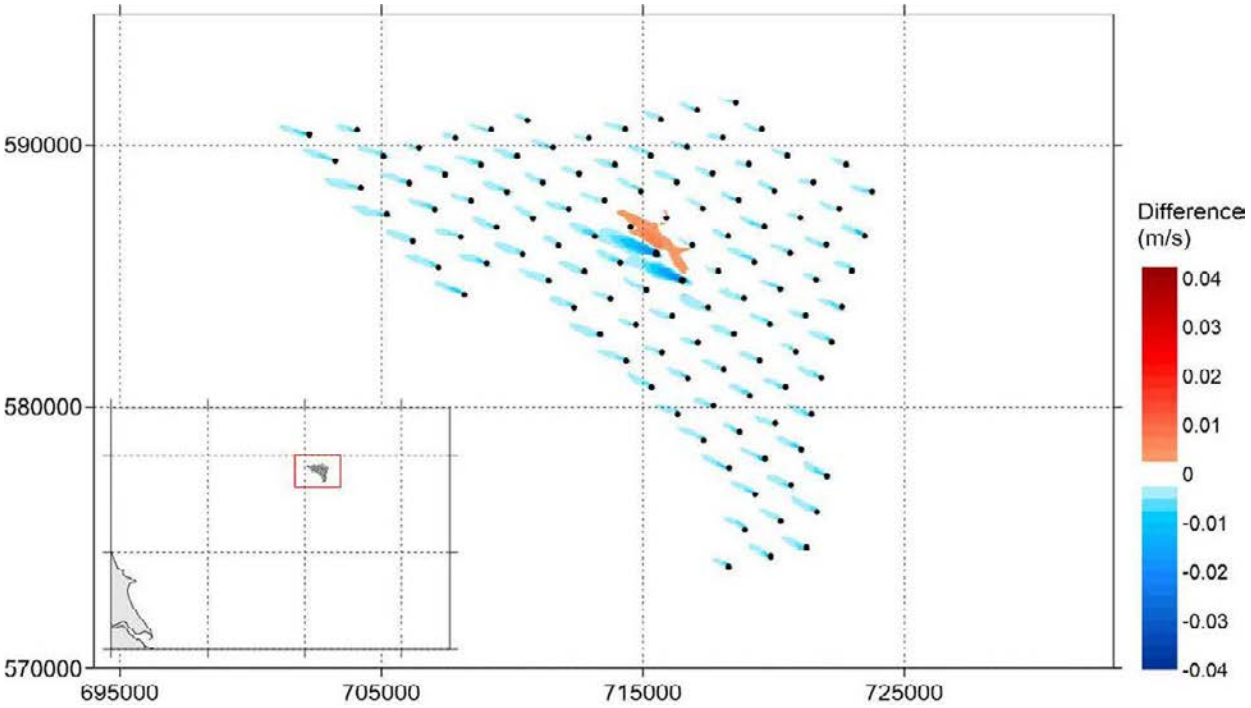

Figure A.167 Change of Speed of Peak North-west-going Currents in a Spring Tide (Layout C-OSP2 – Baseline)

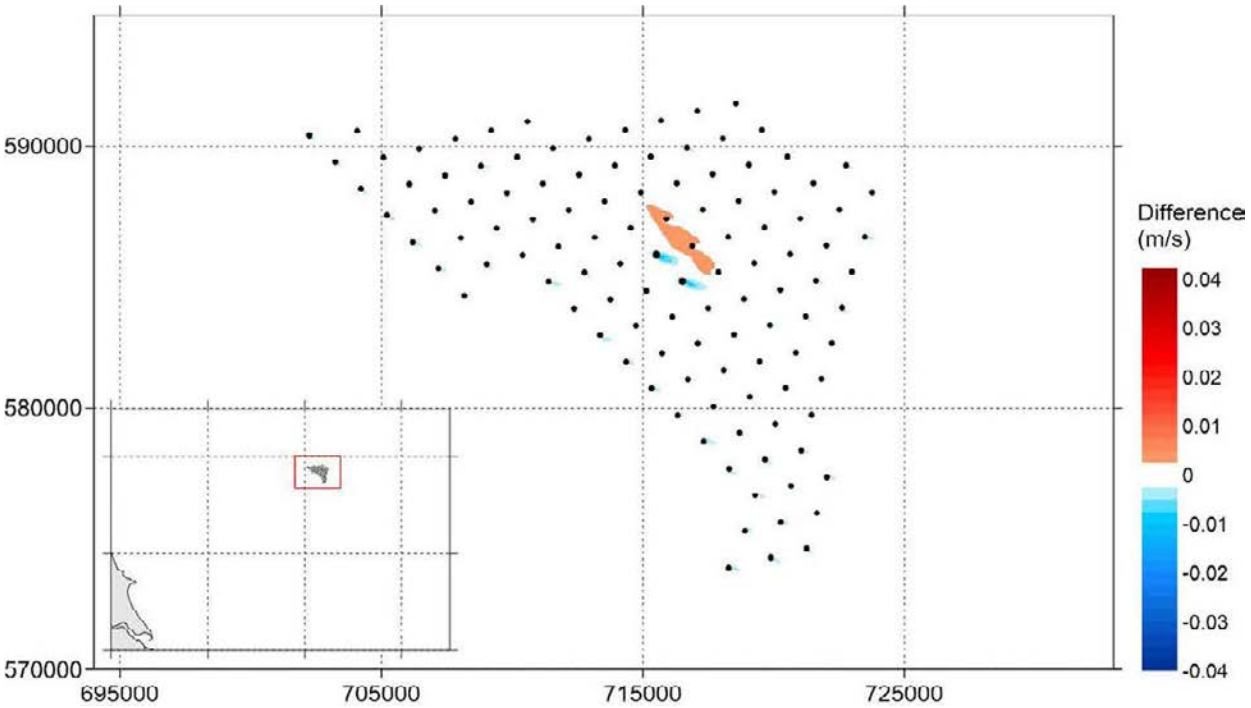

Figure A.168 Change of Speed of Peak South-east-going Currents in a Neap tide (Layout C-OSP2 – Baseline)

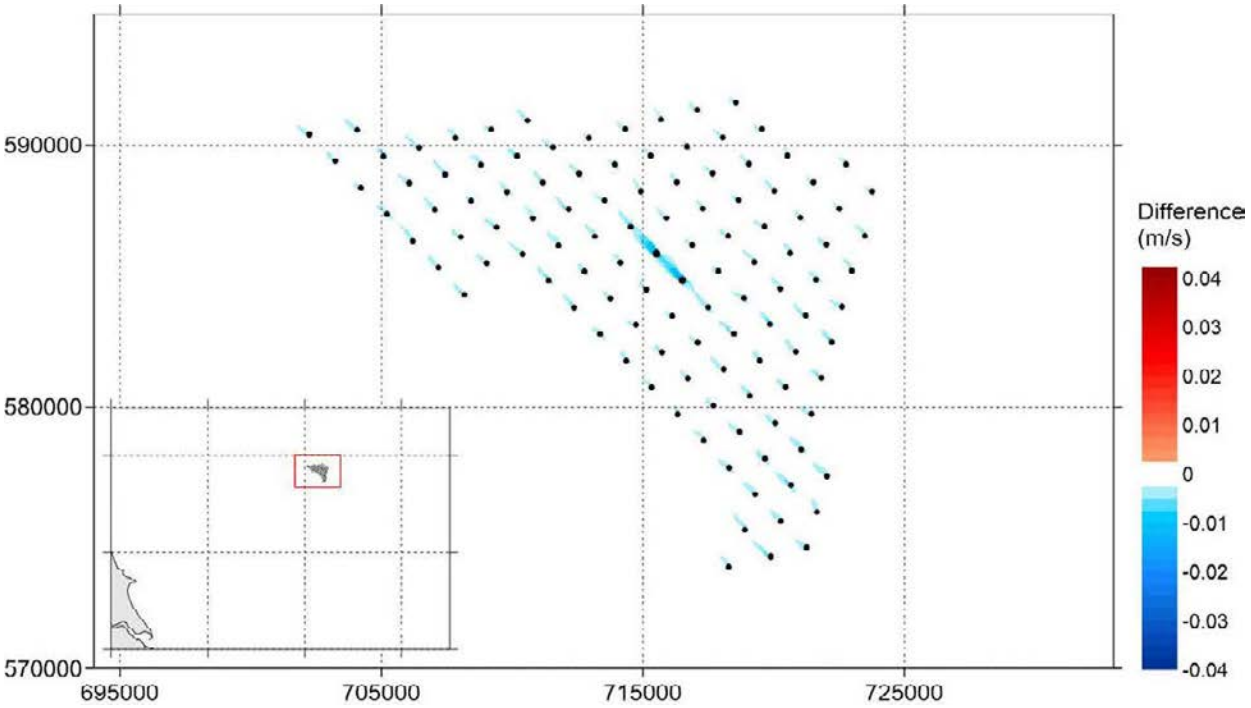

Figure A.169 Change of Speed of Peak North-west-going Currents in a Neap tide (Layout C-OSP2 – Baseline)

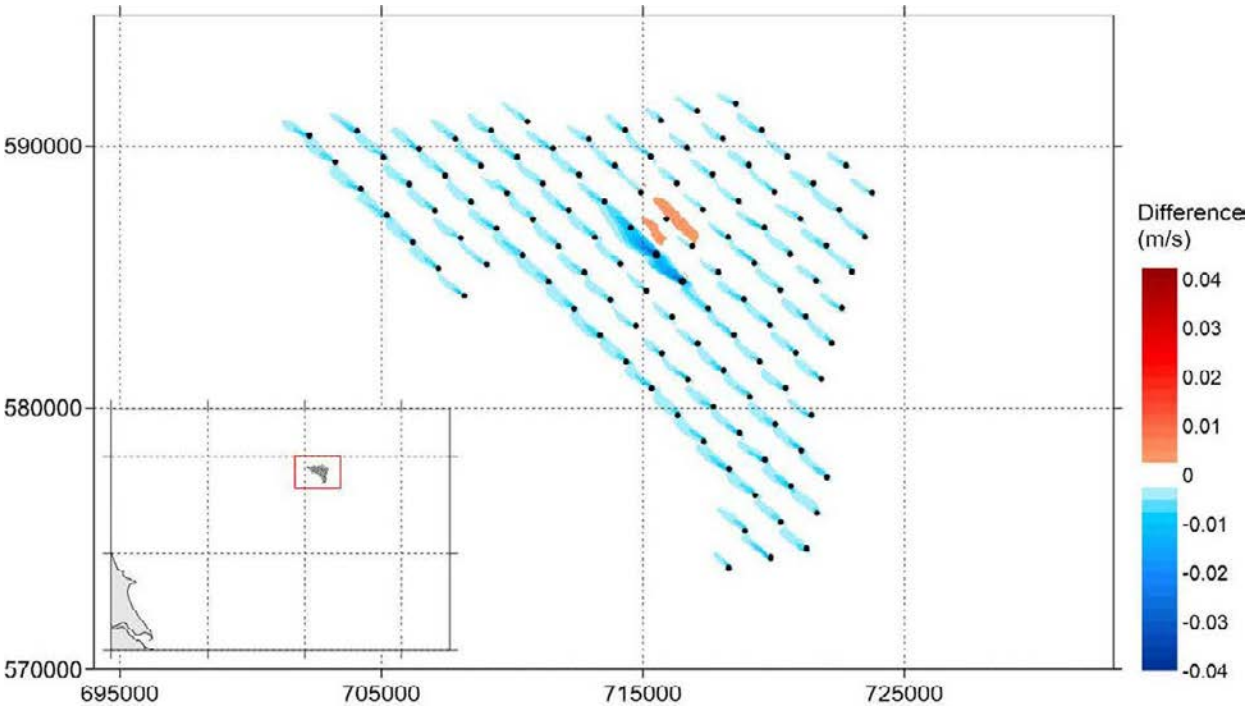

Figure A.170 Change of Maximum Current Speed Over 30 days (Layout C-OSP2 – Baseline)

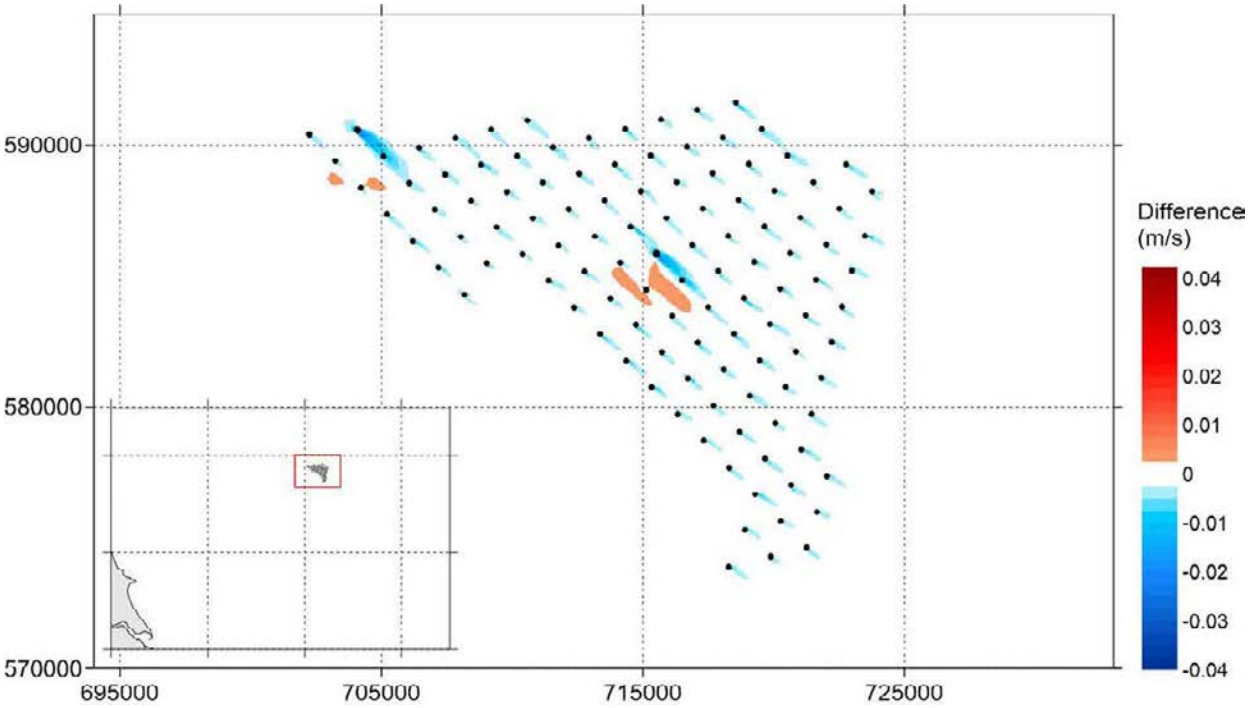

Figure A.171 Change of Speed of Peak South-east-going Currents in a Spring Tide (Layout C-OSP3 – Baseline)

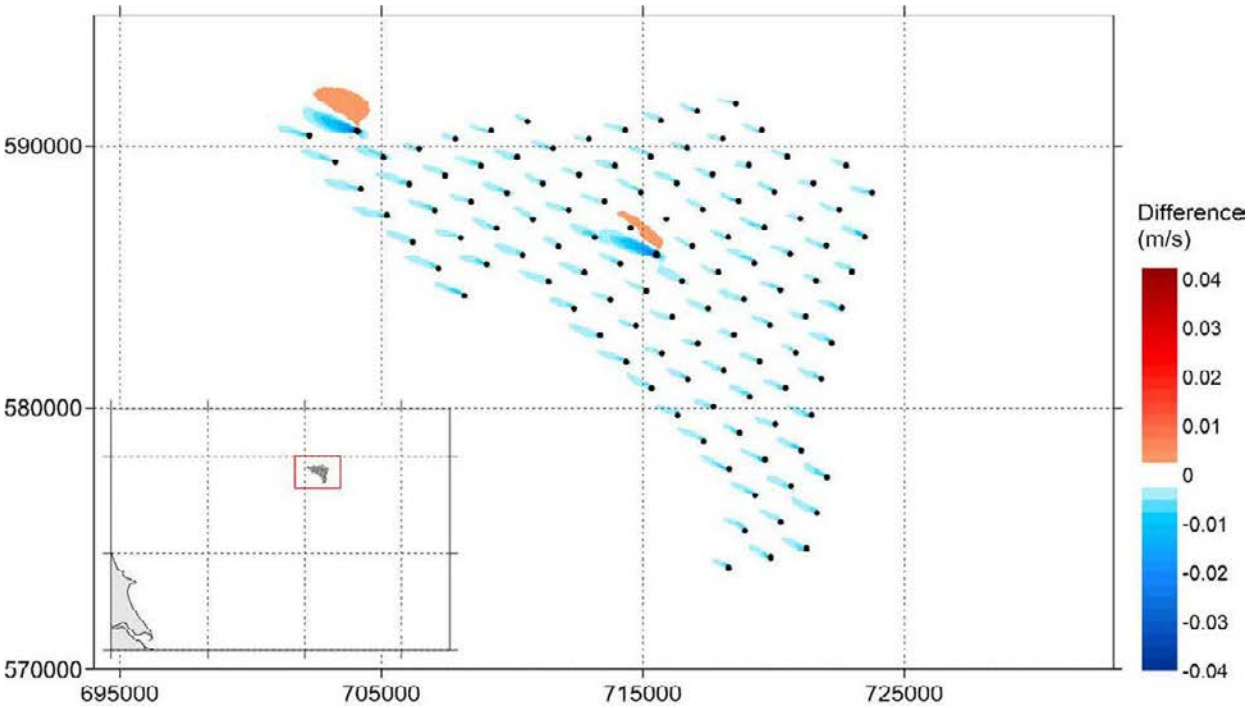

Figure A.172 Change of Speed of Peak North-west-going Currents in a Spring Tide (Layout C-OSP3 – Baseline)

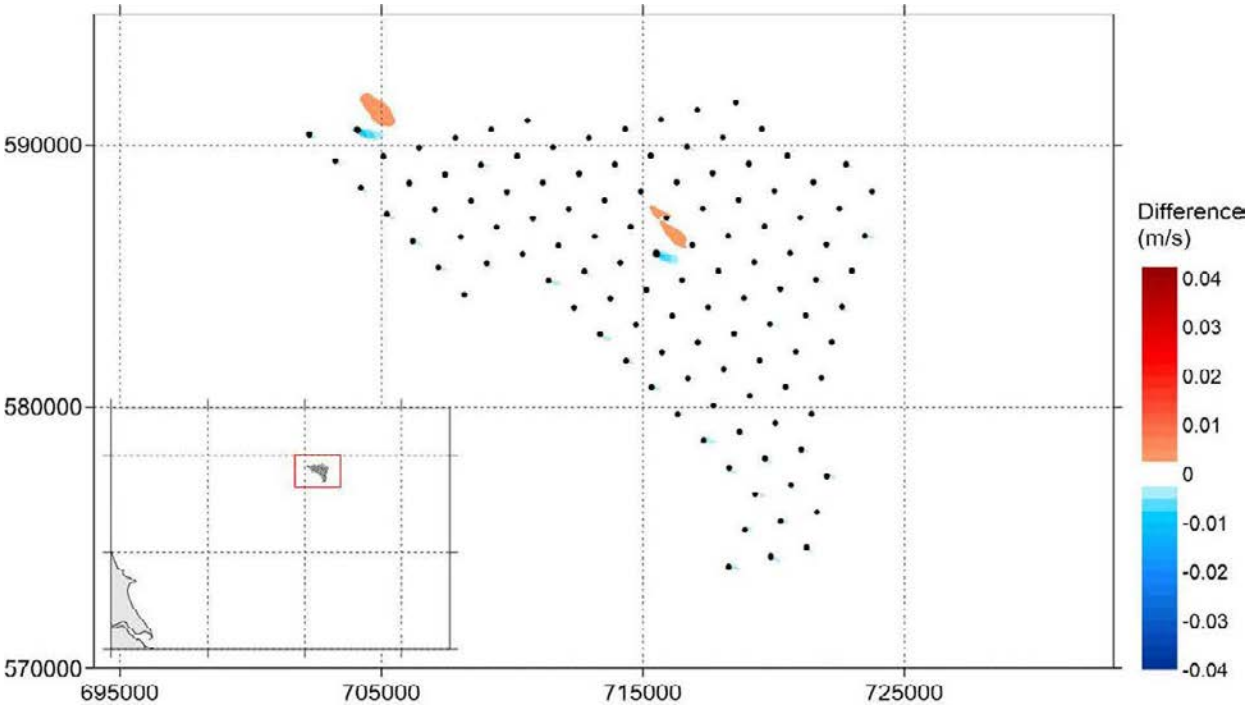

Figure A.173 Change of Speed of Peak South-east-going Currents in a Neap tide (Layout C-OSP3 – Baseline)

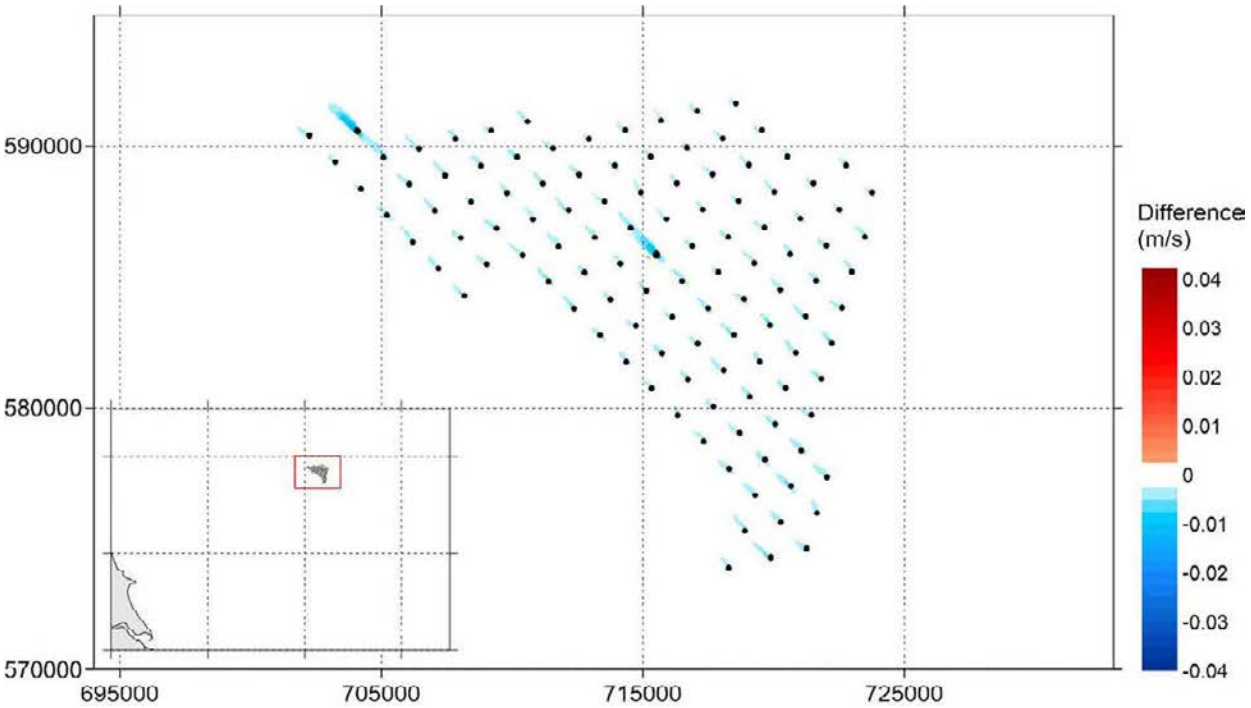

Figure A.174 Change of Speed of Peak North-west-going Currents in a Neap tide (Layout C-OSP3 – Baseline)

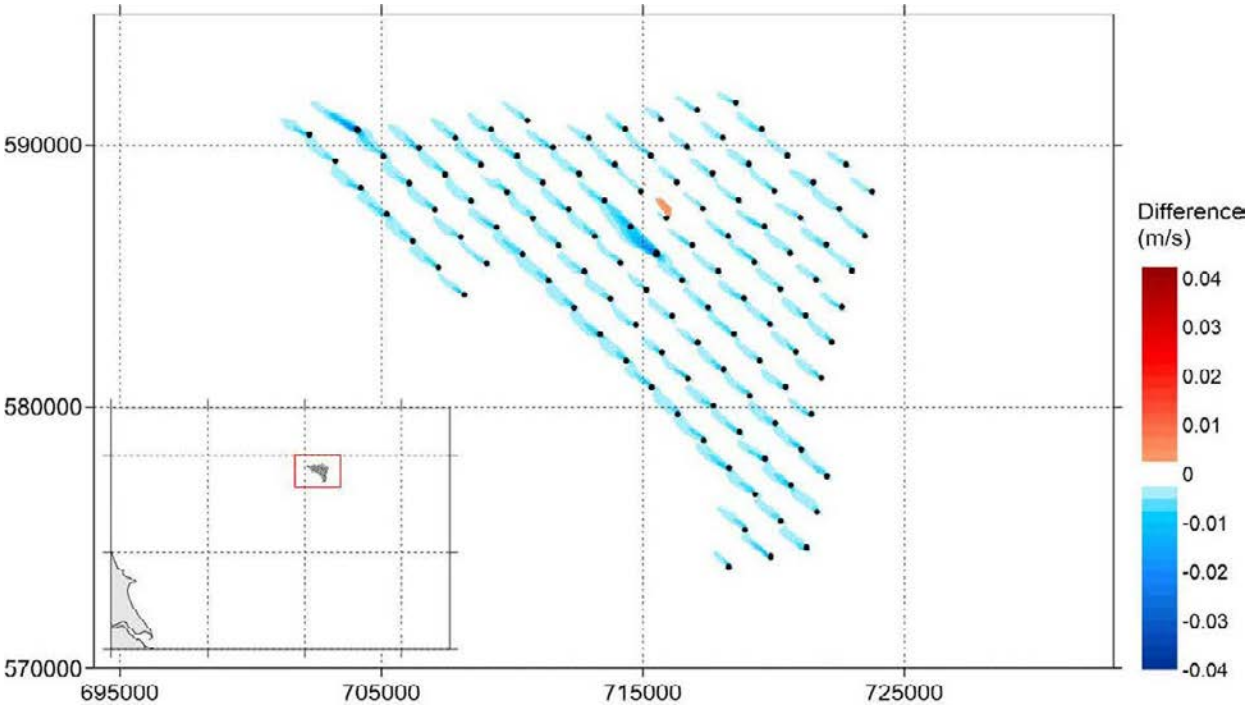

Figure A.175 Change of Maximum Current Speed Over 30 days (Layout C-OSP3 – Baseline)

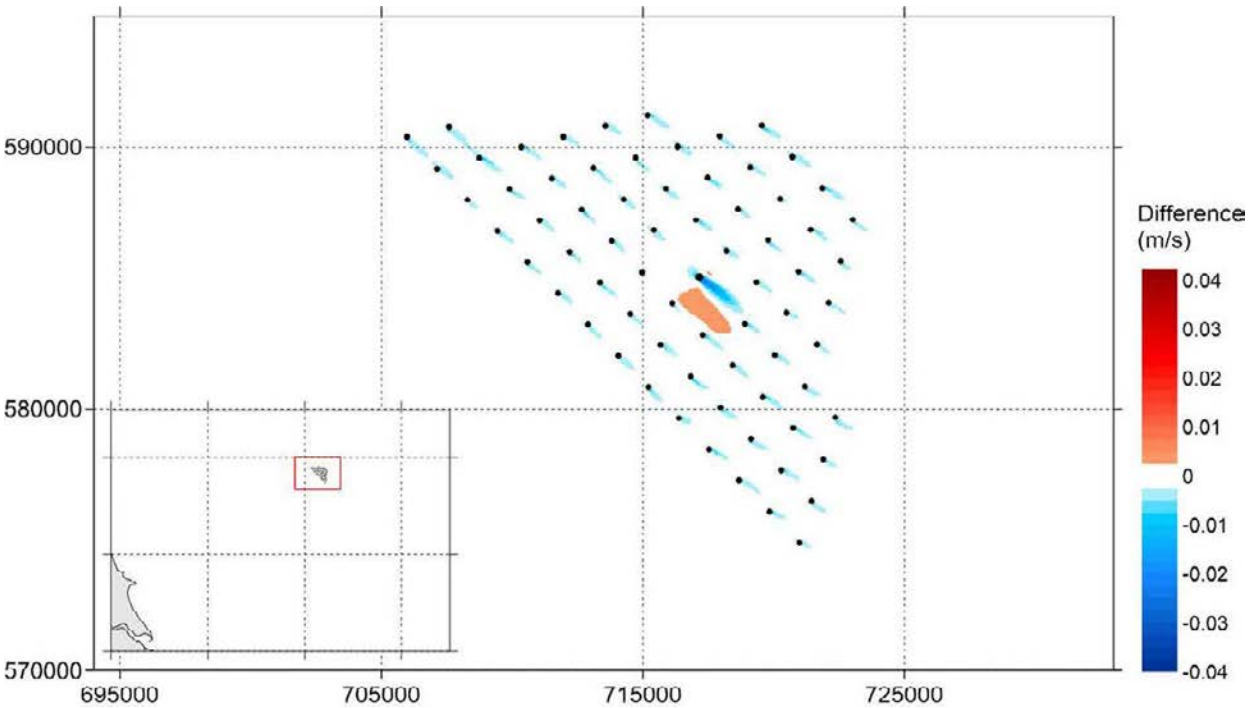

Figure A.176 Change of Speed of Peak South-east-going Currents in a Spring Tide (Layout D-OSP1 – Baseline)

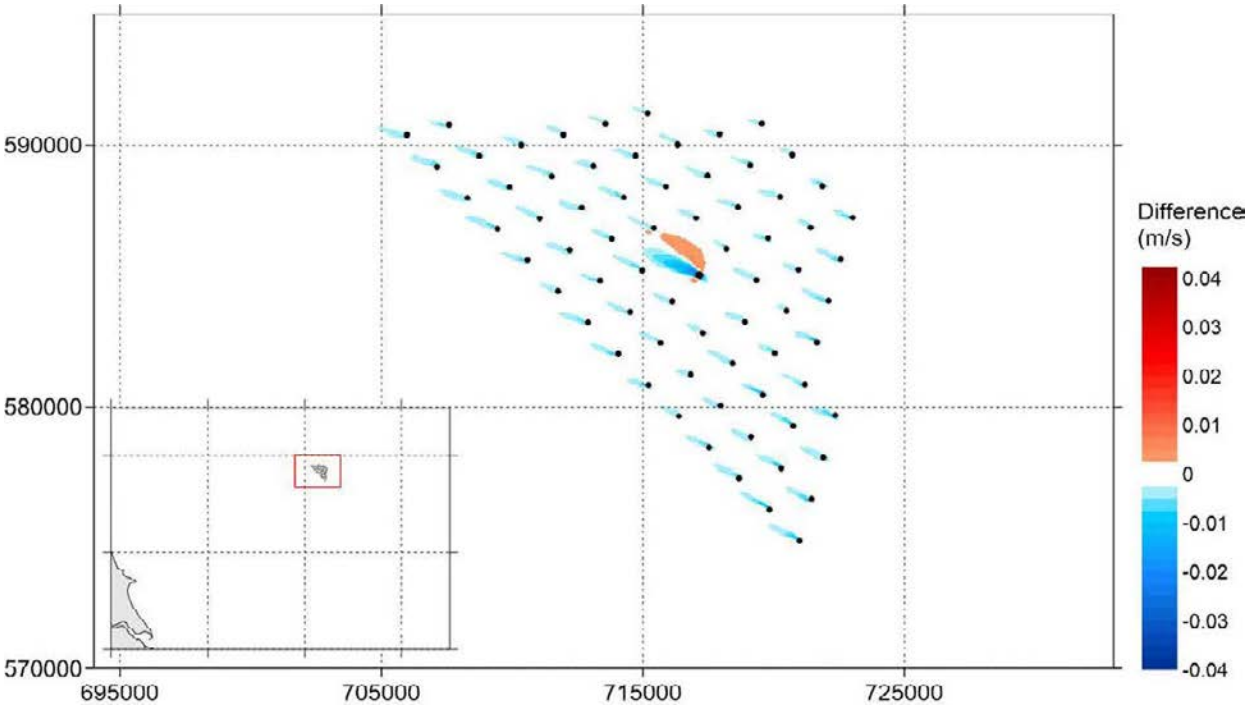

Figure A.177 Change of Speed of Peak North-west-going Currents in a Spring Tide (Layout D-OSP1 – Baseline)

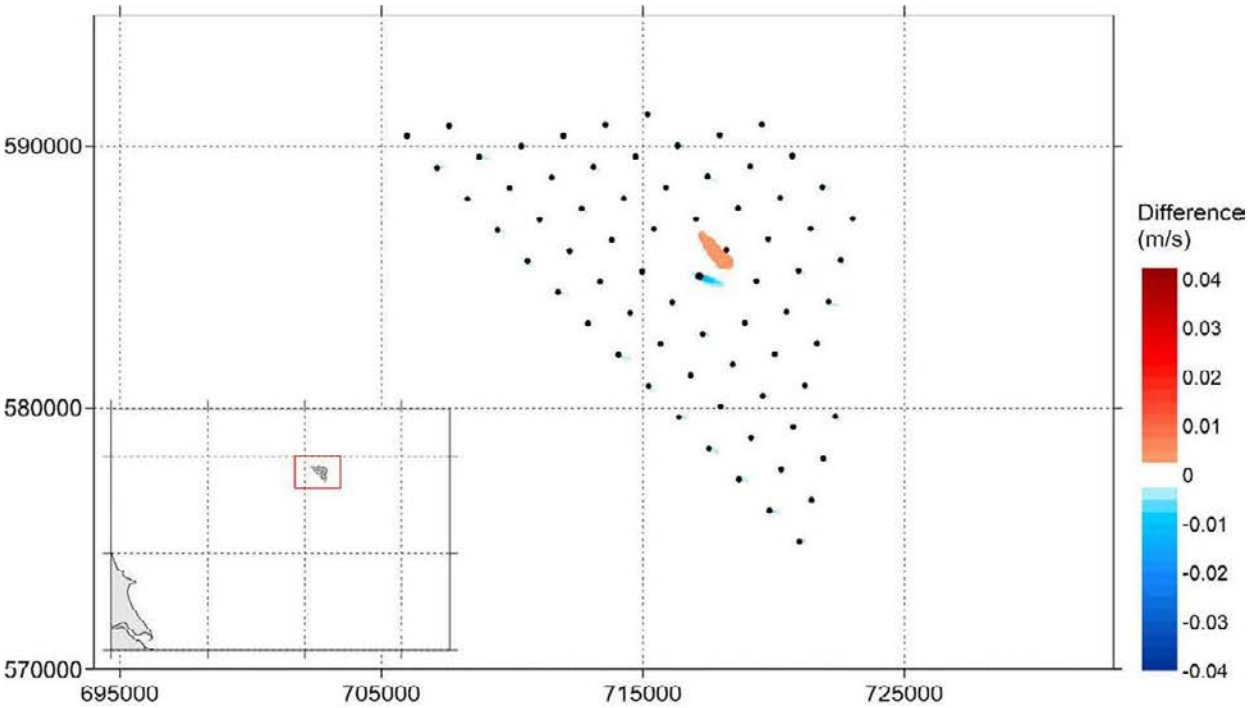

Figure A.178 Change of Speed of Peak South-east-going Currents in a Neap tide (Layout D-OSP1 – Baseline)

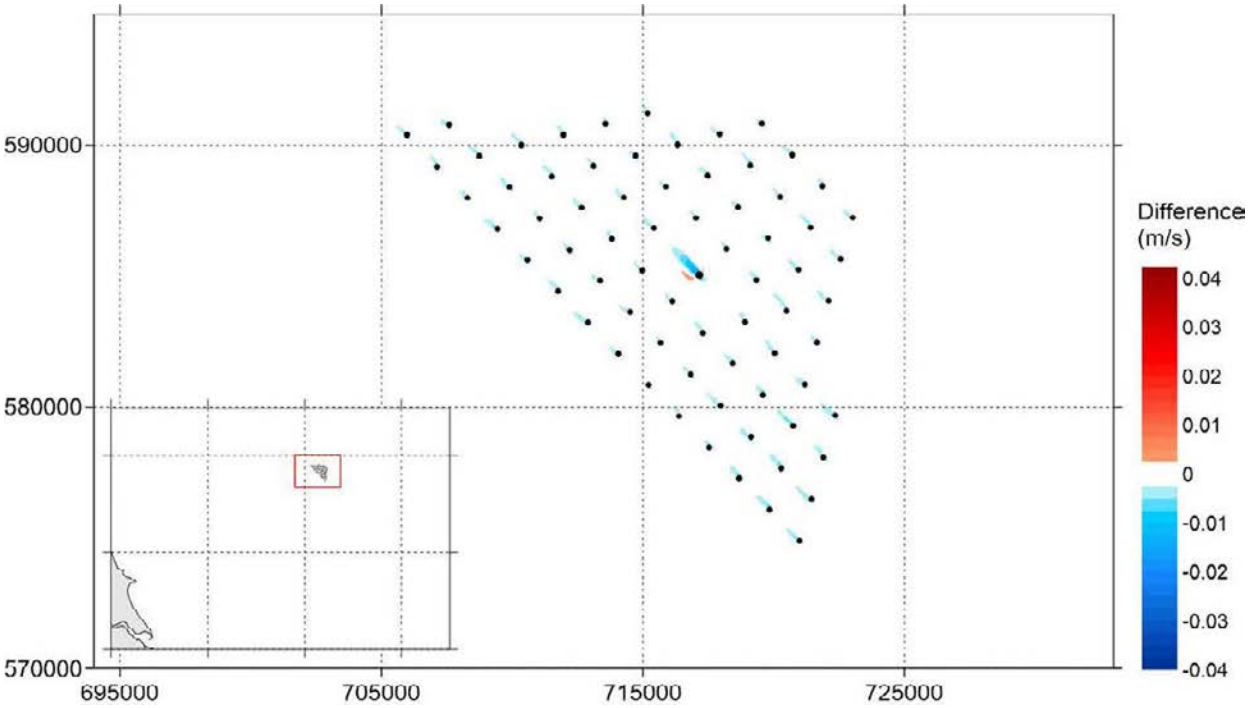

Figure A.179 Change of Speed of Peak North-west-going Currents in a Neap tide (Layout D-OSP1 – Baseline)

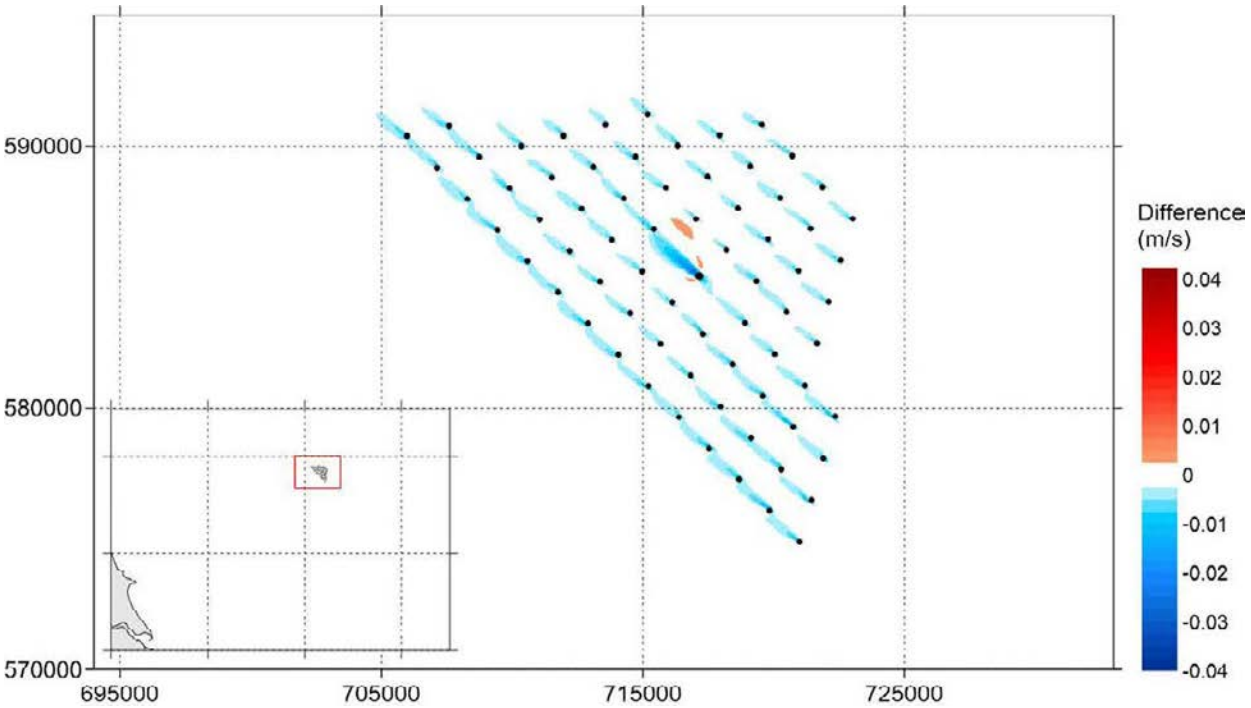

Figure A.180 Change of Maximum Current Speed Over 30 days (Layout D-OSP1 – Baseline)

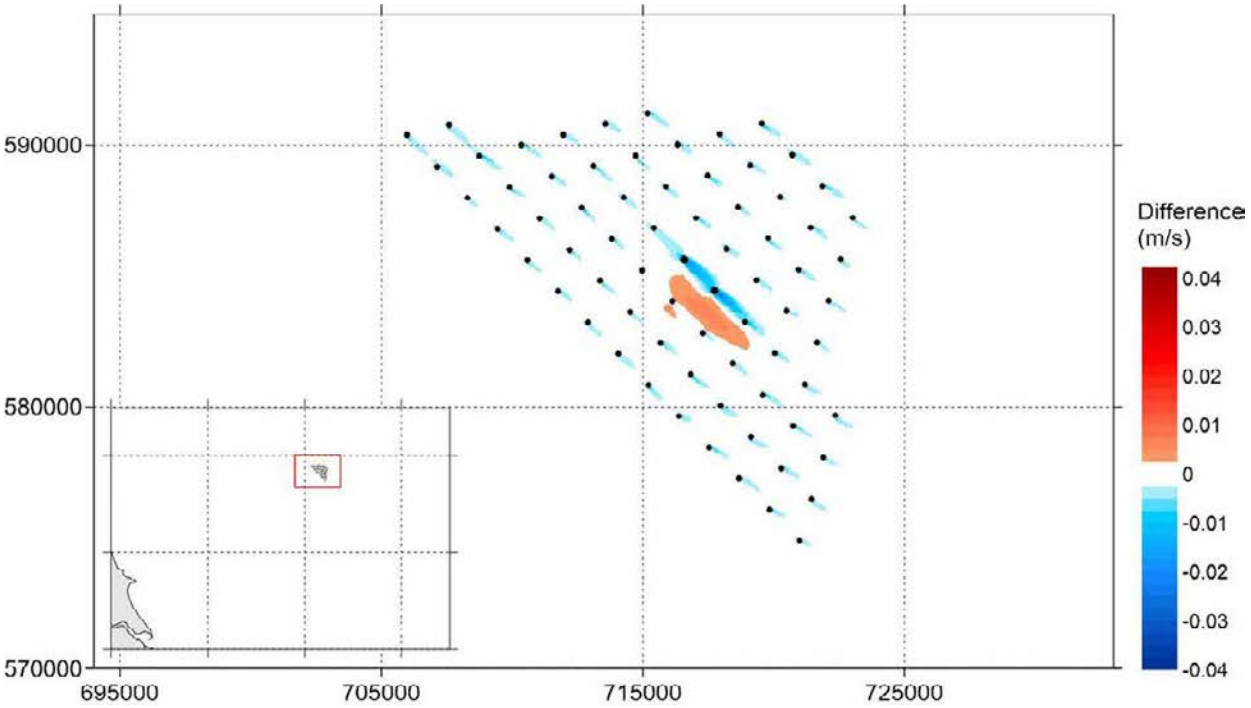

Figure A.181 Change of Speed of Peak South-east-going Currents in a Spring Tide (Layout D-OSP2 – Baseline)

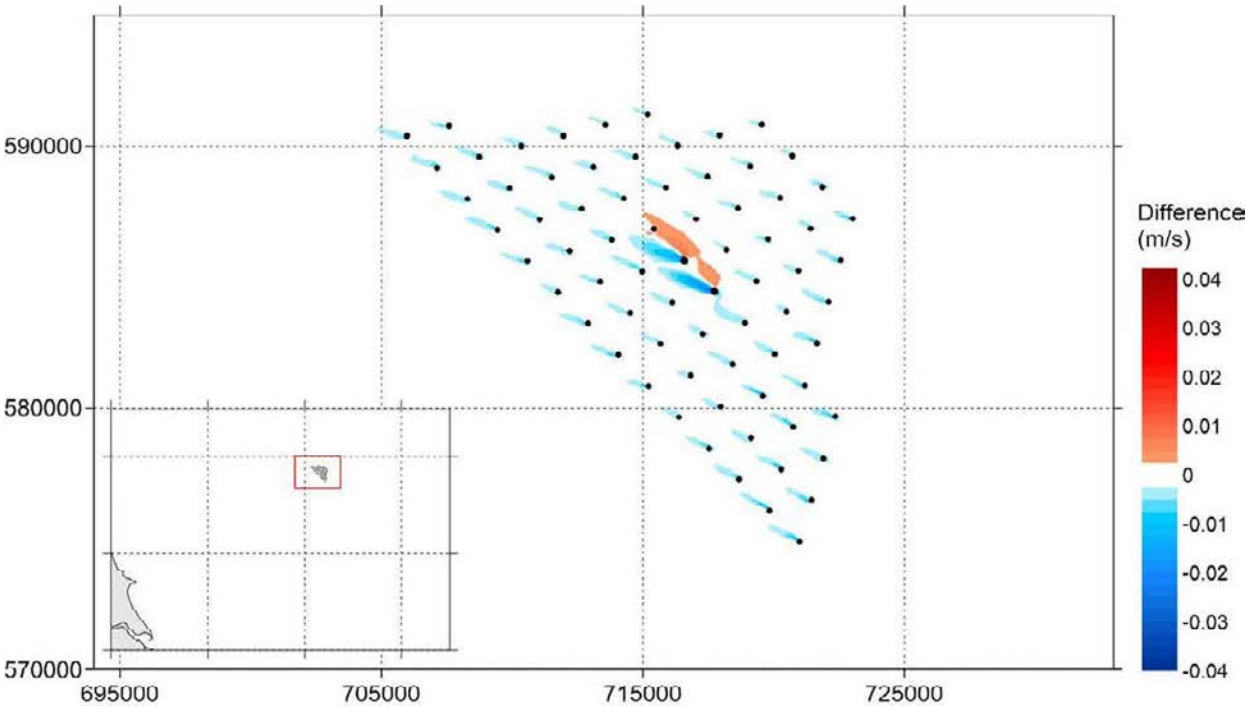

Figure A.182 Change of Speed of Peak North-west-going Currents in a Spring Tide (Layout D-OSP2 – Baseline)

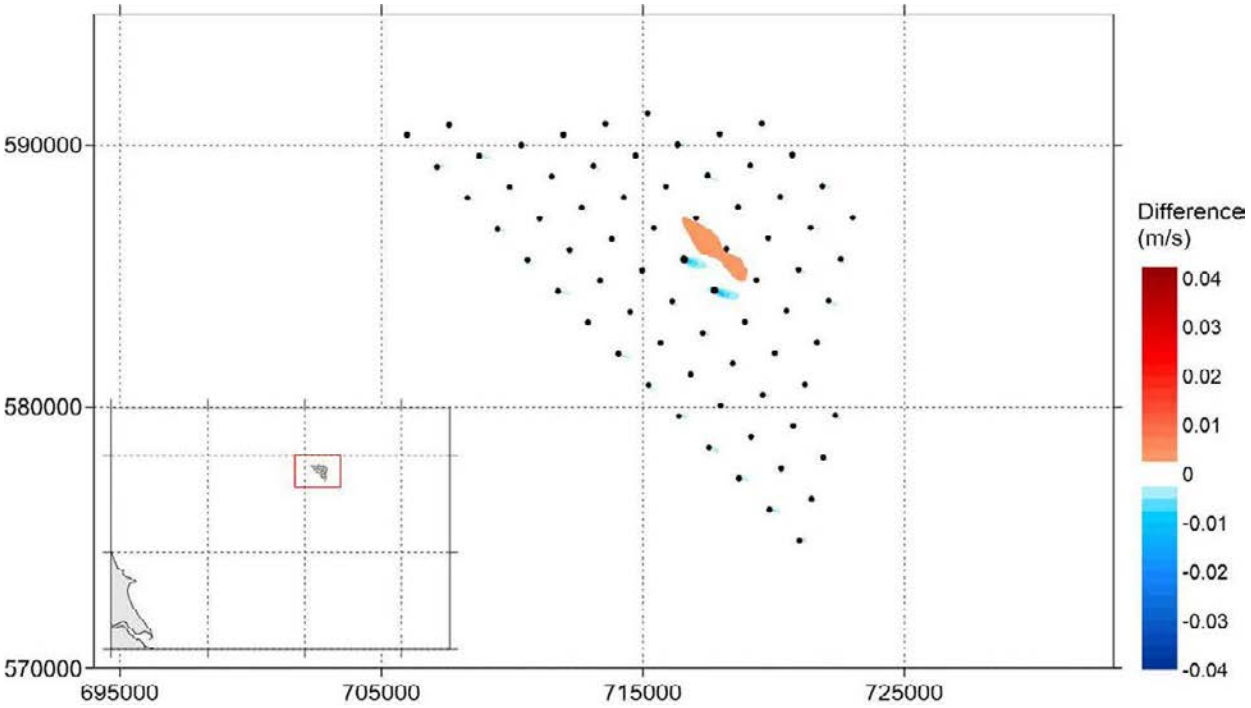

Figure A.183 Change of Speed of Peak South-east-going Currents in a Neap tide (Layout D-OSP2 – Baseline)

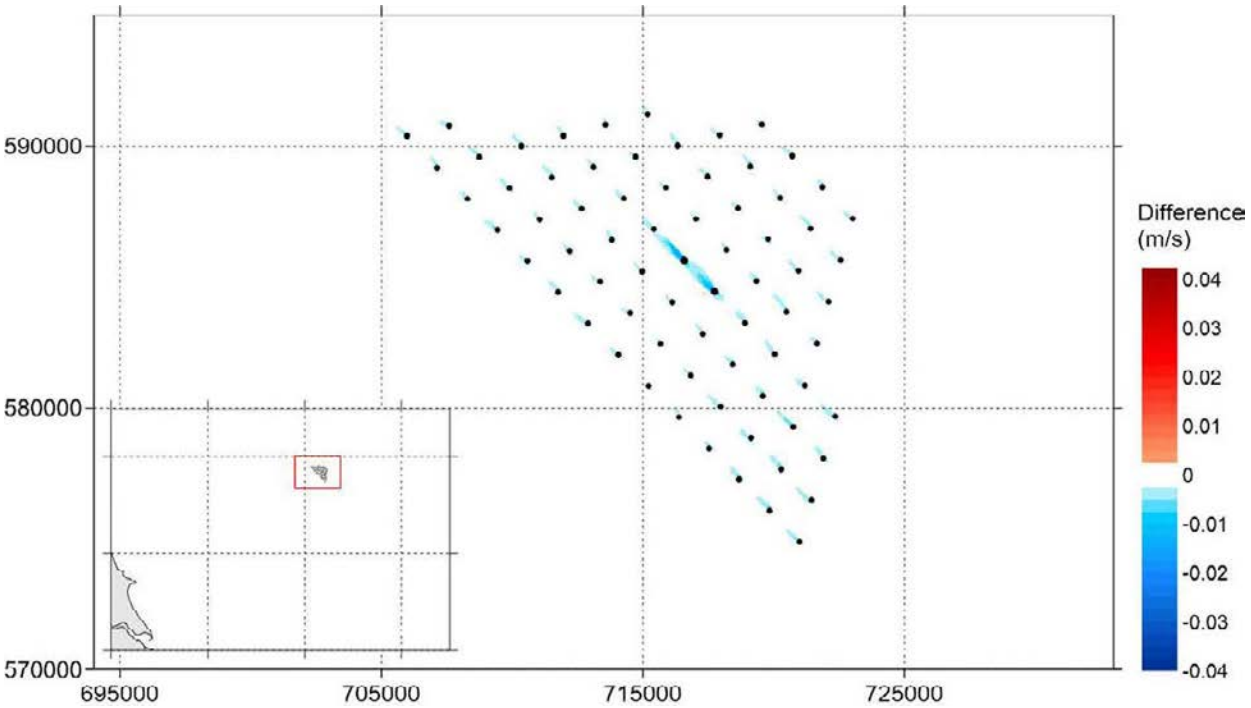

Figure A.184 Change of Speed of Peak North-west-going Currents in a Neap tide (Layout D-OSP2 – Baseline)

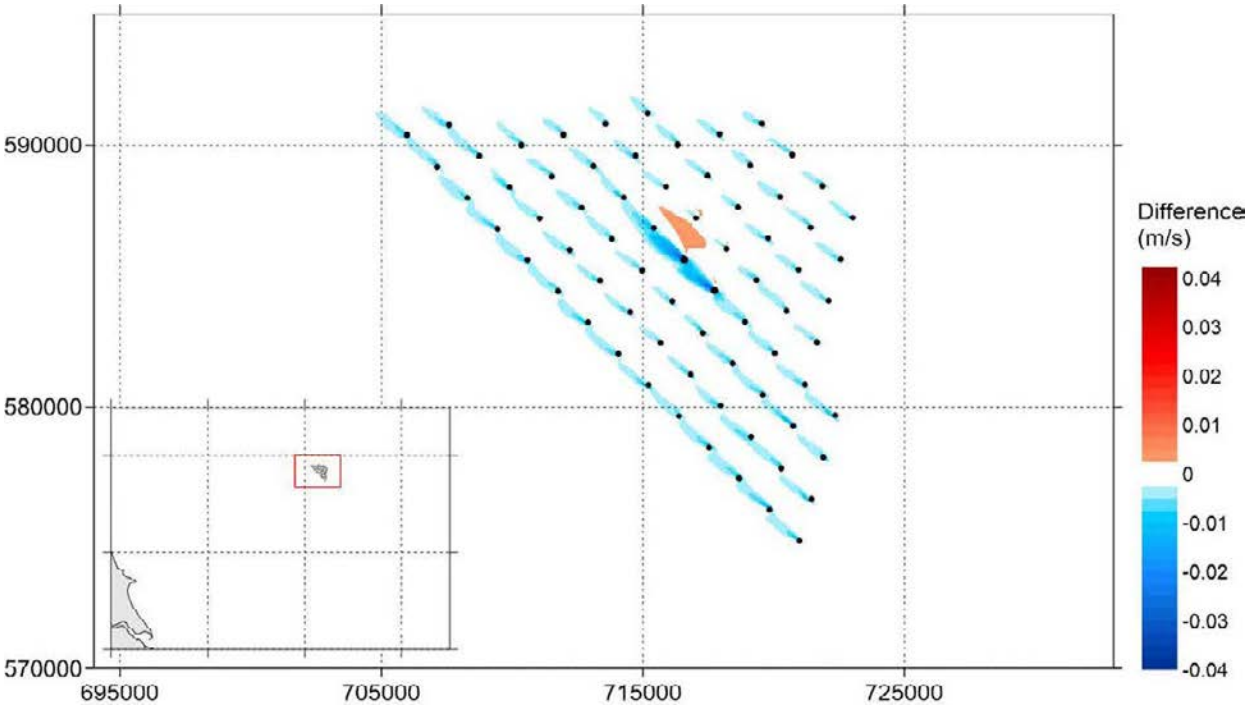

Figure A.185 Change of Maximum Current Speed Over 30 days (Layout D-OSP2 – Baseline)

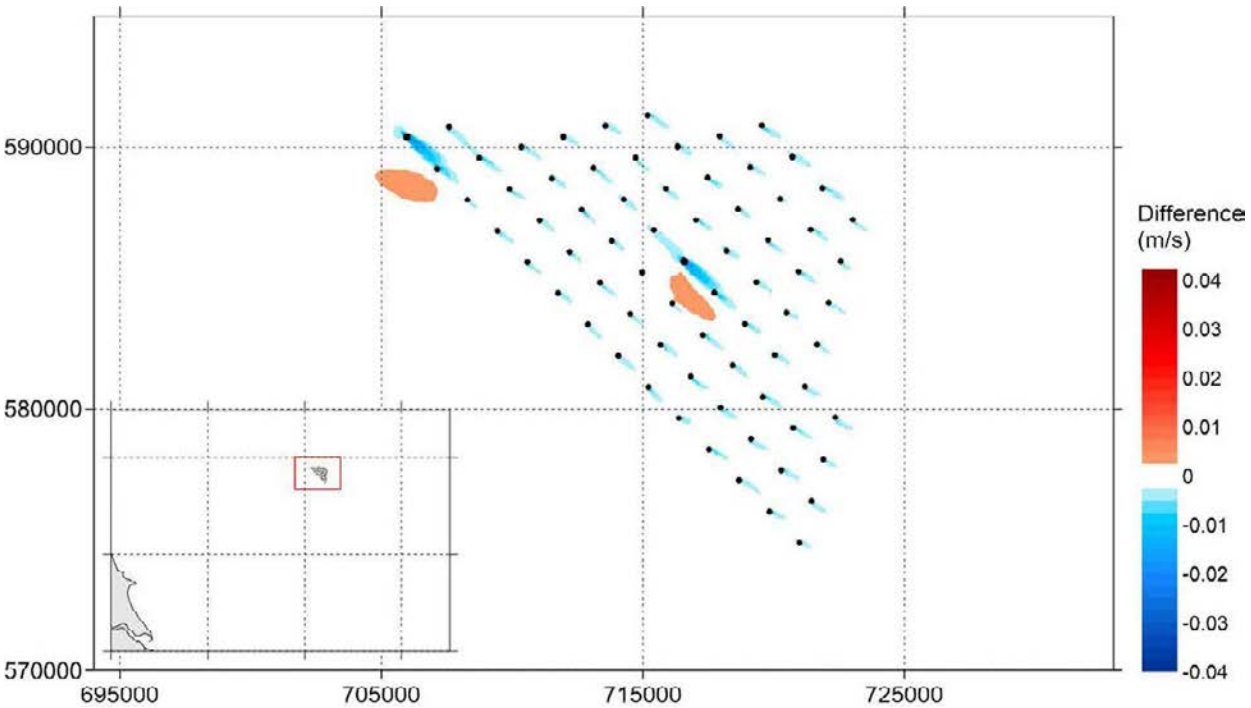

Figure A.186 Change of Speed of Peak South-east-going Currents in a Spring Tide (Layout D-OSP3 – Baseline)

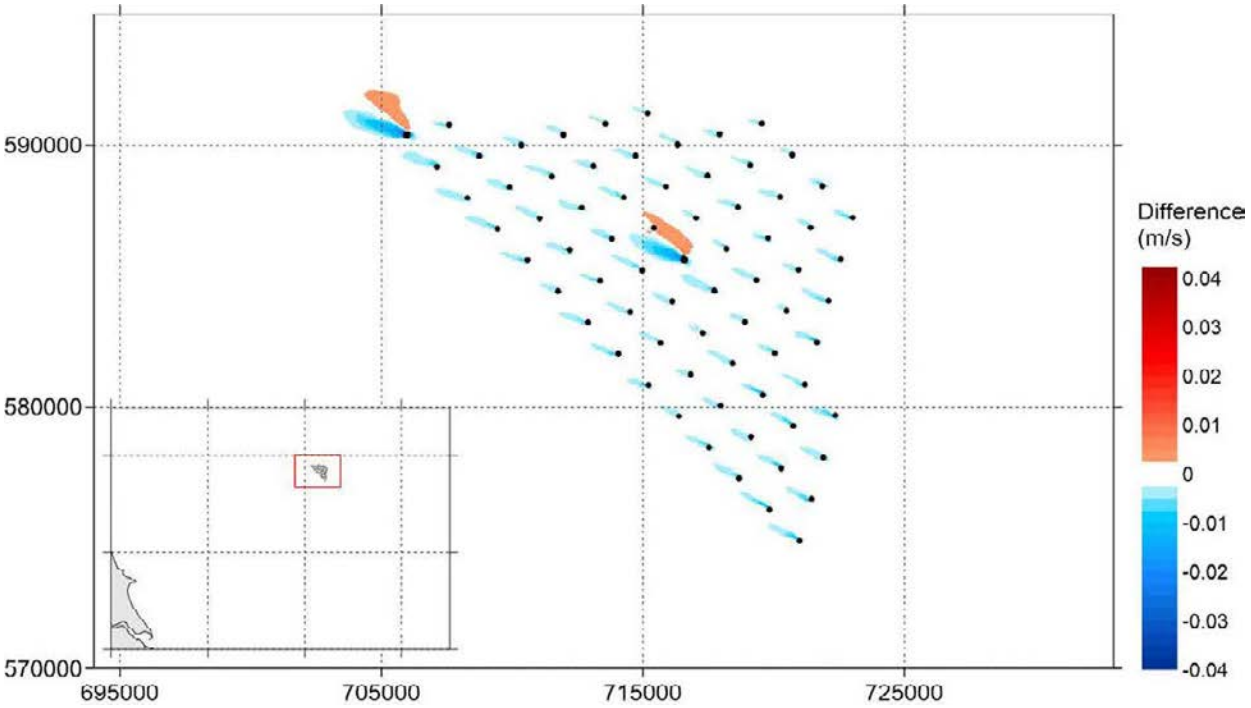

Figure A.187 Change of Speed of Peak North-west-going Currents in a Spring Tide (Layout D-OSP3 – Baseline)

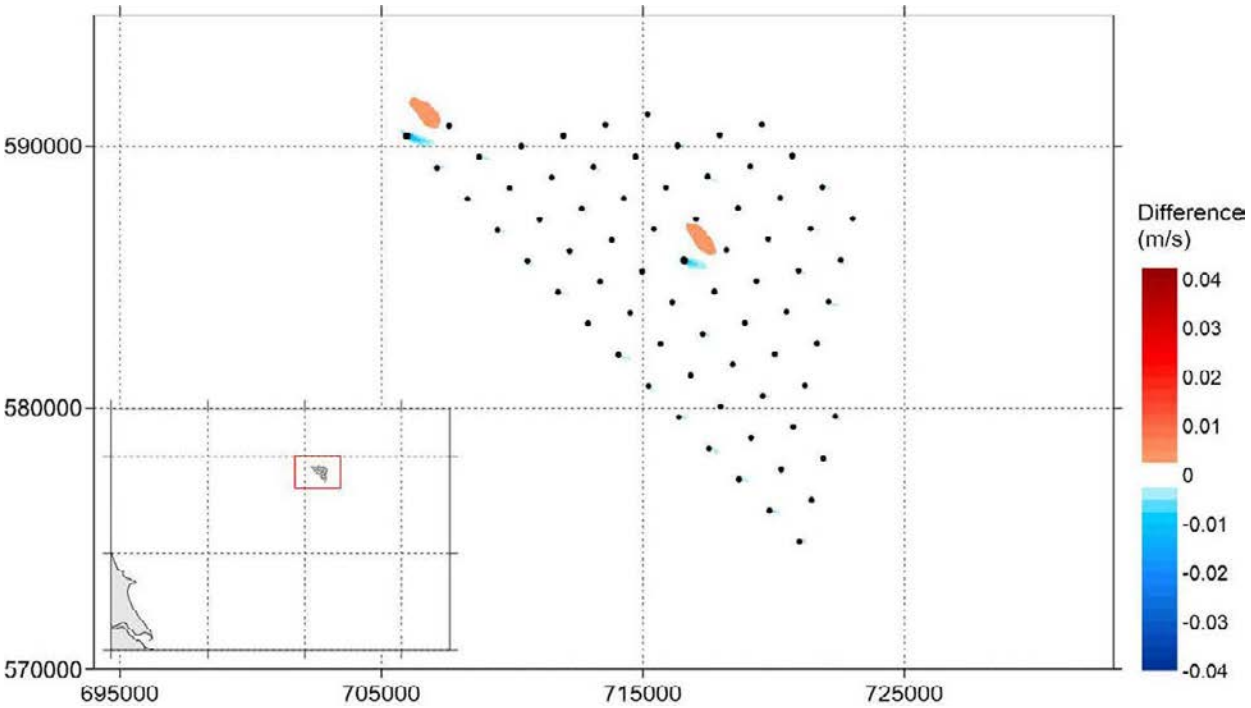

Figure A.188 Change of Speed of Peak South-east-going Currents in a Neap tide (Layout D-OSP3 – Baseline)

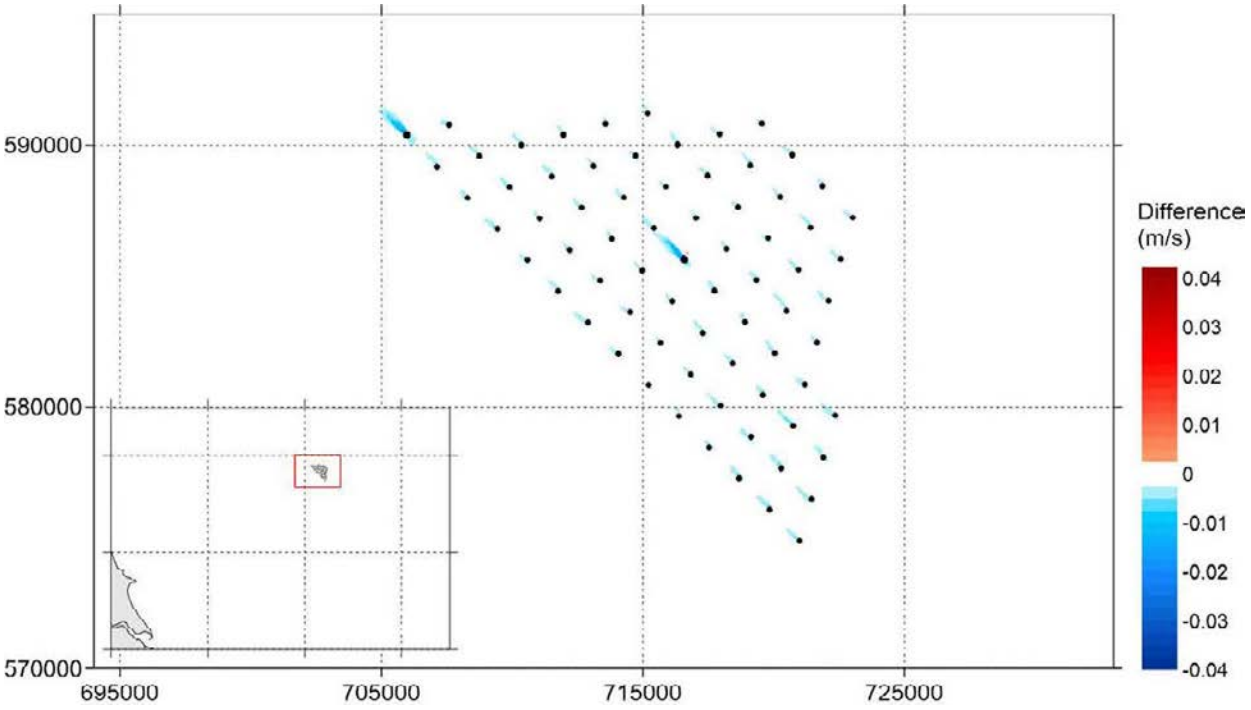

Figure A.189 Change of Speed of Peak North-west-going Currents in a Neap tide (Layout D-OSP3 – Baseline)

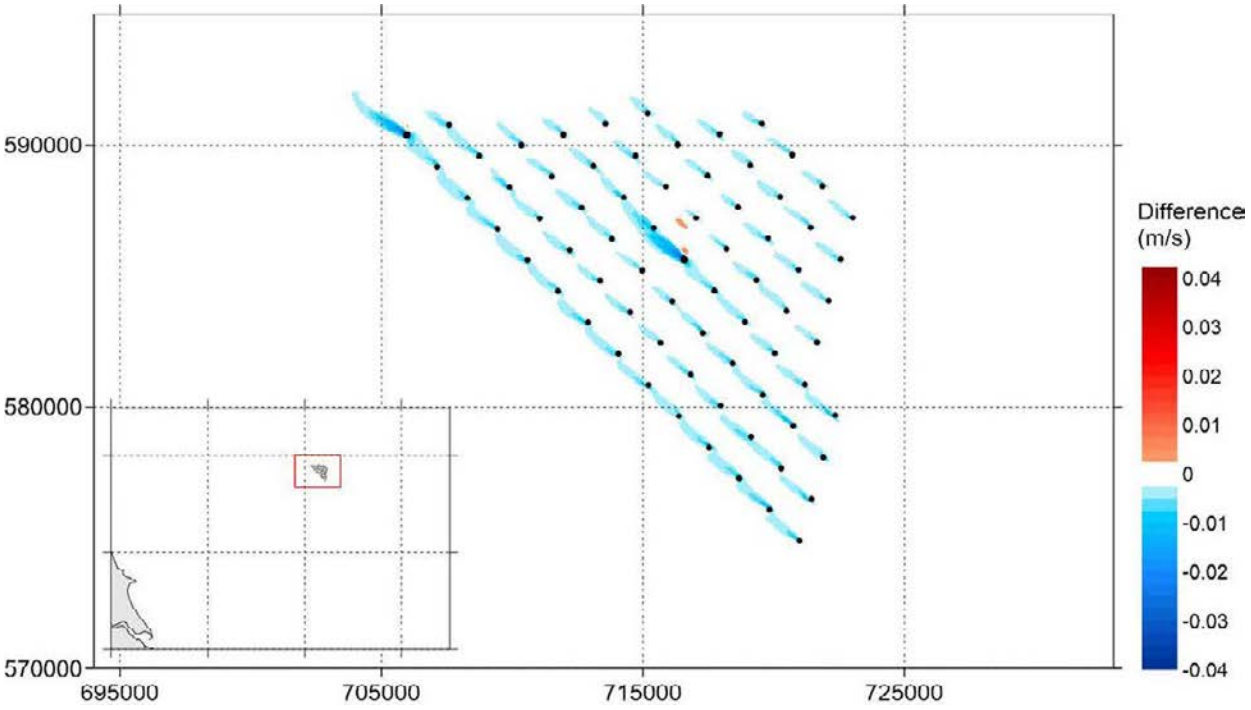

Figure A.190 Change of Maximum Current Speed Over 30 days (Layout D-OSP3 – Baseline)

Appendix B: Hydrodynamic Modelling Cumulative Run Results – Layout C, Offshore Platform 2

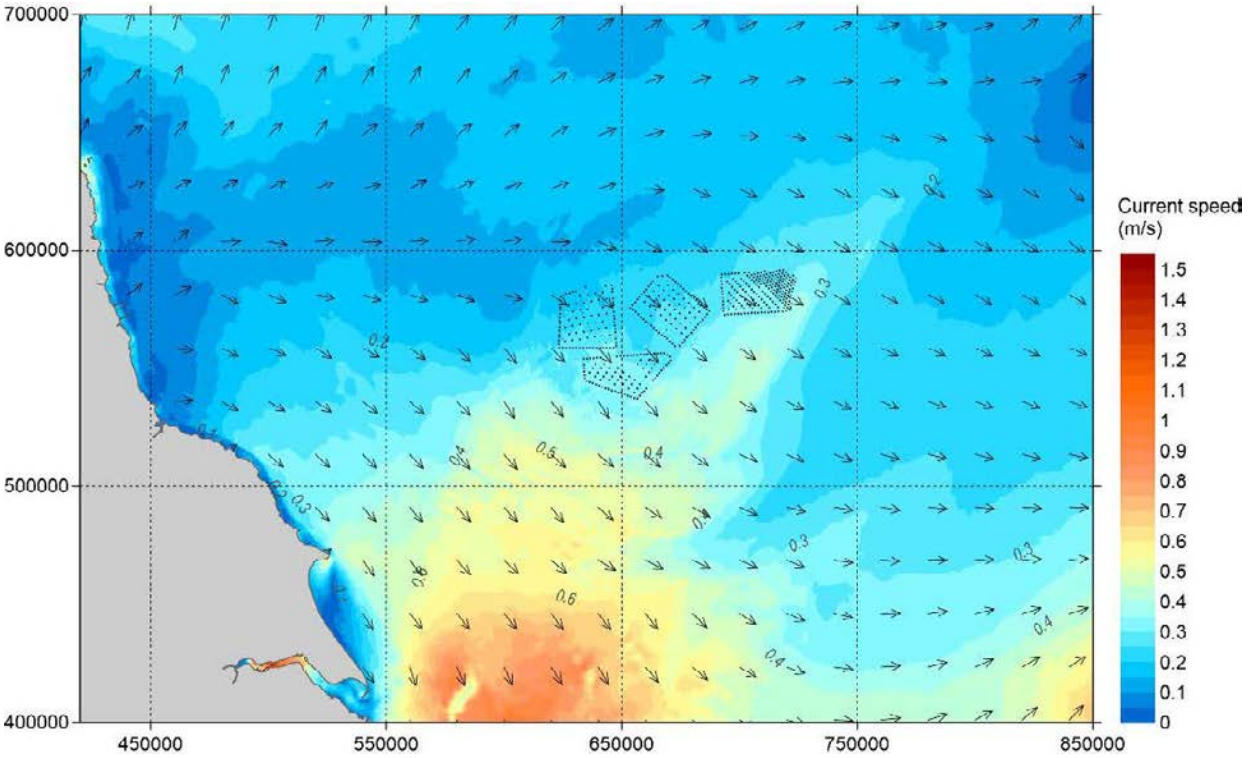

Figure B.1 Overview of Spatial Variation of Peak South-east-going Currents in a Spring Tide – Scenario 1

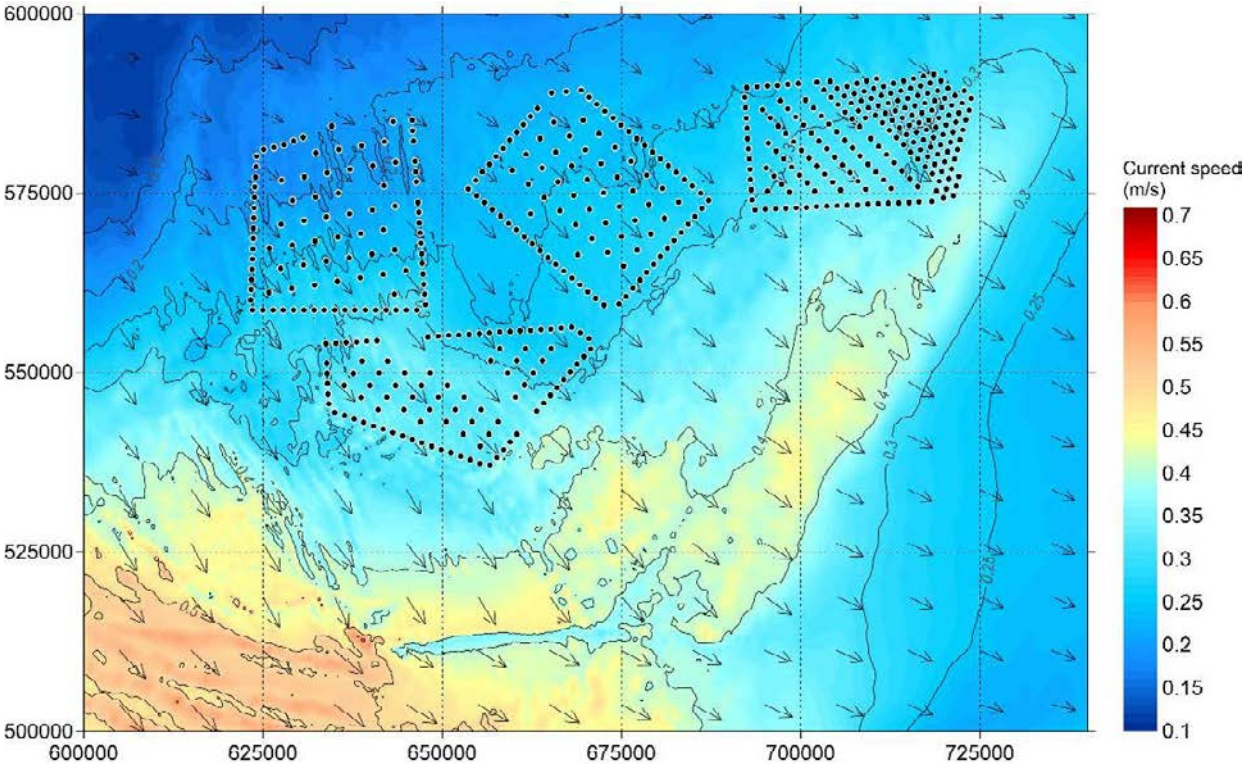

Figure B.2 A Closer View of Spatial Variation of Peak South-east-going Currents in a Spring Tide – Scenario 1

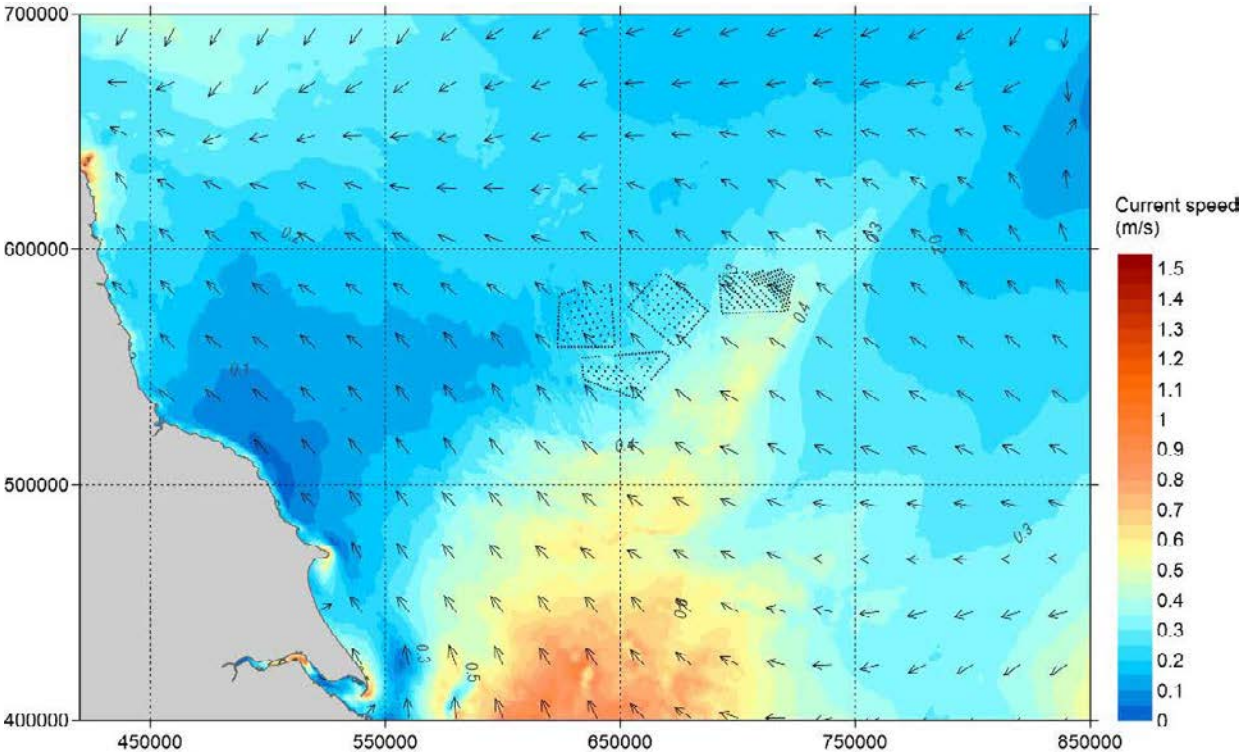

Figure B.3 Overview of Spatial Variation of Peak North-west-going Currents in a Spring Tide – Scenario 1

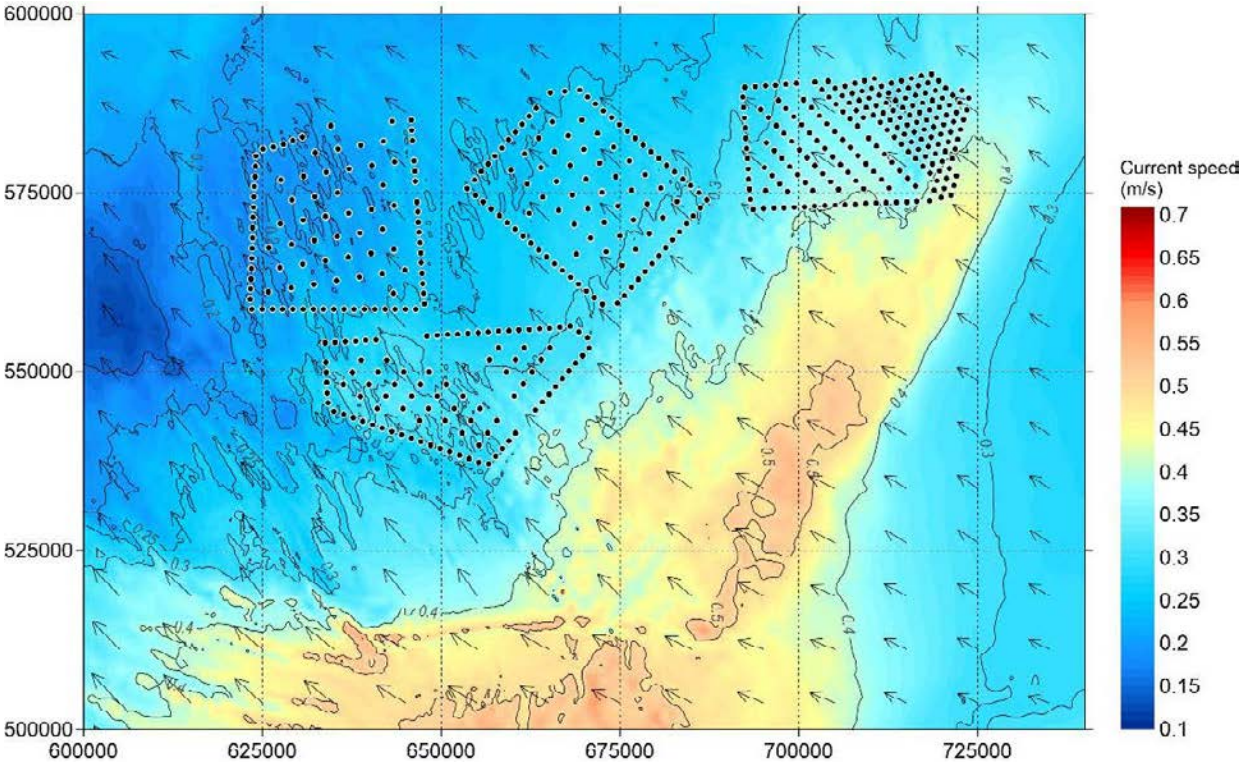

Figure B.4 A Closer View of Spatial Variation of Peak North-west-going Currents in a Spring Tide – Scenario 1

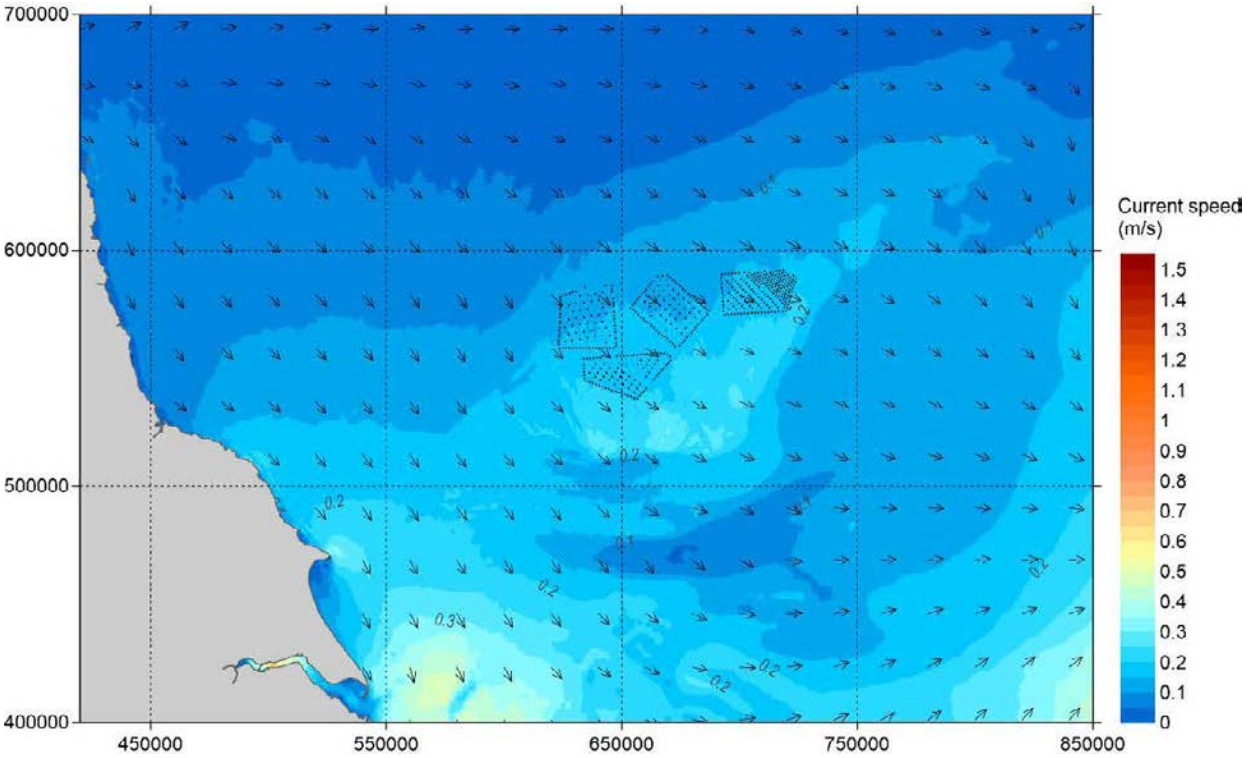

Figure B.5 Overview of Spatial Variation of Peak South-east-going Currents in a Neap Tide – Scenario 1

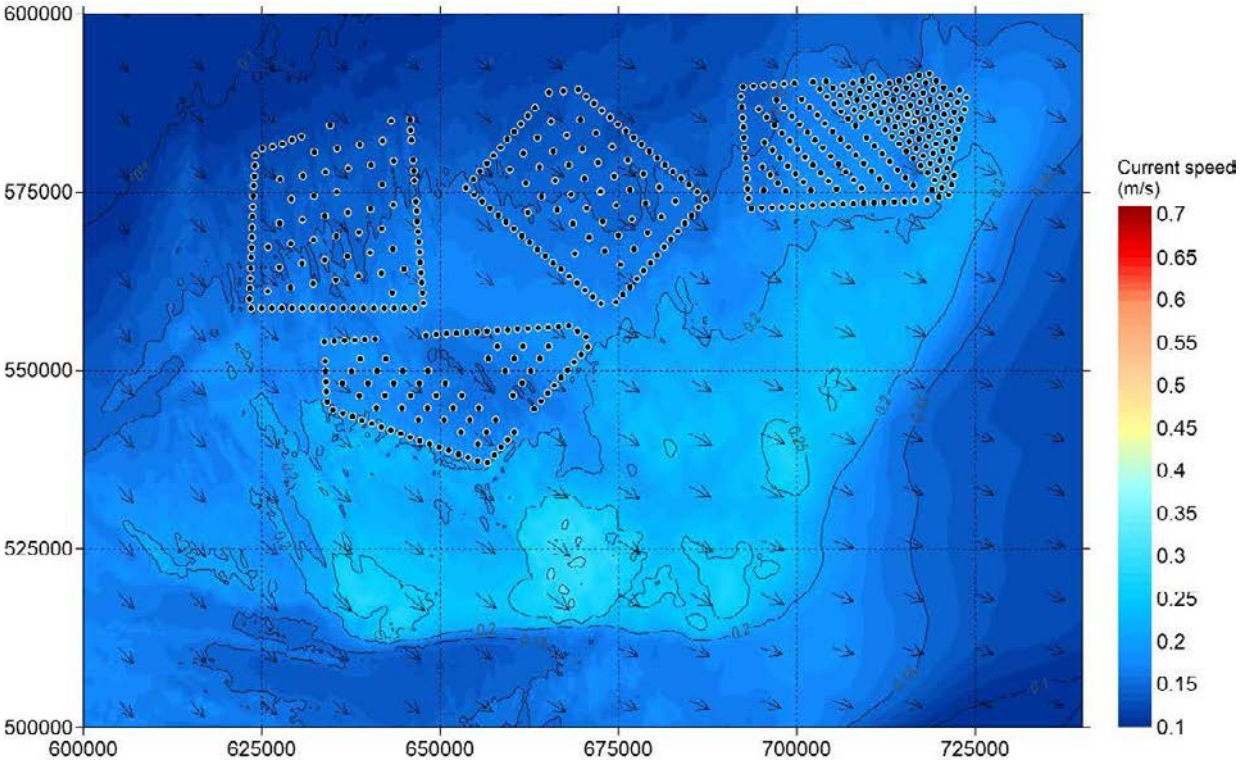

Figure B.6 A Closer View of Spatial Variation of Peak South-east-going Currents in a Neap Tide – Scenario 1

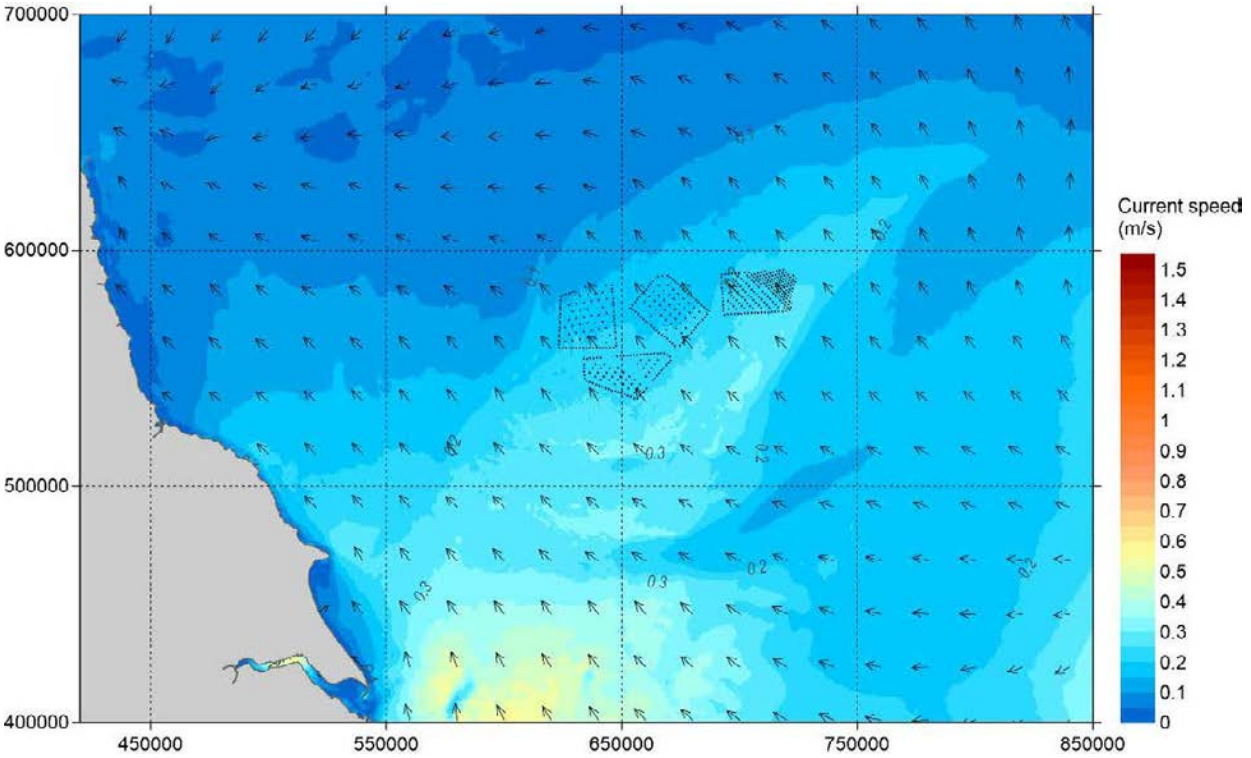

Figure B.7 Overview of Spatial Variation of Peak North-west-going Currents in a Neap Tide – Scenario 1

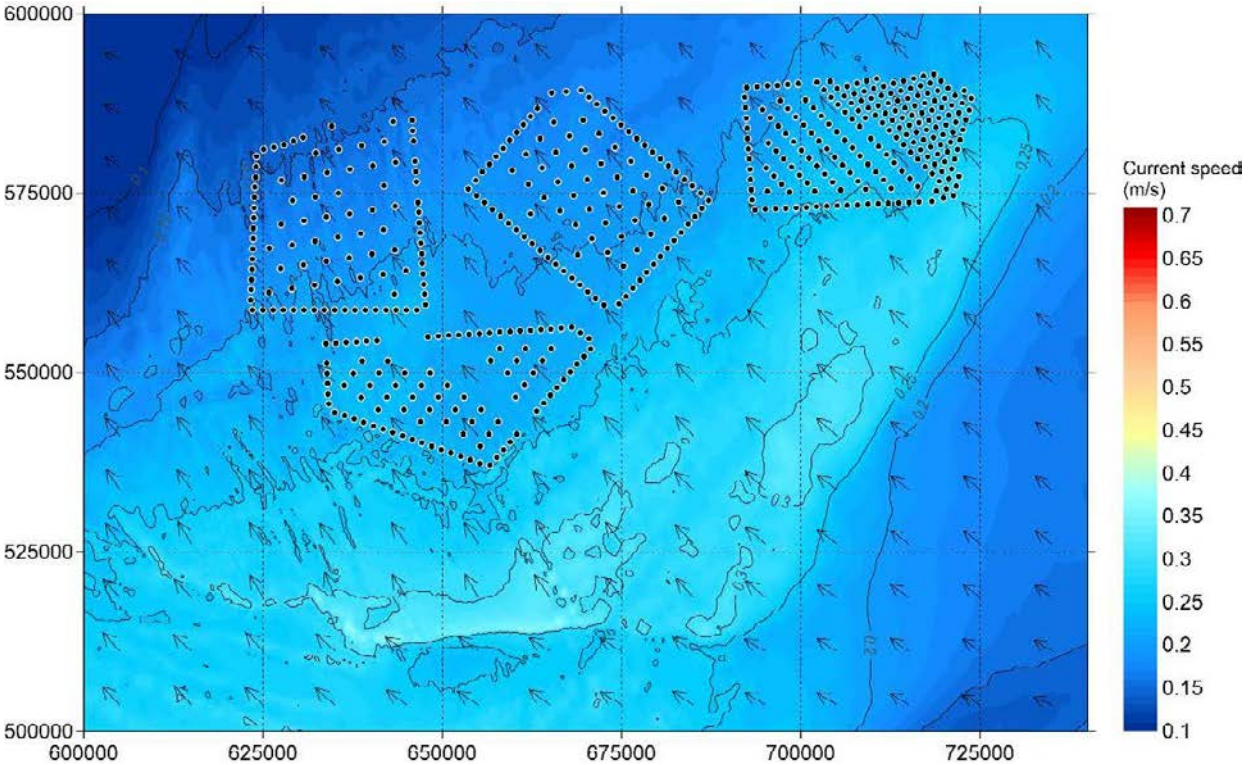

Figure B.8 A Closer View of Spatial Variation of Peak North-west-going Currents in a Neap Tide – Scenario 1

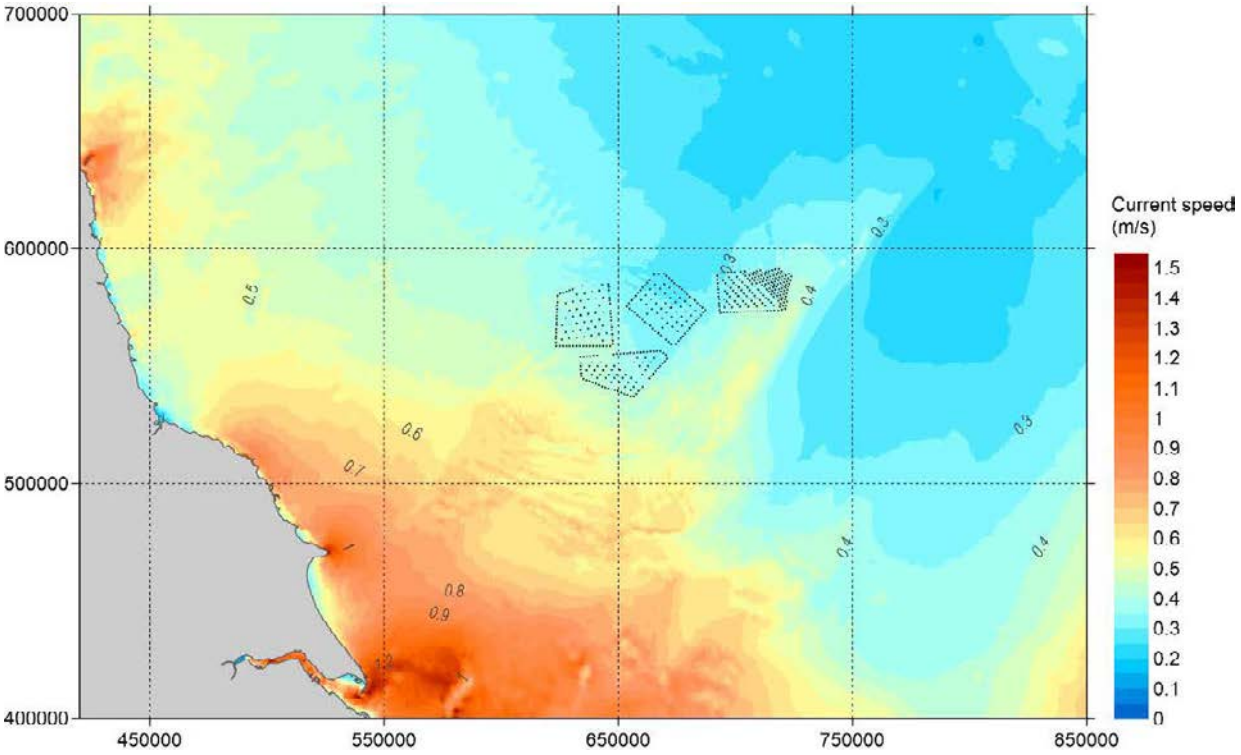

Figure B.9 Overview of Spatial Variation of Maximum Current Speed Over 30 days- Scenario 1

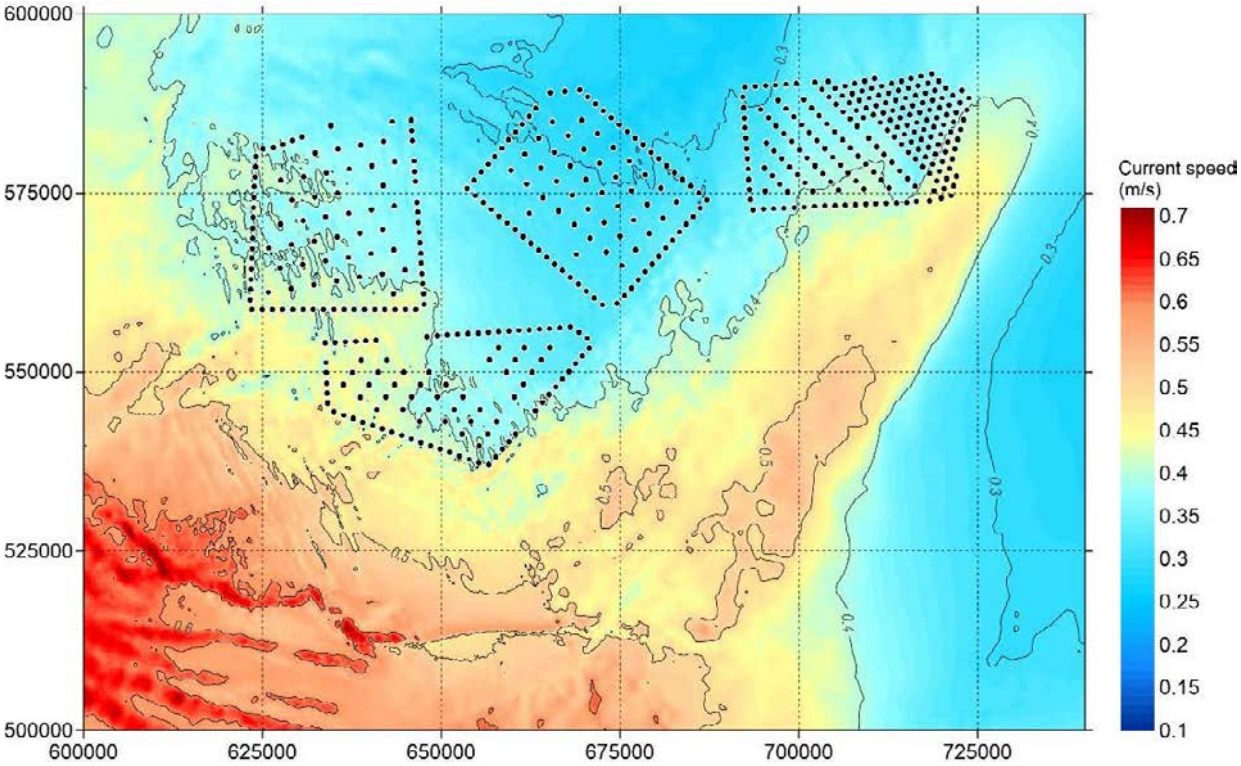

Figure B.10 A Closer View of Spatial Variation of Maximum Current Speed Over 30 days- Scenario 1

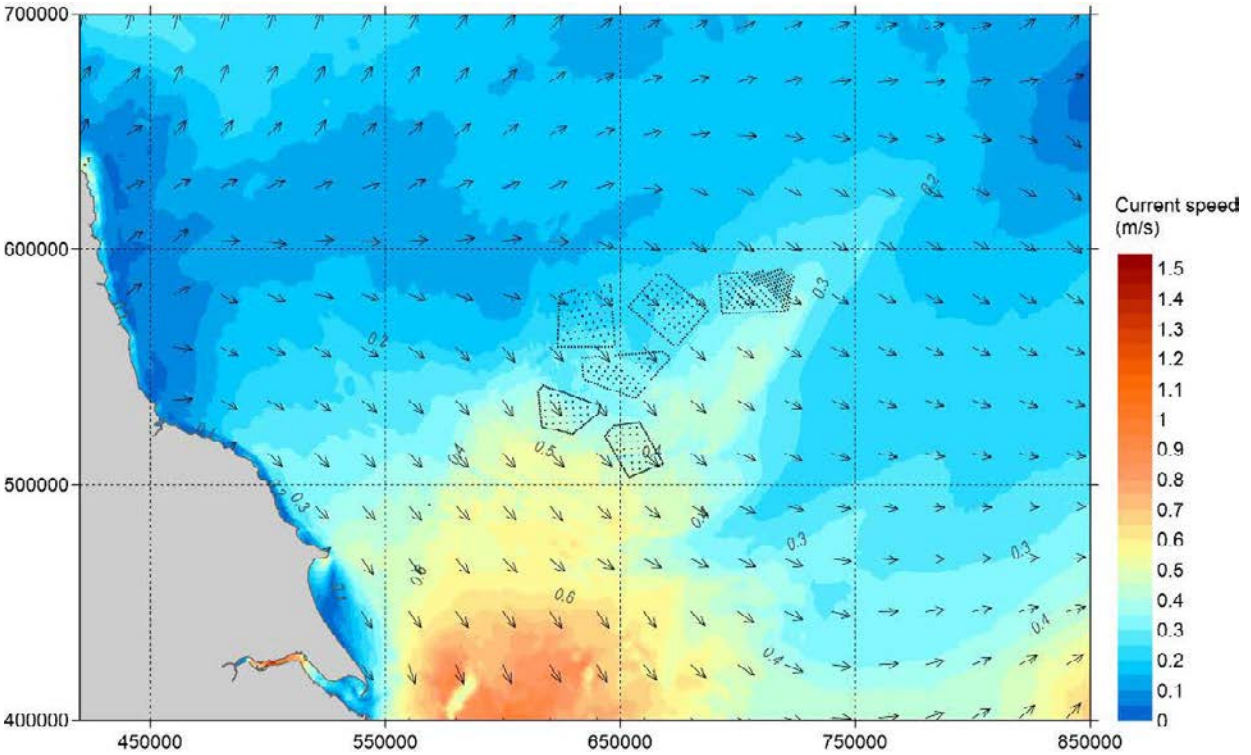

Figure B.11 Overview of Spatial Variation of Peak South-east-going Currents in a Spring Tide – Scenario 2

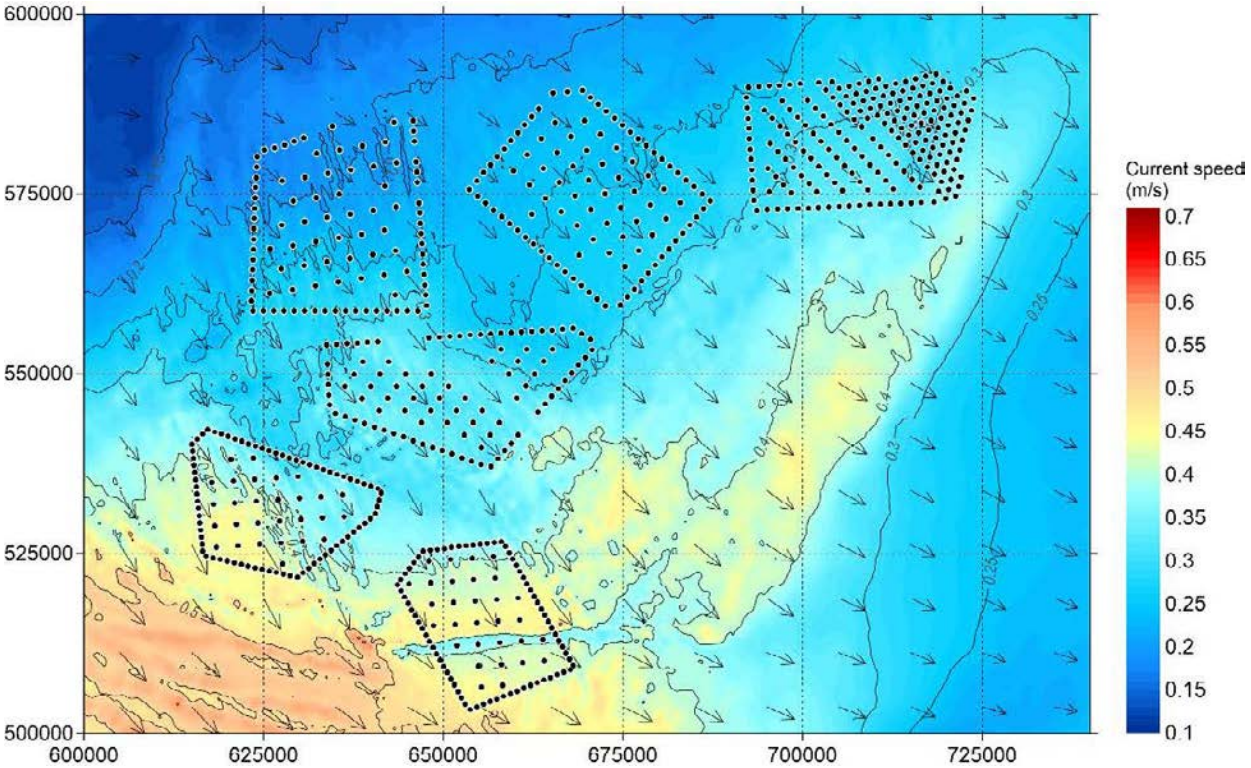

Figure B.12 A Closer View of Spatial Variation of Peak South-east-going Currents in a Spring Tide – Scenario 2

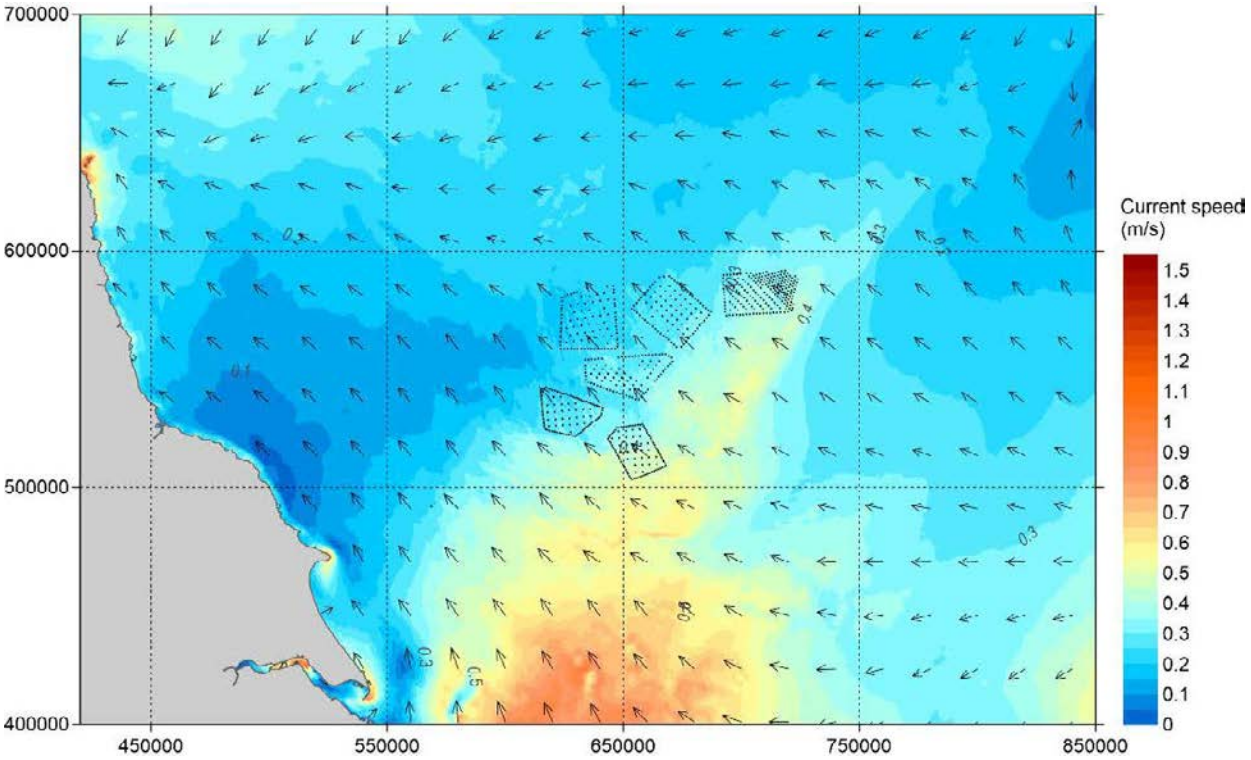

Figure B.13 Overview of Spatial Variation of Peak North-west-going Currents in a Spring Tide – Scenario 2

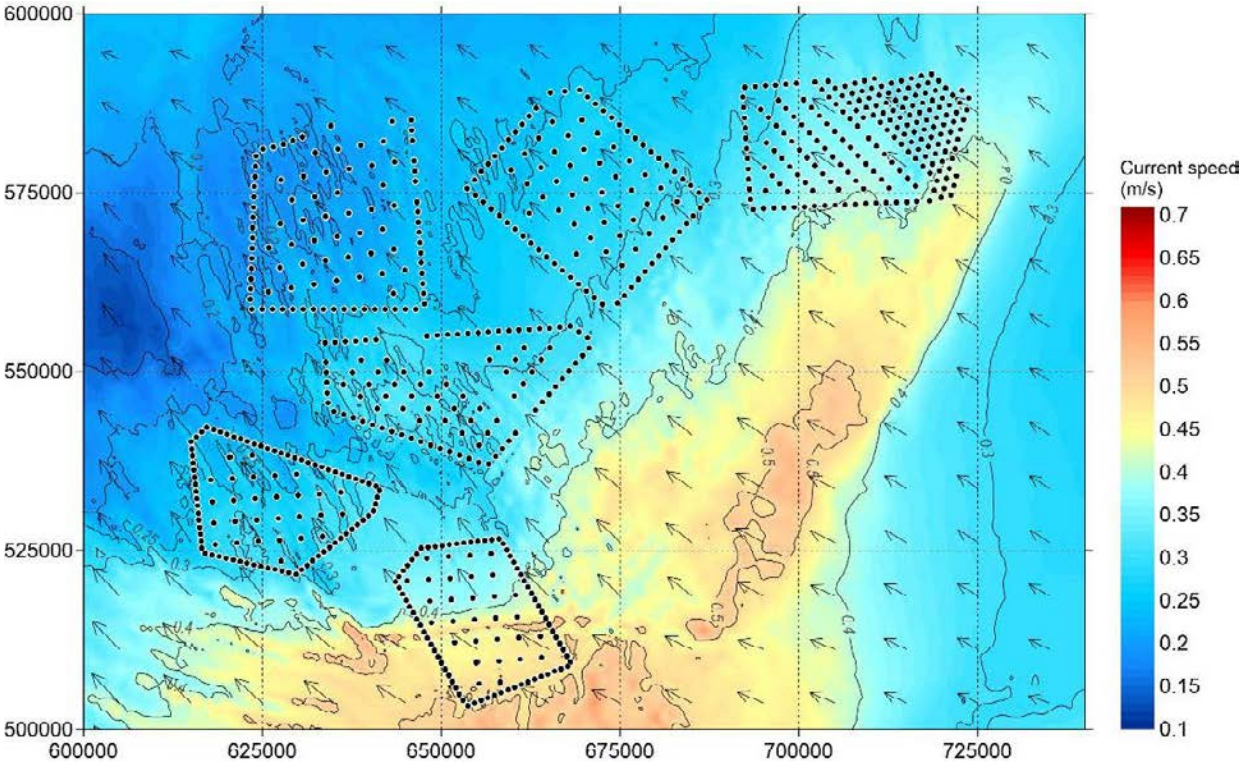

Figure B.14 A Closer View of Spatial Variation of Peak North-west-going Currents in a Spring Tide – Scenario 2

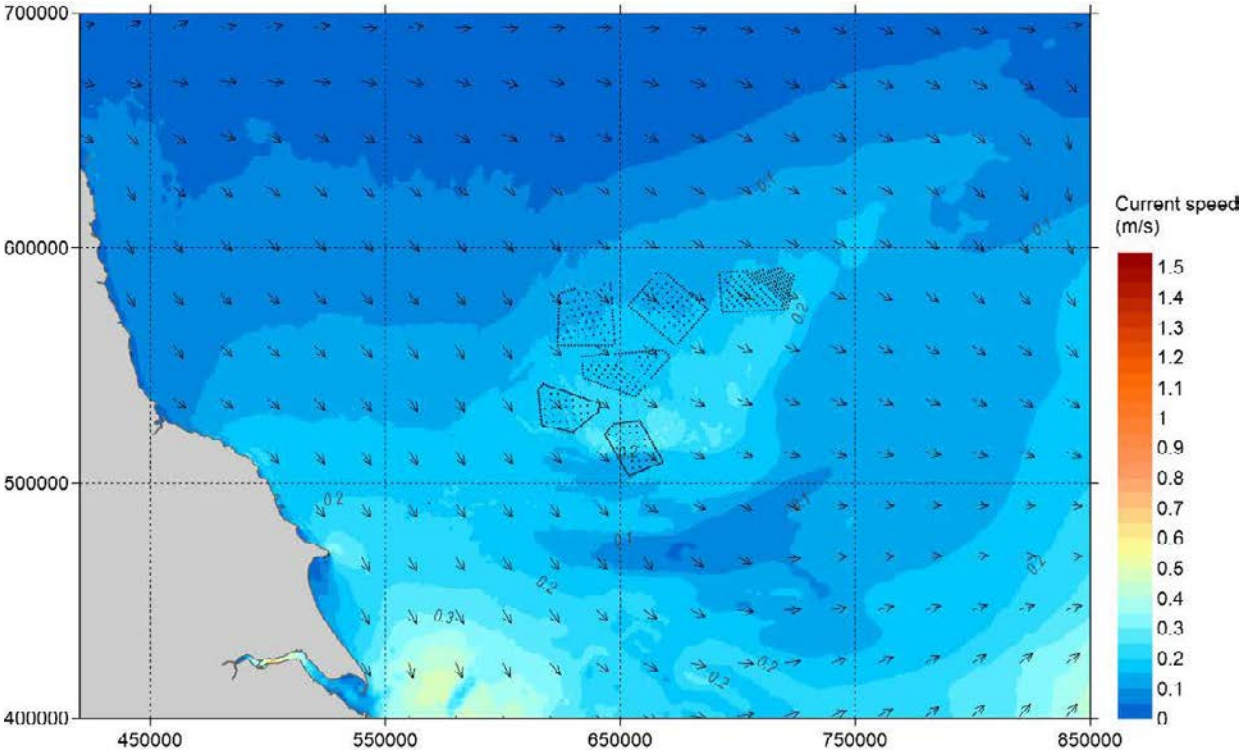

Figure B.15 Overview of Spatial Variation of Peak South-east-going Currents in a Neap Tide – Scenario 2

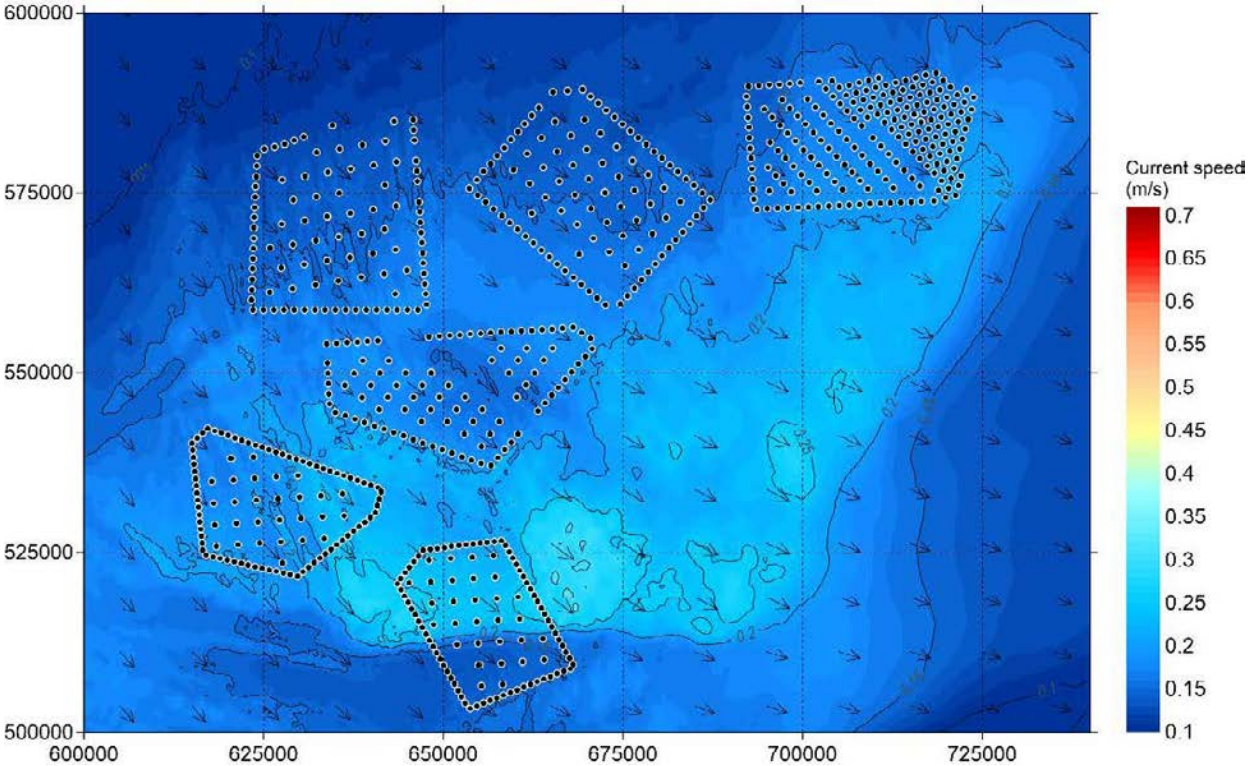

Figure B.16 A Closer View of Spatial Variation of Peak South-east-going Currents in a Neap Tide – Scenario 2

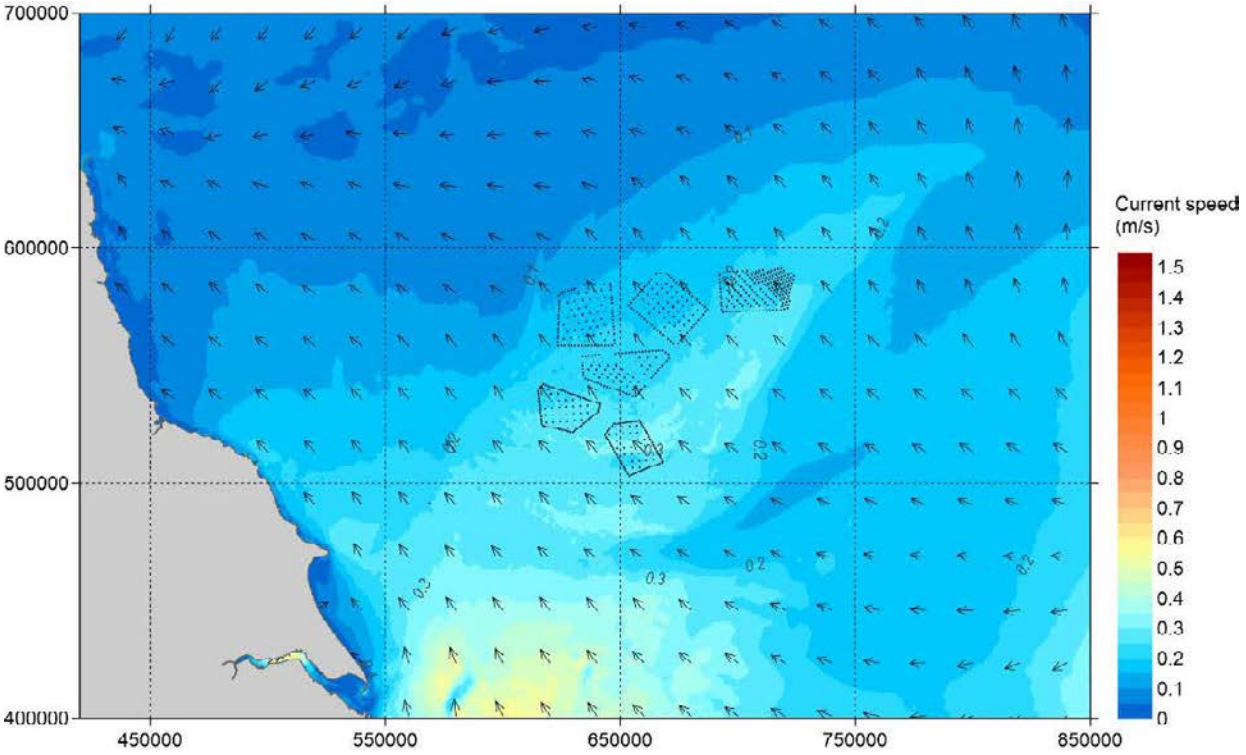

Figure B.17 Overview of Spatial Variation of Peak North-west-going Currents in a Neap Tide – Scenario 2

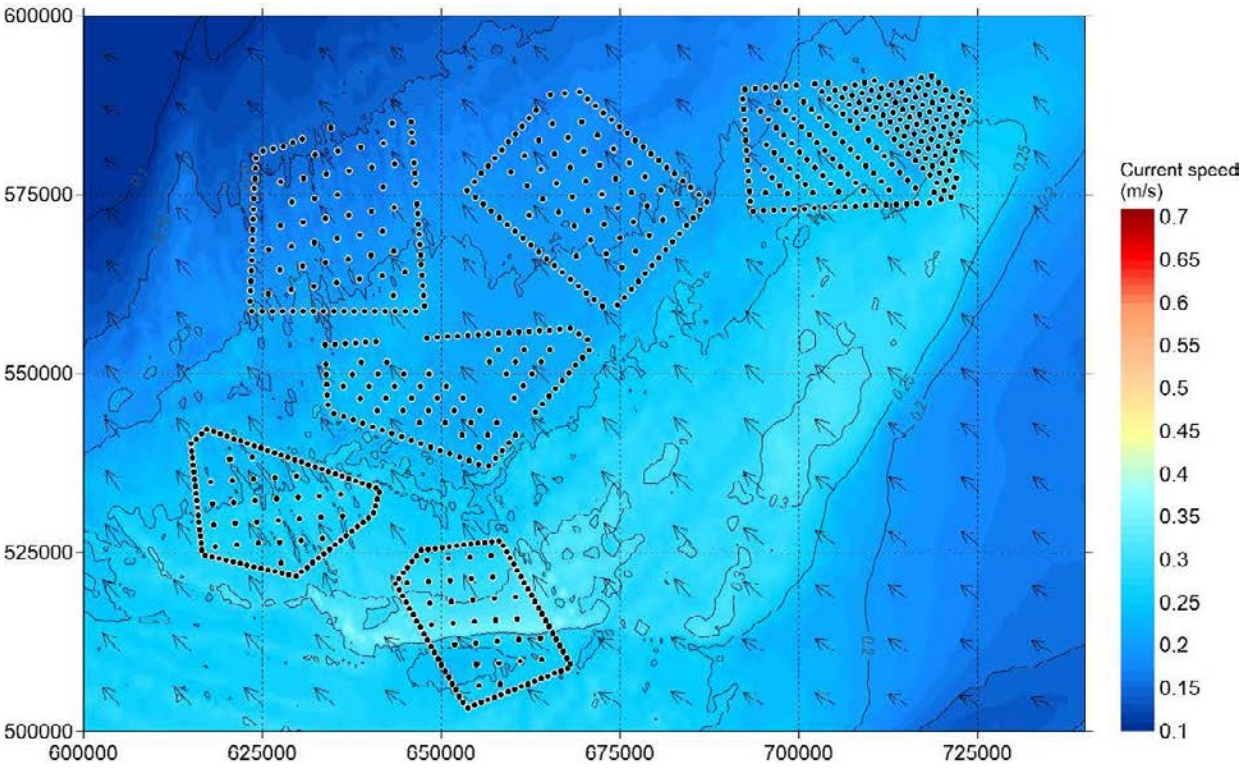

Figure B.18 A Closer View of Spatial Variation of Peak North-west-going Currents in a Neap Tide – Scenario 2

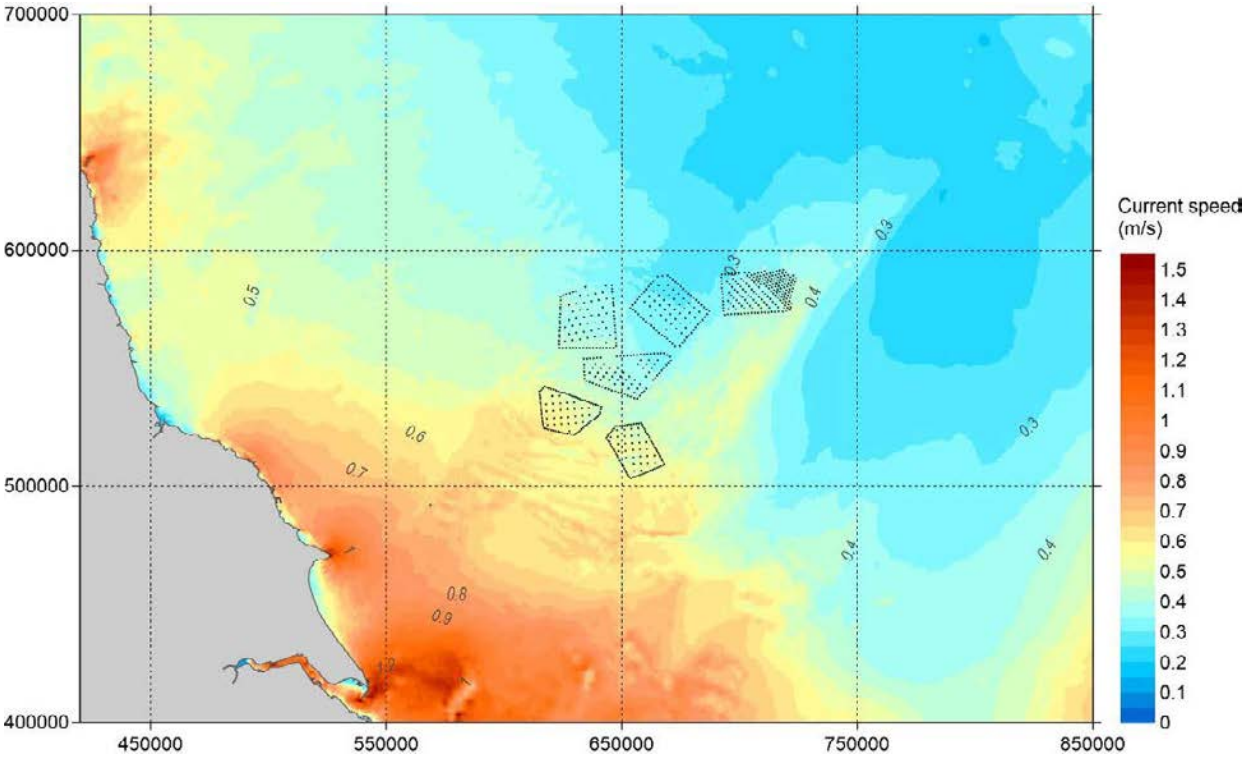

Figure B.19 Overview of Spatial Variation of Maximum Current Speed Over 30 days- Scenario 2

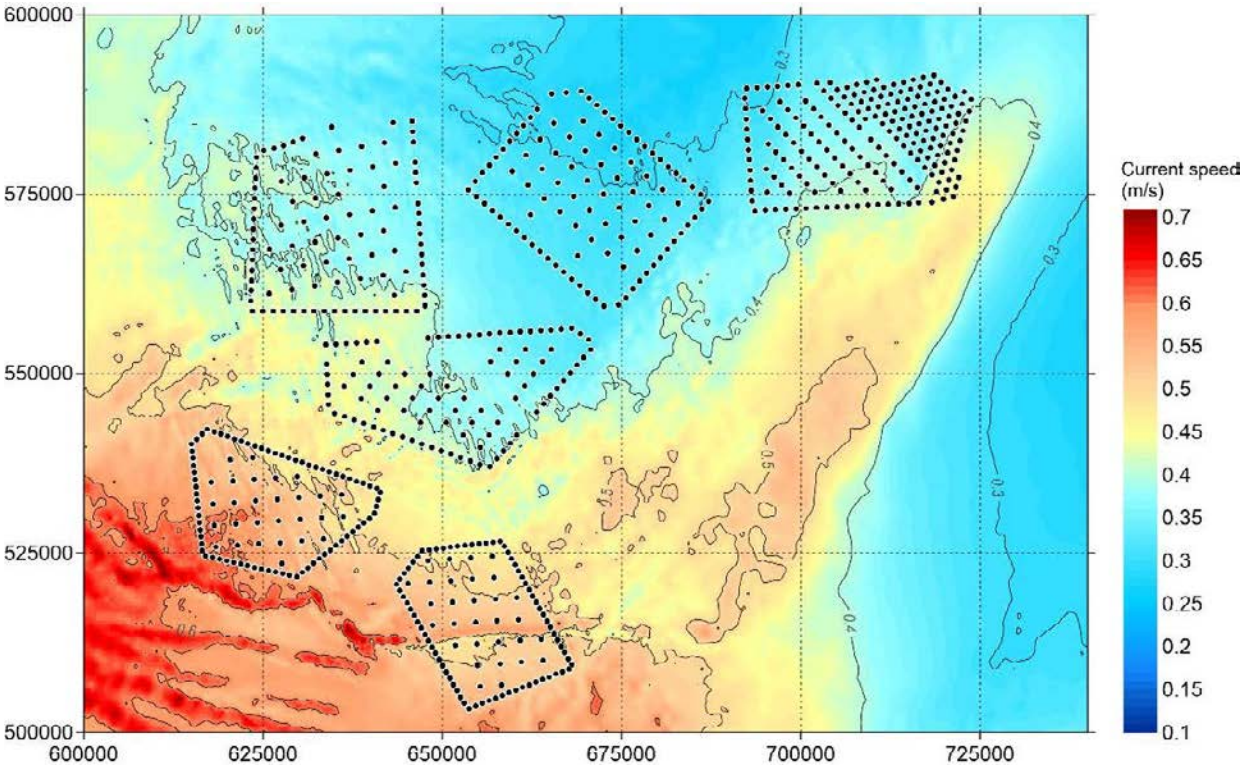

Figure B.20 A Closer View of Spatial Variation of Maximum Current Speed Over 30 days- Scenario 2

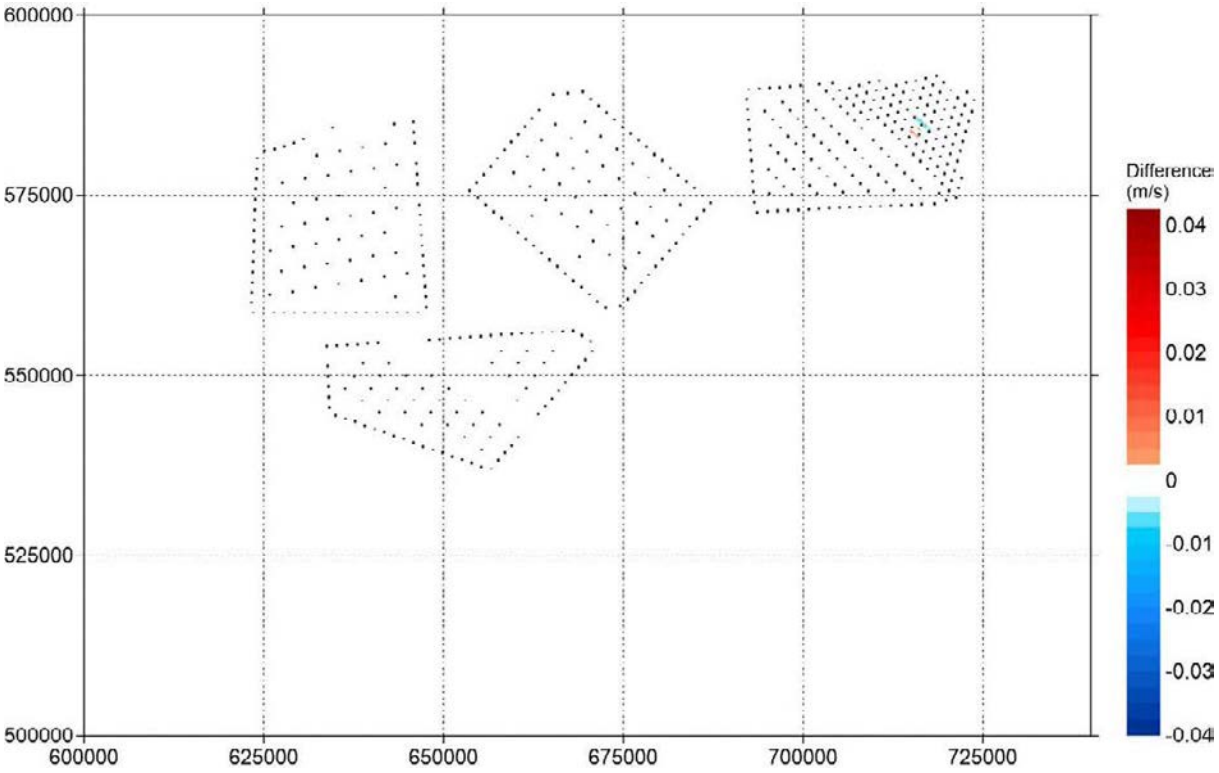

Figure B.21 Change of Speed of Peak South-east-going Currents in a Spring Tide (Scenario 1)

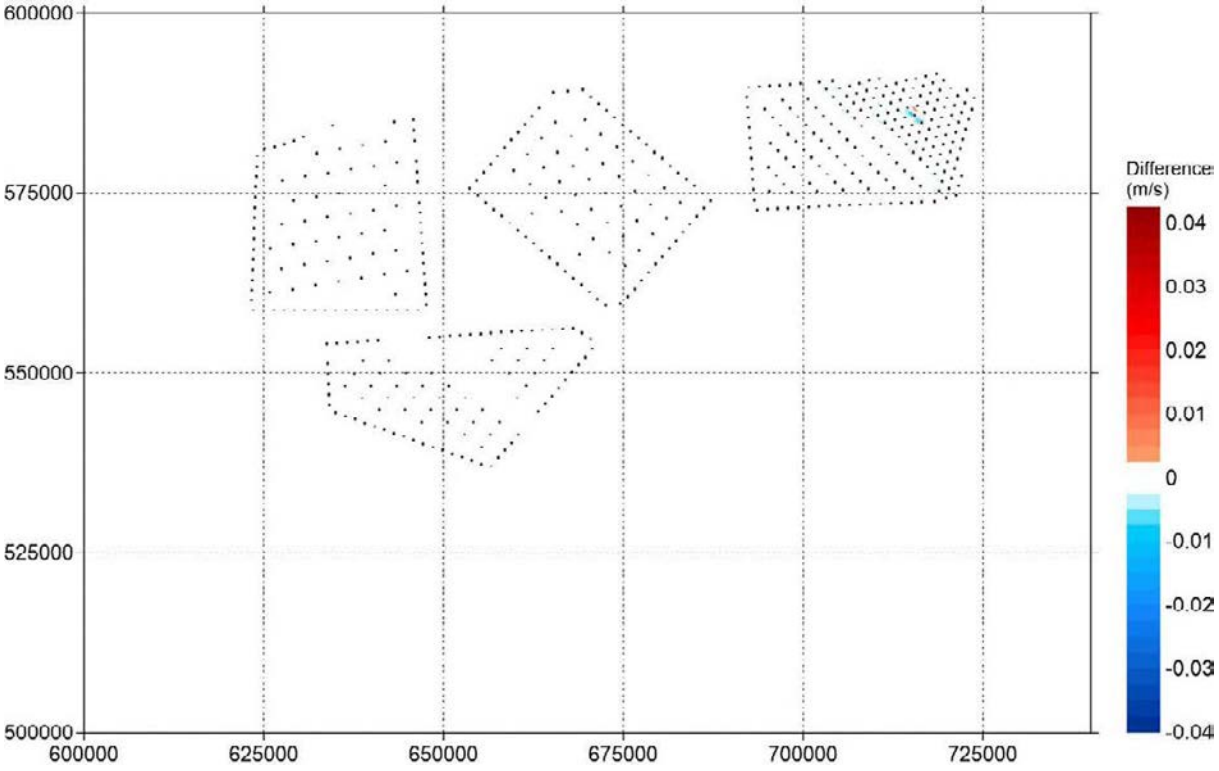

Figure B.22 Change of Speed of Peak North-west-going Currents in a Spring Tide (Scenario 1)

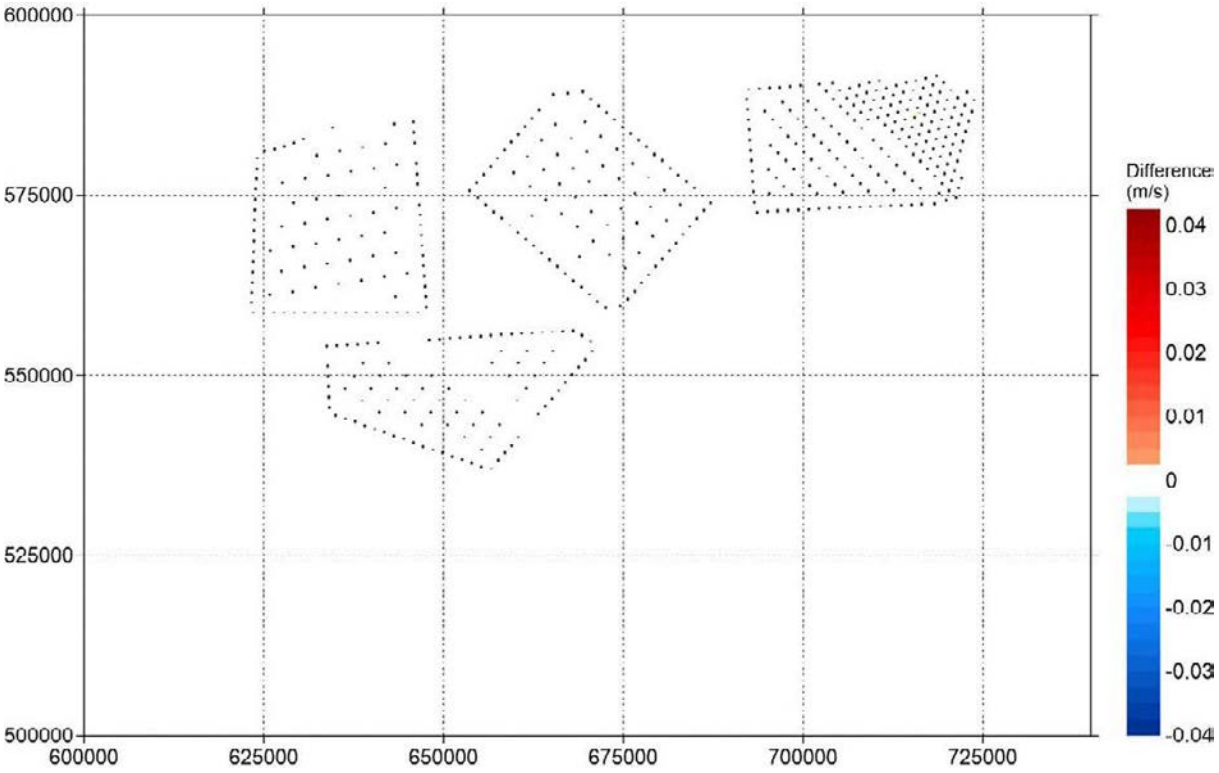

Figure B.23 Change of Speed of Peak South-east-going Currents in a Neap Tide (Scenario 1)

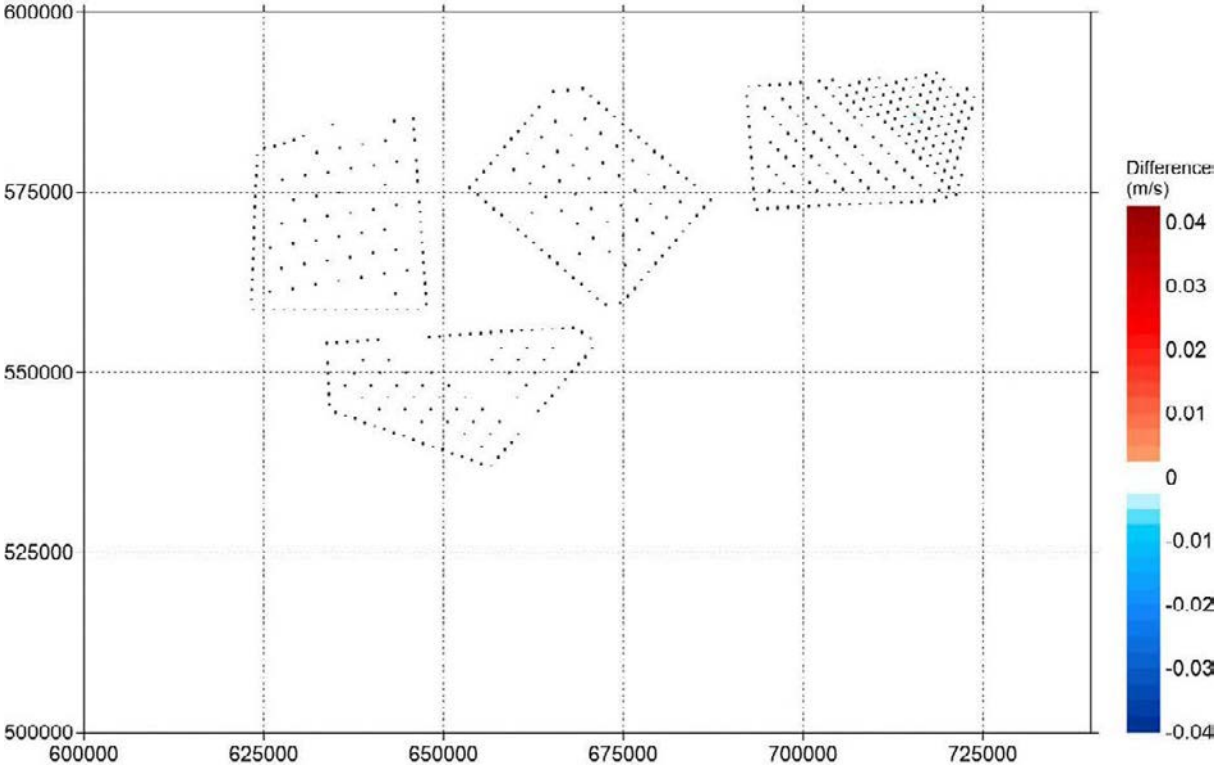

Figure B.24 Change of Speed of Peak North-west-going Currents in a Neap Tide (Scenario 1)

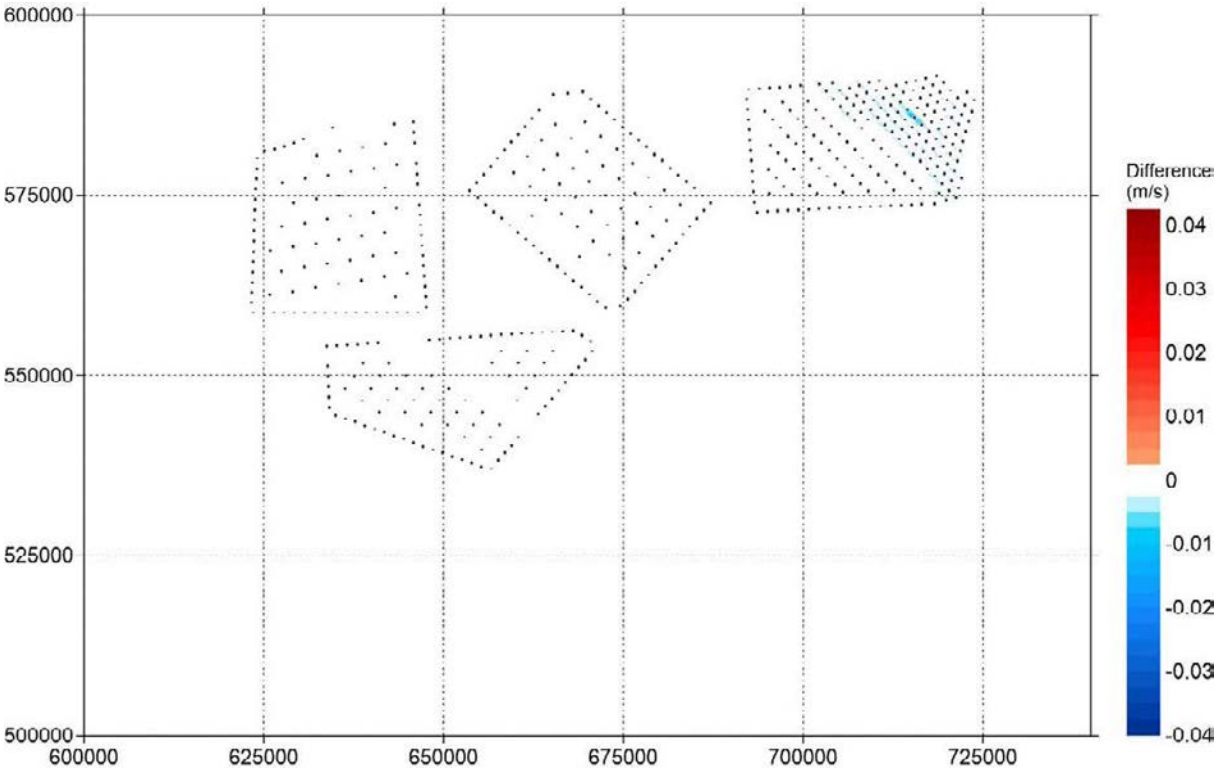

Figure B.25 Change of Maximum Current Speed Over 30 days (Scenario 1)

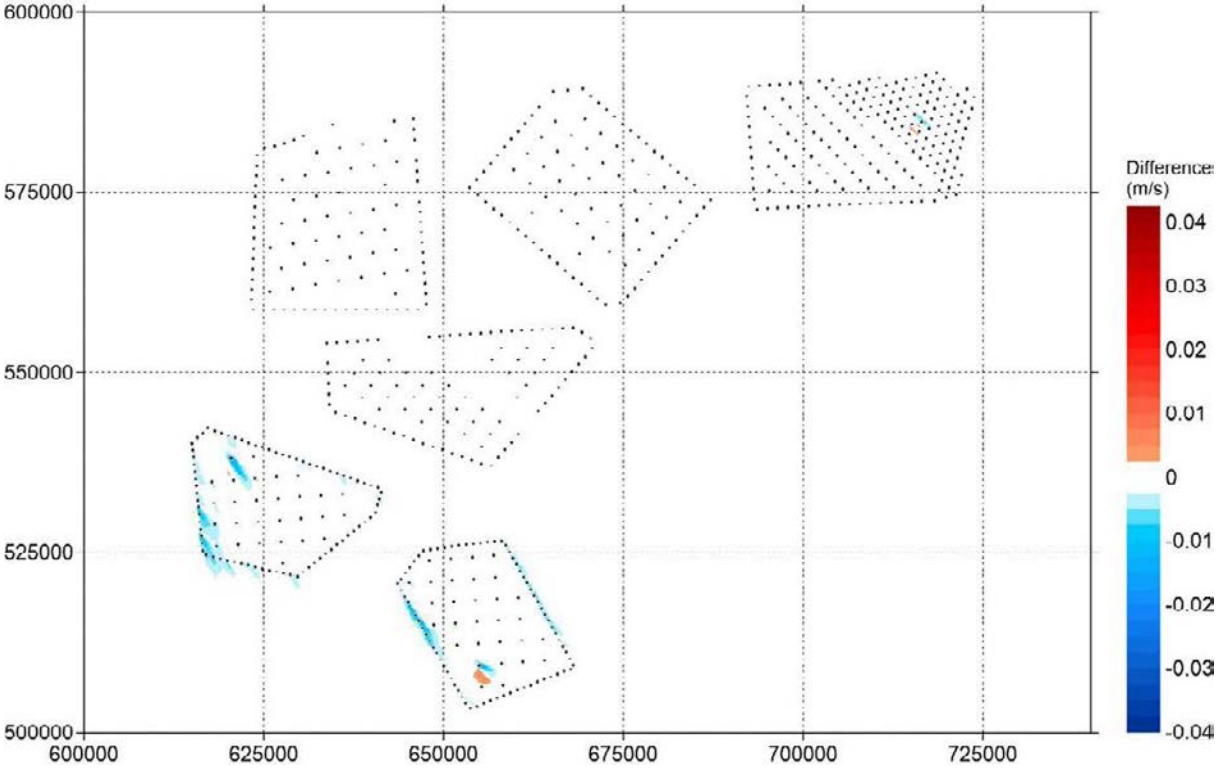

Figure B.26 Change of Speed of Peak South-east-going Currents in a Spring Tide (Scenario 2)

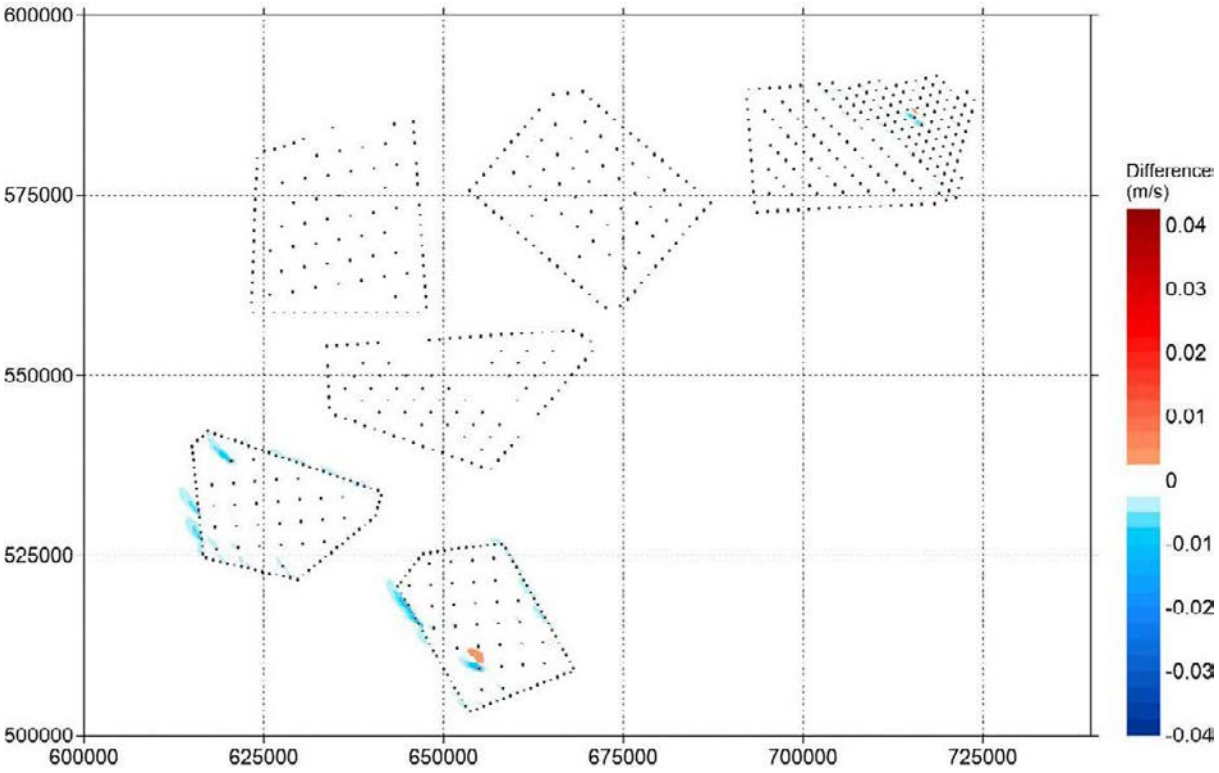

Figure B.27 Change of Speed of Peak North-west-going Currents in a Spring Tide (Scenario 2)

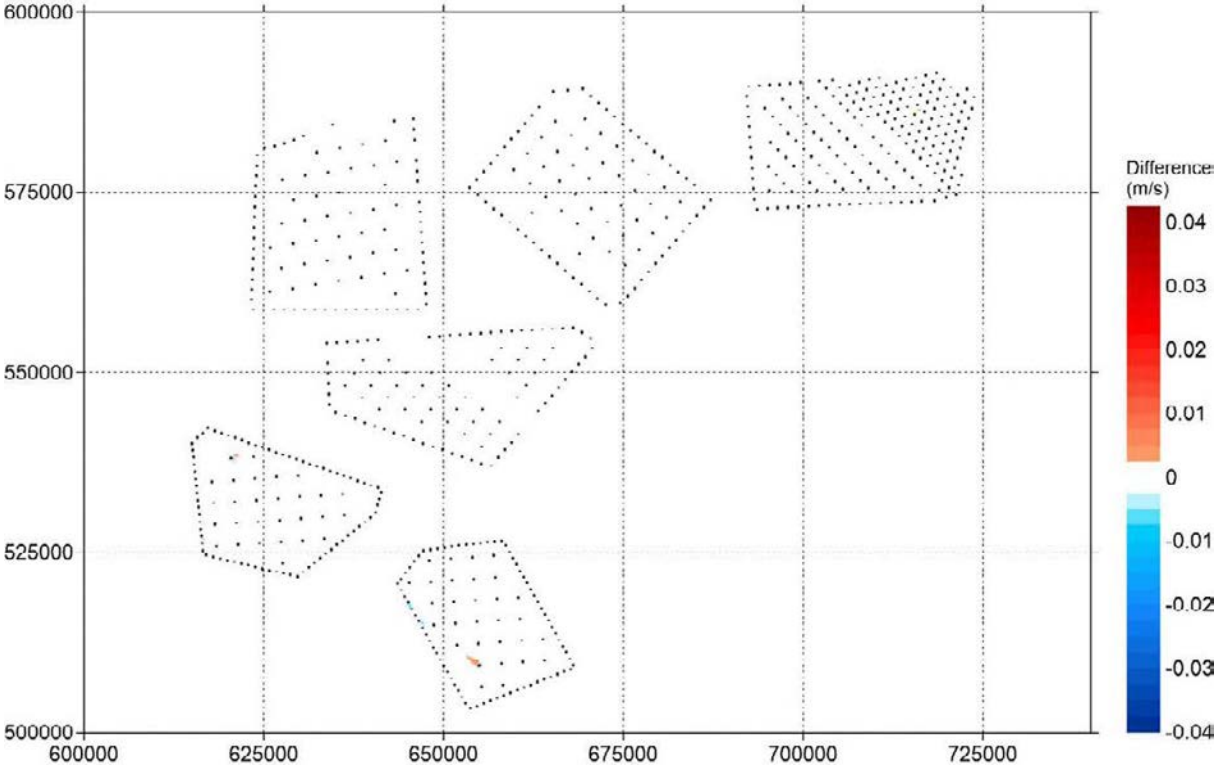

Figure B.28 Change of Speed of Peak South-east-going Currents in a Neap Tide (Scenario 2)

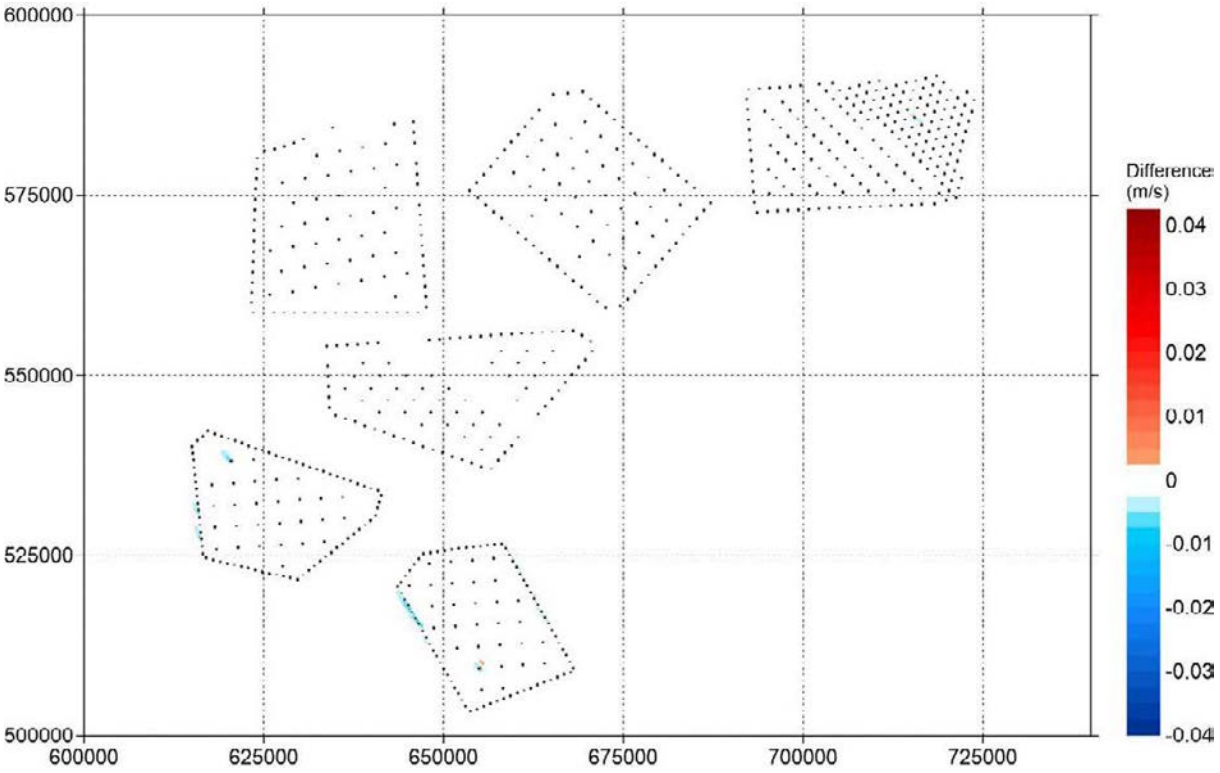

Figure B.29 Change of Speed of Peak North-west-going Currents in a Neap Tide (Scenario 2)

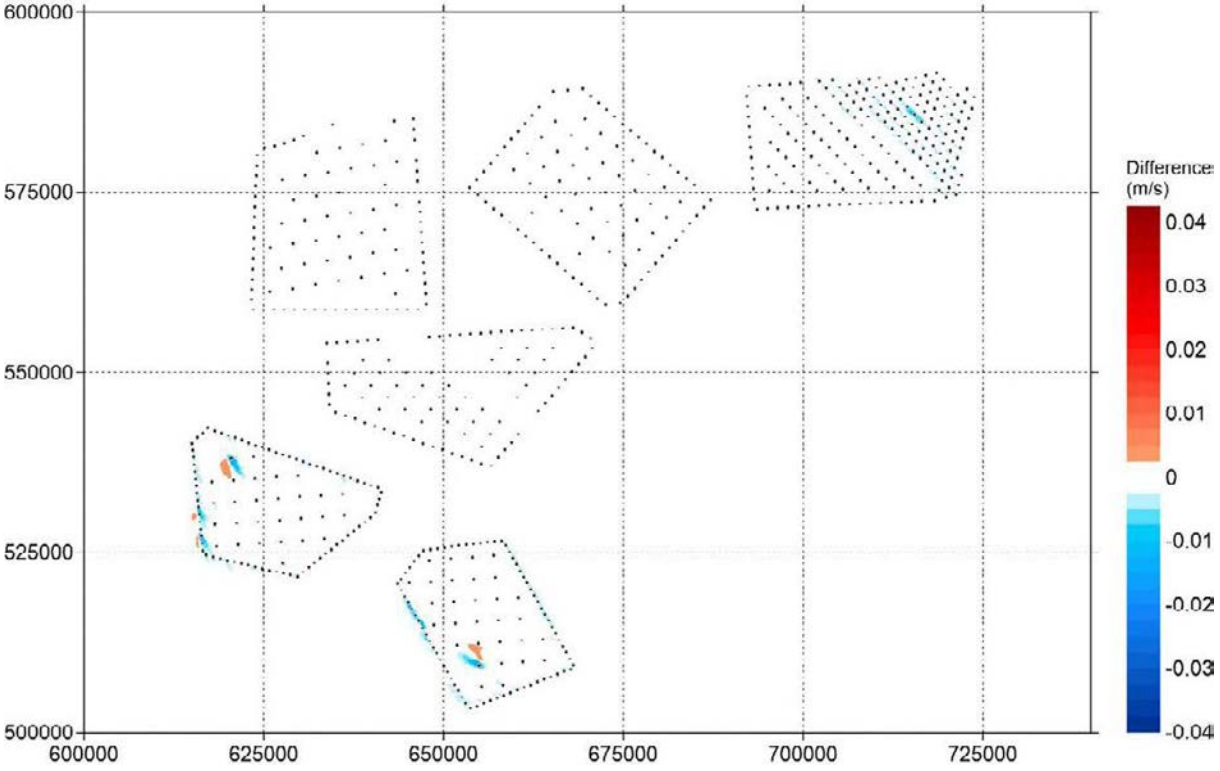

Figure B.30 Change of Maximum Current Speed Over 30 days (Scenario 2)

Appendix C: Hydrodynamic Modelling Cumulative Run Results – Layout B, Offshore Platform 2

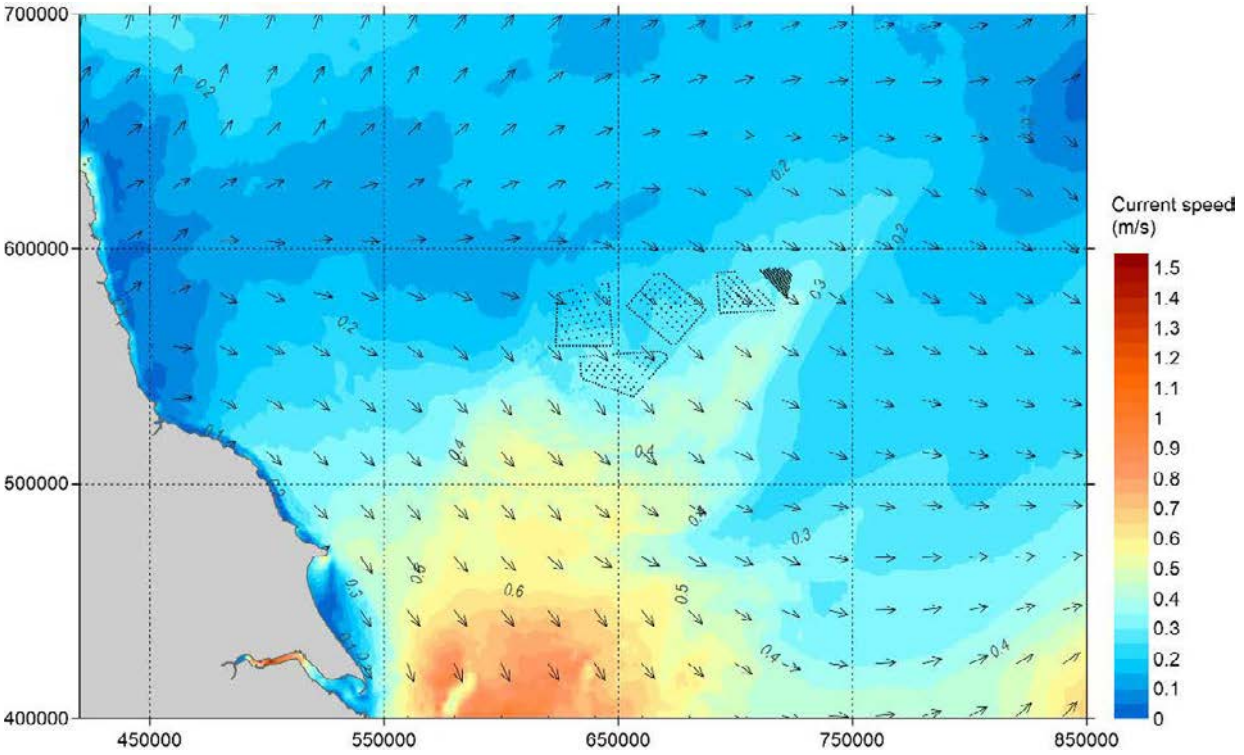

Figure C.1 Overview of Spatial Variation of Peak South-east-going Currents in a Spring Tide – Scenario 1

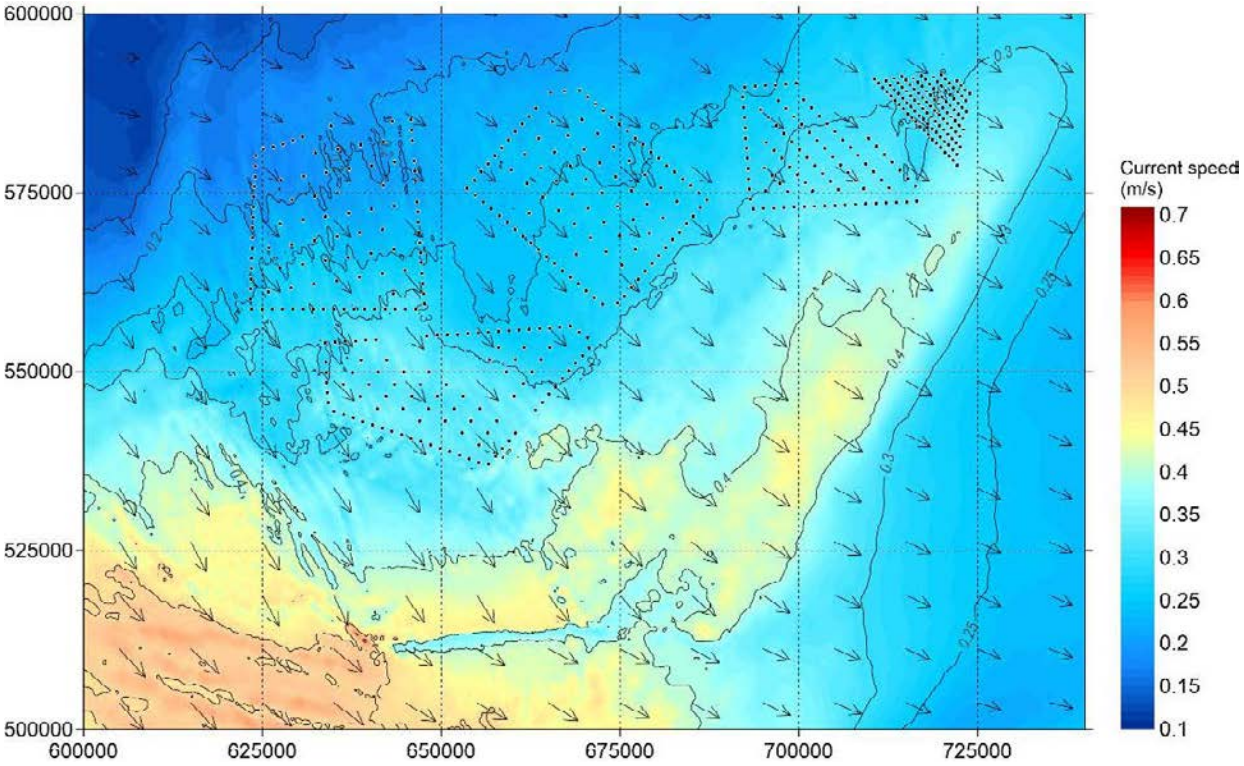

Figure C.2 A Closer View of Spatial Variation of Peak South-east-going Currents in a Spring Tide - Scenario 1

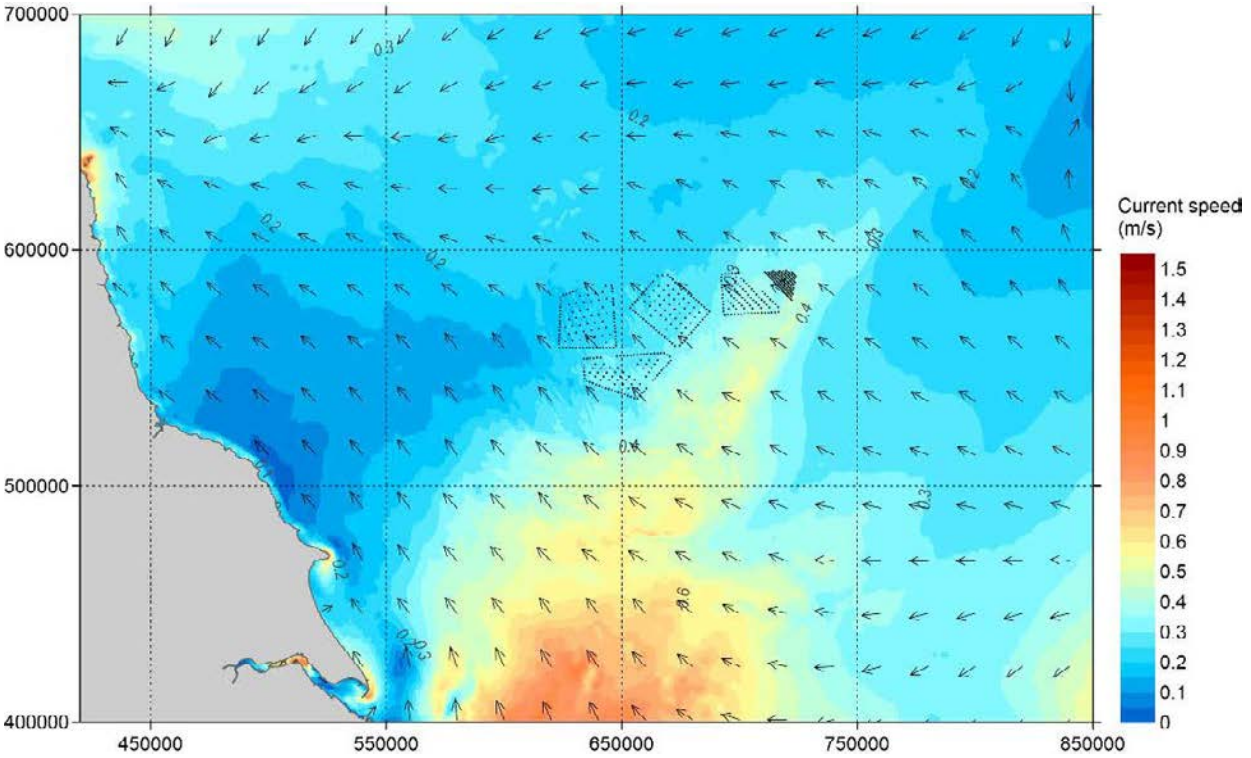

Figure C.3 Overview of Spatial Variation of Peak North-west-going Currents in a Spring Tide – Scenario 1

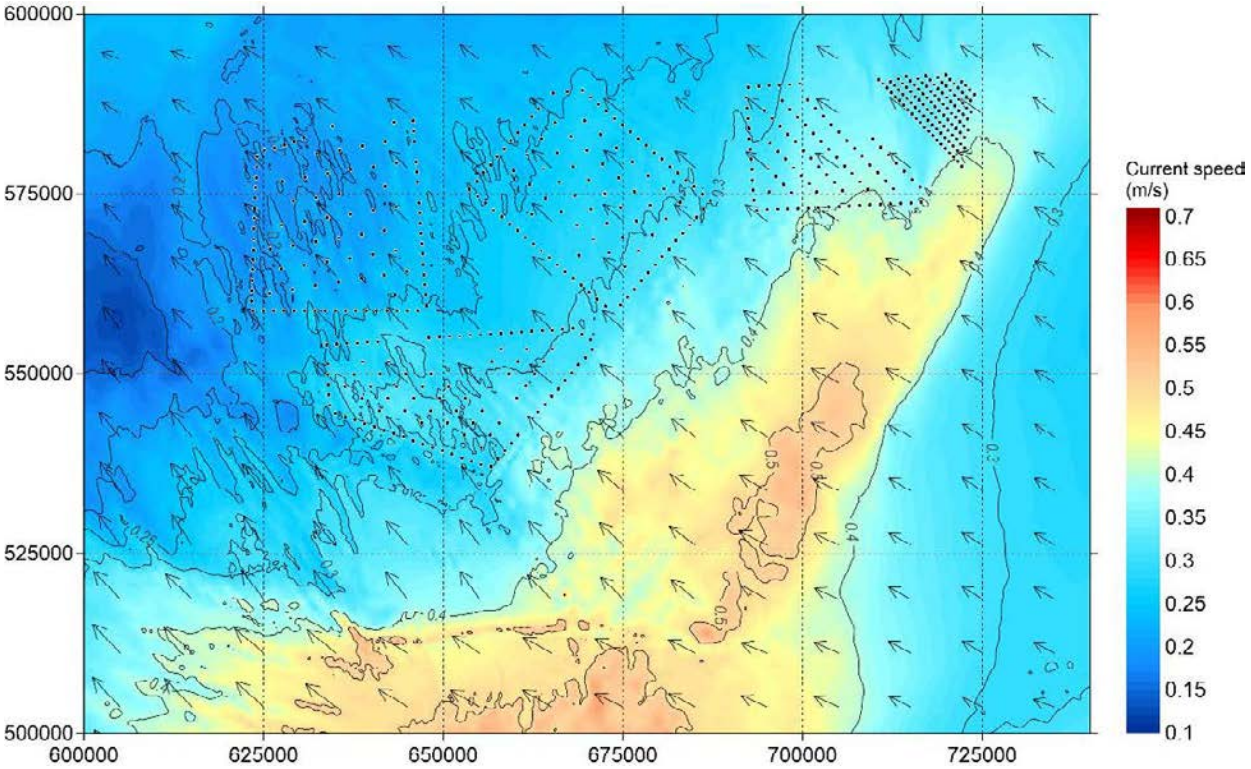

Figure C.4 A Closer View of Spatial Variation of Peak North-west-going Currents in a Spring Tide – Scenario 1

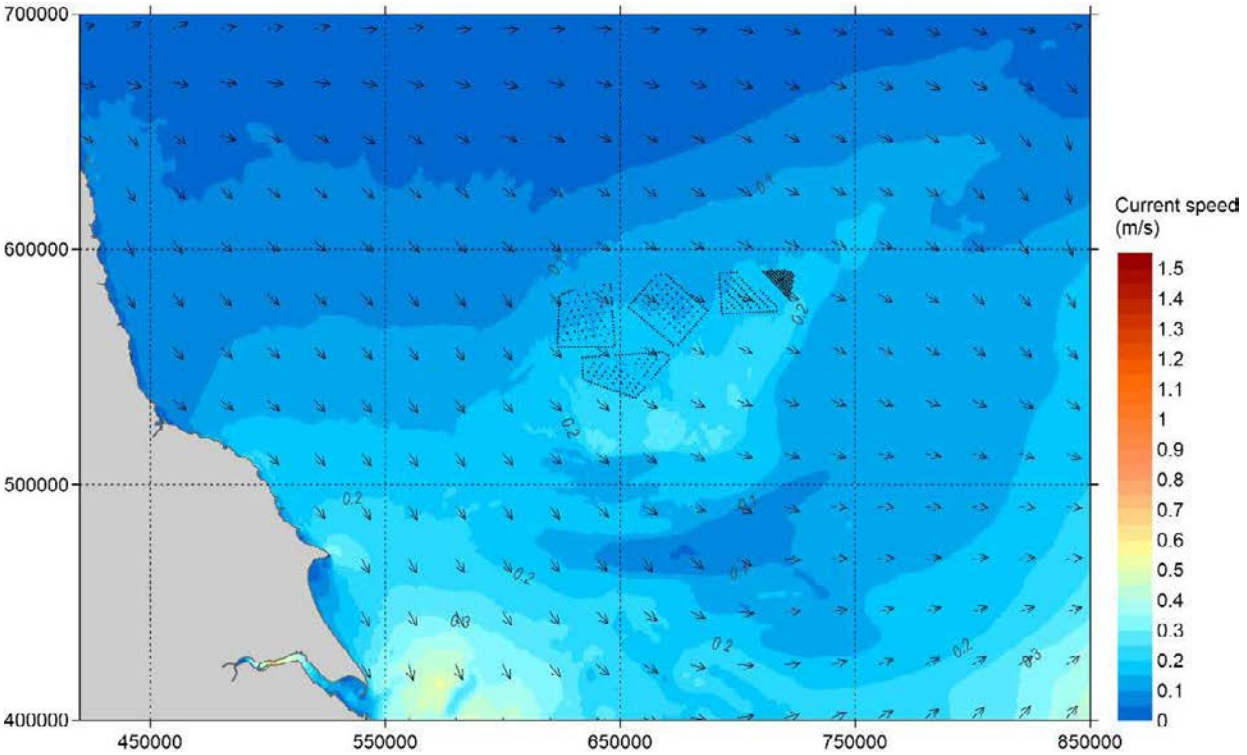

Figure C.5 Overview of Spatial Variation of Peak South-east-going Currents in a Neap Tide – Scenario 1

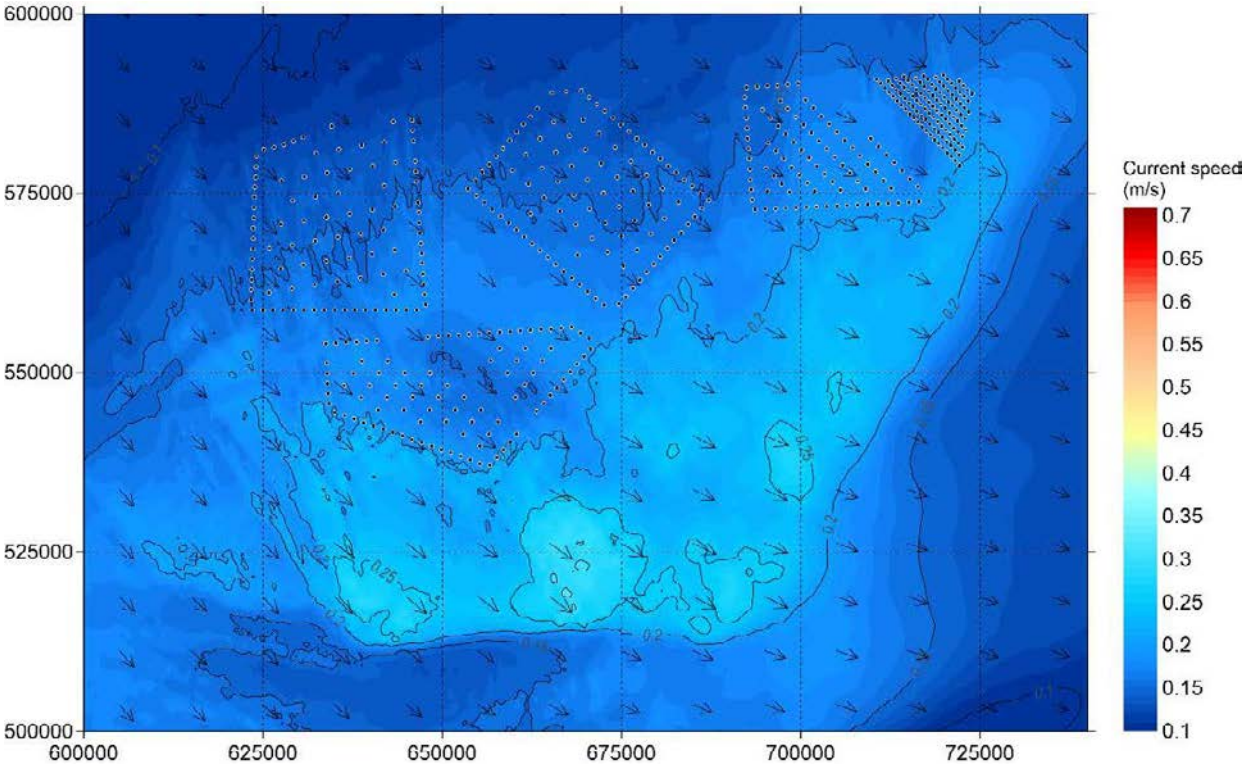

Figure C.6 A Closer View of Spatial Variation of Peak South-east-going Currents in a Neap Tide – Scenario 1

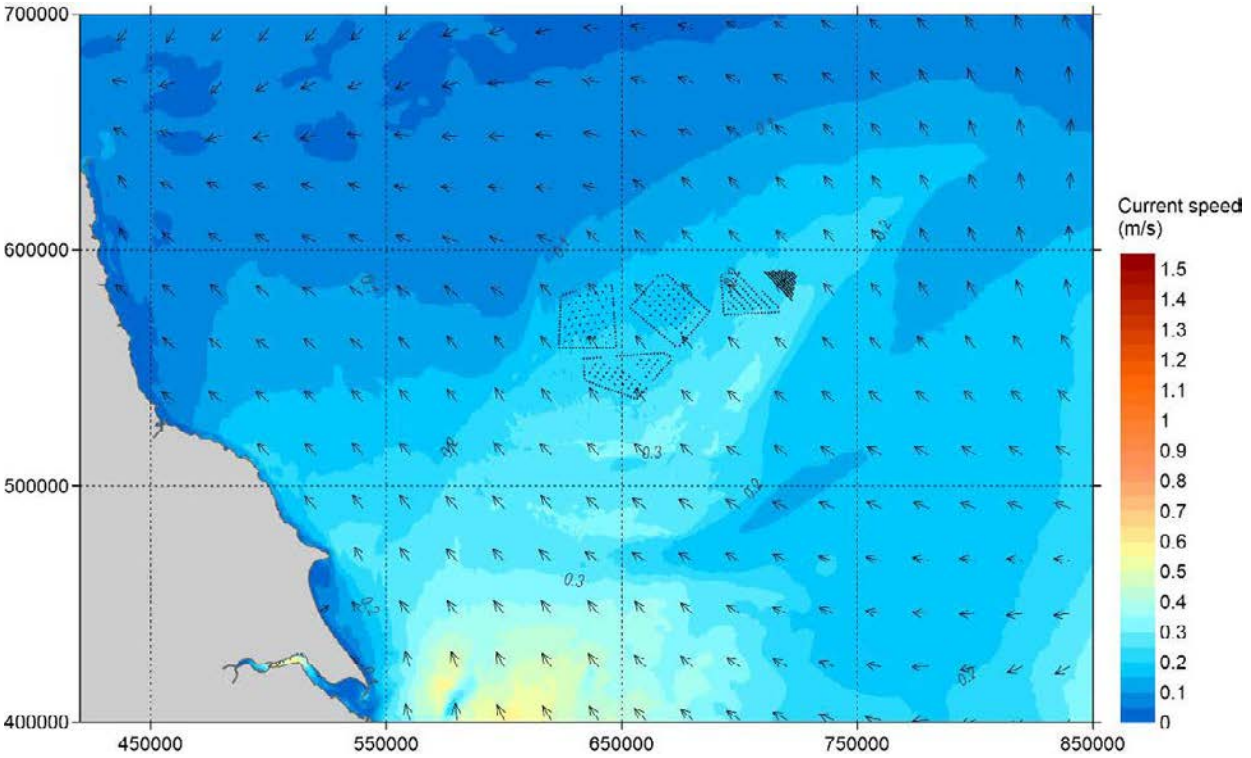

Figure C.7 Overview of Spatial Variation of Peak North-west-going Currents in a Neap Tide – Scenario 1

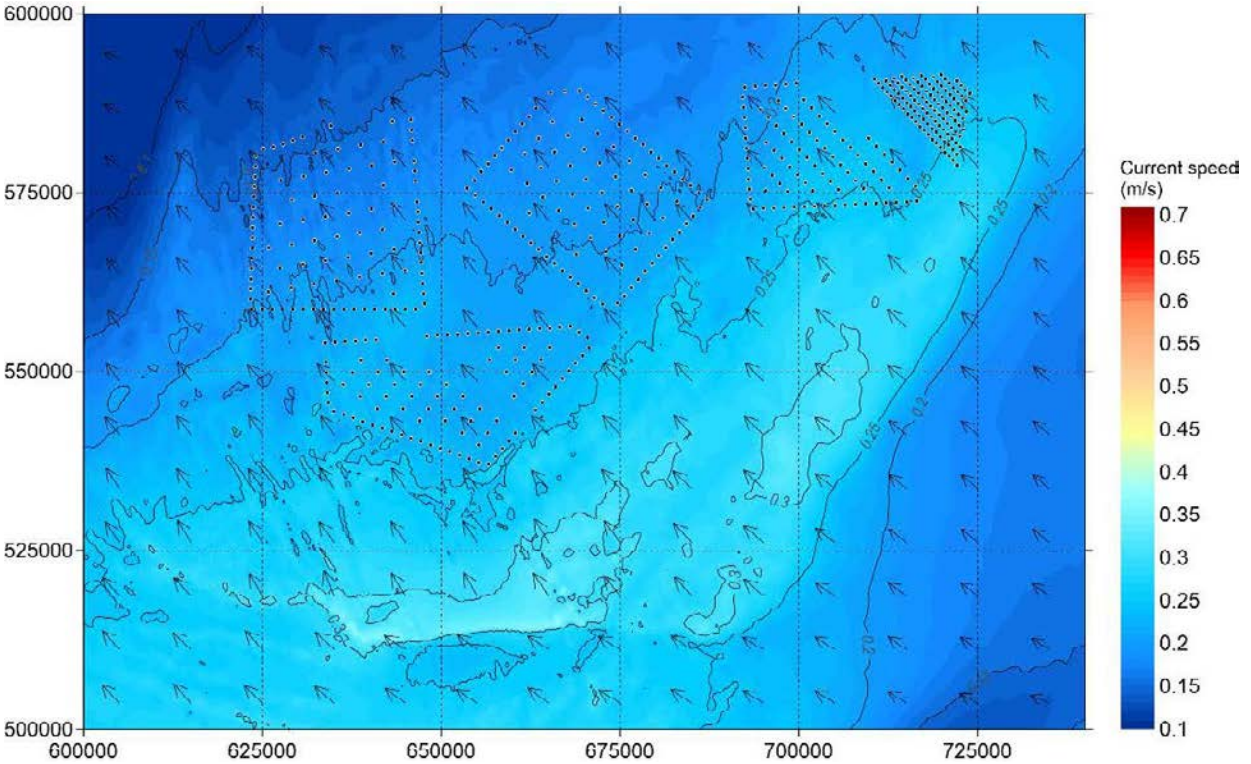

Figure C.8 A Closer View of Spatial Variation of Peak North-west-going Currents in a Neap Tide – Scenario 1

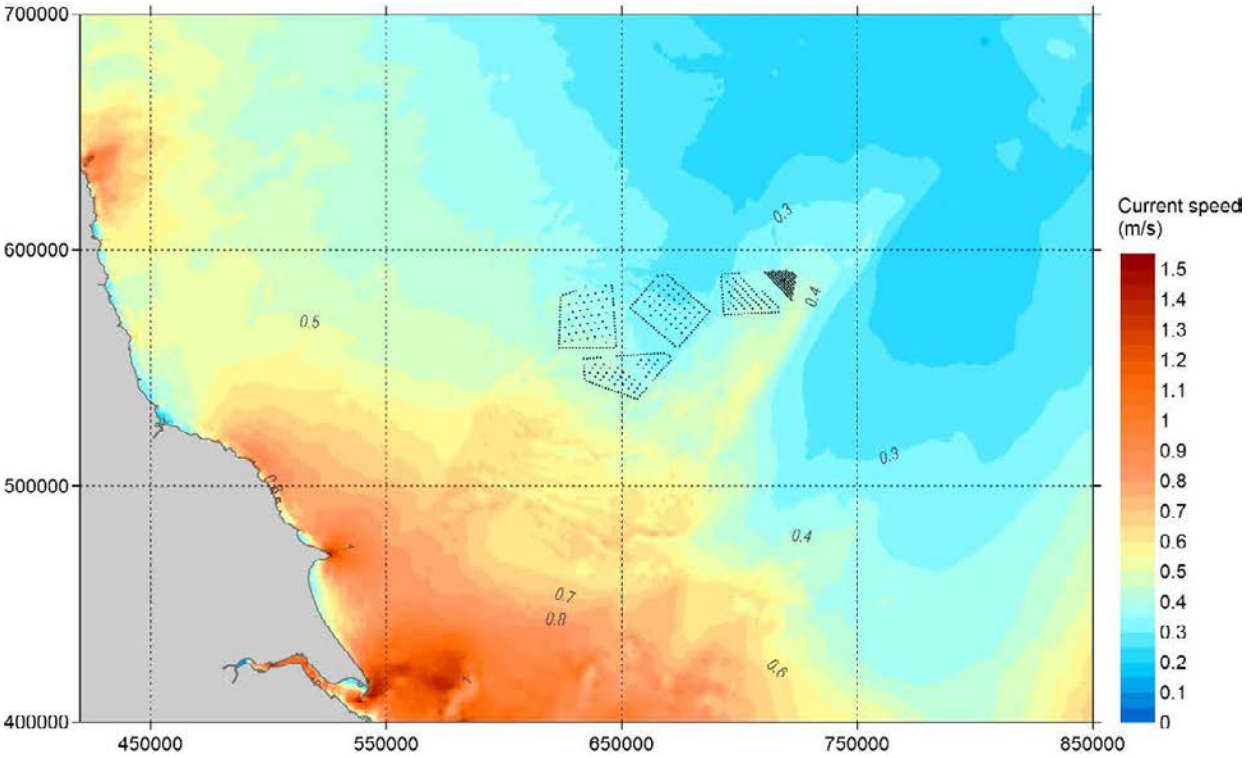

Figure C.9 Overview of Spatial Variation of Maximum Current Speed Over 30 days- Scenario 1

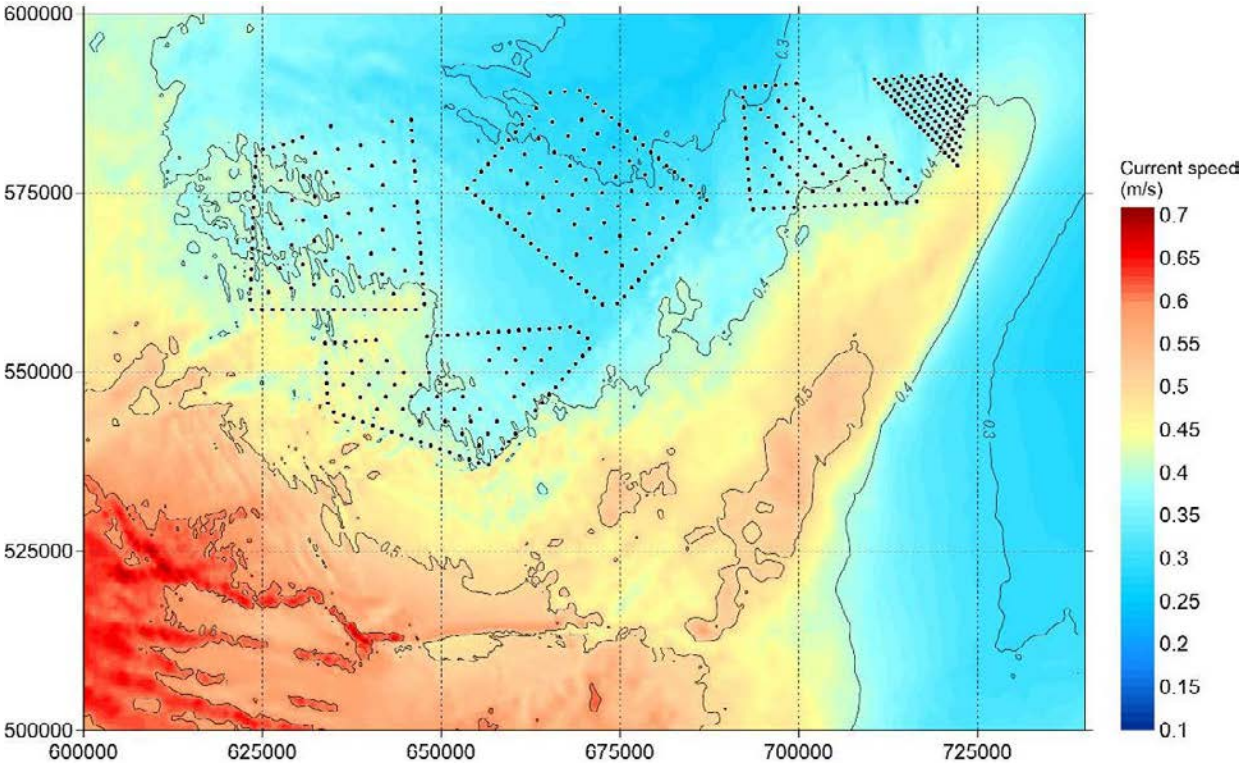

Figure C.10 A Closer View of Spatial Variation of Maximum Current Speed Over 30 days- Scenario 1

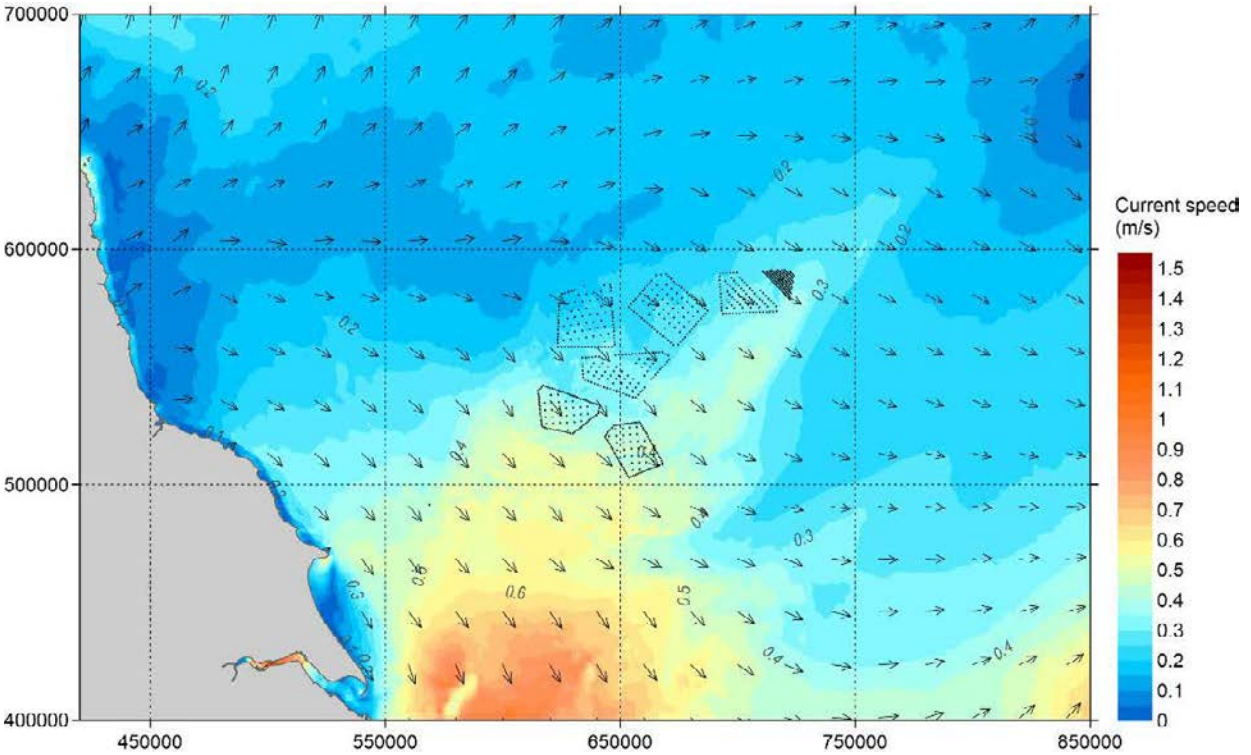

Figure C.11 Overview of Spatial Variation of Peak South-east-going Currents in a Spring Tide – Scenario 2

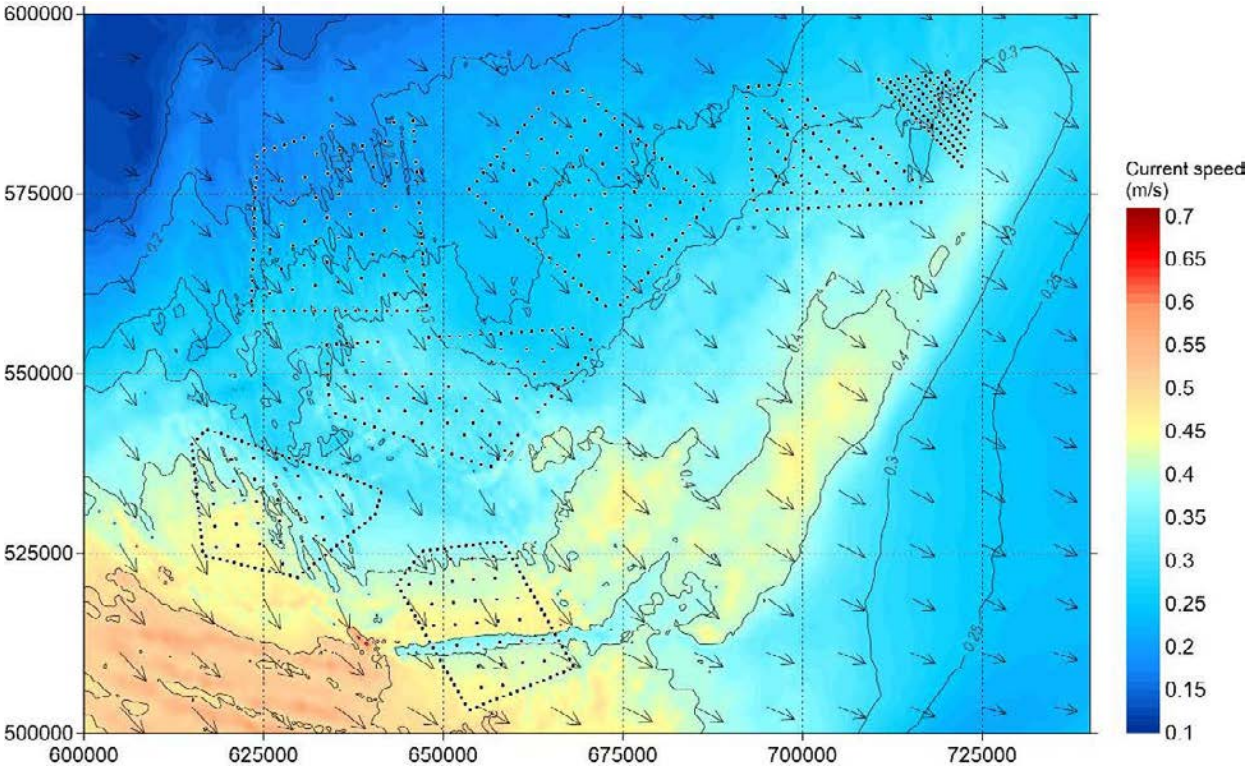

Figure C.12 A Closer View of Spatial Variation of Peak South-east-going Currents in a Spring Tide - Scenario 2

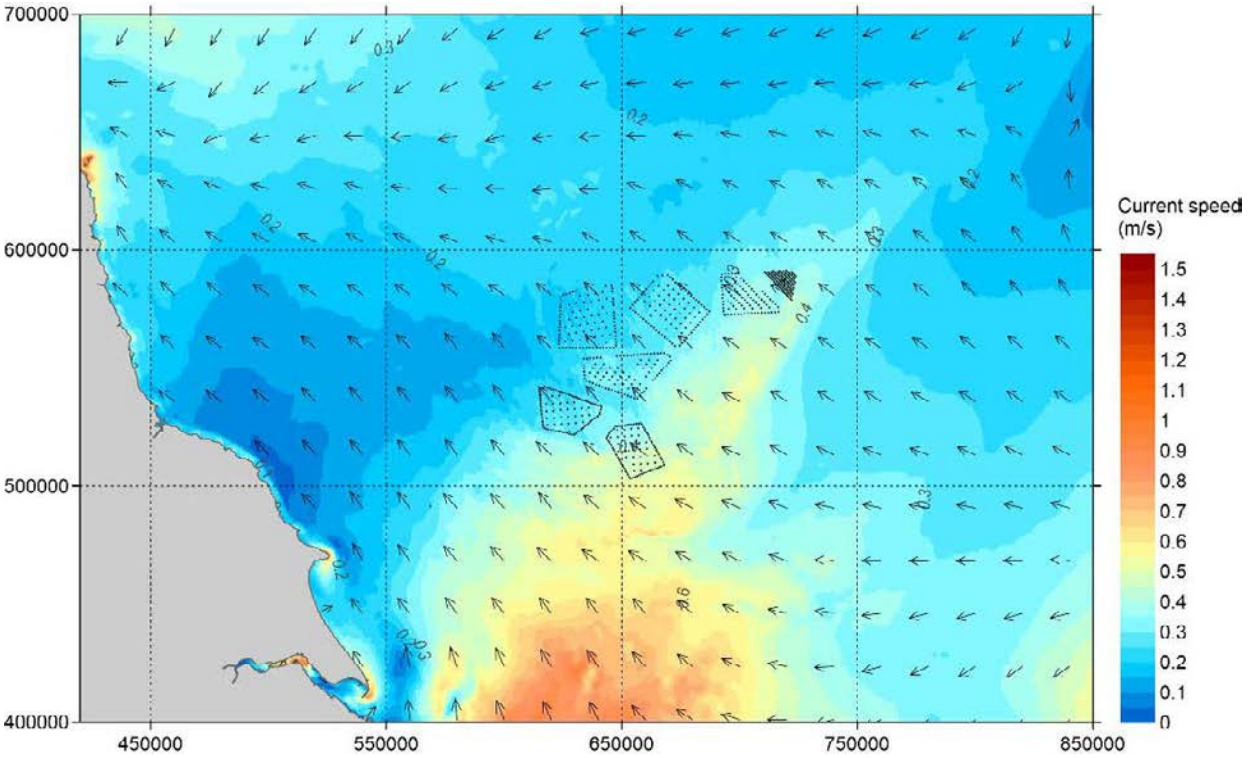

Figure C.13 Overview of Spatial Variation of Peak North-west-going Currents in a Spring Tide – Scenario 2

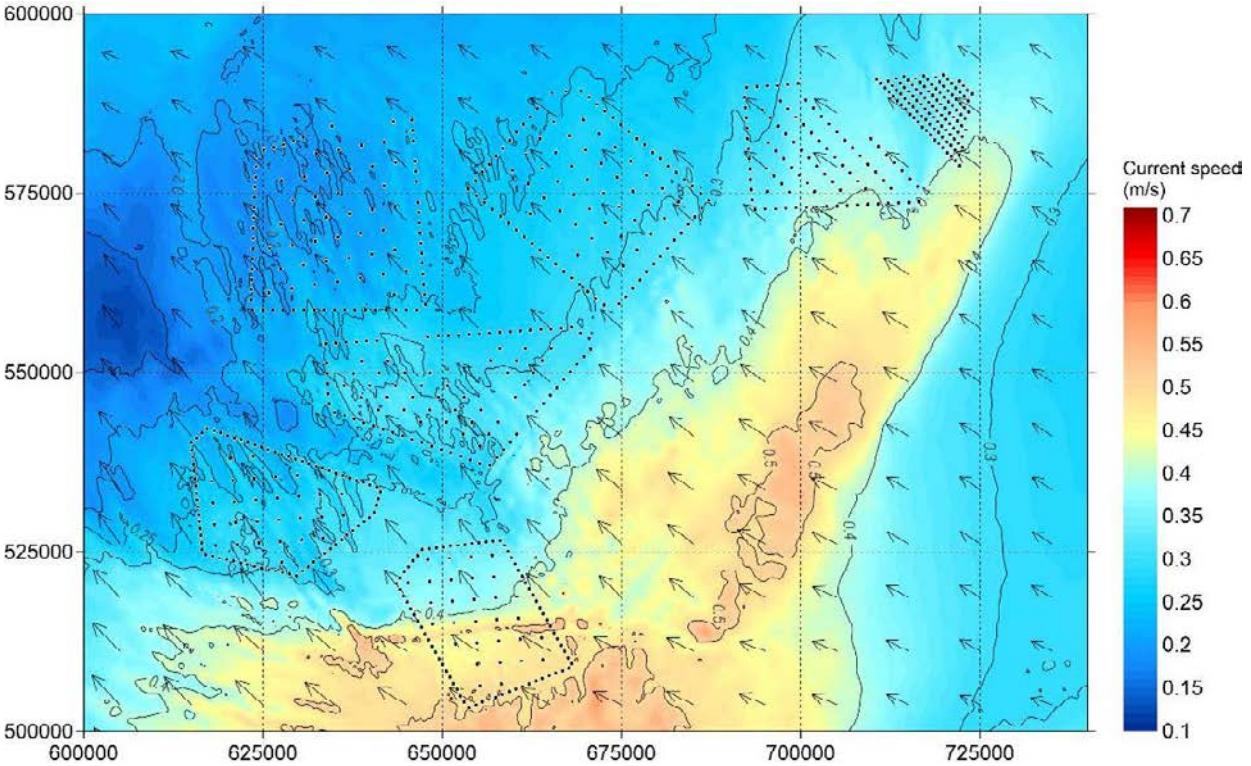

Figure C.14 A Closer View of Spatial Variation of Peak North-west-going Currents in a Spring Tide – Scenario 2

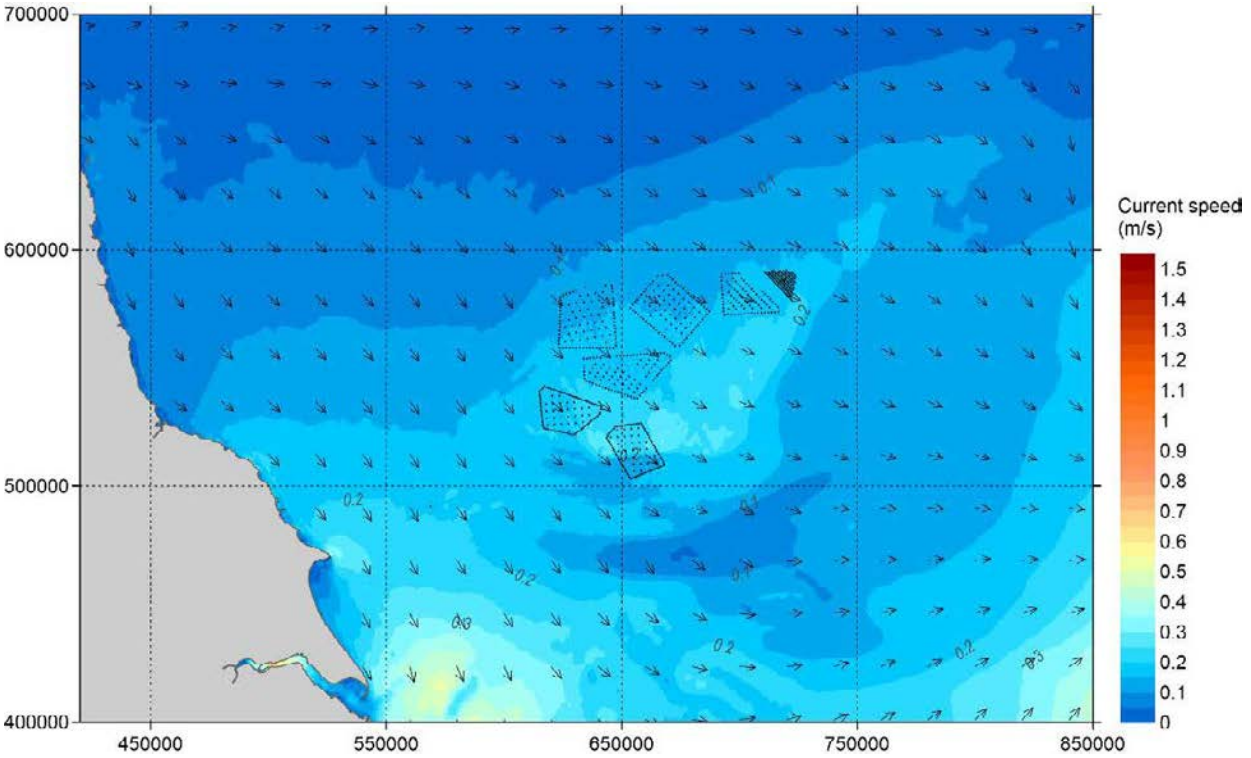

Figure C.15 Overview of Spatial Variation of Peak South-east-going Currents in a Neap Tide – Scenario 2

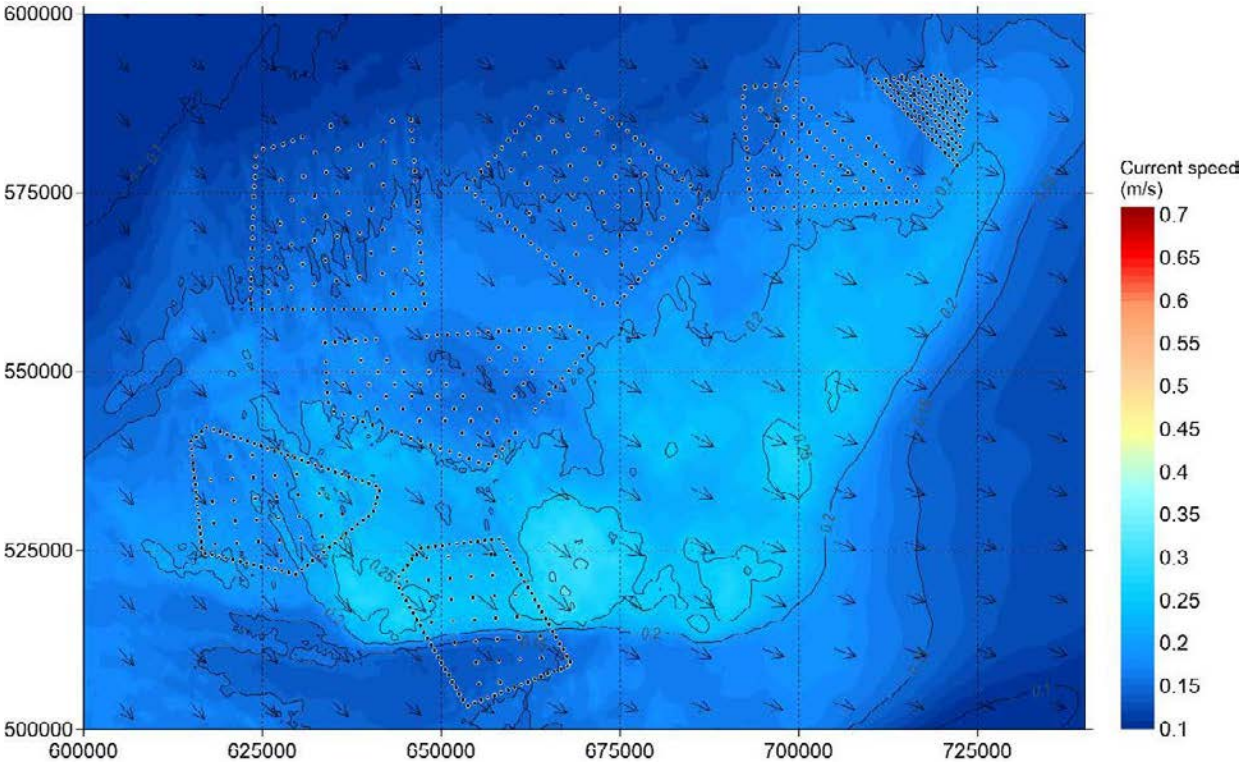

Figure C.16 A Closer View of Spatial Variation of Peak South-east-going Currents in a Neap Tide – Scenario 2

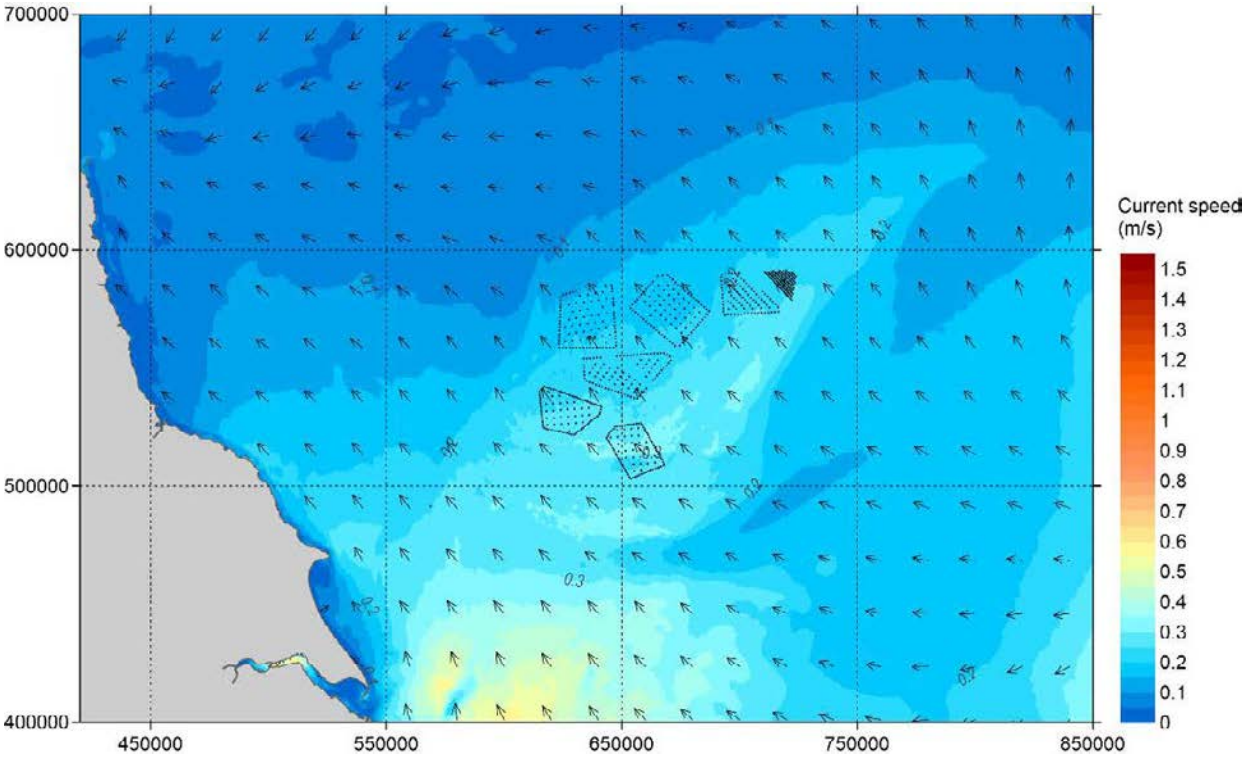

Figure C.17 Overview of Spatial Variation of Peak North-west-going Currents in a Neap Tide – Scenario 2

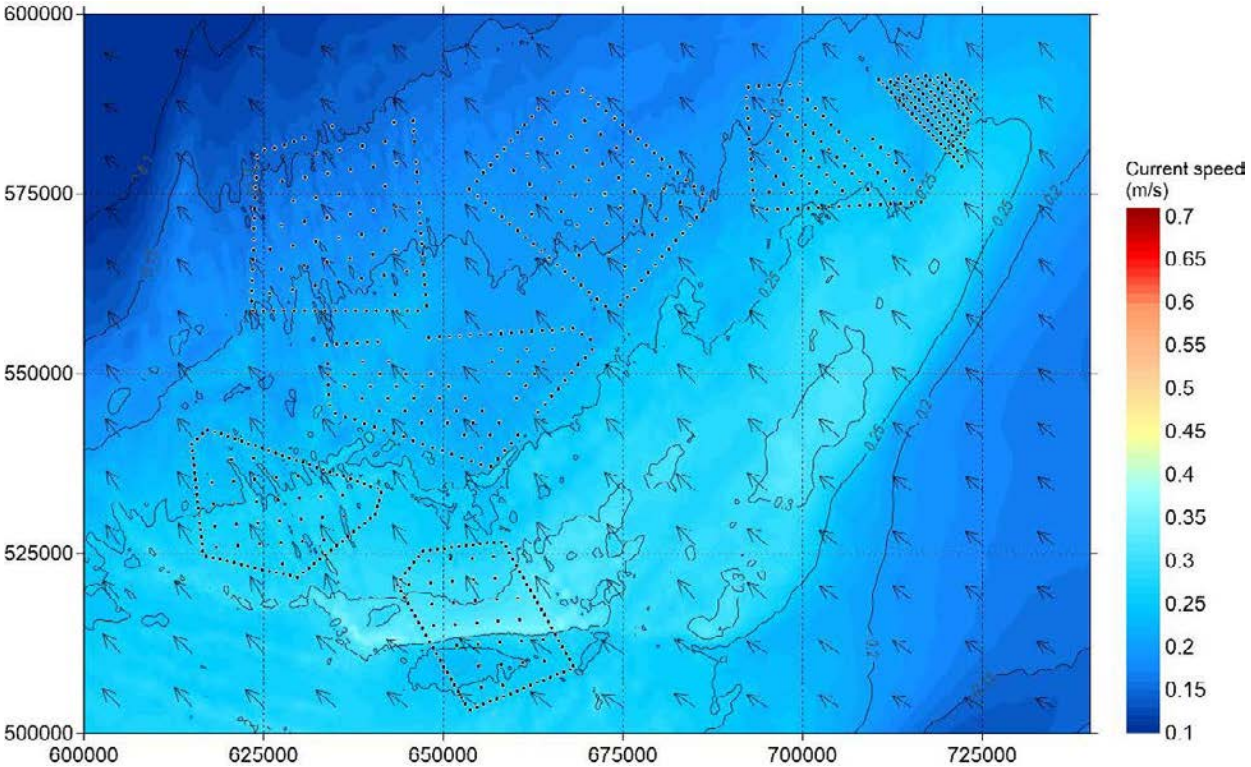

Figure C.18 A Closer View of Spatial Variation of Peak North-west-going Currents in a Neap Tide – Scenario 2

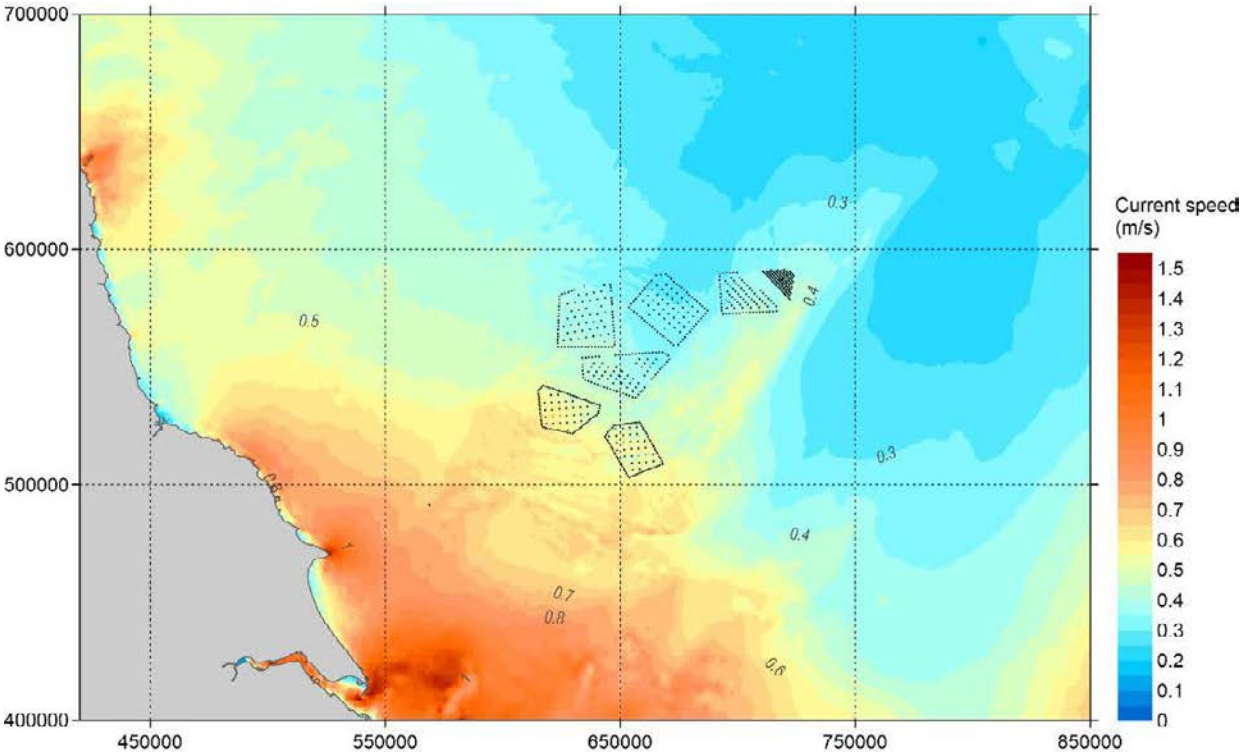

Figure C.19 Overview of Spatial Variation of Maximum Current Speed Over 30 days- Scenario 2

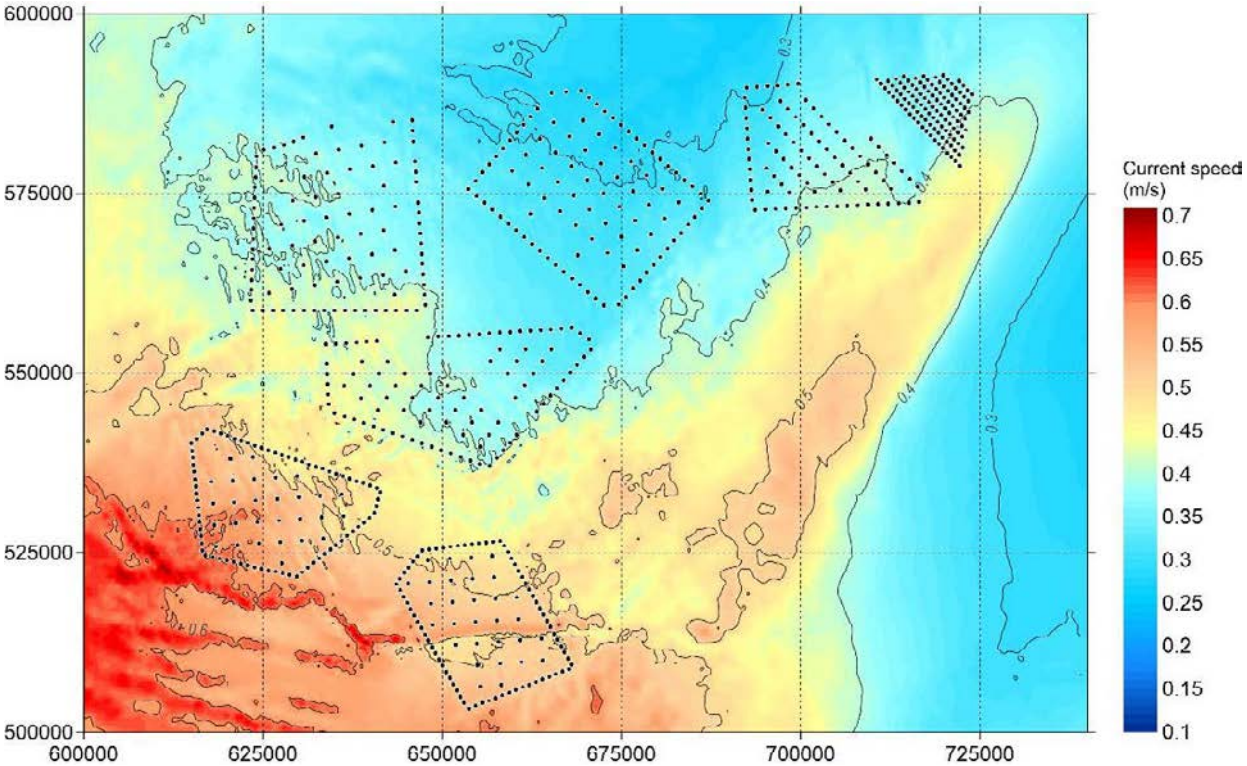

Figure C.20 A Closer View of Spatial Variation of Maximum Current Speed Over 30 days- Scenario 2

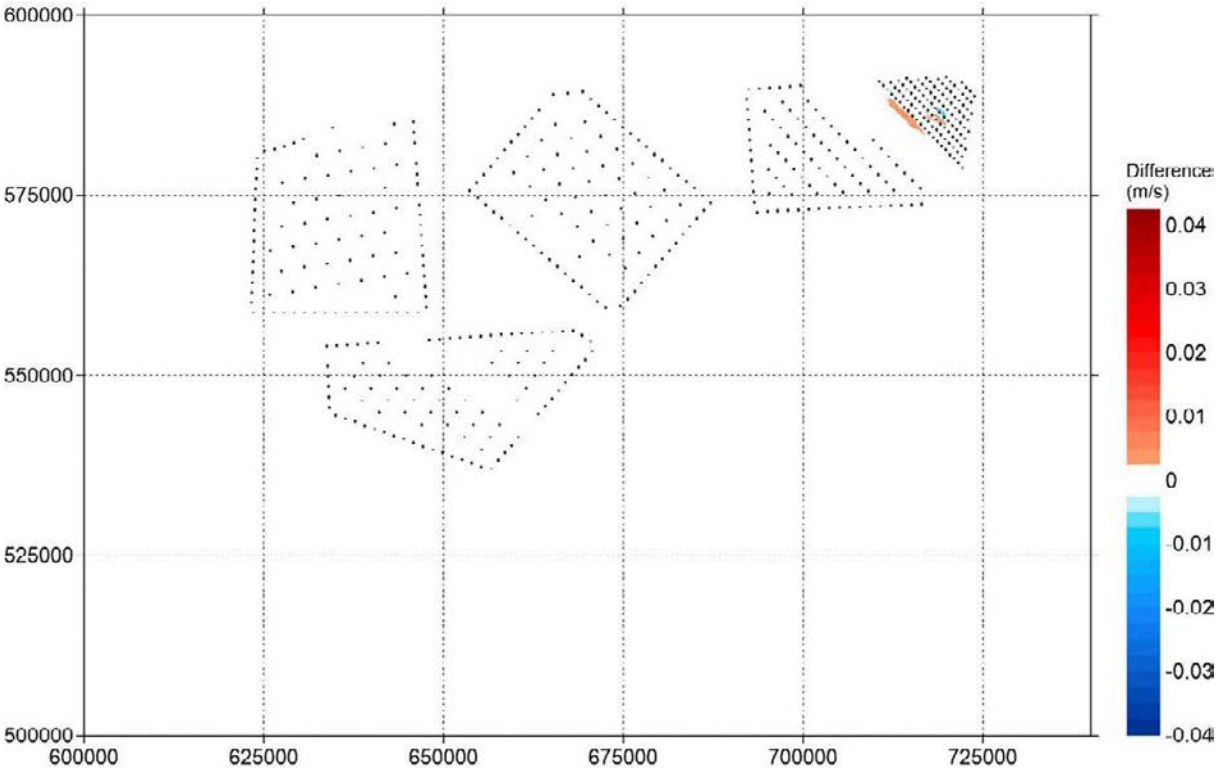

Figure C.21 Change of Speed of Peak South-east-going Currents in a Spring Tide (Scenario 1)

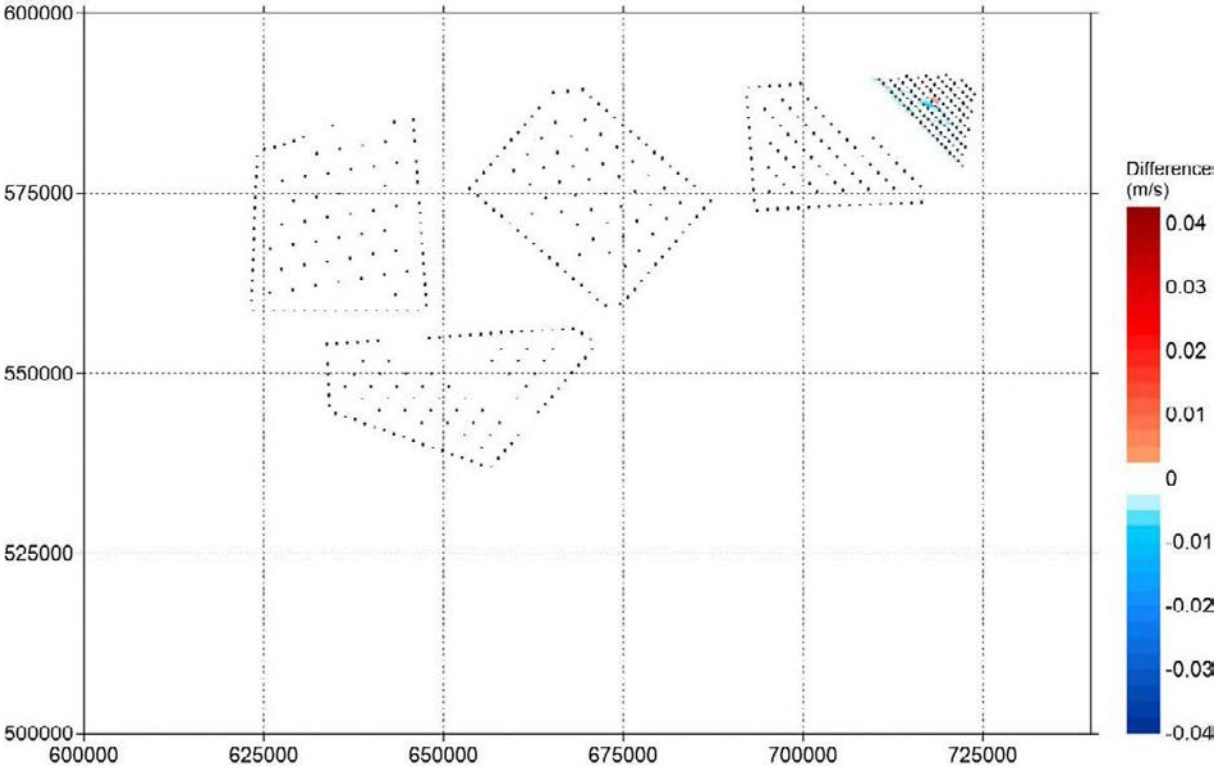

Figure C.22 Change of Speed of Peak North-west-going Currents in a Spring Tide (Scenario 1)

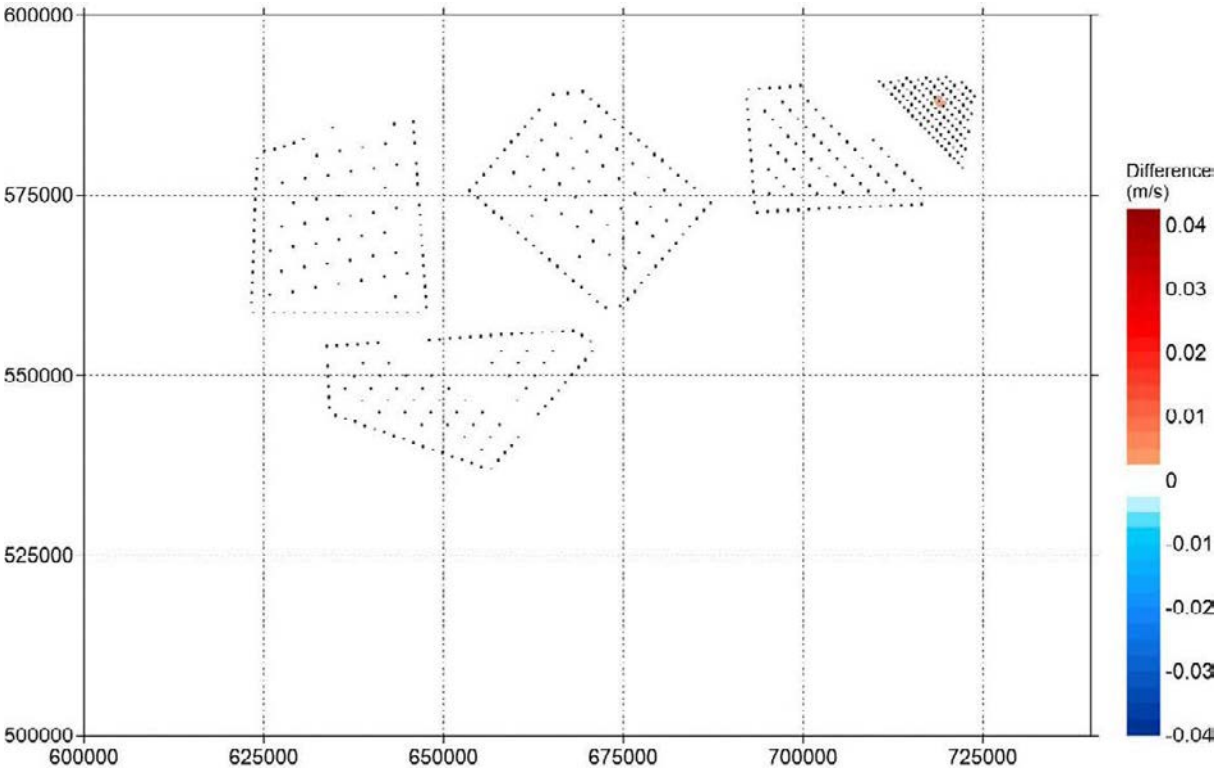

Figure C.23 Change of Speed of Peak South-east-going Currents in a Neap Tide (Scenario 1)

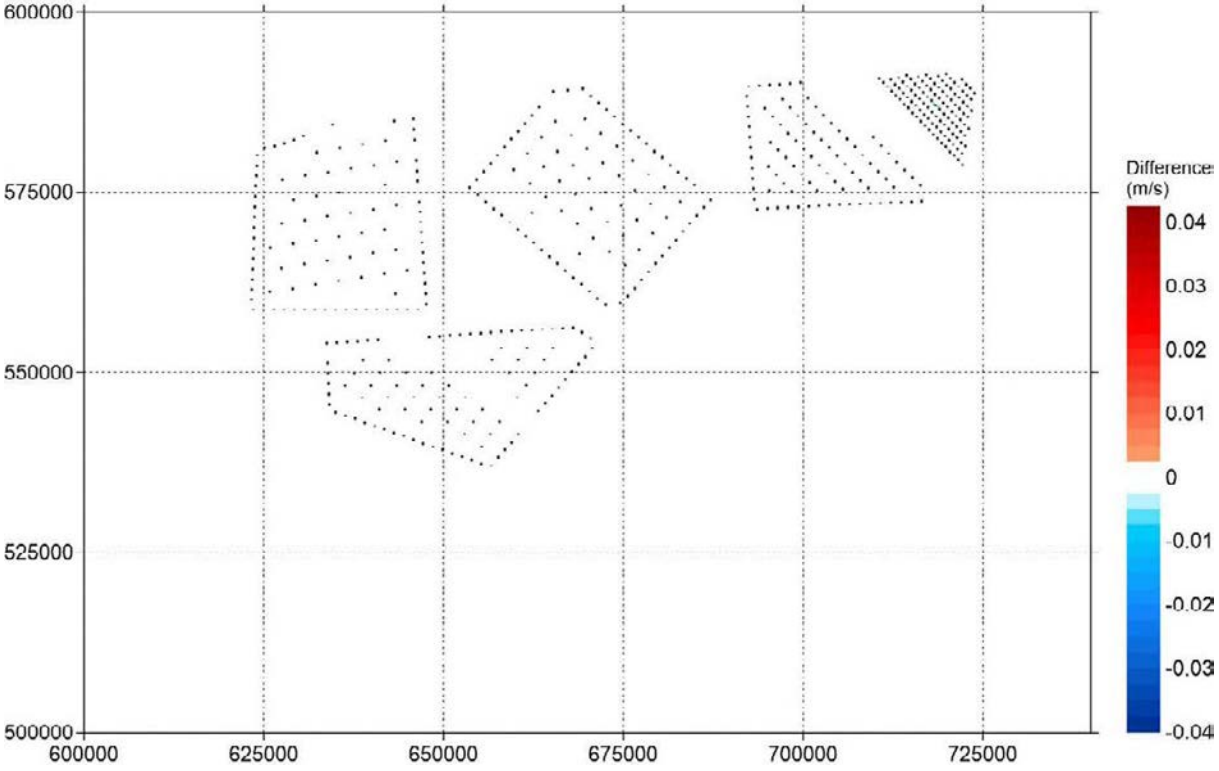

Figure C.24 Change of Speed of Peak North-west-going Currents in a Neap Tide (Scenario 1)

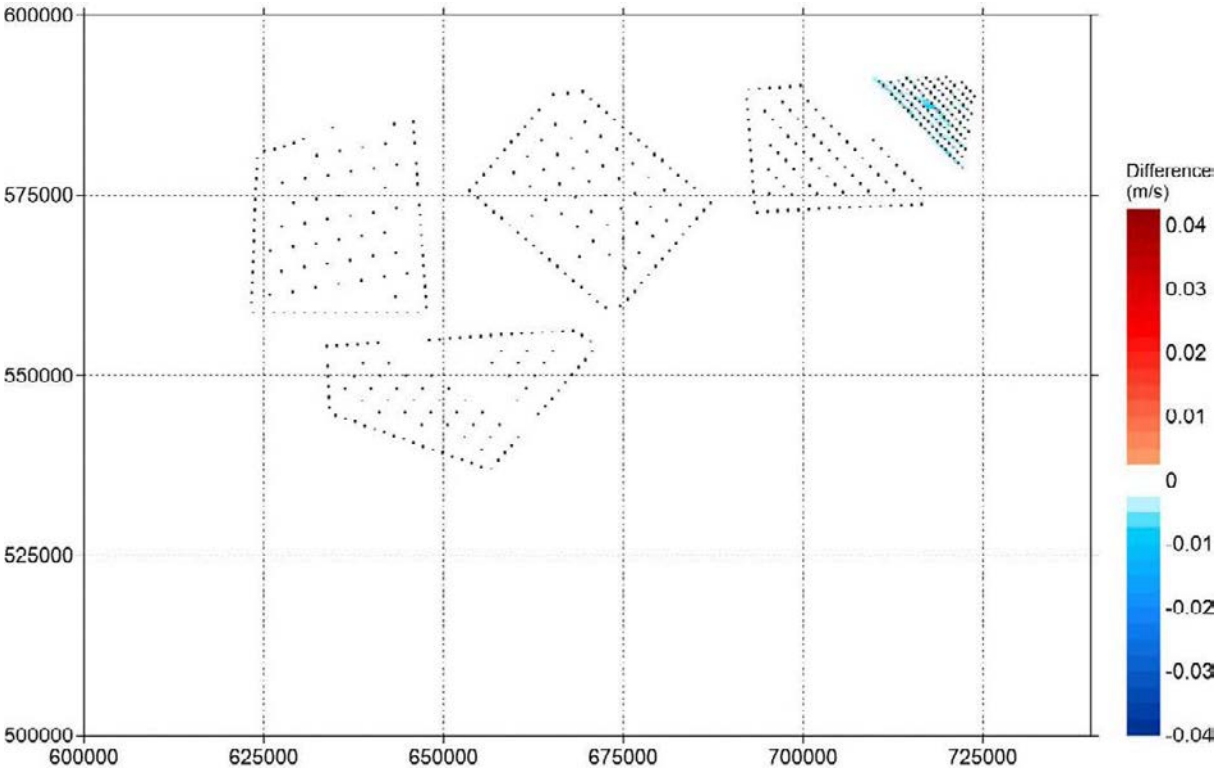

Figure C.25 Change of Maximum Current Speed Over 30 days (Scenario 1)

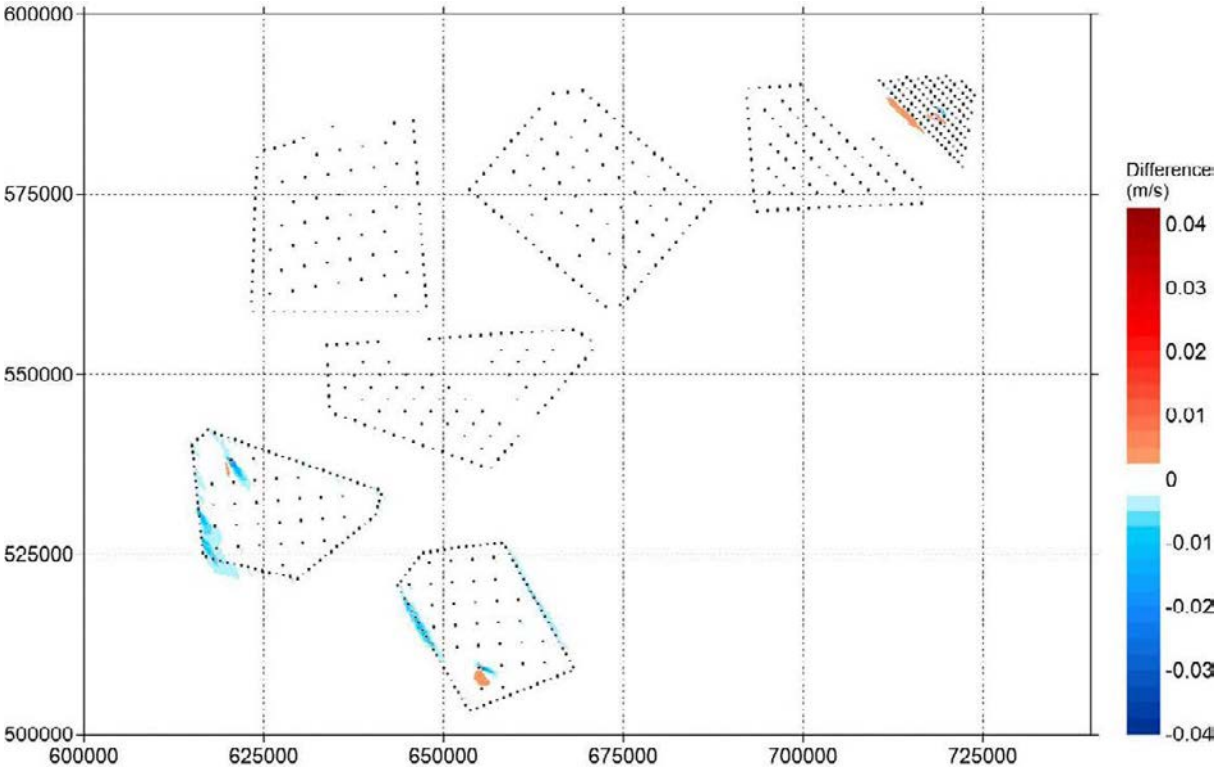

Figure C.26 Change of Speed of Peak South-east-going Currents in a Spring Tide (Scenario 2)

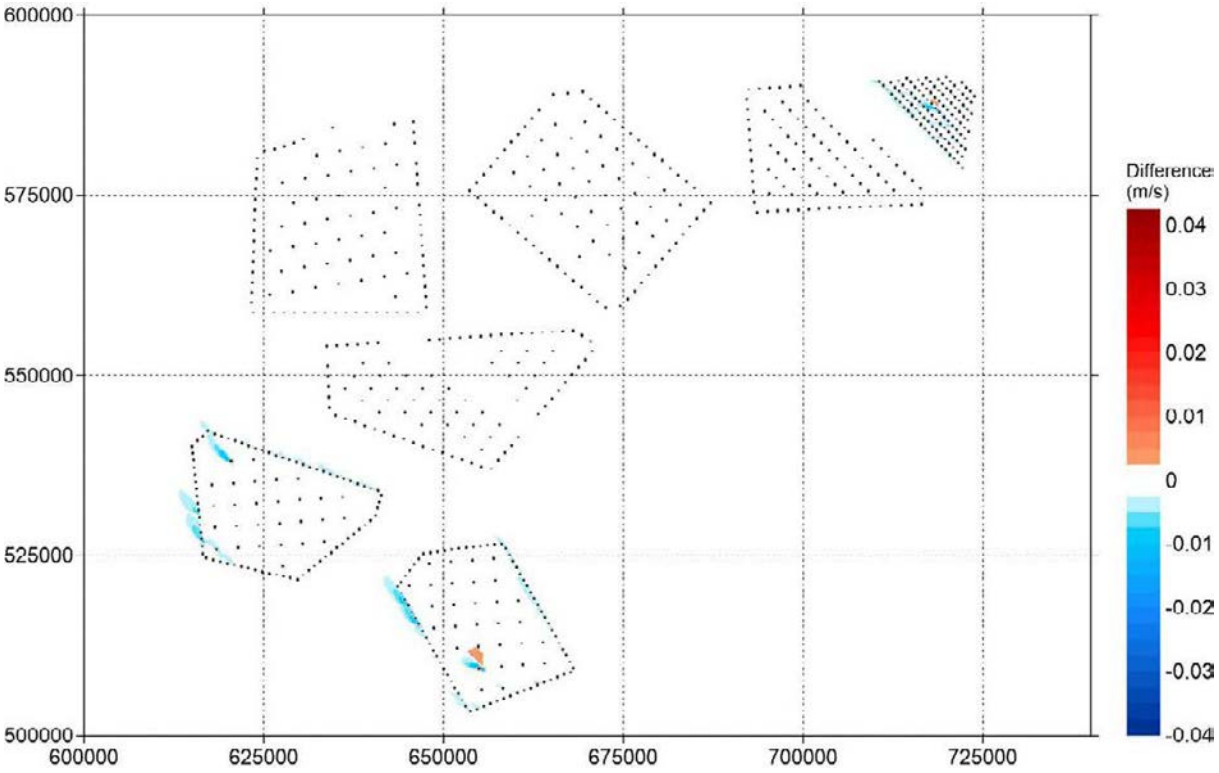

Figure C.27 Change of Speed of Peak North-west-going Currents in a Spring Tide (Scenario 2)

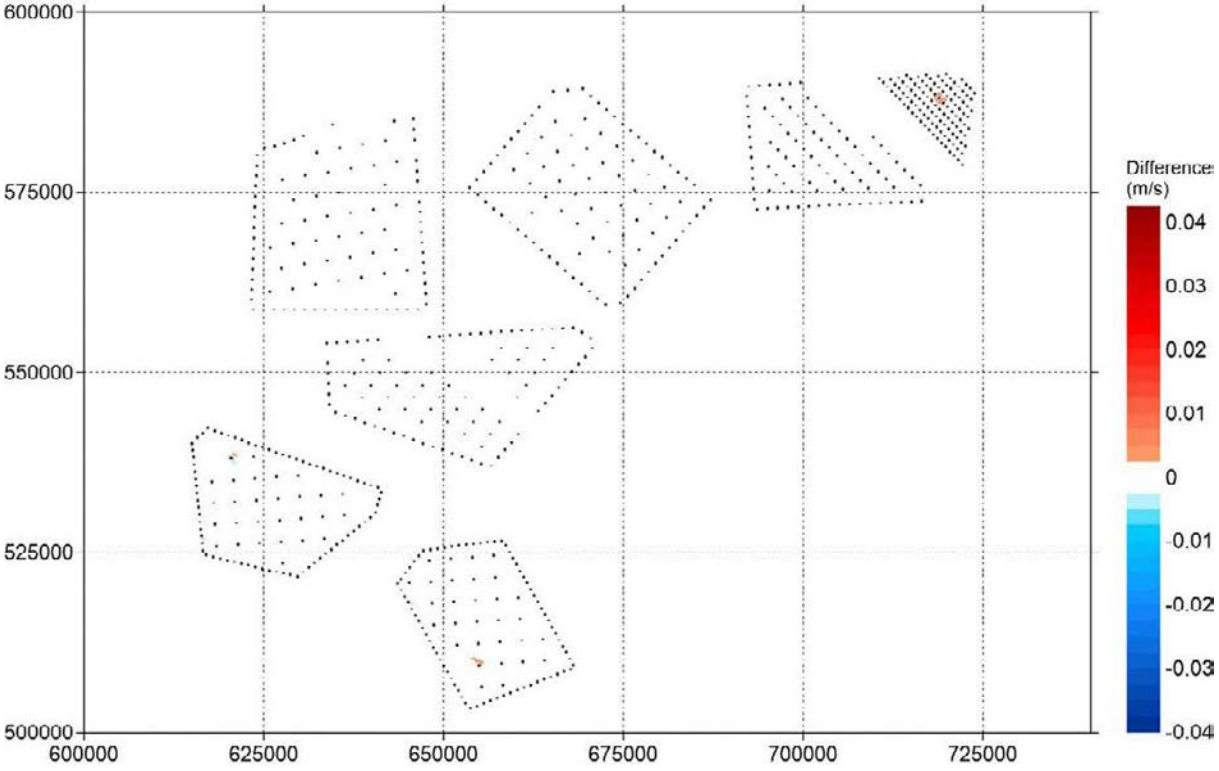

Figure C.28 Change of Speed of Peak South-east-going Currents in a Neap Tide (Scenario 2)

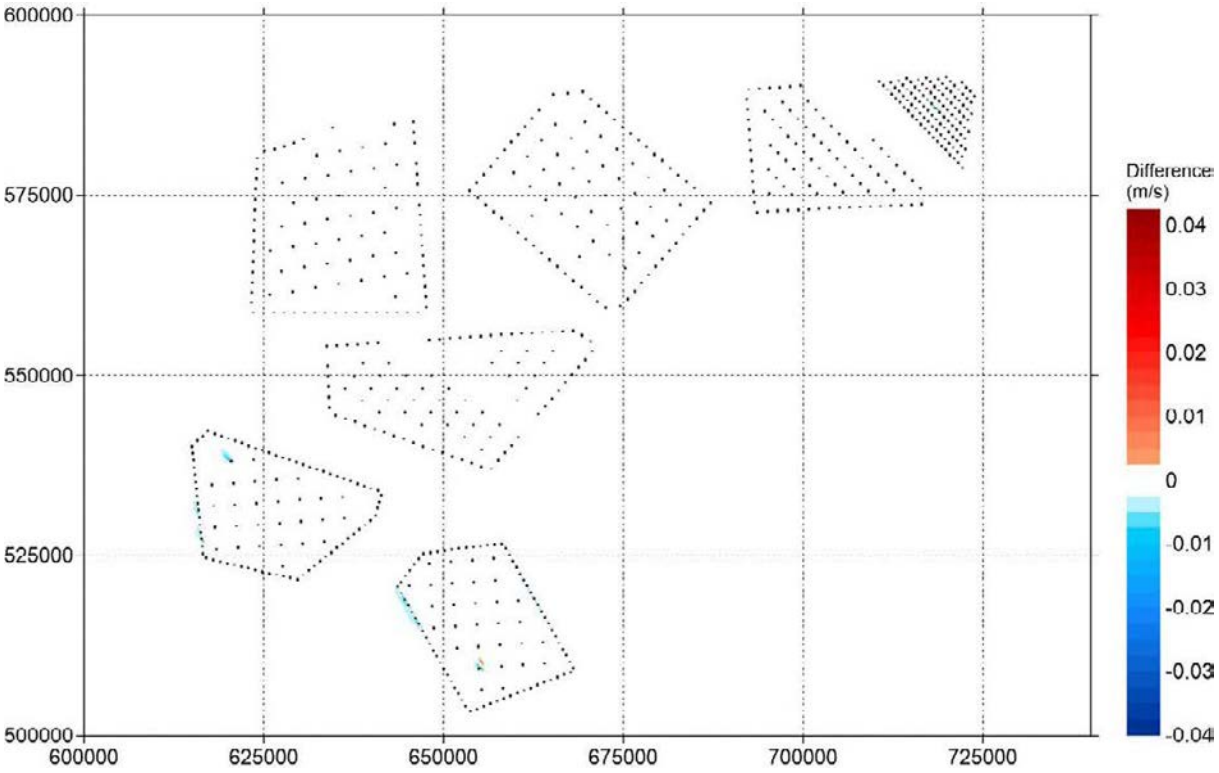

Figure C.29 Change of Speed of Peak North-west-going Currents in a Neap Tide (Scenario 2)

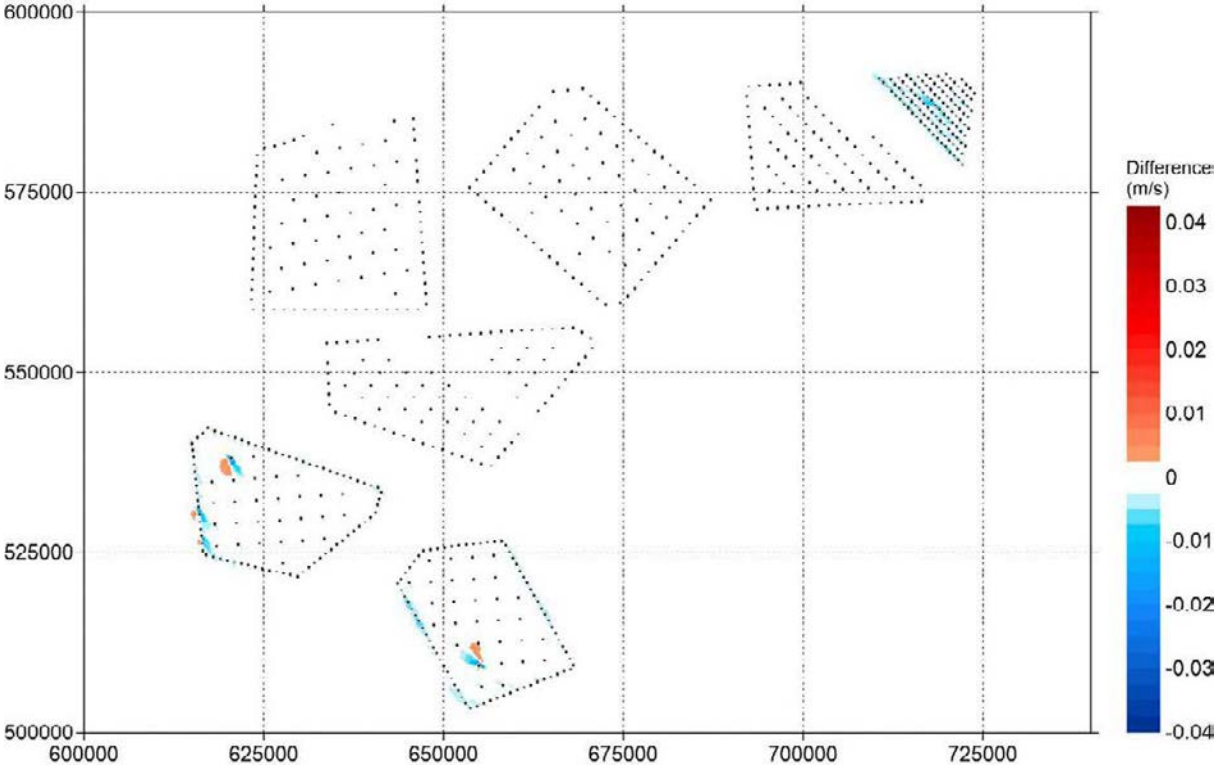

Figure C.30 Change of Maximum Current Speed Over 30 days (Scenario 2)

Appendix D: Predicted Maximum Suspended Sediment Concentration and Sediment Depositions from Laying Export Cables

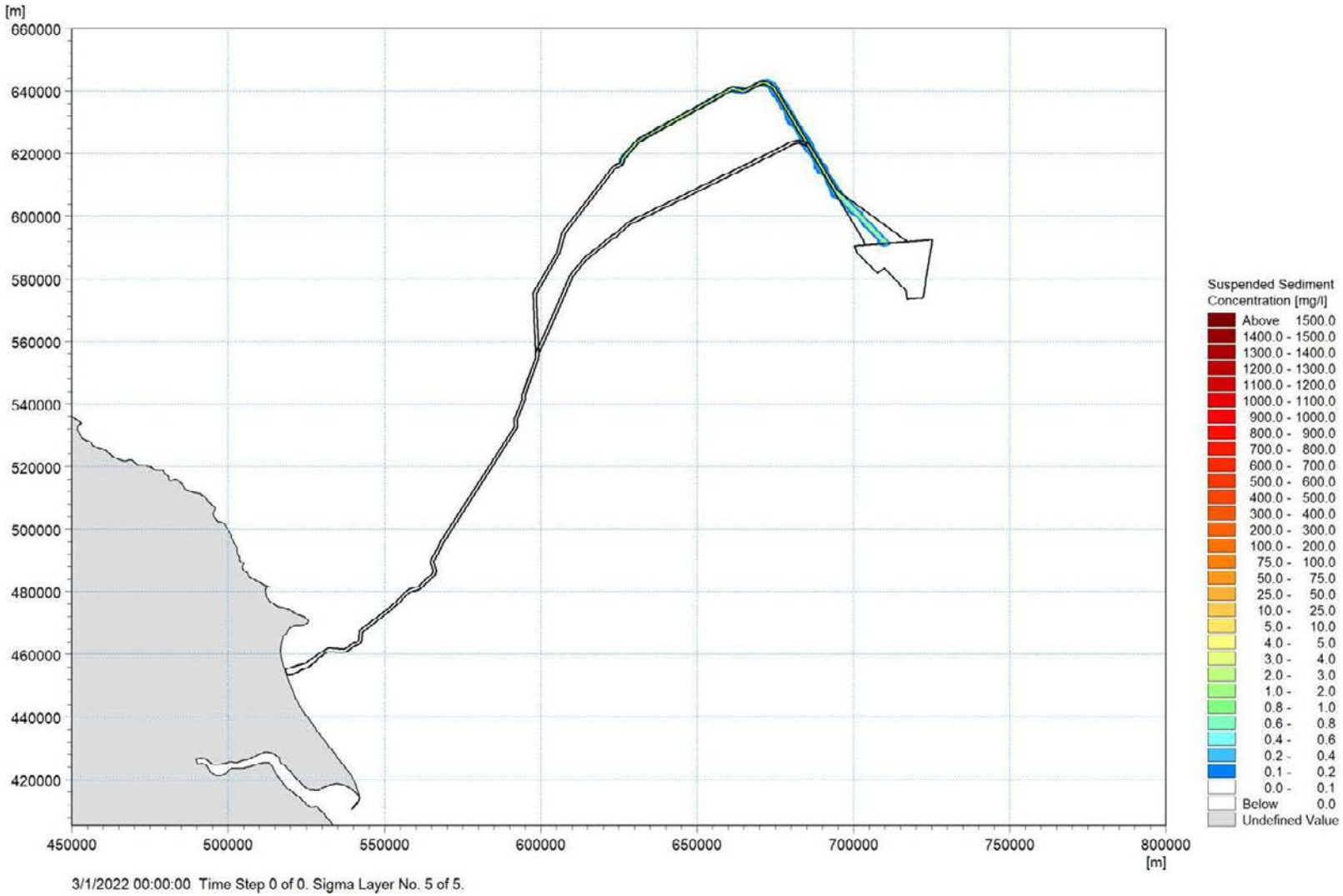

Figure D-1: Maximum Suspended Sediment Concentration (surface layer) – Export Cable Route Option 1– Levelling

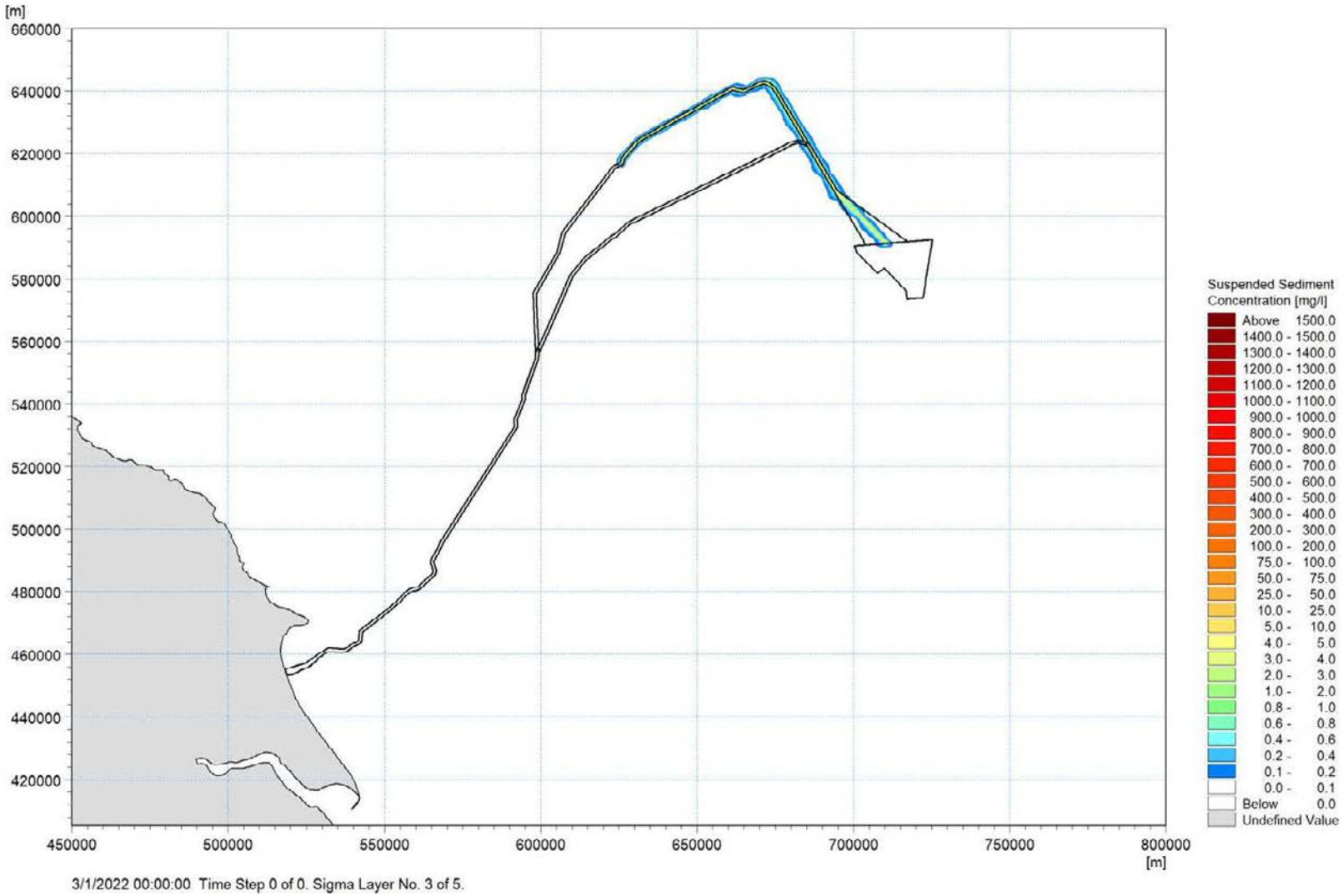

Figure D-2: Maximum Suspended Sediment Concentration (middle layer) – Export Cable Route Option 1– Levelling

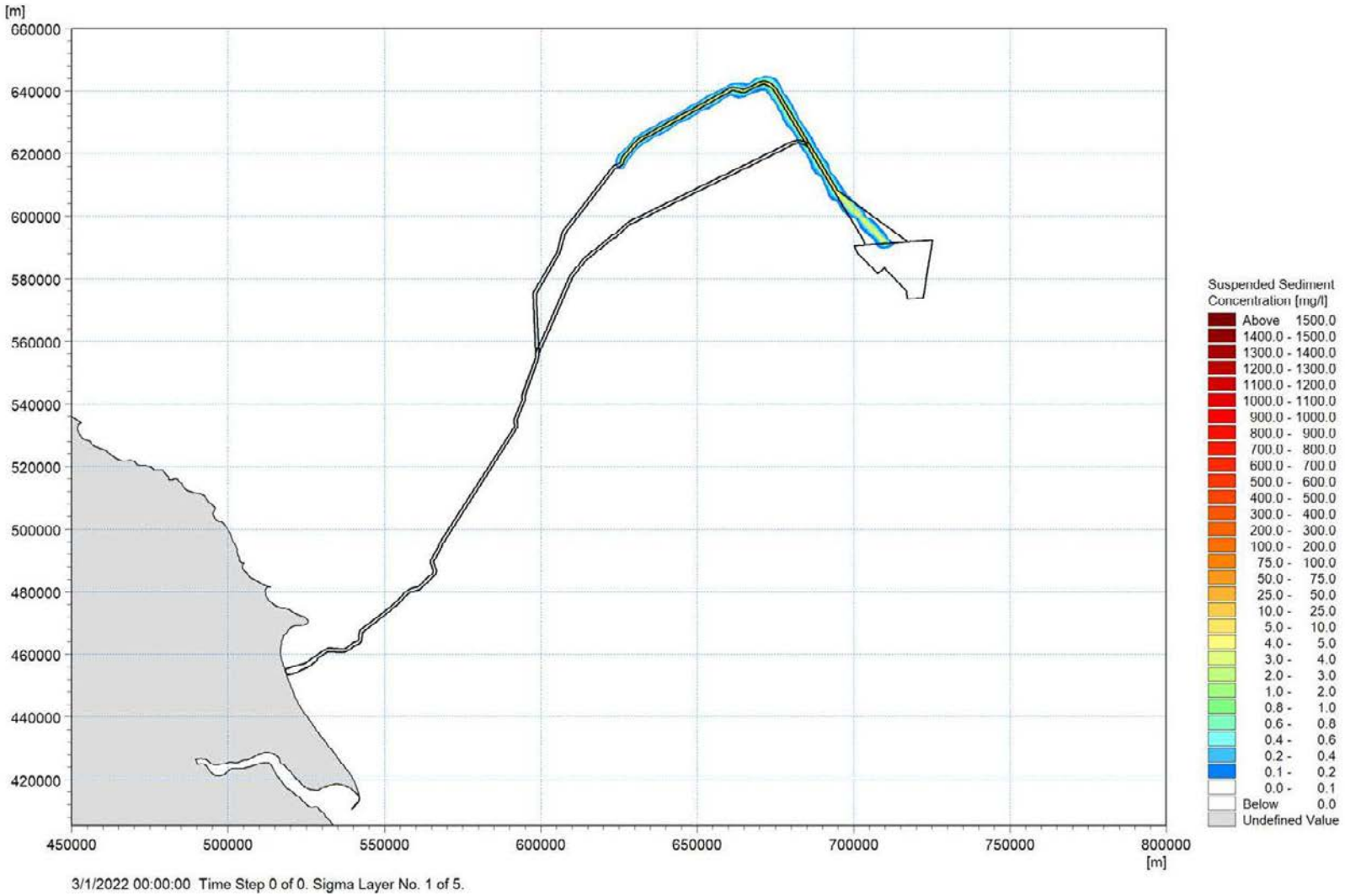

Figure D-3: Maximum Suspended Sediment Concentration (bottom layer) – Export Cable Route Option 1– Levelling

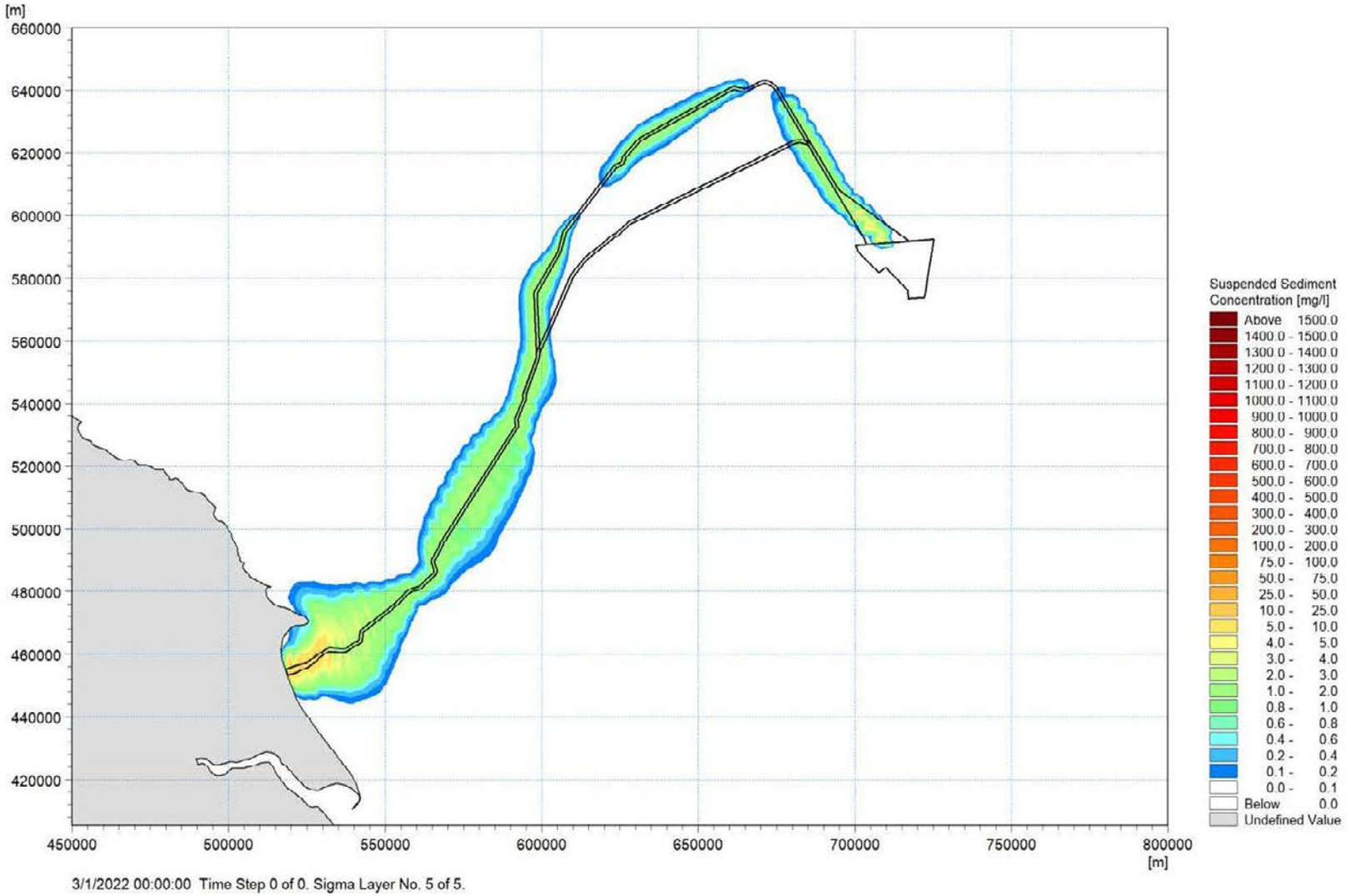

Figure D-4: Maximum Suspended Sediment Concentration (surface layer) – Export Cable Route Option 1– Trenching

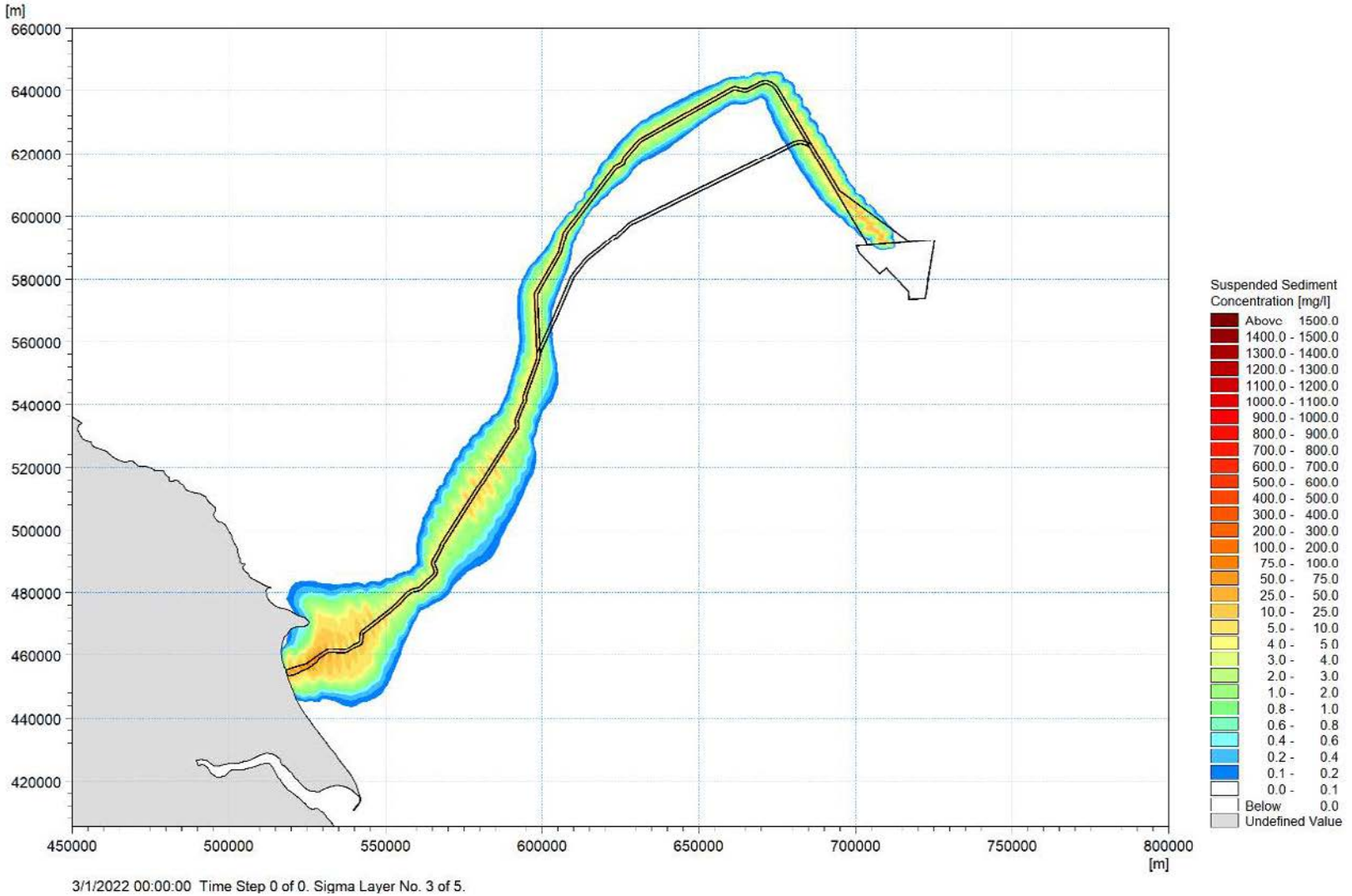

Figure D-5: Maximum Suspended Sediment Concentration (middle layer) – Export Cable Route Option 1– Trenching

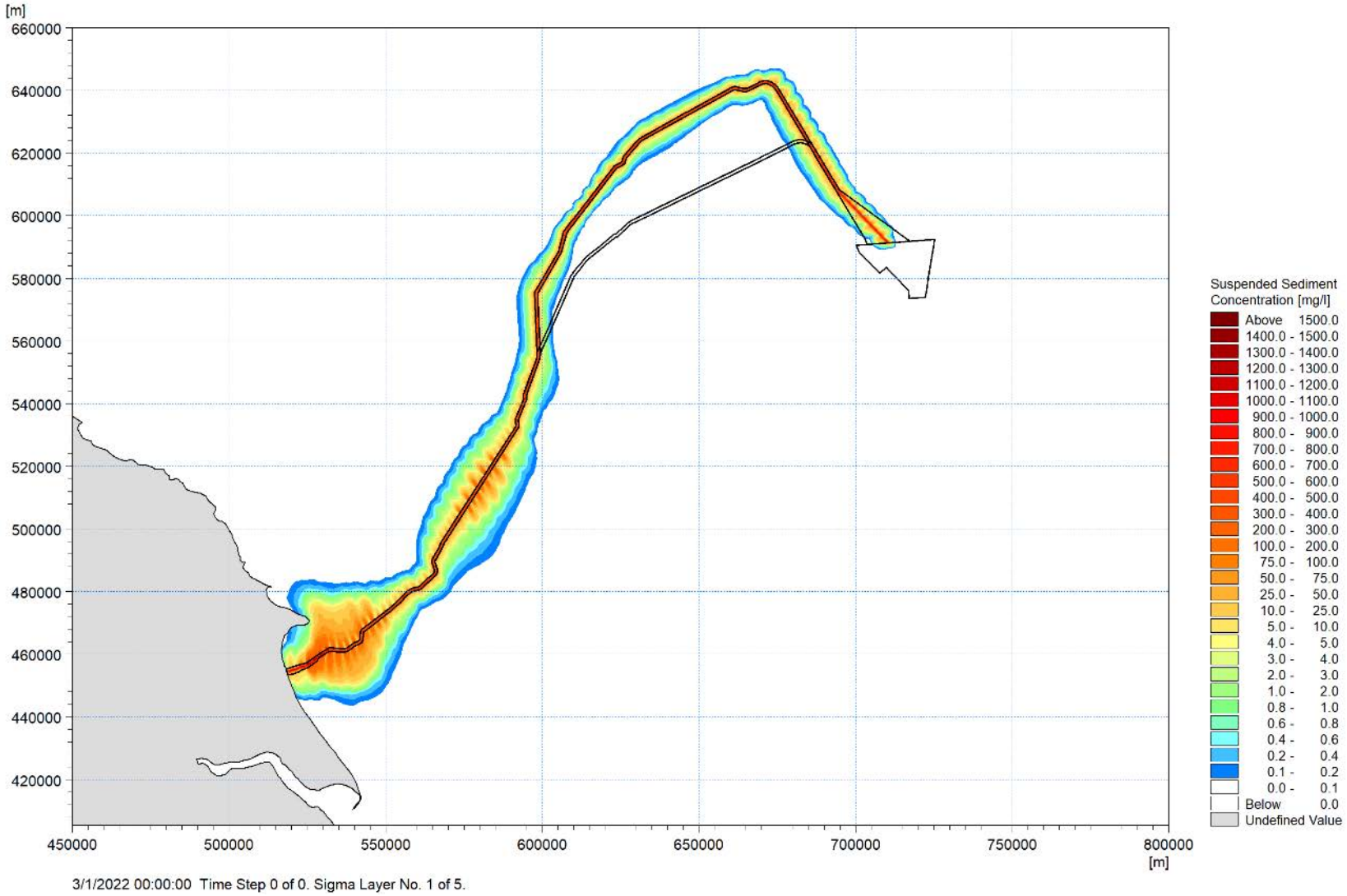

Figure D-6: Maximum Suspended Sediment Concentration (bottom layer) – Export Cable Route Option 1– Trenching

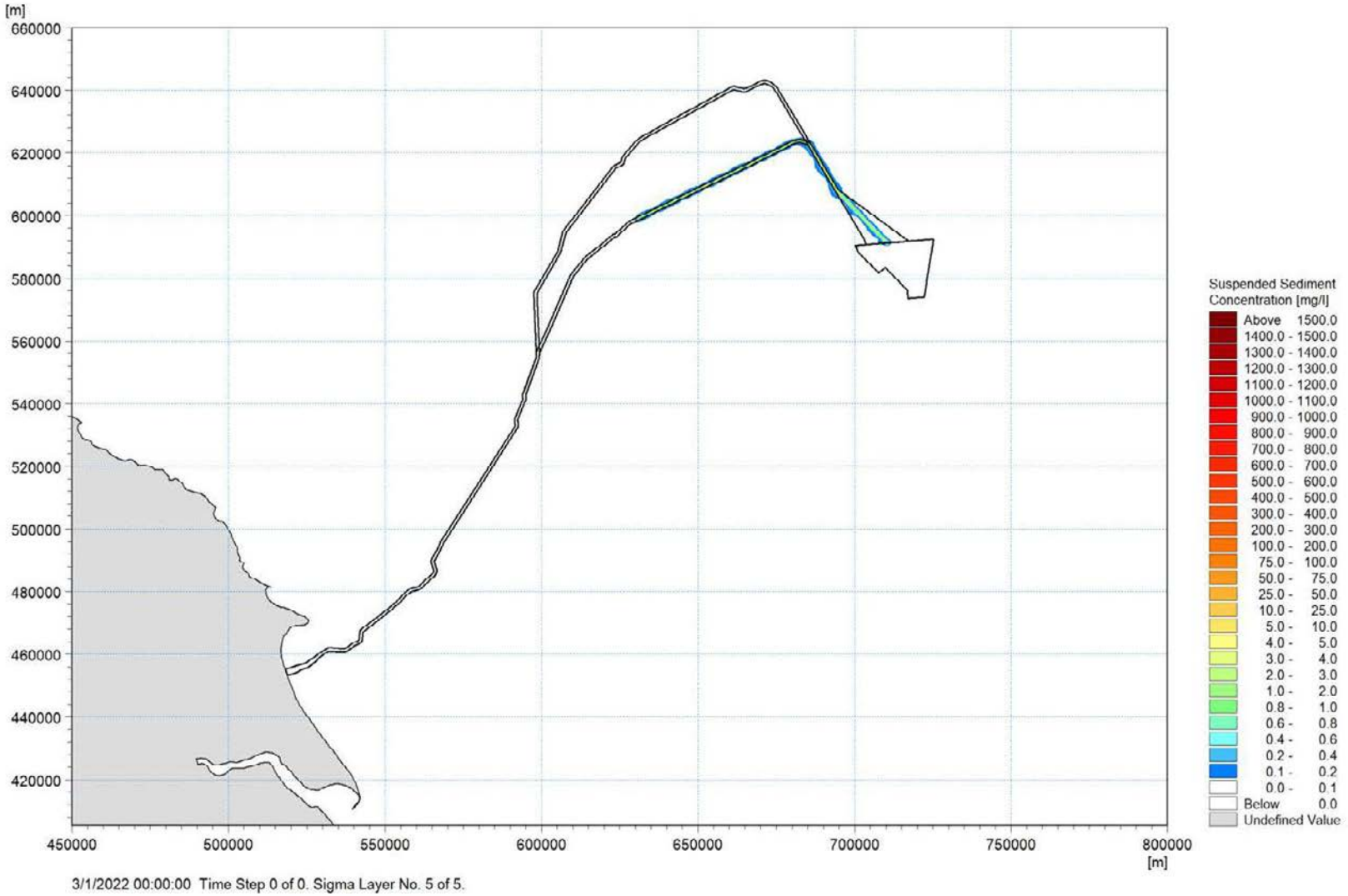

Figure D-7: Maximum Suspended Sediment Concentration (surface layer) – Export Cable Route Option 2– Levelling

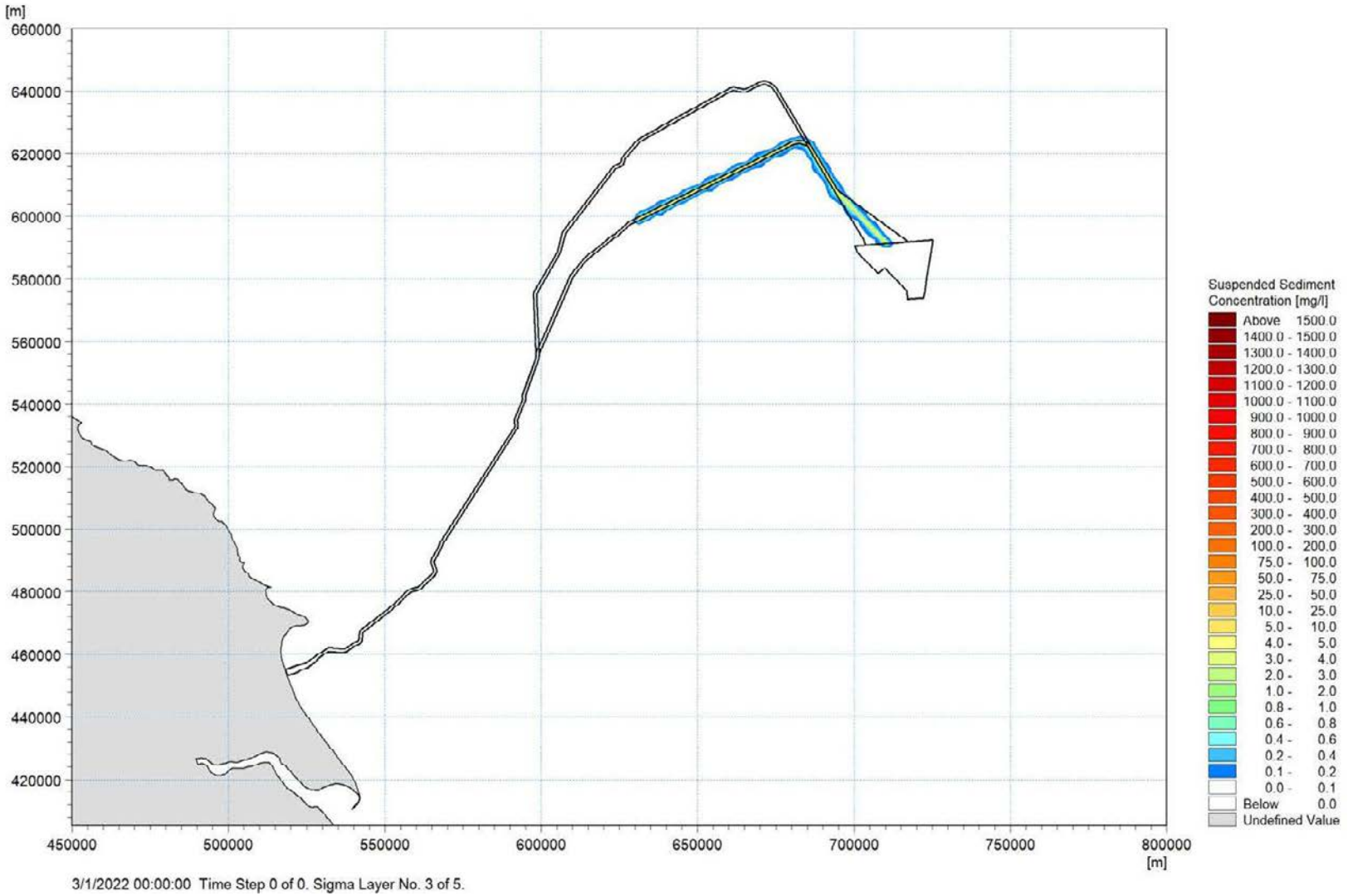

Figure D-8: Maximum Suspended Sediment Concentration (middle layer) – Export Cable Route Option 2– Levelling

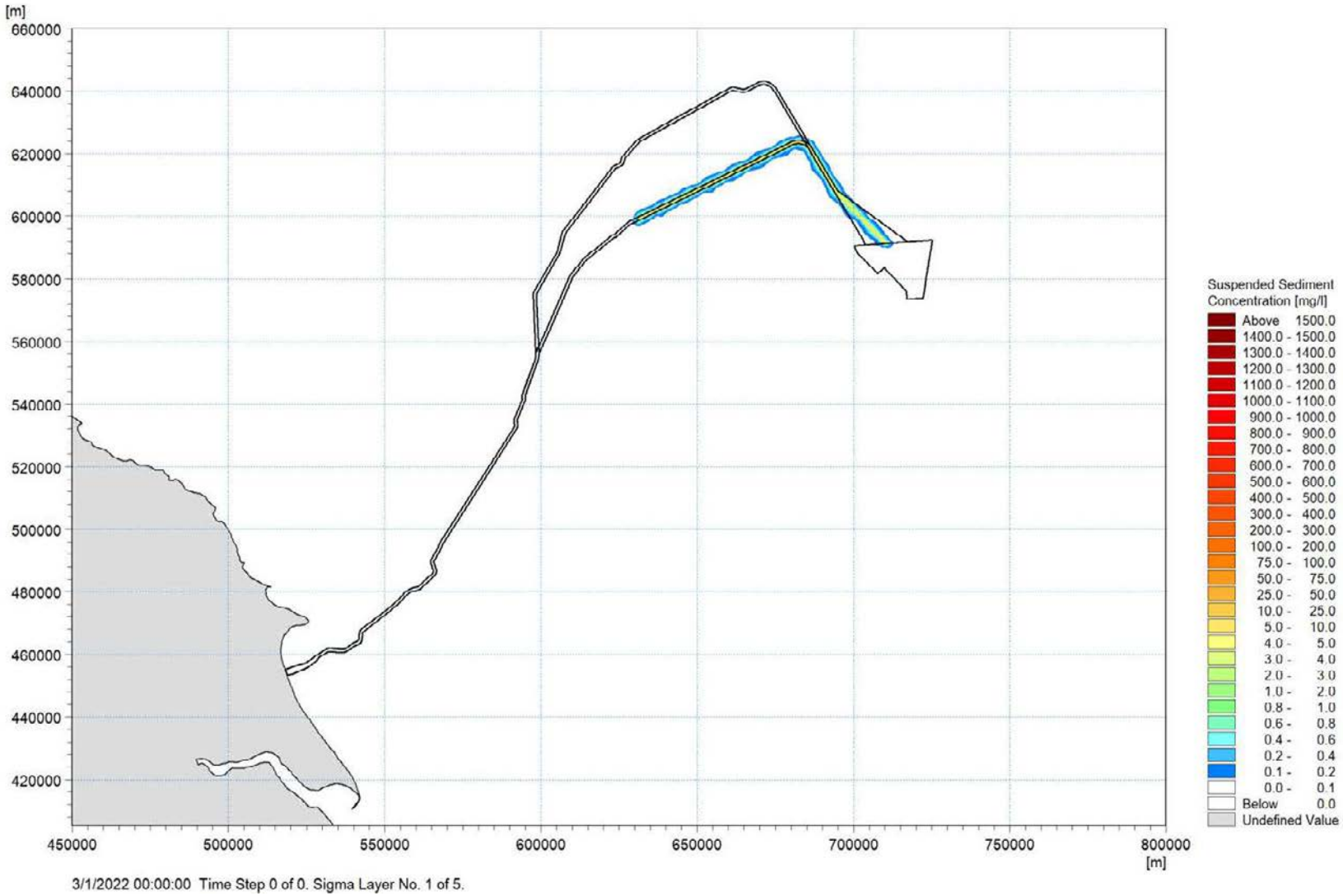

Figure D-9: Maximum Suspended Sediment Concentration (bottom layer) – Export Cable Route Option 2– Levelling

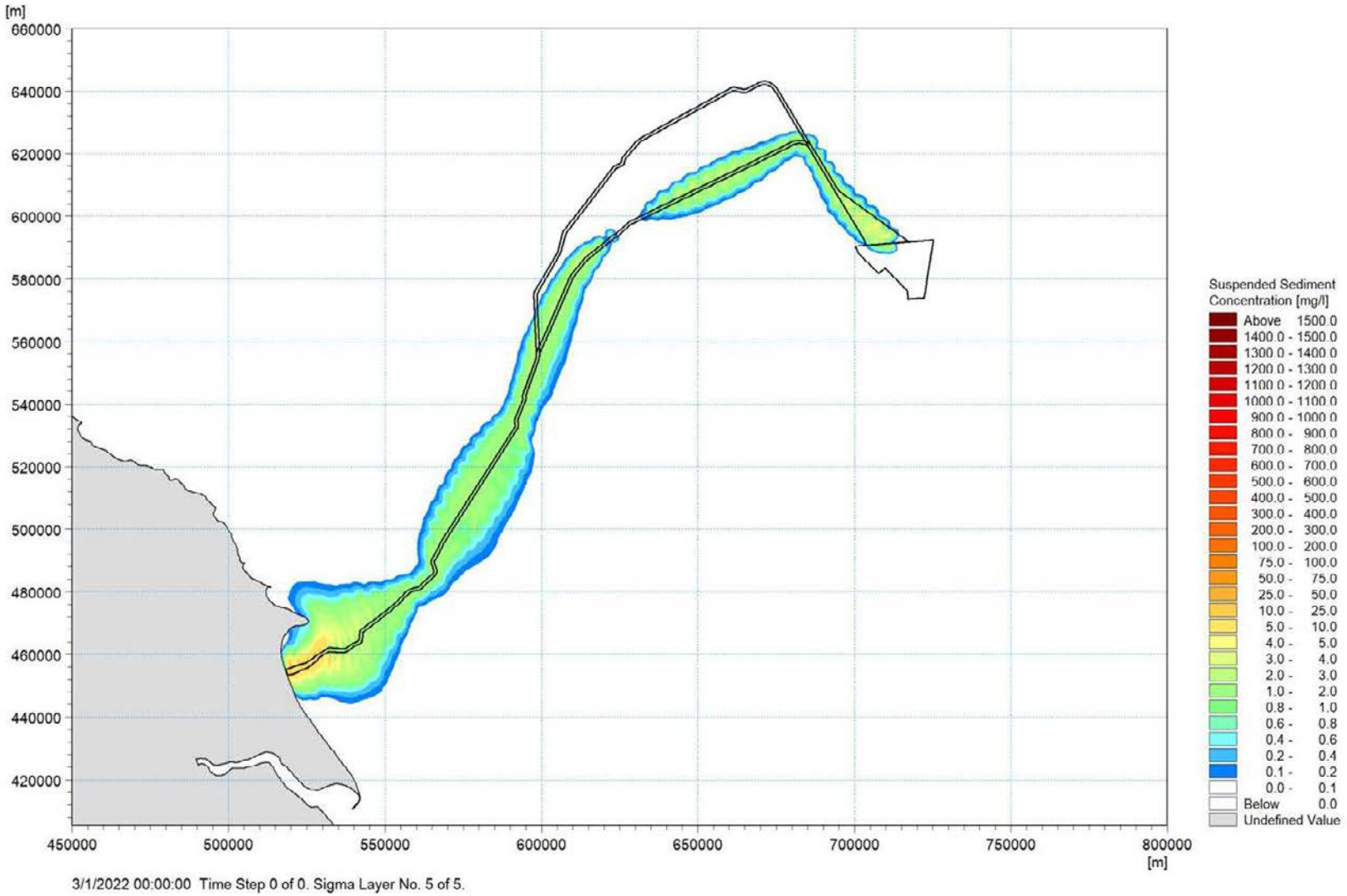

Figure D-10: Maximum Suspended Sediment Concentration (surface layer) – Export Cable Route Option 2– Trenching

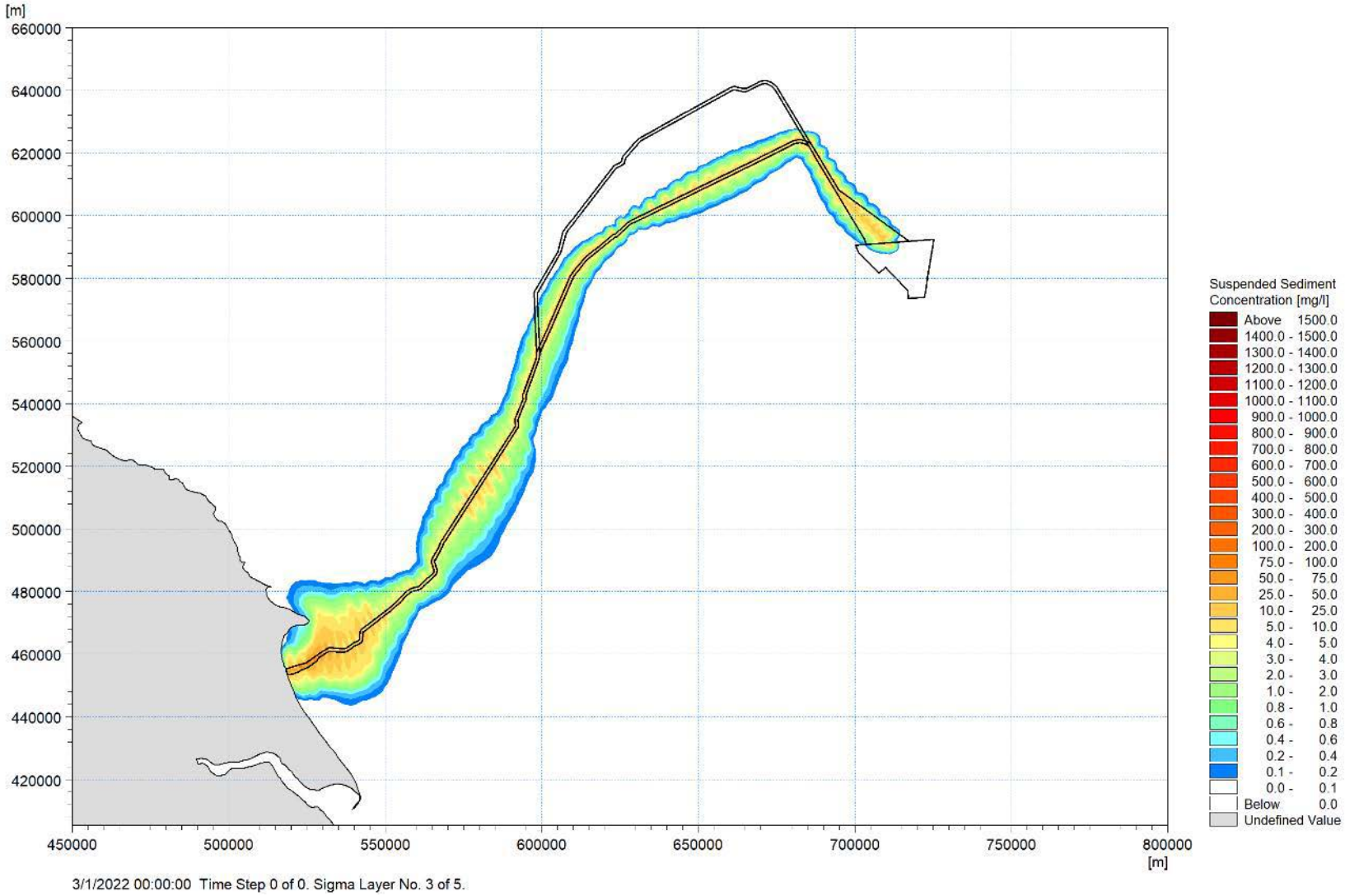

Figure D-11: Maximum Suspended Sediment Concentration (middle layer) – Export Cable Route Option 2– Trenching

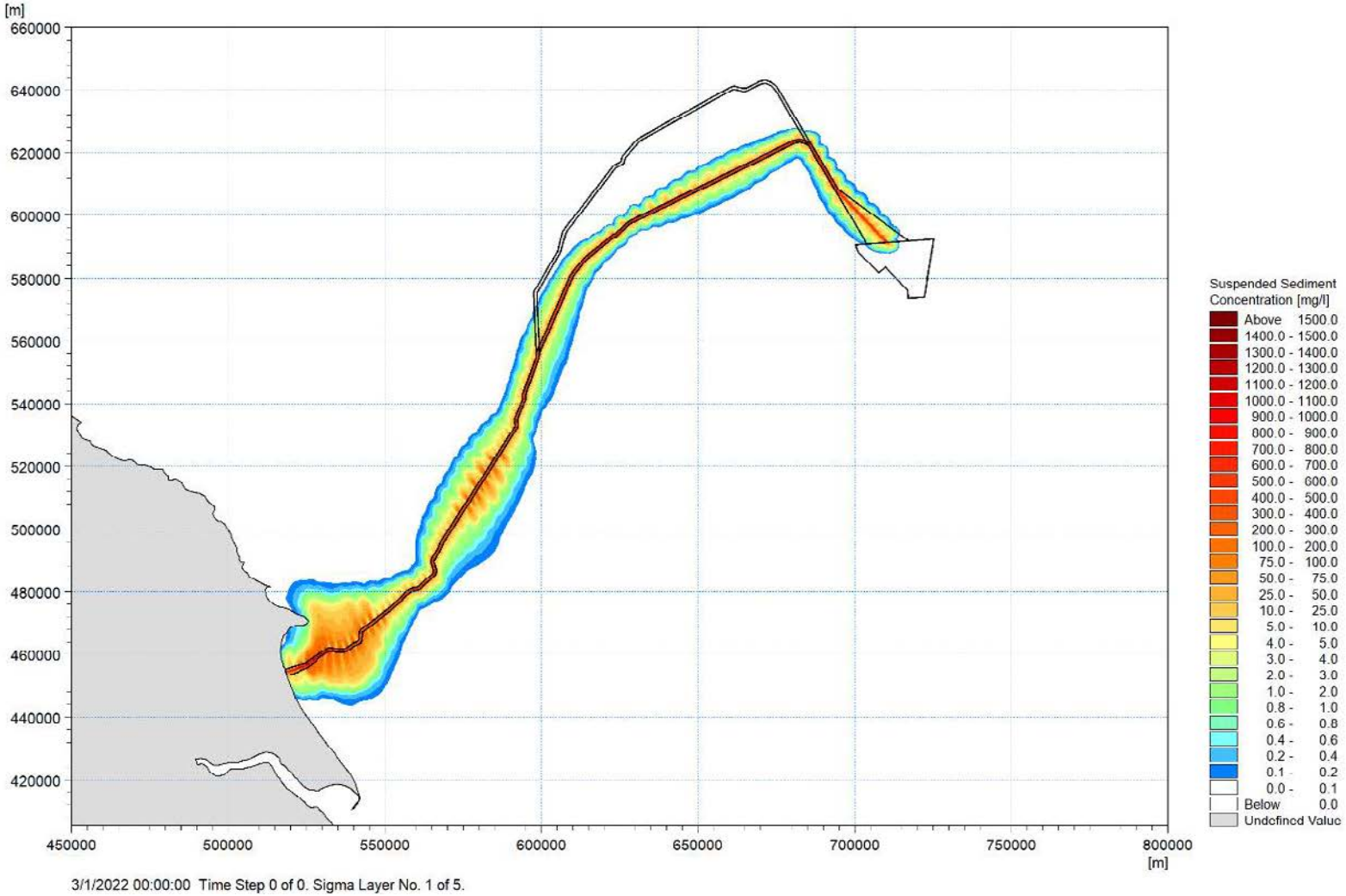

Figure D-12: Maximum Suspended Sediment Concentration (bottom layer) – Export Cable Route Option 2– Trenching

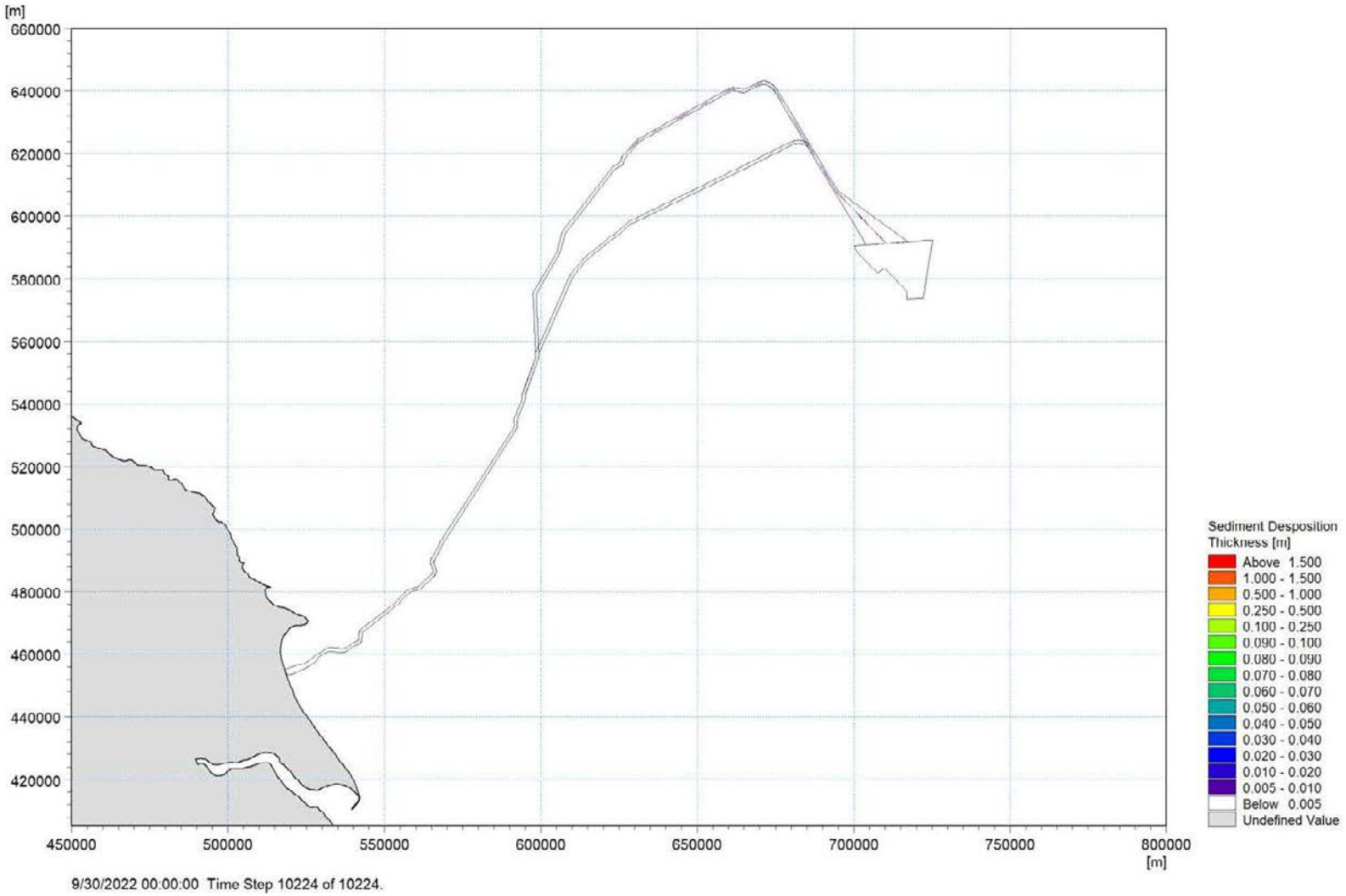

Figure D-13: Total Sediment Deposition Thickness – Export Cable Route Option 1 – Levelling

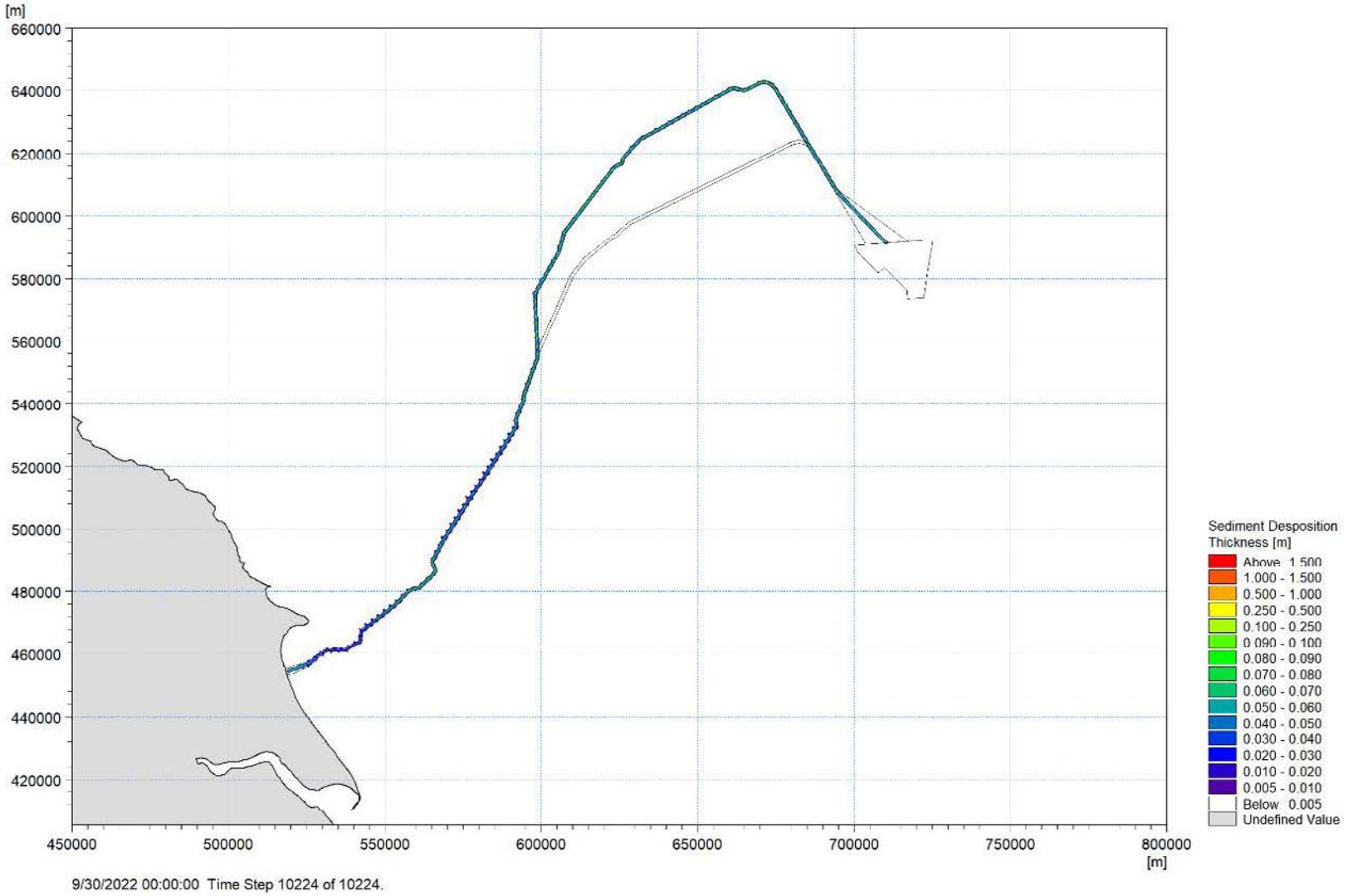

Figure D-14: Total Sediment Deposition Thickness – Export Cable Route Option 1 – Trenching

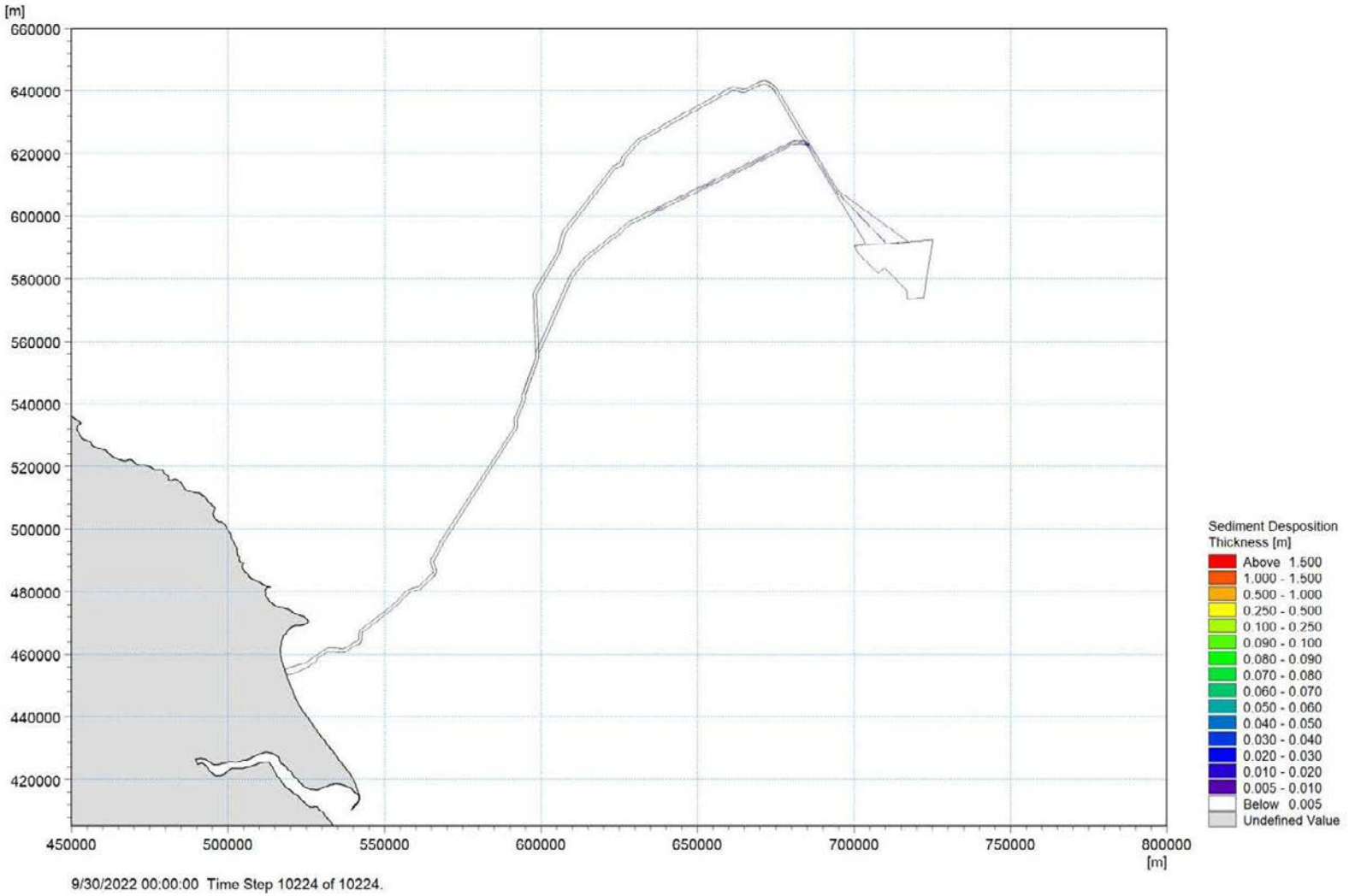

Figure D-15: Total Sediment Deposition Thickness – Export Cable Route Option 2 – Levelling

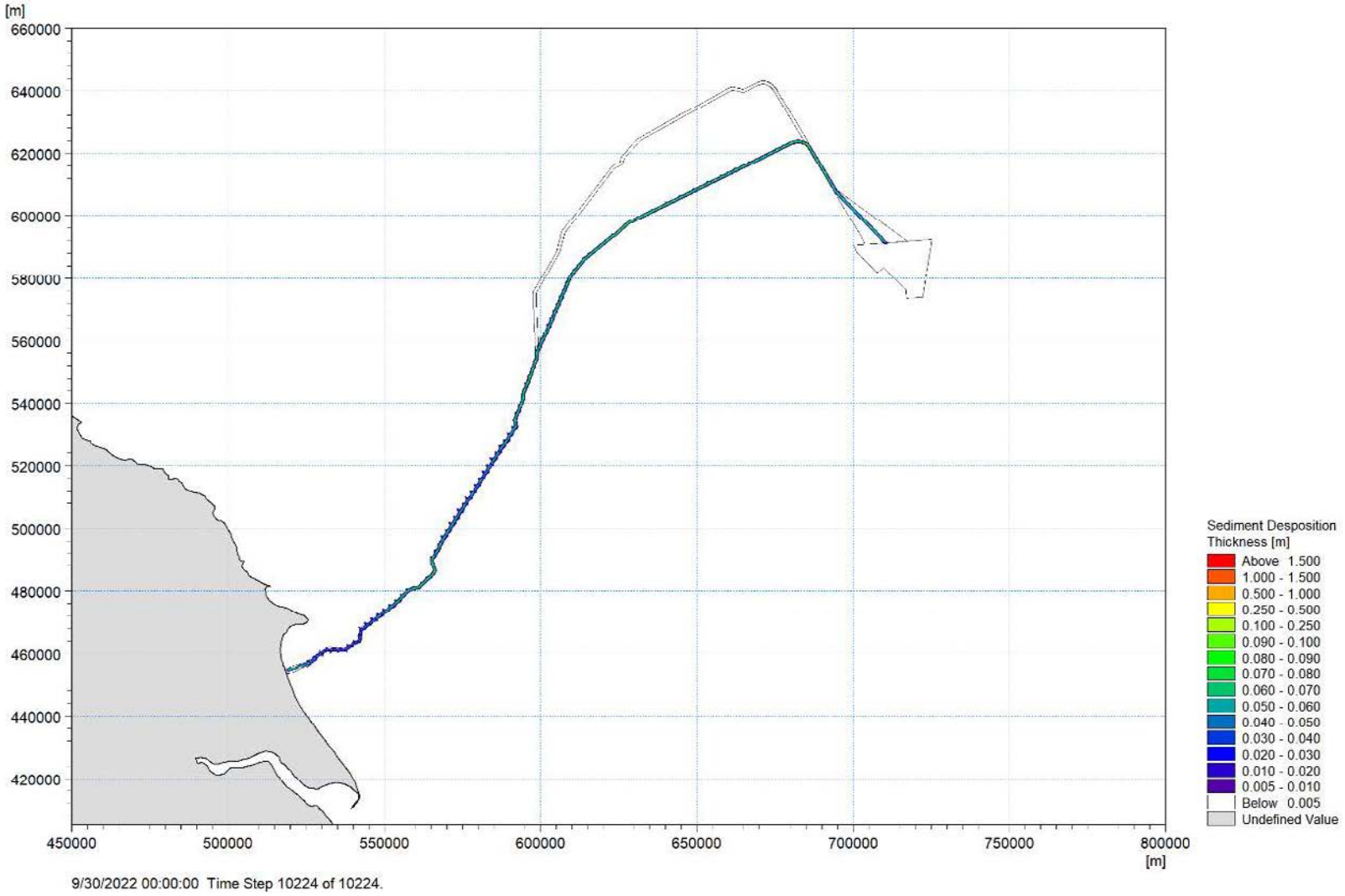

Figure D-16: Total Sediment Deposition Thickness – Export Cable Route Option 2 – Trenching

Appendix E: Predicted Maximum Suspended Sediment Concentration and Sediment Depositions from Drilling Foundation of Turbines and Platforms

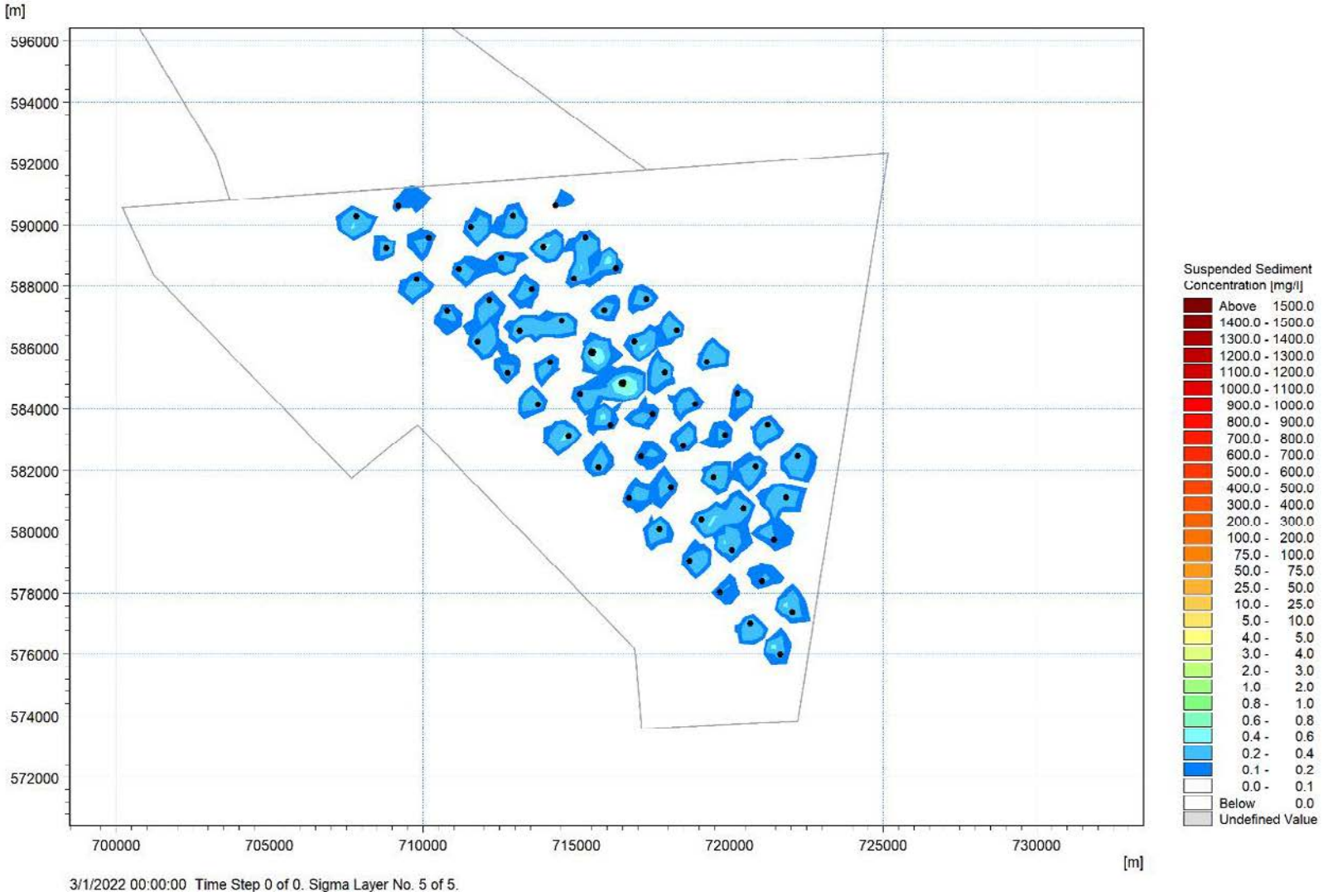

Figure E-1: Maximum Suspended Sediment Concentration (surface layer) – Turbine and Platform Foundations – Drill Arising

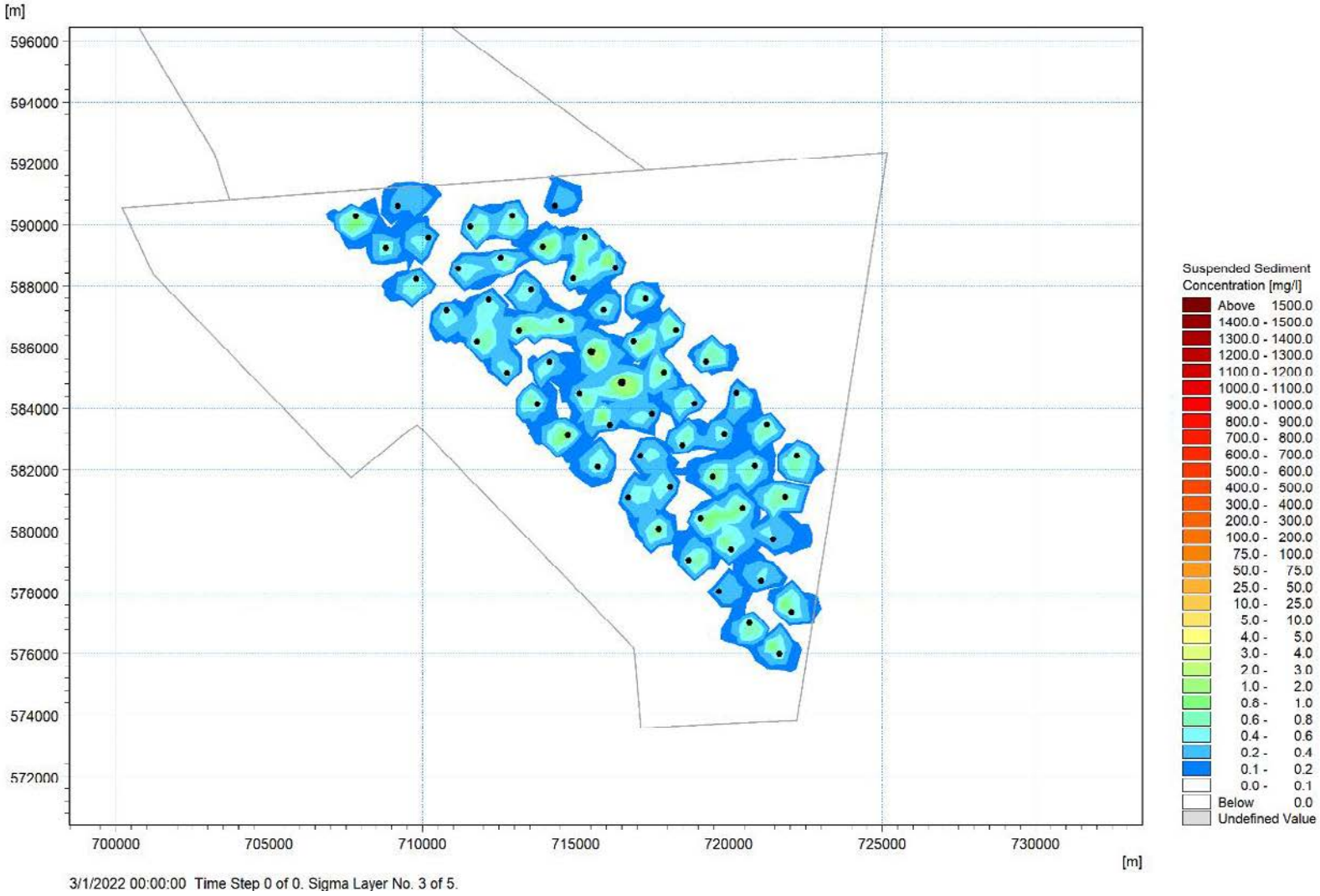

Figure E-2: Maximum Suspended Sediment Concentration (middle layer) – Turbine and Platform Foundations – Drill Arising

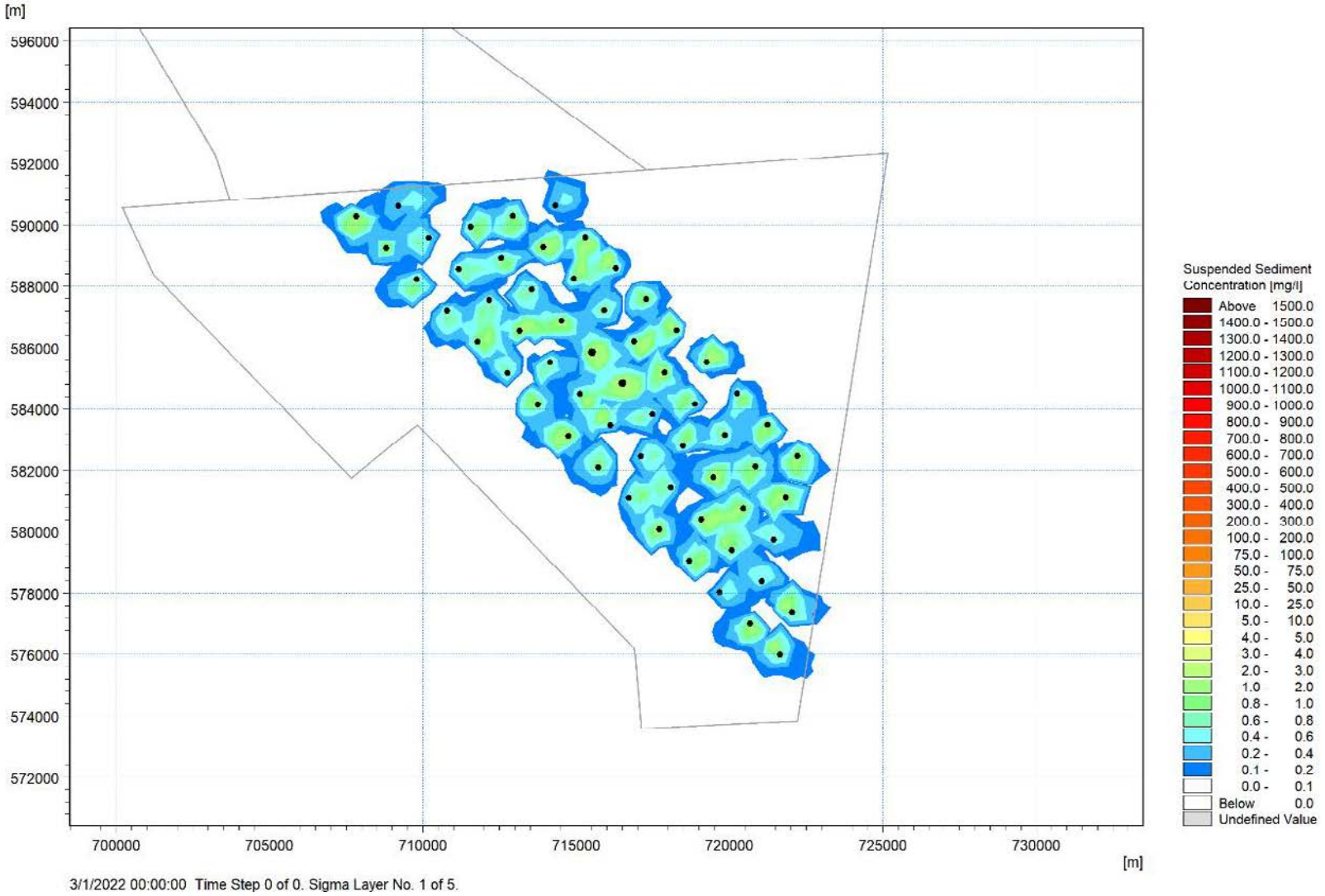

Figure E-3: Maximum Suspended Sediment Concentration (bottom layer) – Turbine and Platform Foundations – Drill Arising

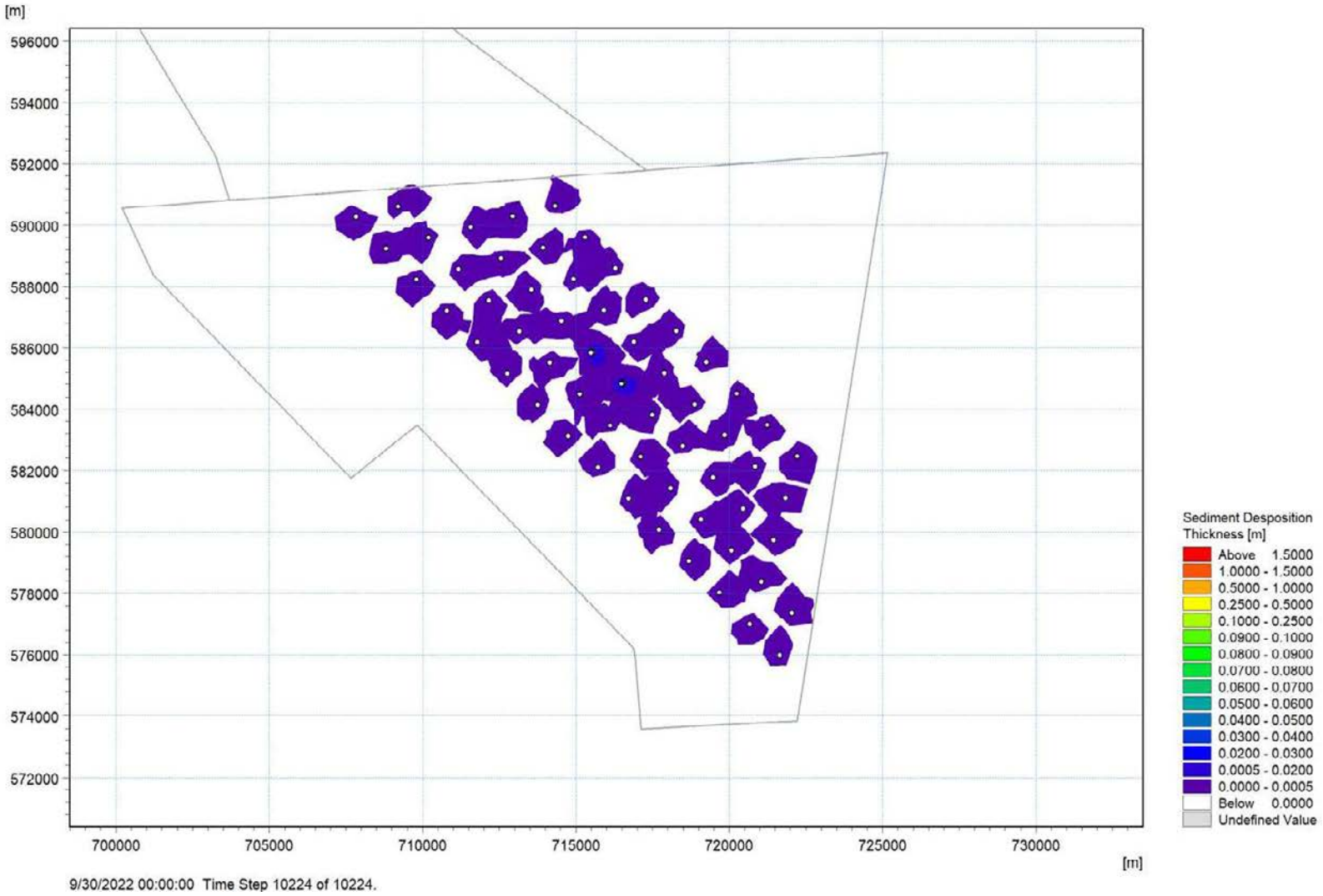

Figure E-4: Total Sediment Deposition Thickness – Turbine and Platform Foundations – Drill Arising

Appendix F: Time Series of Predicted Suspended Sediment Concentration at Selected Points during Trenching Export Cable Corridor

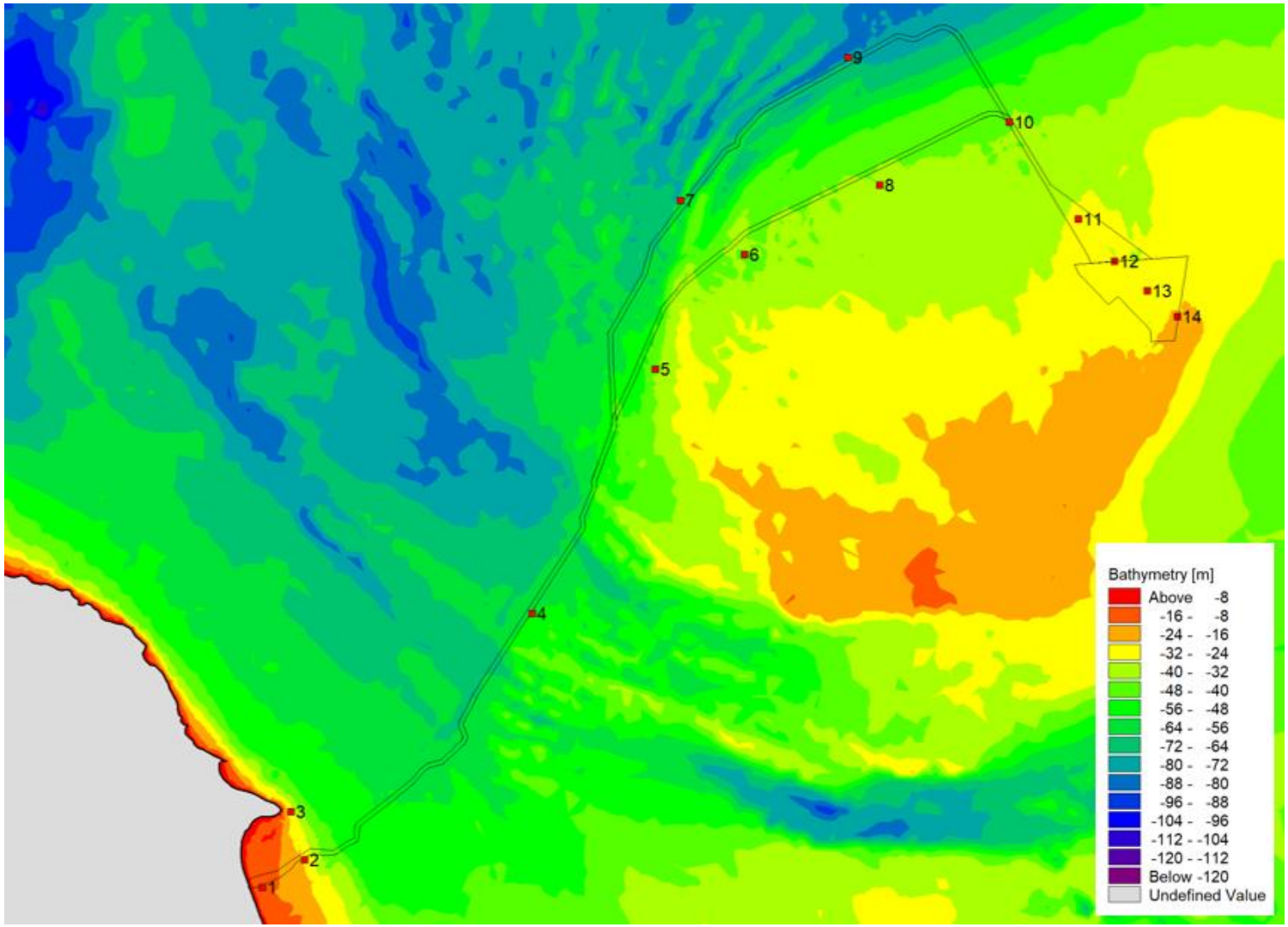

Figure F-1: Locations of Time Series Plots of Predicted Suspended Sediment

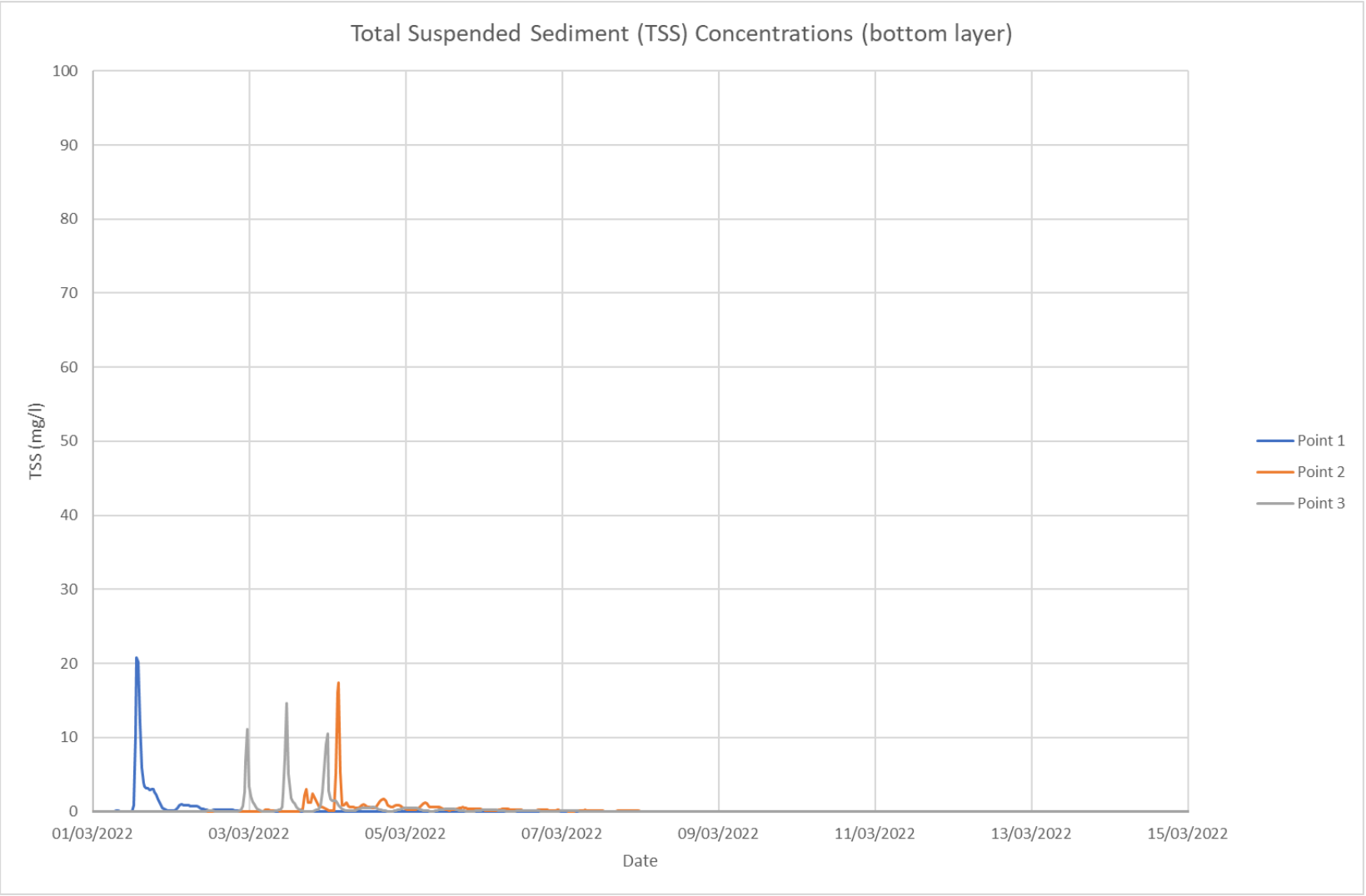

Figure F-2: Predicted Suspended Sediment Concentration (bottom layer) at Points 1, 2 and 3 – Offshore Export Cable Route Option 1

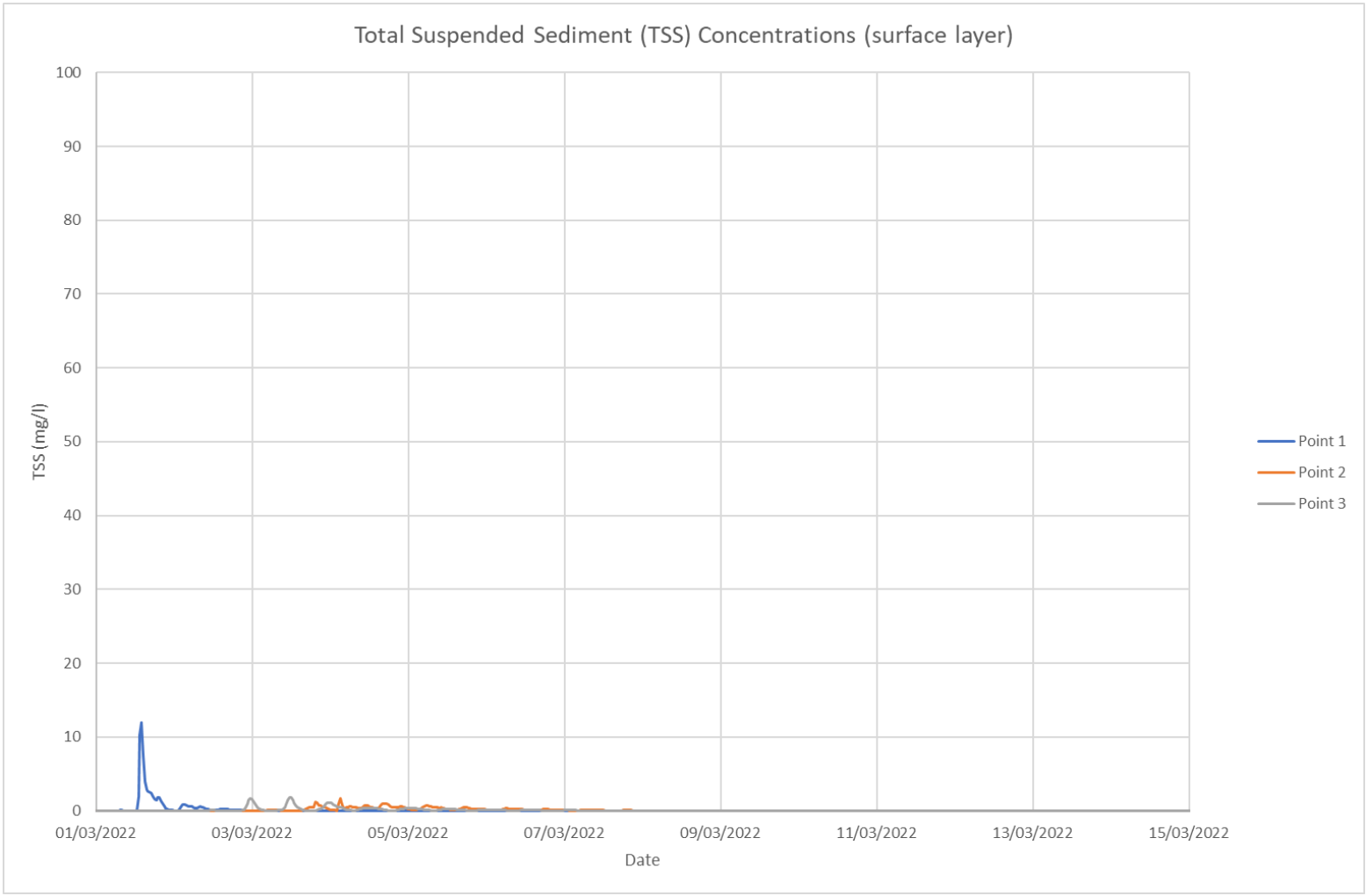

Figure F-3: Predicted Suspended Sediment Concentration (surface layer) at Points 1, 2 and 3 – Offshore Export Cable Route Option 1

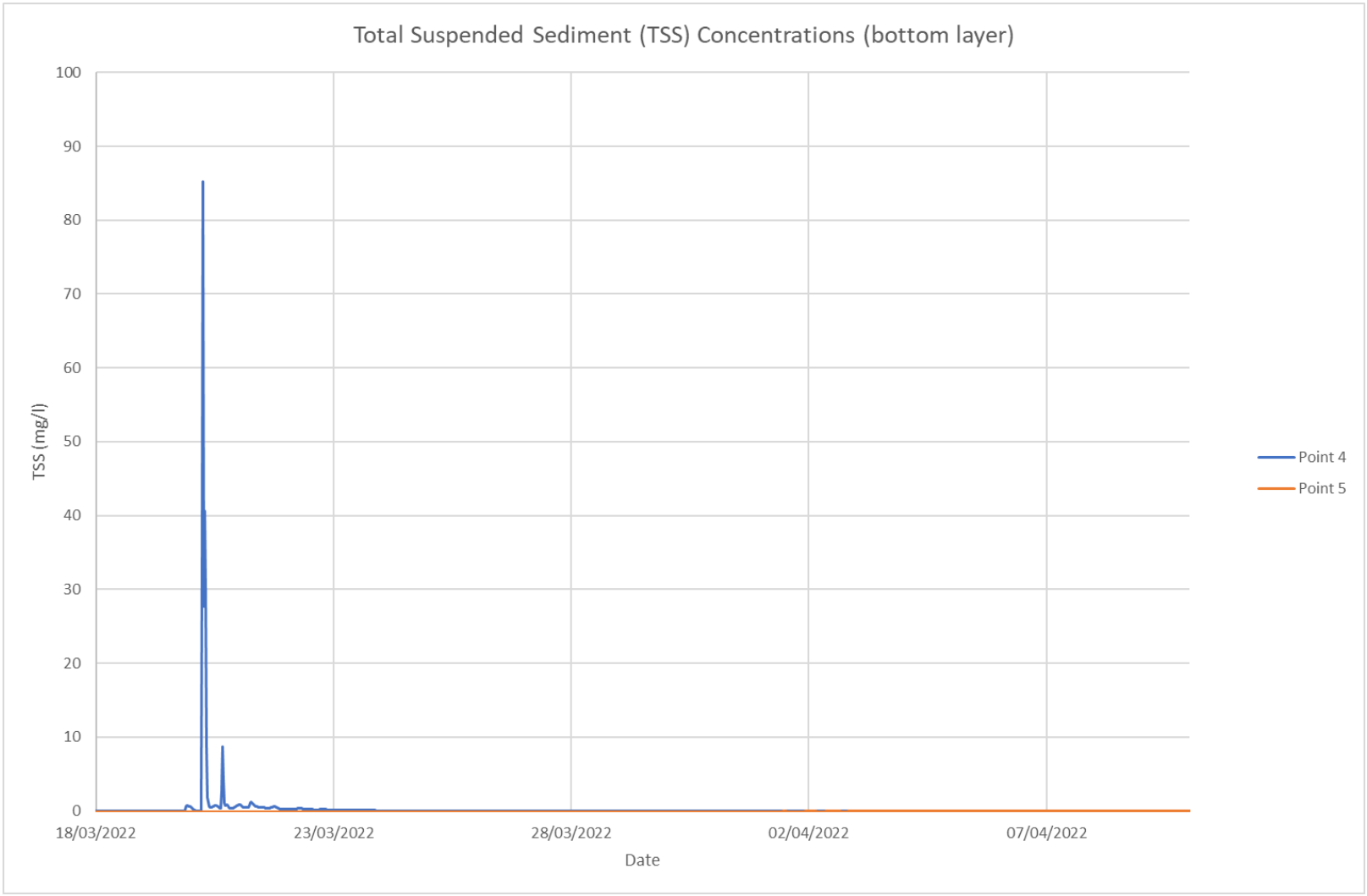

Figure F-4: Predicted Suspended Sediment Concentration (bottom layer) at Points 4 and 5 – Offshore Export Cable Route Option 1

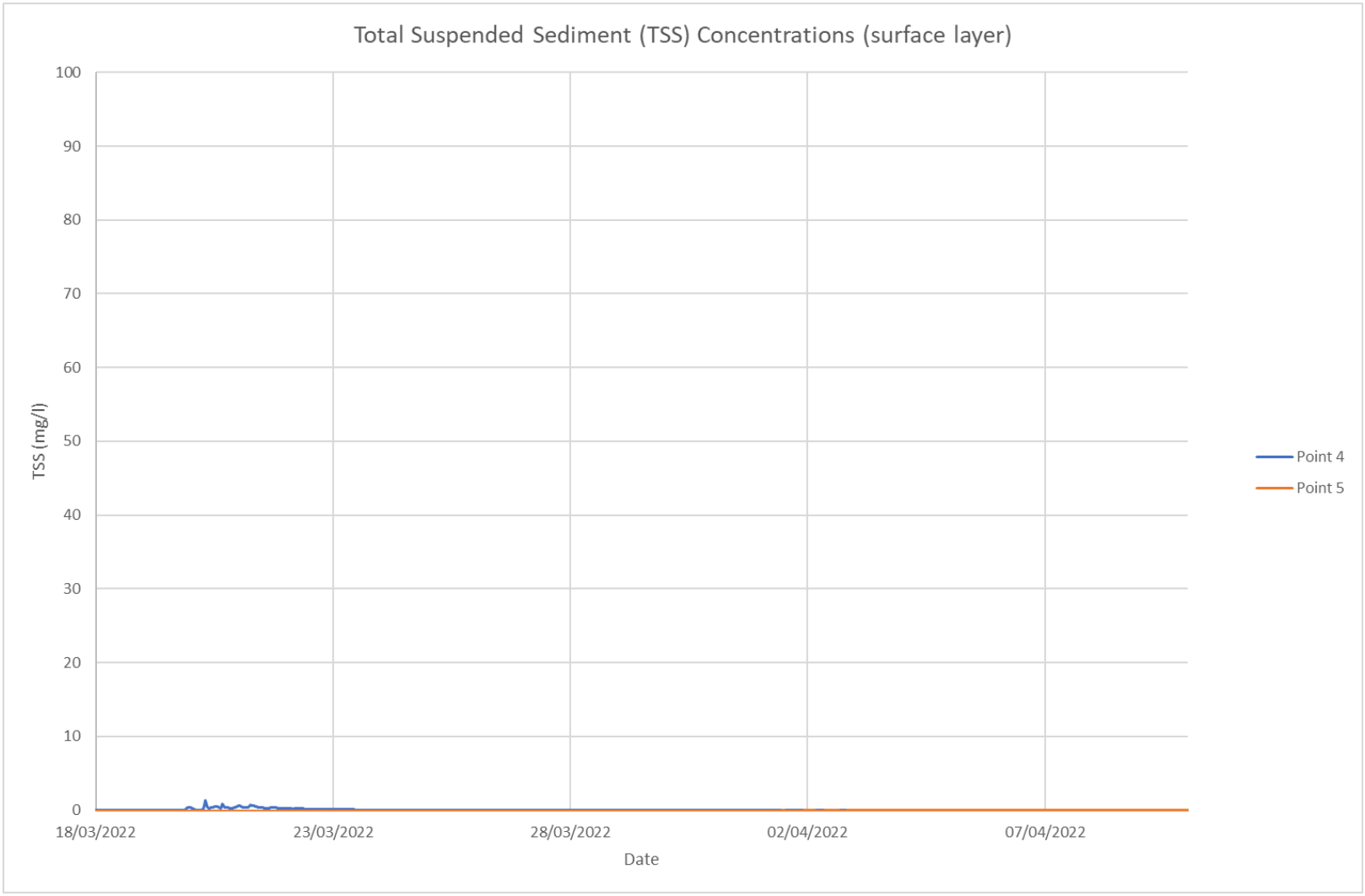

Figure F-5: Predicted Suspended Sediment Concentration (surface layer) at Points 4 and 5 – Offshore Export Cable Route Option 1

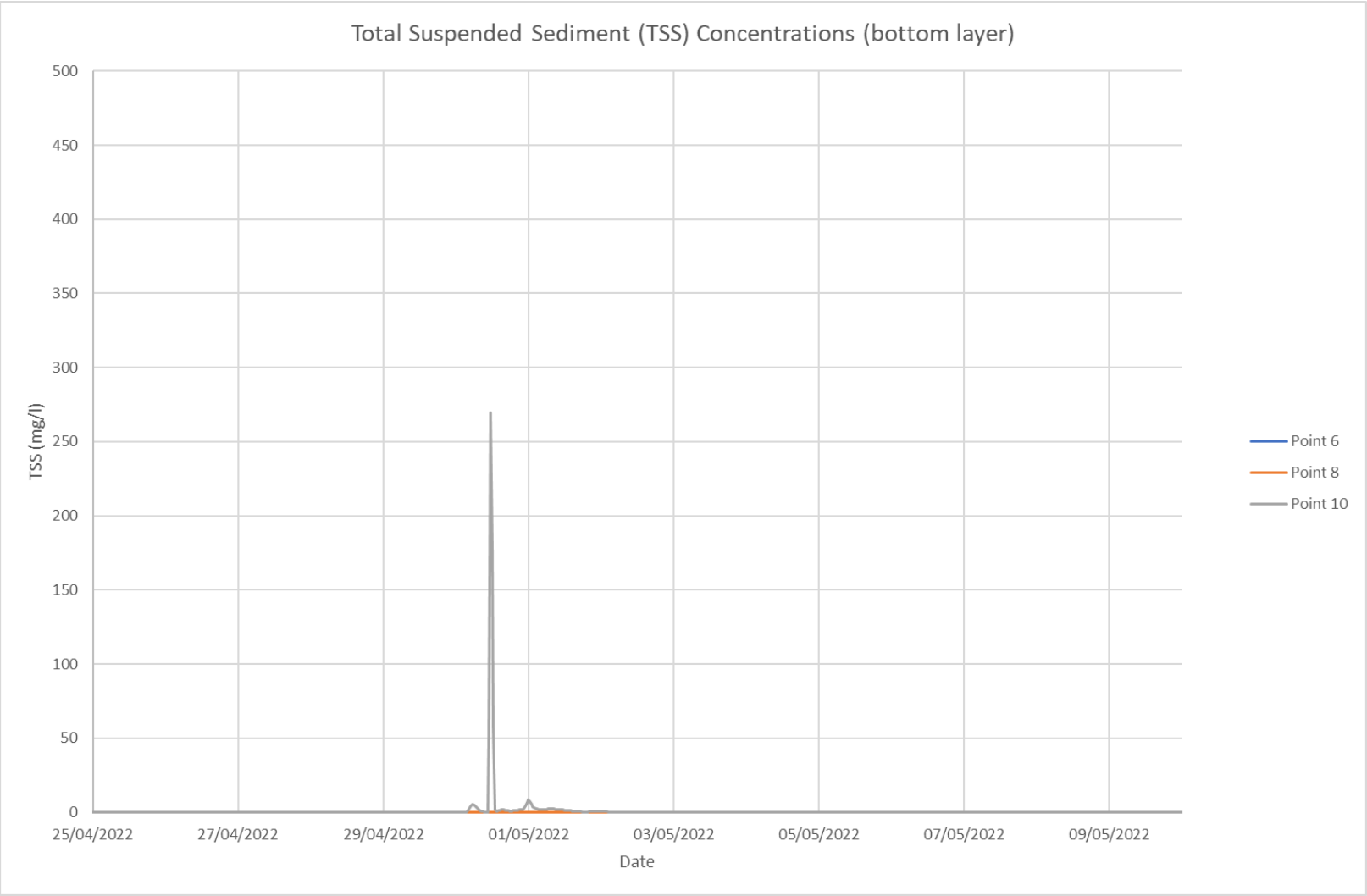

Figure F-6: Predicted Suspended Sediment Concentration (bottom layer) at Points 6, 8 and 10 – Offshore Export Cable Route Option 1

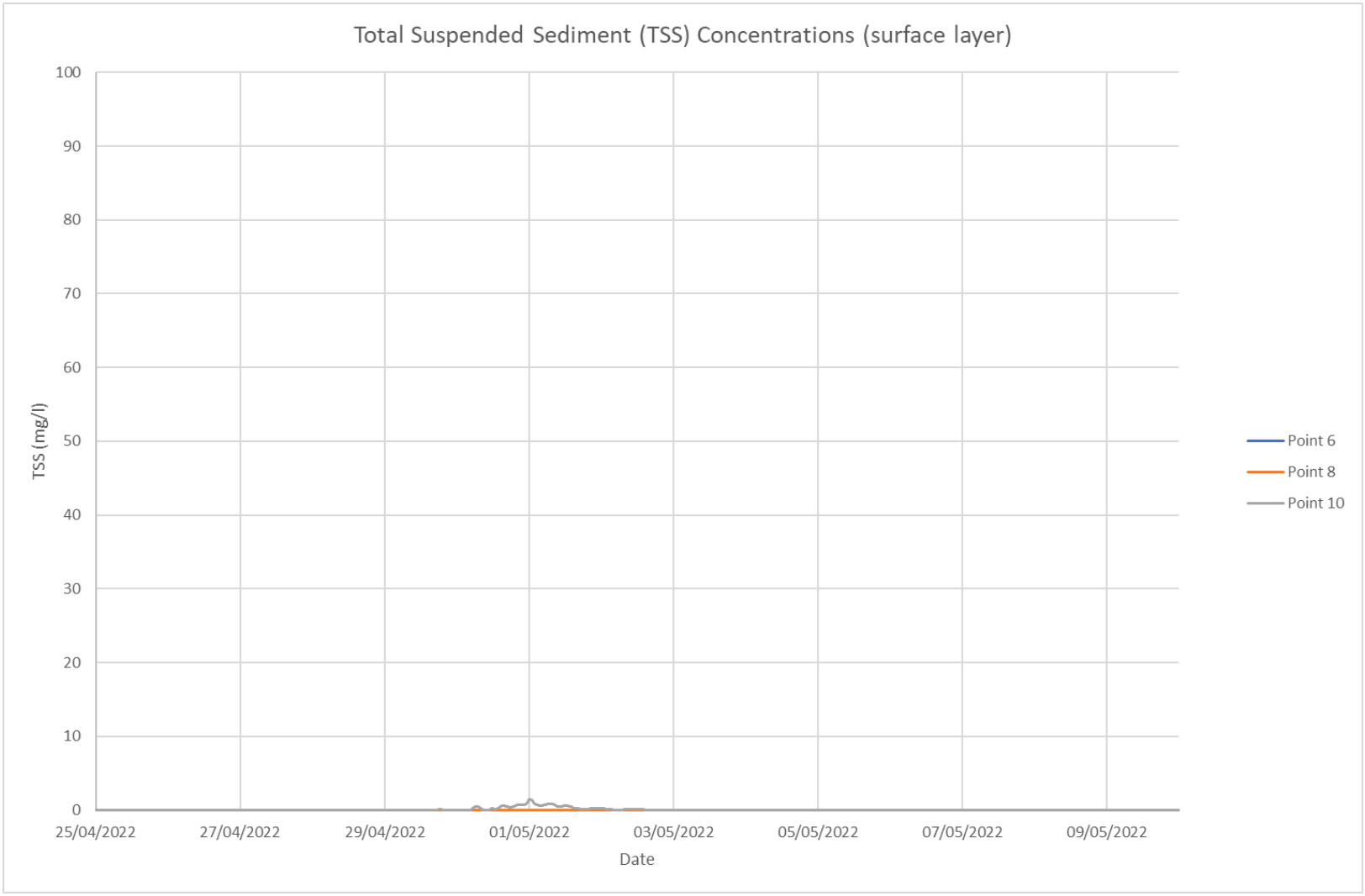

Figure F-7: Predicted Suspended Sediment Concentration (surface layer) at Points 6, 8 and 10 – Offshore Export Cable Route Option 1

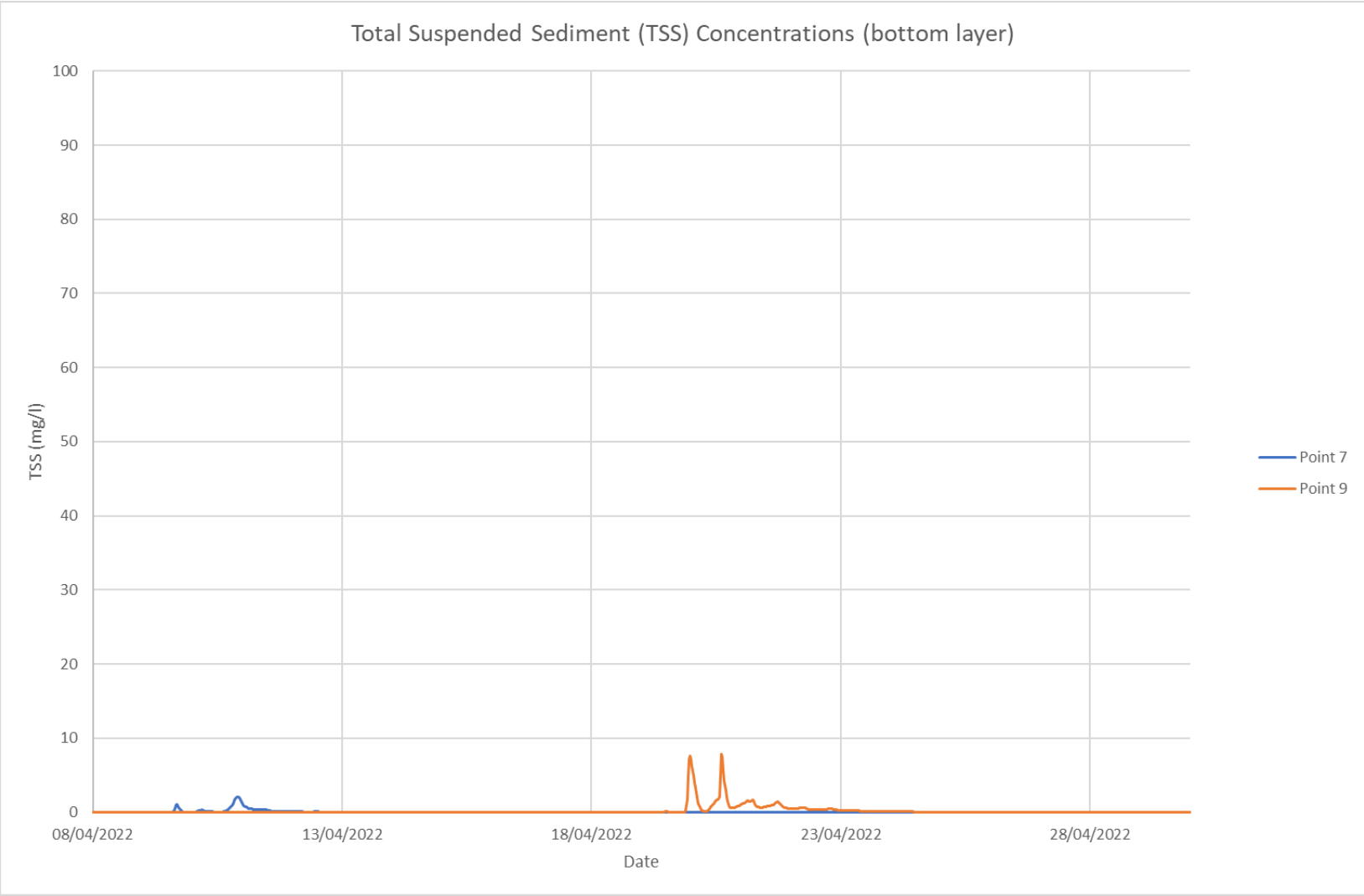

Figure F-8: Predicted Suspended Sediment Concentration (bottom layer) at Points 7 and 9 – Offshore Export Cable Route Option 1

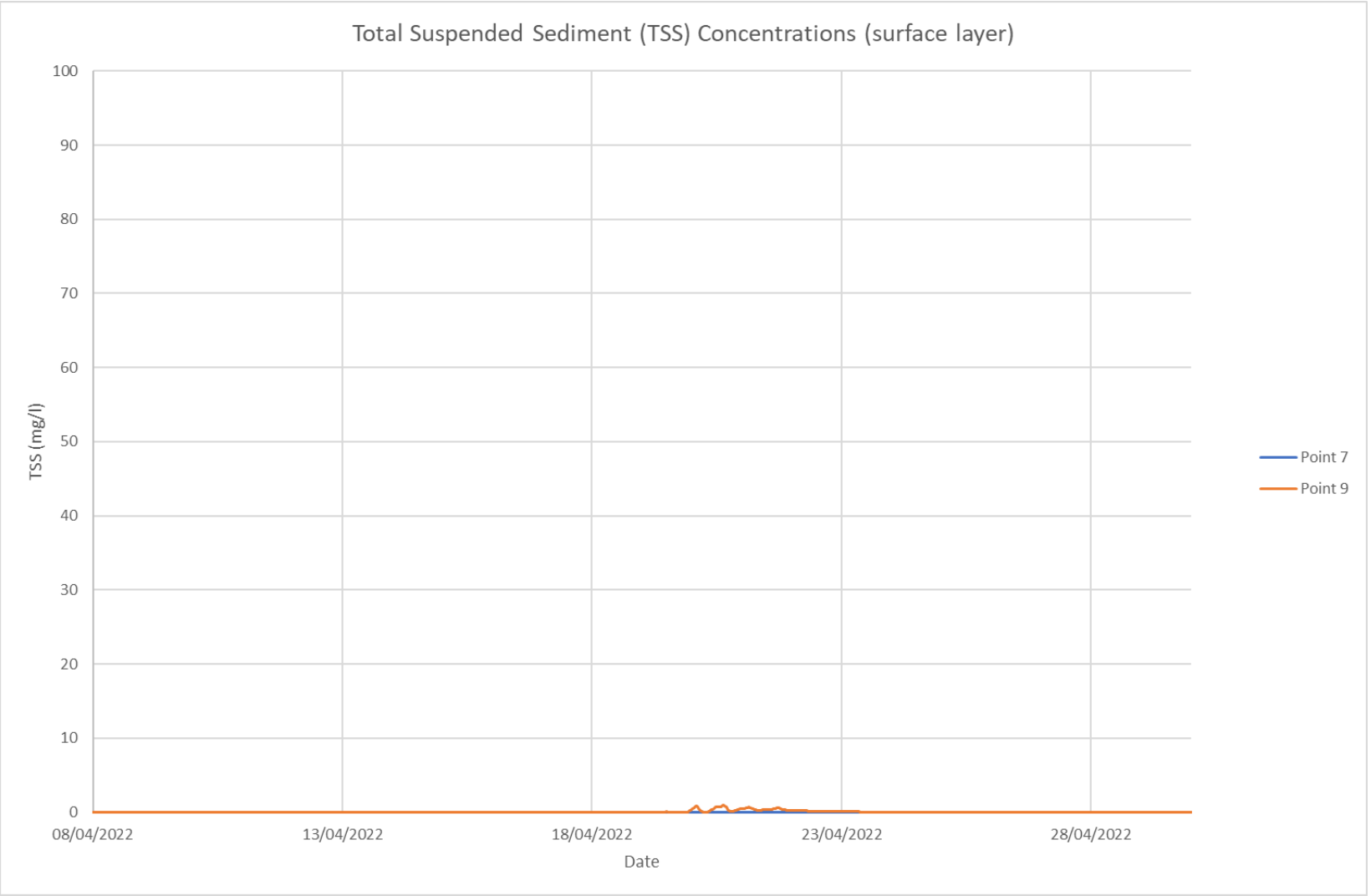

Figure F-9: Predicted Suspended Sediment Concentration (surface layer) at Points 7 and 9 – Offshore Export Cable Route Option 1

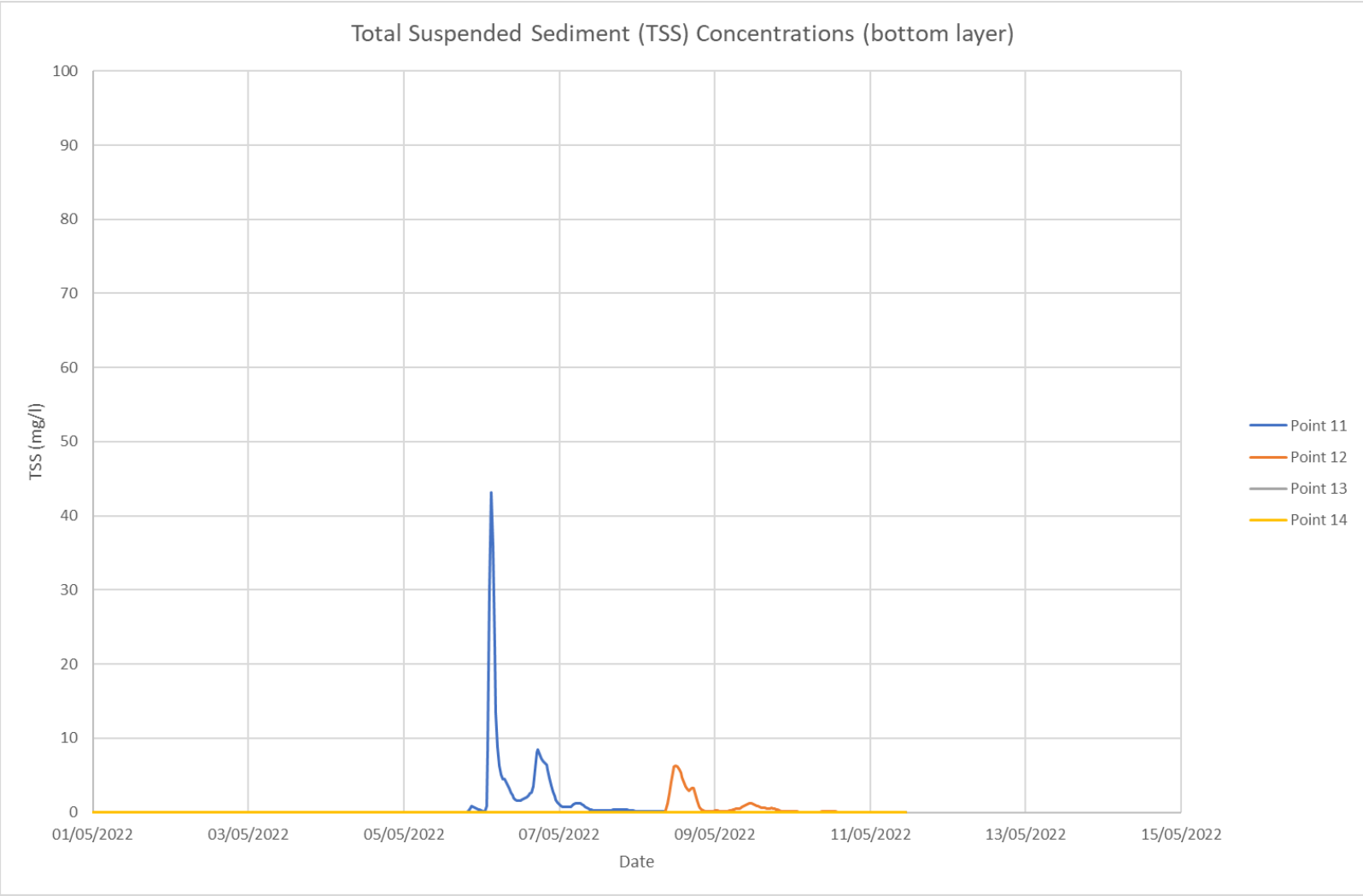

Figure F-10: Predicted Suspended Sediment Concentration (bottom layer) at Points 11 - 14 – Offshore Export Cable Route Option 1

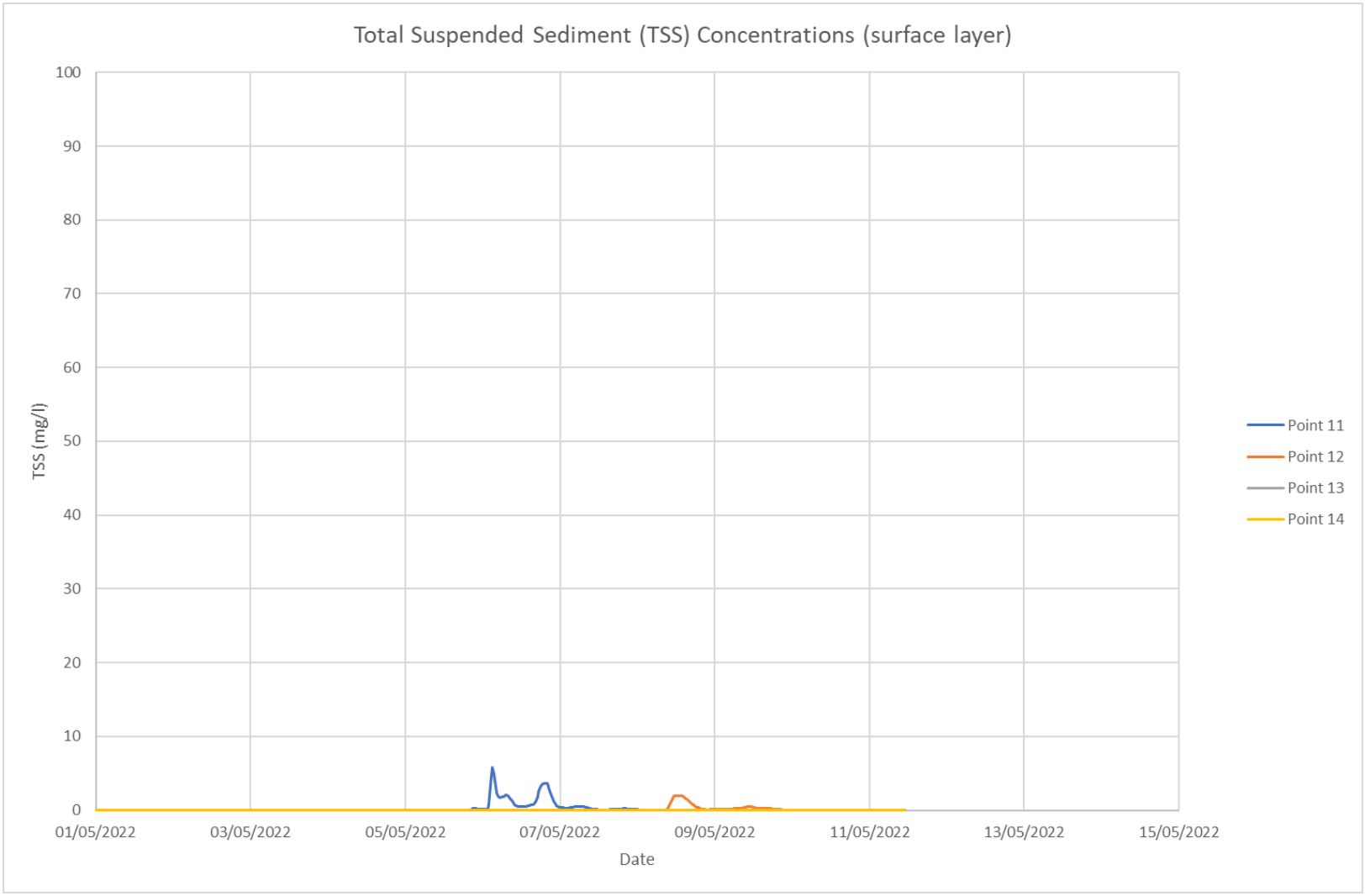

Figure F-11: Predicted Suspended Sediment Concentration (surface layer) at Points 11 - 14 – Offshore Export Cable Route Option 1

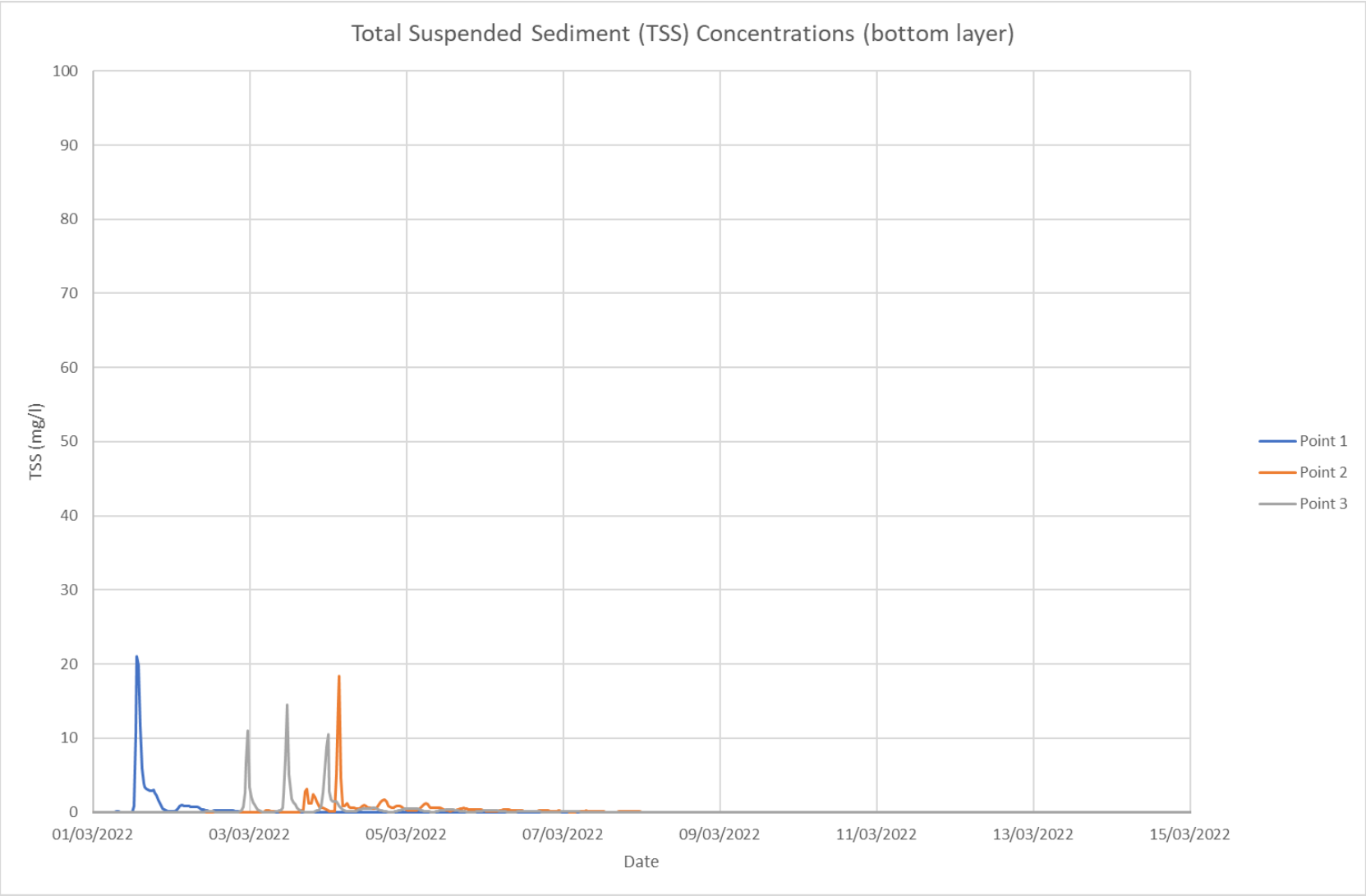

Figure F-12: Predicted Suspended Sediment Concentration (bottom layer) at Points 1, 2 and 3 – Offshore Export Cable Route Option 2

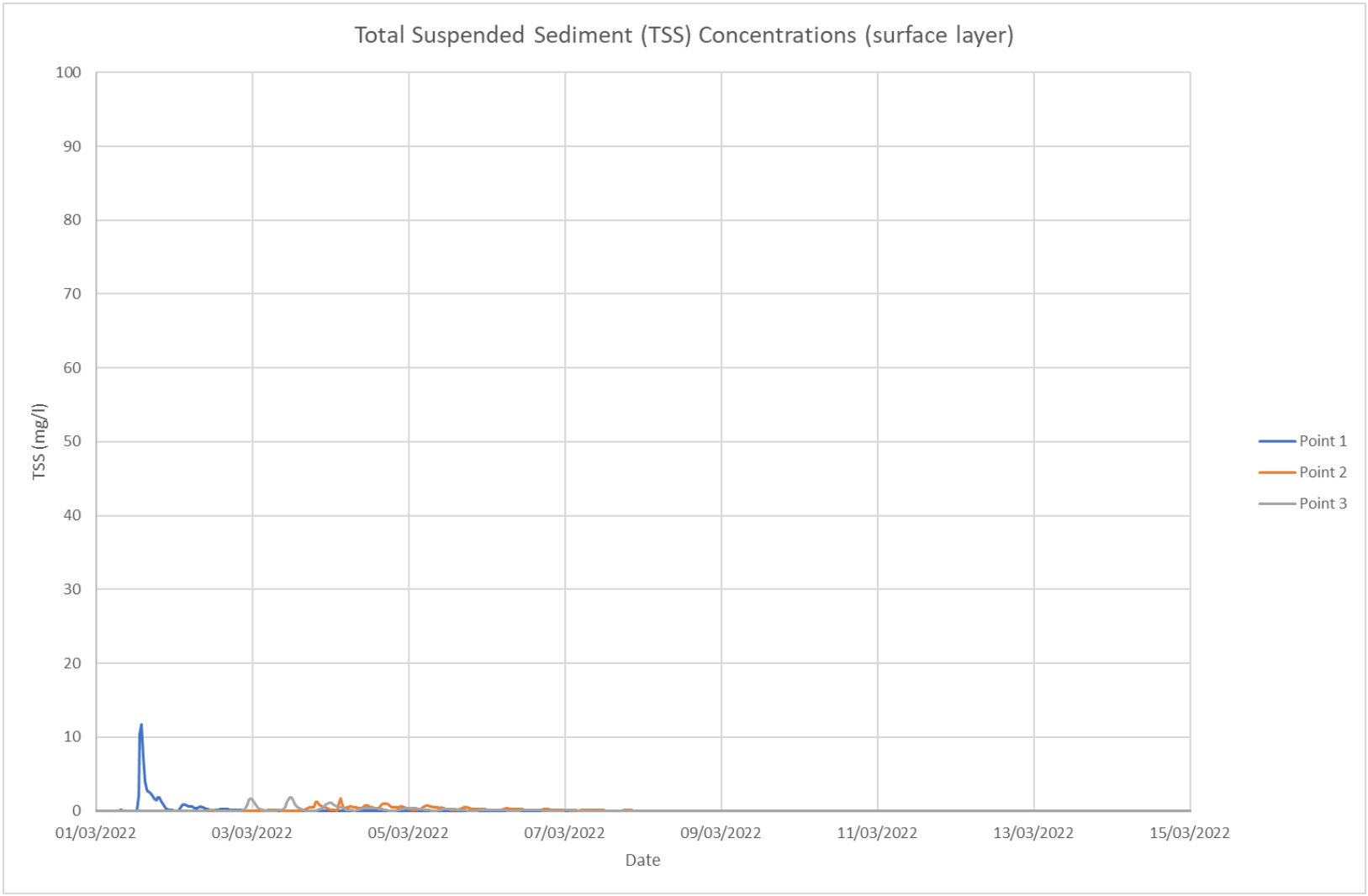

Figure F-13: Predicted Suspended Sediment Concentration (surface layer) at Points 1, 2 and 3 – Offshore Export Cable Route Option 2

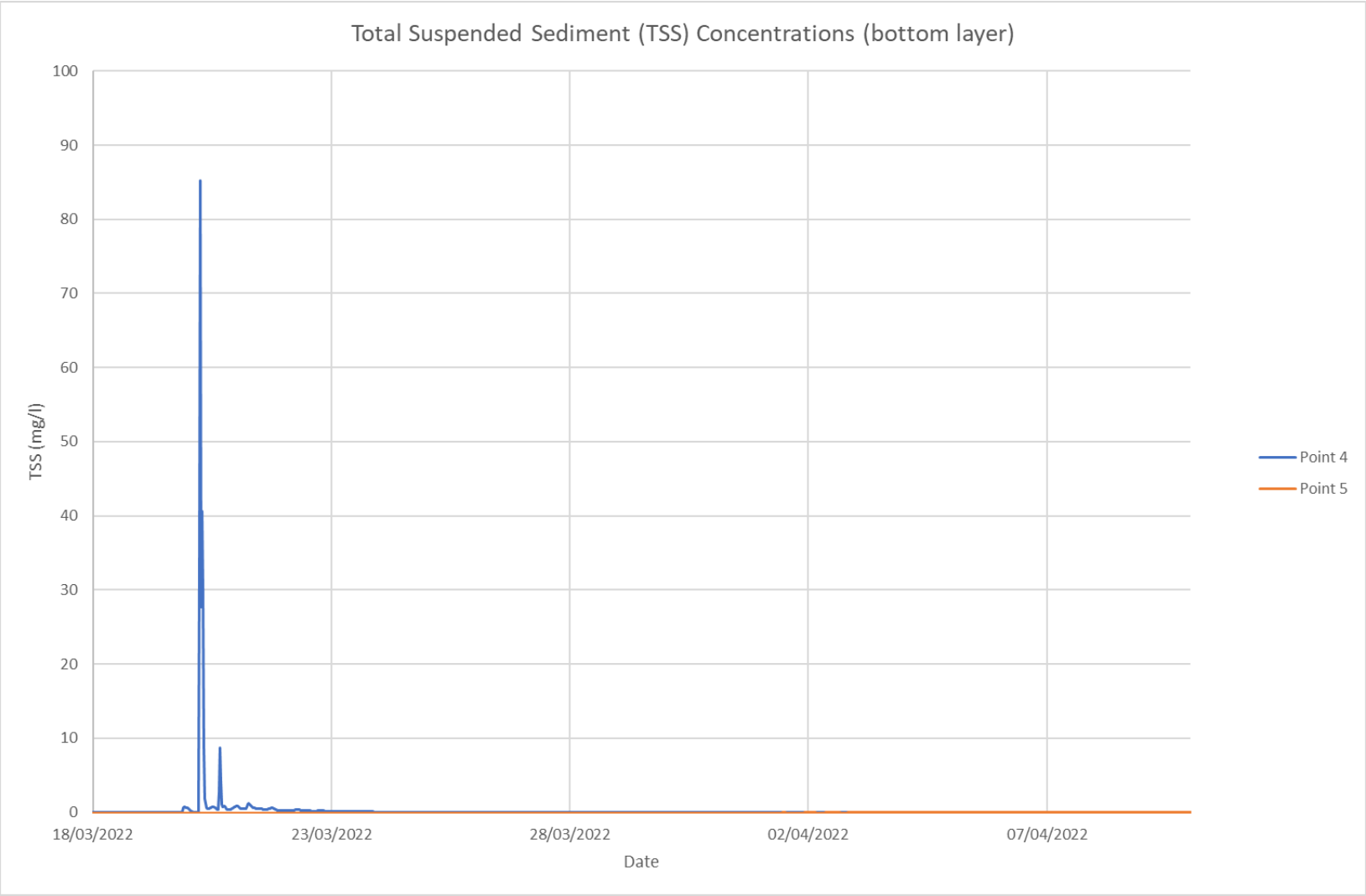

Figure F-14: Predicted Suspended Sediment Concentration (bottom layer) at Points 4 and 5 – Offshore Export Cable Route Option 2

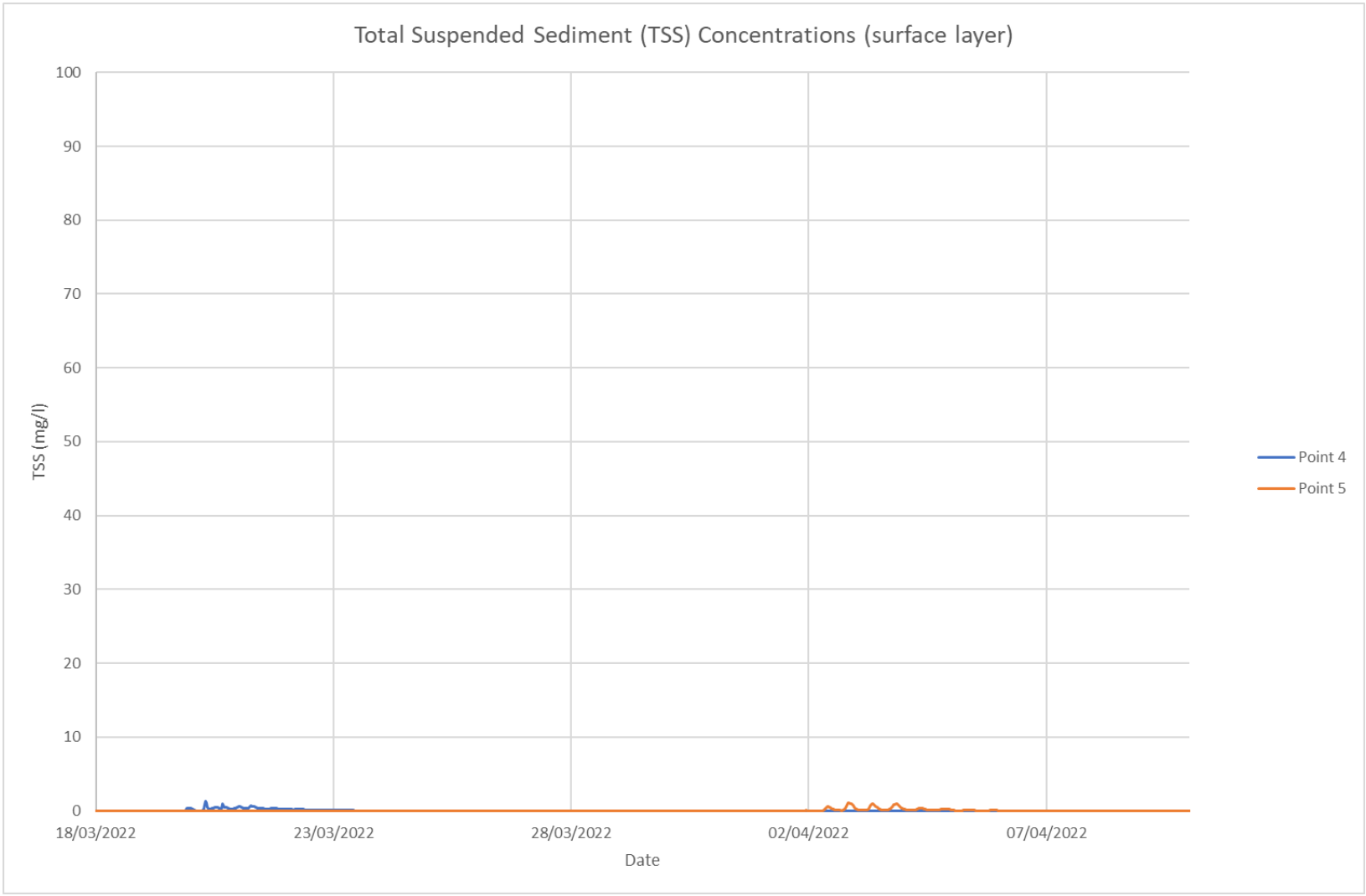

Figure F-15: Predicted Suspended Sediment Concentration (surface layer) at Points 4 and 5 – Offshore Export Cable Route Option 2

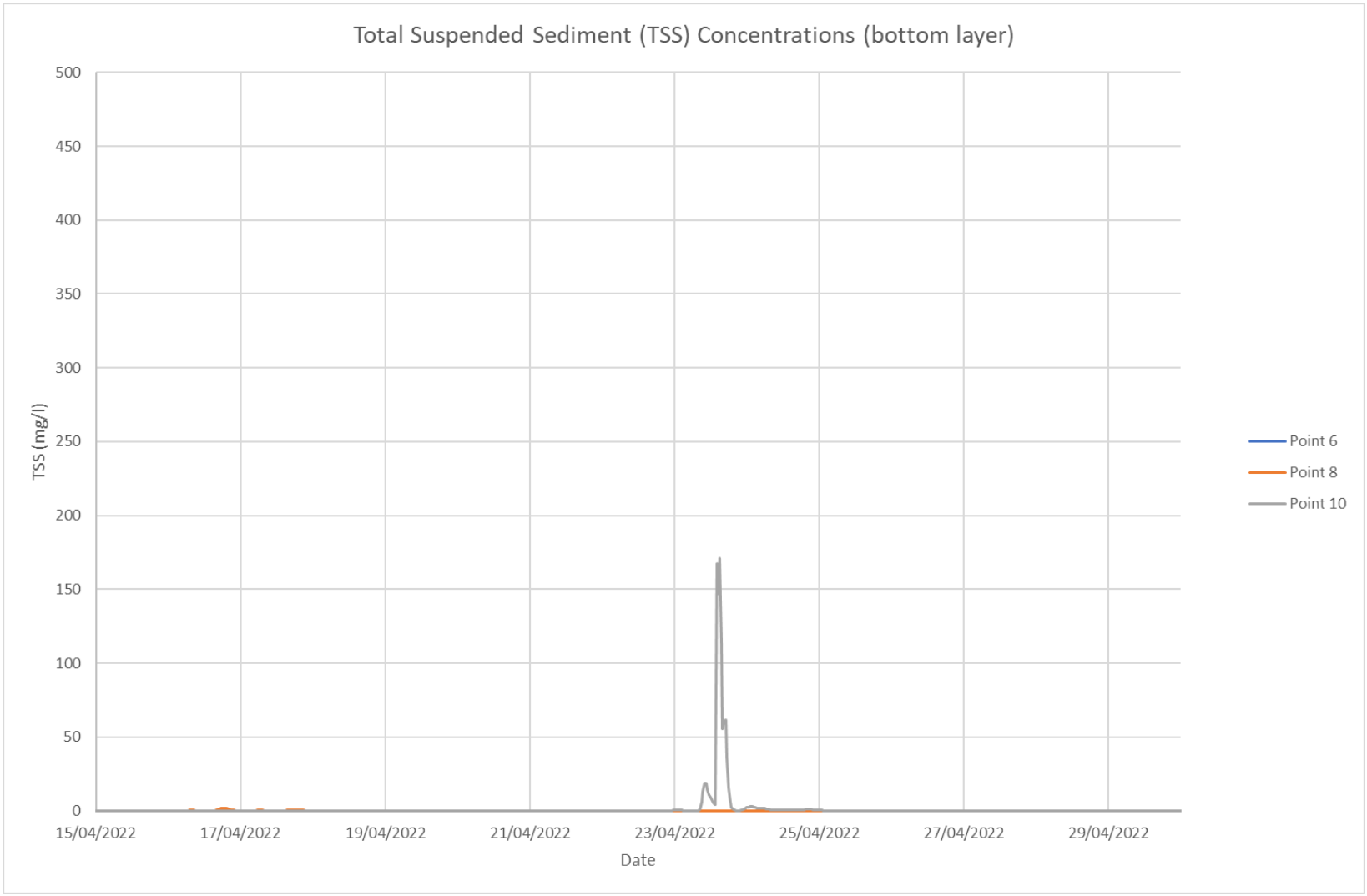

Figure F-16: Predicted Suspended Sediment Concentration (bottom layer) at Points 6, 8 and 10 – Offshore Export Cable Route Option 2

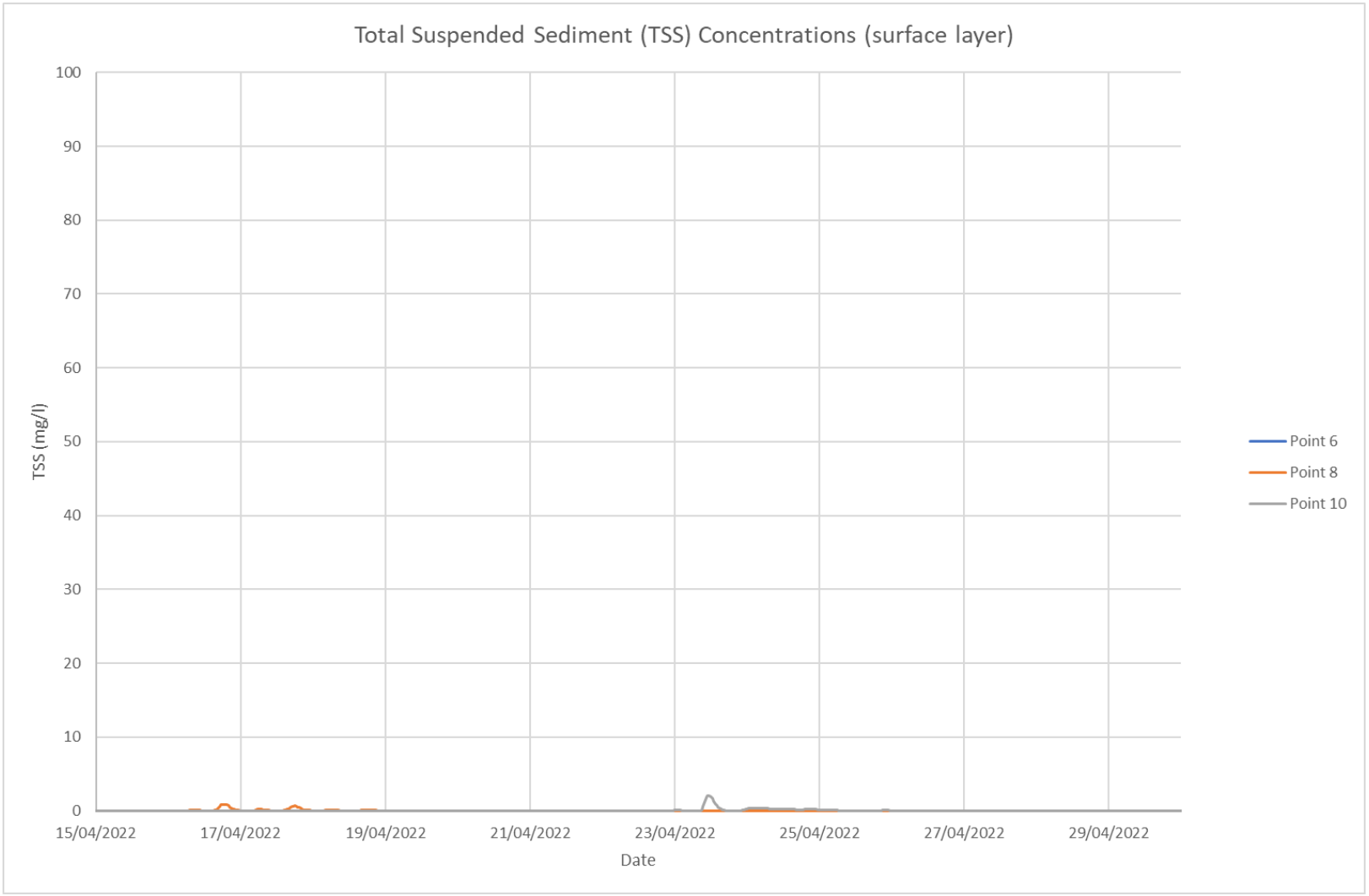

Figure F-17: Predicted Suspended Sediment Concentration (surface layer) at Points 6, 8 and 10 – Offshore Export Cable Route Option 2

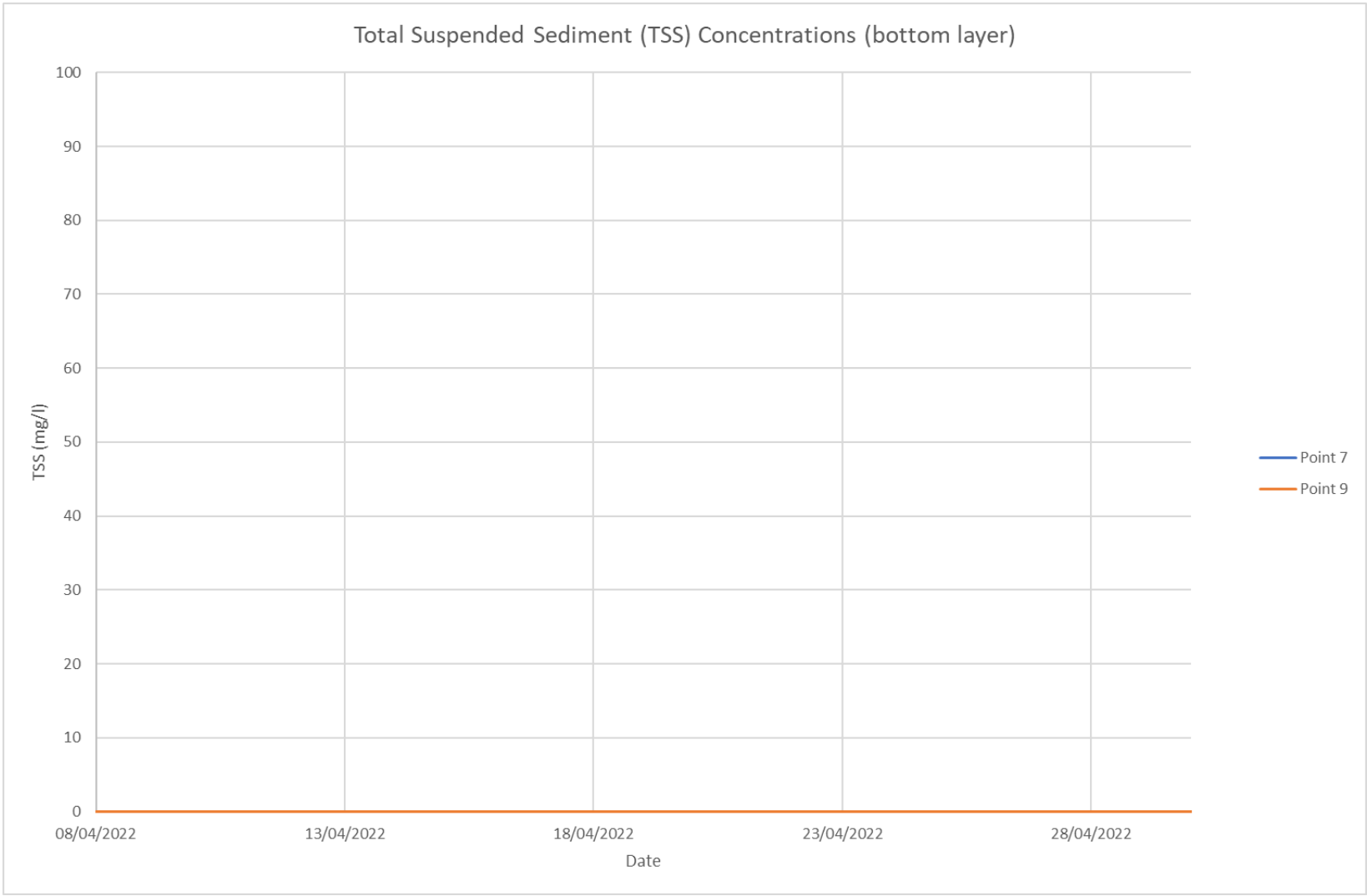

Figure F-18: Predicted Suspended Sediment Concentration (bottom layer) at Points 7 and 9 – Offshore Export Cable Route Option 2

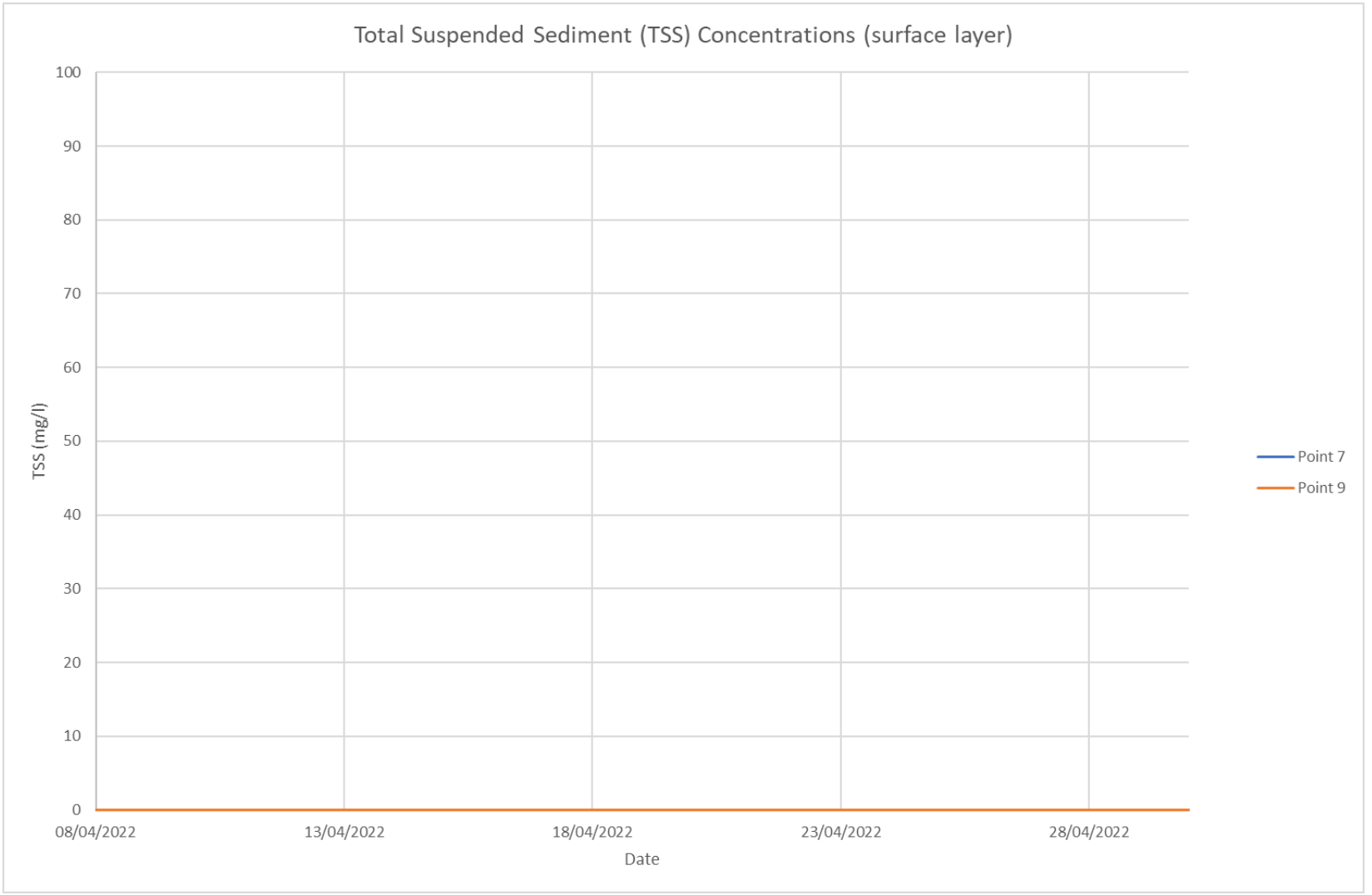

Figure F-19: Predicted Suspended Sediment Concentration (surface layer) at Points 7 and 9 – Offshore Export Cable Route Option 2

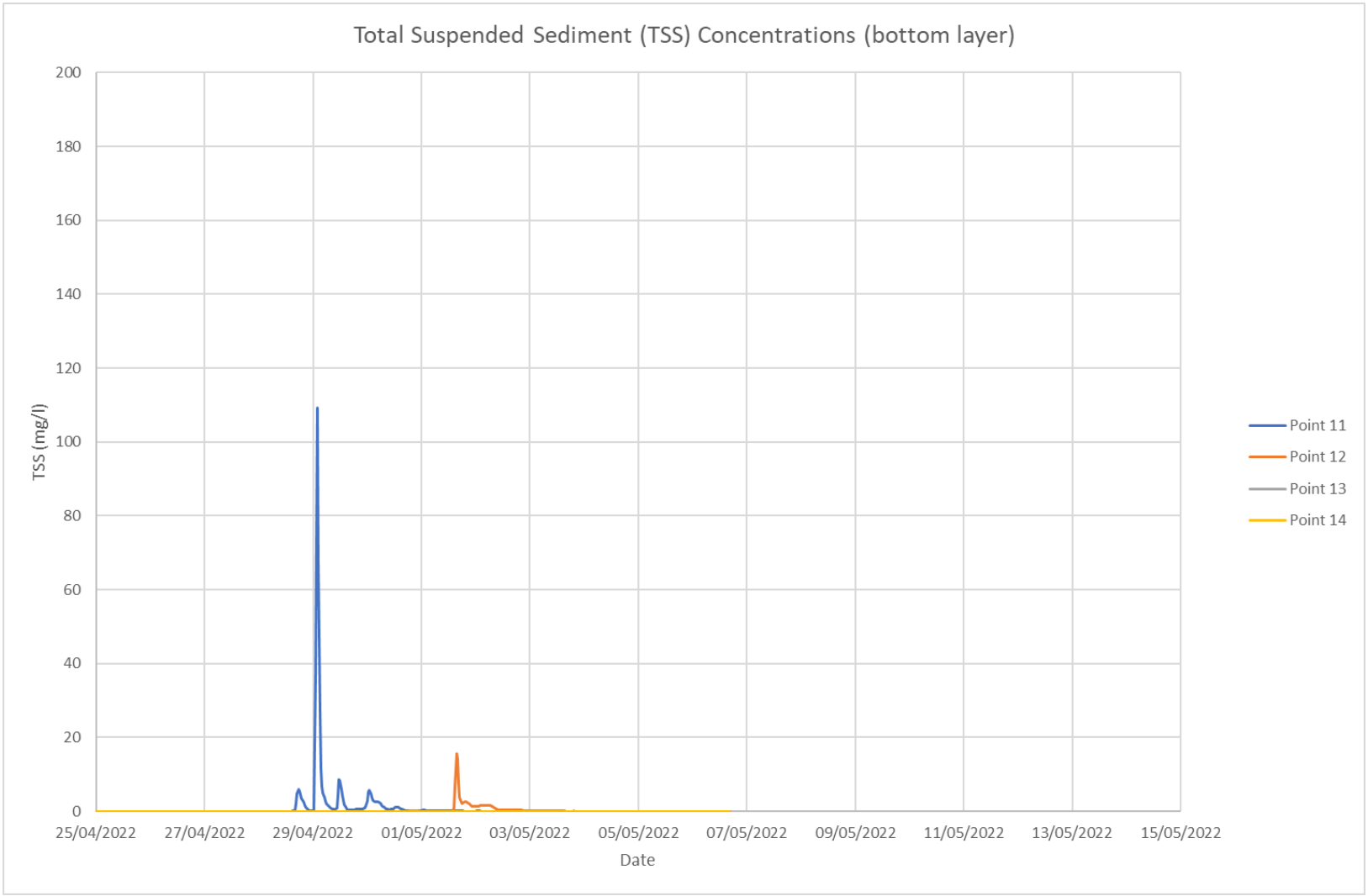

Figure F-20: Predicted Suspended Sediment Concentration (bottom layer) at Points 11 - 14 – Offshore Export Cable Route Option 2

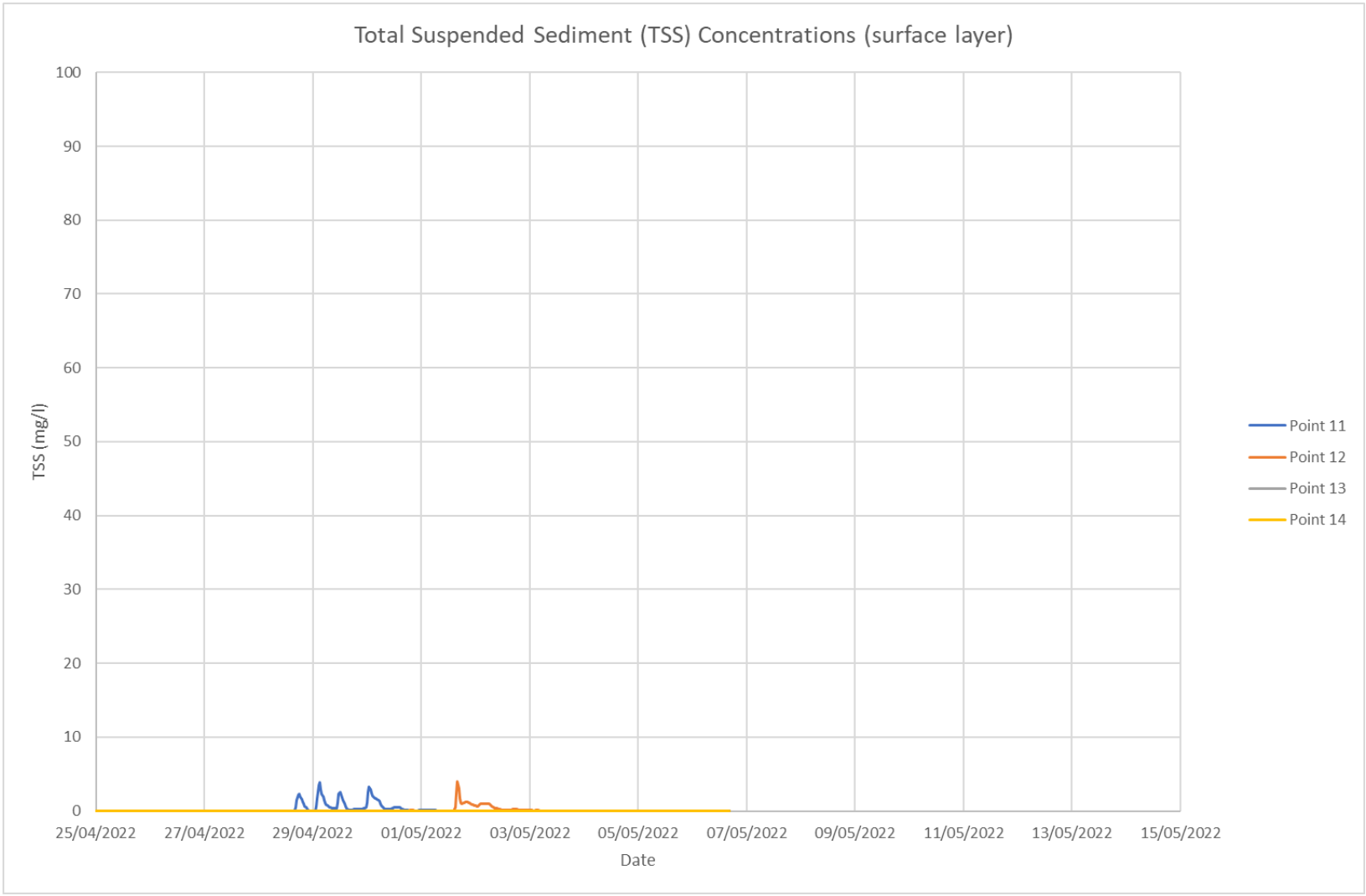

Figure F-21: Predicted Suspended Sediment Concentration (surface layer) at Points 11 - 14 – Offshore Export Cable Route Option 2